# A HYDROINFORMATIC APPROACH TO BASIN/COASTAL WATER MANAGEMENT

By

SHERIF NAOUM, B.A.Sc., M.A.Sc., P.Eng.

A Thesis

Submitted to the School of Graduate Studies

in Partial Fulfilment of the Requirements

for the Degree

Doctor of Philosophy

McMaster University

Half-Title Page

# HYDROINFORMATICS IN BASIN/COASTAL WATER MANAGEMENT

DOCTOR OF PHILOSOPHY (2003) McMaster University

(Civil Engineering) Hamilton, Ontario

TITLE: A Hydroinformatic Approach to Basin/Coastal Water Management

AUTHOR: Sherif Naoum,
B.A.Sc. (Cairo University), M.A.Sc. (McMaster University),
P.Eng. (Professional Engineer)

SUPERVISOR: Professor Ioannis K. Tsanis

NUMBER OF PAGES: xxv, 307, A.51

## ABSTRACT

A geographical information system has been creatively utilized to assist in the study and better understanding of the spatial variation and distribution of certain processes in water resources and coastal engineering. Hydroinformatics is the contemporary term that best describes the interactive knowledge-based non-expert decision support systems (DSSs) developed in this study in the form of GIS-based algorithms.

The spatial distribution of the annual orographic rainfall on the island of Crete (Greece) was modelled by using the multiple linear regression (MLR) method. The MLR models, developed and applied through the GIS interface, provided better estimates/predictions of rainfall at un-gauged locations than the conventional spatial interpolation techniques. This, in turn, resulted in more realistic spatial distribution of rainfall. A new DSS was developed that was applied to the island of Crete and Switzerland to assess rain gauge worth within an established network. This system provided the tools needed to reduce the number of gauges, if necessary, in an existing network, which means eliminating redundant gauges while maintaining an efficient network. Another tool was also developed to provide a ranking system that is based on performance evaluation of a number of spatial interpolation techniques in large and small rain gauge networks. Recommending the usage of certain techniques over others for a certain set-up of gauges and their records should improve the gridded precipitation input to distributed hydrological models. The same procedure may be followed for any other spatial variable (hydrological, meteorological, etc). Switzerland and the municipality of Hamilton-Wentworth (Ontario, Canada) were used as test cases for system evaluation.

A new GIS module was developed to estimate reference evapotranspiration based on the Penman-Monteith and Class A Pan Evaporation methods and using the station- and grid-based approaches. Although the combination of the grid-based approach and the Penman-Monteith method is recommended, the collection of significant amount of meteorological data from a relatively dense meteorological network is required for better results.

GIS was also used to facilitate the estimation of irrigation water requirements for different scales. Zooming in from large-scale (in the island of Crete) with limited number of meteorological stations to smaller scales with more "representative" stations provided support for the usage of the grid-based approach for calculating irrigation requirements.

For coastal engineering, a GIS pre-processor was developed for pollutant transport modelling in coastal areas. It provides accurate input to the models in the form of user-specified well-descritized bathymetry and shoreline, which are also used for post-processing purposes (i.e. graphical display). In addition to saving time in generating input files, this GIS pre-processor provides higher spatial accuracy, since all themes are geographically-referenced, which eliminates the possibility of overlapping or misplacing. It also shows great flexibility in generating grids of different cell sizes, interpolation techniques, and spatial extent. Transferability of the project between users and terminals makes it more accessible and convenient.

## ACKNOWLEDGMENTS

Thanks must first go to my supervisor Dr. Ioannis K. Tsanis for his continuous support and encouragement throughout the course of the program. His supervision and guidance greatly contributed to the successful completion of the thesis.

Thanks are also due to the members of the supervisory committee, Dr. Syed M.A. Moin (Department of Civil Engineering) and Dr. John Vlachopoulos (Department of Chemical Engineering) for keeping track of the work progress. Their contributions are very much appreciated.

The author would also like to thank the following organizations for their direct or indirect assistance with this work: the Department of Civil Engineering at McMaster University and the Ontario Graduate Scholarship Program.

## TABLE OF CONTENTS

## LIST OF FIGURES

## LIST OF TABLES

# CHAPTER 1

# BACKGROUND

The natural growth in population and industrial activities (which can be very rapid in some areas) represents a continuous challenge to various government organizations. Higher demand for good quality drinking water, increasing in frequency and intensity of disposable effluent by residential and industrial areas, and need for growing more crops by providing sufficient irrigation water - are only few of the concerns that face municipal, provincial, as well as federal governments. With the continuous flow of data of different types in different fields, the need for comprehensive systems that can be used for managing the quantity and controlling the quality of such data is certain. The other challenge is that efficient use of this data requires a good knowledge of the data itself, the system of data management, the purpose it will be used for, and the system that will make use of this data.

Decision makers and managers are regularly faced with such challenges as they try to evaluate different options and plans. This may require different professional databases and data acquisition systems, expert software and models, and plotting and graphical packages. In some cases the pace of development in one area may or may not be paralleled by a same-pace development in a complementary area (e.g. models and graphics or models and databases).

The purpose of this chapter is to familiarize the reader with some of the related terminologies found in the literature.

## 1.1 Decision Support Systems

### 1.1.1 Definitions

*A Short Definition.* A decision support system (DSS) is a specific class of computerized information systems that support decision-making activities. DSS is an interactive computer-based system and subsystems intended to help decision makers use data, documents, knowledge and/or models to identify and solve problems and make decisions.

*A Long Definition.* A decision support system (DSS) is both a process and a tool for solving problems that are too complex for humans alone, but usually too qualitative for only computers. Multiple objectives can complicate the task of decision-making, especially when the objectives conflict. *As a process*, a DSS is a systematic method of leading decision-makers through the task of considering all objectives and then evaluating options to identify a solution that best solves an explicit problem while satisfying as many objectives as possible. *As a tool*, a DSS consists of mathematical models, data, and point-and-click interfaces that connect decision-makers directly to the models and data they need to make informed scientific decisions. A DSS collects, organizes, and processes information and then translates the results into management plans that are comprehensive and justifiable.

### 1.1.2 Where is a DSS typically used?

Often, water resources groups have very diverse goals and values, including environmental, economic and ecological interests. What complicates this process even further is that water resources managers must try to achieve numerous and often conflicting objectives, such as achieving peak sustainable yield, minimizing environmental impact, managing costs, maintaining adequate water quality, controlling floods, minimizing energy use, and providing recreational opportunities.

DSS programs have been used to develop water resources management plans, adaptable operating rules for water and wastewater systems, and regional policies. Many municipalities and water authorities often derive their water supplies from several sources, which may include surface reservoirs, rivers, groundwater wells or combinations of these sources. To identify the best combination of supply sources in the long term, or to determine the most effective way of managing existing systems, decision-makers need a lot of information to account for all of the hydrologic, hydraulic, water quality, and economic relationships within the system.

### 1.1.3 What are the benefits of this technology for water resources management?

DSS recommendations are based on scientific data and models and can account for all objectives, cause/effect relationships, risks, costs, and reliability. DSS programs are adaptable and custom-designed for specific systems to help achieve system-specific management objectives.

A DSS is capable of aggregating all competing objectives to identify the best strategy, that is, a strategy that is truly optimal. Moreover, as a process, decision support techniques involve the decision-makers in defining the problems and the objectives.

### 1.1.4 What are the challenges of using this technology?

One of the biggest challenges is changing people's perceptions about both water resource management and environmental models. A common misconception is that competing objectives will necessarily result in a stalemate. However, a DSS is designed to consider all objectives and then produce an optimal solution. A computer model is often seen as a black box, but in the case of a DSS, a graphical interface links the decision-makers with the models. Decision-makers can set up scenarios and even view the modeling relationships in familiar formats (spreadsheets or graphical displays). Finally, rather than generating output that is cryptic and disaggregated, a DSS presents management plans graphically or with organized familiar terminology. Refer to Watkins and McKinney (1995) for a documentation of the developments associated with decision support systems in water resources.

## 1.2 Water Resources Planning and Management

The water resources planning and management field is unique in providing a linkage of the technologies available in the existing water-related disciplines in civil engineering, including hydrology, hydraulics, groundwater, and environmental engineering, with interdisciplinary studies in economics, sociology, political science, natural science, mathematics, computer science, and systems science for the purpose of providing graduate training and conducting interdisciplinary research in water resource systems planning and management.

The decision-making focus of this field places emphasis on application of advanced computer technology, decision support systems, geographic information systems, mathematical programming, and artificial intelligence to water resources and environmental systems. These tools are applied to complex multiple objective problems involving analysis of multi-facility multi-purpose systems requiring coordinated planning, management, and operations for water supply, hydropower, flood control, irrigation, wastewater management, water quality control, and conjunctive use of groundwater and surface water.

As it is widely known, effective water resources planning and management is mainly influenced by three types of groups: political, financial, and technical with different backgrounds and roles. This fact reflects a need for an effective way of simply communicating the different aspects of the planning and management process which may be accomplished by using GIS.

Applications include hydrologic modeling using geographic information systems; computer and statistical methods in water resources; spatial water balances; flood mapping; water resources systems analysis; groundwater modeling and management; multi-phase flow; and optimization, uncertainty and reliability analysis.

## 1.3 Watersheds

A watershed is a geographic area in which all sources of water, including lakes, rivers, estuaries, wetlands, and streams, as well as ground water, drain to a common surface water body. Because all watersheds are defined by natural hydrology and ultimately drain to coastal waters, they are good focal points for managing water and coastal resources.

## 1.4 Surface Hydrology

It is the part of hydrology (*The Concise Oxford Dictionary defines hydrology as: The science of properties of the earth's water, especially of its movement in relation to land. Hydrology is primarily concerned with the amounts and quality of water moving and accumulating on the land surface and in the soils and rocks near the surface. It therefore encompasses water in rivers, lakes, aquifers and glaciers. Hydrology embraces a wide range of interests including scientific and engineering applications*) that takes care of the water on

and above the Earth's surface. That includes precipitation, evaporation, evapotranspiration (transpiration and evaporation), interception, overland flow, surface runoff, and runoff to streams and the ocean. Examples of surface hydrology applications are: estimating rainfall and evapotranspiration amounts, calculating irrigation water requirements, assessing damages caused by floods, and examining water quality in coastal (near-shore) areas.

## 1.5 Geographic Information Systems

A Geographic Information System (GIS) is an organized collection of computer hardware, software, geographic data and personnel designed to efficiently capture, store, update, manipulate, analyze, and display all forms of geographically referenced information. A GIS is not a standalone technology but rather an integration of other technologies and disciplines. GIS technology also integrates common database operations, such as queries and statistical analysis, with the unique visualization and geographic analysis benefits offered by maps and spatial databases. These abilities distinguish GIS from other information systems and make GIS valuable to a wide range of public and private enterprises for explaining events, predicting outcomes, and planning strategies. Geographic Information Systems are being used by governments, business and academia (teaching and research). Particularly in the area of water resources, as part of the civil engineering discipline, the use of GIS is becoming more common, bringing together the expertise of professional hydrologists, professional engineers and GIS specialists. The diversity in data types suggests an efficient data storage engine. ArcView GIS provides a great potential for creating a GIS-based multimedia computer application. It relates numbers to locations (i.e. spatially identified information) which helps in the effective management of physical, biological, chemical, hydrological, hydrogeological, environmental, and political information about counties, cities, municipalities, watersheds, streets, rivers, lakes, etc.

## 1.6 Hydroinformatics

Hydroinformatics is the new and rapidly developing field which integrates knowledge and understanding of both water quantity and quality with the latest developments in information technology to improve technical and business decision making within the water industry.

Hydroinformatics embraces not only methods of data capture, storage, processing, analysis and graphical display, but the use of advanced modelling, simulation, optimization and knowledge-based tools and systems to plan and manage the water environment and water engineering infrastructure. Modelling of rivers, river basins, groundwater flow and contaminant transport, crisis management, strategic management, the management of assets and infrastructure, the use of data and computation, hydrological risks and climate change, flood risk estimation, the assessment, management and remediation of contaminated land and groundwater and mine water pollution, and water conservation are just some of the topics

covered by this field.

Hydroinformatics use simulation modelling and information and communication technologies to help us understand and solve problems of hydraulics, hydrology and environmental engineering for better management of water-based systems. It utilizes web-based information and knowledge systems, and computer-based modelling tools for urban drainage and water supply networks, rivers, estuaries and coastal waters, to provide support for decision making at all levels of management and operations. There is a growing need for professionals and managers to appreciate and work with these new technologies and tools.

## 1.7 Geostatistics

Geostatistics is concerned with spatial data. That is, each data value is associated with a location in space and there is at least an implied connection between the location and the data value. "Location" has at least two meanings; one is simply a point in space (which only exists in an abstract mathematical sense) and secondly with an area or volume in space.

The application of statistics to problems in geology and mining as well as to hydrology date back a considerable time. Geostatistics is very much an applied discipline and its development has been the work of mining engineers, petroleum engineers, hydrologists, soil scientists, geologists as well as statisticians. There are applications in epidemiology, plant pathology or entomology as well as forestry, atmospheric sciences, global change, geography. There is some overlap with geographic information systems and spatial statistics in general.

In one respect geostatistics might be viewed as simply a methodology for interpolating data on an irregular pattern but this is too simplistic. A number of interpolation methods/algorithms were already well known when geostatistics began to be known. Inverse Distance Weighting and Trend Surface Analysis as well as the much simpler Nearest Neighbor Algorithm.

## 1.8 Geomatics

Geomatics is a field of activities which, using a systematic approach, integrates all the means used to acquire and manage spatial data required as part of scientific, administrative, legal and technical operations involved in the process of the production and management of spatial information. Geomatics can also be defined as the modern scientific term referring to the integrated approach of measurement, analysis, and management of the descriptions and locations of Earth-based data, often termed spatial data. These data come from many sources, including earth orbiting satellites, air and sea-borne sensors and ground based instruments. It is processed and manipulated with state-of-the-art information technology using computer software and hardware.

Geomatics has applications in all disciplines which depend on spatial data, including environmental studies, planning, engineering, navigation, geology and geophysics, land development and land ownership. It is thus fundamental to all geoscience disciplines which use spatially related data, such as Surveying, Geodesy, Remote Sensing and Photogrammetry, Cartography, Geographic Information Systems and Global Positioning Systems.

## 1.9 Summary

In the water resources area, the design of general easy-to-use decision support tools requires an interaction between many disciplines, experiences, technologies and concepts. In this study, hydroinformatics are considered a specific branch of the more general decision support systems that use geographic information systems as their platform for data acquisition and model execution. The purpose and performance of such systems are determined by the type and quality of the integrated components derived from the broad areas of water resources management, surface hydrology, geostatistics, geomatics ..etc. The development of such tools should be well documented, which allows for an efficient and continuous update of these tools as new technologies and ideas emerge.

# CHAPTER 2

# INTRODUCTION

Encapsulating of information in a digital-electronic form occupied roughly the period of 1960 to 1980 and made way for the knowledge representation to take a similar course. The available information and knowledge in their new digital-electronic form are used to produce *new kinds of information* that have a particular value to us. Present day modelling systems have evolved from not so distant relatives that first appeared in the 1950's. These "first generation" models consisted of simple procedures that automated the calculation of mathematical formulas. Soon after, second generation models emerged incorporating these computational methods within problem specific code. This evolution continued through the development of third generation models that enabled users to apply these systems in a variety of situations and conditions, without altering the program, breaking away from the site or case specific applications. In more recent times, the fourth generation of water resources models appeared. These models provided users with elaborate pre- and post- processing functions, fully integrated simulation models, fronted by a graphic menu driven interface, taking advantage of database integration, that together provide a comprehensive and reliable simulation environment (Vieira et al., 1994).

The evolution continues and with the active involvement of society in many water resources issues bringing together a wide spectrum of individuals with varying perception, attitudes, and experiences, many questions arise influencing the decisions that are made at all management levels with regard to environmental regulation, policy, and design. Water resources modelling systems are now in the midst of their fifth generation. The fifth generation of models is "hydroinformatics" (Abbott, 1994).

Water resources problems are normally solved by using data, physical model testing or mathematical simulation and often by a combination of these techniques. A practical problem is how to handle the vast amount of data and yet come up with practical solutions within budget and time constraints. Present day information technology enables the integration of data obtained from on-site measurements, from model scale experiments or from numerical simulations. Libraries of mathematical functions (often distributed over worldwide networks), modelling support, libraries of components for the construction of models, program generators, graphical presentation tools and intelligent front ends, high speed computing systems and local and worldwide networks. They all facilitate interactive modelling over a wide range of applications. These problem-solving environments can be used to obtain practical engineering solutions for realistic problems in the field of hydroscience, as demonstrated here in case of hydrodynamic applications. Gallopoulos et al.

(1992) give the following steps towards the solution of a problem in some physical domain:

1. Construction of a mathematical model of the phenomenon under study.
2. Selection of relevant physical parameters and geometry.
3. Manipulation of equations and associated conditions, and making simplifications to allow for suitable solution methods to be applied.
4. Specification of a solution method based on analytical and approximate techniques.
5. Construction [test] problems and data sets.
6. Using appropriate specification and programming languages and specifying and creating (building or evolving from existing material) a program for a solution method, including documentation.
7. Application of the program(s) to the [test] data.
8. Validation of the results.
9. Comparison of the quality of the results and performance of the solution method with alternative solution procedures.
10. Collection and manipulation of output data.
11. Recording of the steps of the experiment.
12. Communication of the results to the client.

In many cases several additional issues become necessary, such as:

1. Assessment of the total problem and decomposition into component-problems
2. Identification of sub-problems which can be solved by mathematical models.
3. Evaluation of the solution of the sub-problems.
4. Integration of the results of the different component-problems.
5. Validation of the total solution.
6. Two-way interaction between the consultant and the client.

Of course, not all steps are needed in all projects and some steps will present no substantial problems in many situations. Some of the steps are completely pre-determined by the problem, others by the tools which are available. At this moment, tools are available to support the solution of specific problems in the academic environment, but the decomposition into and the integration of a great number of component-problems is much more difficult to support.

## 2.1 Goal and Objectives

### 2.1.1 General

Contribution is the general outcome when conducting research at the Ph.D. level. Two types of contribution are: contribution to the researcher and contribution to research. The first is mainly concerned with personal and professional development. To name a few topics under the personal development category: leadership, communication, administrative, and presentation skills; financial wisdom; group work; enhancing professional writing;

perseverance and perspective. On the professional level: an academic degree, publications, related computer knowledge (e.g software), computer skills, updated knowledge, etc. Contribution to research can be categorized as educational, inspirational and original. Proper documentation is the focus of the educational component. The documentation can be integrated into the undergraduate learning in any form. This can also motivate senior students to conduct research in the form of graduate work or any other form. Inspiring new researchers can be done through a good documentation of the technical and the general aspects of the project and providing a list of suggestions for future research. The original component includes: engineering applications, scientific investigations, software development, and reported results.

2.1.2 Specific

*Goal of Research:* The development of a series of well documented hydroinformatics to solve/tackle problems in the areas of water resources and coastal engineering

*Objectives of the Thesis:* the thesis is a treatment of a variety of issues that surfaced during the literature review phase. It emphasizes originality and avoids repetition through a number of original research publications of different interest and focus (Appendix A). The publications are concerned with:

1) organizing a common hydrometric database under one platform that is an assembly of hydrological, meteorological, water quality, water quantity, and land use data together with many other supporting data sets. The database should easily be managed (i.e. access, store, retrieve, extract, display, and update) and should also provide support for multi-disciplinary projects in the water resources area.
2) establishing a standard procedure to study the spatial and temporal variation of hydrological variables.
3) assessing existing raingauge networks and recommending a set of candidate gauges to be removed with a minimum loss of information. Being done through a decision-support system, locations for new gauges may also be suggested.
4) ranking spatial interpolation techniques for regional studies in small and big networks. This should assist in the decision making process and provides better input (and output) for distributed hydrological models.
5) modelling orographic precipitation via the multiple linear regression (MLR) method using spatial variables. More information is obtained about the spatial distribution of rainfall as the MLR method has emerged as a new spatial interpolation technique. Predicting rainfall at ungauged locations with higher accuracy can be achieved.
6) estimating reference evapotranspiration (ETo) using the grid based method by using all pieces of information available. Predicting ETo at any location in a given region with higher accuracy can be achieved. Comparing the station based method and grid based method using the Penman-Monteith and the Pan Coefficient methods provides more understanding of the importance of collecting various meteorological data.

7) developing a pre-processor for pollutant transport modelling that facilitates the modelling process by preparing high quality input and provides more enhanced and presentable results.

## 2.2 The Tool

ArcView GIS® is a Geographic Information System (GIS) software package for the display and manipulation of digital data keyed to geographic locations. It can create maps in a variety of projections and scales. In more sophisticated applications, it can be used to perform spatial query and analysis based on attributes or location, or to display images or documents linked to a map location.

ArcView was found to be an attractive tool for the purpose of this study because it can:

1) manipulate and use dBASE or ASCII tabular data;
2) display images (e.g., a remotely sensed image);
3) read vector data (points, lines, and polygons) as well as raster data (e.g. grids);
4) communicate with a digitizer so that features from a paper map can be stored in digital format in the desired units and projection;
5) read CAD drawings as AutoCAD files (.DWG and .DXF formats);
6) interact with the Graphical User Interface (GUI) by adding or eliminating buttons, menus, etc with assigned tasks;
7) interact with other applications through Remote Procedure Calls (RPC) by establishing client/server relationship (e.g. ARC/INFO server);
8) make conversations with Dynamic Data Exchange (DDE) which is a special client/server mechanism supported by Microsoft (e.g. Visual Basic and Excel);
9) customize and develop ArcView through its own programming language (Avenue);
10) use Dynamic Link Libraries (DLLs) through Avenue to add more functionality to ArcView (e.g. create a new directory or execute a Fortran code);
11) create windows and pop-up menus through ArcView's own dialog designer or using Visual Basic; and
12) interact with other applications that can work in ArcView environment (e.g. the statistical package S-Plus).

Geographic Information Systems have been increasingly used in supporting water resources management applications. These systems can be linked to/integrated with different environmental simulation models that provide functions for data storage, calculation of required input parameters, data manipulation, and output processing (Ross and Tara, 1993; Maidment, 1993; Greene and Cruise, 1995; Brimicombe and Bartlett, 1996; Tsanis et al., 1996; Naranjo and Larsen, 1998; Lichy, 1998). GIS technology is also central to these

models because it provides the system with spatial data management, analysis, display and interface functions (Boyle et al. 1998; Boyle and Tsanis 1998).

## 2.3 The System

Any developed system within this study is a combination of coupled and integrated components. An example for the coupled component is pollutant transport modelling application (Chapter 8). An example for the integrated component is concerned with estimating reference evapotranspiration (Chapter 7). The tools and modules required for the interactive usage of the system and the proper documentation of the system are also major components.

Documentation should provide the preliminary vision and suggested components of the system and it is normally drafted at the outset of the project and it has to:

1) include all needed information to design, upgrade, or use the system;
2) include true statements such that the system should satisfy every statement;
3) explicitly state the areas of incompleteness;
4) state the changes that likely or unlikely to take place;
5) be easy to change;
6) allow personnel turnover;
7) assume basic knowledge of the system (provide separate overview); and
8) give quick access for details (i.e. no searching).

## 2.4 Thesis Structure

The thesis consists of 9 chapters and 8 appendices (CD is attached). Additional information is included in the appendices to discuss in more detail the contents of the chapters. In Chapter 1, the reader is familiarized with the topic by introducing definitions and concepts, which largely comprise the main body of the thesis. In Chapter 2, the goal, objectives, and structure of the thesis are presented. The temporal and spatial variation of annual precipitation on the island of Crete (Greece) is investigated in Chapter 3, while Chapter 4 introduces a GIS-based multi-criteria analysis for assessing raingauge worth within an established network with two case studies from Crete and Switzerland. In Chapter 5, a number of spatial interpolation techniques in the ArcView GIS package are evaluated using two test cases from Hamilton (Ontario, Canada) and Switzerland. Modelling the annual orographic precipitation using GIS-based multiple linear regression method for the island of Crete (Greece) is discussed in Chapter 6. Estimating reference evapotranspiration and irrigation demand is presented in Chapter 7 with two case studies in Greece and Crete (Greece). Chapter 8 is devoted to the documentation of a GIS-based pre-processor for 3D pollutant transport modelling. Finally, Chapter 9 is discussing the achievement of the study and recommendations for future research.

## 2.5 ArcView GIS in the Thesis

The use of ArcView GIS in this study has gone through phases of maturation. Before the use of ArcView had been focused on being and defined as a platform for developing hydroinformatics, it aimed primarily at the spatial analysis and display capabilities of the software.

# CHAPTER 3

# TEMPORAL AND SPATIAL VARIATION OF ANNUAL RAINFALL ON THE ISLAND OF CRETE, GREECE

In this chapter, the annual rainfall records from the island of Crete in Greece were used with the aid of a geographical information system to study the temporal and spatial rainfall characteristics. The GIS was used to produce a digital elevation model, delineate watersheds and estimate the areal rainfall from a network of raingauges by using different interpolation schemes. The rainfall-elevation correlation was examined. Frequency analysis of the rainfall records was used to estimate areal rainfall for the island of Crete and its main watersheds for return periods of 2, 5, and 10 years.

## 3.1 Introduction

Owing to its variability according to the general pattern of atmospheric circulation and according to local factors, precipitation (i.e. rain and the liquid water equivalent of the various form of frozen water) is measured in time and space. The measured precipitation is useful in a variety of hydrologic applications. Raingauges that fail to capture the actual amount of precipitation result in an underestimation of flood assessment or an overestimation of irrigation water requirements. Rainfall duration and intensity are key factors in assessing floods, while estimating irrigation water needs requires a water balance between available water, represented by rain, and losses, which are mainly caused by crop evapotranspiration in addition to other factors. Sevruk (1982) indicated that the commonly used methods of measurement may underestimate actual precipitation from 5 to 30 percent, depending upon the type of instrument and its installation, the climatology of the region and, the form of precipitation. The underestimation can be owing to the effects of wind, splashing, wetting, evaporation and blowing snow.

There is a seasonal variation and a geographic variation of precipitation. Pronounced seasonal variation occurs where the annual oscillation in the atmospheric circulation changes the amount of moisture inflow over the regions (Chow et al., 1988). Although the tropics may not really have seasons, other parts of the world have better defined rainy seasons, which may occur in summer or in winter (Singh, 1992). Southern Africa has its rainy season during the summer, whereas Greece has one in winter. Egypt, like other parts of Northern Africa, has no rainy season. The geographical distribution of precipitation depends upon latitude, orographic factors and the distance the air mass moves away from the source of moisture. Rainfall tends to be heaviest near the equator and diminishes as the air flows toward higher latitudes. Other factors reported in the literature that may have an impact on the variability of precipitation include continentality, direction of prevailing wind,

topography, orientation of topography and aspect.

Analysis of precipitation data is essential in any water resources application. The variation is partly predictable, or deterministic, and partly random. In some cases, the random variability is so large compared to its deterministic variability that treating the variation as purely random may be justified. This type of treatment is appropriate for hydrologic data averaged over long time intervals, such as annual precipitation (Chow et al., 1988). Statistical methods can be used to describe the random variation of a set of observations and to focus attention on the observations themselves, rather than on the physical processes that produced them.

## 3.2 Orographic Effects

The orographic influence occurs only in the proximity of high ground in the case of stable atmosphere. There are three main mountain effects: orographic lifting, thermal forcing, and obstacle effects which include mountain blocking, flow deflection, and the production of lee-side flow disturbances. Two major roles that mountains have in forming clouds and precipitation. First, mountains are *obstacles* to atmospheric flow. As stable approaching airflow encounters a mountain barrier, it is forced to ascend the mountain (Banta, 1990). If the necessary atmospheric conditions exist, particularly the stability and moisture content of the atmosphere, clouds and precipitation may be produced owing to the forced-orographic uplift of the air. To a large extent, the stability of the atmosphere determines how the obstacle will affect the flow. In particular, the stability determines the maximum orographic lifting realized by the air. If the atmosphere is more stable, there will be less vertical displacement and more flow around the mountains. Mountains also cause *blocking* of stable flow. As stable air approaches the mountain, it slows down owing to the blocking effect. Flow retardation can result in horizontal-mass convergence upstream of the mountain, and may produce upward air motion and cloud formation before the mountain slope is reached. Similar to mountain blocking is flow *deflection* by a mountain. Airflow deflection can also produce regions of horizontal-mass convergence, but in a different location. Stable airflow may be forced to split and flow around the mountain. The airflow then convergences on the lee side of the obstacle and may create a region of enhanced instability. The stable airflow may also be *forced to flow upslope* and over the mountain top on the windward side, and then descend to its original level on the lee side. Disturbances in the flow on the lee side and down stream of the mountains can play a major role in cloud and precipitation formation as well (Banta, 1990).

The second major role that mountains have on forming clouds and precipitation is that they are elevated heat sources (Banta, 1990; Orville 1965, 1968). The slopes of the mountain protrude into the atmosphere and air next to the mountain slopes is warmed by the

heated slopes. Air next to the mountain becomes warmer than that at the same level away from the mountain and over the plains. This produces a relative low pressure in the air next to the mountain. The low pressure induces convergence of flow toward the mountain. Air begins to flow up the slope. Provided there is sufficient heating and low stability, the airflow will eventually rise over the peak and break away from the slope. Updrafts then form over the mountain. Mountains are elevated moisture sources as well (Orville 1965, 1968). Mountains typically have fairly dense vegetation that holds moisture in the vegetation itself and facilitates moisture retention in the topsoil on the mountain slopes (Oke, 1987). The addition of water vapor to the atmosphere from evaporation and evapotranspiration at the surface of the mountain slope creates enhanced buoyancy effects. This causes air flowing up the mountain slope to be more moist and less dense than that at the same level away from the mountain and over the plains (Orville, 1968). In addition, the moisture is a critical component for the formation of clouds.

## 3.3 Study Area

The increased demand for water for agricultural use on the island of Crete (Greece), which constitutes approximately 80% of the water use, cannot be always met (Angelakis and Diamadopoulos, 1995). This is especially true in the summer months, when there is little or no precipitation and the water demand is the highest. Temporal and regional variations of precipitation and the difficulty in transporting water owing to the mountainous terrain make the water imbalance more evident. These uneven spatial and temporal distributions, although common in many Mediterranean areas, have significant impact when compounded by the water demands associated with intensive agricultural activities and the tourism industry, (Marecos do Monte et al., 1996) both of which are applicable to the island of Crete. There has been little emphasis on quantifying the variation in climatic conditions and/or the relative distribution of irrigated areas and their respective impact on irrigation estimates on the island of Crete.

Rainfall is the largest component of annual precipitation on the island of Crete in Greece. The objective of this chapter is to investigate the temporal and spatial variation of annual rainfall in the region, where orographic effects are expected to increase with the intensity of winter precipitation, by employing statistical methods and a Geographic Information Systems (GIS). It should be noted that the term "annual rainfall" which will be used throughout the chapter represents water years (September to August) rather than calendar year (January to December).

Greece covers an area of 130000 $km^2$ and is located in the Mediterranean region at the south of Europe and facing northern Africa as shown in Figure 3.1a. It is divided to 51 political counties as shown in Figure 3.1b. The island of Crete occupies the southern part of

Greece with an area of 8265 km$^2$, which is 6.3% of the area of Greece and is divided into four counties (prefectures) Lassithi, Iraklion, Rethymno, and Chania as shown in Figure 3.1b. Most of the agricultural activity takes place in the county of Iraklion (2626 km$^2$), while the remaining counties, in order of agricultural activity, are: Lassithi (1810 km$^2$), Chania (2342 km$^2$) and Rethymno (1487 km$^2$).

Monthly precipitation data were compiled by the Hellenic National Meteorological Service for 54 meteorological stations and 27 precipitation gauges (as shown in Figure 3.2a) for periods ranging from 12 to 50 years. There was no daily rain data available and the gauges used were of the cylindrical weighing type, with a diameter of 10 cm$^2$. A small amount of oil is added to the gauge to prevent excessive evaporation losses. The stations covered the more agricultural eastern part of the island, while there were fewer gauges on the western side. The gauges were located at different elevations, ranging from mean sea level (MSL) in the county of Iraklion, to 905 m above MSL for the county of Lassithi. As shown in Figure 3.2b, high elevations (mountains) are situated east-west that reach in some parts an altitude of 2500m.

## 3.4 Methods

### 3.4.1 Spatial Data Analysis

Spatial data was handled through the use of the software ArcView GIS, where a small database was created for that purpose. The database included spot elevation data, contour lines, shorelines, political boundaries, location of gauges (x,y) in decimal degrees, rain gauges altitude (Z) (in meters) above MSL, and monthly rainfall values. The GIS coverages used in this study were based on maps developed by the Greek Army Geographical Service. A GIS layer was generated for the gauges where their locations were identified (after conversion from degrees-minutes-seconds "DMS") by decimal degrees. The layers were then projected (for more information about projection, refer to Appendix B) using the Transverse Mercator projection (Appendix B) and the GRS 80 Spheroid with a Central Meridian of 24°, Scale Factor of 0.9996, and False Easting of 500000. This projection is also referred to as EGSA units. From the spot elevation values, together with a 20m contour map, a Digital Elevation Model (DEM) was also generated with a cell size of 30m, resulting in a grid of 3027 rows and 8659 columns. The DEM was used to check the altitude of the gauges and to delineate watersheds as shown in Figure 3.2c.

#### 3.4.1.1 Delineating Watersheds

The GIS facilitates the generation of hydrologic regions (watersheds) as they are delineated by the use of the DEM through a multi-step procedure (refer to Appendix C) that includes:

*Filling the DEM.* Sinks are cells with undefined flow direction owing to the fact that all

neighboring cells are higher than the processing cell. Sinks can be interpreted in two ways. One group of hydrologists deals with them as depression storage or ponds and should be left unfilled. The other group deals with them as errors in the data and have to be corrected. The latter explanation is, conditionally, more acceptable taking into account the location and the number of sinks. Filling sinks is an iterative process. When a sink is filled, the boundaries of the filled area may create new sinks, which then need to be filled.

*Flow Direction Grid Generation.* The direction of flow is determined by finding the direction of steepest descent from each cell. The Flow Direction grid is an integer square grid whose values range from 1 to 128. The processing cell is surrounded by 9 cells. Each of these cells, starting from the east cell, to the right of the processing cell, is assigned a number starting with a value of 1 and, moving clockwise, the values 2, 4, 8, 16, 32, 64, 128. For example, if the direction of largest decrease was to the left of the current processing cell, its flow direction would be 16... and so on (Jenson and Domingue, 1988).

*Flow Accumulation Grid Generation.* This is a grid that represents the accumulated flow to each cell by accumulating the weight for all of the cells that flow into each downslope cell. The accumulated flow is based upon the number of cells flowing into each cell in the output grid. The current processing cell is not considered in this accumulation. Output cells with a high flow accumulation are areas of concentrated flow and may be used to identify stream channels. Output cells with a flow accumulation of "0" are local topographic highs and may be used to identify watershed divides. A Stream Network can then be generated and vectorized. Visually comparing the generated network with the given one is a reasonable way of checking the accuracy of the DEM.

*Delineating Watersheds.* This requires a depression-less digital elevation model and it is done by defining some minimum threshold. Watershed delineation is a primary use of GIS in hydrologic modelling. There are many other examples to follow where information on computing contributing areas, mean elevation, areal precipitation over the basin, flow length, land slope, and channel slope can be derived from raster and vector data layers.

3.4.1.2 Estimating Areal Precipitation

Using the annual records, the areal rainfall is estimated using the conventional spatial interpolation techniques in addition to the multiple linear regression (MLR) technique (will be discussed in more detail in Chapter 6). The conventional interpolation techniques are considered station-based methods, while the MLR method is a grid-based method. In other words, these models use the point rainfall values to estimate rainfall at ungauged locations, while the MLR method use these point values to construct the model and then apply it to the "gridded" island where each cell has a known altitude, latitude, and longitude. If there exists

an area that is not covered by gauges, the error associated with the conventional methods is greater than that associated with the MLR method (as in Chapter 6). The methods are used to estimate mean annual rainfall for the different years as well as for return periods of 2, 5, and 10 years.

*Multiple Linear Regression (MLR).* The method of analysis used is the method of Least Squares (LS), which is simply a minimization of the sum of squares of the deviations of the observed response from the fitted response. This involves the initial assumption that a certain type of relationship, linear in unknown parameters, holds. With rainfall being the dependent (response) variable, the model function is of a specified form that involves both the predictor variables (altitude, longitude, and latitude) and the parameters. Interaction effects between the variables can also be considered. These are represented in the models by adding three more terms. The use of a second-order model, also a possibility, results in the addition of three more terms, leading to a ten-parameter model. The general form of the final model is:

$$\begin{aligned} y = {} & \beta_o + \beta_1 x_1 + \beta_2 x_2 + \beta_3 x_3 \\ & + \beta_4 x_1^2 + \beta_5 x_2^2 + \beta_6 x_3^2 \\ & + \beta_7 x_1 x_2 + \beta_8 x_1 x_3 + \beta_9 x_2 x_3 \end{aligned} \qquad (3.1)$$

where y: rainfall (mm/year); $x_1$: altitude (m); $x_2$: longitude (km); and $x_3$: latitude (km).

*Spline Interpolation.* It is referred to as the basic minimum curvature technique, or thin plate interpolation, because it possesses two main features: (a) the surface must pass exactly through the data points, and (b) the surface must have minimum curvature. The latter is accomplished by minimizing the cumulative sum of the squares of the second derivative terms of the surface, taken over each point on the surface. The *Regularized Spline* modifies the minimization criterion so that the third derivative terms are incorporated into the minimization criteria ensuring both a smooth surface and smooth first-derivative surfaces. The *Tension Spline* modifies the minimization criterion, so that first derivative terms are incorporated into the minimization criteria. The *Regularized* option usually produces smoother surfaces than those created with the *Tension* option. Although it has been used to simulate the spatial distribution of precipitation, the smooth spline surface was occasionally found to fail or erratic predictions were obtained (Franke, 1982; Mitas and Mitasova, 1988).

*IDW.* The Inverse Distance Weighted technique determines cell values using a linearly weighted combination of a set of sample points. The weight is a function of inverse distance. IDW allows the user to control the significance of known points upon the interpolated values based upon their distance from the output point. The best results from IDW are obtained when sampling is sufficiently dense with regard to the local variation the user is attempting to simulate. If the sampling of input points is sparse or very uneven the results may not

sufficiently represent the desired surface. The IDW is known for its tendency to isolate high values thus providing unrealistic interpolation results (Tung, 1983; Watson and Philip, 1985).

*Kriging.* Unlike the other interpolation models, Kriging involves an interactive investigation of the spatial behavior of the phenomenon before generating the output surface. It is based on the regionalized variable theory, which assumes that the spatial variation in the phenomenon is statistically homogeneous throughout the surface; that is, the same pattern of variation can be observed at all locations on the surface. The spatial variation is quantified by the semi-variogram. The semi-variogram is estimated by the sample semi-variogram, which is computed from the input point data set. The value of the sample semi-variogram for a separation distance, referred to as the lag, is the average squared difference in value between pairs of input sample points separated by that distance and is modeled by fitting a theoretical function to the sample semi-variogram. The extent of the horizontal axis of the semi-variogram is determined by the distance between the most widely separated pair of points in the input sample data. Data sets known to have spikes or abrupt changes are not appropriate for the Kriging technique. In cases where the gauges are sparse, using kriging is also problematic as the semi-variogram can not be constructed (Burrough, 1986; Heine, 1986; McBratney and Webster, 1986; Oliver, 1990; Press, 1988; Royle et al, 1981);

*Trend Surface.* The linear trend surface uses a polynomial regression to fit a least-squares surface to the input points. It allows the user to control the order of the polynomial used to fit the surface. The surface generated will seldom pass through the original data points since it performs a best fit for the entire surface. As the order of the polynomial is increased, the surface being fitted becomes progressively more complex. Because a higher order polynomial is dependent upon the data, it will not always generate the most accurate surface. More details about these techniques can be found in Appendix D.

### 3.4.2 Time Series Data Analysis

#### 3.4.2.1 Missing Records

Some monthly values for precipitation may be missing. Two arithmetic methods (Paulhus and Kohler, 1952) were used to estimate missing records.

*Arithmetic Mean.* This method requires that the three adjacent stations have mean annual precipitation within 10% of the station with missing data. The arithmetic mean of the three stations is used as the missing record.

*Normal-Ratio.* This method is used where the mean annual precipitation of one or more of the adjacent stations exceeds the station with missing data by more than 10% and is calculated as:

$$P_x = \frac{1}{3}\left[\frac{N_x P_a}{N_a} + \frac{N_x P_b}{N_b} + \frac{N_x P_c}{N_c}\right] \tag{3.2}$$

where $P_x$: precipitation for the station with missing records; $P_{a,b,c}$: adjacent stations' precipitation values; and $N_{a,b,c,x}$ : long-term mean annual precipitation values at the respective stations.

3.4.2.2 Record Extension

The simplest version of the maintenance of variance extension (MOVE.1) by Hirsch (1982) was used to extend the shorter time series by deriving a set of coefficients for the model that transforms the X data to estimates of Y in such a way that the expected values of the statistics of the estimated Y values equal the true, but unknown, values of the statistical properties of Y. MOVE.1 preserves the mean and variance of Y using the equation

$$\tilde{Y}_i = a + bX_i \tag{3.3}$$

where $b = \sqrt{S_{yy}/S_{xx}}\ \mathrm{sgn}(r)$, $a = \bar{y} - b\,\bar{x}$, $S_{yy} = \sum (y_i - \bar{y})^2$, $S_{xx} = \sum (x_i - \bar{x})^2$, and sgn (r) is the sign of r (the correlation coefficient). A numerical example is shown in Appendix E.

Because MOVE.1 can also preserve the distribution shape and serial correlation structure rather well if the stations are in similar hydrologic settings, it seemed suitable to use for rainfall records in this application.

3.4.2.3 Data Consistency

Although systematic errors owing to wind, wetting loss, and evaporation (as mentioned earlier) can be adjusted, other errors in rainfall measurement owing to observer error, instrument malfunction, instrument changes, site relocations, and environmental changes can only be identified through site inspections and well-documented data or inter-comparison of data with nearby gauges. The double-mass curve tests the consistency of the rainfall record at a given station by comparing its accumulated annual record with the accumulated annual values of several other nearby stations whose history have been checked regularly (Kohler, 1949). The following points should be taken into account when using the method: (a) the plotting should start from the most recent year of available data and move backwards to the early years of observations; (b) the points can fluctuate in a random fashion around a fitted line, especially if the records of the station of concern are compared to records from only one or two stations. It is more favorable that the records of the station are

compared to the average of records of many neighboring stations if they are available; (c) if values on the plot continue to follow a parallel path after deviating from the fitted line at some point, no correction is needed. For precipitation, this may imply a dry or wet year; (d) corrections should only be done if there is a permanent slope change. Changes in slope should be accepted only when substantiated by historical evidence of a change and continuing over a period of 5 years; and (e) data of the earlier years are the ones that should be corrected by multiplying each record by a factor that is the ratio between the original slope to the new slope. Using this method to assess each station's data within the study area, no correction was needed as will be discussed in the following section.

3.4.2.4 Trend Analysis

This test is intended to determine the significance of each slope for time series data. If X-variable denotes time and the Y-variable represents rainfall taken over time, then Kendall's tau (1907) or Spearman's rho (1904) are calculated for these observations (X, Y). If the null hypothesis is that the $Y_1, Y_2, ..., Y_n$ are independent and identically distributed, then the alternative hypothesis is that the Y measurements (rainfall) exhibit a trend. A large positive value for tau (t) or rho ($r_s$) indicates that the rainfall measurements tend to become larger as time goes on (positive trend). A large negative trend value for tau (t) or rho ($r_s$) indicates the opposite (negative trend). The test for trend based on Kendall's tau was developed by Mann (1945) and the one based on Spearman's rho was suggested by Daniels (1950).

3.4.2.5 Testing the Goodness of Fit

The goodness of fit of the normal distribution can be tested by comparing the theoretical and sample values of the relative frequency function by means of the $\chi^2$ test. When a confidence level is chosen for the test it is often expressed as $100(1-\alpha)\%$, where $\alpha$ is termed the *significance level.* A typical value for the confidence level is 95%. The *null hypothesis* for the test is that the proposed probability distribution fits the data adequately. This hypothesis is rejected (i.e., the fit is deemed inadequate) if the calculated value of $\chi^2$ is larger than a limiting value ( $\chi^2_{\upsilon,1-\alpha}$ ) determined from the $\chi^2$ distribution with $\nu$ degrees of freedom as the value having cumulative probability $1-\alpha$, which is normally followed by checking for high or low outliers (Montgomery and Runger, 1994).

3.4.2.6 Checking for Outliers

Outliers are data points that depart significantly from the trend of the remaining data. The retention or deletion of these outliers can significantly affect the magnitude of statistical parameters computed from the data, especially for small samples. If the station skew is greater than +0.4, tests for high outliers [ $x_h = \bar{x} + k_n s$ ] are considered first; if the station

skew is less than -0.4, tests for low outliers [ $x_l = \bar{x} - k_n s$ ] are considered first. $K_n$ values are given for each sample size *n* and are used in one-sided tests, which detect outliers at the 10% level of significance in normally distributed data (USWRC, 1981). A numerical example can be found in Chow et al. (1988, pp. 401-405). The following polynomial can be used for estimating the tabulated values for $k_n$:

$$k_n = -3.62201 + 6.28446\, n^{1/4} - 2.49835\, n^{1/2} + 0.491436\, n^{3/4} - 0.037911\, n \qquad (3.4)$$

Where n = sample size. Truncating the values of $K_n$ beyond the third decimal place should give results identical to the tabulated ones.

It should be emphasized that automatic rejection of outliers is not always a very wise procedure. Sometimes the outlier provides information that other data points cannot because it may reflect an unusual combination of circumstances. These circumstances may be of vital interest and require further investigation, rather than rejection. As a general rule, outliers should be rejected only if they can be traced to causes such as errors in recording observations; otherwise careful investigation is required (Draper and Smith, 1998).

3.4.2.7 Frequency Analysis

Although some hydrologic variables, such as annual precipitation, calculated as the sum of the effects of many independent events, tend to follow the normal distribution (Chow et al, 1988), they are more commonly skewed. Because it is generally necessary to extrapolate beyond the range of observed events in a frequency analysis, several theoretical transformations have been developed for normalizing a skewed distribution. It is generally easier to draw statistical conclusions from the normal distribution whose exact theoretical properties are well known (Pilon et al, 1985). Two types of transformations are used in this study: (1) Three-Parameter Lognormal distribution and (2) Log Pearson Type III distributions. For a lognormal transformation, the theoretical coefficients of skewness and kurtosis of the transformed data should be 0.0 and 3.0, respectively. If the coefficient of skewness is between -0.025 and 0.125, the first transformation was used. If it is higher, the second transformation was implemented. Refer to Appendix E for more details.

## 3.5 Results and Discussion

It should be pointed out that despite the fact that records were filled and extended to cover periods of unavailable data, analysis in some cases was performed on raw data sets (i.e. prior to filling and extending the records). In this case, the data set is normally referred to as an "incomplete data set"; otherwise it is a "complete data set".

3.5.1 Spatial Rainfall Characteristics

Six watersheds each of which contained 3 or more raingauges were included in the analysis (refer to Figure 3.1c and Table 3.1). The double-mass curve analysis was performed on the six watersheds. Figure 3.3 shows an example where precipitation at the Zaros gauge was compared to the remaining gauges of the Geropotamou basin for the water years 1969-70 to 1996-97.

This watershed-based analysis aimed at studying the mean annual precipitation-elevation correlation and the temperature-elevation gradient (lapse rate). A complete common data set of 20 water years (1977-78 to 1996-97) was used in the analysis. The simple linear regression between rainfall (response variable) and elevation (predictor variable) was used to study the degree of association between the two variables for small scale areas represented in this case by watersheds. The coefficient of determination ($r^2$) is often used to judge the adequacy of the regression model. For the purpose of studying the local (watershed-based) correlation between elevation and rainfall, the coefficient is a qualitative, rather than quantitative, measure. This is owing to the relatively few number of gauges in each watershed which is likely to result in a high association and possibly perfect fit in some cases. The results are summarized in Table 3.2. When the low elevation gauges record less rain than mountainous gauges, it is likely that orographic effects control precipitation. The precipitation-elevation relation is not as strong for the whole island as it is for individual basins; $r^2$ = 37%. Significant difference in precipitation recorded on the windward slope of the island (north) than the leeward slope (south).

For individual watersheds, introducing boundary and/or neighbouring gauges changed the precipitation-elevation relation considerably. For the Anapodiaris basin, when using all inside nine gauges and closest seven neighbouring gauges the precipitation-elevation gradient decreases significantly from 1.02 (Table 3.2) to 0.64 mm/m with the intercept increasing from 312 to 436 mm. A decrease in ($r^2$) from 59% to 52% was calculated. This can be attributed to both the location of the watershed and the fact that the additional stations used were towards the east, where less precipitation is recorded. For the Gerapotamou basin, using all inside nine gauges and closest five neighbouring gauges did not significantly affect the slope (decreased from 1.17 to 0.94 mm/m) with the intercept increasing from 296 to 389 mm and ($r^2$) decreasing from 58% to 51%. The neighbouring gauges were located to the east of the watershed and to the west of the Anapodiaris basin. Although the station of Demati, established for the Anapodiaris basin, was installed at an elevation of 210m, which is close to the 200m (at which the stations of Kalyvia and Asimi are installed), it collected only an average of 350mm, while the Kalyvia and Asimi stations collected 595mm and 613mm, respectively. This difference is owing to the aspect factor. Similarly, while Agios Kirillos and Gergeri, the stations for the Gerapotamou basin, were installed at an elevation of 450m, Agios Kirillos station collected an average of only 544mm, while Gergeri collected 910mm.

The same can be said about the gauge of Finikias, in the Giofyro basin. When using three inside gauges and closest five boundary gauges, the slope increased from 0.65 to 0.79 mm/m with the intercept decreasing from 572mm to 522mm because all new gauges are northern gauges and ($r^2$) from 74% to 55%. The Platis and Petras basins are average in terms of their slope, while the intercept in Platis is slightly greater owing to its location to the west of the island. Using more stations for Platis basin (four inside gauges and three neighbouring gauges) increased the slope from 0.86 to 1.09 mm/m with a decrease in intercept from 541 to 479 mm; while the introduction of three neighbouring in addition to the three inside gauges caused the slope for Petras to decrease from 0.86 to 0.68 mm/m with an intercept increase from 460 to 525mm. Tavronitis basin, which is located to the far west of the island, has the highest slope of 1.96 mm/m that goes down to 1.88 mm/m when using two neighbouring gauges with an intercept increasing to 681mm from 644mm.

To summarize, although a strong precipitation-elevation correlation may exist for watersheds, some gauges within a watershed may not be well represented by regression models. Despite the fact that using information obtained from boundary and neighboring gauges is always encouraged, it seems that selecting these gauges should be practiced with caution as results have significantly changed after introducing these gauges to the analysis. It is also clear that the slope decrease in the models was always accompanied by an intercept increase and vice versa, which simply means that, for example, if rainfall is not well predicted by elevation, the model will adjust itself by increasing the average precipitation over the watershed, which in this case is represented by the intercept term.

### 3.5.2 Temporal Rainfall Characteristics

#### 3.5.2.1 Testing The Goodness of Fit

The goodness of fit test was performed on all precipitation stations. Figure 3.4 shows: a) a time series plot of the annual precipitation of the Agia Barbara station, b) the frequency histogram, c) the relative frequency function and d) the cumulative frequency function. From Figure 3.4d and based on 20% and 80% exceedence limits, precipitation $\geq$ 1050 mm/year is a wet year and $\leq$680 mm/year is a dry year. The wet years can be listed as 67-68, 75-76, 77-78, 80-81, 81-82, 83-84, 84-85, 86-87, and 87-88; while the dry years can be listed as 76-77, 89-90, and 92-93 for the Agia Barbara gauge. Note that the water year starts from September of a calendar year to August of the following calendar year with three phases: start, peak, and end. Precipitation values that lie between these two values represent average years. Out of the sixty eight stations analyzed, only seventeen stations did not fit the normal distribution (nine in Iraklion, two in Lassithi, three in Rethymno, and three in Chania). For those stations that did not fit the normal distribution, removing the highest record from the time series data and re-analyzing the remaining data showed that twelve stations out of the seventeen fit the normal distribution.

3.5.2.2 Checking For Outliers

Following the procedure described in the previous section, results show that there were no low outliers among the fifty one stations that fit the normal distribution. However, twelve stations showed high outliers. The departure from the general trend was not significant except for the case of the station of Sitia in Lassithi, where the precipitation recorded for the water year 1986-87 exceeded a $\mu + 3\sigma$ limit. Sixty two stations showed positive skewness, while only six stations showed negative skewness.

3.5.2.3 Wet, Average, and Dry Years

A two-stage station-based analysis first aimed to classify each year as dry, wet or average according to data collected from different stations for that particular year. An overall classification emerged when new information from all stations for each year was collected. Fifty nine out of sixty seven stations proved the water year 1977-78 to be the wettest, while sixty one out of sixty three stations indicate that the water year 1989-90 is the driest. Examples of average years are 1974-75, 1971-72, and 1972-73; while examples for wet years are 1975-76, 1980-81, and 1986-87 as shown in Table 3.3.

3.5.2.4 Rainfall Trend

Nineteen stations were selected to examine the temporal change in precipitation amounts over a relatively long period of time. Long record periods (from 34 to 54 years) for stations installed at different altitudes and locations were chosen so that each county (prefecture) would be represented by at least three stations, as shown in Figure 3.5. Although in fourteen out of the nineteen stations, annual rainfall totals show a decreasing linear trend in rainfall amounts that ranged from -0.36 mm/year for the station of Askifu, to -9.7 mm/year for the station of Palea Rumata, the slopes were not significant, based on the Mann-Kendall test (Hirsch et al., 1991). There were only two cases where the slope was found to be significant. For Palea Rumata station (county of Chania), the slope is significant at $p<0.05$; while for Anogia station (county of Rethymno), the slope is not significant at $p<0.05$ but significant at $p<0.1$ (Figure 3.6). Since there is no proof of change in location, exposure, or gauge type, it is believed that this decline can be attributed to natural variability.

A data set that included 42 stations was selected to study the "gain/loss" in rainfall over the thirty years between 1967-68 and 1996-97. The "gain/loss" term is used to describe the amount of rain for each station, which is estimated as the yearly change in precipitation (slope of the line) multiplied by the number of years (the period of observation, i.e. 30 years). Elevation is positively correlated with precipitation as shown in Figure 3.7a, there is also a correlation between "gain/loss" and elevation. Figure 3.7b shows that there is a greater decrease or loss in precipitation recorded at higher elevations than that at lower elevations. This probably is an indication that higher elevations are more sensitive to changes in precipitation patterns than lower elevations as they are away from urbanization effects and exposure issues. The results also show that fifteen out of forty two stations showed a positive slope, which ranged from 0.1 to 6.5 mm/year for the stations of Profilias and Finikias,

respectively. The remaining stations showed a negative slope, which ranged from -0.4 to -15.7 mm/year for the stations of Zaros and Palea Rumata, respectively. Refer to Figure 3.8 for the spatial distribution of both categories of rainfall stations. The stations that are marked with a "+" sign show a positive change, while the rest of the stations show a negative change. Per watershed (as shown in the inserted table of the figure) it is clear that precipitation/elevation ratio is higher in north western and northern parts of the island as in the case of Tavronitis and Giofyro basins, respectively. The ratio is less in south and east as in the case of the Anapodiaris, Platis, Geropotamou, and Petras basins.

### 3.5.3 Areal Rainfall Depth Estimation

#### 3.5.3.1 Missing Records

Missing monthly data were estimated using the methods previously described. However, for the purpose of comparison, the maintenance of variance extension (MOVE.1) technique was used to extend the records for twenty three stations from 1991 to 1997. This extension was constructed by using the records of neighboring stations. Figure 3.9 shows the station of Kasteli as an example for the method application. As a result, three sets of data were generated: data set (1) includes eighty one stations of *complete* data for the 20 years 1977-1997; data set (2) includes fifty eight stations of *incomplete* data for the 20 years 1977-97; and data set (3) includes forty two stations of *incomplete* data for the 30 years 1967-97.

#### 3.5.3.2 Spatial Interpolation

Different spatial interpolation techniques such as Spline, IDW, Trend, and Kriging, in addition to MLR, have been applied to the yearly data for each of the three data sets separately. Results show that MLR estimates of areal rainfall as shown in Figure 3.10, which is an illustration of the 30-year incomplete data set, are intermediate between high estimates obtained using the Spline technique and low estimates obtained using the Trend interpolator. The trend in the annual estimates for mean areal rainfall using MLR (Figure 3.10) is sinusoidal reflecting the natural variability of rainfall over the island. Results also show that all spatial interpolation techniques estimated less mean areal rainfall when more stations were used. As shown in Figure 3.11, for example, smaller values of mean areal rainfall were estimated when using the 20-year complete data set with 81 stations than when using the 30-year incomplete data set with 42 stations. This can be attributed to the lack of 30-year precipitation data for the stations in the western part of Crete. When comparing all methods, the smallest difference between estimates using 20 years of incomplete data and estimates using 20 years of complete data was obtained when using the MLR technique. This indicates that the MLR method can be used as a reliable estimator of missing records (refer to Figure 3.11). Figure 3.12 shows that the MLR method can be a good replacement for the other interpolation methods when fewer stations are available for interpolation. In fact, the Regularized Spline and the Trend techniques produce high negative values for rainfall at some ungauged locations, which is illustrated by the circled areas in Figure 3.12. This is not

possible with the MLR method. It should be noted that the high rainfall estimates in the western and northwestern parts of the island caused by interpolation problems as in the case of the Regularized Spline and the Trend techniques.

3.5.3.3 Return Periods

Using the logarithmic transformation described earlier, estimates for 2, 5, and 10 year return periods were obtained at each of the 42 stations for the 30 year incomplete data set. Figure 3.13 shows the frequency analysis results obtained for four stations. Two scenarios for estimating the areal rainfall for the island for the 2, 5, and 10 year return periods were adopted. Scenario (a): using the MLR technique, areal rainfall is evaluated by interpolating values at the individual stations for the 2, 5, and 10 year return periods using data set (3). Figure 3.14 shows the spatial distribution of the 10 year return period of rainfall across the island and the four watersheds. Precipitation in the western part of the island is slightly overestimated owing to the fact that there are only three gauges available for the area for the 30 years. Scenario (b): the frequency analysis on the mean areal rainfall is calculated for every year using the MLR method. Results are within 2% of those estimated by the first scenario, as shown in Table 3.4, which also shows results obtained for watersheds for 2, 5, and 10 year return periods using scenario (a).

## 3.6 Conclusion

The spatial and temporal variation of annual precipitation was investigated for the island of Crete in Greece. The annual records of precipitation from various meteorological and precipitation stations were used. Spatially, it was evident that precipitation is of an orographic type (i.e. precipitation is strongly correlated with elevation). Temporally, 75% of the stations included in the analysis fit the normal distribution according to the goodness of fit test performed on the time series data of the stations. Although real outliers were almost non-existent, the 1977-78 records caused deviation from the norm in some cases. It was clear that the year 1977-78 was the wettest, while the year 1989-90 was the driest. Twenty seven out of forty two stations showed insignificant downward trends, indicating a decline of precipitation over the period of 1967-1997. The decrease in precipitation was found to be greater on higher elevations. The MLR technique was used for the purpose of spatial interpolation because: 1) it provides reasonable estimates for areal rainfall for different scales, 2) it yields realistic spatial distribution of rainfall, and 3) it is not greatly influenced by either the number or the spatial distribution of the gauges when estimating mean areal rainfall and its spatial distribution. Frequency analysis of the annual precipitation records revealed that Crete is expected to receive mean areal rainfall of 1010, 1228 and 1324 mm every 2, 5 and 10 years, respectively. Results from representative watersheds in Crete indicate that the 10 year return period can vary from 928 mm (Eastern Crete) to 1875 mm (Western Crete). These findings should assist in improving the water resources planning and management of the island of Crete.

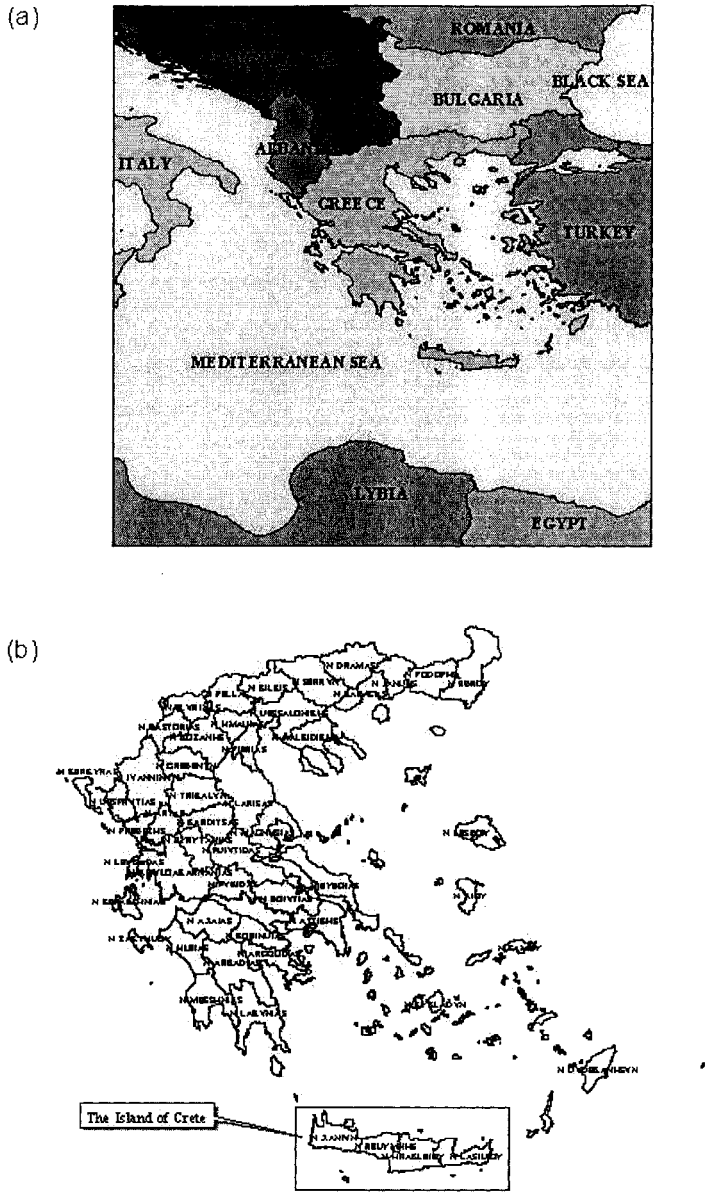


**Figure 3.1:** (a) The country of Greece and its neighbors in the Mediterranean region at the south of Europe and facing northern Africa. (b) The 51 political counties of Greece with the island of Crete divided into four counties (from left to right: Chania, Rethymno, Iraklion, and Lassithi).

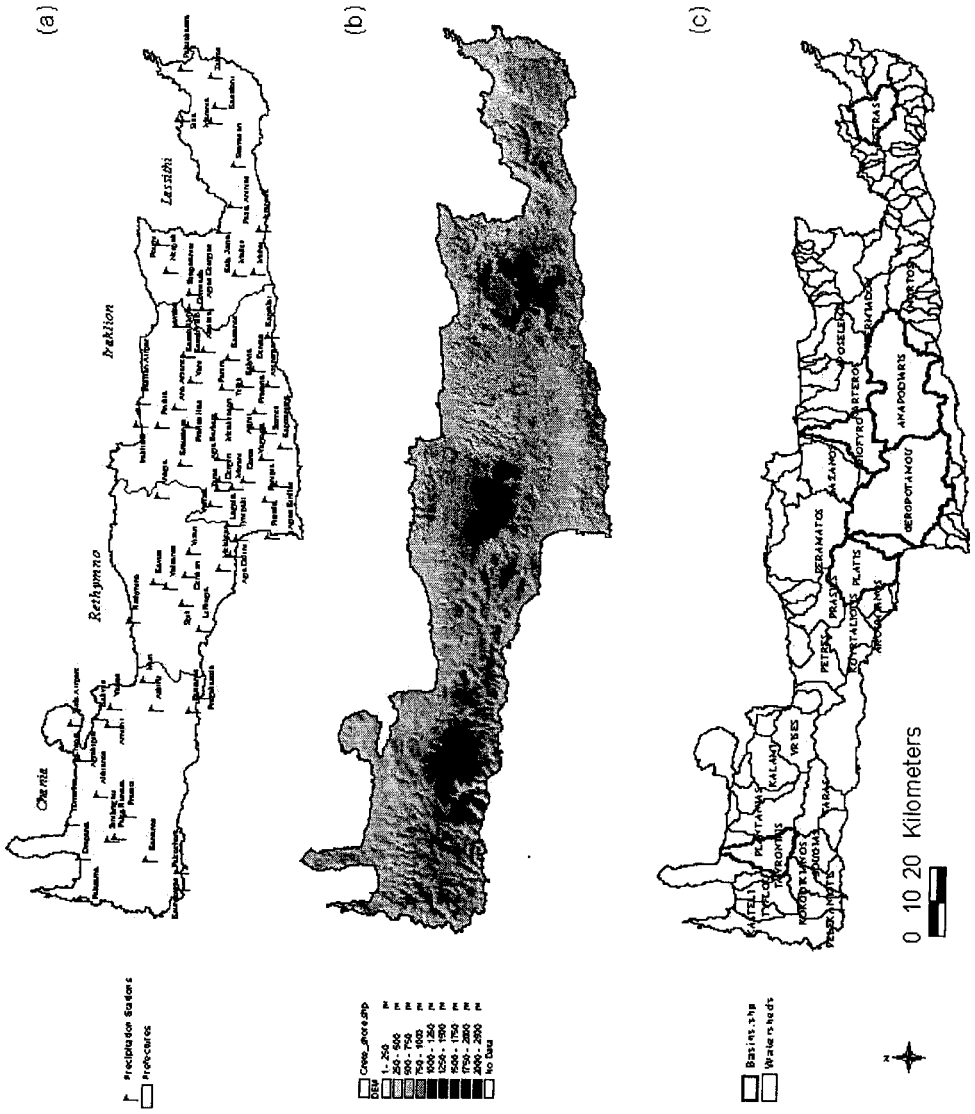


**Figure 3.2:** (a) Names and locations of the gauges on the island of Crete. The majority of the gauges are located on the county (prefecture) of Iraklion. (b) A map of the Digital Elevation Model (DEM) for the island. (c) Delineated watersheds of the island. Thehighlighted basins are the ones considered for analysis.

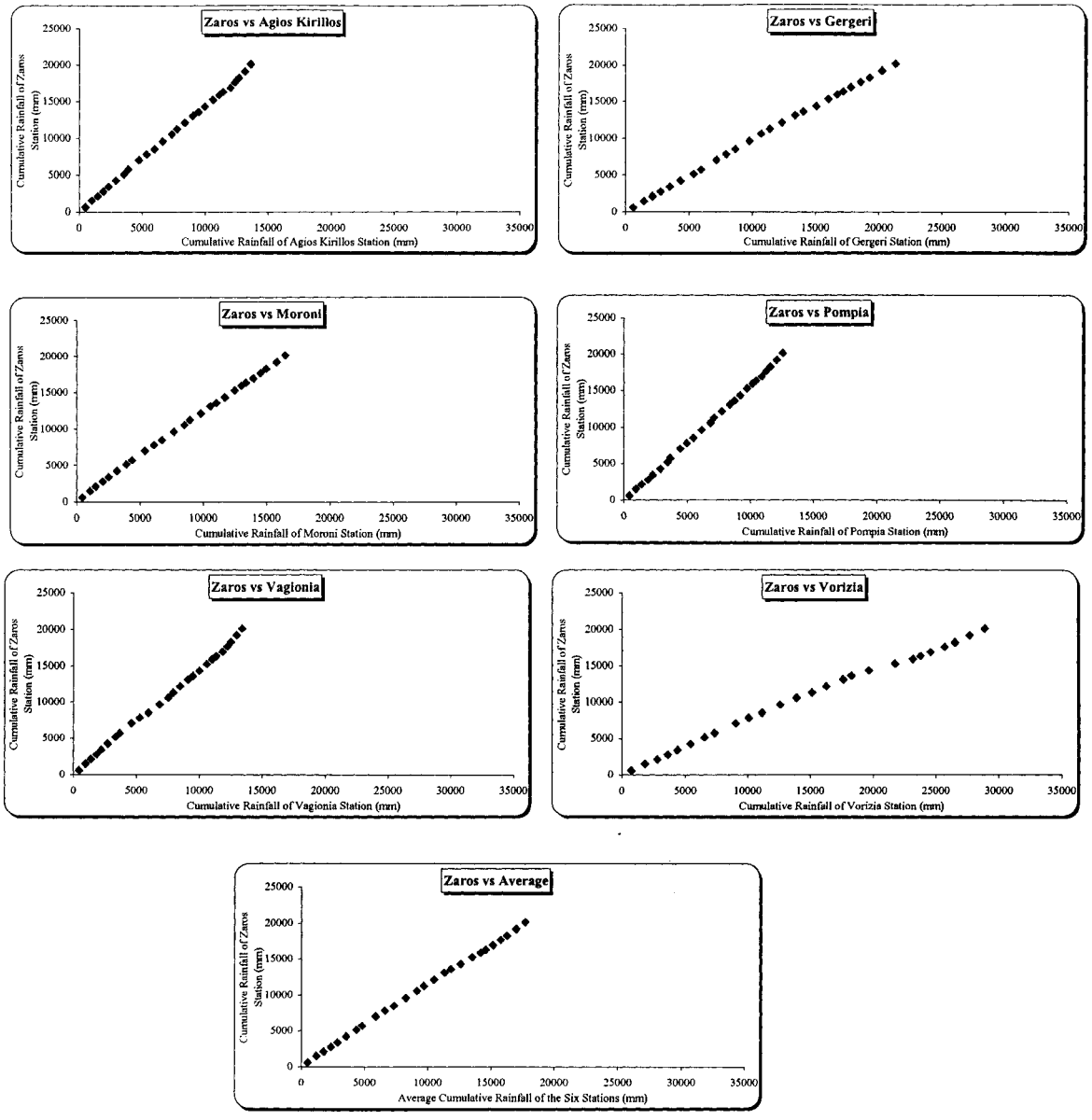


**Figure 3.3:** Double-mass curve plots using records of annual rainfall obtained for precipitation gauges in Gerapotamou basin for the water years 1969-70 to 1996-97.

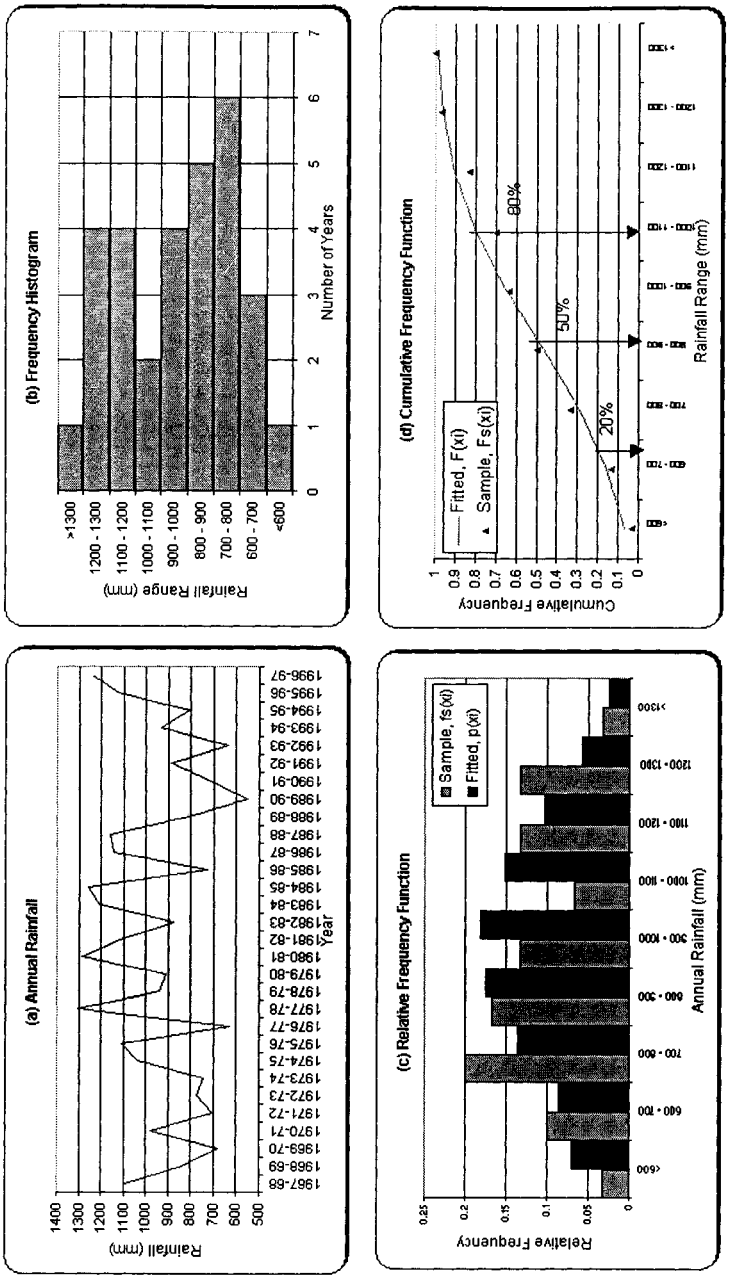


**Figure 3.4:** Goodness of fit test for Agia Barbara station. (a) a time series plot of the annual precipitation. (b) the frequency histogram. (c) the relative frequency function. (d) the cumulative frequency function.

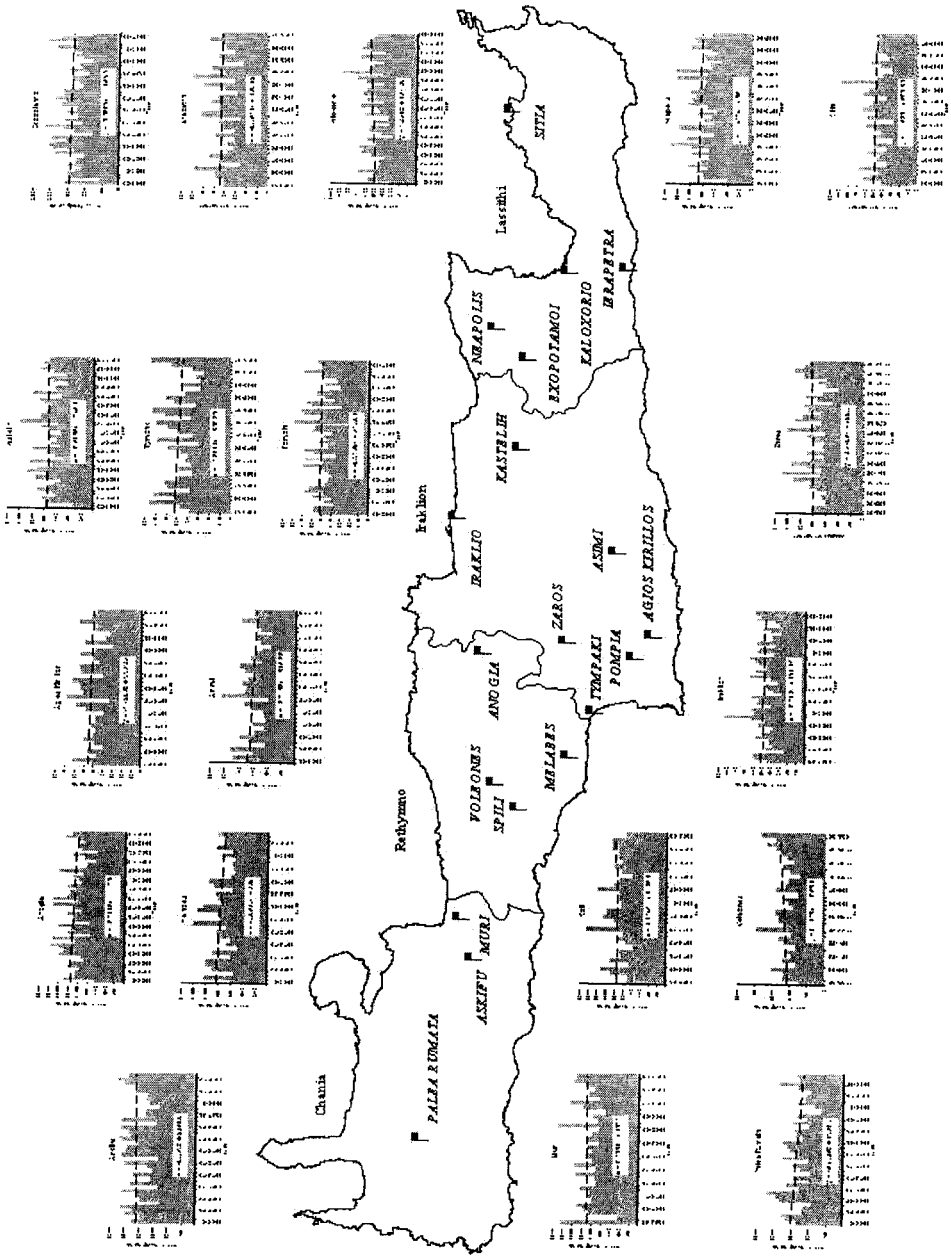


**Figure 3.5:** Rainfall time series for selected precipitation stations.

(a)

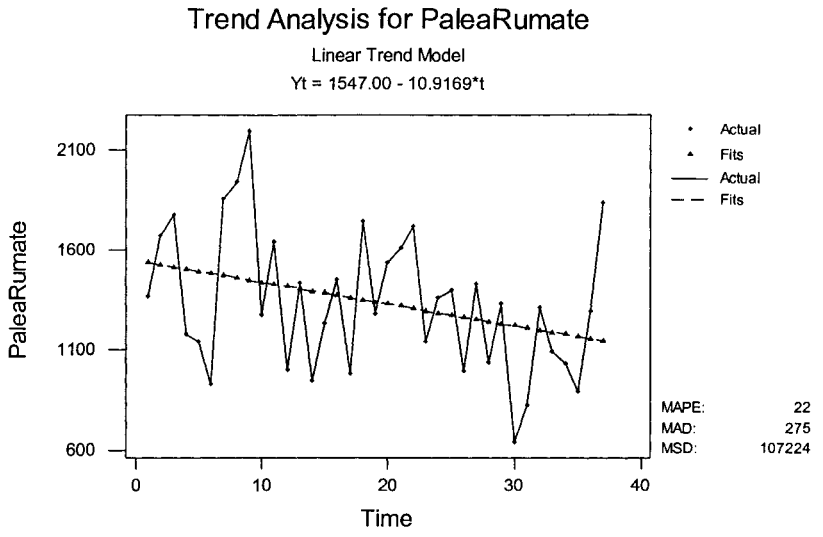


(b)

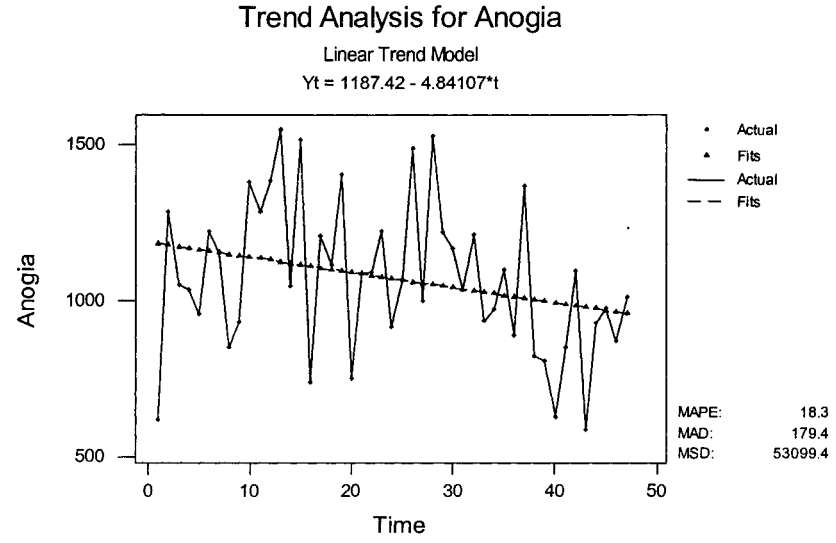


**Figure 3.6:** (a) Trend analysis results for Palea Rumata station (county of Chania) where the slope is found to be significant at $p<0.05$. (b) Trend analysis results for Anogia station (county of Rethymno) where the slope is found to be not significant at $p<0.05$, but significant at $p<0.1$. The slopes at the remaining gauges were not significant.

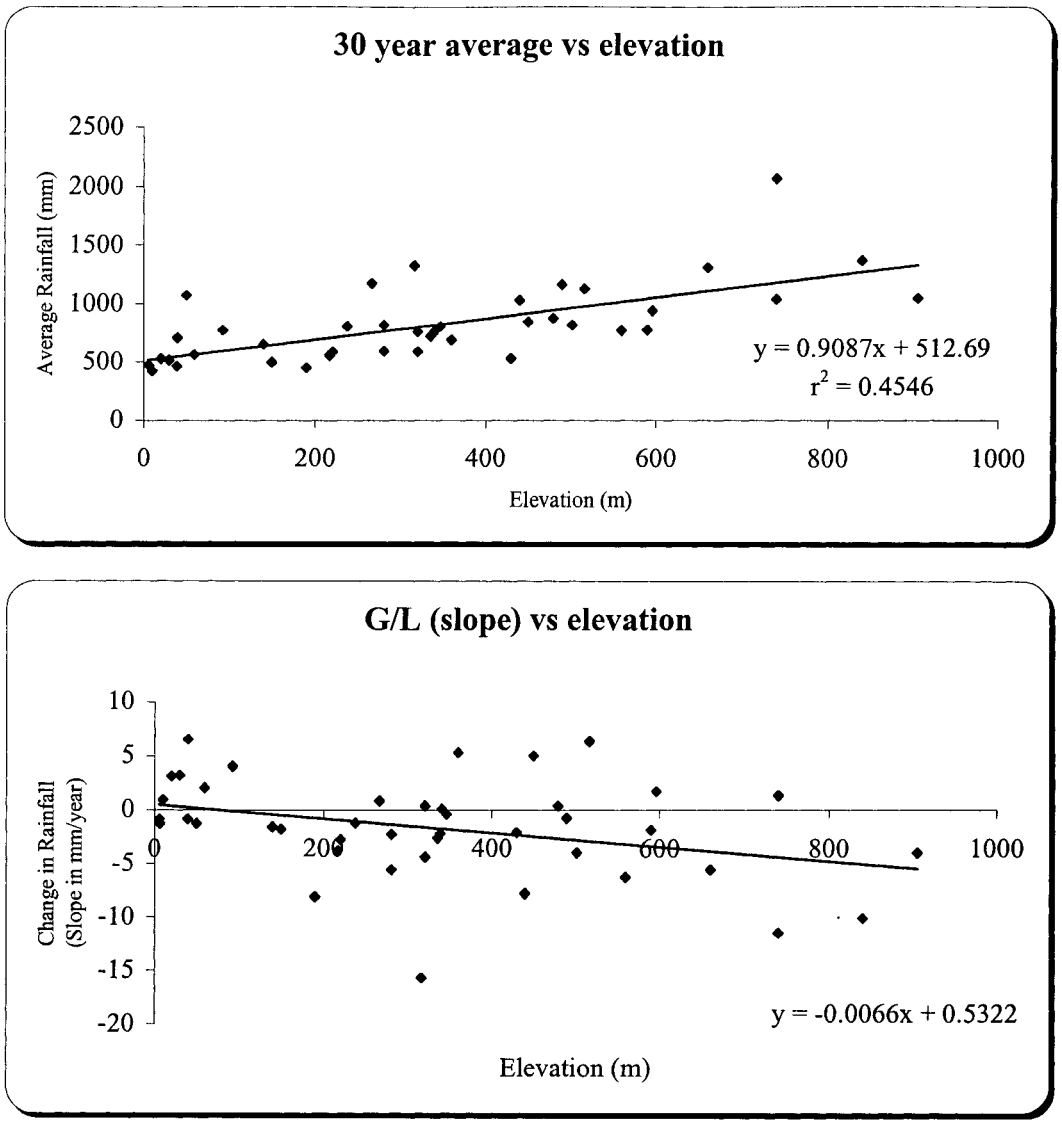


**Figure 3.7:** (a) 30-average rainfall in mm vs station elevation in m for the whole island. (b) The change in rainfall for each of the stations vs elevation.

| Basin | Mean Elevation (m) | Average Rainfall (mm/year) | Rainfall/Elevation Ratio (mm/year/m) |
|---|---|---|---|
| Tavronitis | 439 | 1503 | 3.42 |
| Giofyro | 345 | 820 | 2.38 |
| Gerapotamou | 478 | 822 | 1.72 |
| Anapodiaris | 461 | 755 | 1.64 |
| Platis | 659 | 1288 | 1.95 |
| Petras | 409 | 756 | 1.85 |

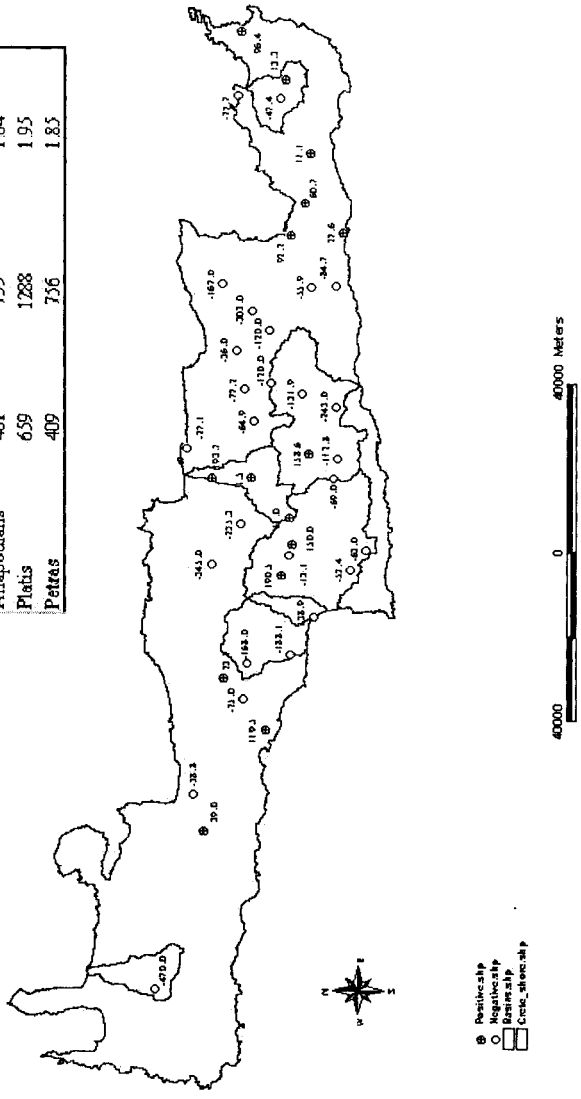


**Figure 3.8:** The estimated change in rainfall over the years for selected stations. After calculating the mean elevation (using the DEM) and the average rainfall for each basin, the rainfall-elevation ratio shows that Tavronitis basin (northwest) receives per meter of elevation an estimated 3.42 mm/year, while Petras basin (east) receives per meter of elevation an estimated 1.85 mm/year. This shows that north western and northern parts receives (established by the records) more rain than the eastern and southern parts of the island.

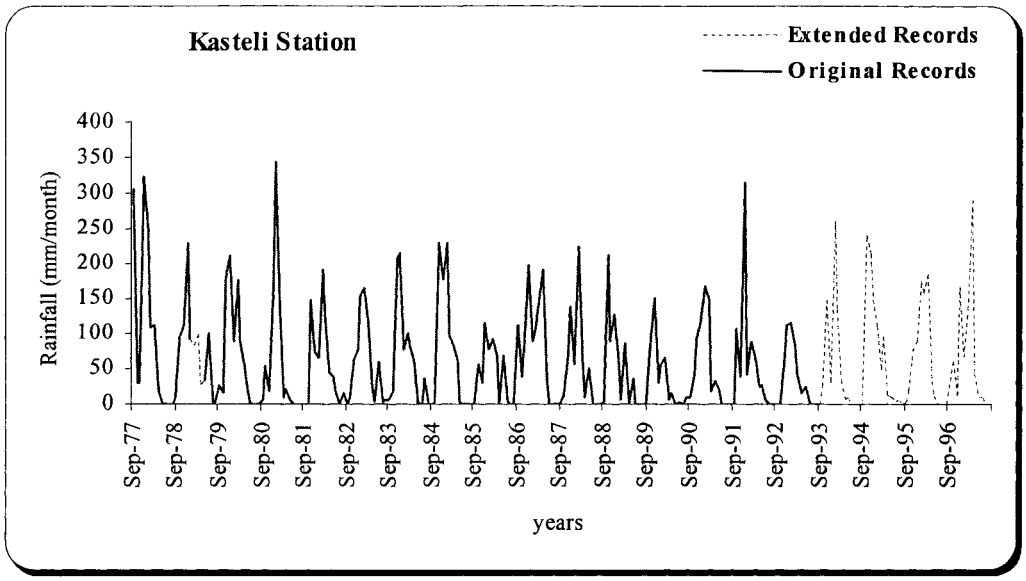


**Figure 3.9:** An illustration of extending and filling missing records for Kastelih station (county of Iraklion).

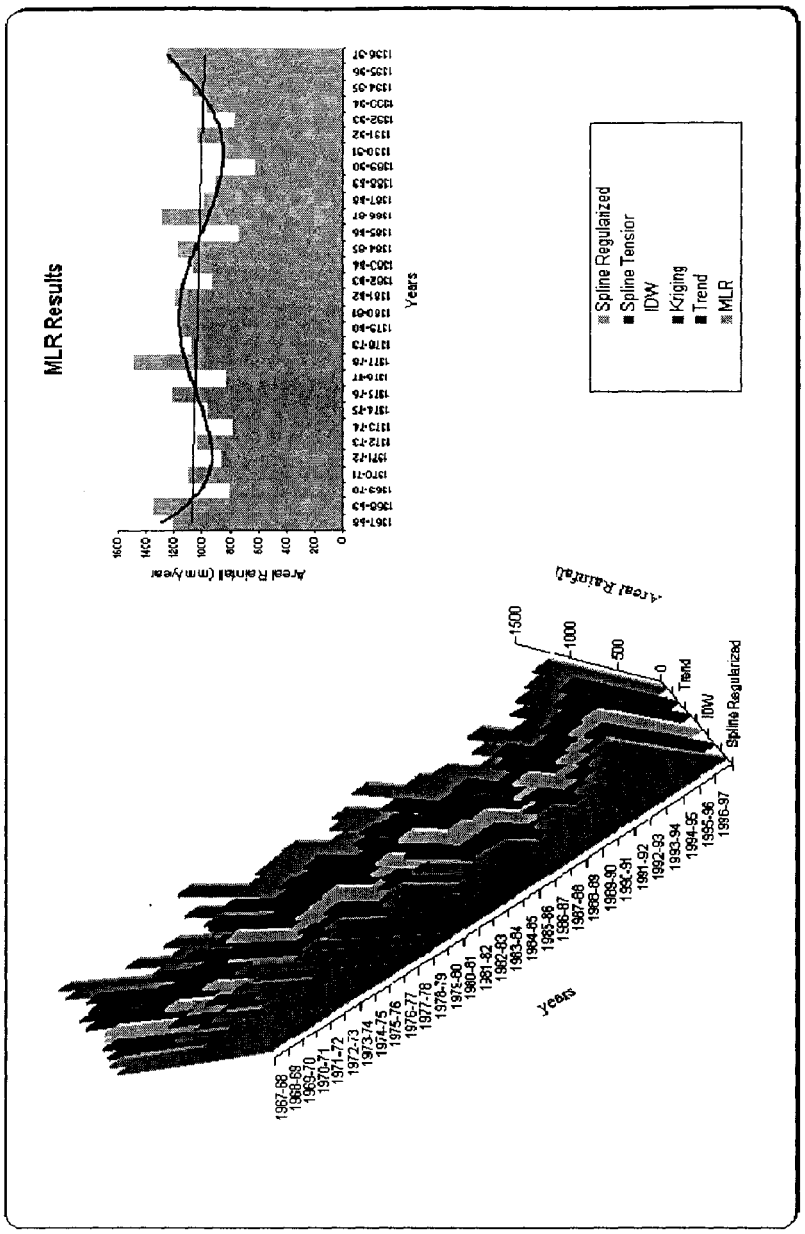


**Figure 3.10:** Using 30 years of annual records, the areal rainfall depth is estimated via the different spatial interpolation techniques. The values obtained for each year differ using each technique, yet they all show similar trend. The MLR is considered more acceptable.

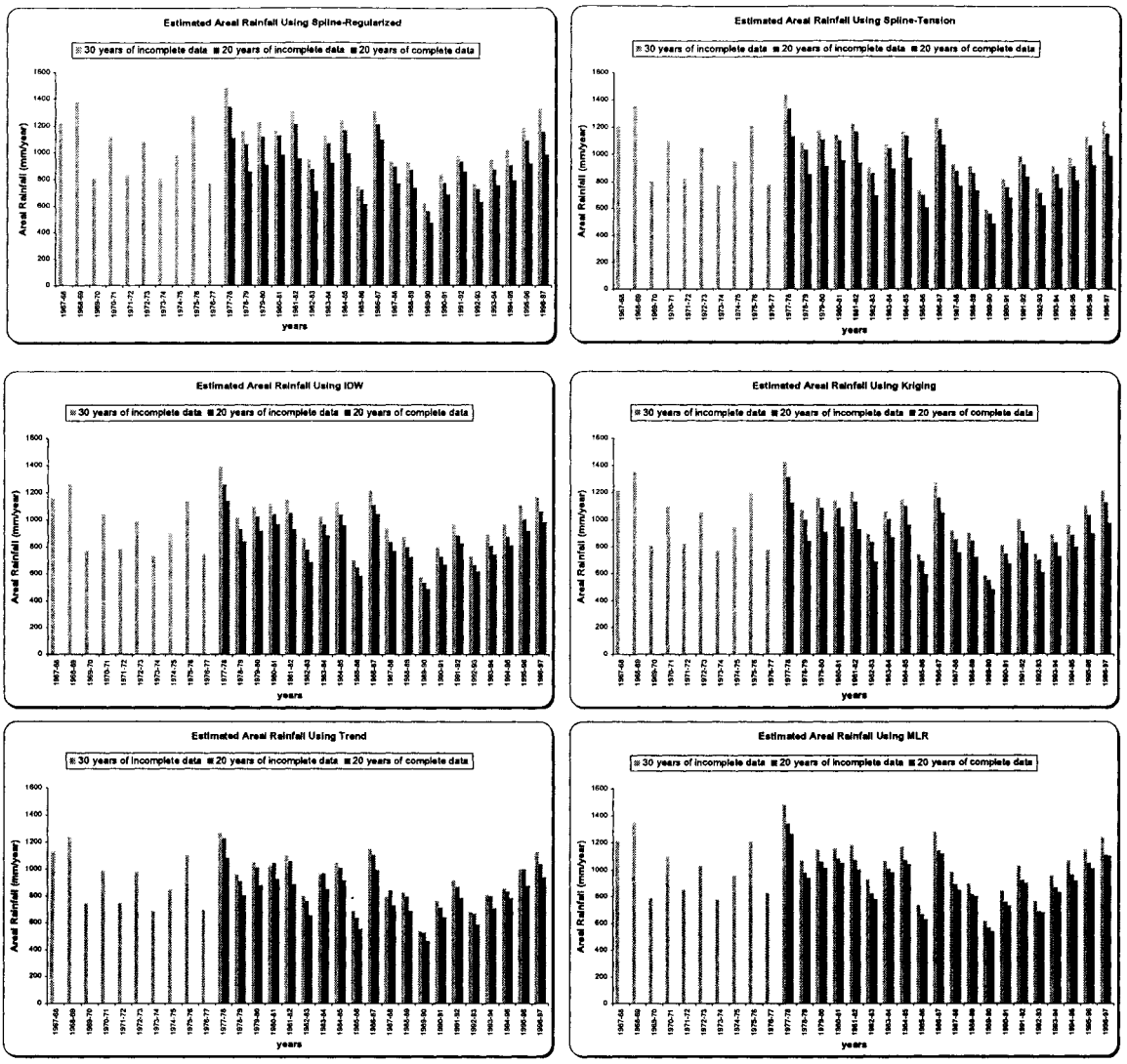


**Figure 3.11:** Estimated areal rainfall for three data sets using different spatial interpolation techniques. This analysis is done for data sets before and after filling missing records. If the records of one station are not complete, the station is dropped out of the analysis.


**Figure 3.12:** Spatial distribution of rainfall for the year 1977-78 across the island using 42 gauges by means of the different spatial interpolation techniques. Due to the fact that less gauges with complete records exist on the western part of the island, the conventional spatial interpolation methods can not accurately estimate rainfall at ungauged locations. This results in either underestimation (negative values as in the case of regularized-spline and trend methods) or overestimation (high positive values as in the case of the tension-spline method).

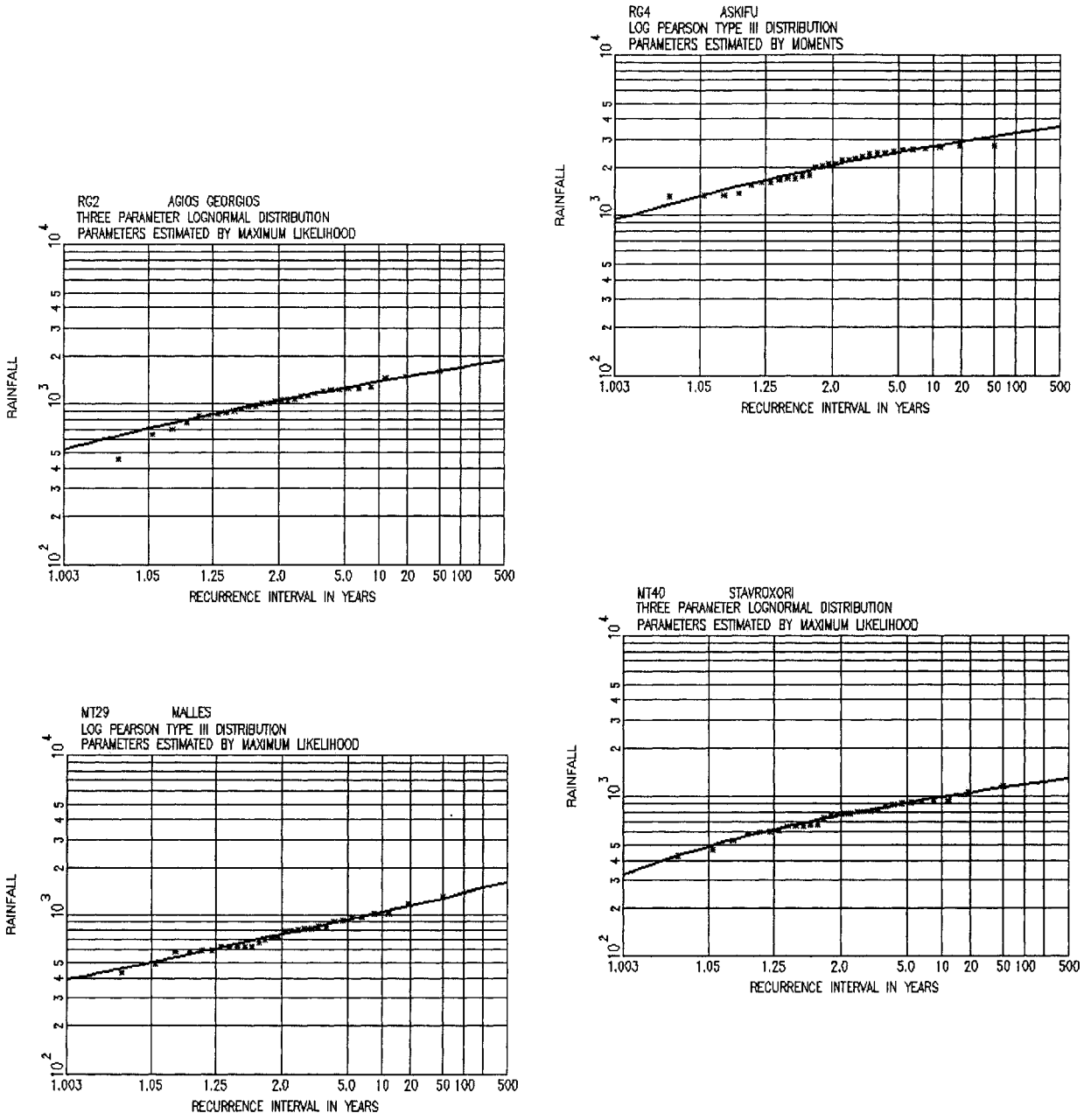


**Figure 3.13:** Frequency analysis results for the station of Askifu (Chania), Agios Geogrios (Iraklion), and Stavroxori and Malles (Lassithi). The analysis was performed on 42 stations using the three parameter lognormal and log pearson type III distributions.

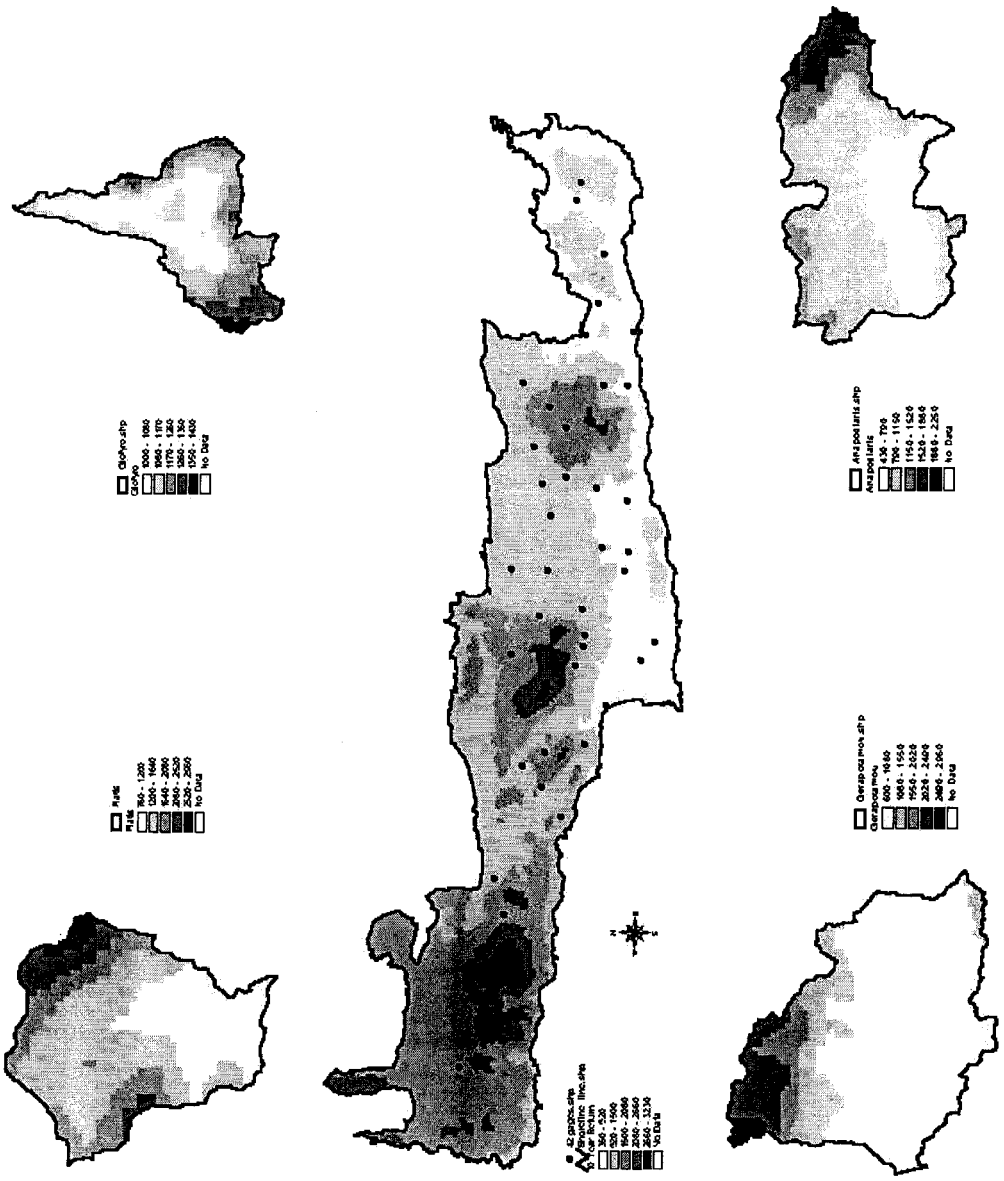

**Figure 3.14:** The spatial distribution of 10-year return period estimated rainfall across the island and for selected basins.

**Table 3.1:** The attributes of selected basins for the analysis including precipitation gauges within each basin, the area of each basin, altitude of each gauge, the 20-year average rainfall for each gauge, and the number of years of available data for each gauge.

| Watershed | Station Name | Elevation (m) | 20-year Average Rainfall (mm/year) | Years of Available Data |
|---|---|---|---|---|
| **Anapodiaris** | Armaxa | 450.0 | 832.9 | 63-64 .. 96-97 / 34 |
| (Area = 520 km2) | Asimi | 200.0 | 612.9 | 61-62 .. 96-97 / 36 |
| (*Mean Elevation = 310.6 m) | Demati | 210.0 | 349.9 | 64-65 .. 96-97 / 33 |
| | Kalyvia | 200.0 | 594.9 | 69-70 .. 96-97 / 28 |
| | Kassanos | 320.0 | 582.5 | 63-64 .. 96-97 / 34 |
| | Metaksoxori | 430.0 | 736.8 | 68-69 .. 96-97 / 29 |
| | Partira | 400.0 | 645.8 | 69-70 .. 96-97 / 28 |
| | Protoria | 225.0 | 556.5 | 67-68 .. 96-97 / 30 |
| | Tefeli | 360.0 | 743.2 | 63-64 .. 96-97 / 34 |
| **Gerapotamou** | Agios Kirillos | 450.0 | 543.8 | 61-62 .. 96-97 / 36 |
| (Area = 602 km2) | Gergeri | 450.0 | 910.3 | 63-64 .. 96-97 / 34 |
| (Mean Elevation = 349.1 m) | Gortis | 182.0 | 537.0 | 71-72 .. 96-97 / 26 |
| | Moroni | 400.0 | 688.9 | 69-70 .. 96-97 / 28 |
| | Pompia | 150.0 | 504.8 | 45-46 .. 96-97 / 52 |
| | Sternes | 300.0 | 607.9 | 68-69 .. 87-88 / 20 |
| | Vagionia | 190.0 | 545.7 | 69-70 .. 96-97 / 28 |
| | Vorizia | 520.0 | 1169.3 | 63-64 .. 96-97 / 34 |
| | Zaros | 500.0 | 822.7 | 52-53 .. 96-97 / 45 |
| ***Giofyro*** | Agia Barbara | 570.0 | 982.2 | 66-67 .. 96-97 / 31 |
| (Area = 189 km2) | Finikias | 40.0 | 728.6 | 66-67 .. 96-97 / 31 |
| (Mean Elevation = 251.3 m) | Iraklio B | 15.0 | 480.8 | 75-76 .. 96-97 / 22 |
| | Profilias | 380.0 | 750.9 | 65-66 .. 96-97 / 32 |
| ***Petras*** | Katsidoni | 480.0 | 866.7 | 65-66 .. 96-97 / 32 |
| (Area = 128 km2) | Maronia | 150.0 | 668.5 | 49-50 .. 96-97 / 48 |
| (Mean Elevation = 248 m) | Sitia | 114.1 | 486.8 | 60-61 .. 96-97 / 37 |
| ***Platis*** | Agia Galini | 20.0 | 605.7 | 69-70 .. 96-97 / 28 |
| (Area = 228 km2) | Gerakari | 660.0 | 1325.2 | 67-68 .. 96-97 / 30 |
| (Mean Elevation = 387.5 m) | Melabes | 560.0 | 778.6 | 63-64 .. 96-97 / 34 |
| | Vizari | 310.0 | 791.7 | 69-70 .. 96-97 / 28 |
| ***Tavronitis*** | Palea Rumata | 316.0 | 1276.1 | 60-61 .. 96-97 / 37 |
| (Area = 140 km2) | Prasses | 520.0 | 1682.9 | 62-63 .. 91-92 / 30 |
| (Mean Elevation = 271.6 m) | Tavronitis | 15.4 | 701.2 | 71-72 .. 89-90 / 19 |
| | Zimbragou | 235.0 | 1049.1 | 71-72 .. 89-90 / 19 |

** Mean elevation of the stations in the watershed*

**Table 3.2:** Summary of the watershed-based analysis including the intercept (average rainfall over the basin), the slope (rate of change of rainfall with respect to elevation), the coefficient of determination for the simple regression model, and the lapse rate (the decrease in temperature for each 1000m of elevation).

| Watershed Name | Number of Stations | a (mm/year) | b (mm/year.m) | r2 (%) | Lapse Rate (°C/km) |
|---|---|---|---|---|---|
| *Anapodiaris* | 9 | 312 | 1.02 | 59 | 5.7 |
| *Gerapotamou* | 9 | 296 | 1.17 | 58 | 5.3 |
| *Giofyro* | 4 | 572 | 0.65 | 74 | 3.0 |
| *Petras* | 3 | 460 | 0.86 | 84 | 6.2 |
| *Platis* | 4 | 541 | 0.86 | 63 | 4.9 |
| *Tavronitis* | 4 | 644 | 1.96 | 98 | 6.0 |

**Table 3.3:** The water years from 1945-46 to 1994-1995 are classified as dry, average, or wet years based on the number of gauges available during a specific year. For example, a total of 65 gauges recorded precipitation for the water year 1982-83. For fifty five of the gauges this year is considered average year, while for ten gauges it is considered a dry one. This water year is then classified as an average year

| No. | Water Year | Dry Year | Average Year | Wet Year | No. of Gages | No. | Water Year | Dry Year | Average Year | Wet Year | No. of Gages |
|---|---|---|---|---|---|---|---|---|---|---|---|
| 1 | 1945-46 | 0 | 1 | 0 | 1 | 26 | 1970-71 | 1 | 49 | 9 | 59 |
| 2 | 1946-47 | 0 | 0 | 1 | 1 | 27 | 1971-72 | 6 | 58 | 0 | 64 |
| 3 | 1947-48 | 0 | 1 | 1 | 2 | 28 | 1972-73 | 0 | 58 | 6 | 64 |
| 4 | 1948-49 | 0 | 1 | 1 | 2 | 29 | 1973-74 | 17 | 47 | 0 | 64 |
| 5 | 1949-50 | 0 | 4 | 2 | 6 | 30 | 1974-75 | 0 | 63 | 3 | 66 |
| 6 | 1950-51 | 7 | 1 | 0 | 8 | 31 | 1975-76 | 0 | 21 | 46 | 67 |
| 7 | 1951-52 | 0 | 6 | 2 | 8 | 32 | 1976-77 | 23 | 44 | 0 | 67 |
| 8 | 1952-53 | 0 | 9 | 0 | 9 | 33 | 1977-78 | 0 | 8 | 59 | 67 |
| 9 | 1953-54 | 0 | 8 | 1 | 9 | 34 | 1978-79 | 0 | 55 | 12 | 67 |
| 10 | 1954-55 | 0 | 6 | 3 | 9 | 35 | 1979-80 | 0 | 42 | 25 | 67 |
| 11 | 1955-56 | 0 | 6 | 3 | 9 | 36 | 1980-81 | 0 | 23 | 42 | 65 |
| 12 | 1956-57 | 0 | 9 | 0 | 9 | 37 | 1981-82 | 2 | 29 | 34 | 65 |
| 13 | 1957-58 | 0 | 9 | 0 | 9 | 38 | 1982-83 | 10 | 55 | 0 | 65 |
| 14 | 1958-59 | 1 | 8 | 0 | 9 | 39 | 1983-84 | 0 | 45 | 20 | 65 |
| 15 | 1959-60 | 0 | 5 | 4 | 9 | 40 | 1984-85 | 0 | 24 | 41 | 65 |
| 16 | 1960-61 | 0 | 13 | 2 | 15 | 41 | 1985-86 | 28 | 37 | 0 | 65 |
| 17 | 1961-62 | 0 | 8 | 9 | 17 | 42 | 1986-87 | 0 | 23 | 42 | 65 |
| 18 | 1962-63 | 0 | 3 | 17 | 20 | 43 | 1987-88 | 4 | 47 | 14 | 65 |
| 19 | 1963-64 | 0 | 27 | 2 | 29 | 44 | 1988-89 | 4 | 57 | 2 | 63 |
| 20 | 1964-65 | 0 | 6 | 27 | 33 | 45 | 1989-90 | 61 | 2 | 0 | 63 |
| 21 | 1965-66 | 22 | 17 | 0 | 39 | 46 | 1990-91 | 6 | 46 | 3 | 55 |
| 22 | 1966-67 | 0 | 33 | 9 | 42 | 47 | 1991-92 | 2 | 44 | 8 | 54 |
| 23 | 1967-68 | 0 | 20 | 27 | 47 | 48 | 1992-93 | 27 | 24 | 0 | 51 |
| 24 | 1968-69 | 0 | 21 | 28 | 49 | 49 | 1993-94 | 1 | 46 | 3 | 50 |
| 25 | 1969-70 | 16 | 42 | 1 | 59 | 50 | 1994-95 | 1 | 31 | 18 | 50 |

**Table 3.4:** Summary of the frequency analysis results for the whole island and selected basins for 2, 5, and 10 years return period.

| Region | Average Rainfall (mm/year) | 2-year (mm/year) | 5-year (mm/year) | 10-year (mm/year) |
|---|---|---|---|---|
| **Crete (A)** | 1086 | 1010 | 1228 | 1324 |
| **Crete (B)** | 1086 | 1030 | 1200 | 1290 |
| **Gerapotamou** | 822 | 765 | 937 | 993 |
| **Giofyro** | 820 | 863 | 1052 | 1139 |
| **Anapodiaris** | 755 | 752 | 922 | 981 |
| **Platis** | 1288 | 1077 | 1309 | 1391 |
| **Tavronitis** | 1503 | 1434 | 1730 | 1875 |
| **Petras** | 756 | 694 | 852 | 928 |

# CHAPTER 4

# INTEGRATING MULTI-CRITERIA ANALYSIS AND GIS FOR ASSESSING RAINGAUGE WORTH WITHIN AN ESTABLISHED NETWORK

Geographic Information Systems technology is used to develop automated methods for assessing raingauge networks. An ArcView GIS module has been developed by incorporating simple statistical methods with the software's spatial analysis capabilities, visualization, and AVENUE scripts (the ArcView programming language). The main purpose of the module is to provide a decision support for reducing the number of gauges in an existing network without compromising the reliability and quality of the information obtained. Two test cases were used, one from the country of Switzerland for demonstration and the other is the island of Crete, in Greece for validation of the module.

## 4.1 Introduction

Evaluating an existing meteorological network necessitates a thorough analysis of the available data to find out the strengths and weaknesses of the network as far as density, spatial distribution, and representativeness of stations are concerned. A meteorological network should be designed to sample a phenomenon in both time and space in order to obtain adequate knowledge of its spatial and temporal variation with an acceptable error (Fortin *et al.* 1978; Charbonneau 1979).

Many articles have been written that deal with designing and optimizing raingauge network configurations. A perfect network, however, does not exist and the fact remains that the denser the network the better. Hendrick and Comer (1970), raised many questions that are the main concern of hydrologists such as: "How many gauges are enough?", "Are they in the right place?", "What are the precipitation measurement requirements for watershed research?", "To what degree should spatial variations in rainfall and snowfall be specified to determine quantitative effects on the subsequent hydrologic processes of runoff, evapotranspiration, sediment movement, or water quality?". Earlier studies attempted to answer these questions. To name a few, Watt (1956) found that in a tropical area of 66 square miles, one gauge indicated rainfall on 47% of the days while with 21 gauges the rainy days increased to 58%. Sharp *et al.* (1961) reported only an insignificant difference of average rainfall amounts between 39 gauges and 10 gauges for an area of 62 square miles. However, when the number of gauges was reduced to 5, a noticeable difference occurred. Nicks (1963) stated that if the existing network of rain gauges were installed with a uniform spacing, fewer gauges would give better results. In his study of 15 networks in the United States, Hershfeld (1965) adopted the inter-gauge correlation coefficient of 0.9 as the criterion for raingauge spacing (i.e. 81% of the rainfall variation at any ungauged point will be accounted for by

variations at a gauged point). Hendrick and Comer (1970) investigated the required raingauge density over a watershed to measure daily rainfall amounts. They calculated the error of the raingauge estimation of daily precipitation by comparison of the arithmetic mean of raingauge measurements from a dense network with the arithmetic means of raingauge measurements from various sub-networks. By applying Hershfeld's criterion of 0.9 inter-gauge correlation, they determined the required number of raingauges and the error of the estimate and pointed out that the correlation coefficient is not always a sufficient criterion for establishing the spacing of raingauges. However, Zawadzki (1973) concluded that the 0.9 inter-gauge correlation criterion gives a good precision in area-average rainfall amounts. Eagleson (1967) stated that incorporating the catchment dynamics into the design of flood forecasting networks reduces the number of gauges needed when compared with the number of gauges obtained solely through consideration of precipitation variability. Eagleson also added that little advantage is gained by utilizing more than two properly located stations for the determination of long-term areal mean rainfall. Alvarez and Henry (1970) figured that the number of gauges should depend on the topography of the region, the mean diameter of the rainstorms, and the type of data required (daily, monthly, or yearly totals). Charbonneau (1979) demonstrated that errors of interpolation caused by microclimatic irregularities and by observational errors in the initial data are greater than those resulting from the reduction of the network.

Some networks start with few gauges and are then expanded. Gauges are added one or two at a time (at locations of undetected patterns) to enhance the performance of the network as measured by flood forecasting ability, where the catchment dynamics become a major factor in gauge allocation, or potential rainfall predictability. At some point, networks may be downsized due to cost or accessibility constraints. At the same time, radar (or radar/satellite) rainfall estimates are becoming more popular and reliable, making dense networks increasingly unnecessary.

A number of methods are reported in the literature for network design. Some of them are simple, while others are more sophisticated. Examples are: the systematic approach (Rodda *et al.* 1976), the simulation approach (Bras and Rodrigues-Iturbe 1976), the correlation analysis technique (Hutchinson 1969; Stole 1972), the isocorrelation method (Hershfield 1965), the regionalization approach (Creutin and Obled 1982; Dingman *et al.* 1988), the rational approach (Desi *et al.* 1965), the smallest standard error approach (Bradsley and Manly 1985), and Decision Theory (Hoffmann 1974). Most of these network design methods can be applied to special cases. Some of them assume linear variation between stations; others assume homogeneous areas.

Due to their spatial analysis capabilities, Geographic Information Systems can be used effectively as a platform for studying the network problem. In this study, the goal is to identify which stations are redundant and could be removed should it become necessary. The process initiates by listing the evaluation criteria and determining groups of homogeneous stations as sub-networks. This chapter describes the development of a GIS tool that is used to assess existing raingauge networks. The developed module is applied to a 467-gauge network in Switzerland and two 9-gauge networks in two watersheds in the island of Crete, in Greece.

## 4.2 Methodology

Information of sufficient detail and accuracy on how much water falls onto a watershed is a basic requirement to estimate the yield of a watershed when it rains. Also, due to the fact that many local water resources management projects are watershed-based projects, watersheds of "reasonable sizes" are delineated using a DEM. These watersheds are used to divide the main network into many smaller sub-networks. The gauges located within each watershed are then extracted.

### 4.2.1 Evaluation Criteria

This is done by suppressing one sampling point (station) and values for that point are interpolated based on the remaining (n-1) points. Then, the interpolated values are compared with those observed for that point. The same procedure is followed and repeated for all points for each sub-network. The criteria for comparison are:

#### 4.2.1.1 Correlation Coefficient (r)

The sample correlation coefficient between observed and estimated rain values is an empirical measure of their linear association.

$$r_{UW} = \frac{\sum_{i=1}^{n}(U_i - \overline{U})(W_i - \overline{W})}{\{\sum_{i=1}^{n}(U_i - \overline{U})^2\}^{1/2}\{\sum_{i=1}^{n}(W_i - \overline{W})^2\}^{1/2}} \qquad (4.1)$$

where $r_{UW}$ : correlation coefficient ($-1 \leq r_{UW} \leq 1$); $U_i$ : observed values; $\overline{U}$ : mean of observed values; $W_i$ : estimated values; $\overline{W}$ : mean of estimated values; n: number of sample points.

#### 4.2.1.2 Mean of Absolute Residuals ($\bar{e}_{abs}$)

This is an average of the residuals not considering their sign. Given that there are negative errors, this value will be greater than a normal average of residuals ( $\bar{e}$ ).

$$\bar{e}_{abs} = \sum_{i=1}^{n} \frac{|U_i - W_i|}{n} \tag{4.2}$$

4.2.1.3 Standard Deviation of Absolute Residuals ($S_{abs}$)

This value determines how much deviation there is from the mean (spread of the distribution about the mean).

$$S_{abs} = \sqrt{\sum_{i=1}^{n} \frac{(|e_i| - \bar{e}_{abs})^2}{n-1}} \tag{4.3}$$

where $|e_i|$: absolute value of the individual residual ($|U_i - W_i|$).

4.2.1.4 Variance of Absolute Residuals ($S^2_{abs}$)

$$S^2_{abs} = \sum_{i=1}^{n} \frac{(|e_i| - \bar{e}_{abs})^2}{n-1} \tag{4.4}$$

4.2.2 Approach

The adopted gauge elimination approach marks the gauge with the least effect in terms of estimating both rainfall at ungauged locations and/or mean areal rainfall and consider it a candidate for removal. The definition of a redundant gauge is the gauge that produces the lowest value for ($\bar{e}_{abs}$), (S), ($S^2$), and the highest value for (r) within the sub-network. After the sub-networks (each sub-network represents a watershed) have been identified, two rain surfaces (grids) {*a grid refers to a two-dimensional array of regularly spaced grid cells. A grid cell refers to a single pixel that has dimensions equivalent to the resolution of the grid. For example, each cell in a 1-km resolution grid is 1 km * 1 km in size. A value assigned to a pixel, such as a precipitation estimate, is positioned at the cell center. However, it is not a point value; rather, it represents an average value over the entire cell.*} are generated based on a user-specified interpolation technique and cell size. The first grid is based on the gauges only located within the watershed (local grid), while the second grid is based on the main network (global grid). Each sub-network will then be modified by eliminating one gauge at a time from the local grid and deriving a new local rain surface (new grid) based on the remaining gauges. The five statistics previously mentioned are calculated each time a (new grid) is generated. Three approaches were used to suggest the elimination of less influencing gauges.

4.2.2.1 Based on Correlation Coefficient

The correlation coefficient is calculated using the observed and estimated rainfall

values at the suppressed gauge. The number of calculated correlation coefficients equals the number of gauges within a sub-network setting. If the correlation coefficient is high at one point, this implies that the other gauges provided a good estimated value of rainfall at that site (point) and vice versa.

4.2.2.2 Based on the Variance (VAR)

This approach is executed by calculating a number of parameters:

1) the estimated value of rainfall (by extracting the value from the "new grid");
2) the error between the estimated value "new grid" and the value extracted from the "local grid" as an absolute value;
3) the error between the estimated value "new grid" and the value extracted from the "global grid" as an absolute value;
4) the error between the estimated value "new grid" and the observed value "Obs" as an absolute value; {the mean and variance are then calculated for the errors (residuals) determined in steps 2, 3, and 4 as *MeanAbsErrLoc*, *MeanAbsErrGlb*, *MeanAbsErrObs*, *VarAbsErrLoc*, *VarAbsErrGlb*, and *VarAbsErrObs*. For a given rain surface (grid), the sum of the rainfall values at each grid cell divided by the total number of cells in the grid represents the mean areal rainfall *MAR*. A grid-based MAR over the watershed is estimated using the "new grid", "local grid", and "global grid"}; and
5) The difference between MAR from "new grid" and MAR from "local grid" is *Diff_Loc*, and between "new grid" and "global grid" is *Diff_Glb* are then obtained as absolute values.

The previous procedure is automatically repeated for every gauge in the sub-network for each sub-network in the main network. Generally, for a gauge to be ineffective:

1) the mean absolute error and the variance for all categories should be minimal (steps 2, 3, and 4);
2) the difference between averages should be minimal (step 5); and finally
3) given equal weights for all statistical measures MeanAbsErrLoc, MeanAbsErrGlb, MeanAbsErrObs, VarAbsErrLoc, VarAbsErrGlb, VarAbsErrObs, Diff_Loc, and Diff_Glb; the *AVG* value should also be minimal. It should be noted that the *AVG* value is used for comparison only (i.e. the value itself is not a measure), therefore assigning equal weights seems appropriate and justifiable.

As mentioned earlier, the procedure is repeated for each sub-network a number of times that is equal to the number of gauges in the watershed. The gauge corresponding to the minimum AVG value in each watershed is then marked for elimination. The new (modified) sub-networks are then generated and aggregated to form the new main network. It should be noted that by using this approach, the variance is the dominating factor because all values

have the same weight. The mean was used to differentiate between variances that are equal (or close) in value. This indicates that there is more emphasis on estimating rainfall at ungauged locations than estimating mean areal rainfall over the region. In hydrologic modelling, for example, in a case where "lumped" models are used, areal-averaged values for different parameters are often used as input to such models.

4.2.2.3 Based on the Standard Deviation (STDEV)

The same VAR procedure is followed for STDEV, however, in this case the emphasis is on estimating mean areal rainfall over the region more than estimating rainfall at ungauged locations. In this case, the AVG value will be calculated based on: MeanAbsErrLoc, MeanAbsErrGlb, MeanAbsErrObs, StdevAbsErrLoc, StdevAbsErrGlb, StdevAbsErrObs, Diff_Loc, and Diff_Glb.

## 4.3 Test Cases

The module is applied to raingauge networks in Switzerland and Crete.

### 4.3.1 Switzerland

It lies at the heart of Western Europe and covers an area of 41,284 $km^2$. Both the region's digital elevation model and a rain surface (interpolated from observed values) are shown in Figure 4.1a. The set of data being used is related to the period of Chernobyl Nuclear Power Plant accident (April, 26$^{th}$ 1986) (Dubois 1998). During the days following the accident, a radioactive plume crossed many European countries. Atmospheric flow and rain resulted in radioactive contamination, which occurred in almost all European countries. Radioactive deposition on the ground was mainly a function of the rainfall. The primary set of data includes 467 daily rainfall records made in Switzerland on May 8$^{th}$ 1986. The collection of the data was carried out by the Air Pollution Group at Imperial College in London. The location of the data points are also shown in Figure 4.1a. A DEM with a 1km resolution was provided as secondary information along with the country border used to define the area under study. The rainfall records were tabulated in a text file format in 1/10$^{th}$ of a millimeter. The DEM is a normal ASCII ARC/INFO file format and the country border was available as an AutoCad Interchange Drawing file.

By looking at Figure 4.1b, which is a spatial distribution of rainfall-elevation ratio over the country, it seems that topography did not have a great effect on rainfall. In fact higher ratios were located on the moderate topography of the northwestern part. From the first plot (elevation vs rainfall), it is clear that various amounts of rainfall is scattered along a low elevation line. Low elevations received considerable amount of precipitation. The second plot shows that the there is a positive association between rainfall-elevation ratio and rainfall. This is another indication that the elevation was not a factor in

determining/predicting the amount of precipitation (i.e. no orographic effects). If there were any orographic effects, we would have expected a trend line of a very small slope (almost horizontal). Big and heavy storms dominating the whole region would result in a trend line of a very large slope (almost vertical).

### 4.3.2 Crete

As shown in Figure 4.2a, the island of Crete occupies the southern part of the country of Greece, with an area of 8265 $Km^2$, which is almost 6.3% of the area of Greece. Two watersheds on the island were chosen for the second test case: Geropotamou (with an area of 602 $km^2$) and Anapodiaris (with an area of 520 $km^2$). Each of the watersheds is covered with 9 gauges , which are located at different locations and different elevations. The data sets used are annual rainfall for: wet years (1977 and 1986), an average year (1974), a dry year (1989), a short term average (1975-85), and a long term average (1970-95). The data for the wet month of January 1981 is also included. Monthly precipitation for all data were compiled by the Hellenic National Meteorological Service. The locations of the data points were also provided. A 50m DEM was generated and the island boundary is used to define the area under study. The rainfall measurements were in the form of database files and the borders were available as an ARC/INFO export file. Figure 4.2b shows the DEM for Gerapotamou and Anapodiaris basins, the stream systems in the basins, and the raingauges.

## 4.4 GIS Module Structure

GIS technology has been used for numerous applications in supporting water resources management. GIS applications linked to (or integrated with) different computer models provide functions for data storage, calculation of required input parameters, data manipulation, and output processing (Ross and Tara 1993; Maidment 1993; Greene and Cruise 1995; Brimicombe and Bartlett 1996). A GIS becomes more powerful when some added features (represented in this case by statistical methods) are combined with its many capabilities, as described above, to produce a good decision support system. This GIS module interface, as shown in Figure 4.3, was developed in the ArcView GIS environment using AVENUE (the ArcView programming language).

The programming language AVENUE provides a well-defined mechanism for allowing user-written routines to be called from within the normal user interface of the GIS package. In addition, this language also provides the capability to customize a menu-driven graphical user interface that makes it possible to guide a user with prompts and explanations throughout the application.

The project is composed of AVENUE scripts, dynamic link libraries (dlls), and designed dialogs. A dialog was created for the convenience of the user, which included all

spatial interpolation techniques available in ArcView (see Appendix D), including those that are not available in the normal interface of the software. As the name implies, the "makedir.dll" and "deldir.dll" dynamic link libraries were built to create and delete directories without the use of batch files. The main module uses four main pieces of information to perform its task and generate new network: the location of gauges, rainfall data, region boundary, and a DEM as shown in Figure 4.4. The main module consists of five sub-modules:

### 4.4.1 Project Description

This module documents the project by informing the user of the different parts of the main module using many graphic illustrations. It can be viewed as either a Word Perfect Document (help.wpd) or an HTML (help.htm). The advantage of the HTML is that it provides links to all AVENUE scripts and examples of output tables and text files (Figure 4.5).

### 4.4.2 Data Preparation

This is a five-phase module that basically prepares the project for modules to follow. The data input requirements for this part include information on the boundary of the region, the DEM, and the data and location of the gauges in the original network.

#### 4.4.2.1 Watersheds

In this step a watersheds shapefile is generated from the DEM through a multi-step process that starts from generating a FILLED DEM grid, and moves on to generate a FLOW DIRECTION grid, a FLOW ACCUMULATION grid, a WATERSHEDS grid, a Watersheds shapefile, and finally a Streams shapefile (Jenson and Domingue 1988) (refer to Section 3.4.1.1 and Appendix C for more details). The users will then be asked if they would like to edit the watersheds shapefile before proceeding to the following steps, in which case the shapefile will be editable and ready for the user to make any correction deemed necessary. Otherwise, a column that includes the areas for all watersheds will be generated in the attribute table of that shapefile.

#### 4.4.2.2 Calculate Areas

If the user chooses to edit the watersheds shapefile, this step will allow them to calculate the areas of the final watersheds shapefile by adding a column to the attribute table. The calculated area of the watersheds will be used in a later stage to assess the possibility of removing a number of gauges according to the desired density condition.

#### 4.4.2.3 Clip Watersheds

The generated watersheds are based on the original DEM, which may be of larger

extent than the country (region) borders. This allows for the exclusion of parts of the watersheds that are located outside the boundary of the region. This menu item allows the user to clip the generated watersheds using the Country.shp (polygon) as shown in Figure 4.3. Areas of the watershed should be re-calculated if the clipping takes place.

4.4.2.4 DEM Clipping

The given DEM can be clipped at this stage by the border shapefile (polygon), creating a new grid "DEM" and renaming the source DEM grid as "DEM_Original" (Figure 4.6).

4.4.2.5 Rain Surface

Using the new developed dialog (Figure 4.7), a grid of interpolated precipitation values from all given gauges is formed (Figure 4.1a). The interpolation technique is stored as a global variable "_anInterp" to be used, assuming there is no interruption throughout the project. Otherwise, the dialog will be re-presented to the user to reassign the technique.

4.4.3 Views Preparation

Assuming that the preliminary work is being performed in "view1", this step is responsible for carrying out the following tasks:

1. creating a number of views that are equal to the number of watersheds generated in the first step of this module, including "view1";
2. creating and setting a working directory for each view that is named after the view inside the main working directory (for example: "C:Net\");
3. copying the themes "Rain.shp", "Watersheds.shp", "Rain Surface", and "DEM" from "view1" to each of the created views;
4. setting the "watersheds.shp" active for future work;
5. setting the properties of each view (i.e. distance units and map units); and
6. running the script responsible for cycling through the views and selecting the watershed whose ID number is equal to the view number.

For example, all work performed on watershed with ID # 3 will be done within "view3" and saved in working directory "C:\Net\view3" (refer to Figure 4.8). This is achieved by selecting each record in the attribute table of the "Watersheds.shp" according to a "loop" statement and then running another script from within the "For" statement. Assuming that we are looking at "view3", the script is responsible for:

1. creating a shapefile for each individual watershed "example: wat3";
2. using that new shapefile to:
   - a- clip the DEM. (Example: "DEM3");
   - b- clip the Rain Surface. (Example: "Rain_Global3"); and
   - c- select the rain gauges that are located within the borders of that

watershed and create a new point shapefile. (Example: "Rain3");

3. create a "local" rain surface that is interpolated based on the local rain gauges inside the watershed. (Example: "Rain3" using the "_anInterp" global variable).

4.4.4 Design Criteria and Execution

At this stage, the elimination process takes place for each sub-network in each watershed preparing to establish the new network (as shown in Figure 4.9). The "Execution" menu item is attached to a script that is responsible for prompting the user to specify the desired gauge density and choose the number of gauges to be removed for each watershed (as shown in Figure 4.10). Based on the user's choice, different scripts may be run. Script "Net_Execute1_S" will run if one gauge is selected, "Net_Execute2_S" will run if two gauges is selected, ... and so on to script "Net_Execute5_S". All scripts, except for script "Net_Execute1_S", will run script "Net_EXE" as a subroutine. Common features of the "Net_Execute*_S" scripts include:

1. adding 11 columns to the attribute table of the rain gauges shapefile. The first 2 columns include extracted rain values for each gauge from both the local and global rain surfaces. The columns are named "Est_Loc" and "Est_Glb", respectively;
2. satisfying the design criteria (network density and number of gauges to be removed). If the conditions are met, the script will continue running, otherwise a lower script will be triggered to run. For example, if "Net_Execute4_S" is running but the "new" density condition is not satisfied for any of the watersheds, the script "Net_Execute3_SS" will run ... and so on. If the density criterion is still not met by a watershed, the "rain" shapefile will simply be copied in the same view with a new name: "Final.shp". Scripts with the double "S" are similar to the ones with the single "S". Unlike Single-S scripts, double-S scripts run only for one case (one watershed);
3. cycling (looping) through all rain gauges and:
   - a- eliminating one gauge at a time;
   - b- generating a rain surface from the remaining gauges;
   - c- comparing:
     - i- the average of each generated grid with the average of both the local and global rain surfaces. The difference is recorded in the added columns "Dif_M_Loc" and "Dif_M_Glb", respectively.
     - ii- the average of the absolute error resulting from the difference between the estimated rain from each generated rain surface and the estimated rain from both the local and global rain surfaces and the observed rain. Those values are recorded in the columns "M_Abs_Loc", "M_Abs_Glb", and "M_Abs_Obs", respectively.
     - iii- the variance of the absolute error resulting from the difference

between the estimated rain from each generated rain surface and the estimated rain from both the local and global rain surfaces and the observed rain. Those values are recorded in the columns "Var_Abs_Loc", "Var_Abs_Glb", and "Var_Abs_Obs", respectively. Refer to Figure 4.11.

iv- the AVG value is then recorded in the column "Average".

4. locating the smallest value in the "Average" column. Excluding the gauge with the smallest AVG value, a new point shapefile from the remaining gauges named "Final.shp" is generated as shown in Figure 4.12; and
5. adding that new point shapefile to a global list "_ThemesToMerge" and preparing for the merge job when generating the new network.

As mentioned earlier, the script "Net_EXE" is run from within a loop statement in the execute scripts 2, 3, 4, and 5. It performs similar tasks to script "Net_Execute1_S", which means it eliminates one gauge every time it is run through the Loop statement. For example, if script "Net_Execute4_S" is run, we should expect script "Net_EXE" to run 3 times, eliminating 3 gauges before it returns back to script "Net_Execute4_S" for the final (fourth) gauge elimination.

### 4.4.5 New Network

This is the final step of the project, in which all the generated shapefiles "Final.shp" in every view of the project are merged into one shapefile, which represents the new network. Two ways of generating the "New Network" are adopted. The first is accomplished by recalling the global list "_ThemesToMerge" to merge all the shapefiles in that list and generate the "New Netwrok.shp" shapefile in View1, which represents the recommended gauge distribution. The second is achieved by adding all the "Final.shp" from all views to a new view "View9999" and merging them. The latter method is normally used if the number of watersheds (sub-networks) is large. A summary file is also generated in the main working directory of the project, as shown in Figure 4.13. The summary is a list of actions that took place with the design criteria heading the file. Each view is represented by its name, number of remaining gauges, number of eliminated gauges, and number of generated grids (rain surfaces) for that view. At the end of the file the total number of remaining gauges, eliminated gauges, and number of grids are summarized. To check for any errors or dysfunctions during project execution, the summary file should be reviewed at the end of the run. The number of grids in each view can be verified by using a simple formula (for calculating the sum of terms of an arithmetic sequence) for each sub-network. The number of grids generated for each view should agree with the formula:

$$\text{The Sum} = a*(a-z)+s\frac{(a-z)}{2}(a-z-1) \qquad (4.5)$$

where a: original number of stations in a sub-network; z: remaining number of stations in a sub-network; and s: -1 (in this case)

which can be further simplified to:

$$\text{No. of Grids} = n*(a-\frac{n-1}{2}) \tag{4.6}$$

where a: original number of stations in a sub-network; and n: number of eliminated stations in a sub-network.

4.4.6 Project Accessories

The project is equipped with more scripts, which are automatically executed upon opening and closing the project. These scripts perform additional functions, which are intended to facilitate the project/user interaction and results presentation.

## 4.5 Results and Discussion

It should be noted that although the user can specify the desired sub-network density, they cannot eliminate more than 5 gauges per sub-network for this version of the module.

4.5.1 Switzerland

The Inverse Distance Weighted (IDW) interpolation with a grid cell size of 500m was used for this case. The country was divided into 31 watersheds of different sizes, which ranged from 155 $km^2$ in area, that had only one raingauge, to 6017 $km^2$ with 44 raingauges. A total of 25 runs were performed to test all components of the module, generating a total of 25,825 local grids.

Using the VAR approach, a total of 25 new networks were generated for this one data set based on a combination of criteria, as shown in Figure 4.14 (the rest of the Figures can be found in Appendix F). In Figure 4.14, for example, when the user only allows the removal of two gauges per subnetwork, only 10 gauges can be removed for six watersheds and the density within the watershed remains one gauge per 100 $km^2$ or less. But if the density within the watershed is required to remain one gauge per 200 $km^2$ or less and the user allows the removal of two gauges per watershed, 35 gauges can be removed with Watershed "31" has one more candidate gauge than is required by the design criterion.

One of many ways to perform the task of eliminating gauges based on the design criteria of network density and number of gauges is by using tables (or spreadsheets). Writing a macro within a spreadsheet or a simple Fortran code can do that. Although Table 4.1 represents a comparison of results obtained by both a spreadsheet and the developed module, tables are neither able to provide information on which gauge to remove nor can they provide

the location of the gauge and the interaction between the whole network and its sub-networks. There also were cases where the module detected that more gauges can be eliminated for a subnetwork because those gauges share the same *AVG* value. This could not have been determined using only spreadsheet calculations, which are strictly based on density. Let us use watershed "31" and the design criteria of "one gauge/200 $km^2$" and "two gauges to be removed" as an example. Although the design criteria do not allow for eliminating more than one gauge, the module detected that two gauges, which both had the same AVG value, can be removed, allowing the decision maker to choose either one or both of the gauges.

Figure 4.15 shows the results using the STDEV approach (similarly, the rest of the Figures can be found in Appendix F). Because the networks are relatively dense and measuring only daily values, there is not a big difference in the precipitation amounts recorded by the gauges. The results in both cases are similar with one more or less gauge for each network to be eliminated. The correlation coefficient approach did not provide valuable information for this case. The coefficient was very high (i.e. 99% and higher) for all gauges within the whole networks and its sub-networks.

Repeated runs for different data sets is required to verify the results obtained. For example, wet, moderate, and dry conditions; hourly, daily, monthly, and yearly data; short and long term average..etc. The one available data set used as a test case in this study does not provide enough evidence that certain gauges should be removed from the original network.

### 4.5.2 Crete

The Inverse Distance Weighted (IDW) interpolation with a grid cell size of 100m was used for this case. The local distribution of rainfall within a network is different from the global rainfall distribution, as previously mentioned, where more outside (the watershed) gauges are used in the interpolation. This can be illustrated in Figures 4.16 and 4.17. Figures 4.16a and 4.16b show the local and global rainfall distribution, respectively, in Gerapotamou basin for the wet years 1977-78 and 1986-87, the dry year 1989-90, the short term average (74-84), long term average (60-95), and a wet month (January 1981). Figures 4.17a and 4.17b show the same for Anapodiaris basin. Notice the difference between the local and global distribution for the northwestern part of Gerapotamou basin and the northeastern part of Anapodiaris basin.

In this case, the VAR and STDEV approaches yielded different results. Because annual rainfall amounts vary greatly in their spatial distribution, a gauge that can be eliminated according to one approach is the most important using the other approach. To give

an example, in Gerapotamou basin, using the year 1977-78 records, the VAR approach proved Vorizia gauge to be very significant within the network. The same gauge, however, was recommended as the first candidate for removal when using the STDEV approach. The type of records obtained from this gauge are usually unpredictable by the other gauges within the basin. The error was always high when using the VAR method. For the same reason, the gauge was recommended for elimination using the STDEV approach because records from that gauge do not represent the rainfall spatial distribution within the basin. The correlation coefficient, being an error-based estimator, agreed with the VAR approach results. The same can be said about Armaxa gauge in Anapodiaris basin. For dry year and monthly precipitation records, where there is low spatial variation in precipitation, the three approaches were almost in agreement as in the case of Vorizia station in Gerapotamou basin and Armaxa station in Anapodiaris basin. Refer to Figure 4.18 and Table 4.2 for the results obtained by applying the three approaches for the two basins. The correlation coefficients are presented as contour lines for the two basins for the different years used in the analysis in Figures 4.19 and 4.20. By looking at the DEM of the basins in Figure 4.2b, it is clear that the correlation coefficients are smaller on higher elevations. This means that estimated precipitation values on the mountain are significantly different from the observed ones. This could be attributed to the under representation on high elevation because most of the gauges are located in the valleys.

For Gerapotamou basin, the elevation-precipitation ratio ranges from 0 to 2 for a wet year, and from 0 to 8 for a dry year, and from 0 to 4 for an average year. That means, for example, that for a wet year there is a possible increase of precipitation of 0.5 mm/m, 0.25 mm/m for an average year, and 0.125 mm/m for a dry year. Similarly, for Anapodiaris basin, the elevation-precipitation ratio ranges from 0 to 2 for a wet year, 0 to 3 for an average year, and from 0 to 4 for a dry year. In fact, for both basins, the correlation coefficient was found to be greater than 85% for the areas where the elevation-precipitation ratio was less than half its maximum value. This means that:

| For Gerapotamou basin, | | | For Anapodiaris basin, | | |
|---|---|---|---|---|---|
| $r \geq 85\%$ | if $0 < E/R < 1$ | for wet year | $r \geq 85\%$ | if $0 < E/R < 1$ | for wet year |
| | if $0 < E/R < 2$ | for average year | | if $0 < E/R < 1.5$ | for average year |
| | if $0 < E/R < 4$ | for dry year | | if $0 < E/R < 2$ | for dry year |

which is an indication that precipitation patterns are not detectable on higher elevations.

Other results:

1) the Vorizia, Pompia, Moroni, and Vagionia gauges are valuable within the Gerapotamou basin.
2) the Gortis gauge provided good information when records were available. The gauge was

put out of service in 1982. It is suggested that another gauge should be placed in the same location. The Sternes gauge also stopped recording in 1988 which is a reasonable decision, as it did not prove valuable for depicting the rainfall spatial distribution within the basin.

3) the Armaxa, Protoria, Demati, and Kassani gauges are important ones for the Anapodiaris basin.

## 4.6 Conclusion

Integrating concepts with a GIS provides a good decision support tool for mangers and decision makers. It was clearly demonstrated in this chapter how tackling an engineering problem can be achieved by integrating simple statistical methods with a GIS. The module performed satisfactorily according to the purpose for which it was developed. This tool provides the means for continuous evaluation of raingauge networks. Visualizing precipitation grids can be of great help in determining areas (locations) of proposed new gauges. The location of (a) new gauge(s) is/are expected to be around the gauges that produce the highest AVG values or lowest correlation coefficients. In its current form, this module is suitable for watershed-based management. In other words, it deals with each watershed individually, taking into account the effect of all other sub-networks in their original condition (i.e. before eliminating any gauges). Removing gauges from a sub-network is likely to affect results obtained for a neighboring watershed more than a far one. This can easily be overcome by running the program for each new scenario in a sub-network in order to generate the new "global rain surface". Due to the different spatial distribution of gauges in each sub-network and the amount of rain they record, it is recommended that the program be run using different interpolation techniques and grid cell sizes. Three approaches were used to evaluate the significance of gauges. Results were in agreement when the spatial variation of precipitation was not big (i.e. daily, monthly, dry years, etc.). However, the correlation coefficient and the VAR-based methods provided different results from those obtained by the STDEV-based approach when there was a high spatial variability (i.e. wet years). Gauges should be candidates for elimination if they can depict neither the areal distribution of rainfall nor the point estimates at ungauged locations. Finally, it should be noted that there may be additional factors that should be taken into account in the selection of gauges for removal from a network other than using the criteria described in this chapter. These factors may include: cost of maintenance, length of available record (keep the long ones), gauge altitude, aspect and perhaps others. It is also important to point out that gauge network design greatly depends on the intended or potential uses for a particular network. For example, if the purpose of a network is to provide flash flood warning, it would have a different configuration (spatial and temporal resolution) from the one that is intended for research and monitoring purposes. When using hourly data, for example, gauges will jump up and down on the priority list.

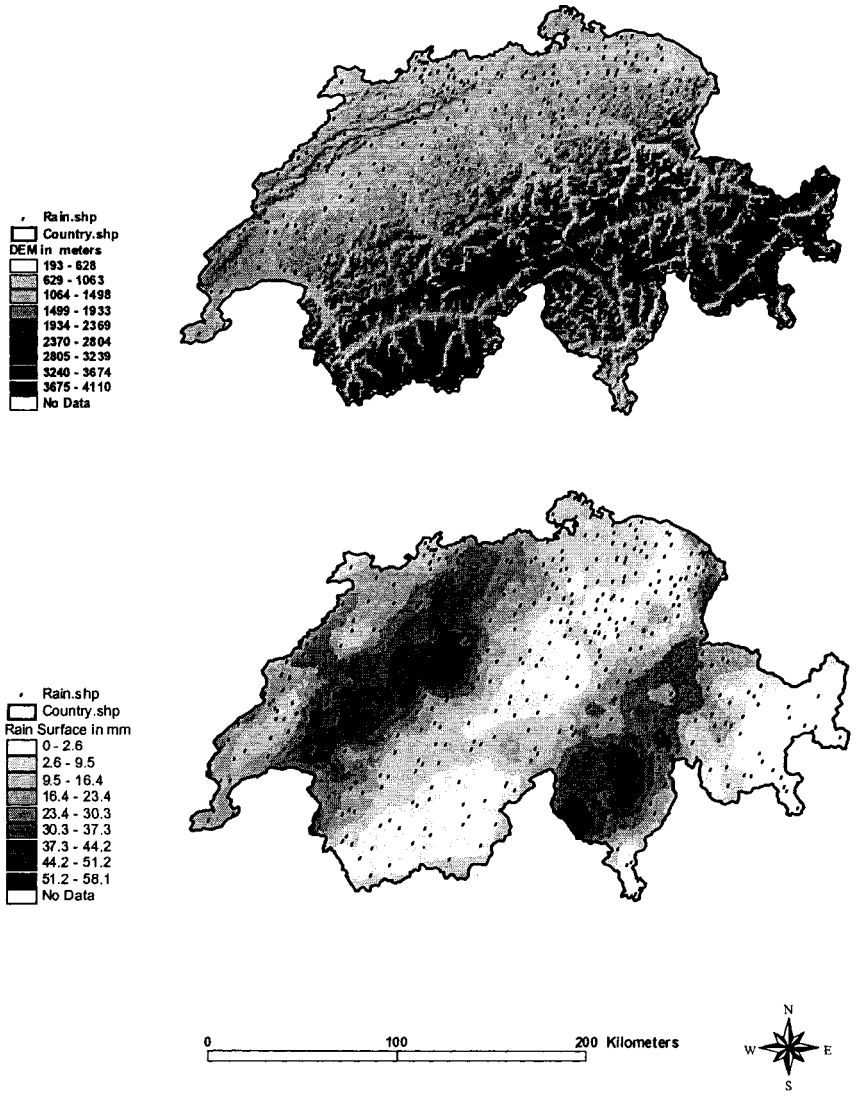


**Figure 4.1a:** Digital Elevation Model (DEM) and the rain surface of Switzerland.

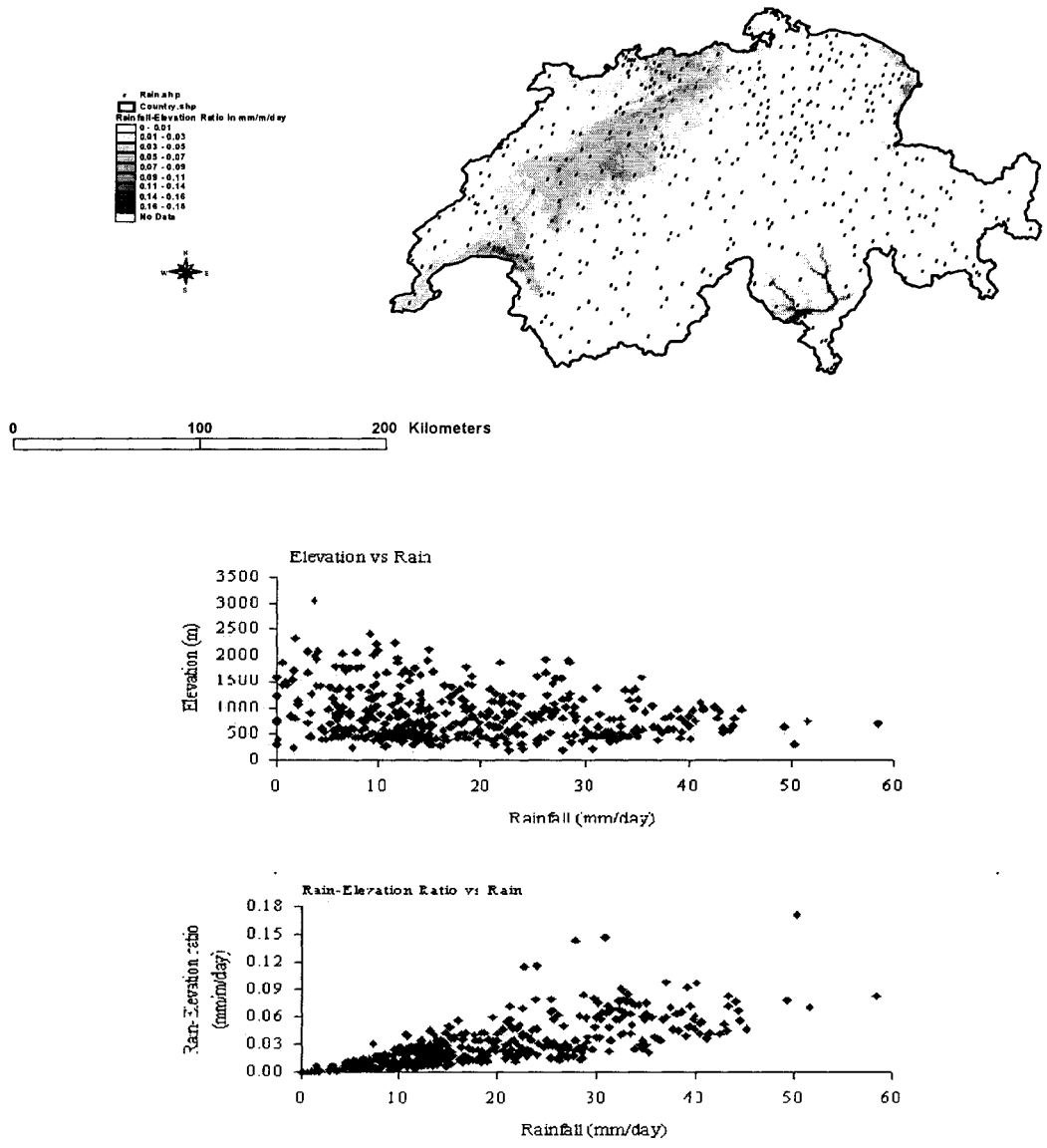


**Figure 4.1b:** A grid representation of the rainfall-elevation ratio over the country and two plots of elevation vs rainfall and rainfall-elevation ratio vs rainfall.

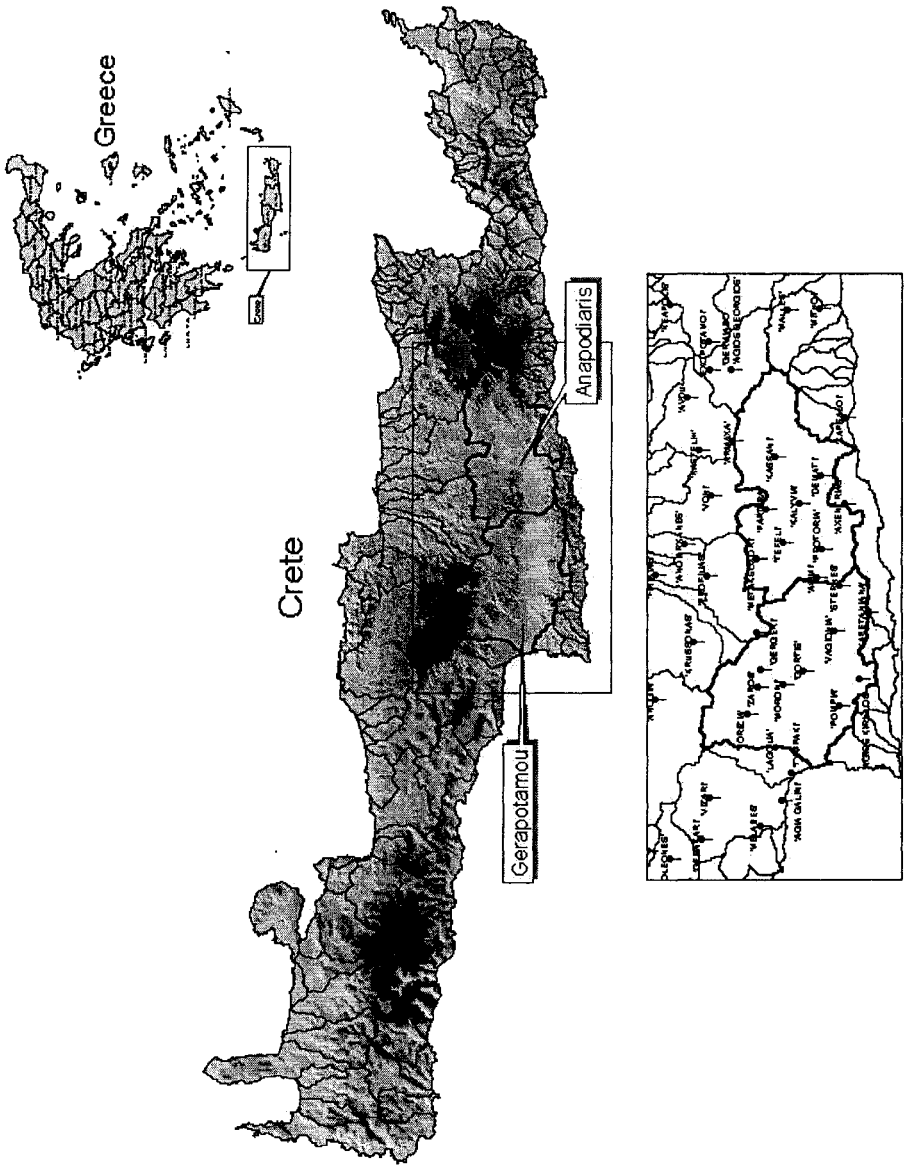


**Figure 4.2a:** Digital Elevation Model (DEM) and watersheds of Crete.

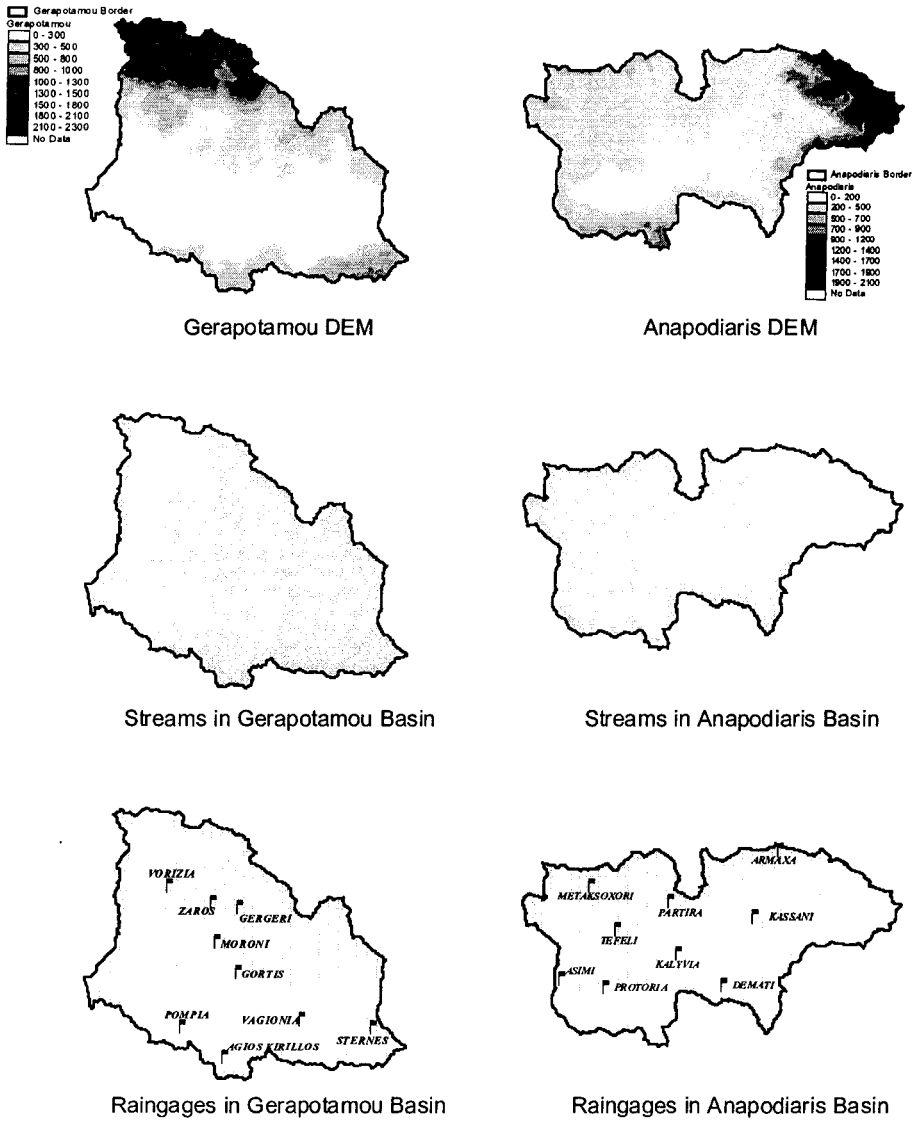


**Figure 4.2b:** DEM, streams, and raingauge networks for Gerapotamou and Anapodiaris basins.

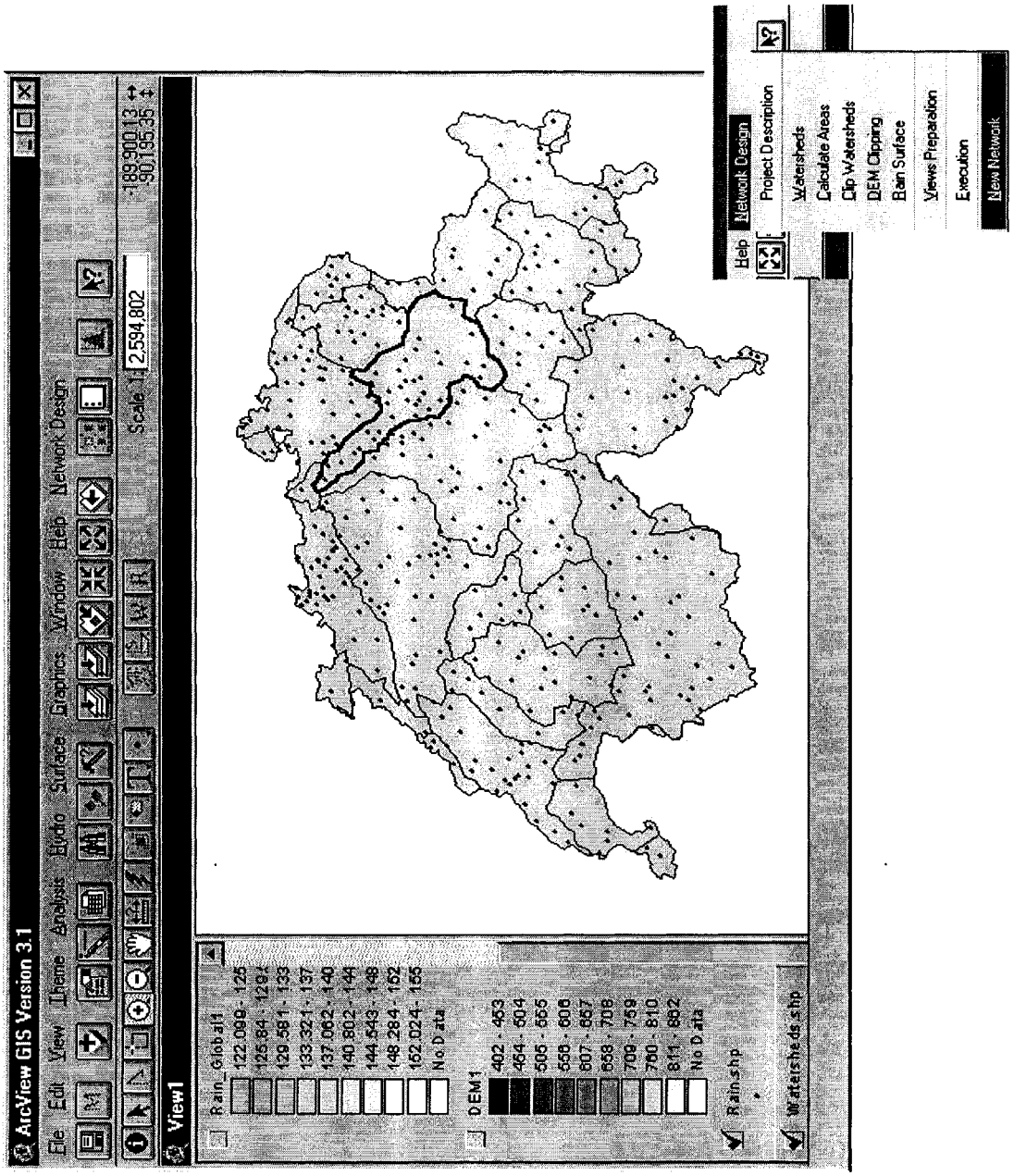


**Figure 4.3:** The GIS module interface of the network design project. The Figure also shows the clipped watersheds using the menu item "Clip Watersheds". Elevation values in "meters" and rain values in $1/10^{th}$ of "mm".

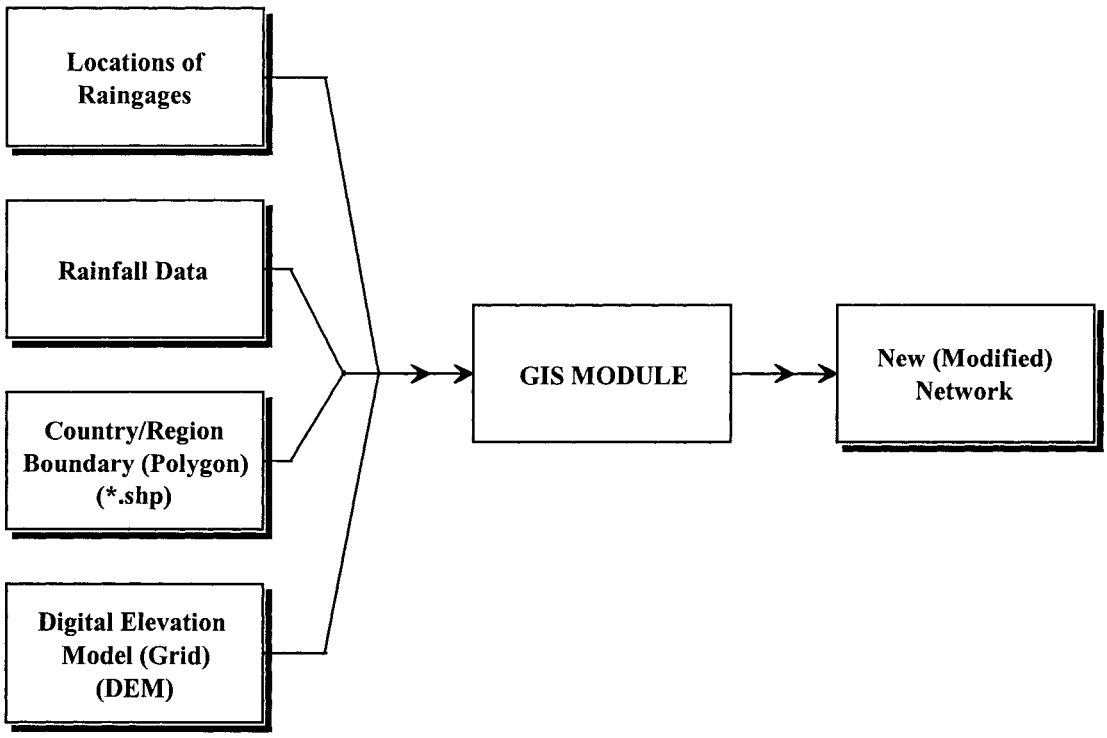


**Figure 4.4:** A simple flow chart representing input and output of the main module.

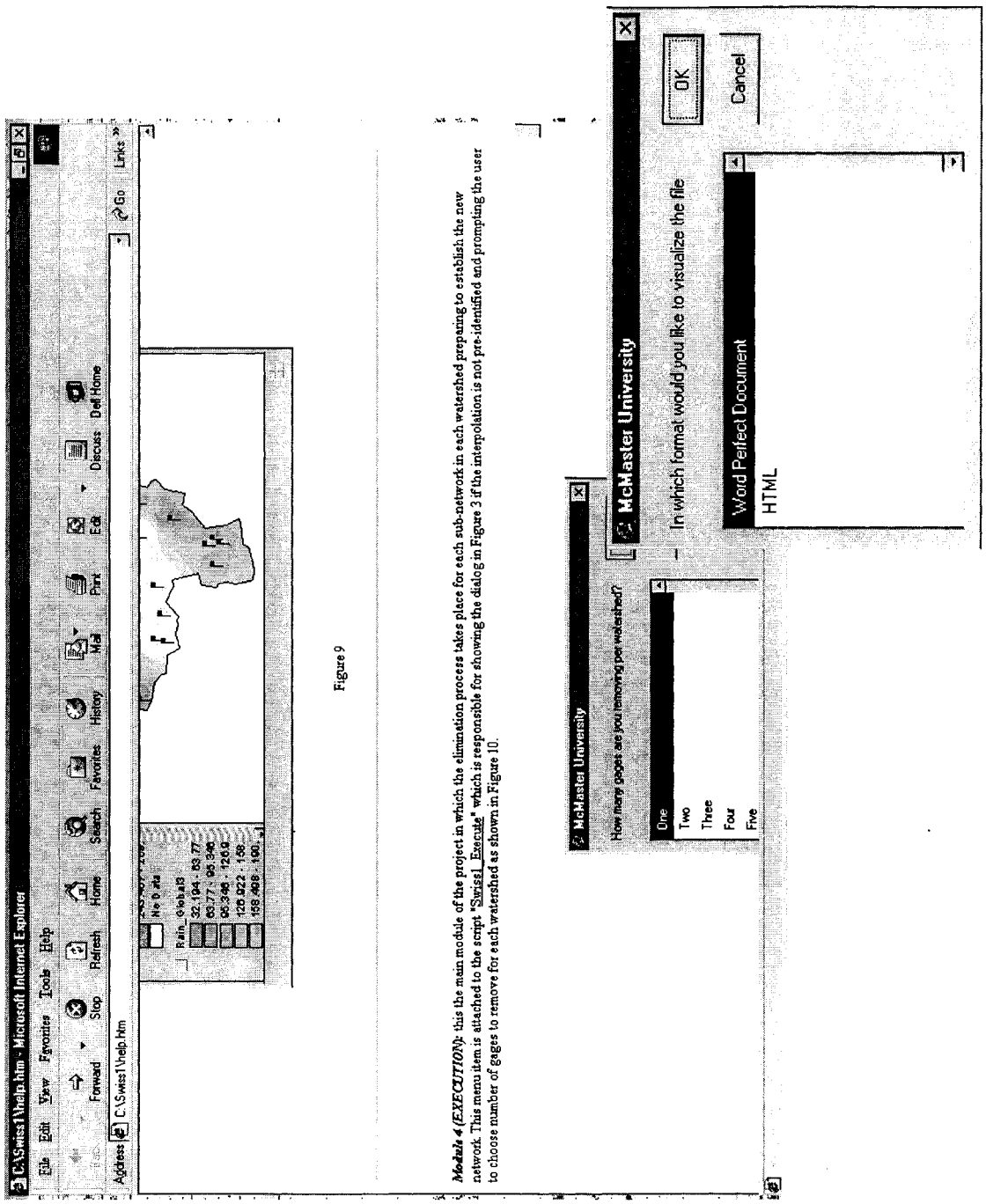


**Figure 4.5:** Module 1: Project Description. Rain values in $1/10^{th}$ of "mm".

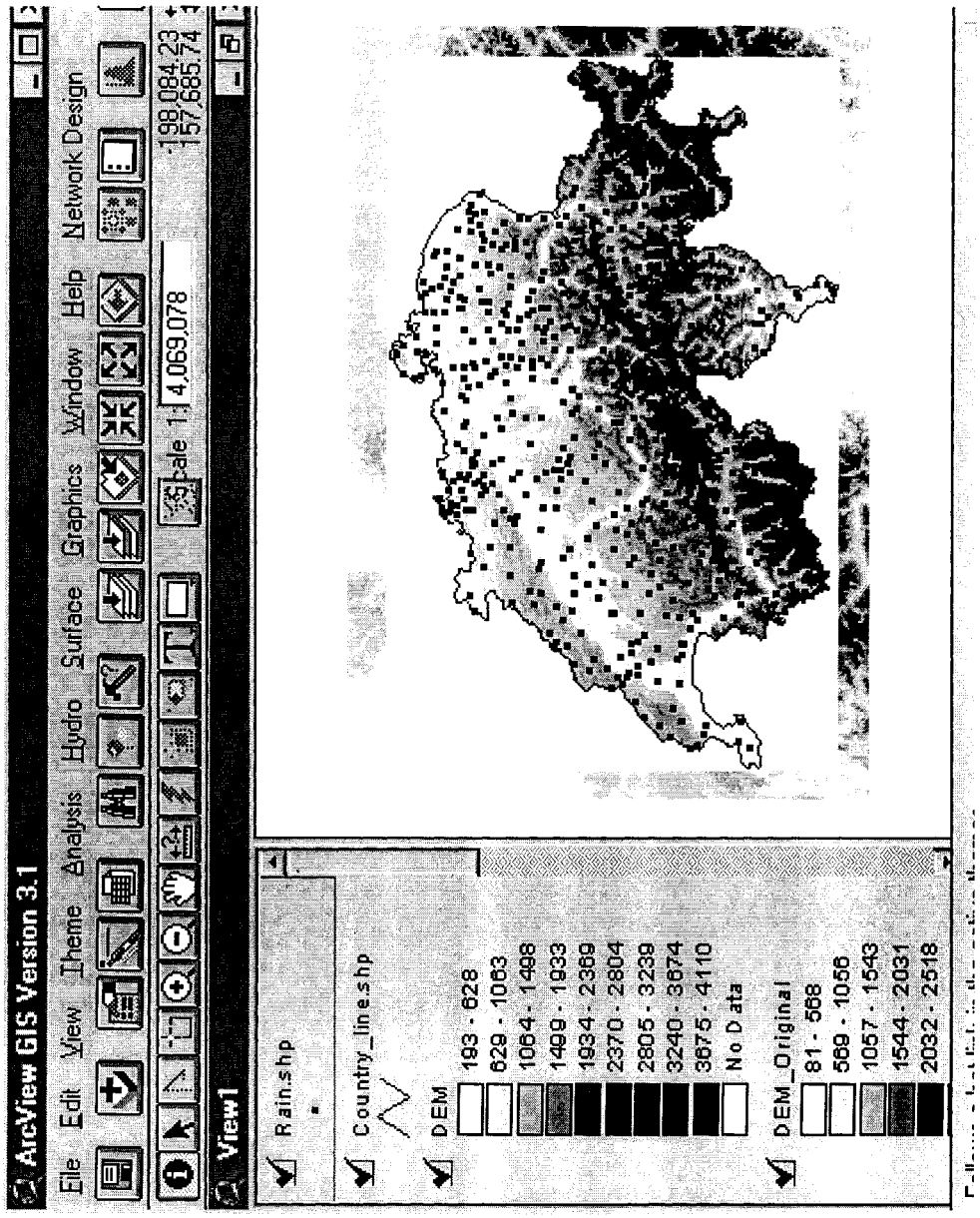


**Figure 4.6:** Clipped DEM using the menu item "DEM Clipping". Elevation values in "meters".

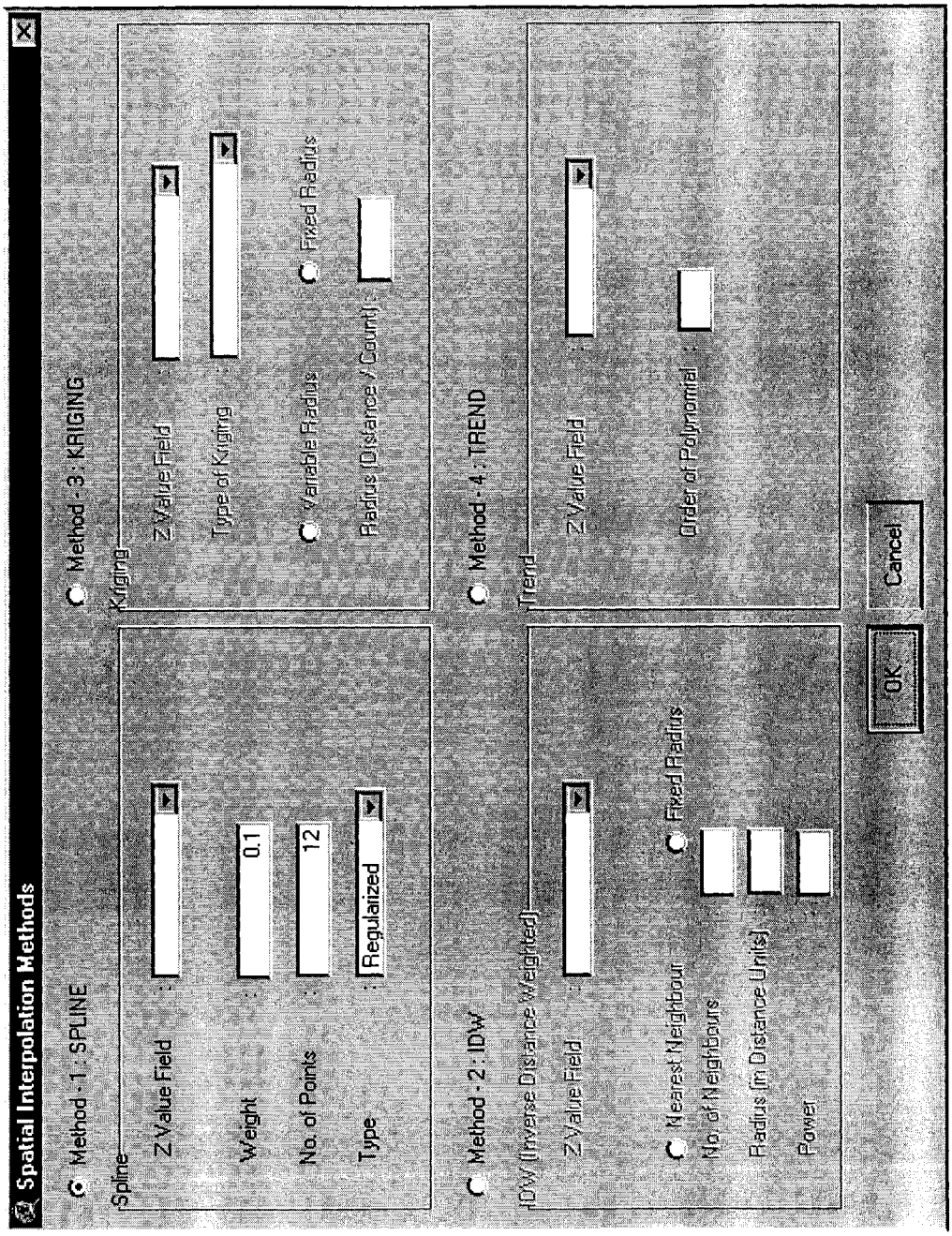


**Figure 4.7:** The developed interpolation dialog as part of module (2).

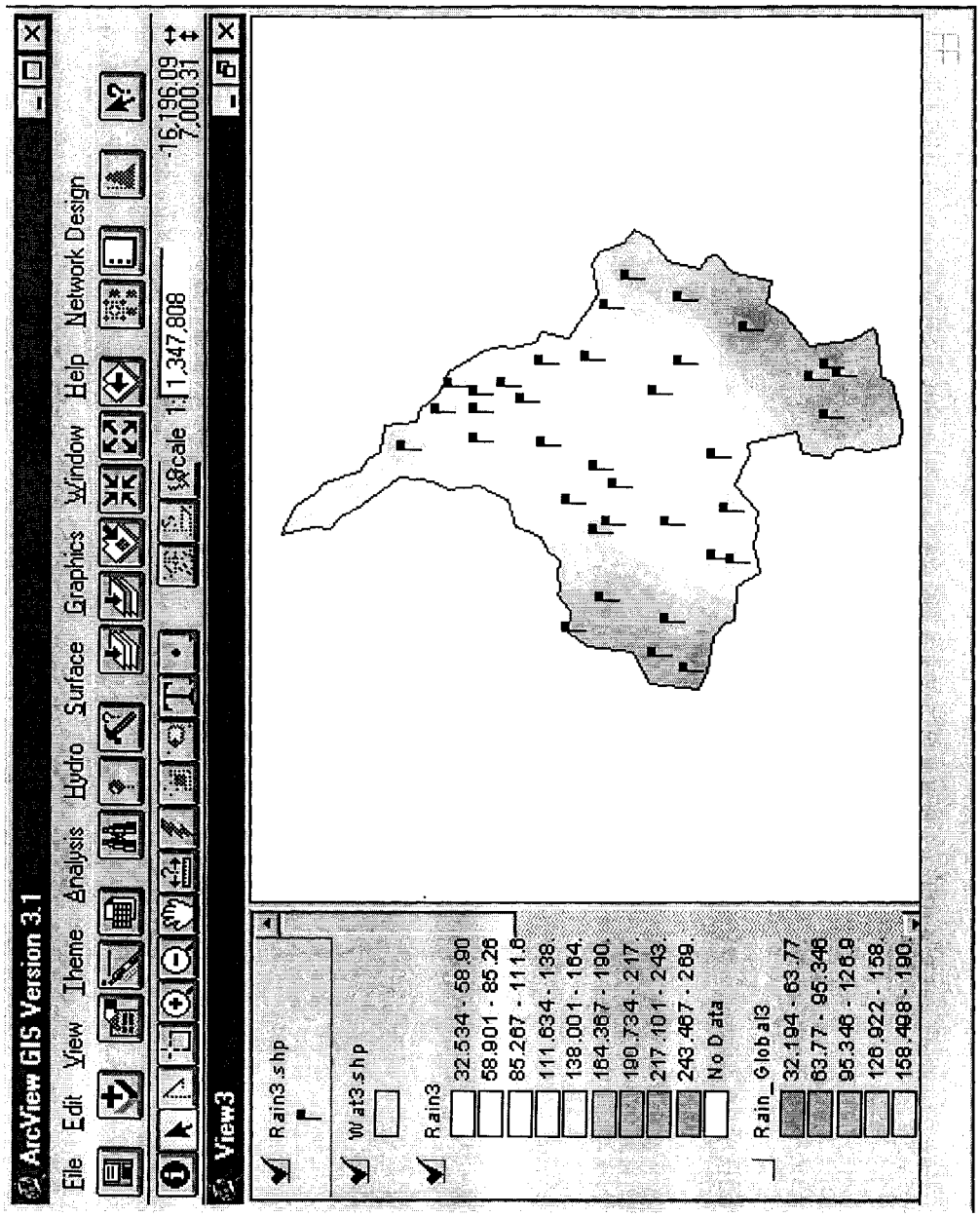


**Figure 4.8:** Clipped watershed with the ID number 3. Rain values in $1/10^{th}$ of "mm".

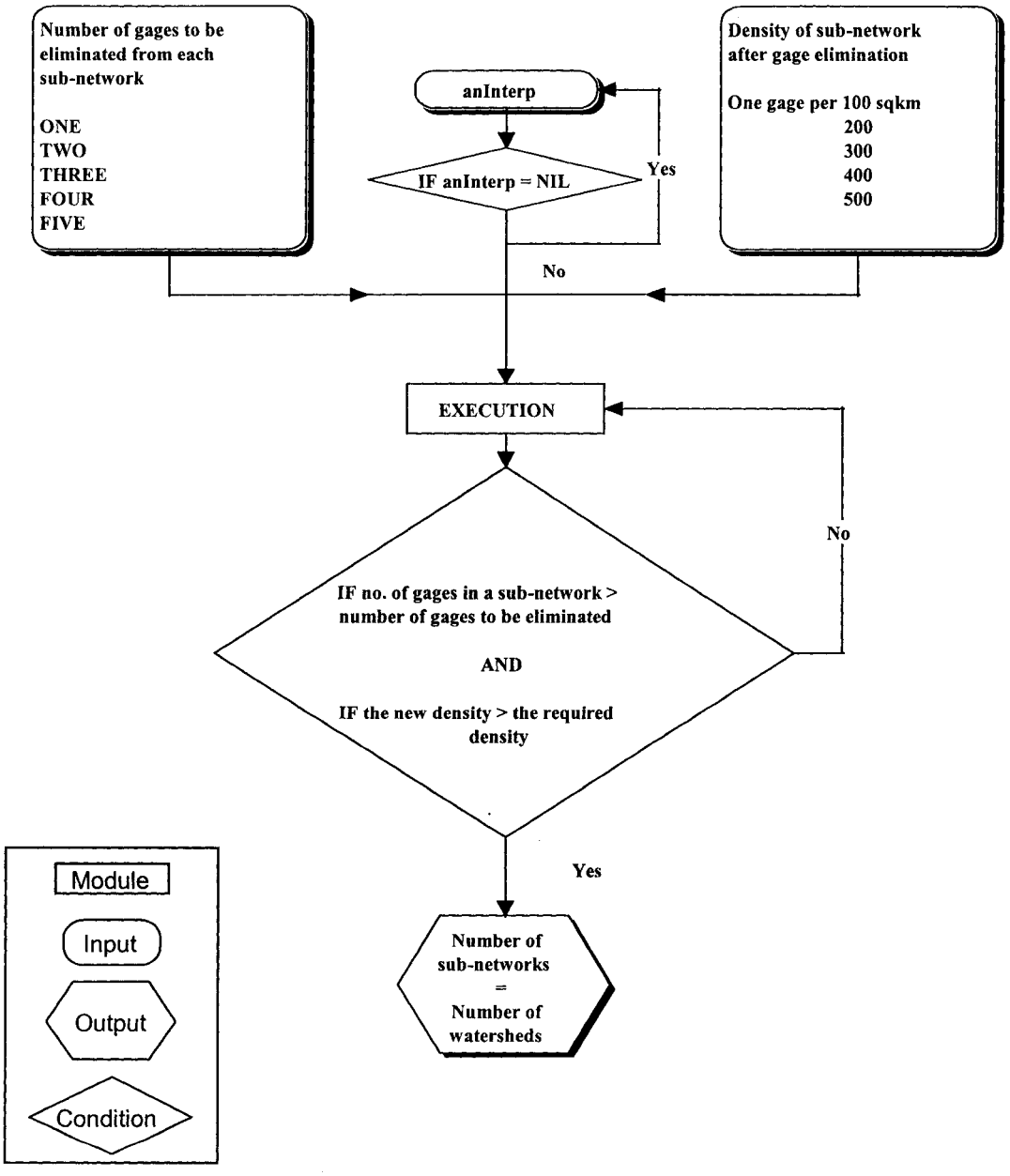


**Figure 4.9:** Input and output of the execution module (module 4).

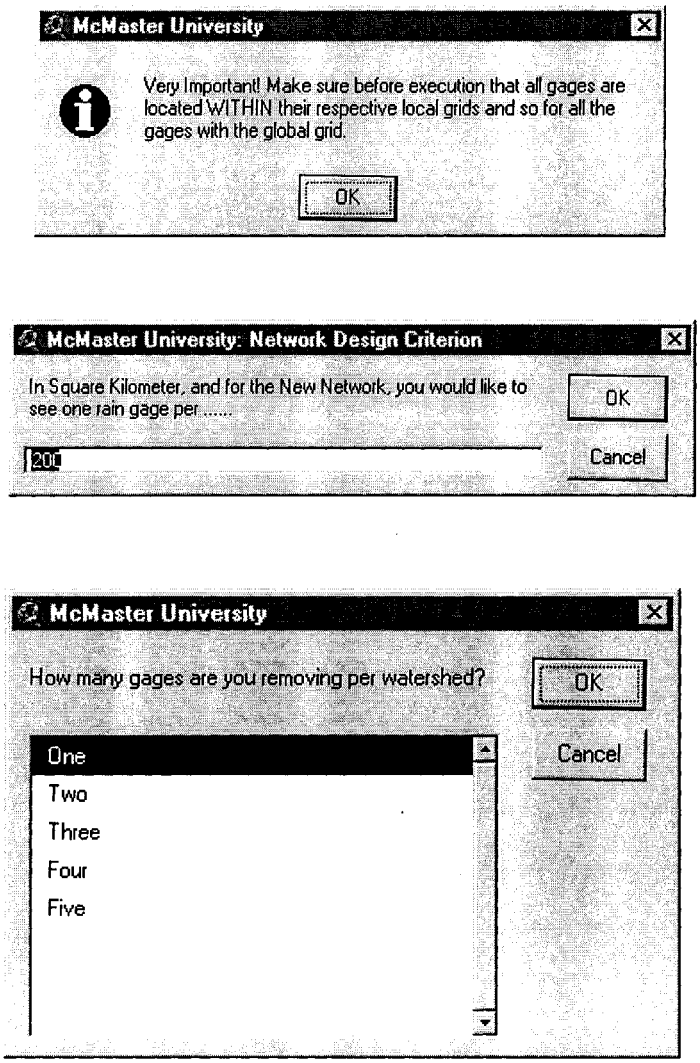


**Figure 4. 10:** Interactive pop-up menus (dialogs) for design criteria specification.

ArcView GIS Version 3.1

File Edit Table Field Window Help

0 of 40 selected

Attributes of Wanted.shp

| Est_Loc | Est_Gib | Dif_M_Loc | Dif_M_Gib | M_Abs_Loc | M_Abs_Gib |
|---|---|---|---|---|---|
| 211.751 | 211.606 | 0.762 | 6.189 | 1.114 | 1.518 |
| 182.997 | 183.038 | 0.144 | 5.570 | 0.031 | 0.443 |
| 132.258 | 132.167 | 0.557 | 4.869 | 1.019 | 1.430 |
| 163.857 | 163.965 | 0.455 | 5.881 | 0.501 | 0.915 |
| 162.804 | 162.780 | 0.624 | 6.051 | 0.927 | 1.342 |
| 124.123 | 124.313 | 0.065 | 5.362 | 0.290 | 0.696 |
| 119.974 | 119.537 | 0.200 | 5.627 | 0.377 | 0.771 |
| 75.203 | 76.667 | 0.690 | 4.737 | 1.179 | 1.520 |
| 123.821 | 123.288 | 0.565 | 5.991 | 0.716 | 1.105 |
| 77.349 | 77.694 | 0.589 | 4.837 | 0.877 | 1.274 |
| 67.055 | 67.008 | 0.313 | 5.114 | 0.270 | 0.684 |
| 93.935 | 93.944 | 0.193 | 5.620 | 0.397 | 0.812 |
| 112.656 | 112.430 | 0.358 | 5.785 | 0.698 | 1.100 |
| 65.118 | 65.195 | 0.288 | 5.139 | 0.454 | 0.862 |
| 45.183 | 45.419 | 0.613 | 4.814 | 0.606 | 1.006 |
| 91.094 | 91.479 | 0.372 | 5.054 | 0.510 | 0.905 |
| 90.479 | 90.304 | 0.113 | 5.540 | 0.444 | 0.850 |
| 58.351 | 59.337 | 0.334 | 5.092 | 0.402 | 0.765 |

ArcView GIS Version 3.1

File Edit Table Field Window Help

0 of 40 selected

Attributes of Wanted.shp

| M_Abs_Gib | M_Abs_Obs | Var_Abs_Loc | Var_Abs_Gib | Var_Abs_Obs | Averages |
|---|---|---|---|---|---|
| 1.518 | 1.286 | 50.268 | 49.336 | 50.474 | 20.118 |
| 0.443 | 0.199 | 0.026 | 0.318 | 0.049 | 0.848 |
| 1.430 | 1.189 | 42.087 | 41.734 | 42.300 | 16.898 |
| 0.915 | 0.673 | 10.143 | 10.143 | 10.145 | 4.857 |
| 1.342 | 1.095 | 34.643 | 34.129 | 34.728 | 14.192 |
| 0.696 | 0.458 | 3.310 | 3.282 | 3.316 | 2.097 |
| 0.771 | 0.547 | 5.680 | 5.375 | 5.602 | 3.022 |
| 1.520 | 1.353 | 56.561 | 52.582 | 56.664 | 21.911 |
| 1.105 | 0.884 | 20.688 | 19.679 | 20.735 | 8.795 |
| 1.274 | 1.048 | 31.130 | 30.130 | 31.481 | 12.671 |
| 0.684 | 0.445 | 2.910 | 3.020 | 2.878 | 1.954 |
| 0.812 | 0.570 | 6.330 | 6.314 | 6.275 | 3.314 |
| 1.100 | 0.872 | 19.710 | 19.137 | 19.984 | 8.455 |
| 0.862 | 0.608 | 7.947 | 7.819 | 7.941 | 3.882 |
| 1.006 | 0.781 | 14.762 | 14.303 | 14.804 | 6.461 |
| 0.905 | 0.677 | 10.384 | 9.907 | 10.341 | 4.769 |
| 0.850 | 0.605 | 7.753 | 7.556 | 8.104 | 3.871 |
| 0.765 | 0.567 | 6.351 | 5.611 | 6.530 | 3.207 |

**Figure 4.11:** The attribute table of the "final.shp" shapefile showing the calculated statistical values.

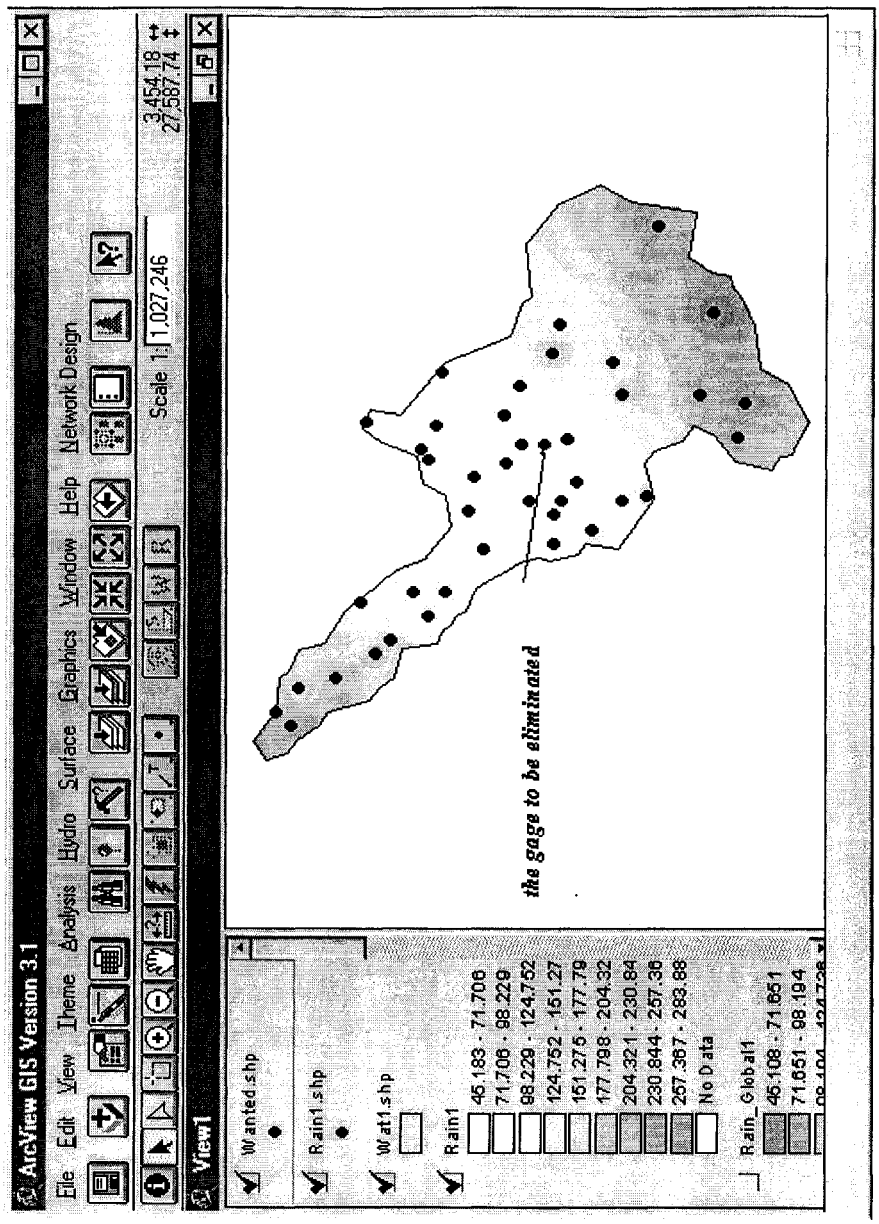


**Figure 4.12:** An example of a sub-network with one gauge marked for elimination. Rain values in $1/10^{th}$ of "mm".

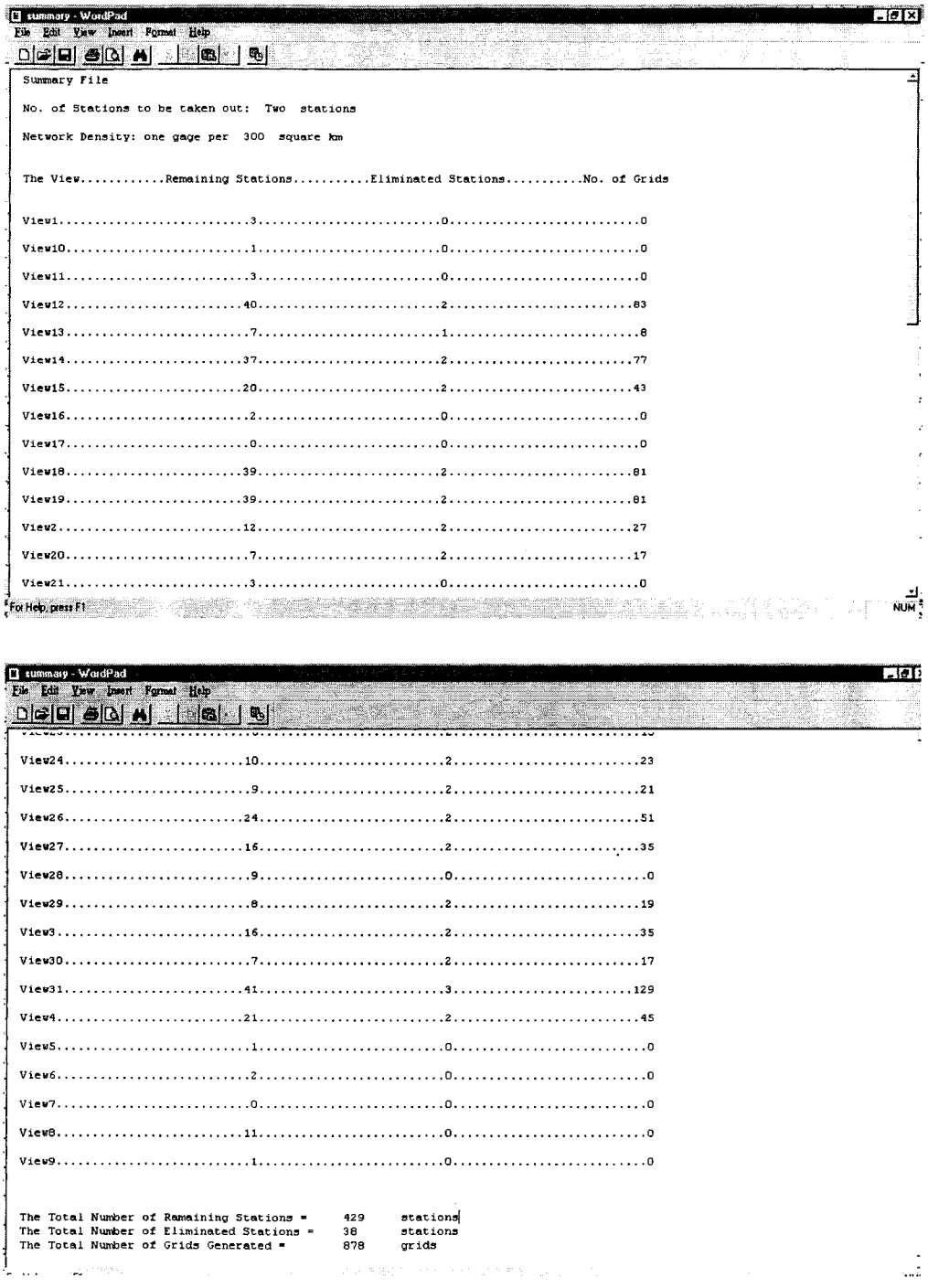


**Figure 4.13:** The text file "Summary.txt" generated as a final output.

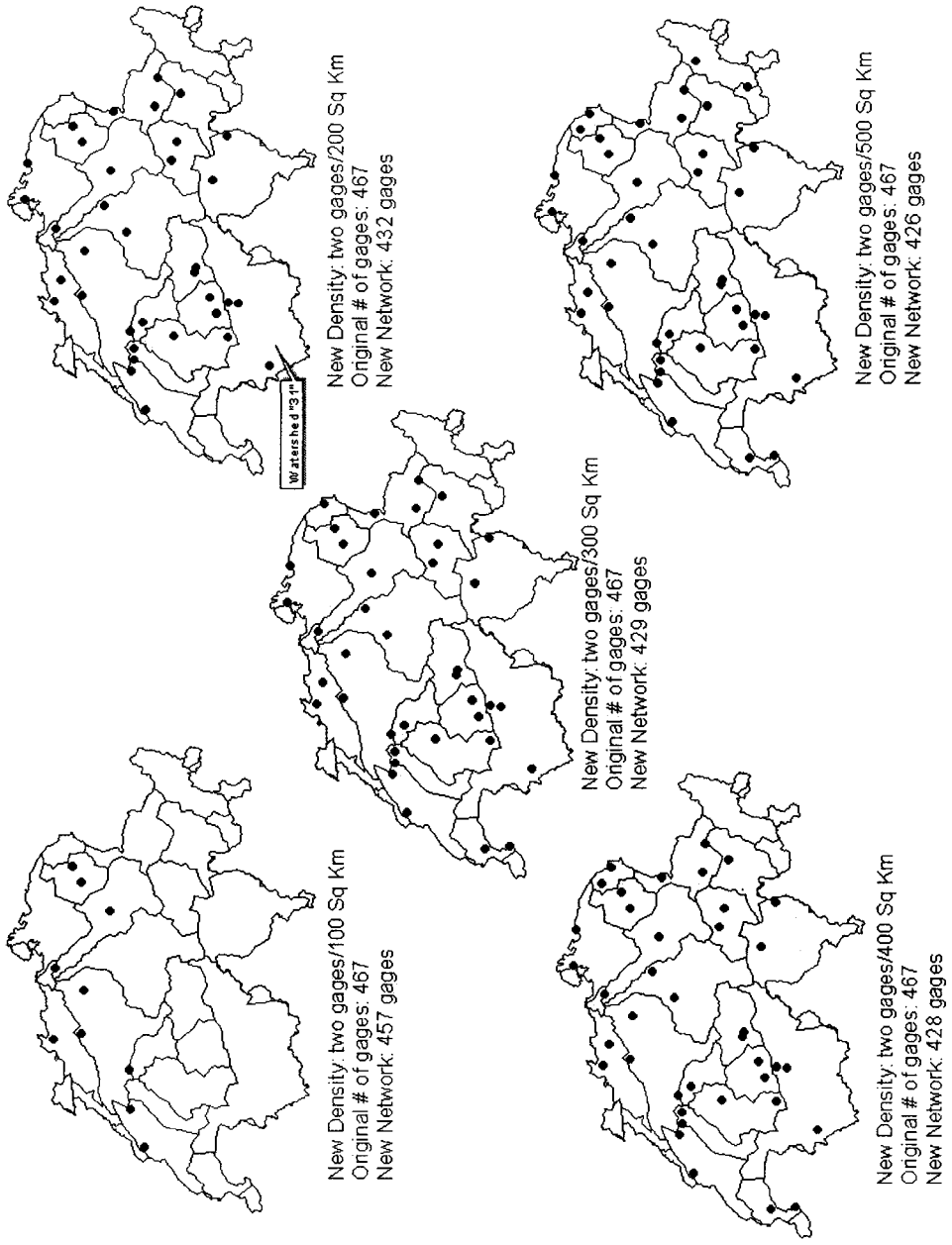


**Figure 4.14:** Based on the VAR approach, the candidate gauges for removal based on the criterion: eliminate two gauges per watershed/subnetwork.

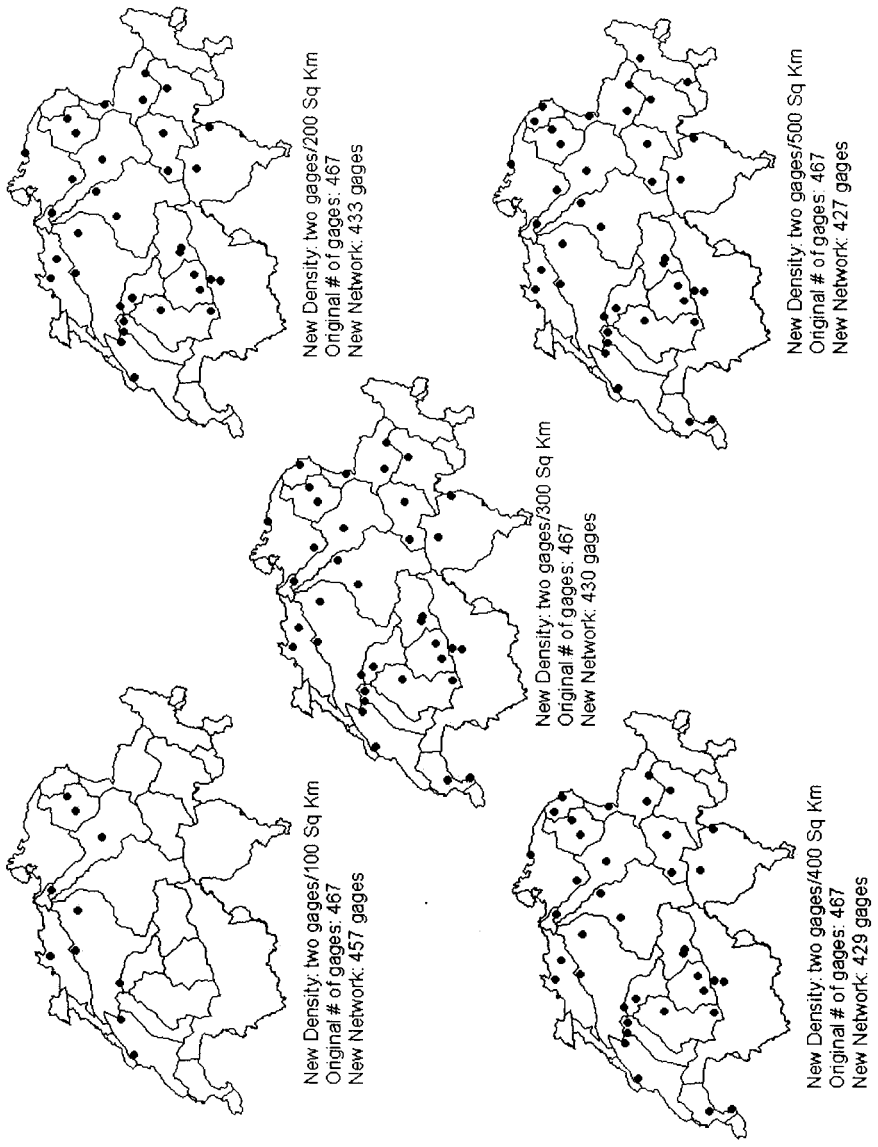


**Figure 4.15:** Based on the STDEV approach, the candidate gauges for removal based on the criterion: eliminate two gauges per watershed/subnetwork.

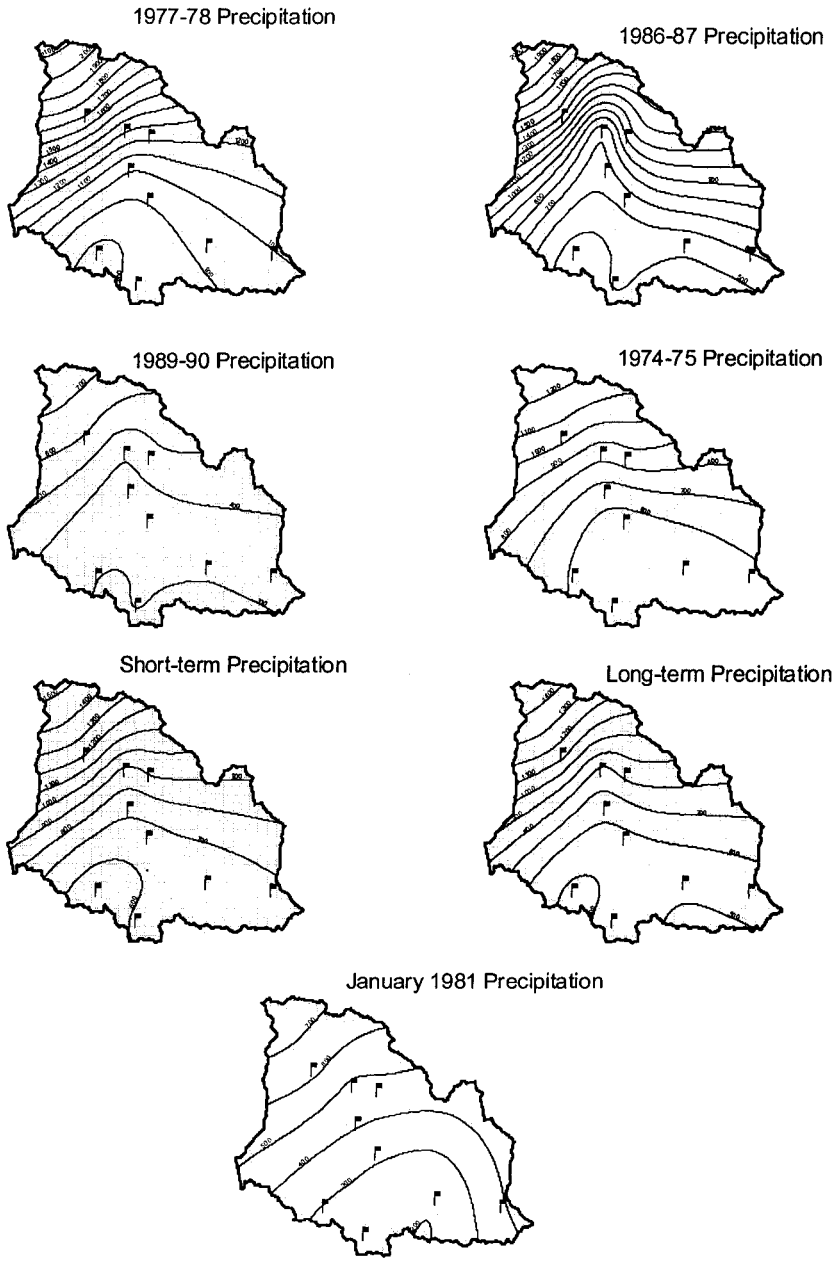


**Figure 4.16a:** Precipitation contour lines (isohyets) representing the local precipitation grid in Gerapotamou basin.

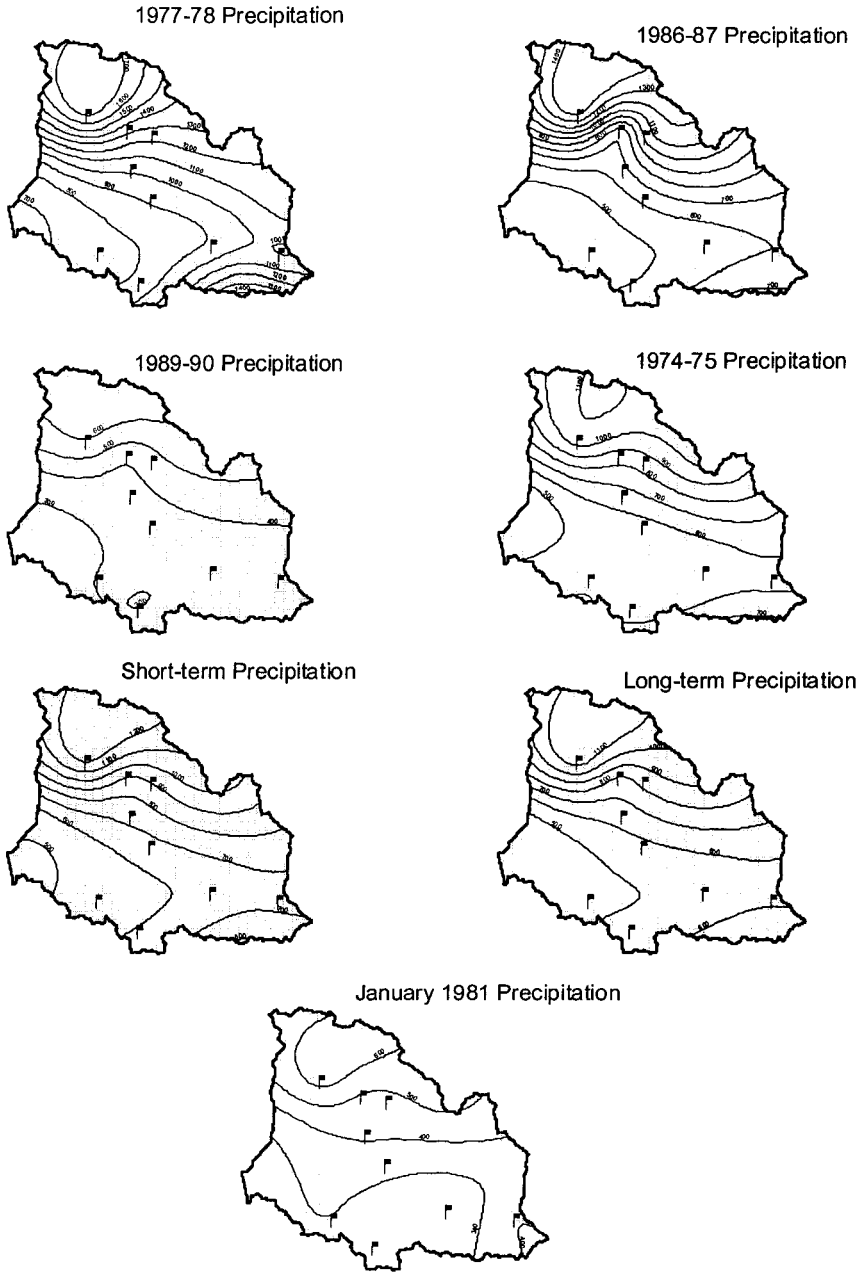


**Figure 4.16b:** Precipitation contour lines (isohyets) representing the global precipitation grid in Gerapotamou basin.

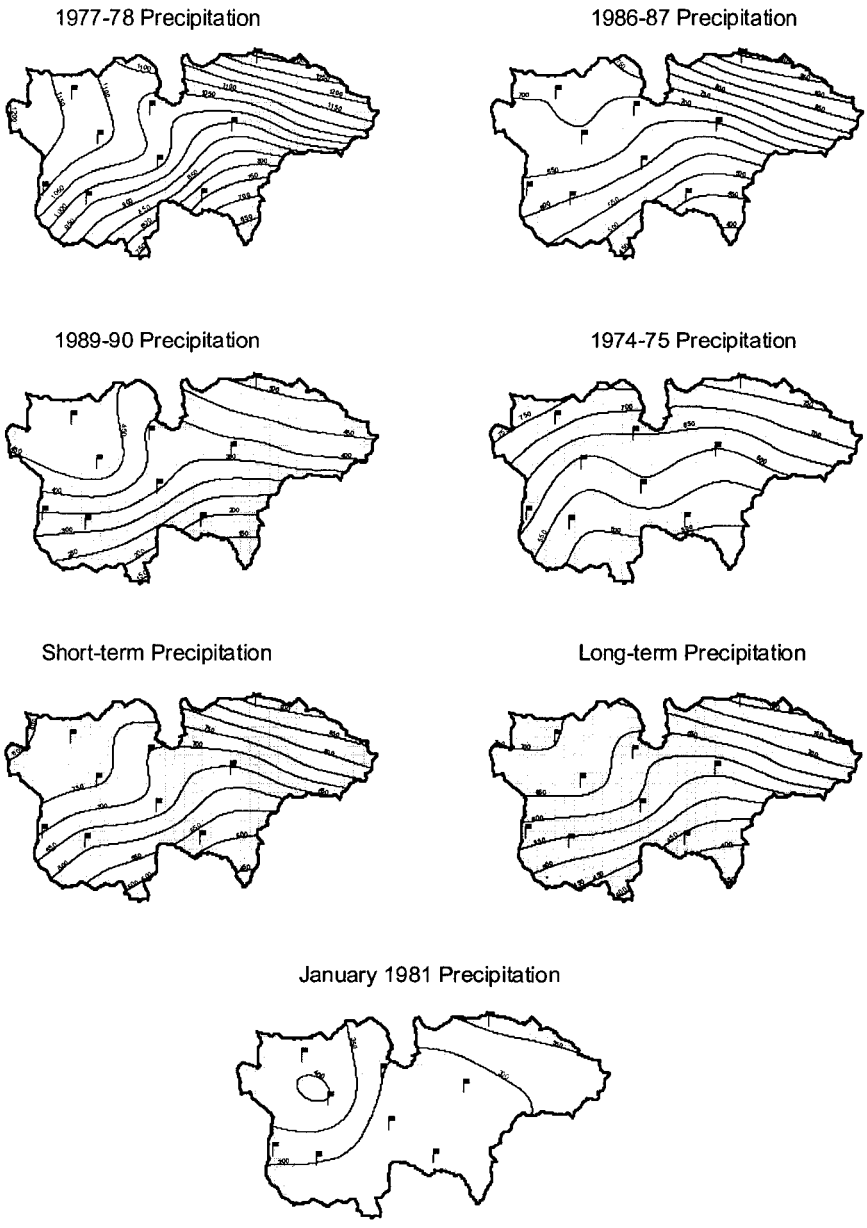


**Figure 4.17a:** Precipitation contour lines (isohyets) representing the local precipitation grid in Anapodiaris basin.

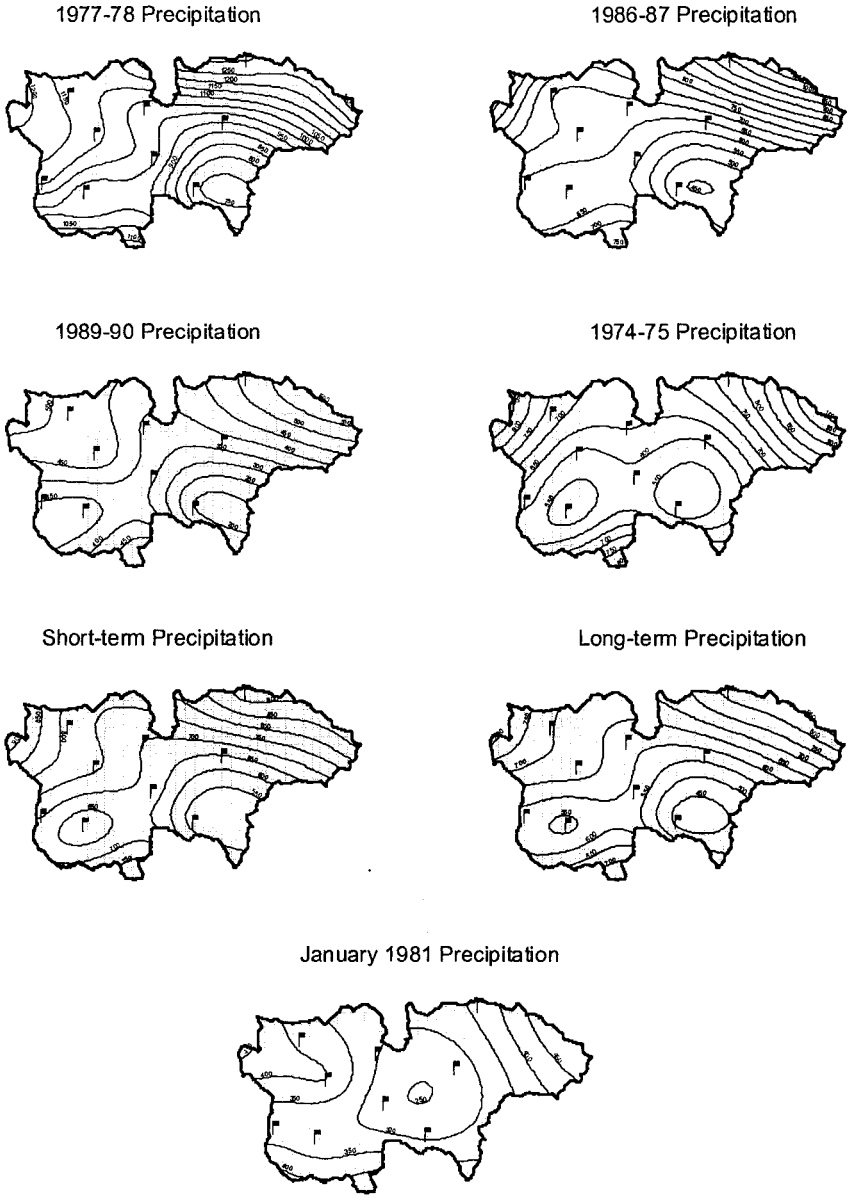


**Figure 4.17b:** Precipitation contour lines (isohyets) representing the global precipitation grid in Anapodiaris basin.

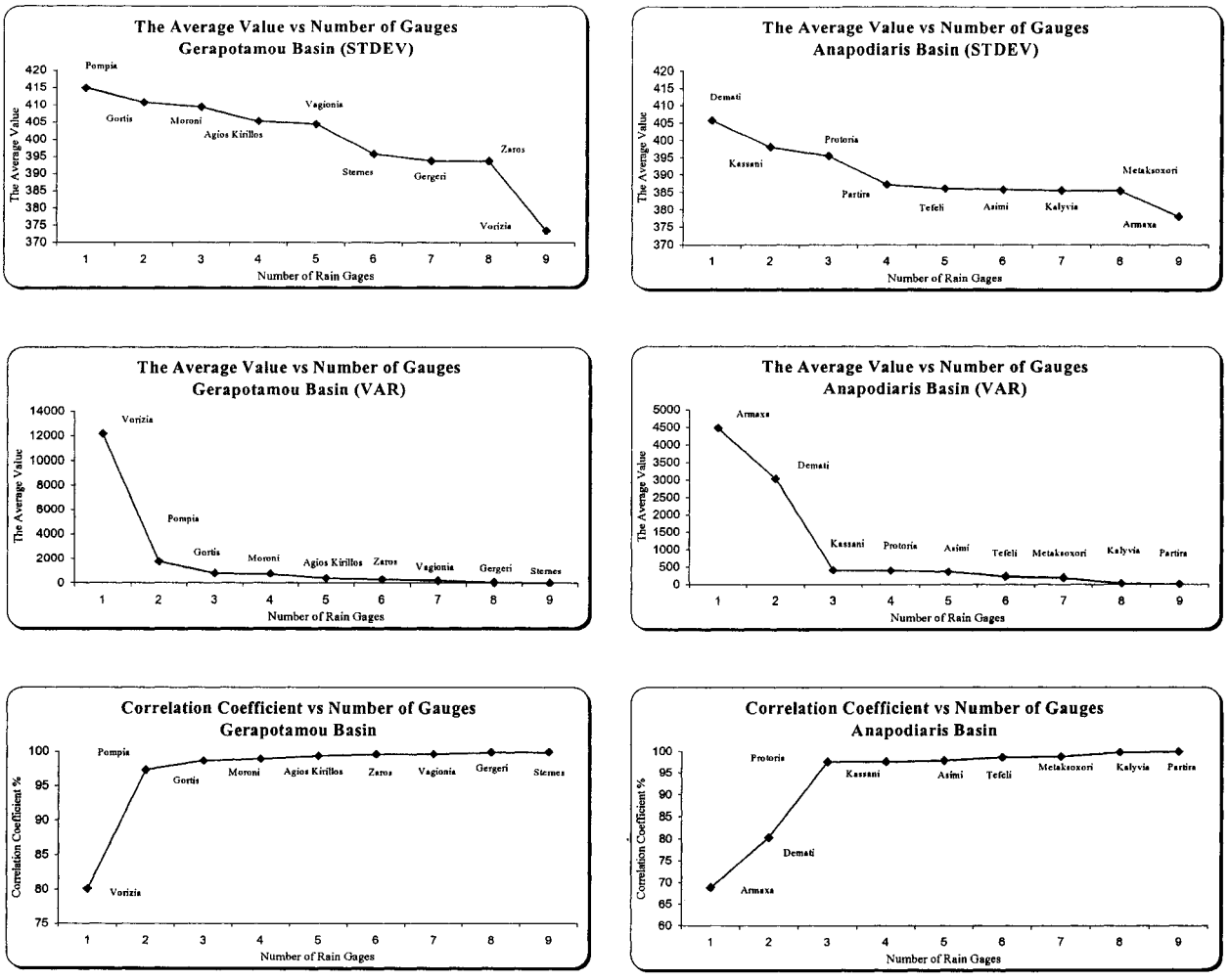


**Figure 4.18:** The ranking of gauges using the three approaches for the Gerapotamou and Anpodiaris basins in Crete for the year 1977-78. Higher values for the STDEV or VAR approaches and low values for correlation coefficients mean important gauges.

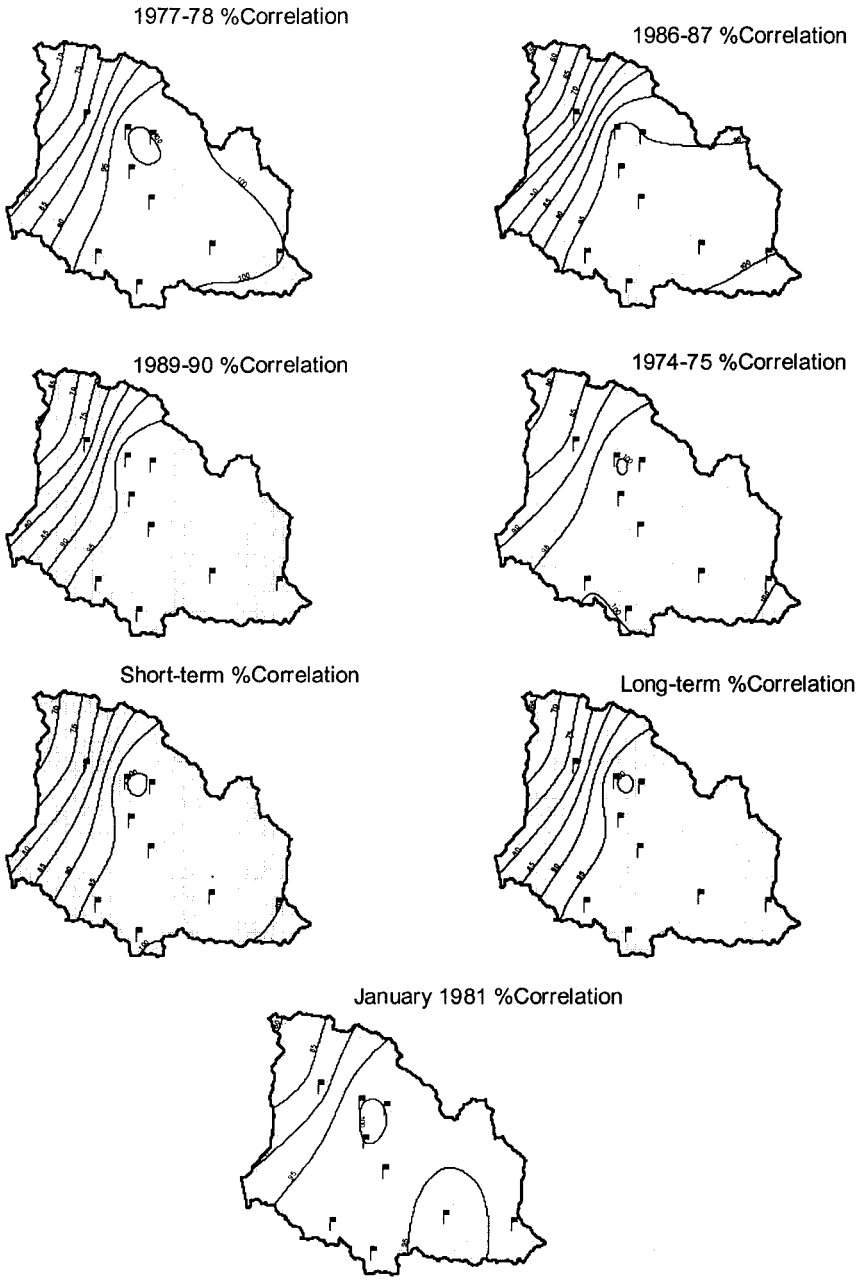


**Figure 4.19:** Correlation coefficient contour lines for Gerapotamou basin.

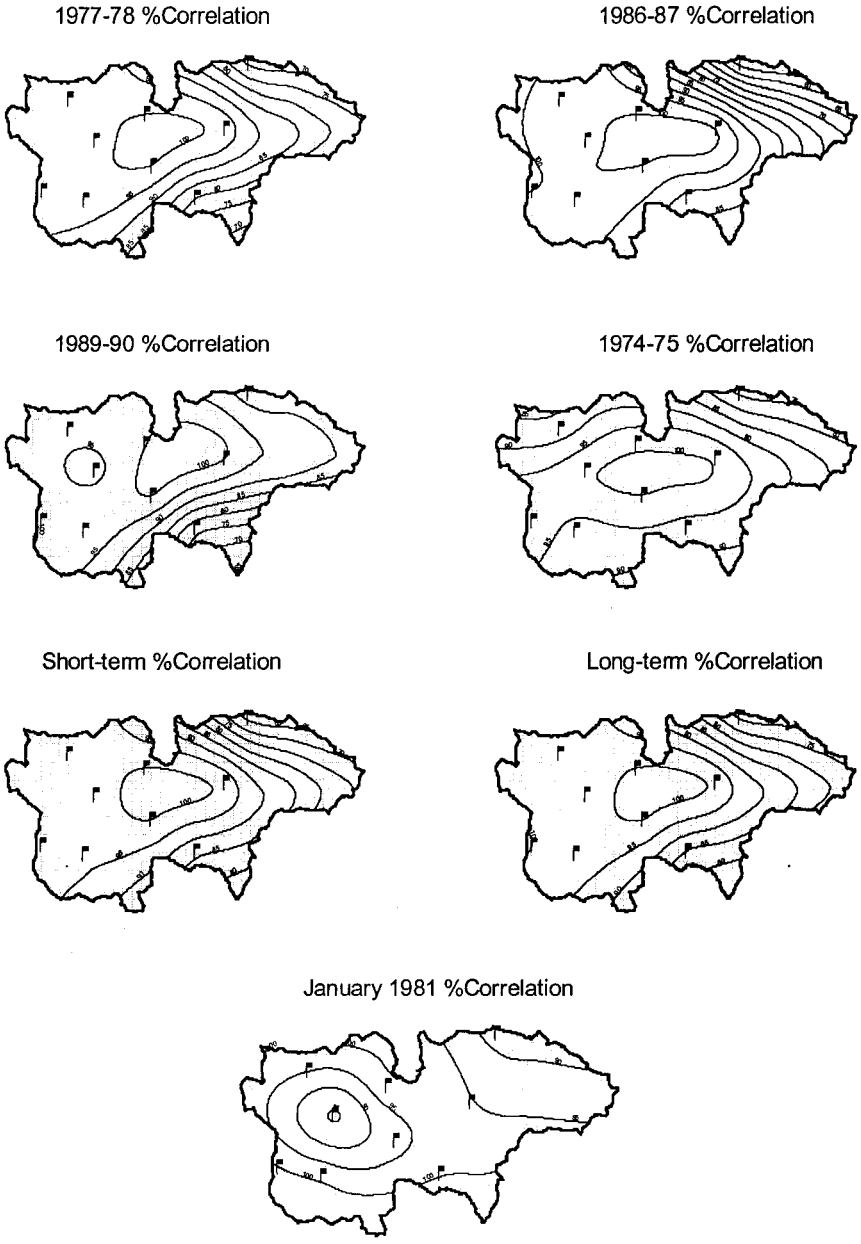


**Figure 4.20:** Correlation coefficient contour lines for Anapodiaris basin.

**Table 4.1:** A comparison between module output and Excel spreadsheet calculations.

| | | | | | | | | | ONE | | | | | TWO | | | |
|---|---|---|---|---|---|---|---|---|---|---|---|---|---|---|---|---|---|
| View | Area | Stations | density | a/n-1 | a/n-2 | a/n-3 | a/n-4 | a/n-5 | 100 | 200 | 300 | 400 | 500 | 100 | 200 | 300 | 400 |
| 1 | 1127 | 3 | 376 | 564 | 1127 | | | | 3 | 3 | 3 | 3 | 3 | 3 | 3 | 3 | 3 |
| 2 | 1749 | 14 | 125 | 135 | 146 | 159 | 175 | 194 | 14 | 13 | 13 | 13 | 13 | 14 | 12 | 12 | 12 |
| 3 | 1838 | 18 | 102 | 108 | 115 | 123 | 131 | 141 | 18 | 17 | 17 | 17 | 17 | 18 | 16 | 16 | 16 |
| 4 | 4146 | 23 | 180 | 188 | 197 | 207 | 218 | 230 | 23 | 22 | 22 | 22 | 22 | 23 | 21 | 21 | 21 |
| 5 | 2144 | 1 | 2144 | | | | | | 1 | 1 | 1 | 1 | 1 | 1 | 1 | 1 | 1 |
| 6 | 3241 | 2 | 1621 | 3241 | | | | | 2 | 2 | 2 | 2 | 2 | 2 | 2 | 2 | 2 |
| 7 | 1671 | 0 | - | | | | | | 0 | 0 | 0 | 0 | 0 | 0 | 0 | 0 | 0 |
| 8 | 5130 | 11 | 466 | 513 | 570 | 641 | 733 | 855 | 11 | 11 | 11 | 11 | 11 | 11 | 11 | 11 | 11 |
| 9 | 220 | 1 | 220 | | | | | | 1 | 1 | 1 | 1 | 1 | 1 | 1 | 1 | 1 |
| 10 | 155 | 1 | 155 | | | | | | 1 | 1 | 1 | 1 | 1 | 1 | 1 | 1 | 1 |
| 11 | 2221 | 3 | 740 | 1111 | 2221 | | | | 3 | 3 | 3 | 3 | 3 | 3 | 3 | 3 | 3 |
| 12 | 5509 | 42 | 131 | 134 | 138 | 141 | 145 | 149 | 42 | 41 | 41 | 41 | 41 | 42 | 40 | 40 | 40 |
| 13 | 1851 | 8 | 231 | 264 | 309 | 370 | 463 | 617 | 8 | 8 | 7 | 7 | 7 | 8 | 8 | 7 | 6 |
| 14 | 3746 | 39 | 96 | 99 | 101 | 104 | 107 | 110 | 38 | 38 | 38 | 38 | 38 | 38 | 37 | 37 | 37 |
| 15 | 1138 | 22 | 52 | 54 | 57 | 60 | 63 | 67 | 21 | 21 | 21 | 21 | 21 | 20 | 20 | 20 | 20 |
| 16 | 2794 | 2 | 1397 | 2794 | | | | | 2 | 2 | 2 | 2 | 2 | 2 | 2 | 2 | 2 |
| 17 | 1286 | 0 | - | | | | | | 0 | 0 | 0 | 0 | 0 | 0 | 0 | 0 | 0 |
| 18 | 2428 | 41 | 59 | 61 | 62 | 64 | 66 | 67 | 40 | 40 | 40 | 40 | 40 | 39 | 39 | 39 | 39 |
| 19 | 3830 | 41 | 93 | 96 | 98 | 101 | 104 | 106 | 40 | 40 | 40 | 40 | 40 | 39 | 39 | 39 | 39 |
| 20 | 791 | 9 | 88 | 99 | 113 | 132 | 158 | 198 | 8 | 8 | 8 | 8 | 8 | 8 | 7 | 7 | 7 |
| 21 | 2648 | 3 | 883 | 1324 | 2648 | | | | 3 | 3 | 3 | 3 | 3 | 3 | 3 | 3 | 3 |
| 22 | 3538 | 36 | 98 | 101 | 104 | 107 | 111 | 114 | 36 | 35 | 35 | 35 | 35 | 36 | 34 | 34 | 34 |
| 23 | 888 | 8 | 111 | 127 | 148 | 178 | 222 | 296 | 8 | 7 | 7 | 7 | 7 | 8 | 6 | 6 | 6 |
| 24 | 1466 | 12 | 122 | 133 | 147 | 163 | 183 | 209 | 12 | 11 | 11 | 11 | 11 | 12 | 10 | 10 | 10 |
| 25 | 1378 | 11 | 125 | 138 | 153 | 172 | 197 | 230 | 11 | 10 | 10 | 10 | 10 | 11 | 9 | 9 | 9 |
| 26 | 1823 | 26 | 70 | 73 | 76 | 79 | 83 | 87 | 25 | 25 | 25 | 25 | 25 | 24 | 24 | 24 | 24 |
| 27 | 1707 | 18 | 95 | 100 | 107 | 114 | 122 | 131 | 18 | 17 | 17 | 17 | 17 | 18 | 16 | 16 | 16 |
| 28 | 3220 | 9 | 358 | 403 | 460 | 537 | 644 | 805 | 9 | 9 | 9 | 9 | 8 | 9 | 9 | 9 | 9 |
| 29 | 1091 | 10 | 109 | 121 | 136 | 156 | 182 | 218 | 10 | 9 | 9 | 9 | 9 | 10 | 8 | 8 | 8 |
| 30 | 1744 | 9 | 194 | 218 | 249 | 291 | 349 | 436 | 9 | 9 | 8 | 8 | 8 | 9 | 9 | 7 | 7 |
| 31 | 6017 | 44 | 137 | 140 | 143 | 147 | 150 | 154 | 44 | 43 | 43 | 43 | 43 | 44 | ***42*** | ***42*** | ***42*** |
| | 72535 | 467 | | | | | | | 461 | 450 | 448 | 448 | 447 | 457 | 433 | 430 | 429 |
| | | | | | | | | Module Output | 461 | 450 | 448 | 448 | 447 | 457 | 432 | 429 | 428 |

| | | | | | | THREE | | | | | FOUR | | | | | FIVE | | | |
|---|---|---|---|---|---|---|---|---|---|---|---|---|---|---|---|---|---|---|---|
| View | Area | Stations | density | 100 | 200 | 300 | 400 | 500 | 100 | 200 | 300 | 400 | 500 | 100 | 200 | 300 | 400 |
| 1 | 1127 | 3 | 376 | 3 | 3 | 3 | 3 | 3 | 3 | 3 | 3 | 3 | 3 | 3 | 3 | 3 | 3 |
| 2 | 1749 | 14 | 125 | 14 | 11 | 11 | 11 | 11 | 14 | 10 | 10 | 10 | 10 | 14 | 9 | 9 | 9 |
| 3 | 1838 | 18 | 102 | 18 | 15 | 15 | 15 | 15 | 18 | 14 | 14 | 14 | 14 | 18 | 13 | 13 | 13 |
| 4 | 4146 | 23 | 180 | 23 | 21 | 20 | 20 | 20 | 23 | 21 | 19 | 19 | 19 | 23 | 21 | 18 | 18 |
| 5 | 2144 | 1 | 2144 | 1 | 1 | 1 | 1 | 1 | 1 | 1 | 1 | 1 | 1 | 1 | 1 | 1 | 1 |
| 6 | 3241 | 2 | 1621 | 2 | 2 | 2 | 2 | 2 | 2 | 2 | 2 | 2 | 2 | 2 | 2 | 2 | 2 |
| 7 | 1671 | 0 | - | 0 | 0 | 0 | 0 | 0 | 0 | 0 | 0 | 0 | 0 | 0 | 0 | 0 | 0 |
| 8 | 5130 | 11 | 466 | 11 | 11 | 11 | 11 | 11 | 11 | 11 | 11 | 11 | 11 | 11 | 11 | 11 | 11 |
| 9 | 220 | 1 | 220 | 1 | 1 | 1 | 1 | 1 | 1 | 1 | 1 | 1 | 1 | 1 | 1 | 1 | 1 |
| 10 | 155 | 1 | 155 | 1 | 1 | 1 | 1 | 1 | 1 | 1 | 1 | 1 | 1 | 1 | 1 | 1 | 1 |
| 11 | 2221 | 3 | 740 | 3 | 3 | 3 | 3 | 3 | 3 | 3 | 3 | 3 | 3 | 3 | 3 | 3 | 3 |
| 12 | 5509 | 42 | 131 | 42 | 39 | 39 | 39 | 39 | 42 | 38 | 38 | 38 | 38 | 42 | 37 | 37 | 37 |
| 13 | 1851 | 8 | 231 | 8 | 8 | 7 | 5 | 5 | 8 | 8 | 7 | 5 | 4 | 8 | 8 | 7 | 5 |
| 14 | 3746 | 39 | 96 | 38 | 36 | 36 | 36 | 36 | 38 | 35 | 35 | 35 | 35 | 38 | 34 | 34 | 34 |
| 15 | 1138 | 22 | 52 | 19 | 19 | 19 | 19 | 19 | 18 | 18 | 18 | 18 | 18 | 17 | 17 | 17 | 17 |
| 16 | 2794 | 2 | 1397 | 2 | 2 | 2 | 2 | 2 | 2 | 2 | 2 | 2 | 2 | 2 | 2 | 2 | 2 |
| 17 | 1286 | 0 | - | 0 | 0 | 0 | 0 | 0 | 0 | 0 | 0 | 0 | 0 | 0 | 0 | 0 | 0 |
| 18 | 2428 | 41 | 59 | 38 | 38 | 38 | 38 | 38 | 37 | 37 | 37 | 37 | 37 | 36 | 36 | 36 | 36 |
| 19 | 3830 | 41 | 93 | 39 | 38 | 38 | 38 | 38 | 39 | 37 | 37 | 37 | 37 | 39 | 36 | 36 | 36 |
| 20 | 791 | 9 | 88 | 8 | 6 | 6 | 6 | 6 | 8 | 5 | 5 | 5 | 5 | 8 | 4 | 4 | 4 |
| 21 | 2648 | 3 | 883 | 3 | 3 | 3 | 3 | 3 | 3 | 3 | 3 | 3 | 3 | 3 | 3 | 3 | 3 |
| 22 | 3538 | 36 | 98 | 36 | 33 | 33 | 33 | 33 | 36 | 32 | 32 | 32 | 32 | 36 | 31 | 31 | 31 |
| 23 | 888 | 8 | 111 | 8 | 5 | 5 | 5 | 5 | 8 | 5 | 4 | 4 | 4 | 8 | 5 | 3 | 3 |
| 24 | 1466 | 12 | 122 | 12 | 9 | 9 | 9 | 9 | 12 | 8 | 8 | 8 | 8 | 12 | 8 | 7 | 7 |
| 25 | 1378 | 11 | 125 | 11 | 8 | 8 | 8 | 8 | 11 | 7 | 7 | 7 | 7 | 11 | 7 | 6 | 6 |
| 26 | 1823 | 26 | 70 | 23 | 23 | 23 | 23 | 23 | 22 | 22 | 22 | 22 | 22 | 21 | 21 | 21 | 21 |
| 27 | 1707 | 18 | 95 | 18 | 15 | 15 | 15 | 15 | 18 | 14 | 14 | 14 | 14 | 18 | 13 | 13 | 13 |
| 28 | 3220 | 9 | 358 | 9 | 9 | 9 | 9 | 7 | 9 | 9 | 9 | 9 | 7 | 9 | 9 | 9 | 9 |
| 29 | 1091 | 10 | 109 | 10 | 7 | 7 | 7 | 7 | 10 | 6 | 6 | 6 | 6 | 10 | 6 | 5 | 5 |
| 30 | 1744 | 9 | 194 | 9 | 9 | 6 | 6 | 6 | 9 | 9 | 6 | 5 | 5 | 9 | 9 | 6 | 5 |
| 31 | 6017 | 44 | 137 | 44 | ***41*** | ***41*** | ***41*** | ***41*** | 44 | ***40*** | ***40*** | ***40*** | ***40*** | 44 | ***39*** | ***39*** | ***39*** |
| | 72535 | 467 | | 454 | 417 | 412 | 410 | 408 | 451 | 402 | 395 | 392 | 389 | 448 | 390 | 378 | 375 |
| | | | Module Output | 454 | 416 | 411 | 409 | 407 | 451 | 401 | 394 | 391 | 388 | 448 | 389 | 377 | 374 |

* shaded areas in the module output are results different from Excel® calculations.

**Table 4.2** The rank of rain gauges in two sub-networks in Crete using the three approaches.

**Correlation**

| | Geropotamou | | | | | | | Anapodiaris | | | | | |
|---|---|---|---|---|---|---|---|---|---|---|---|---|---|
| RANK | 1977-78 | 1986-87 | 1989-90 | 1974-75 | short-term | long-term | Jan-81 | 1977-78 | 1986-87 | 1989-90 | 1974-75 | short-term | long-term |
| 1 | Vorizia | Vorizia | Vorizia | Vorizia | Vorizia | Vorizia | Vorizia | Armaxa | Armaxa | Demati | Armaxa | Armaxa | Armaxa |
| 2 | Pompia | Gergeri | Moroni | Gortis | Pompia | Moroni | Vagionia | Demati | Demati | Armaxa | Metaksoxori | Demati | Demati |
| 3 | Gortis | Zaros | Vagionia | Vagionia | Moroni | Pompia | Sternes | Protoria | Protoria | Tefeli | Demati | Protoria | Metaksoxori |
| 4 | Moroni | Moroni | Gergeri | Gergeri | Vagionia | Vagionia | Agios Kirillos | Kassani | Kassani | Metaksoxori | Protoria | Metaksoxori | Protoria |
| 5 | Agios Kirillos | Pompia | Pompia | Moroni | Gergeri | Gergeri | Gortis | Asimi | Tefeli | Protoria | Asimi | Kassani | Tefeli |
| 6 | Zaros | Vagionia | Zaros | Agios Kirillos | Agios Kirillos | Agios Kirillos | Pompia | Tefeli | Metaksoxori | Asimi | Partira | Tefeli | Kassani |
| 7 | Vagionia | Agios Kirillos | Agios Kirillos | Pompia | Zaros | Zaros | Gergeri | Metaksoxori | Partira | Partira | Tefeli | Asimi | Partira |
| 8 | Gergeri | Sternes | - | Sternes | Sternes | - | Zaros | Kalyvia | Kalyvia | Kalyvia | Kassani | Kalyvia | Asimi |
| 9 | Sternes | - | - | Zaros | - | - | Moroni | Partira | Asimi | Kassani | Kalyvia | Partira | Kalyvia |

**Variance**

| | Geropotamou | | | | | | | Anapodiaris | | | | | |
|---|---|---|---|---|---|---|---|---|---|---|---|---|---|
| RANK | 1977-78 | 1986-87 | 1989-90 | 1974-75 | short-term | long-term | Jan-81 | 1977-78 | 1986-87 | 1989-90 | 1974-75 | short-term | long-term |
| 1 | Vorizia | Vorizia | Vorizia | Vorizia | Vorizia | Vorizia | Vorizia | Armaxa | Armaxa | Demati | Armaxa | Armaxa | Armaxa |
| 2 | Pompia | Gergeri | Moroni | Gortis | Pompia | Moroni | Vagionia | Demati | Demati | Armaxa | Metaksoxori | Demati | Demati |
| 3 | Gortis | Zaros | Vagionia | Vagionia | Moroni | Pompia | Sternes | Kassani | Kassani | Tefeli | Demati | Protoria | Metaksoxori |
| 4 | Moroni | Moroni | Gergeri | Gergeri | Vagionia | Vagionia | Agios Kirillos | Protoria | Protoria | Metaksoxori | Protoria | Kassani | Protoria |
| 5 | Agios Kirillos | Pompia | Pompia | Moroni | Gergeri | Gergeri | Gortis | Asimi | Tefeli | Proptoria | Asimi | Metksoxori | Tefeli |
| 6 | Zaros | Vagionia | Agios Kirillos | Agios Kirillos | Agios Kirillos | Agios kirillos | Pompia | Tefeli | Metaksoxori | Asimi | Partira | Tefeli | Kassani |
| 7 | Vagionia | Agios Kirillos | Zaros | Pompia | Sternes | Zaros | Gergeri | Metaksoxori | Partira | Partira | Tefeli | Asimi | Asimi |
| 8 | Gergeri | Sternes | - | Zaros | Zaros | - | Zaros | Kalyvia | Kalyvia | Kalyvia | Kassani | Kalyvia | Kalyvia |
| 9 | Sternes | - | - | Sternes | - | - | Moroni | Partira | Asimi | Kassani | Kalyvia | Partira | Partira |

**Standard Deviation**

| | Geropotamou | | | | | | | Anapodiaris | | | | | |
|---|---|---|---|---|---|---|---|---|---|---|---|---|---|
| RANK | 1977-78 | 1986-87 | 1989-90 | 1974-75 | short-term | long-term | Jan-81 | 1977-78 | 1986-87 | 1989-90 | 1974-75 | short-term | long-term |
| 1 | Pompia | Zaros | Vorizia | Vagionia | Pompia | Vagionia | Vorizia | Demati | Demati | Demati | Demati | Demati | Demati |
| 2 | Gortis | Moroni | Vagionia | Gortis | Moroni | Moroni | Vagionia | Kassani | Kassani | Protoria | Protoria | Kassani | Kassani |
| 3 | Moroni | Pompia | Agios Kirillos | Moroni | Vagionia | Pompia | Agios Kirillos | Protoria | Protoria | Tefeli | Kassani | Protoria | Protoria |
| 4 | Agios Kirillos | Vagionia | Pompia | Pompia | Agios Kirillos | Agios Kirillos | Sternes | Partira | Kalyvia | Asimi | Tefeli | Tefeli | Tefeli |
| 5 | Vagionia | Agios Kirillos | Moroni | Agios Kirillos | Sternes | Zaros | Gortis | Tefeli | Tefeli | Partira | Metaksoxori | Asimi | Asimi |
| 6 | Sternes | Sternes | Gergeri | Sternes | Zaros | Gergeri | Pompia | Asimi | Metaksoxori | Metaksoxori | Asimi | Partira | Metaksoxori |
| 7 | Gergeri | Gergeri | Zaros | Vorizia | Gergeri | Vorizia | Gergeri | Kalyvia | Asimi | Kalyvia | Kalyvia | Metaksoxori | Kalyvia |
| 8 | Zaros | Vorizia | - | Zaros | Vorizia | - | Zaros | Metaksoxori | Partira | Kassani | Partira | Kalyvia | Partira |
| 9 | Vorizia | - | - | Gergeri | - | - | Moroni | Armaxa | Armaxa | Armaxa | Armaxa | Armaxa | Armaxa |

| | | | | | | | | | | | | | |
|---|---|---|---|---|---|---|---|---|---|---|---|---|---|
| Missing | - | Gortis | Gortis | - | Gortis | Gortis | - | - | - | - | - | - | - |
| | - | - | Sternes | - | - | Sternes | - | - | - | - | - | - | - |

***Rank 1: Gage to stay***
***Rank 9: Gage to go***
***These results assuming that the outside gages are remaining without change***

# CHAPTER 5

# INVESTIGATING SPATIAL INTERPOLATION TECHNIQUES IN A GIS

One of the problems which often arises in hydrologic and hydraulic design is the attempt to estimate data at a given site where the data is missing or the site is ungauged. Such estimates can be made by spatial interpolation of data available at other sites. Geographic Information Systems offer a number of embedded ready-to-use spatial interpolation techniques. The interpolation techniques in the ArcView GIS® software are used. These are: IDW, Spline (Tension and Regularized), 2nd Order Polynomial, and Kriging (Universal 1, Universal 2, Circular, Gaussian, Linear, Spherical, and Exponential).
It is the intent of this chapter to:

a) document the development of a GIS-based Decision Support System (DSS) to select the appropriate interpolation technique used in studying rainfall spatial variability. The DSS used the ArcView GIS platform by incorporating its spatial analysis capabilities, the programming language "AVENUE", and simple statistical methods. The system consists of a series of modules and can be applied in spatial studies of other hydrological parameters. A test case from the country of Switzerland is used to demonstrate the applicability of the system. The primary set of data included 467 daily rainfall records made in Switzerland on May 8th 1986.

b) compare these interpolation techniques for estimating rainfall at a selected area in the Province of Ontario, Canada. One-minute rainfall data for sixteen events were extracted from ten rainy days during the summer of 1989. The study area, located in the Hamilton-Wentworth region, is 8km by 8km and it is covered by a nine-gauge network.

## 5.1 Spatial Interpolation Techniques

Details about the techniques can be found in Appendix D.

## 5.2 Ranking Spatial Interpolation Techniques

### 5.2.1 Case 1: Switzerland

#### 5.2.1.1 Introduction

The analysis and interpretation of spatial data sets form an important part of geostatistics and is, unfortunately, highly human dependent (Genton and Furrer, 1998). For instance, it is well known that different individuals will take different approaches, yielding a large assortment of distinct solutions. It is often the case where judgement and experience play a key role in selecting the proper spatial interpolation technique for each individual case

(Englund, 1990). This is partly due to the variety of available spatial interpolation methods, which range from simple intuitive predictions to more sophisticated and complex procedures (Cressie, 1991). Estimating both rainfall at ungauged locations and mean areal rainfall over an area (e.g. catchment) based on the results of meteorological observations, motivated the development of gridded estimates of precipitation to provide inputs to spatially distributed hydrologic and management models.

Although numerous articles have been written that are concerned with spatial interpolation, there is little or no agreement among the authors on the superiority of some techniques over others. Additionally, the increasing interest in Geographic Information Systems with their broad usage and popularity, made it crucial to simply investigate the applicability of the different ready-to-use spatial interpolation techniques that are embedded in those systems. This work has been inspired by the Journal of Geographic Information and Decision Analysis's special edition on spatial interpolation (Spatial Interpolation Comparison SIC97). For this case, Theissen polygons were used as another additional technique for interpolation. The twelve spatial interpolation techniques employed in this case are listed in Figure 5.1a.

5.2.1.2 Approach and Procedure

Variability is often a result of changes in conditions under which observations are made, differences in the way people do the work, difference in process variables, difference in environmental factors, the measurement system, or sampling. Statistical techniques are used to describe and understand variability. To provide a basis of comparison between the different techniques/models in this work, simple statistical methods are adopted. Since the method is data-driven and fully automated it does not require preprocessing. This could be of value in an emergency situation where quick, yet justifiable, results are required. The process initiates by randomly eliminating some of the available gauges. The different interpolation techniques are then applied to estimate the "unobserved/missing" values on the basis of the "observed/remaining" ones. The purpose of the random selection of gauges, which in this case takes the form of twenty tries, is intended to overcome the problem of outliers, if they exist. Experience shows that measured data contains between 10 to 15 per cent of outlying values due to gross errors, measurement mistakes, and faulty recording. Identifying and rejecting, or removing, outliers is highly opinion dependent and is not normally recommended since they, being extremes, represent critical cases or worst case scenarios. The errors/residuals for the unobserved/ungauged locations are then calculated as the difference between observed and estimated values and categorized as positive and negative residuals. If the absolute value of the sum of the positive residuals is greater than the absolute value of the sum of the negative residuals, it implies that the observed values are greater than estimated ones. The model is then said to be *underestimaing*. If the absolute value of the sum of the positive residuals is less than the absolute value of the sum of the

negative residuals, it implies that the estimated values are greater than observed ones. The model is then said to be *overestimating*. The errors at the ungauged (unobserved) locations are grouped in one column as absolute values, where the mean and the standard deviation are calculated as in equations (4.2) and (4.3).

Generally, for a model/technique to be considered satisfactory, the mean ($\bar{e}$: MeanAbsErr) and standard deviation (S: StDevAbsErr) of the absolute values of residuals are expected to be as low as possible among the other techniques. From the rain surface (grid), which is generated using the observed values, the average value is calculated as the sum of the rain values at each grid cell divided by the total number of cells in the grid. This represents the mean areal precipitation (MeanEst). The average of the observed values at all locations (observed and unobserved) is then calculated (MeanObs). A good model should generate a value (MeanEst) that matches (or be as close as possible to) the (MeanObs) and the difference between these two values is minimal. The difference is then calculated (Diff). The main criterion for judging the best model for each run is based on the minimum value obtained by averaging (Avg) the values (Diff, MeanAbsErr, StDevAbsErr), assuming equal weights for all. The twelve techniques are ranked accordingly from best (MinAvg) to the worst (MaxAvg) in addition to many other statistics in a report format.

5.2.1.3 Test Case

The module is applied to a group of raingauges in Switzerland. Switzerland lies at the heart of Western Europe and covers an area of 41,284 km$^2$ (Figure 5.1b). A Digital Elevation Model (DEM) and some interpolated rain surfaces (interpolated from observed values using different techniques) are shown in Figure 5.1a. The data set being used is related to the period of Chernobyl Nuclear Power Plant accident (April, 26$^{th}$ 1986) (Dubois, 1998). During the days following the accident, a radioactive plume, led by the action of atmospheric flow, was crossing many European countries. Radioactive deposition on the ground was mainly a function of the rainfall. The primary set of data includes 467 daily rainfall records made in Switzerland on May 8$^{th}$ 1986. The collection of the data was carried out by the Air Pollution Group at Imperial College in London under financial support of JRC-Ispra. The location of the data points was also provided. Both the DEM, with a resolution of around 1 km * 1 km, and the country border were provided. The rainfall measurements were in the form of text files, the DEM in the form of a normal ASCII file and the country border was available as an AutoCad Interchange Drawing file.

5.2.1.4 Structure and Description of the Project

The GIS module, as shown in Figure 5.2, was developed in the ArcView GIS environment using AVENUE (the ArcView programming language). The main module uses four main pieces of information to perform its task and generate the new network: the

location of gauges, rainfall data, region boundary, and a DEM and it consists of five sub-modules:

*Module 1: ReadMe.* This module documents the project by informing the user of the different parts of the main module using many graphic illustrations. It can be viewed as either a Word Perfect Document (help.wpd) or an HTML (help.htm). The advantage of the HTML is that it provides links to all AVENUE scripts and examples of output tables and text files (Figure 5.3).

*Module 2: Data Preparation.* This is a five-step module that prepares the project for the modules to follow. The data input requirements for this module include information on the boundary of the region, the DEM, the rainfall data and location of raingauges (refer to Figure 4.4).

a) DXF to Shapefile Converter. In many cases, data is provided as AutoCad drawing files (for example: dxf files) which must then be converted to ArcView Shapefiles. This menu item is responsible for the conversion.

b) Polyline to Polygon Converter. After converting the AutoCad drawing file to an ArcView shapefile, the user should convert the resultant "polyline" shapefile into a "polygon" shapefile, which will be used in a later step.

c) Import Grid From ASCII Format. A grid, DEM in many cases, will be saved in the *ASCII ARC/INFO* format. In this case, it has to be imported into an ArcView grid format. This menu item is responsible for the importing job.

d) Grid Clipping. An area has to be extracted (clipped) from the original imported grid from the previous step in order to calculate mean areal rainfall or mean elevation over a specific region. The clipping process (refer to Figure 4.6) is accomplished by using the "polygon" shapefile generated in step 2 and the imported grid from step 3.

e) Generate Theme from Database File. A *database file* that contains information about location of raingauges and amounts of rainfall can be converted to a "point" shapefile and added to the project.

It should be noted that this module was created specifically for the purpose of this study. If all input requirements are satisfied and the data is in the proper format, there is no need to go through these five steps.

*Module 3: Interpolators.* This is a key four-step module that is responsible for executing many tasks as shown in Figure 5.4, where a number of gauges are selected randomly and a rain surface (grid) is generated. The remaining number of gauges (the unselected ones) is then projected on the generated grid, and estimated values for rainfall at those locations are then extracted. A comparison between the observed and estimated precipitation values is held and residuals/errors are calculated. The results of the comparison are summarized in a text file and a database file from which illustrative charts can be generated, if desired. The

last item of the module generates Theissen Polygons for the selected gauges.

a) Random Selection. In this step, the user is prompted to enter the required number of gauges that should be randomly selected. The result is two shapefiles. One represents the selected gauges and the other represents the unselected ones.

b) Spatial Interpolation (ONE). The user is presented with the interpolation dialog (refer to Figure 4.7) so that they may select the type of interpolation technique they will be using to generate the rain surface from the selected gauges (as shown in Figure 5.5).

c) Statistics. This task is executed on the shapefile of the unselected gauges. There is some interaction between the user and the program. The user is prompted by some messages and a text file and a database file are then generated, as shown in Figure 5.6, in the working directory.

d) Theissen Polygons. This task is executed on the shapefile of the selected gauges. The mean areal rainfall will be calculated and presented to the user.

*Module 4: Spatial Interpolation (MANY).* This module is an extended (advanced) version of module 3, where the user interference is minimized. It simply generates grids using all the spatial interpolation techniques available (including Theissen polygons) by using the shapefile of the selected gauges. Twelve grids are then generated using the interpolation techniques and the estimated values are compared to the observed values of the unselected gauges. The result is a text file and twelve database tables. Each table represents the results of each interpolation technique in the same sequence as in the text file. At the end of the text file, the different interpolation techniques are ranked from the best to the worst according to their performance.

*Module 5: (Automated Interpolation Operations).* This module is an advanced version of module 4, with the least interference from the user. Three inputs are required from the user at the start of the operation: the number of iterations, the cell size, and the number of gauges to be randomly selected; also the DEM, Rain.shp, and Country.shp as shown in Figure 5.7. The main script, when executed, opens new views that are equal to the number of iterations specified by the user. It also generates new working directories for each one of the views inside the main working directory "C:\Inter", sets the properties of the views (map units and distance units), sets the analysis properties (extent, cell size, and mask), and copies the input files (Rain.shp, Country.shp, and DEM) from the main view to the other views. The main script, then, triggers another script which, in turn, opens each of the views and performs the random selection of the gauges according to the number that was initially specified by the user. A third script is run from within the second, which is responsible for opening each of the previously generated views and performing the spatial interpolation task using the different methods. As shown in Figure 5.8, a text file and 12 database files are generated. All output files are located in the respective working directory of each view, each of which is

named after the view (e.g. all work done in view1 is stored in the sub-directory "C:\Inter\View1"). In some cases, the user will choose to terminate the run. For example, if the technique is not suitable for a certain data set or the user would like to run the same case with different cell size, the run may be terminated. The user will then choose to resume execution without generating new views or new shapefiles. At this point, the menu item "Continue Operations ..." will be used to work with the existing files. This menu item is attached to the script "Inter_Continue" which will run the script "Inter_Continue1" or it will run the script "Inter_DifferentCellSize" if the user would like to run the "Automated Operations" using different cell size on multiple views that had been previously generated.

*Project Accessories.* The project is equipped with more scripts that are automatically executed upon opening and closing the project. These perform additional functions which are intended to facilitate the project/user interaction and results presentation.

#### 5.2.1.5 Execution

Speculating that the cell size and the number of available gauges may influence the ranking of the interpolation techniques, a total of 12 runs were performed. The first 4 runs were done using only 40% of the available gauges (187 out of 467 gauges) as observed records with a cell size of 500m, 1000m, 5000m, and 10000m. The second set of 4 runs used 60% of the available gauges (280 out of 467 gauges) as observed records with a cell size of 500m, 1000m, 5000m, and 10000m. The third and final set of 4 runs used 80% of the available gauges (374 out of 467 gauges) as observed records with a cell size of 500m, 1000m, 5000m, and 10000m. Each of the 12 techniques was then evaluated based on the average value of the 20 tries within each of the 12 runs. The evaluation was done on a scale of 0 to 10 with "10" being a perfect technique which means the smallest average value for the 20 (Avg) values; while a "0" is the worst technique which means the largest average value for the 20 (Avg) values.

### 5.2.2 Case 2: Hamilton

#### 5.2.2.1 Introduction

The regional municipality of Hamilton-Wentworth is developing a Real Time Control (RTC) system to help reduce combined sewer overflows (CSOs) to local receiving waters. Knowledge of rainfall and resulting flows at key points in the region's combined sewer system is essential to minimize CSOs. The region has set up a monitoring network of nine gauges to provide data for rainfall and flow forecasting. Accurate gridded rainfall information is needed to compute expected rainfall intensities at ungauged locations as input to hydrologic/hydraulic distributed models of the region and its combined sewer system. In

hydrologic modeling, the random spatial variability of rainfall is often accounted for by spatial interpolation techniques with varying degrees of complexity. This results in better prediction of rainfall storms in real time for flood warning systems and the minimization of the discharge of untreated sewage into the receiving water bodies. The purpose of this section of the chapter is to: 1) document the development of a general procedure that is developed to define the most acceptable interpolation technique; 2) rank the interpolation techniques for this rainfall network from most to least acceptable; and 3) provide a classification of the monitoring network gauges according to their contribution in depicting the spatial variability of rainfall for different storms. It should be emphasized that the primary objective of the paper is to document the development of the decision support tool. Evaluating the gauges and the spatial interpolation techniques is to be verified using more data by the region's officials. The recommendation was strictly based on the limited data available (i.e. 16 events).

#### 5.2.2.2 Study Area

The analysis is performed on a square area of approximately 8 km by 8 km of the municipality of Hamilton-Wentworth, which is located to the west of Lake Ontario. Lake Ontario lies at the borders between the Province of Ontario (Canada) and the State of New York (the United States), as shown in Figure 5.9a. The area under study is located in the southwestern part of the Province (Ontario), as shown in Figure 5.9a and 9b. Due to its location within the Hamilton-Wentworth region and with respect to the lake, as shown in Figure 5.9b, this area is mostly urbanized. The municipality is comprised of the cities of Hamilton and Stoney Creek, the towns of Ancaster, Dundas, and Flamborough, and the township of Glanbrook (refer also to Appendix G). Figure 5.10a shows the digital elevation model of the area and its surroundings. Figure 5.10b shows the main features of the area such as: 1) Ancaster basin: is the main basin in the area, which occupies an area of around 40 $km^2$. Its main three tributaries are: Sulphur Creek, Tiffany Creek, and Ancaster Creek; 2) Cootes Paradise: is a wildlife sanctuary and is located in the Dundas Valley at the western end of Hamilton Harbour, Lake Ontario. Approximately 250 hectares of Cootes Paradise is wetland, the majority of which is open water surrounded by marshy areas and woodland. Cootes Paradise is connected to Hamilton Harbour by the Desjardins Canal. Several streams and creeks drain into Cootes Paradise, including Sulphur, Tiffany, and Ancaster Creeks. The Dundas Sewage Treatment Plant (STP) also drains into Cootes Paradise (Figure 5.10b); 3) Hamilton Harbour: lies at the western edge of Lake Ontario. It is separated naturally from the Great Lake by a sandbar. Some 46 percent of the harbour's 45-kilometer shoreline is given to industrial uses; 10 percent is residential, while 44 percent is private, institutional or public open space. Major causes of impairment include: point and non-point source pollution, contaminated sediments, combined sewer overflows, loss of shoreline access, and degradation or loss of fish and wildlife habitat (BARC, 2002). Figure 5.11a is a zoom-in to

the area of interest and shows the 9-gauge network location within the municipality.

5.2.2.3 Precipitation in the Area

Precipitation records are considered to be estimates rather than measurements. Sevruk (1982) indicated that the commonly used methods of measurement may underestimate actual precipitation from 5 to 30 percent, depending upon the type of instrument and its installation, the climatology of the region and the form of precipitation. The underestimation can be caused by the effects of wind, splashing, wetting, evaporation and blowing snow. The interpolation techniques enable estimates of the spatial variation in precipitation to be acquired at a field level by providing data for a network of grid points at a user-specified resolution. This "distributed" concept is using a limited number of points within the area to predict precipitation values at tens, hundreds, or thousands of individual points, as shown in Figure 5.11b.

The greatest rainfall events in the area are associated with convective precipitation (Shifter, 1981). Orographic uplift over the Niagara Escarpment rarely leads to rainfall, however it does contribute to the formation of clouds (Shifter, 1981). All rainfall storms are comprised of "cells". Each cell has its own characteristics. Cells vary in size and shape and in the level of precipitation intensity. When a cell has a given level of rainfall intensity, the actual amount of rainfall falling on any point will depend on the speed of the cell's movement. A slow moving cell will drop more rain on a given point than a fast moving cell with the same level of rainfall intensity will. These convective storms produce intense and heavy rainfall, cover a small area, and move relatively fast. In Southern Ontario, thirty to forty "thunderstorm days" are reported annually (Kendall and Petrie, 1962). Approximately 95 percent of the storms are approaching the region from the west or south west with a speed ranging from 40 to 80 km/hr (Tsanis and Gad, 2001).

The region has maintained nine tipping bucket raingauges between the period of 1989 and 1993, which recorded precipitation at 1-minute intervals. The locations and descriptions of the gauges are provided in Table 5.1 and Figure 5.12a. By using GIS, and based on this information, the longitude and latitude coordinates were converted to a point shapefile that was then transformed to the UTM projection. The position of each individual gauge was inspected and adjusted, if necessary. Figure 5.12b shows the position and location of the gauges relative to the region and each other.

The area is mainly dominated by two types of storms : 1) typical convective storms, which are characterized by high intensity, high variation, and short duration, and 2) wide-

spread storms, which are characterized by low intensity, low variation, and long duration (Tsanis, 1999). The data used for the purpose of this analysis represented these two types of storms. Sixteen events, extracted from ten rainy days during the summer of 1989 were used. The events, their duration, the start time, the end time, and the accumulated rainfall at each gauge are summarized in Tables 5.2a and 5.2b. Rainfall events in the area may be classified generally as either small (1-4mm), medium (4-12mm), or large (>12mm). The graphical representation (hyetographs) of some events are shown in Figures 5.13a (average, wide-spread), 5.13b (average, convective) and 5.13c (average, mix of convective and wide-spread).

5.2.2.4 Methodology

*Evaluation Criteria.* The validity and applicability of the foregoing interpolation techniques is examined by the so-called "fictitious-point" method (Delhomme, 1978; Tabios III and Salas, 1985). This is done by suppressing one sampling point (station) and values for that point are interpolated based on the remaining (n-1) points. Then, the interpolated values are compared with those observed for that point. The same procedure is followed for all points in the network. The criteria for comparison are:

a) Correlation Coefficient (r). The sample correlation coefficient between observed and estimated rain values is an empirical measure of their linear association. Refer to equation (4.1).

b) Coefficient of Simple Determination ($r^2$). The coefficient of determination for simple linear regression is related to simple correlation coefficient by the relationship:

$$r_{UW} = (\text{sign of the slope of the line}) (r^2)^{1/2} \tag{5.1}$$

c) Mean of Absolute Residuals ($\bar{e}_{abs}$). This is an average of the residuals not considering their sign. The smaller the value, the better the technique. Refer to equation (4.2).

d) Standard Deviation of Absolute Residuals ($S_{abs}$). This value determines how much deviation there is from the mean (spread of the distribution about the mean). The smaller the value, the better the technique. Same as in equation (4.3).

e) Error Variance ($S^2$).

$$S^2 = \sum_{i=1}^{n} \frac{(e_i - \bar{e})^2}{n-1} \tag{5.2}$$

where $S^2$: error variance; $e_i$: error at point (i); $\bar{e}$ : the mean of residuals. The smaller the

value, the better the technique.

*The GIS Approach.* The process is data-driven and fully automated. The GIS project interface is shown in Figure 5.14.

a) GIS Project Description. An ArcView project in its basic format is a collection of views, tables, scripts, layouts, and charts. The saved project, with all its contents, is transferable under the condition that the source location of the themes displayed in the views is transferred along with it. In addition to the necessary input for the project, the user can choose to add any geographical features in the study area (e.g. streets). Upon running the scripts, the output is a group of database files for each technique for each storm (as shown in Figure 5.15).

b) Project Execution. The execution of the project can be summarized in the following steps:

b.1) LOAD. The storm rainfall data of all gauges in the area are extracted from the ASCII file to a database file, which is automatically added to the GIS project.

b.2) SETUP. This setup phase is developed to prepare for the execution step. It: 1) spatially links the extracted data to the gauges ArcView shapefile; 2) generats "eleven" Views and assign each of the views the a name of an interpolation technique; 3) assigns each View its own working directory (e.g. "C:\Interp\IDW") in which all files generated during execution will be stored; 4) allows the user to generate sixteen empty directories named after the sixteen events under study (e.g. "C:\Interp\01091989_G1"); 5) converts the gauges shapefile, after the join, to a new shapefile "rain.shp"; 6) copies all information within the view (i.e. DEM, Border.shp, Rain.shp) to all views within the project and makes the "Rain.shp" the active theme; and 7) sets the map units in all views to "meters".

b.3) EXECUTE. The automated execution process recognizes each view of the project and thus assigning one interpolation technique for each view according to its name. For example, for view "Spline_Regularized", the Regularized Spline technique will be used. For each time step (minute) of the event/storm, each of the gauges will be suppressed and interpolated values will be estimated for all gauges. The process will be repeated nine times for each gauge for each time step. In addition to the interpolated rainfall values, values for correlation coefficient, coefficient of determination, mean absolute error, error variance, and standard deviation of absolute errors are also estimated. These values are stored in five database files for each interpolation technique in its respective working directory. A total of 55 database files are generated for each run (storm). Figure 5.16a shows a sample run for all gauges for Event 22091989 at minute 1244, which is 8:44 PM. By removing the RBG gauge for Event 22091989 at minute 1244, each of the generated interpolated grids (using a cell size of 100m) is different, to an extent, (as shown in Figure 5.16b). For example, the Kriging_Gaussian technique was not able to predict reasonably, while IDW was more stable and provided more

reliable estimates, estimates which were close to what was generated in Figure 5.16a.

b.4) REPAIR & PREPARE. This phase prepares the project for a new run. After completing the run, all working directories are copied by the user to the empty directory, that was previously generated bearing the storm name. The following also is done: 1) disconnecting the database table from the attribute table of the gauges point shapefile; 2) deleting all working directories; and 3) deleting all tables from the project. The project is then ready to perform the LOAD phase for the next run of a new storm.

## 5.3 Results and Discussion

### 5.3.1 Case 1: Switzerland

#### 5.3.1.1 Results

Relying on the multiple random selection of gauges to eliminate the effect of any errors or outliers, no statistical data preparation or preliminary analysis was done. Descriptive statistics were employed to provide inferences for the different models. The module output takes various forms:

1) Visual Grids (Surfaces): as shown in Figure 5.17, where the user can see the distribution of selected (solid dots) and unselected gauges (x-marked locations). In addition to this, the different techniques can be visually compared to each other.

2) Text Files (Report Format): as shown in Figures 5.6 and 5.8, the user is able to obtain permanent records of the various runs for comparison purposes with helpful statistics listed for each technique. In addition, the techniques are listed in performance sequence.

3) Database Files: as shown in Figure 5.6, database files are permanently stored in their respective locations, which can be used to generate different plots (as shown in Figure 5.18).

4) The results of the 12 runs are shown in Figure 5.19, where the horizontal axis represents the interpolation techniques in the same order as in Figure 5.1a and the vertical axis represents the 0-to-10 scale. The following can be concluded:

   a. the Spline_Regularized and the 2$^{nd}$ Order Polynomial techniques showed poor performance in almost all cases.

   b. Theissen Polygons and Kriging (Linear; Gaussian; Circular; Universal_2) techniques fluctuated from one case to the other.

   c. the Spline_Tension, IDW, and Kriging (Spherical; Exponential; Universal_1) techniques were able to provide reliable estimates. The Kriging_Exponential

and Kriging_Universal_1 models are recommended.

Results show that changing the cell size of the interpolated grid did not significantly affect the classification/rank of the interpolation techniques when using small number of gauges (187 gauges), as shown in Figure 5.20a, except for the Theissen Polygons method which dropped on the scale significantly when a cell size of 10000m was used. However, by increasing the number of gauges, the cell size started to show a more noticeable influence as some techniques show higher performance while the others show lower performance. It should be noted that the 2nd order polynomial (technique 11) did not respond to any changes throughout the analysis. It was always ranked 12. Figure 5.20b shows that changing the number of gauges used in the interpolation when using a cell size of 10000m did not have any effect on the performance of the different techniques. It is clear that increasing the number of gauges available for interpolation enhanced the performance of the techniques except for three techniques: Spline_Regulaqrized, Spline_Tension, and Theissen Polygons. Because Spline is set to fit a smooth surface that passes through the points, increasing the number of gauges does not help the technique, especially if there is abrupt changes in rain records resulting in erratic estimated values.

#### 5.3.1.2 Discussion

This network is a relatively dense network with a density of one gauge per 88.4 $km^2$ and it records daily precipitation. Due to the high density of the network, it is unlikely that techniques such as Trend and Spline_Regularized would provide good estimates. Trend surfaces are always smooth surfaces which do not normally pass through the original data points but performs a best fit for the entire surface. They provide an approximate direction of the intensity of rain rather than an accurate description of the spatial variability of rain. On the other hand, surfaces generated using Spline_Regularized try to pass through the points which, in this case, is not suitable because of the rapid changes in gradient/slope in the vicinity of the data points. However, Spline_Tension is a more relaxed version of Spline, which could fit a less smooth curves.

Kriging is generally a good interpolator. The Ordinary Kriging is represented in this case by the Spherical, Circular, Exponential, Gaussian, and Linear methods. With these options, Kriging uses the mathematical function specified by the method to fit a line or curve to the semi-variance data in the semi-variogram. These five models are provided to ensure that the necessary conditions of the variogram model are satisfied. The Exponential and Spherical methods seem to better fit the spatial variation of this data set. The Universal Kriging, represented by the Universal1 and Universal2 methods, assumes that the spatial variation across the surface has a structural component (drift). Drift is a systematic change in the cell values at a particular scale. This scale is related to the radius of the search area.

The goal is to change the search radius to find the scale at which the drift can be detected and the variance is lowest. Universal1 uses a first order polynomial to approximate the drift and Universal2 uses a second order. The first derivative (Universal1) was appropriate for this specific application.

Theissen polygons and IDW techniques provide better results when used for relatively dense networks as in this case. However, increasing the number of gauges can be problematic for the Theissen polygons technique.

It should be noted that repeated runs for different data sets are required to verify the results obtained. For example: wet, moderate, and dry conditions; hourly, daily, monthly, and yearly data; short and long term average; ...etc. The one available data set used as a test case in this study does not provide enough evidence that certain techniques are better than others.

### 5.3.2 Case 2: Hamilton

At each time step and for each technique, an average value was obtained for each evaluation criteria (as shown in Figure 5.21a). Similarly, at each gauge and for each technique, an average value was obtained for each evaluation criterion (as shown in Figure 5.21b). Figure 5.21a shows a comparison between the IDW and Kriging_Gaussian techniques for the storm 15081989_G4 based on correlation coefficient, mean absolute error, and error variance at each time step. Figure 5.21b shows a comparison between all techniques for the storm 15081989_G4 based on correlation coefficient, mean absolute error, and error variance at each gauge. The techniques are sorted from the best (IDW) to the worst (Kriging_Gaussian). Generally, the techniques that provided better results were IDW, Spline_Tension, and Kriging_Universal_1; while the Kriging_Gaussian and 2$^{nd}$ Order Polynomial techniques were found to be bad estimators. Taking into account results from all storms, the techniques were ranked based on each criterion and then an overall ranking was obtained (as shown in Table 5.3a). Similarly, gauges were ranked based on each criterion. An overall ranking was then obtained as shown in Table 5.3b. For example, most of the techniques were able to provide good estimates of rainfall at the "CHE" gauge location, which is an indication that this gauge does not provide significant information within the network and can be replaced. On the contrary, most of the techniques were not able to provide good estimates of rainfall at the "LEE" gauge location, which is an indication that this gauge provides significant information within the network. Figure 5.22 shows the areas where more gauges can be added on and around the contours of low rank values. These areas are located to the west, northwest, and southeast of the region.

## 5.4 Conclusion

### 5.4.1 Case 1: Switzerland

This work establishes an approach by using GIS and historical data to locate the best spatial interpolation technique. The performance of a certain technique applied to a partial data set is likely to be different when applied to a larger data set. By taking a sample of the data set, the problem scale is changed, and the boundary between large and small scale variation is modified. For that reason, data sets with different sizes are recommended. Finally, it is highly advisable for any region to obtain data from the closest parts of neighboring regions or at least to have as many data as possible from locations within the region. Based on the one data set available for this study, it was clear that the Kriging_Exponential and Kriging_Universal_1 models showed consistent performance and provided reliable estimates regardless of the number of gauges or the cell size used in the interpolation.

### 5.4.2 Case 2: Hamilton

The study reported herein describes the comparison of a number of spatial interpolation techniques in a GIS for estimating rainfall in a high temporal and spatial resolution. A brief description of the techniques was given. The techniques were then applied and compared for a nine-gauge network with 1-minute data in an area of 8 km by 8 km in the province of Ontario, Canada. The techniques included the following: IDW, Spline (Tension and Regularized), 2$^{nd}$ Order Polynomial, and Kriging (Universal 1, Universal 2, Circular, Gaussian, Linear, Spherical, and Exponential). These techniques were compared based on the following criteria: correlation coefficient, coefficient of determination, mean absolute error, error variance, and standard deviation of absolute errors. Results showed that, for this area and using 1-minute rainfall data for events that took place during the summer of 1989, the IDW was the most suitable technique, while the Kriging_Gaussian and 2$^{nd}$ Order Polynomial did not provide any good estimates. The "LEE" gauge was also found to be a key gauge in the specified area, while the "CHE" gauge did not play a significant role in detecting the spatial variability of rainfall in the region. More gauges can be added around R11, LEE, and BUN gauges.

Finally, it should be noted that judging the performance of the spatial interpolation techniques cannot be based on the results of this study. More data is required to verify such an outcome. The results, however, can be considered a useful warning of the instability of interpolation techniques with limited/sparse data, particularly in the context of commercial software.

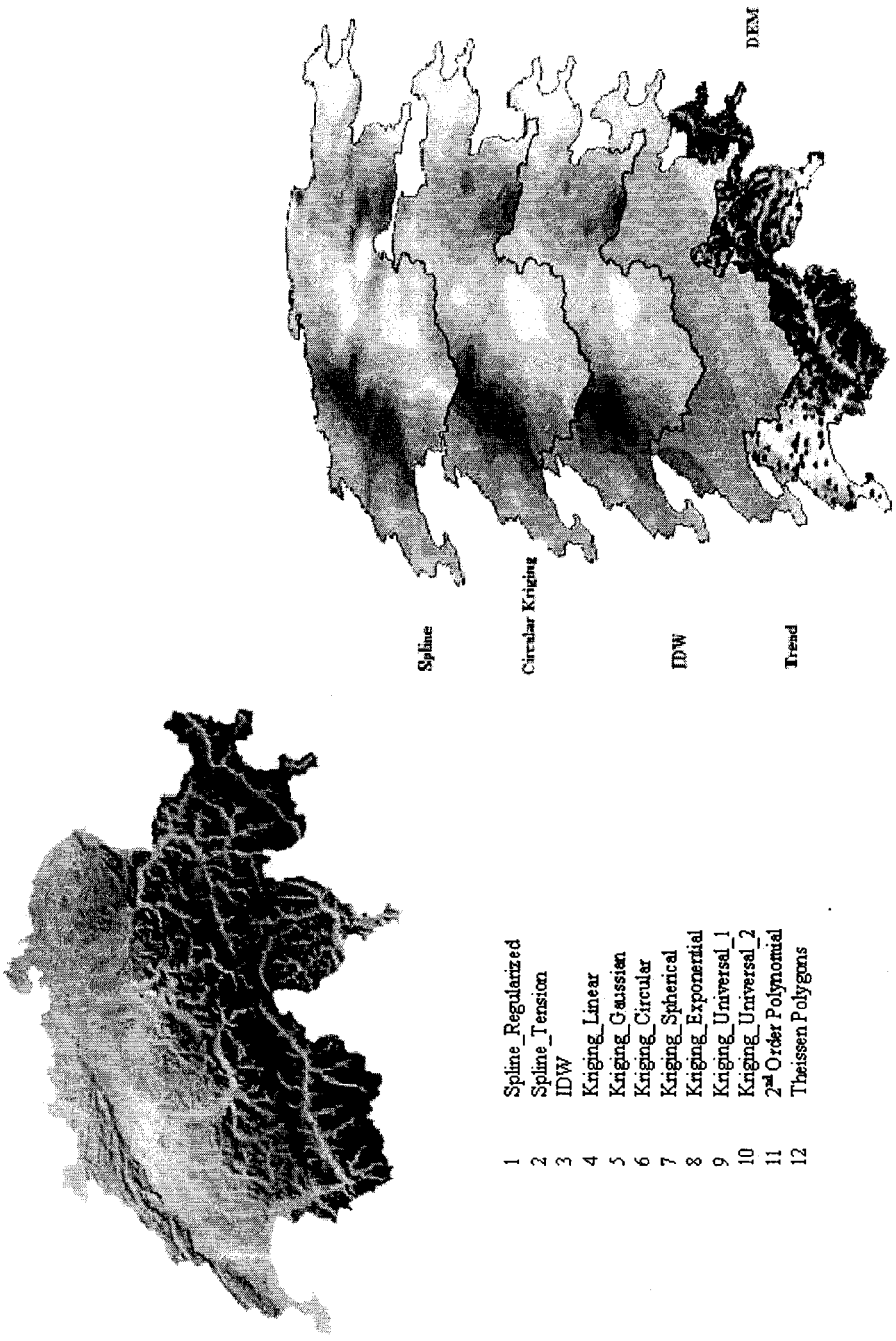


**Figure 5.1a:** Digital Elevation Model (DEM) and interpolated rain surfaces in Switzerland

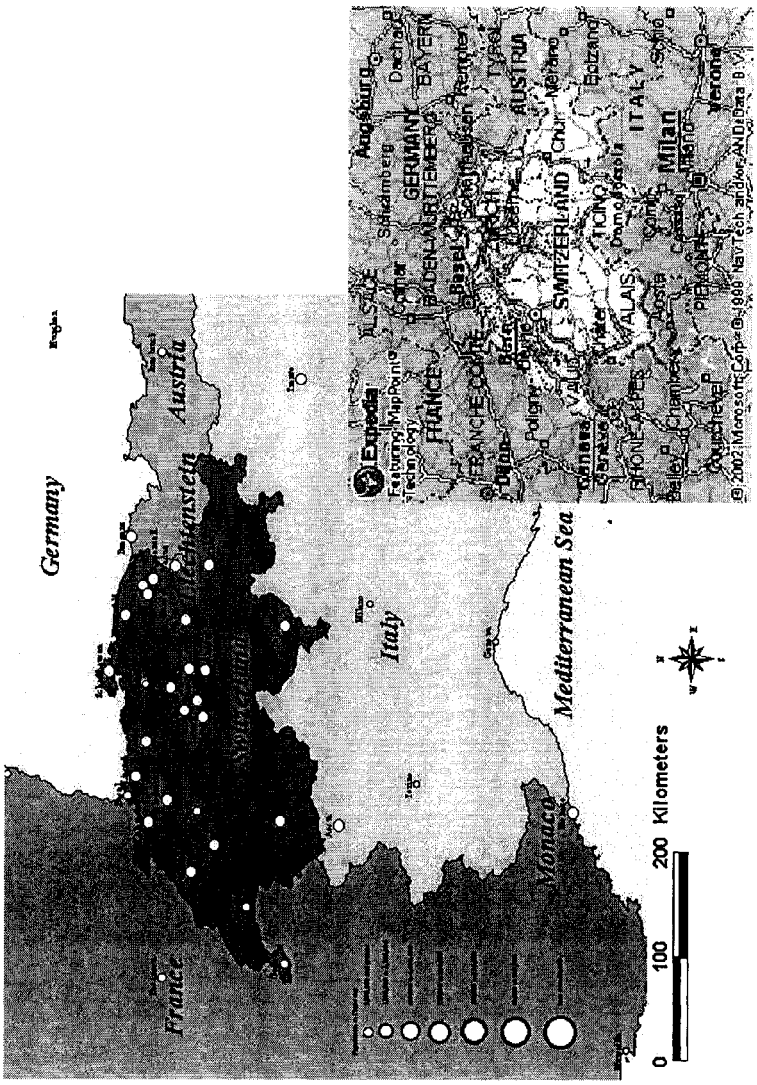


**Figure 5.1b:** Geographical location of Switzerland in Europe.

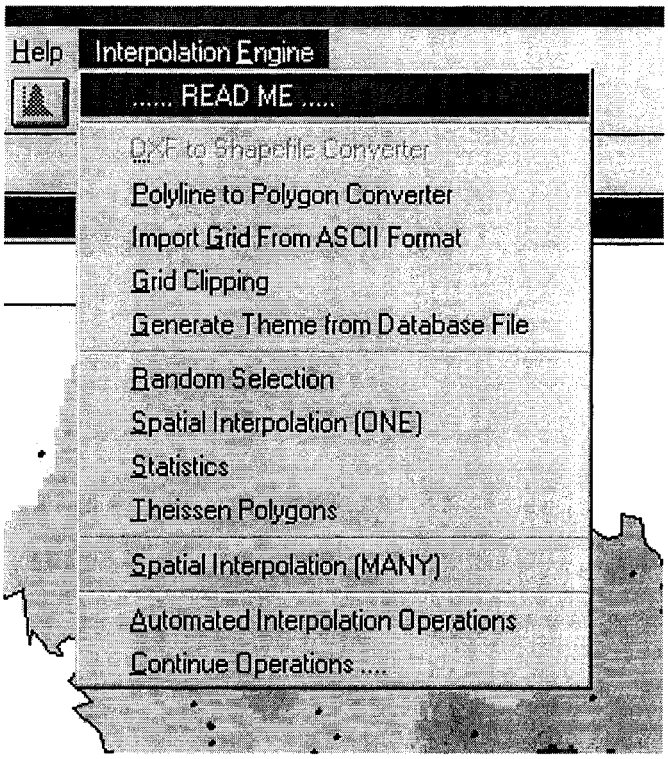


**Figure 5.2:** The main module of the "interpolation engine" project.

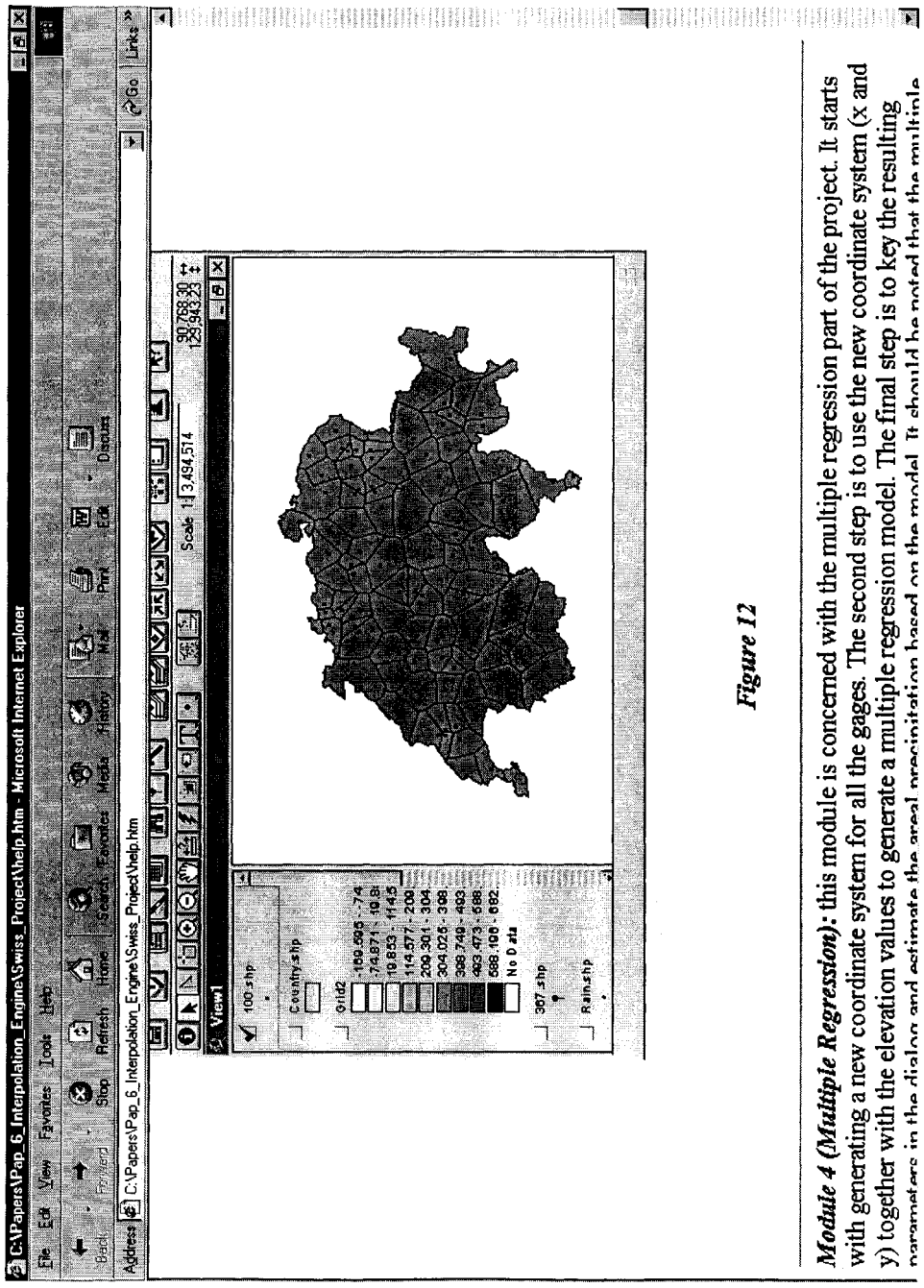


**Figure 5.3:** Module 1: Project Description. Rain values in $1/10^{th}$ of "mm".

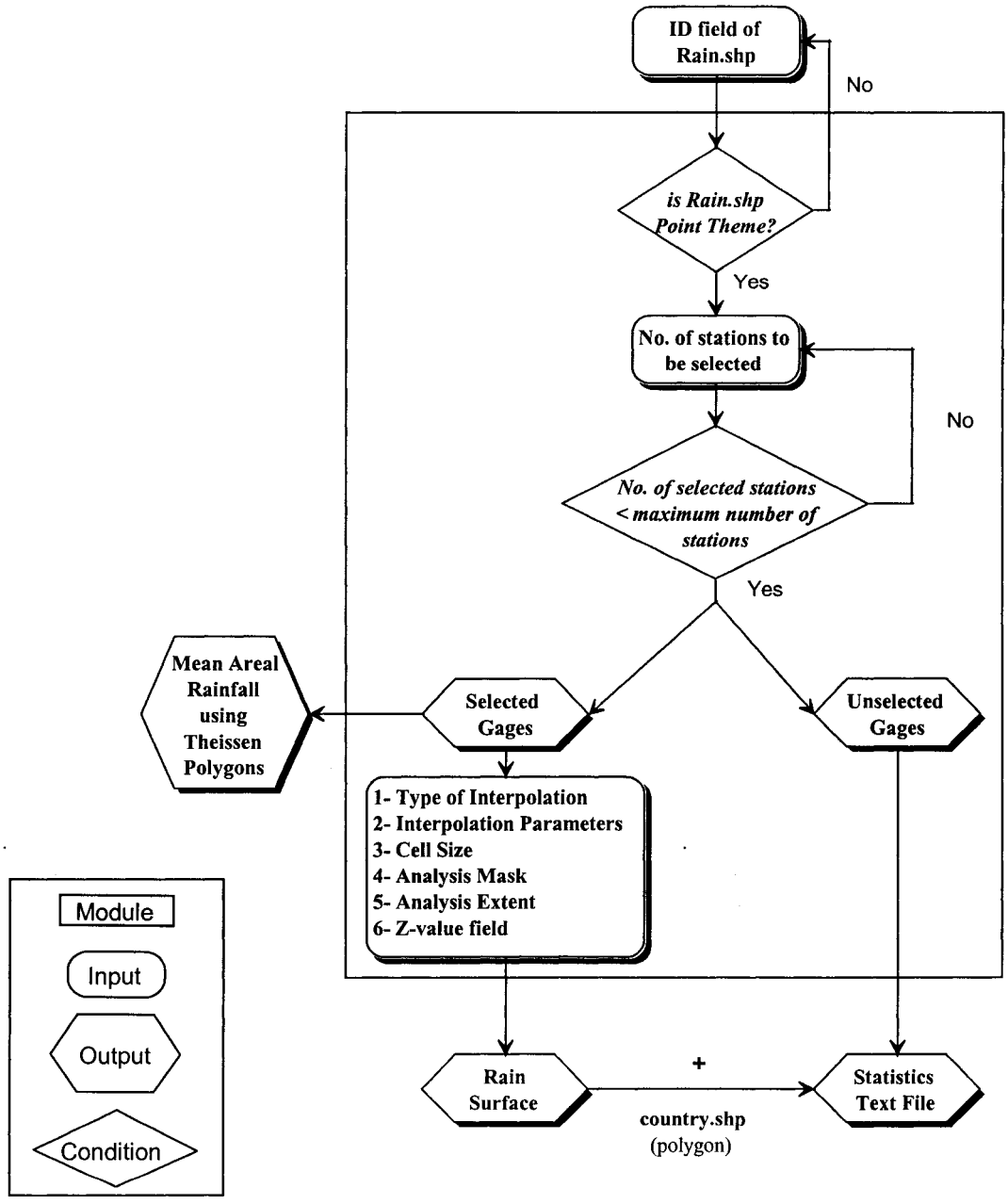


**Figure 5.4**: Module 3 (Interpolators)

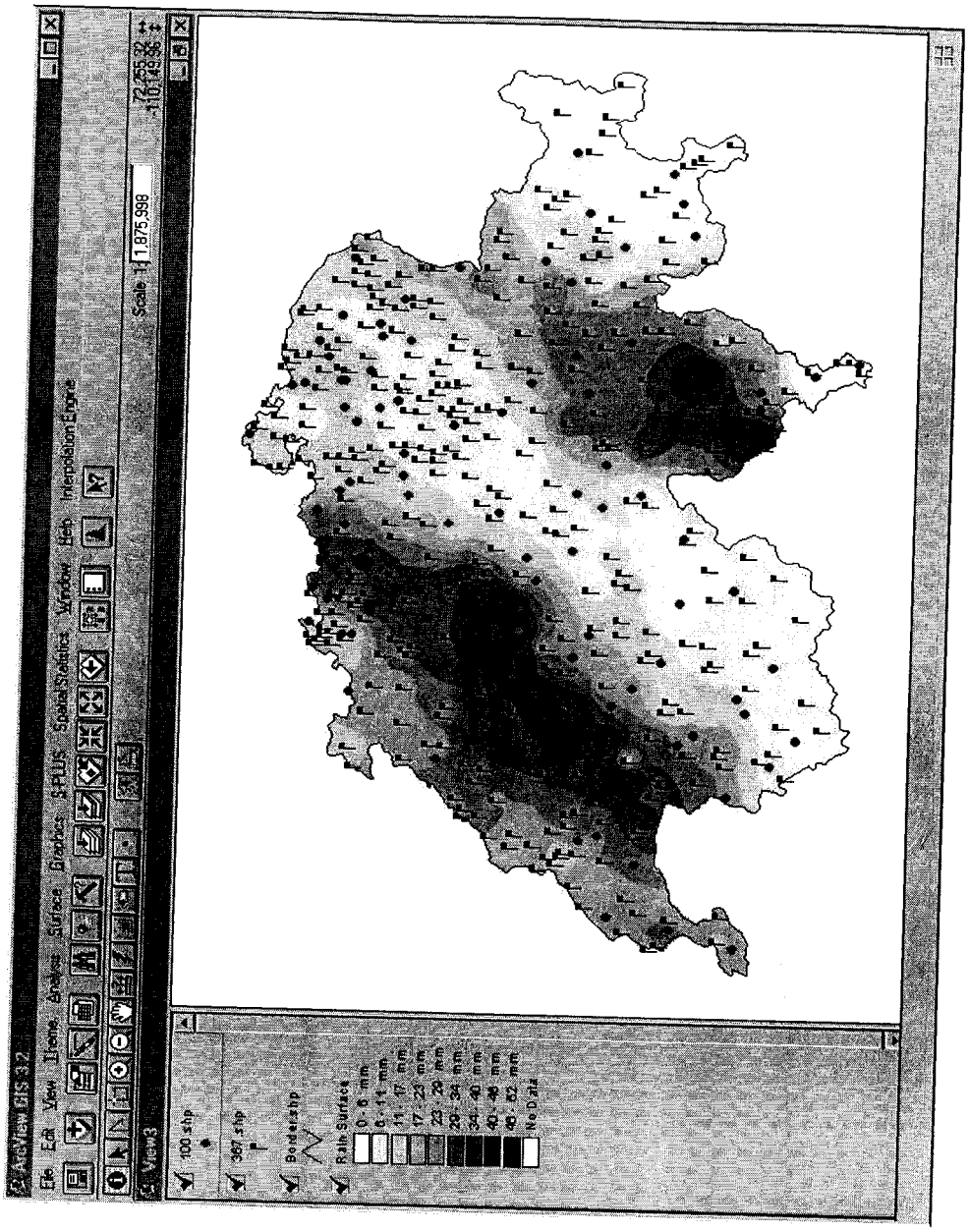


**Figure 5.5:** Output of module 3 using menu item "Spatial Interpolation [ONE]"

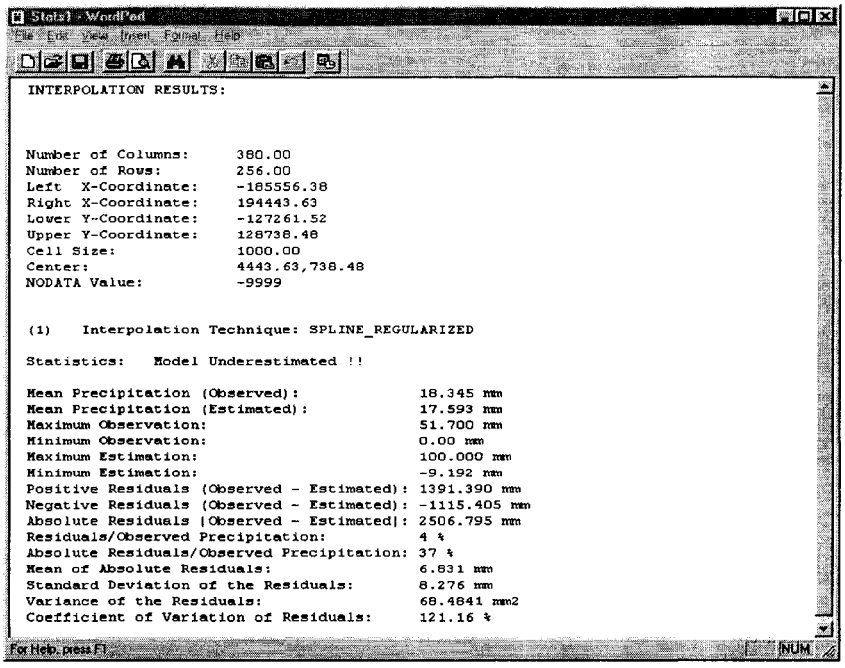

stats1 - WordPad

File Edit View Insert Format Help

```
INTERPOLATION RESULTS:


Number of Columns:      380.00
Number of Rows:         256.00
Left  X-Coordinate:     -185556.38
Right X-Coordinate:     194443.63
Lower Y-Coordinate:     -127261.52
Upper Y-Coordinate:     128738.48
Cell Size:              1000.00
Center:                 4443.63,738.48
NODATA Value:           -9999


(1)    Interpolation Technique: SPLINE_REGULARIZED

Statistics:   Model Underestimated !!

Mean Precipitation (Observed):                  18.345 mm
Mean Precipitation (Estimated):                 17.593 mm
Maximum Observation:                            51.700 mm
Minimum Observation:                            0.00 mm
Maximum Estimation:                             100.000 mm
Minimum Estimation:                             -9.192 mm
Positive Residuals (Observed - Estimated):      1391.390 mm
Negative Residuals (Observed - Estimated):      -1115.405 mm
Absolute Residuals |Observed - Estimated|:      2506.795 mm
Residuals/Observed Precipitation:               4 %
Absolute Residuals/Observed Precipitation:      37 %
Mean of Absolute Residuals:                     6.831 mm
Standard Deviation of the Residuals:            8.276 mm
Variance of the Residuals:                      68.4841 mm2
Coefficient of Variation of Residuals:          121.16 %
```

For Help, press F1 NUM

Microsoft Excel - stats1 [Read-Only]

A1 ID

| | A | B | C | D | E | F | G | H |
|---|---|---|---|---|---|---|---|---|
| 1 | ID | LONG | LAT | OBS_RAIN | EST_RAIN | POS_RES | NEG_RES | RESID |
| 2 | 1 | -159812 | -39393 | 21.50 | 35.99 | 0.00 | -14.49 | -14.49 |
| 3 | 2 | -159806 | -68316 | 16.70 | 32.27 | 0.00 | -15.57 | -15.57 |
| 4 | 3 | -158368 | -42768 | 27.10 | 32.46 | 0.00 | -5.36 | -5.36 |
| 5 | 4 | -156586 | -62838 | 16.60 | 29.58 | 0.00 | -12.98 | -12.98 |
| 6 | 7 | -153090 | -46242 | 14.90 | 24.74 | 0.00 | -9.84 | -9.84 |
| 7 | 8 | -148708 | -24105 | 19.00 | 21.08 | 0.00 | -2.08 | -2.08 |
| 8 | 11 | -145922 | -35296 | 14.90 | 14.60 | 0.30 | 0.00 | 0.30 |
| 9 | 12 | -143939 | -16435 | 22.80 | 17.55 | 5.25 | 0.00 | 5.25 |
| 10 | 13 | -140463 | -30977 | 15.10 | 8.55 | 6.55 | 0.00 | 6.55 |
| 11 | 14 | -136211 | -12166 | 25.50 | 12.47 | 13.03 | 0.00 | 13.03 |
| 12 | 15 | -129848 | -72 | 21.00 | 5.29 | 15.71 | 0.00 | 15.71 |
| 13 | 16 | -128276 | -33474 | 21.00 | 10.58 | 10.42 | 0.00 | 10.42 |
| 14 | 17 | -127684 | -5680 | 23.40 | 6.55 | 16.85 | 0.00 | 16.85 |
| 15 | 19 | -125353 | -3505 | 21.70 | 3.82 | 17.88 | 0.00 | 17.88 |
| 16 | 20 | -124685 | -7968 | 10.00 | 6.95 | 3.05 | 0.00 | 3.05 |
| 17 | 23 | -121276 | 9758 | 19.10 | 4.12 | 14.98 | 0.00 | 14.98 |
| 18 | 24 | -120674 | 1960 | 19.40 | 0.54 | 18.86 | 0.00 | 18.86 |
| 19 | 26 | -118084 | 17479 | 23.40 | 12.04 | 11.36 | 0.00 | 11.36 |
| 20 | 28 | -116742 | 8555 | 18.30 | 3.13 | 15.17 | 0.00 | 15.17 |
| 21 | 29 | -116780 | -32596 | 33.40 | 29.19 | 4.21 | 0.00 | 4.21 |
| 22 | 30 | -115480 | -4816 | 10.70 | 6.36 | 4.34 | 0.00 | 4.34 |
| 23 | 31 | -114528 | -34864 | 37.10 | 35.25 | 1.85 | 0.00 | 1.85 |
| 24 | 32 | -113301 | -10418 | 23.00 | 15.89 | 7.12 | 0.00 | 7.12 |
| 25 | 33 | -111242 | -22691 | 29.00 | 31.46 | 0.00 | -2.46 | -2.46 |
| 26 | 35 | -109680 | 20655 | 29.60 | 17.86 | 11.74 | 0.00 | 11.74 |
| 27 | 37 | -109172 | -34963 | 39.40 | 38.59 | 0.81 | 0.00 | 0.81 |
| 28 | 38 | -108729 | -10503 | 30.00 | 23.29 | 6.71 | 0.00 | 6.71 |
| 29 | 39 | -108027 | -13852 | 27.80 | 29.18 | 0.00 | -1.38 | -1.38 |

stats1

Draw AutoShapes

Ready NUM

**Figure 5.6:** Output of module 3 using menu item "Statistics"

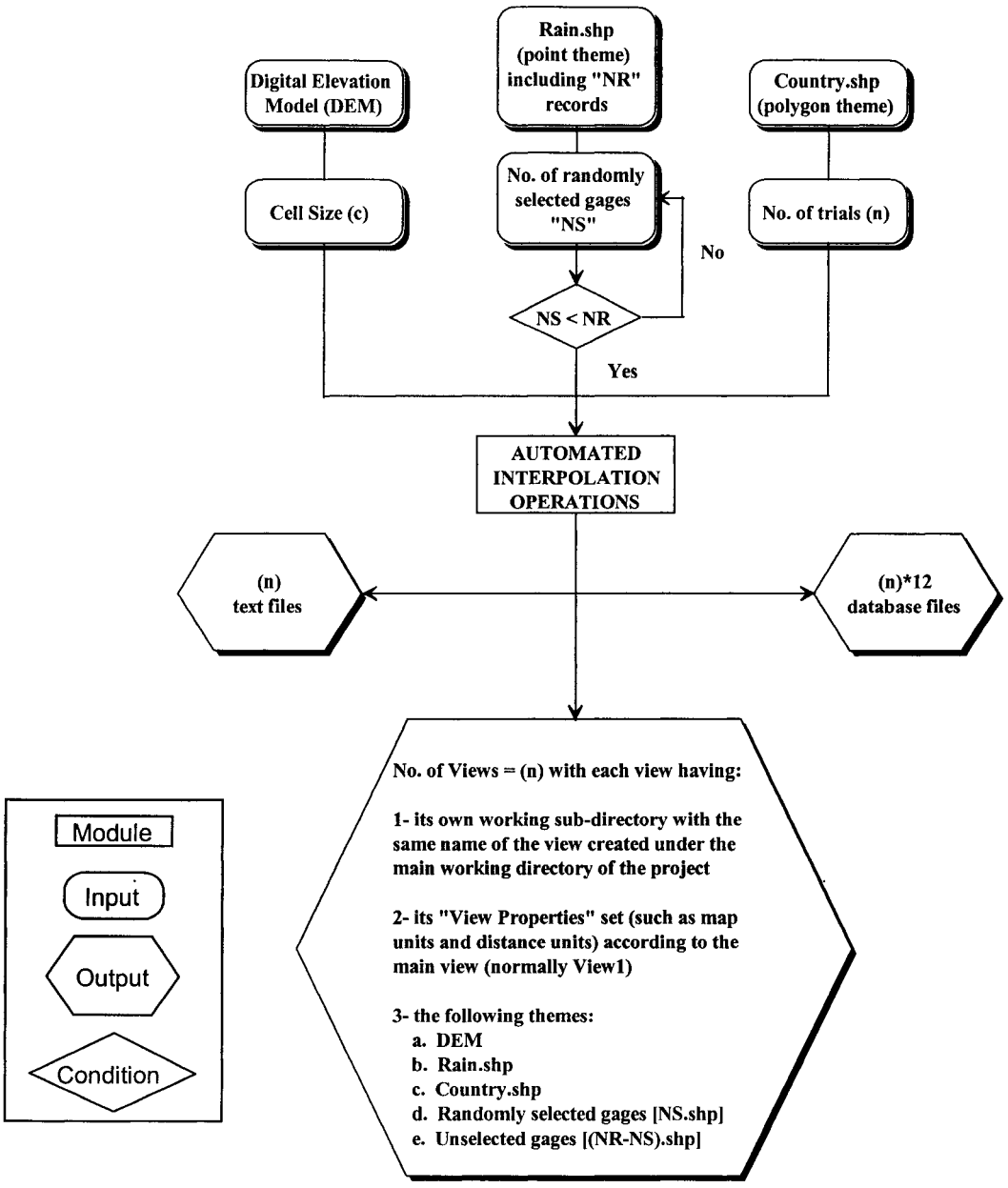


**Figure 5.7**: A flow chart representing module 5 "Automated interpolation Operations"

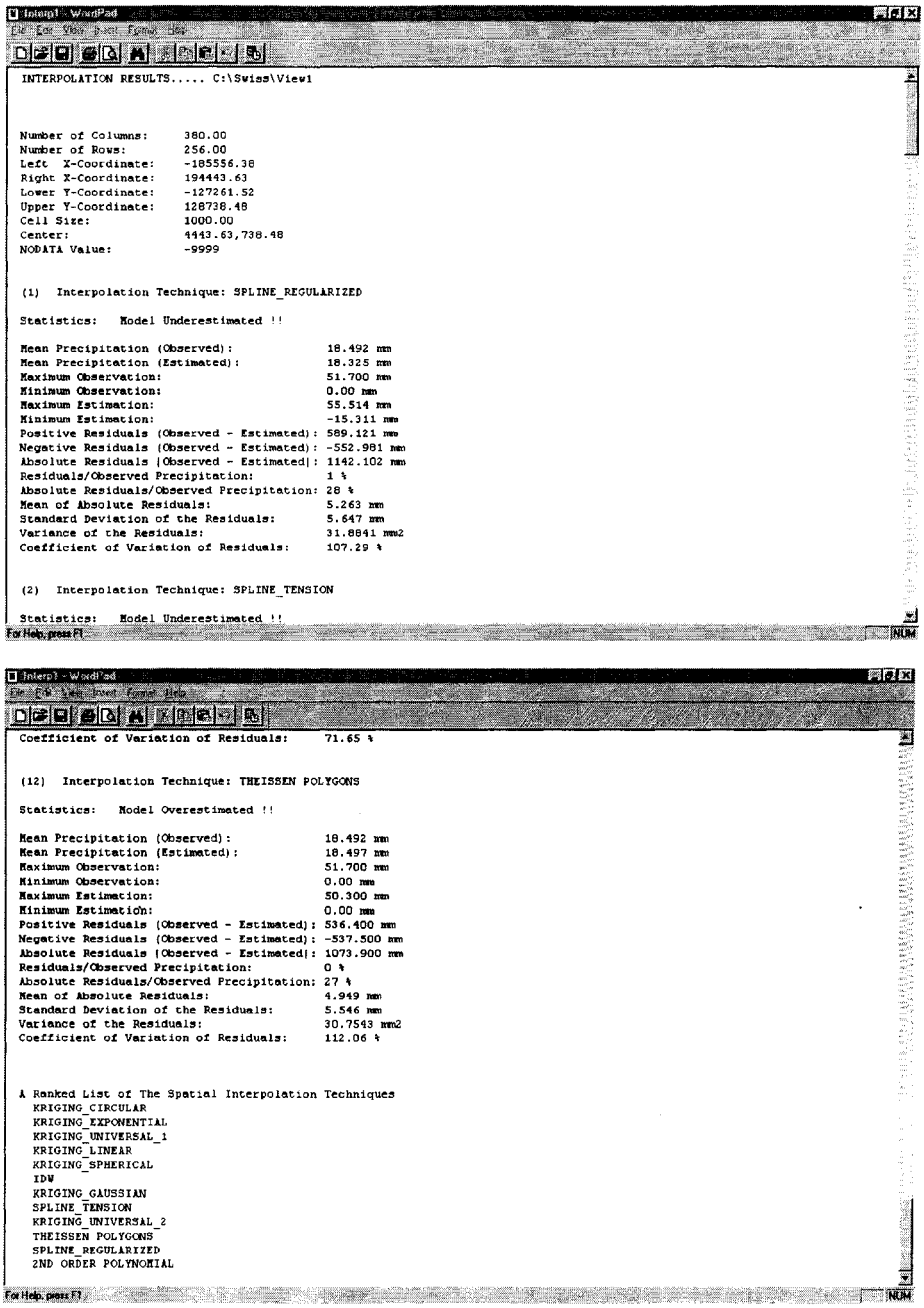

```
INTERPOLATION RESULTS..... C:\Swiss\View1


Number of Columns:      380.00
Number of Rows:         256.00
Left  X-Coordinate:     -185556.38
Right X-Coordinate:     194443.63
Lower Y-Coordinate:     -127261.52
Upper Y-Coordinate:     128738.48
Cell Size:              1000.00
Center:                 4443.63,738.48
NODATA Value:           -9999


(1)  Interpolation Technique: SPLINE_REGULARIZED

Statistics:   Model Underestimated !!

Mean Precipitation (Observed):              18.492 mm
Mean Precipitation (Estimated):             18.325 mm
Maximum Observation:                        51.700 mm
Minimum Observation:                        0.00 mm
Maximum Estimation:                         55.514 mm
Minimum Estimation:                         -15.311 mm
Positive Residuals (Observed - Estimated):  589.121 mm
Negative Residuals (Observed - Estimated):  -552.981 mm
Absolute Residuals |Observed - Estimated|:  1142.102 mm
Residuals/Observed Precipitation:           1 %
Absolute Residuals/Observed Precipitation:  28 %
Mean of Absolute Residuals:                 5.263 mm
Standard Deviation of the Residuals:        5.647 mm
Variance of the Residuals:                  31.8841 mm2
Coefficient of Variation of Residuals:      107.29 %


(2)  Interpolation Technique: SPLINE_TENSION

Statistics:   Model Underestimated !!
```

```
Coefficient of Variation of Residuals:      71.65 %


(12)  Interpolation Technique: THEISSEN POLYGONS

Statistics:   Model Overestimated !!

Mean Precipitation (Observed):              18.492 mm
Mean Precipitation (Estimated):             18.497 mm
Maximum Observation:                        51.700 mm
Minimum Observation:                        0.00 mm
Maximum Estimation:                         50.300 mm
Minimum Estimation:                         0.00 mm
Positive Residuals (Observed - Estimated):  536.400 mm
Negative Residuals (Observed - Estimated):  -537.500 mm
Absolute Residuals |Observed - Estimated|:  1073.900 mm
Residuals/Observed Precipitation:           0 %
Absolute Residuals/Observed Precipitation:  27 %
Mean of Absolute Residuals:                 4.949 mm
Standard Deviation of the Residuals:        5.546 mm
Variance of the Residuals:                  30.7543 mm2
Coefficient of Variation of Residuals:      112.06 %


A Ranked List of The Spatial Interpolation Techniques
  KRIGING_CIRCULAR
  KRIGING_EXPONENTIAL
  KRIGING_UNIVERSAL_1
  KRIGING_LINEAR
  KRIGING_SPHERICAL
  IDW
  KRIGING_GAUSSIAN
  SPLINE_TENSION
  KRIGING_UNIVERSAL_2
  THEISSEN POLYGONS
  SPLINE_REGULARIZED
  2ND ORDER POLYNOMIAL
```

**Figure 5.8:** The text file "Interp1.txt" as an output of module 5 using menu item "Automated Interpolation Operations"

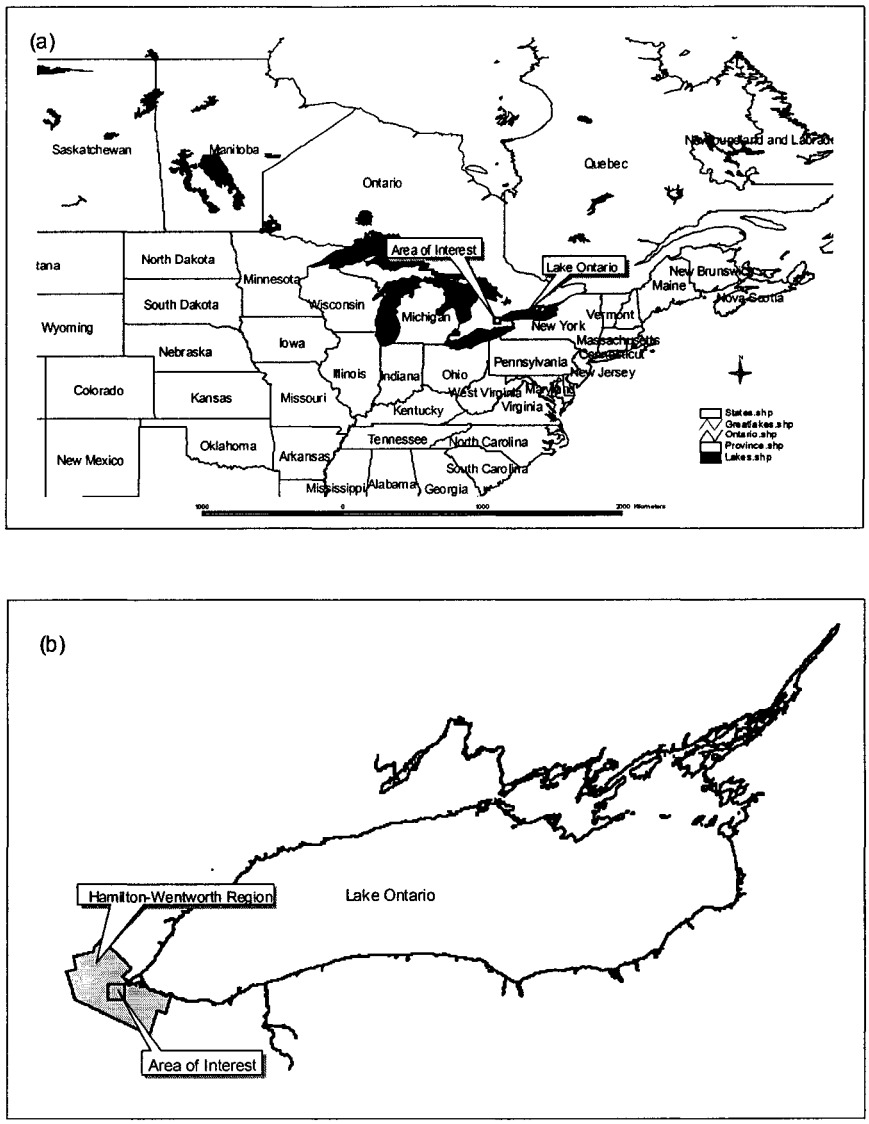


**Figure 5.9**: (a) The location of Lake Ontario on the Canadian-American border. The area of interest is located to the west of the lake. (b) The area of interest within the municipality of Hamilton-Wentworth

(a)

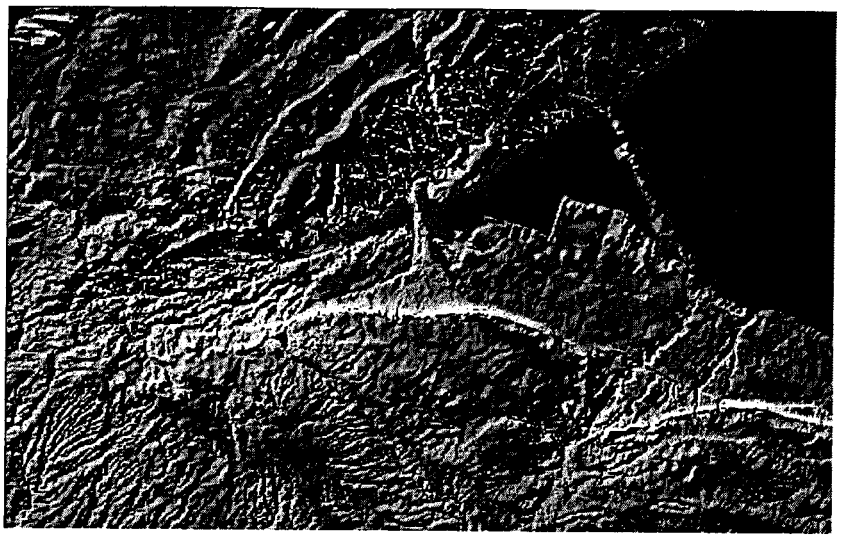

(b)

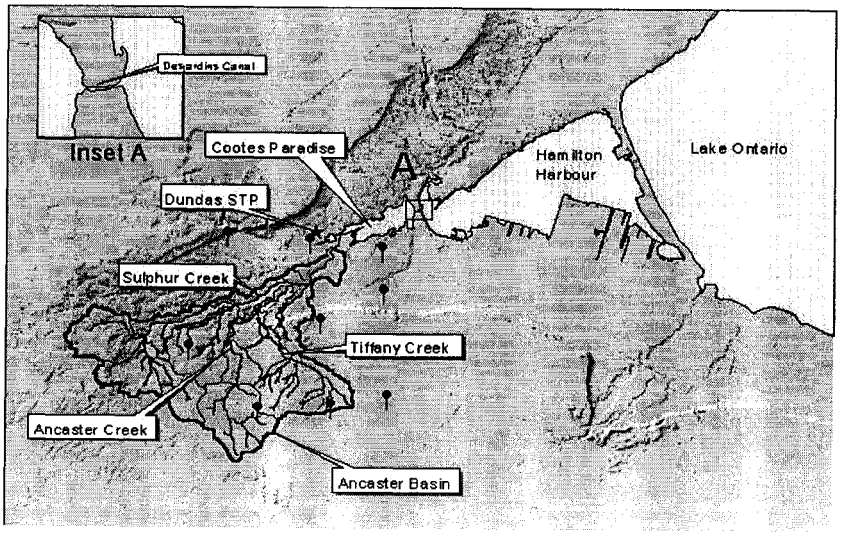


**Figure 5.10:** (a) The digital elevation model of the study area and its surroundings. (b) Ancaster basin with its tributaries discharging to Cootes Paradise. Dundas sewage treatment plant discharging to Cootes Paradise to Hamilton Harbor to Lake Ontario

a)

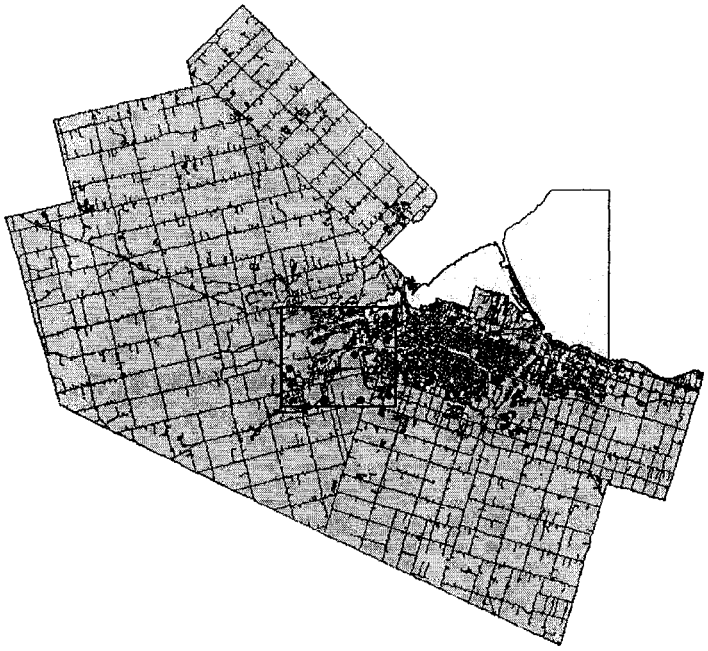

b)

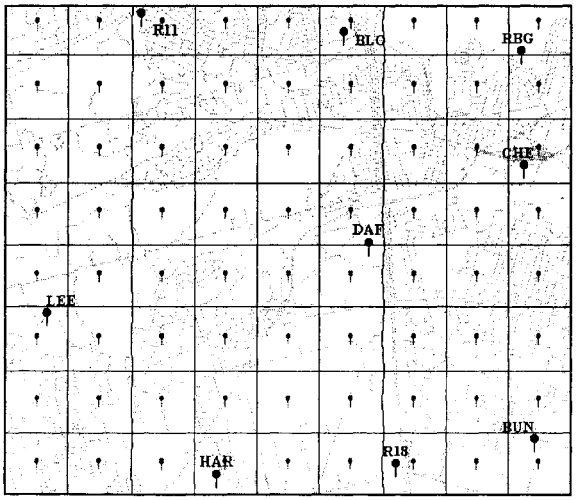


**Figure 5.11**: (a) the location of the 9-gauge network used in the study with respect to Lake Ontario. (b) A big network composed of imaginary gauges (small flags) as an illustration of how spatial interpolation techniques use information from the 9 gauges (bigger flags) to estimate precipitation at the location of these imaginary gauges

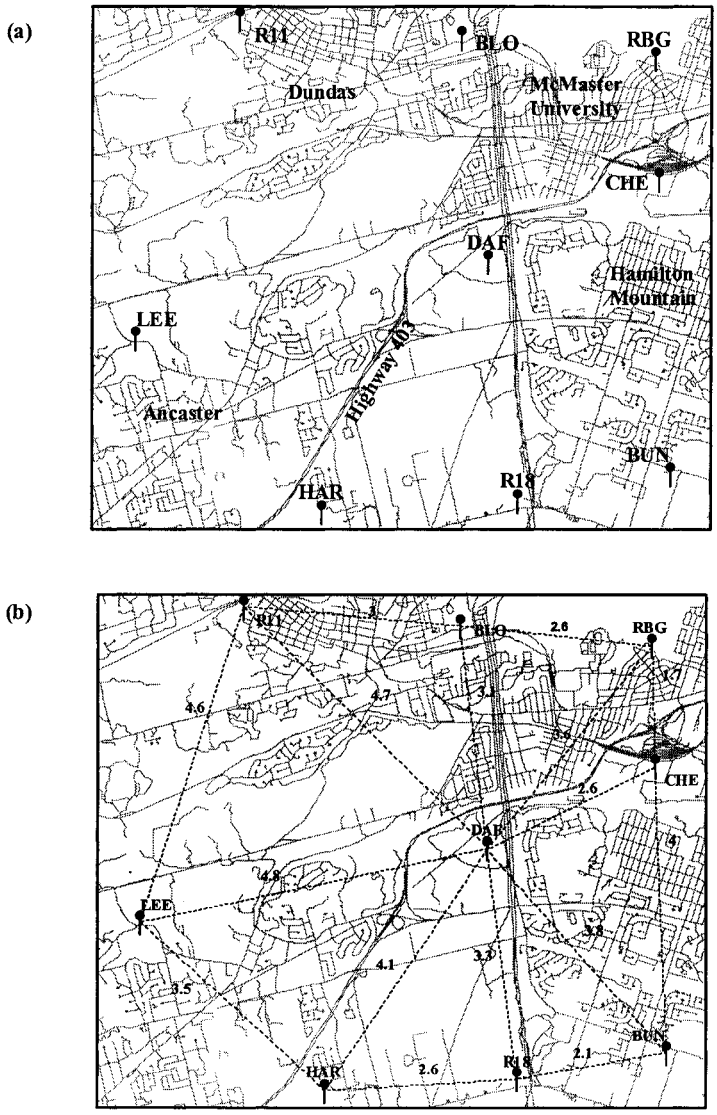


**Figure 5.12:** (a) the 8 km by 8 km study area within the Hamilton-Wentworth Region. The area is monitored by a 9-gauge rainfall network. (b) Distances in km between the gauges.

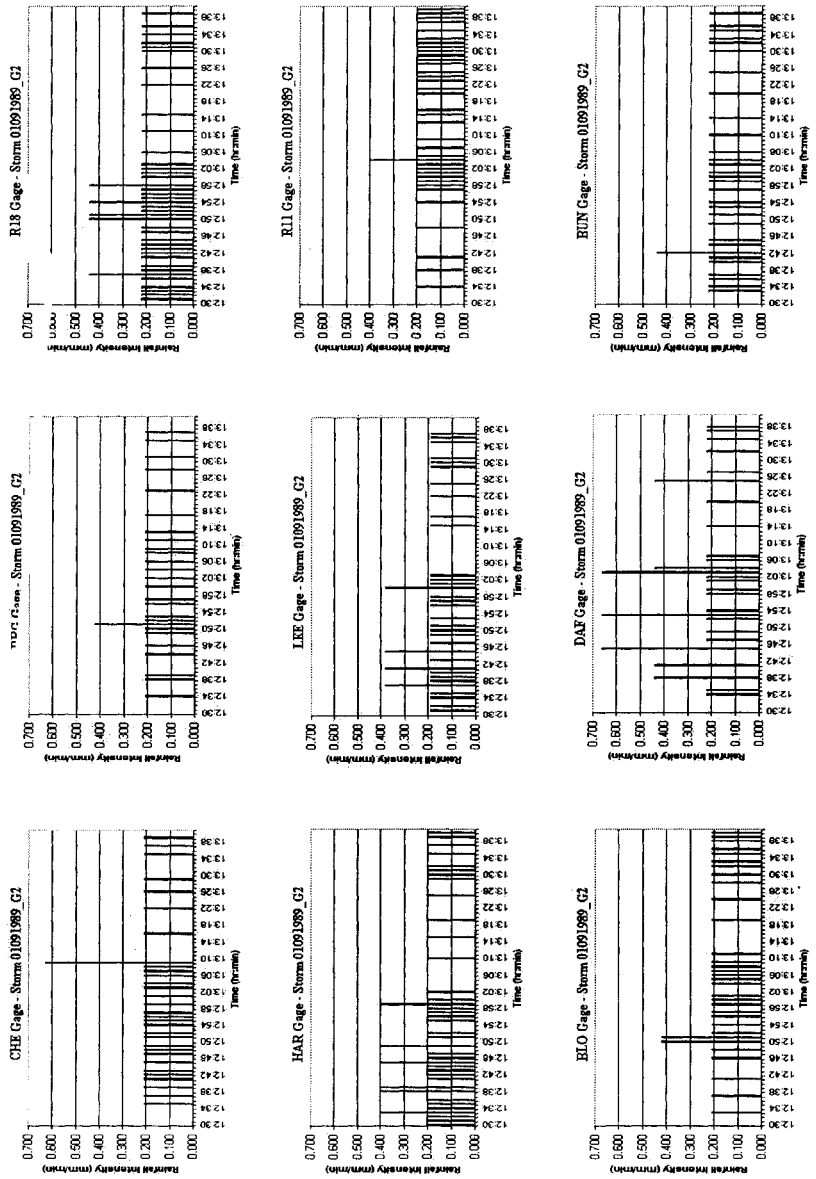


**Figure 5.13a:** Hyetographs of the storm 01091989_G2 at all gauges.
This storm is considered to be an average one and specified as a wide-spread event.

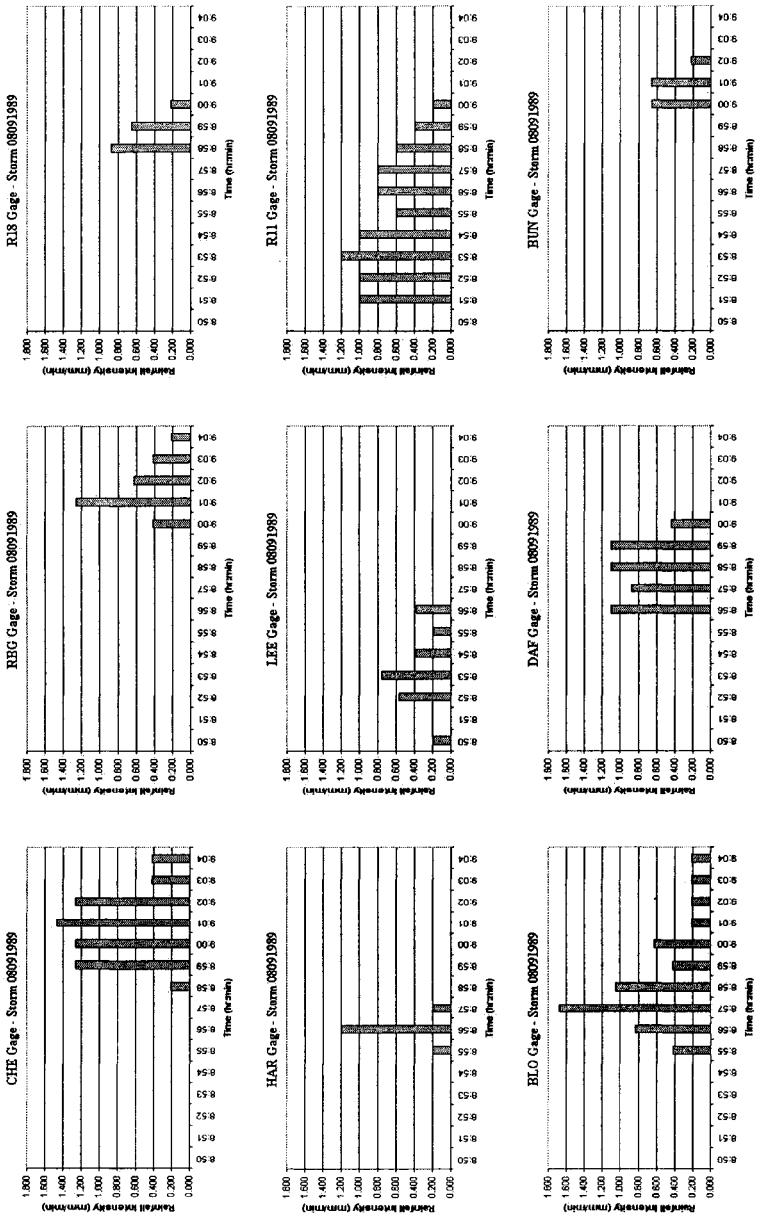


**Figure 5.13b:** Hyetographs of the storm 08091989 at all gauges.
This storm is considered to be an average one and specified as a convective event.

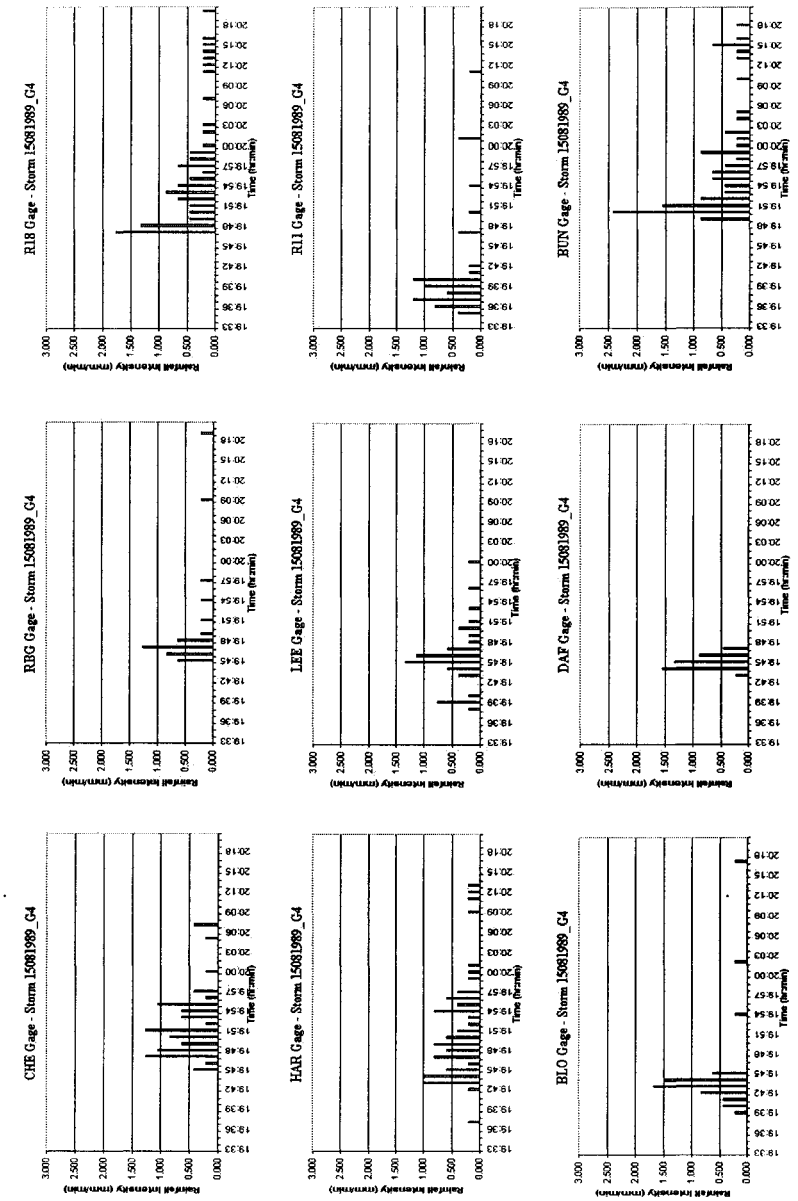


**Figure 5.13c:** Hyetographs of the storm 15081989_G4 at all gauges.
This storm is considered to be an average one and specified as a mix of convective and wide-spread event.

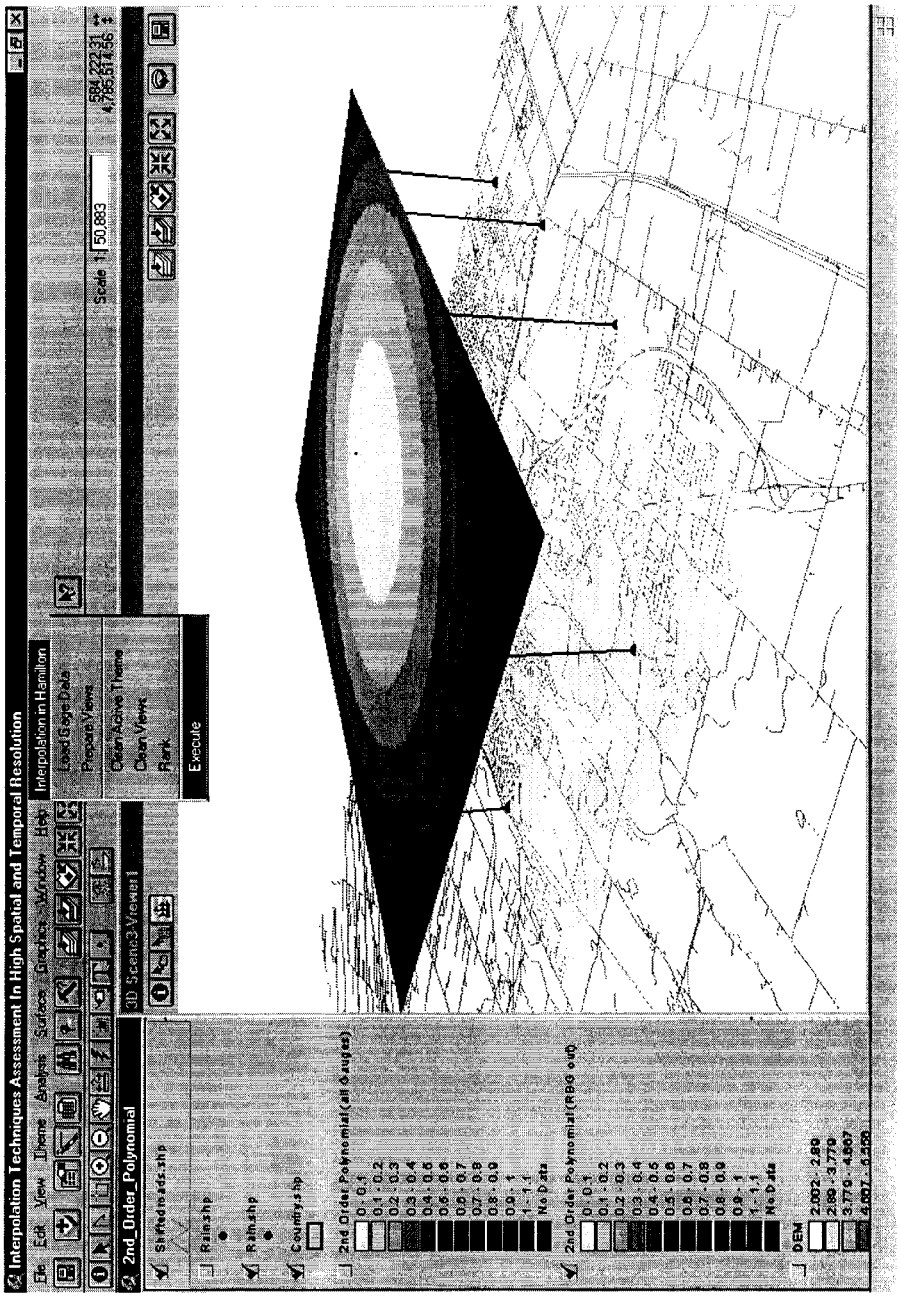


**Figure 5.14:** The ArcView GIS interface, including the developed drop-down menu through which the project was executed

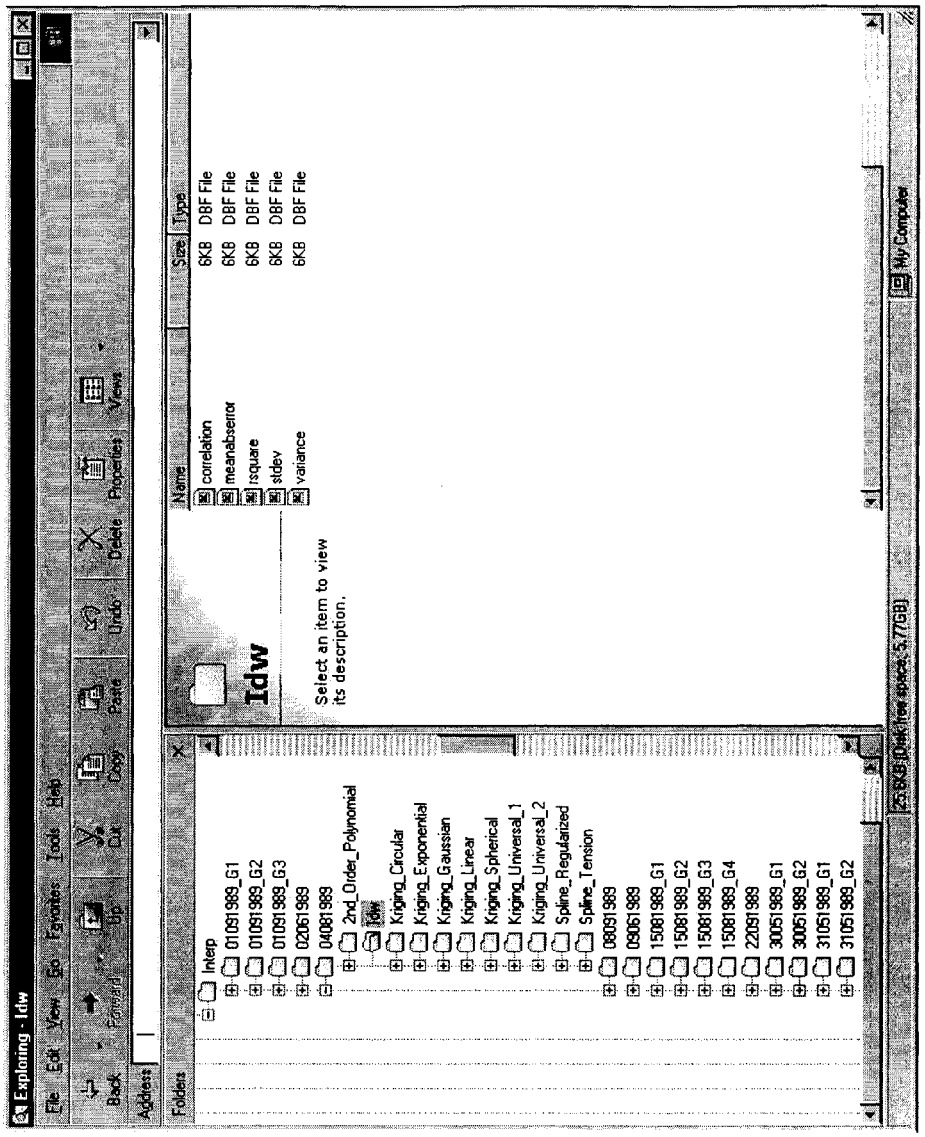


**Figure 5.15:** The layout of the directories and sub-directories created prior to and during the GIS project execution.

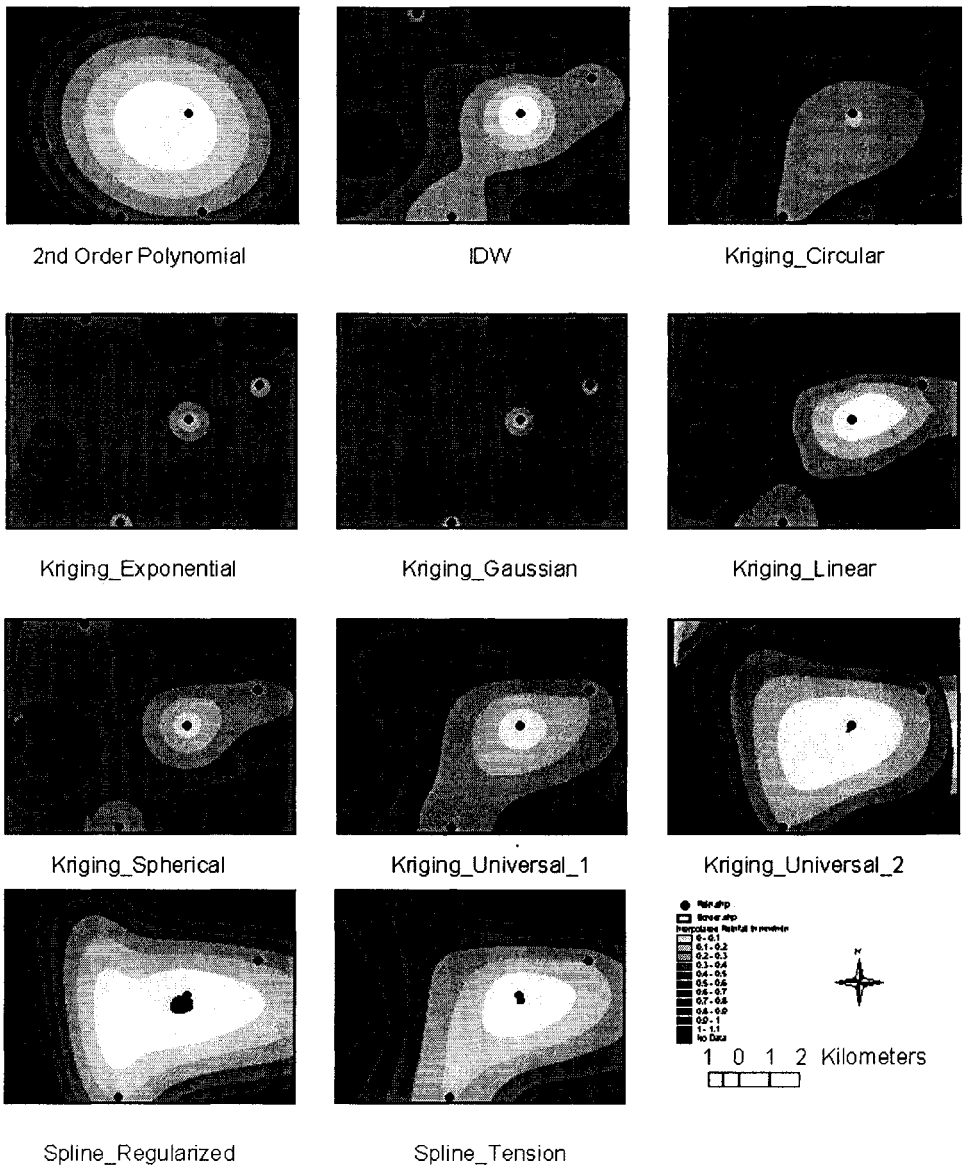


**Figure 5.16a:** Interpolated grids from all gauges using the different interpolation techniques for the Event 22091989 at minute 1244, which is 8:44 PM.

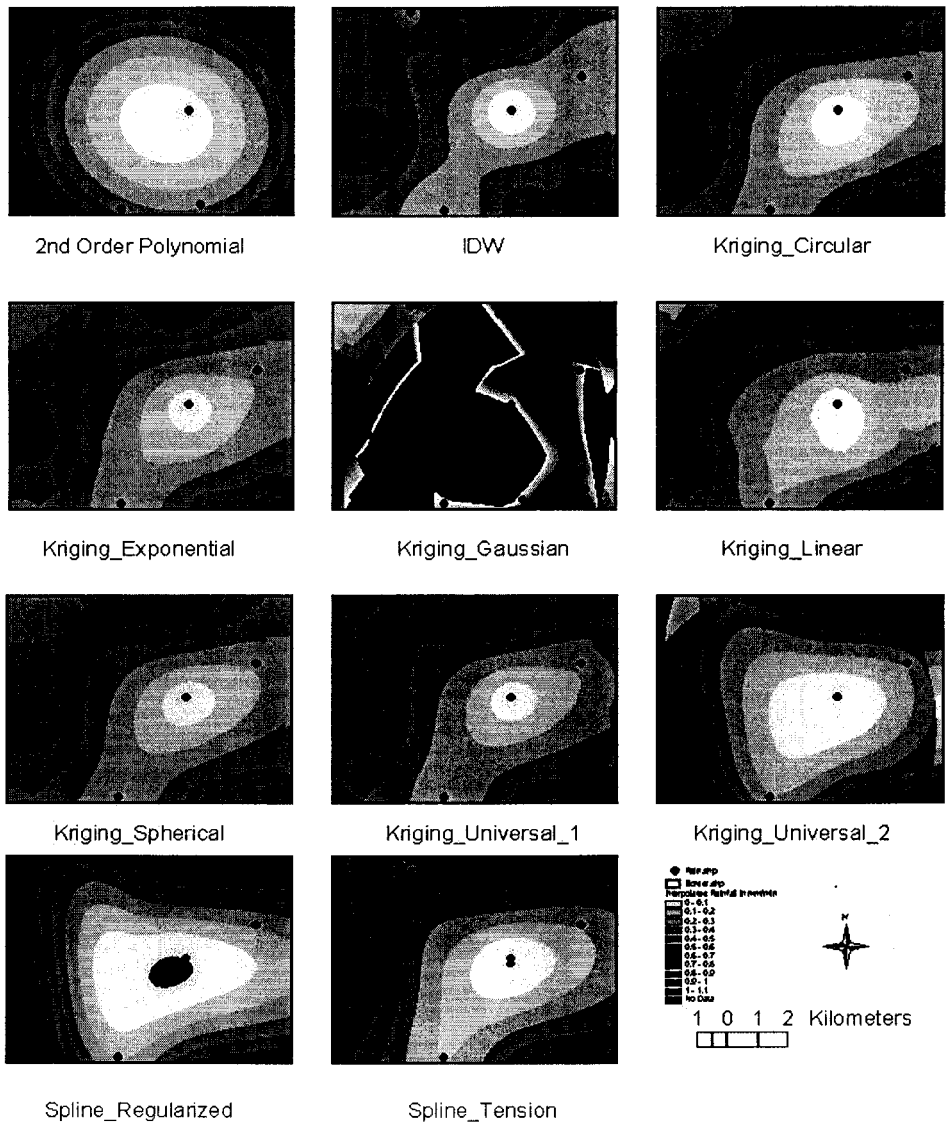


**Figure 5.16b:** Interpolated grids from all gauges (except RBG) using the different interpolation techniques for the Event 22091989 at minute 1244, which is 8:44 PM. Note the black spots at the center of the area when using techniques Kriging_Gaussian, Spline_Regularized, and Spline_Tension. These spots represent negative values in the case of Spline and high positive values in the case of Kriging.

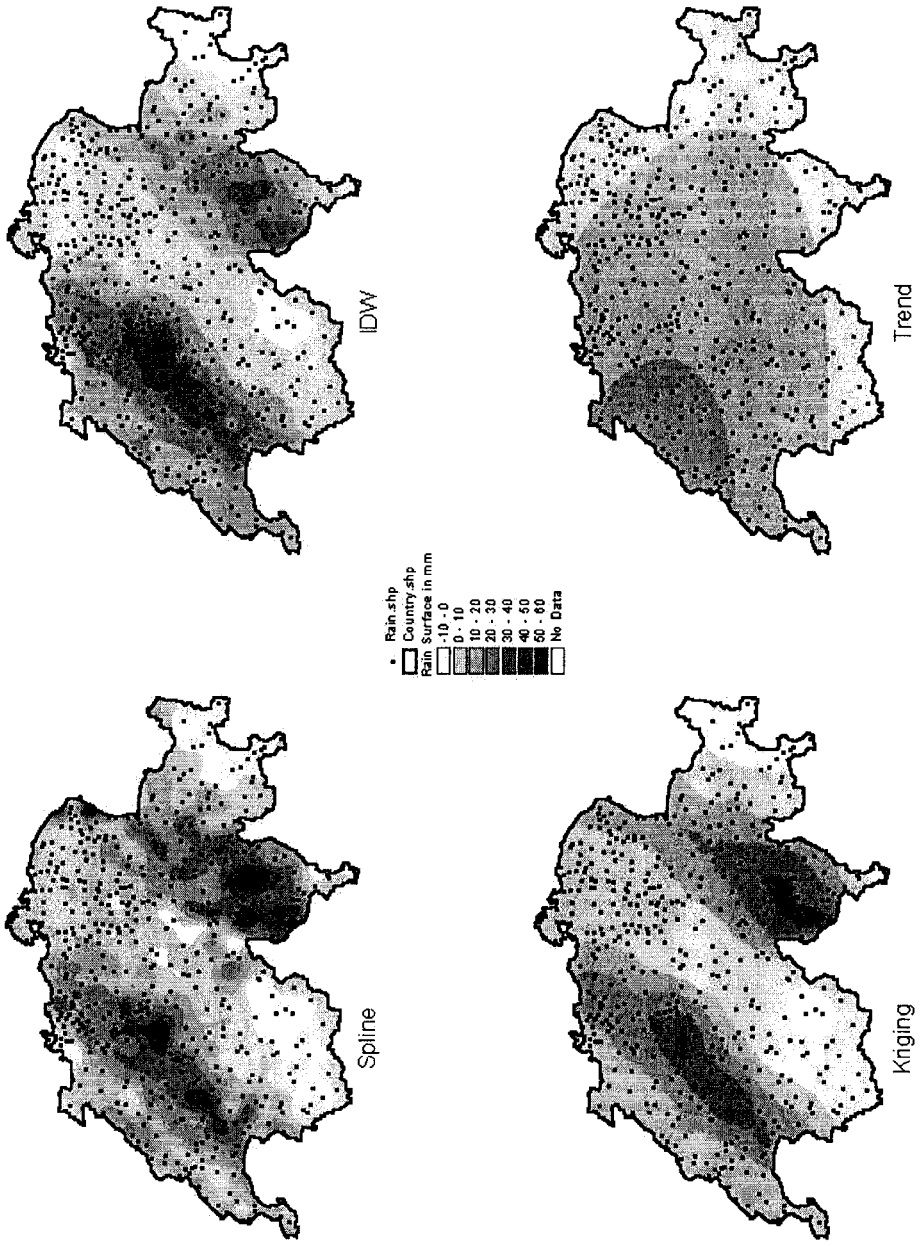


**Figure 5.17:** A visual comparison between four interpolation techniques

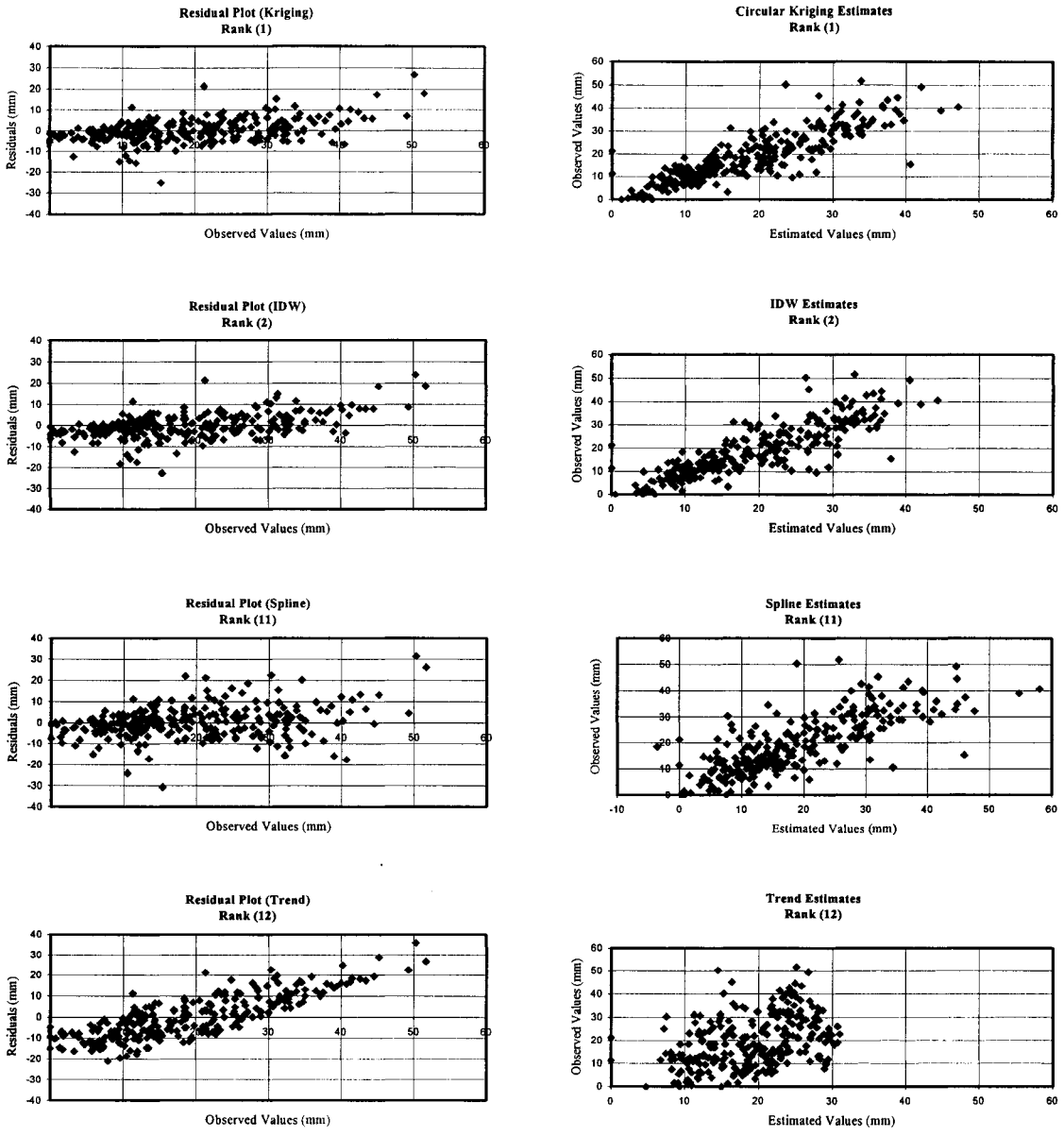


**Figure 5.18:** Observed rainfall versus estimated rainfall plots as well as residual plots using four interpolation techniques.

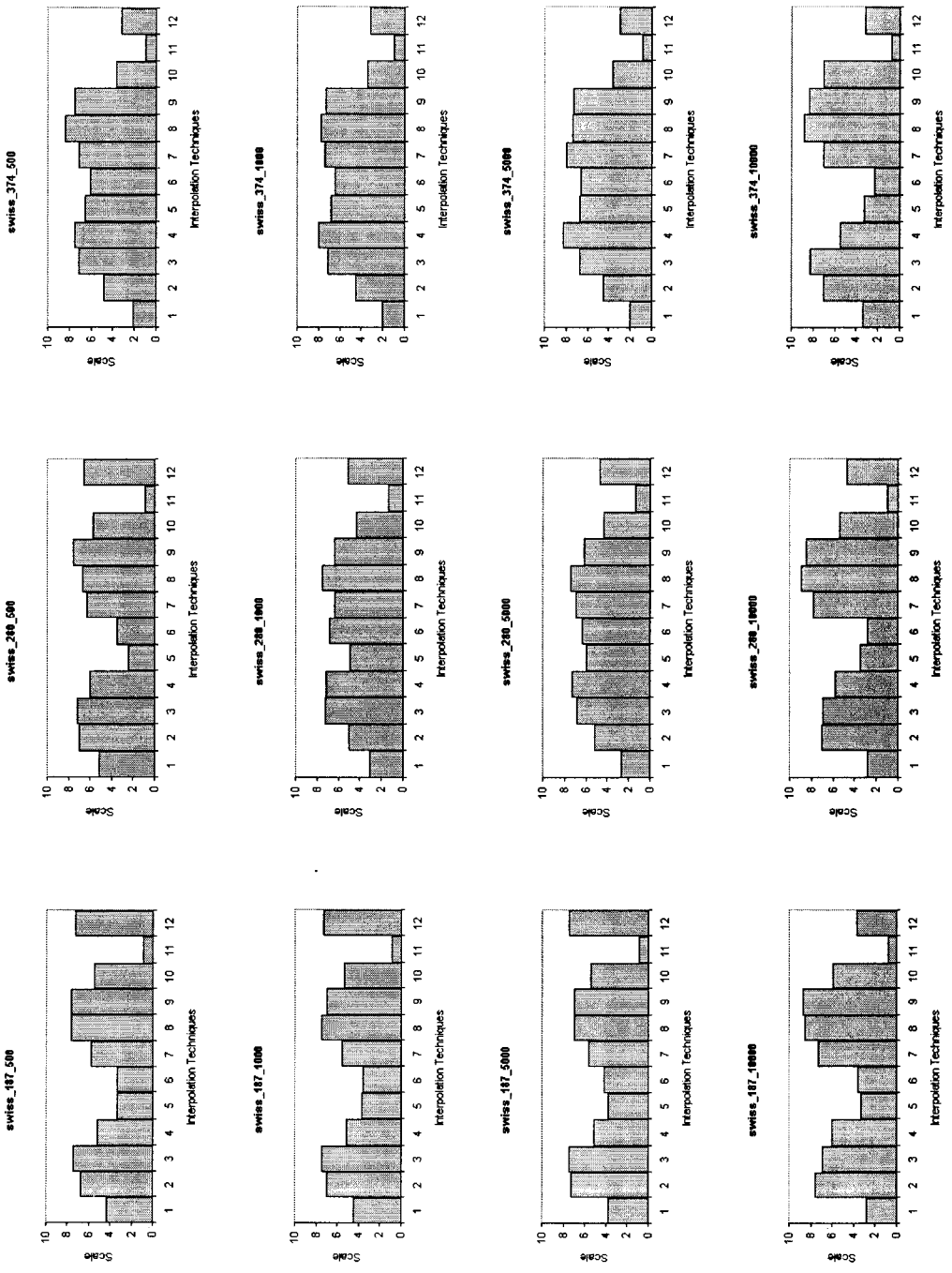


**Figure 5.19:** Performance of all interpolation techniques for the 12 runs.

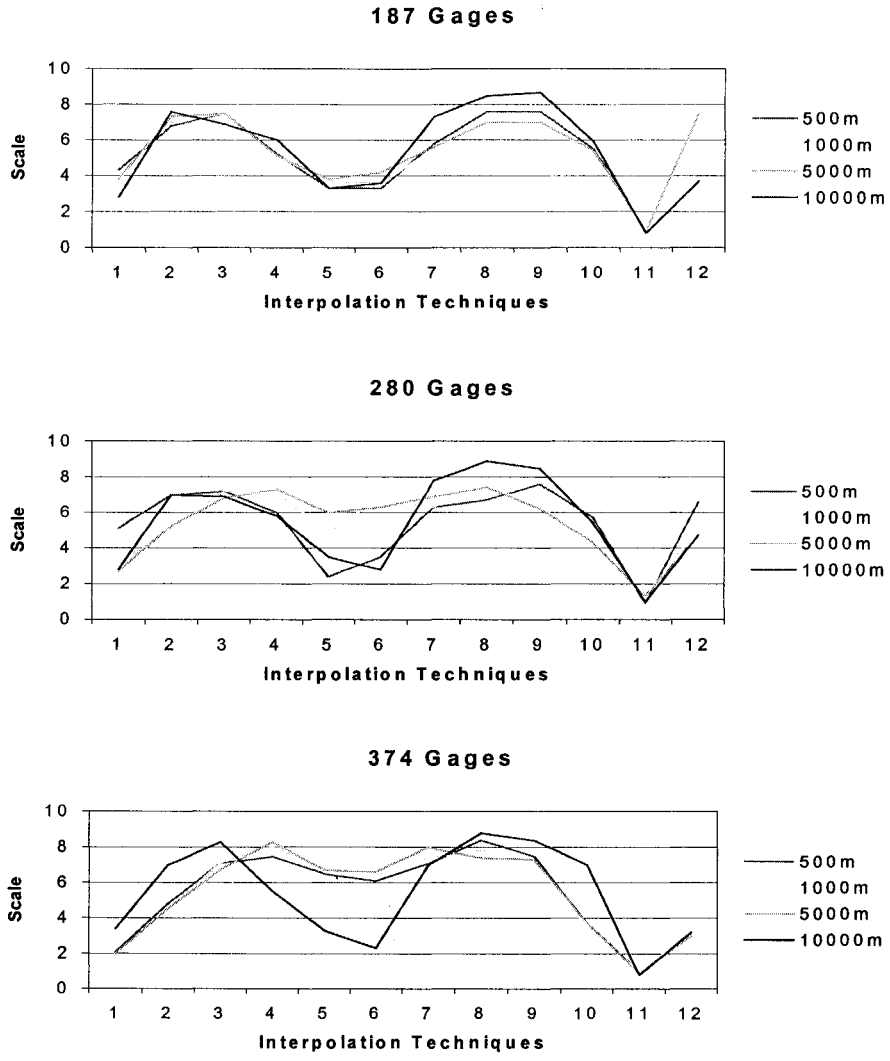


**Figure 5.20a:** The effect of changing the cell size on the performance of the interpolation techniques.

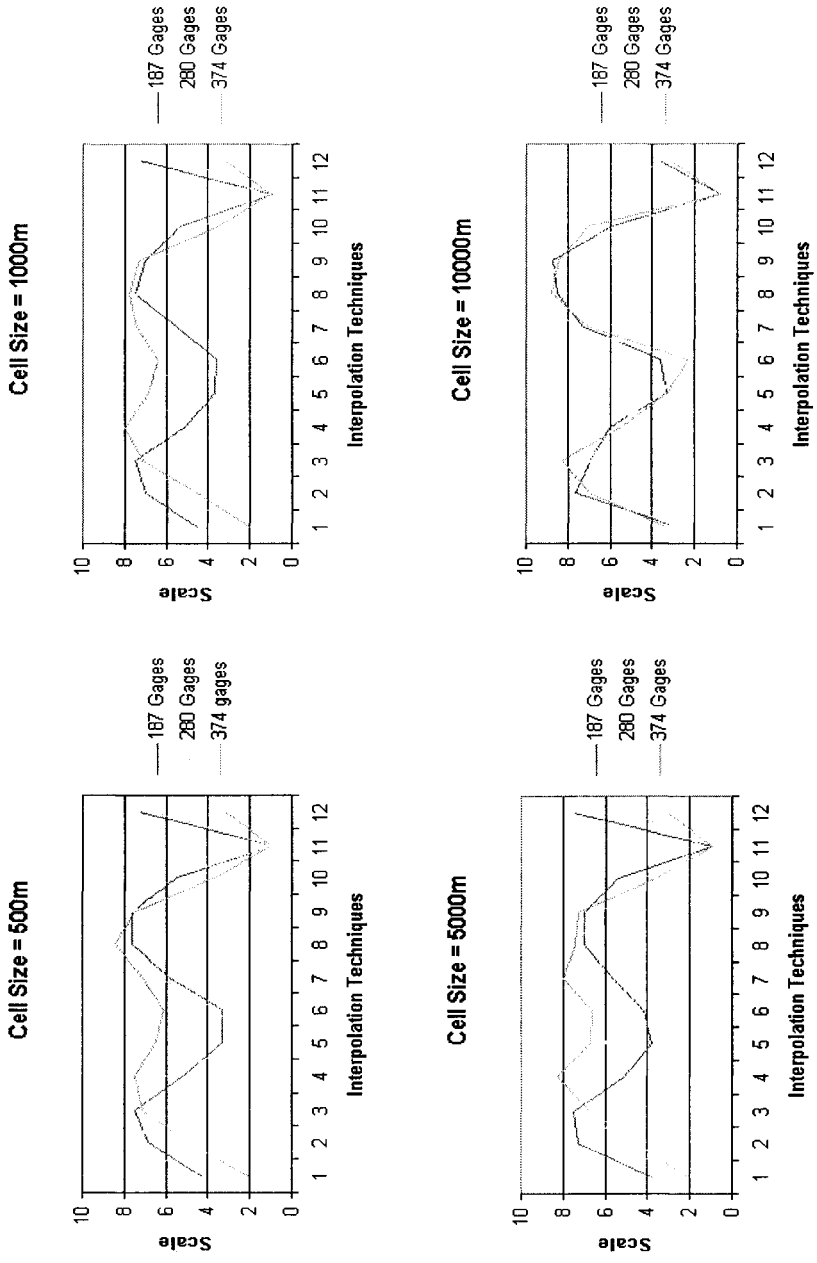


**Figure 5.20b:** The effect of changing the number of gauges used for interpolation on the performance of the interpolation techniques.

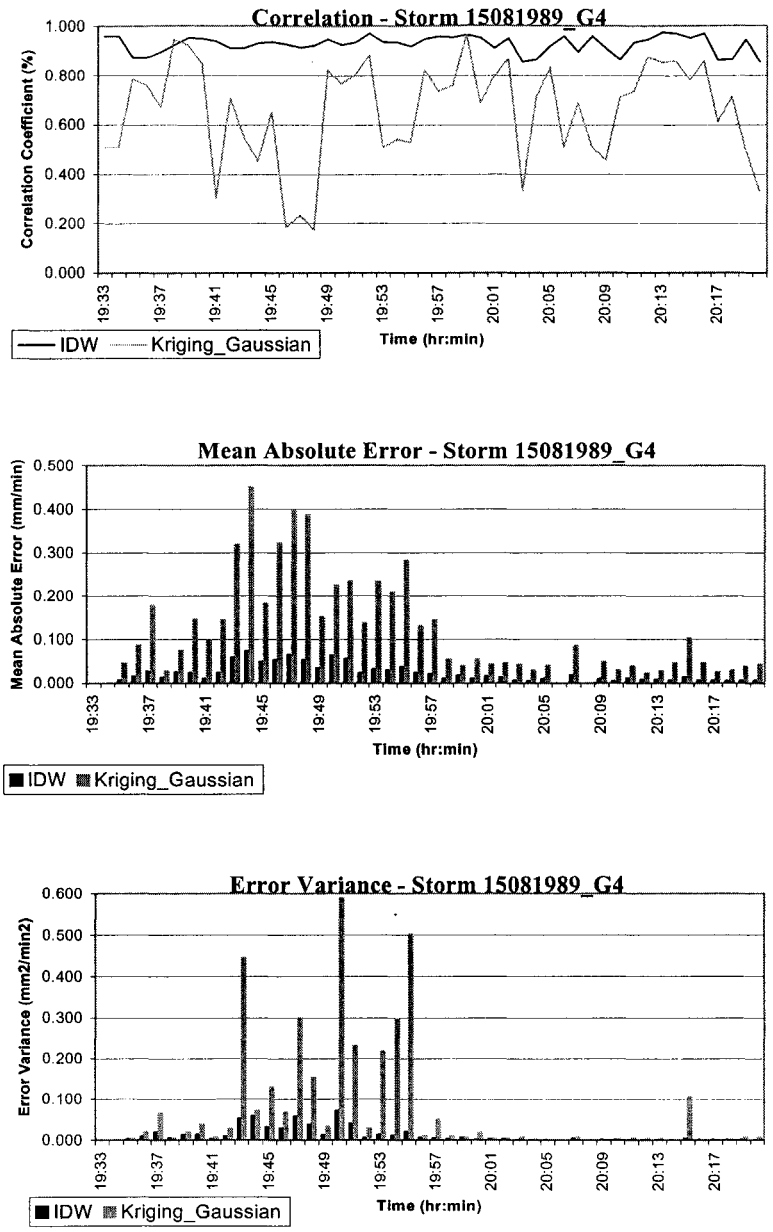


**Figure 5.21a:** A comparison of the IDW and Kriging_Gaussian techniques using the coefficient of correlation, mean absolute error, and error variance for the storm 15081989_G4 at each time step.

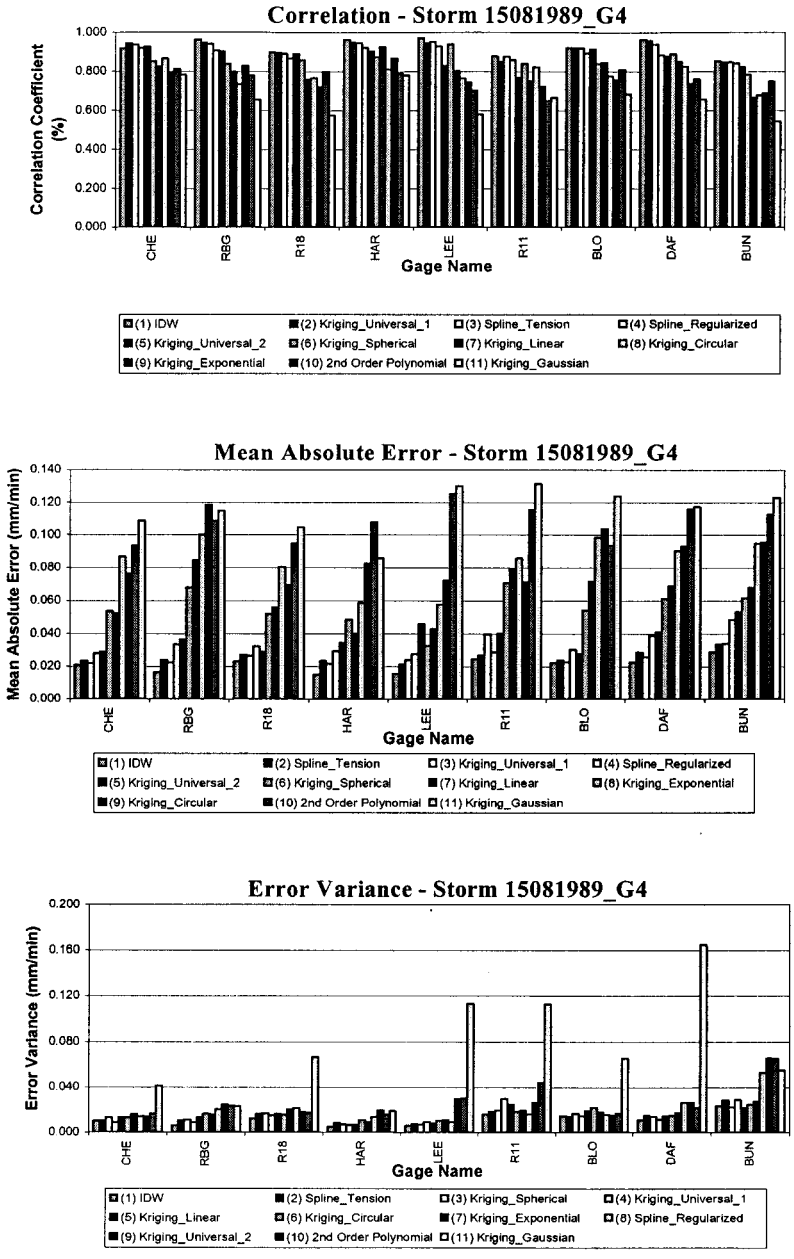


**Figure 5.21b:** A comparison of all techniques using the coefficient of correlation, mean absolute error, and error variance for the storm 15081989_G4 at each gauge.

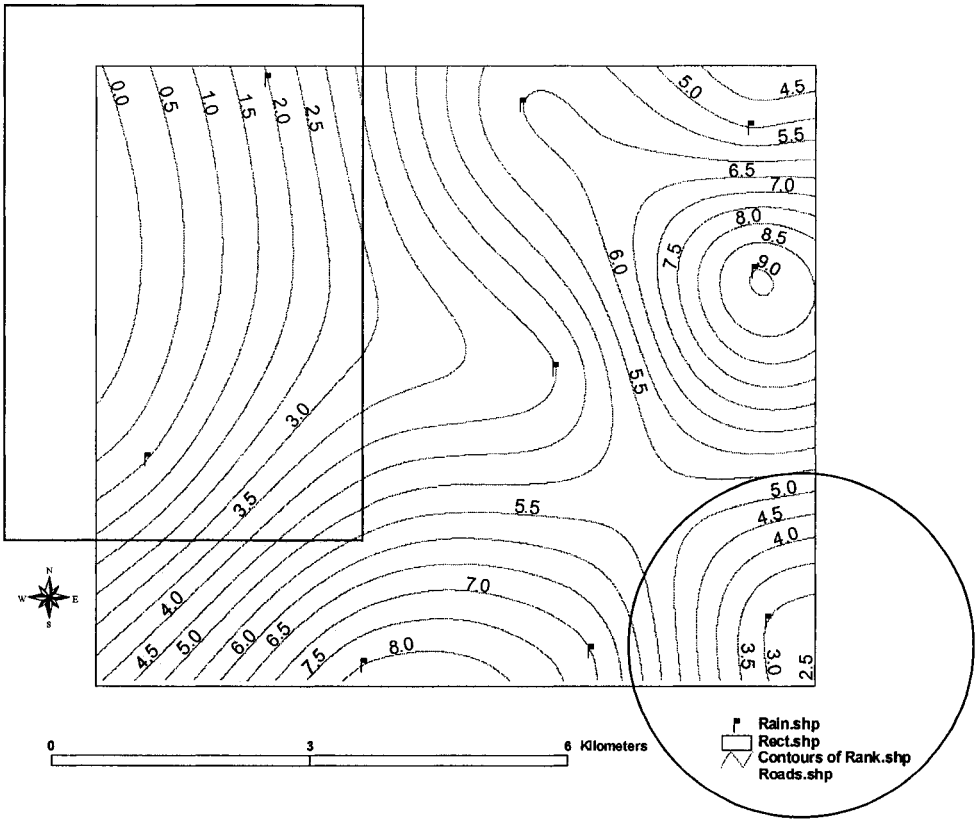


**Figure 5.22:** Contours of the ranked gauges.
Low numbers for rank contours indicate that these areas are of demand for more gauges.
Large numbers show that gauges on this region are sufficient.

**Table 5.1:** The names and locations of the rain gauges within the Hamilton-Wentworth region.

| No. | Station Name | ID | Latitude | Longitude | Location of Raingauge | City/Town |
|---|---|---|---|---|---|---|
| 1 | Chedoke Works Yard | CHE | 43-15-02 | 79-54-26 | Regional Works Yard next to Chedoke Public Golf Course | Hamilton |
| 2 | Westdale Royal Botanical Garden | RBG | 43-15-56 | 79-51-27 | RBG Childrens Garden at North end of Marion Ave. | Hamilton |
| 3 | Ancaster Water Resrvoir 18 | R18 | 43-12-40 | 79-55-52 | Water Res. W-h18 on Rymal Rd. west of Glencaster Rd. | Ancaster |
| 4 | Harmony Hall Sewage P.S. | HAR | 43-12-36 | 79-57-49 | Sewage P.S. S-H8 at south end of Harmony Hall Dr. | Ancaster |
| 5 | Lee Smith Water P.S. | LEE | 43-13-54 | 79-59-39 | Water P.S. W-H22AS on Sulphur Spring Rd. at Woodview Cr. | Ancaster |
| 6 | Dundas Water Reservoir 11 | R11 | 43-16-16 | 79-58-35 | Water Res. W-H11s on Woodley's Lane off Hwy. 8 | Dundas |
| 7 | Dundas WWTP Blower Building | BLO | 43-16-06 | 79-56-23 | Dundas WWTP Blower Bldg. On King St. west of Olympic Dr. | Dundas |
| 8 | Daffodil Cr. Sewage P.S | DAF | 43-14-26 | 79-56-08 | Sewage P.S S-H20 on Daffodil Cr. (north leg) | Ancaster |
| 9 | Garth St. Water Reservoir (The Bunker) | BUN | 43-12-51 | 79-54-21 | Water Res. W-H6A at Garth St. & Stonechurch Rd. | Hamilton |

**Table 5.2a:** The start time, end time, duration, and type of each of the sixteen events used in this study.

| No. | Event | Event Name | Julian Day | Start Time | End Time | Duration | Event Type |
|---|---|---|---|---|---|---|---|
| 1 | Event 1/9/1988 - Group No. 1 | 01091989_G1 | 244 | 6:10 AM (370 min) | 6:50 AM (410 min) | 40 minutes | Average |
| 2 | Event 1/9/1988 - Group No. 2 | 01091989_G2 | 244 | 12:34 PM (754 min) | 1:44 PM (824 min) | 70 minutes | Average |
| 3 | Event 1/9/1988 - Group No. 3 | 01091989_G3 | 244 | 3:10 PM (910 min) | 4:14 PM (974 min) | 64 minutes | Average |
| 4 | Event 2/6/1989 | 02061989 | 153 | 5:40 AM (340 min) | 6:30 AM (390 min) | 50 minutes | Small |
| 5 | Event 4/8/1989 | 04081989 | 216 | 3:20 PM (920 min) | 3:57 PM (957 min) | 37 minutes | Average |
| 6 | Event 8/9/1988 | 08091989 | 251 | 8:50 AM (530 min) | 9:20 AM (560 min) | 30 minutes | Small |
| 7 | Event 9/6/1988 | 09061989 | 160 | 4:00 PM (960 min) | 5:15 PM (1035 min) | 75 minutes | Average |
| 8 | Event 15/8/1989 - Group No. 1 | 15081989_G1 | 227 | 12:00 Noon (720 min) | 12:20 PM (740 min) | 20 minutes | Small |
| 9 | Event 15/8/1989 - Group No. 2 | 15081989_G2 | 227 | 2:05 PM (845 min) | 2:38 PM (878 min) | 33 minutes | Small |
| 10 | Event 15/8/1989 - Group No. 3 | 15081989_G3 | 227 | 6:27 PM (1107 min) | 7:17 PM (1157 min) | 50 minutes | Small |
| 11 | Event 15/8/1989 - Group No. 4 | 15081989_G4 | 227 | 7:33 PM (1173 min) | 8:20 PM (1220 min) | 47 minutes | Average |
| 12 | Event 22/9/1989 | 22091989 | 265 | 7:30 PM (1170 min) | 9:40 PM (1300 min) | 130 minutes | Large |
| 13 | Event 30/5/1989 - Group No. 1 | 30051989_G1 | 150 | 4:00 AM (240 min) | 5:22 AM (322 min) | 82 minutes | Average |
| 14 | Event 30/5/1989 - Group No. 2 | 30051989_G2 | 150 | 8:20 PM (1220 min) | 9:20 PM (1280 min) | 60 minutes | Small |
| 15 | Event 30:31/5/1989 - Group No. 1 | 31051989_G1 | 150/151 | 11:30 PM (1410 min) | 0:40 AM (next day) (1480 min) | 70 minutes | Average |
| 16 | Event 31/5/1989 - Group No. 2 | 31051989_G2 | 151 | 9:50 PM (1310 min) | 10:20 PM (1340 min) | 30 minutes | Small |

**Table 5.2b:** The rainfall accumulation (in mm) at each gauge for all the events.

| No. Event | Rainfall Accumulation (mm) | | | | | | | | |
|---|---|---|---|---|---|---|---|---|---|
| | CHE | RBG | R18 | HAR | LEE | R11 | BLO | DAF | BUN |
| 1 Event 1/9/1989 - Group No. 1 | 4.83 | 7.14 | 3.52 | 4.00 | 4.75 | 6.20 | 8.82 | 5.28 | 2.86 |
| 2 Event 1/9/1989 - Group No. 2 | 6.94 | 5.67 | 9.68 | 8.80 | 7.03 | 7.40 | 7.14 | 7.92 | 6.82 |
| 3 Event 1/9/1989 - Group No. 3 | 14.91 | 12.60 | 11.22 | 12.00 | 9.50 | 10.20 | 11.34 | 1.54 | 12.32 |
| 4 Event 2/6/1989 | 3.18 | 3.18 | 0.44 | 0.40 | 2.85 | 3.00 | 2.73 | 4.18 | 0.66 |
| 5 Event 4/8/1989 | 7.98 | 10.08 | 5.94 | 5.60 | 10.64 | 11.80 | 7.98 | 8.36 | 3.96 |
| 6 Event 8/9/1989 | 6.30 | 2.94 | 1.76 | 1.60 | 2.47 | 7.60 | 5.88 | 4.62 | 1.54 |
| 7 Event 9/6/1989 | 5.05 | 5.46 | 18.70 | 5.60 | 5.51 | 8.40 | 5.88 | 11.44 | 4.84 |
| 8 Event 15/8/1989 - Group No. 1 | 0.02 | 1.69 | 0.00 | 0.00 | 0.38 | 3.20 | 1.26 | 0.00 | 0.00 |
| 9 Event 15/8/1989 - Group No. 2 | 1.08 | 0.43 | 0.00 | 0.00 | 0.00 | 6.60 | 3.15 | 0.22 | 0.00 |
| 10 Event 15/8/1989 - Group No. 3 | 2.55 | 2.96 | 4.62 | 2.20 | 0.95 | 0.80 | 1.89 | 1.54 | 3.96 |
| 11 Event 15/8/1989 - Group No. 4 | 9.67 | 4.62 | 11.22 | 10.40 | 6.65 | 7.00 | 6.30 | 4.40 | 12.54 |
| 12 Event 22/9/1989 | 37.38 | 34.44 | 37.84 | 31.40 | 29.07 | 28.20 | 29.61 | 0.44 | 44.22 |
| 13 Event 30/5/1989 - Group No. 1 | 8.42 | 5.89 | 14.08 | 11.40 | 7.98 | 10.00 | 4.20 | 8.80 | 10.12 |
| 14 Event 30/5/1989 - Group No. 2 | 3.61 | 4.22 | 3.30 | 2.60 | 0.95 | 6.60 | 2.52 | 2.20 | 3.08 |
| 15 Event 30:31/5/1989 - Group No. 1 | 8.83 | 13.66 | 8.14 | 8.60 | 9.12 | 10.40 | 7.14 | 9.24 | 6.38 |
| 16 Event 31/5/1989 - Group No. 2 | 5.26 | 3.79 | 2.42 | 4.00 | 3.42 | 0.00 | 1.89 | 3.08 | 3.08 |

**Table 5.3a:** An ascending ranking of the spatial interpolation techniques based on the evaluation criteria. An overall ranking was also obtained.

| Interpolation Technique | Correlation Coefficient | Mean Absolute Error | Coefficient of Determination | Standard Deviation of Absolute Errors | Error Variance | overall Ranking |
|---|---|---|---|---|---|---|
| IDW | 1 | 1 | 1 | 1 | 1 | 1 |
| Spline_Tension | 3 | 2 | 3 | 2 | 2 | 2 |
| Kriging_Universal_1 | 2 | 3 | 2 | 3 | 3 | 3 |
| Kriging_Spherical | 5 | 6 | 4 | 4 | 4 | 4 |
| Spline_Regularized | 4 | 4 | 5 | 8 | 8 | 5 |
| Kriging_Linear | 7 | 7 | 7 | 5 | 5 | 6 |
| Kriging_Exponential | 8 | 8 | 8 | 6 | 6 | 7 |
| Kriging_Universal_2 | 6 | 5 | 6 | 9 | 10 | 8 |
| Kriging_Circular | 9 | 9 | 9 | 7 | 7 | 9 |
| 2nd Order Polynomial | 10 | 10 | 10 | 10 | 9 | 10 |
| Kriging_Gaussian | 11 | 11 | 11 | 11 | 11 | 11 |

A technique that is very informative should reflect:
1) the highest correlation Coefficient
2) the lowest mean square error
3) the highest coefficient of determination
4) the lowest error standard deviation
5) the lowest error variance

A technique that is NOT very informative should reflect:
1) the lowest correlation Coefficient
2) the highest mean square error
3) the lowest coefficient of determination
4) the highest error standard deviation
5) the highest error variance

**Table 5.3b:** An ascending ranking of gauge importance based on the evaluation criteria. An overall ranking was also obtained.

| Gauge | Correlation Coefficient | Mean Absolute Error | Coefficient of Determination | Standard Deviation of Absolute Errors | Error Variance | overall Ranking |
|---|---|---|---|---|---|---|
| LEE | 1 | 2 | 1 | 2 | 2 | 1 |
| R11 | 2 | 1 | 2 | 1 | 3 | 2 |
| BUN | 3 | 4 | 3 | 4 | 1 | 3 |
| DAF | 5 | 3 | 5 | 3 | 5 | 4 |
| RBG | 4 | 5 | 4 | 5 | 7 | 5 |
| BLO | 7 | 7 | 7 | 6 | 6 | 6 |
| R18 | 6 | 9 | 6 | 9 | 4 | 7 |
| HAR | 8 | 6 | 8 | 7 | 8 | 8 |
| CHE | 9 | 8 | 9 | 8 | 9 | 9 |

A gauge that is very important should reflect:
1) the lowest correlation Coefficient
2) the highest mean square error
3) the lowest coefficient of determination
4) the highest error standard deviation
5) the highest error variance

A gauge that is NOT very important should reflect:
1) the highest correlation Coefficient
2) the lowest mean square error
3) the highest coefficient of determination
4) the lowest error standard deviation
5) the lowest error variance

# CHAPTER 6

# MODELING OROGRAPHIC PRECIPITATION USING GIS-BASED MULTIPLE LINEAR REGRESSION METHOD

In this chapter, the development of a new ArcView GIS-based spatial interpolation module that adopts the multiple linear regression technique is presented. The functionality of the GIS module is illustrated through a case study on the island of Crete in Greece, as the models generated were applied to locations where estimates of annual precipitation were required. The response variable is "Precipitation" and the predictor variables are "Elevation", "Longitude" and "Latitude" or any combination of these. The module is capable of performing a sequence of tasks, leading to the estimation of mean areal and total volume of precipitation. In addition, it can generate up to nine predictor variables and their parameters and can estimate areal rainfall for a user-specified three dimensional extent. The developed module performed satisfactorily. Precipitation estimates at ungauged locations were obtained using the multiple linear regression method in addition to some conventional spatial interpolation techniques (i.e. IDW, Spline, Kriging, etc).

A multi-scale precipitation analysis was performed on areas ranging from larger areas (the whole island and the northern, southern, and eastern parts of the island), to medium size areas (watersheds), to smaller areas (sub-basins).

## 6.1 Introduction

The rapid development in Geographic Information Systems (GIS) originally inspired hydrologists to develop new models to work within the GIS environment. GIS can integrate databases, extract the needed parameters for different modelling applications, and process and display the results. However current GIS packages are in some cases difficult to use and offer limited functions to support environmental modelling (Strebel at al., 1994; Steyaert and Goodchild, 1994; Maidment, 1996; Sui and Maggio, 1999; Paniconi et al., 1999). Such limitations include lack of efficient data conversion algorithms, static representations of multiple temporal and spatial data, weak tools for information extraction and aggregation, limited capabilities for managing large numbers of data sets and dealing with relationships among the data sets, and inability to assess and communicate uncertainties introduced by imprecision and incompleteness (Jelinski et al., 1994; Stafford et al., 1994; Burrough et al., 1996; Goodchild 1996; Taylor et al., 1999; Paniconi et al., 1999; He et al., 2001). To overcome these problems, four approaches are presented in the literature to link GIS to environmental modelling. (1) embedding GIS-like functionality into the models where GIS is used as a mapping tool only. This approach lacks the capabilities of management and visualization of spatial data; (2) embedded modelling in GIS such as ESRI's ArcStorm and ArcView Hydrologic Modelling. This approach utilizes the full capabilities of GIS, but the

modelling functionalities tend to be simplistic and need to be validated; (3) loose coupling where GIS is used to generate model input files and display model output data independent of models; (4) tight coupling where GIS and the models are integrated via a common user interface that is developed by either GIS macros and scripts or by conventional programming. User-written libraries or routines are incorporated into a GIS and are called through the pull-down menu of the GIS package (Sui and Maggio, 1999; He at al., 2001).

In this chapter, the tight coupling approach is adopted using ArcView Avenue (ArcView GIS programming language) scripts, Fortran, International Mathematical and Statistical Libraries (IMSL), ArcView Dialog Designer, and Batch Programming and a developed drop-down menu. The ArcView project consists of six modules:(1) spatial input data preparation; (2) database accessing tool; (3) parameter generator; (4) model executor; (5) output visualizer; (6) output report generator, that includes spatial statistical information in addition to a printing tool. The ArcView GIS Regression Utility (AVRU) was developed to accommodate the great amount of work that initially had to be done using different software simultaneously, including ArcView, S+ for ArcView, Minitab, and MS Office (Word & Excel). The functionality of this module is presented in an application of the spatial variation of orographic precipitation on the island of Crete by means of the multiple linear regression method.

The distribution of precipitation depends upon latitude, orographic factors (as discussed in Chapter 3), and the distance the air mass moves away from the source of moisture. The *continentality* of an area is determined by the distance from the shore. Although there is no simple relation between the distance from the shore and continentality, it is clear that temperature ranges are greater over continental masses than elsewhere. These temperature variations also affect precipitation and the type of precipitation. The *direction of prevailing wind* can be determined by the direction of storm movements. The direction of prevailing wind also indicates the susceptibility of an area to the influence of the storm systems. *Topography* refers to the nature and elevation of land masses. Mountains, valleys, and all variations of these features are part of topography. A low pressure system picks up moisture over the ocean and transports that moisture over land. If that system is forced to move from sea level up over mountains, it will encounter cooler temperature at higher elevations, which will cause loss of moisture. If a low-pressure system moving from west to east and has to cross several high elevations (or mountains) that are situated north-south, it will give out some of its moisture on each one of those mountains. If there is no additional source of moisture, the far east side of the elevations will receive little, if any, moisture. If those mountains are oriented east-west, however, the effect will cause less moisture to be lost. This is known as the *orientation of topography* factor. If two stations are on the same elevation on a mountain slope but on opposite sides of the mountain, the *aspect* factor will

determine which station will get the greater amount of precipitation. The station with less precipitation is recognized as a "rain shadow" station. If the station is situated on a mountain slope, its aspect relative to the main axis of the mountain is measured in directional units of 10° clockwise from north.

## 6.2 Historical Documentation of Areal Precipitation Estimators

Most methods for estimating areal and gridded precipitation from point data would relate to any of these three major groups: graphical, topographical, and numerical. Graphical methods involve mapping of precipitation data, sometimes in combination with precipitation-elevation analyses, and include isohyetal mapping (Reed and Kincer 1917; Peck and Brown 1962) and Thiessen polygons (Thiessen 1911). Topographical methods involve the correlation of point precipitation data with an array of parameters such as slope, exposure, elevation, location of barriers, and wind speed and direction (Spreen 1947; Burns 1953; Schermerhorn 1967; Houghton 1979). Numerical methods involve the spatial interpolation techniques in which a numerical function is used to weight irregularly spaced point data to estimate a regularly spaced prediction grid. Inverse distance weighting (IDW) is an example of a simple numerical interpolation method. In this case, the weighting of the data points is prescribed to decrease as the distance between the points increases. Spline (or thin plate) interpolation is another method, which is distinguished by two main features: (a) the surface must pass exactly through the data points, and (b) the surface must have minimum curvature. Kriging is a geostatistical approach (Matheron 1971) that has been well received and recognized as a tool for the interpolation of many types of data, including precipitation (Chua and Bras 1982; Dingman et al. 1988; Phillips et al. 1992). In kriging, a semivariogram model that best fits the data is developed to derive optimum station weights for interpolation. A potential drawback of kriging is that it implicitly relies on the data to directly represent the spatial variability of the actual precipitation field (Daly et al. 1994). If the data are not representative as is often the case on a complex terrain, the accuracy of the resulting interpolated field will be in question. In addition, more than one semivariogram may be needed to estimate precipitation at various time periods. Another drawback, is the difficulty of developing a semivariogram for sparse networks. Linear trend surface is another interpolation method that uses a polynomial regression to fit a least-squares surface to the input points. It allows the user to control the order of the polynomial used to fit the surface. The surface generated will seldom pass through the original data points since it performs a best fit for the entire surface.

Attempts also were made to use digital elevation models (DEMs) to predict the physical influence of topographic factors on precipitation patterns (Peck and Schaake 1990; Fan and Duffy 1991; Hay et al. 1991; Daly et al. 1994). The PRISM model, which was developed by Daly et al. (1994), somewhat incorporates some general aspects of the physical

nature of the orographic influence on precipitation in addition to the analytical nature of the numerical approaches. However, it is highly unlikely to correctly identify the aspect (and the elevation) of each precipitation gauge using a DEM, especially if only relatively coarse elevation grids are available. Big complex terrain areas are better studied, in this case, when divided into smaller regions each of general aspect (facet).

### 6.2.1 Orographic Effects

The orographic influence occurs only in the proximity of high ground in the case of stable atmosphere. There are three main mountain effects: orographic lifting, thermal forcing, and obstacle effects which include mountain blocking, flow deflection, and the production of lee-side flow disturbances.

#### 6.2.1.1 Precipitation-Elevation Relationships

On a given mountain slope, precipitation typically increases with elevation (Alter 1919; Barrows 1933; Spreen 1947; Schermerhorn 1967; Hibbert 1977; Smith 1979). This phenomenon, commonly called the orographic effect, is evident worldwide. Depending on its size and orientation, a mountain or range of mountains can increase the intensity of cyclonic precipitation by retarding the rate of movement of the storm and causing forced uplift of the air mass (Barry and Chorley 1976; Marwitz, 1987). In summer, the orographic effect may trigger a conditional or convective instability in an otherwise stable air mass, producing a local redistribution of precipitation over the higher grounds (Daly et al. 1994). Under some conditions the relationship between precipitation and elevation may be best described log-linear or exponential functions, but the linear form is easy to use and appears to be an acceptable approximation in most situations (Daly et al. 1994).

#### 6.2.1.2 The Spatial Scale of Orographic Effects

Because we use a DEM as the source of spatially gridded elevation data, the scale at which orographic effects are observed is of great importance. There is an implicit mismatch in scale when using relationships between station point elevations and precipitation to estimate precipitation at DEM grid cells. The elevation at the center of a DEM grid cell does not represent the elevation at that point, but reflects an average elevation representing the entire grid cell. Therefore, the DEM cell elevation will rarely match the station elevation. Generally, the finer the resolution of the DEM, the more closely the elevation of the grid cell will match that of the point (Daly et al. 1994).

Also, the orographic scale depends on the scale of the prevailing storm type. Large-scale frontal systems have inherently larger scales than localized convective cells. The orographic scale illustrated in the data may also depend on the relationship between the scale of the topographic features involved and the density and placement of the data points (Daly

et al. 1994). Another potential factor is the temporal resolution of the data. Small-scale orographic effects may be more likely to be resolved in short term interval data than in data averaged over a long time period (Daly et al. 1994). The best DEM resolution therefore becomes a function of the scale of orographic effects, data density, and temporal resolution of the data.

6.2.1.3 The Spatial Patterns of Orographic Regimes

The characteristics of the relationship between measured precipitation and topographic factors can vary considerably from hillslope to hillslope, and are influenced, in addition to factors previously mentioned, by differences in steepness of the terrain, upwind barriers, and slope orientation. A usable relationship between precipitation and topographic factors is difficult to be determined, unless rainfall stations are grouped into regions that deal with these factors. To effectively model the spatial pattern of orographic precipitation in complex terrain, it is essential that topographic regions be recognized and isolated (Daly et al. 1994). A mountainous landscape can be divided into regions, each of which is assumed to experience a different orographic regime (in Section 6).

To summarize, although the demand for precipitation fields on a regular grid is growing dramatically, the lack of data for mapping orographic precipitation has always represented a problem when trying to develop precipitation grids for complex terrain. The purpose of this study is to develop a method for distributing point measurements of annual orographic precipitation to regularly spaced grid cells at different spatial scales by relating a spatial dependent variable (annual precipitation) to spatial independent or predictor variables (described above) by means of the multiple linear regression method.

## 6.3 Methodology

### 6.3.1 The Multiple Linear Regression Method

Statistical methods can always be used to describe the variation of a set of observations by focusing attention on the observations themselves rather than on the physical processes that produced them. One of those statistical methods is *regression*. Regression analysis is a technique for analyzing raw data and searching for the messages they contain, hence providing certain insights into how to plan the collection of data when the opportunity arises. In any system in which variable quantities change, it is of interest to examine the effects that some variables exert (or appear to exert) on others. There may, in fact, be a simple functional relationship between variables. In most physical processes, however, this is the exception rather than the rule. Often a functional relationship exists that is too complicated to describe in simple terms. In this case we may wish to approximate to this functional relationship by some simple mathematical function, such as polynomial, which contains the appropriate variables and which graduates or approximates to the true function

over some limited ranges of the variables involved. By examining such a graduating function we may be able to learn more about the underlying true relationship and appreciate the separate and joint effects produced by changes in certain important variables. Even where no sensible physical relationship exists between variables, we may wish to relate them by some sort of mathematical equation. While the equation might be physically meaningless, it may, nevertheless, be extremely valuable for predicting the values of some variables from knowledge of other variables, perhaps under certain stated restrictions (Draper and Smith 1998).

In this chapter, one particular method of obtaining a mathematical relationship is used. This involves the initial assumption that a certain type of relationship, linear in unknown parameters, holds. The unknown parameters are then estimated under certain other assumptions with the help of available data so that a fitted equation is obtained. The method of analysis used is the method of least squares (LS), which is simply a minimization of the sum of squares of deviation of the estimated values from the true values. The *ordinary* LS was favored over the *weighted* LS due to the few number of outliers in the area of study and their low departure form the norm. The model function is of a specified form that involves both the predictor variables and the parameters. The distribution of the random errors (random error = response variable - model function) is assumed to be normal distribution with mean zero, and errors are usually assumed to be independent. Various checks are performed thereafter, such as model significance, parameters significance, residual analysis, etc.

6.3.1.1 Inferences on Individual Parameters

Testing the significance of the model parameters ($\beta_i$) is done as follows: if we assume that the variations of the observations about the best-fit line are normal - that is, the errors $\varepsilon_i$ are all from the same normal distribution, $N(0, \sigma^2)$ - it can be shown that we can assign $100(1-\alpha)\%$ confidence limits for $\beta_i$ by calculating

$$\hat{b}_i \pm \frac{t_{(n-p,1-0.5\alpha)} s}{\{\Sigma(x_i - \bar{x})^2\}^{\frac{1}{2}}} \qquad (6.1)$$

where $\hat{b}_i$ : the estimate of $\beta_i$ ; s: the estimate of standard deviation $\sigma$; n: the sample size; $t_{(n-p,\ 1-0.5\alpha)}$ : the $100(1 - 0.5\alpha)$ percentage point of a t-distribution, with (n-p) degrees of freedom (the number of degrees of freedom on which the estimate of the variance $s^2$ is based); p : the number of parameters in the model; and $\bar{x}$ : the average value of $x_i$. On the other hand, if a test is appropriate, we can test the *null hypothesis* ($H_o$) that $\beta_i$ is equal to zero ($H_o$: $\beta_i = 0$)

against the *alternative hypothesis* ($H_1$) that $\beta_i$ is not equal to zero ($H_1$: $\beta_i \neq 0$) by comparing the $|t|$ with $t_{(n-p,\ 1-0.5\alpha)}$ from a t-table with (n-p) degrees of freedom. The test is a two-sided test conducted at the $100\alpha\%$ level of significance. The *null hypothesis cannot be rejected* if it happens that the observed $|t|$ value is smaller than the critical value and the parameter is insignificant; *reject the null hypothesis* however, if the observed $|t|$ value is greater than the critical value, making the parameter significant.

6.3.1.2 Analysis of Variance

The analysis of variance is an attempt to answer the question of how much of the variation in the data has been explained by the regression model. For any given linear model:

$$\begin{pmatrix}\text{Sum of squares}\\ \text{about the mean}\end{pmatrix} = \begin{pmatrix}\text{Sum of squares}\\ \text{due to regression}\end{pmatrix} + \begin{pmatrix}\text{Sum of squares}\\ \text{about regression}\end{pmatrix} \qquad (6.2)$$

This shows that of the variation in the data about their mean, some of the variation can be attributed to the regression and some to the fact that the actual observations do not all lie on the regression line. If they all did, the sum of squares (SS) about regression (residual sum of squares) would be zero, which yields a perfect regression model. Generally, it is favorable to see that the SS due to regression is much greater than the SS about regression. Any sum of squares is associated with a number called its *degrees of freedom*. This number indicates how many independent pieces of information involving the independent numbers are needed to compile the sum of squares. Due to regression, the SS is associated with a ($df_{Reg}$ = p-1) degrees of freedom, while the SS about regression is associated with a ($df_E$ = n-p) degrees of freedom.

6.3.1.3 Model Significance

An F-test is used to test the significance of regression. Since the sample variables are random variables, any function of them is also a random variable. Two particular functions are: 1) the mean square due to regression $\left(MS_{Reg} = \frac{SS_{Reg}}{df_{Reg}} = \frac{SS_{Reg}}{p-1}\right)$, and 2) the mean square due to residual variation $\left(MS_E = S^2 = \frac{SS_E}{df_E} = \frac{SS_E}{(n-p)}\right)$ and the ratio $\left(F = \frac{MS_{Reg}}{MS_E}\right)$, which follows an F-distribution with (p-1) and (n-p) degrees of freedom. If the test is appropriate, we can test the *null hypothesis* ($H_o$) that $\beta_i$ is equal to zero ($H_o$: $\beta_i = 0$) against the *alternative hypothesis* ($H_1$) that at least some $\beta_i$ are not equal to zero ($H_1$: at least some $\beta_i \neq 0$). The ratio $\left(F = \frac{MS_{Reg}}{MS_E}\right)$ is compared to the $100(1-\alpha)\%$ point of the tabulated $F_{(p-1,\ n-p)}$ distribution in order to determine whether or not the model is significant. It should be noted that just significant regressions may not predict well. Suppose we decide a specified risk level "$\alpha$". The fact that the observed

mean square ratio exceeds $F_{(p-1,\ n-p,\ 1-\alpha)}$ means that a "*statistically significant*" regression has been obtained. In other words, the proportion of the variation in the data, which has been accounted for by the fitted equation, is deemed greater than would be expected by chance in similar sets of data with the same values of $n$ and $x$. This does not necessarily mean that the fitted equation is useful for predictive purposes. Unless the range of values predicted by the fitted equation is considerably greater than the size of the random error prediction will often be of no value even though a "significant" F-value has been obtained, since the equation will be "fitted to the errors" only. For the purpose of this study, a ratio $\left(\frac{F_{Calcultaed}}{F_{Table}} \geq 2\right)$ is set as a criterion to reflect what is so-called a "*Descriptive Model*", while a ratio $\left(\frac{F_{Calculated}}{F_{Table}} \geq 4\right)$ reflects a "*Predictive Model*". Note that a predictive model is, in general, a better model than a descriptive one for estimating rainfall at ungauged points (locations).

6.3.1.4 Extra Sum of Squares Principle (Nested F-test)

In this study, the *stepwise regression* was used. The stepwise regression procedure starts off by choosing an equation containing the single best predictor variable and then attempts to build the model up with subsequent additions of predictor variables one at a time as long as these additions are worthwhile. After a variable has been added, the equation is examined to see if any variable should be deleted. The *extra sum of squares principle* simply answers that question by considering the extra portion of the regression sum of squares, which arises due to the fact that the terms under consideration are in the model. The mean square derived from this extra sum of squares can then be compared with the estimate $s^2$ to see if it appears significantly large. If it does, the terms should be included; if it does not, the terms would be judged unnecessary and can (though not necessarily) be removed. Generally, for the two models,

Model 1 (E1): $y = \beta_1 x_1 + \ldots\ldots\ldots\ldots + \beta_q x_q + \varepsilon_1$ (6.3)

Model 2 (E2): $y = \beta_1 x_1 + \ldots\ldots\ldots\ldots + \beta_q x_q + \beta_{q+1} x_{q+1} + \ldots\ldots\ldots\ldots + \beta_y x_y + \varepsilon_2$ (6.4)

There are a few extra terms in Model 2 which, if adequate, should be able to explain some of the residual sum of squares of Model 1, in this case, the *null hypothesis* ($H_o$: $\beta_{q+1} = \ldots\ldots = \beta_y = 0$) against the *alternative hypothesis* ($H_1$: $\beta_{q+1}, \ldots\ldots, \beta_y \neq 0$). The extra sum of squares is explained by ($\beta_{q+1}, \ldots\ldots, \beta_y$) is ($SS_{E1} - SS_{E2}$) with a (y-q) degrees of freedom. If that holds, the ratio $\left(\frac{(SS_{E1} - SS_{E2})/(y-q)}{SS_{E2}/(n-y)}\right)$ should be greater than, or equal to, the 100(1 - α)% point of the tabulated $F_{(y-q,\ n-y)}$ distribution. For the purpose of this study, α is always assigned the value 0.05.

6.3.1.5 $R^2$ Statistic

The coefficient of determination ($R^2$) is often used as a convenient measure of the success of the regression equation in explaining the variation in the data. It is expressed as the percentage ratio of the SS caused by the regression to the total sum of squares. Ideally, the value of $R^2$ could be 100%, however, practically, it should not be no matter how good the model is. The $R^2$ value could increase in some cases where the extra sum of squares test disapproves the extra terms. This takes place when the degrees of freedom are consumed due to the increase in the number of parameters in the model, therefore approaching the saturation point, i.e. number of parameters (y) ≈ sample size (n).

6.3.2 ArcView GIS Project

The ArcView Regression Utility (AVRU) is a project setup to perform the tasks in sequence through a drop-down menu in the ArcView GIS package. The AVRU project is set up as described below.

1. The initial step deals with a projection of the view where the work is taking place. The projection is of a primary importance since the longitude and latitude variables are extracted based on the map units according to the projection.
2. The Digital Elevation Model (DEM) is the backbone of the project as it provides numerical values for the independent variables, and its grid cells are the platform of the execution stage when mean areal precipitation is estimated. The DEM can be generated, clipped to a desired shape, and modified to a set resolution.
3. The rain gauges shapefile is the connection between the database accessing tool and the parameter generator. The user is able to derive the three spatial predictor variables (x, y, z) of the gauges. The three variables will be derived and stored in three columns in the attribute table of the shapefile.
4. The database is then accessed preparing to extract the user-specified data (i.e. the response variable: precipitation), which can be either monthly or yearly. Similarly, the response variable is stored as a column in the attribute table of the raingauges shapefile.
5. The parameter generator uses the information derived in the previous steps to generate the parameters based on the Least Squares (LS) method. The parameters and the coefficient of determination are then stored in one file.
6. Using the parameters generated and the DEM, the mean areal precipitation (in mm) and the total volume of precipitation water (in $m^3$) are estimated.
7. A point shapefile is generated with the amounts of precipitation recorded in one column at each point for future reference.
8. A text format report summarizing the results for the case under investigation is generated, and can be printed from within ArcView.

## 6.4 Case Study

The island of Crete, in Greece, was chosen in order to study the spatial variation in precipitation in small and medium size mid-latitude areas, where orographic effects tend to increase both frequency and intensity of winter precipitation. The island of Crete in Greece occupies the southern part of the country of Greece (as shown in Figure 6.1) with an area of 8265 $km^2$ which is almost 6.3% of the area of Greece. Crete has a mean elevation of 482 m and an average slope of 228 m/km. The island is divided into four counties (Lassithi, Iraklio, Rethymno, and Chania). Most agricultural activity takes place in the county of Iraklio (2626 $km^2$). The remaining counties, in order of agricultural activity, are: Lassithi (1810 $km^2$), Chania (2342 $km^2$) and Rethymno (1487 $km^2$).

Monthly precipitation data was compiled by the Hellenic National Meteorological Service and other government agencies for seventy seven (77) precipitation stations representing the island (refer to Figure 6.1). The locations of the stations were provided in degrees, minutes, and seconds. The stations mainly cover the eastern part of the island, which has a higher level of agricultural activity and tourism than the western part. The counties of Iraklion, Lassithi, Chania and Rethymno were covered by 35, 17, 16 and 9 gauges, respectively. Six gauges (two in Iraklion, one in Lassithi, and three in Chania) recorded only for four or five years, while the rest recorded for 12 to 50 years. The gauges were located at elevations that ranged from mean sea level (MSL) in the county of Iraklio to 905m above MSL in the county of Lassithi. The GIS coverages used in this study were based on maps developed by the Greek Army Geographical Service.

A digital elevation model (DEM) with a cell size of 30 m and a grid of 3027 rows and 8659 columns was generated from the spot elevation values and a 20-m contour map. As can be seen in Figure 6.2, a chain of high elevations lies across the island receiving fairly high amounts of precipitation and produces runoff that is generally greater in the western and northern parts of the island. The DEM is also used to check the altitude of the gauges and to delineate watersheds.

## 6.5 AVRU Structure

The developed drop-down menu of the project is accessed from the ArcView GIS interface as shown in Figure 6.3. In order for this project to work properly, the ArcView Extensions Dialog Designer and Spatial Analyst are part of the project.
In addition to the shapefiles and DEM used for the analysis, the project "mlr.apr" is composed of ten other facilities:

1. Sixty six Avenue scripts. The written scripts are either new or modified versions of existing scripts in the on-line help of ArcView . Some scripts may run independently

performing an individual task, and some can run in sequence performing one or several task(s).

2. Seven dialogs, which are used to facilitate the program-user interaction and execute the scripts.
3. One IMSL Stat Library (RLSE). This library is using the least-squares method to estimate the parameters for multiple linear regression.
4. Five input files - generated by ArcView GIS. Four of which are used by "mlr.exe" (msize.dat, multi.dat, multx.dat, multy.dat) and the fifth (xy.dat) is used by ArcView. The "msize.dat" file stores the sample size (n), which is also the dimension (x) of the arrays. The "multi.dat" stores the data required by the library, which includes the number "1" if there is an intercept in the model or the number "0"if there is no intercept, the number of variables (up to nine), the sample size and the number of terms in the equation (which is equal to the number of parameters). The "multx.dat" has the numerical values for the predictor variables and the "multy.dat" stores the observed values for response variable. The "xy.dat" holds the extent information of the DEM to be used by AVRU when estimating the mean areal precipitation.
5. One output file, generated by "mlr.exe" (mult.out) that has the numerical values for the parameters as well as the coefficient of determination. Any unused variable is assigned a corresponding "zero" parameter value.
6. One database file (par.dbf) in which all generated parameters are stored. The file is used in the final stage (execution) to extract the parameters.
7. An HTML file for project description (help.html). This contains extensive documentation of the study, with text and images using the Microsoft FrontPage® HTML format providing links to the Avenue scripts and samples of input and output files.
8. Two simple Fortran codes (mlr1.f & mlr2.f). In the first file, the IMSL library is included, the dimension (x) of the arrays is read to be used in the second code. The second program (subroutine) is called from within the first. The second file includes read statements for the rest of input files, calls the external IMSL Stat Library (RLSE), and generates the output file.
9. One executable file (mlr.exe) is generated from the Fortran code to estimate the parameters.
10. Two batch files (mlr.bat & print.bat) - which were written and executed from within ArcView. The first file is to execute the "mlr.exe" from its location and the second file is to print the generated report.

AVRU uses four main pieces of information from preparation to execution: the location of gauges, rainfall data, region boundary and a DEM for the region. The project consists of six modules, as described below.

6.5.1 Spatial Input Data Preparation

As shown in Figure 6.4, this module mainly deals with the DEM and the view projection. The user is prompted to specify the type of projection which can be either EGSA87 or any other projection. EGSA87 is the Greek projection that has the following parameters described below.

1. Transverse Mercator. This is a cylindrical projection with the cylinder along the meridian. The result is a conformal projection that maintains small shapes and increasingly distorts larger regions (area and shape) away from the meridian. As meridians run north and south, this projection is best suited for land masses that also stretch north to south.
2. Spheroid. To make mathematical calculations easier, the Earth is often treated as a sphere, having a radius valued at 6,370,997 m. This assumption can be used for small-scale maps where the difference between a sphere and a spheroid cannot be detected. However, to maintain accuracy for larger-scale maps, the Earth must be treated as a spheroid (ellipsoid). For this particular case the spheroid is GRS80 (Geodetic Reference System 1980).
3. Central Meridian. The central meridian is centred on the region of interest. This centering on a specific region minimizes distortion of all properties in that region. For Greece, Central Meridian is 24°E.
4. Reference Latitude. This is the angular distance in degrees north or south of the equator. For this case it is 0.
5. Scale Factor. This is the ratio of the scale at a particular location and direction on a map to the stated scale of the map. In this case it is 0.9996.
6. False Easting. This is the x-coordinate value assigned relative to the point of origin of the projection. For example, if the origin of the projection (in latitude-longitude) is in the center of the map, all areas to the west of the origin would be negative when a false easting of zero is assigned. To make the coordinates positive for the entire map, set the false easting to a positive number. In this case the number is 500,000.
7. False Northing. This is the y-coordinate value assigned relative to the point of origin of the projection. For example, if the origin of the projection (in latitude-longitude) is in the center of the map, all areas to the south of the origin would be negative when a false northing of zero is assigned. To make the coordinates positive for the entire map, set the false northing to a positive number. In this case the number is 0.

The DEM can be generated, if it is not already available, from a TIN (Triangulated Irregular Network), contour lines, spot elevations or a combination of these. The user can then clip the DEM to a specified extent, create a slope grid, or change the resolution of the DEM if desired. It should be noted that the resolution of the DEM has a direct effect on the model results, so higher resolution is recommended although it may take longer execution time. The spatial interpolation tool is also

available for the user to use the conventional spatial interpolation techniques such as Kriging, Spline, and IDW (as shown in Figure 4.7). Most of the techniques use the *Barrier* argument to specify the location of linear features (such as shoreline) to interrupt the surface continuity. Barriers are set to limit the set of the input sample points used to interpolate the z-values to only those samples on the same side of the barrier. Input sample points that lie exactly on the barrier line are included in the sample set for both sides of the barrier. However, when barriers are specified, processing time is significantly extended.

### 6.5.2 Database Accessing Tool

A shapefile that contains the locations and names of the gauges is required as input to this tool. Because the locations should be in decimal degrees in order to be visualized in ArcView, a conversion tool, as shown in Figure 6.5, is added to convert from degrees-minutes-seconds units to decimal degrees. After the conversion, with the view is already projected, the values for the predictor variables longitude and latitude ($x_2$ and $x_3$, respectively) are extracted from the view. If the altitudes of the gauges ($x_1$) are not known, they can be extracted from the DEM.

The database accessing tool is designed to access three different types of databases where the time series data are stored, and then extract the precipitation values (y) for a user-specified period of time and possibly for a specified group of gauges rather than all the gauges:

a) A database that can basically be one column in the attribute table of the raingauges shapefile. This column can represent a previous run or a one time run.

b) a database that is stored in ArcView as a collection of database files (*.dbf) (77 files for our case study). The tool can browse through all the files, extract the required data and add it as a column to the attribute table of the shapefile.

c) a database that is stored somewhere in the PC outside ArcView. The tool can again browse through all the files, extract the required data and add it as a column to the attribute table of the shapefile.

For the purpose of our case study, and to simplify calculations, a relative coordinate system was established by locating an origin (0, 0) at the lower left corner of the island at latitude 3,800,000 m and longitude 461,000 m (refer to Figure 6.1). Therefore, all Y-coordinates employed in the regression were the result of subtracting 3,800,000 from the original latitudes of the different stations and dividing by 1000 to obtain latitudes in kilometers. Similarly, all X-coordinates were the result of subtracting 461,000 from the original longitudes of the different stations and dividing by 1000 to obtain longitude values in kilometers. This manipulation of coordinates is important when performing the regression

analysis. Using large numbers for latitude and longitude could have resulted in small values for model parameters ( i) and any small error could have resulted in significant changes in the model output. It also is more practical in multiple regression to put all variables into approximately the same order of magnitude (i.e., so that elevation, longitude and latitude values have similar order of magnitude) to ensure that they receive appropriate weighting in the multiple regression analysis.

### 6.5.3 Parameter Generator

The number of parameters generated is one more than the number of the variables included in the analysis due to the intercept parameter ($\beta_o$). The user should identify the variables considered for the case being studied through the pop-up menu shown in Figure 6.6. The module will then generate the four input files necessary to run the executable "mlr.exe", run the "mlr.exe", and read the output file generated by the executable and store the new information in the database file "par.dbf". Once the parameters are estimated, the regression model is complete and ready to use. It also is more practical in multiple regression to put all variables into approximately the same order of magnitude (i.e., so that elevation, longitude and latitude values have similar order of magnitude) to ensure that they receive appropriate weighting in the multiple regression analysis.

### 6.5.4 Model Executor

Each grid cell in the DEM has an area, altitude, longitude and latitude. The regression models are applied for each cell in the DEM using the values of parameters generated in the previous step, and the values of the variables are extracted from each cell. The result is a mean areal precipitation value (in mm) and the total volume of precipitation (in $10^6$ $m^3$) over the region which the DEM represents. The model executor is represented by the pop-up menu shown in Figure 6.7. By using the "refresh" button, the module will extract information from the "par.dbf" file concerning the case being studied, such as the case name, number of variables, number of gauges, coefficient of determination, x-coordinate, y-coordinate and the values of the parameters generated. The user also has full control to alter the boundary conditions in the three dimensions of the study area. For example, the user can estimate the mean areal precipitation for a rectangular extent within the region under consideration rather than the full extent. The user is also able to estimate the mean areal precipitation over a range of altitudes within the study area or above or below a certain altitude. This provides the flexibility required for such a decision-support system. The module is equipped with artificial intelligence components that can recognize the user mistakes and correct them automatically, or inform the user to correct them or terminate the application. The results of the execution are then displayed on the same pop-up menu.

6.5.5 Output Visualizer

It is a point shapefile with each point representing a grid cell in the DEM as shown in Figure 6.8. The attribute table of the shapefile contains information about each cell such as the original values for latitude and longitude, altitude, the x- and y-coordinates, and the estimated value of precipitation. If the user is to specify a smaller area than the full extent, the value of precipitation is 0 outside the specified extent. The user will be informed of the ratio of the extent being analyzed to the full extent as shown in Figure 6.9.

6.5.6 Output Report Generator

Using the "write report" button of the same pop-up menu (Figure 6.7), the user can write a report which is normally named "<*casename*.txt>", that is stored in the working directory of the project as shown in Figure 6.10. The report is divided into four sections. Section 1 is the general information about the case. Section 2 is the boundary conditions of the case. Section 3 is the DEM name, mean elevation, and the average slope as a percentage and in degrees {The slope is defined in ArcView as the maximum rate of change in value from each cell to its neighbors). The slope as degrees is "arctan rise/run", while the slope as percentage is "rise/run*100%". So for a slope of 45°, it is 100% in percentage. Thus the slope in percentage = TAN (the slope in degrees)*100}. Section 4 contains the results. An additional feature is added to the module that enables the user to get a copy of the report through ArcView by clicking the "print report" button. The user will be prompted by a name for the default printer. If the user agrees, the printing job will take place; if not, the user will then have to specify a name that can be recognized by the program and the document is sent to the printer.

## 6.6 Analysis

Most natural phenomena such as rainfall vary continuously. The observations (collected data) that describe these phenomena represent a finite number (sample) of the infinity of possible locations (population). Although these processes (phenomena) are continuous and the values at sites that are close together in space are more likely to behave similarly than those farther apart, exceptions do exist. For instance, in the Geropotamou basin (located in southern Crete, as shown in Figure 6.11) the stations of Vorizia and Pompia record more rain than the neighboring stations of Zaros and Agios Kirillos, respectively. The stations Zaros and Agios Kirillos are considered "rain shadow" stations due to the nature and orientation of topography at that area and considering that the prevailing wind direction is northwesterly.

The annual records were used to study the variation in precipitation in time and space. Temporally, and according to the findings of Chapter 3, it was clear that the year 1977-78 was the wettest, while the year 1989-90 was the driest. Spatially, it was evident that

precipitation is of an orographic type. In other words, on a small scale, precipitation can be well explained by the altitude of the gauges. However, more independent variables were introduced in order to construct efficient models for relatively larger areas, as in the case of Gerapotamou basin. For the average year 1974-75, for example, a value of 43.6% for the coefficient of determination for simple regression ($r^2$) was obtained when using equation (6.5)

$$P = 536.0 + 0.65\ E \ldots\ldots 150m \leq E \leq 517m \tag{6.5}$$

where P = precipitation (mm/year) and E: gauge elevation (m); while an $R^2$ value of 87.8% was then obtained according to equation (6.6)

$$P = -290.51 + 0.47E - 3.42L_o + 15.54L_a \tag{6.6}$$

where $L_o$: x-coordinate (longitude) (km), and $L_a$: y-coordinate (latitude) (km).

The two new variables introduced were the latitude and longitude of the gauges. The analysis in this chapter is thus extended to cover the spatial variation of precipitation over the whole island, rather than small watersheds, by introducing additional predictor variables. The analysis is performed on two wet years (1977-78 and 1986-87), a dry year (1989-90), an average year (1974-75), a short-term average (1974-75 to 1984-85), and a long-term average (1969-70 to 1994-95).

In order for the aspect and orientation of topography factors to be considered, the island was divided into regions (divisions) for which the observations of the respective stations would reflect a general regional pattern. Four plots of latitude vs. precipitation for the wet year of 1977-78 were constructed, as shown in Figure 6.12. Each of the plots represents a prefecture (county), starting from Chania west to Lassithi east. The horizontal axis covers 80 km south to north (i.e. latitude values start from 3,860,000m south to 3,940,000m north). Generally, and being of an orographic type, the plots show similar behavior: precipitation is low at the south and north ends of the island and peaks in the middle. Unlike the other three prefectures, the prefecture of Lassithi showed a rather unique behavior (probably for the lack of representativeness of the gauges in that region or the less obvious orographic effects), which suggested that the prefecture represents an independent division. Therefore, and as shown in Figure 6.2, the island was divided into three divisions: namely "Northern Crete", "Southern Crete", and "Eastern Crete". This process is, as will be seen later, most favorable for studying the quantitative influence of the different environmental and geographical variables on the mean annual precipitation. Satisfactory results would not, normally, be obtained if the area studied was large or complex, since the

factors vary inconsistently. The north division occupies around 40% of the island and covers an area of 3354 $km^2$. It has a mean elevation of 446 m and an average slope of 210 m/km. The south division covers an area of 2765 $km^2$ (34% of Crete), with a mean elevation of 536 m and an average slope of 250 m/km. The eastern part covers an area of 2146 $km^2$ (26%), with a mean elevation of 471 m and an average slope of 230 m/km.

Elevation (altitude) was considered to be the primary predictor variable for the regression models and accounts for the topography factor. Figure 6.13 indicates that there is a positive correlation between altitude and precipitation. The $r^2$ value ranged from 31% (in the case of the dry year of 1989-90) to 46% (in the case of the wet year of 1977-78). The two new variables (latitude and longitude) were then added to the models and the $R^2$ values were significantly increased, a possible indication of model improvement. Developing separate regression equations and still using elevation as the only predictor variable for the three divisions of Crete provided even more descriptive models, as in Figure 6.14, which shows the wet year of 1977-78 as an example. The three models of the divisions show a stronger positive elevation-precipitation correlation and were better than one model of the whole island. In the residuals vs observed precipitation plot, which represents the whole island case, there is a linear relation between observed precipitation and model residuals. This is an indication of one (or more) missing predictor variable(s) that could further describe the phenomenon. Residual plots should show no sign of association with the observed sample and must be purely random, as in the three plots of the three divisions.

The four parameters {$\beta_o$ (intercept), $\beta_1$ (elevation), $\beta_2$ (longitude), and $\beta_3$ (latitude)}, have been proposed and adopted to successfully establish multiple linear regression models. However, interaction effects between the variables can be considered. These would be represented in the models by adding three more terms. The use of a second-order model is also a good possibility. Second-order models with, as in this case, three predictor variables are particularly used in response surface studies, where it is desired to graduate, or approximate to, the characteristics of some unknown response surface by a polynomial of low order. Note that all possible second-order terms will be in the model, thus leading to ten-parameter models for Crete and its divisions for the different data sets. The general form of the final product is

$$\begin{aligned} P = {} & \beta_o + \beta_1 x_1 + \beta_2 x_2 + \beta_3 x_3 \\ & + \beta_4 x_1^2 + \beta_5 x_2^2 + \beta_6 x_3^2 \\ & + \beta_7 x_1 x_2 + \beta_8 x_1 x_3 + \beta_9 x_2 x_3 \end{aligned} \qquad (6.7)$$

where P= precipitation (mm/year), $x_1$= elevation (m), $x_2$= x-coordinate (longitude) (km) and $x_3$= y-coordinate (latitude) (km). Although the models improved by introducing the interaction and second-order terms by observing the $R^2$ statistic value in each of these cases, this improvement took place at the expense of the loss of degrees of freedom. This, in turn, raises the question: was it worthwhile adding the new terms to the models?

## 6.7 Results and Discussion

### 6.7.1 Large-Scale (the island and its 3 regions)

Regression analysis results show that for the eastern part of Crete, where the number of gauges is relatively small, using the four-parameter (three-variable) models is more feasible. This is especially true if there is no noticeable improvement in the coefficient of determination. As for the northern and southern parts of the island, the coefficient of determination increased significantly (a 34% increase was reported in the case of the wet year 1986-87 for Northern Crete). Figure 6.15 compares the 4-parameter model output and the 10-parameter model output for Northern Crete for the year 1977-78. Notice the improvement in the estimated values as the residuals tend to scatter over a smaller range around the x-axis for the second case. The estimate for the station of Askifu (an extreme observation) improved from 1824 mm (using the 4-parameter model) to 2386 mm (using the 10-parameter) model, thus approaching the observed value of 2594 mm. Results for the whole island show that the increase in $R^2$ ranged from 7% to 14% which suggests that using the 10-parameter model rather than the 4-parameter model for Crete can be regarded as a justifiable gain with a moderate loss in degrees of freedom.

From a statistical perspective, while the p-value was always within limits, the different statistical diagnostic tests revealed that the effect of adding new terms to the models varied greatly. Using the Southern Crete model as an example, adding the term "$x_2^2$" had almost no effect on the model when applied to the long-term average (1969-70 to 1994-95) data, but the term did have a noticeable effect on the model when applied to the other datasets. Adding the term "$x_1x_2$" had moderate effects in the case of all Northern Crete models. Generally, the parameter "$\beta_4$" (associated with the variable "$x_1^2$") was classified as "not significant" for all models in all cases. Also, the loss of degrees of freedom is very critical. For example, results of the ten-parameter models in the case of Eastern Crete can not be considered reliable, since the loss of degrees of freedom is great when compared to the sample size (number of stations). Generally, the analysis results supported the significance of neither the majority of ten parameter models for Eastern Crete nor, in the case of long-term average, the ten parameter model for Northern Crete. These models proved to be insignificant and, according to the "extra sum of squares" principle, the extra terms were not needed in spite of the high $R^2$ value, which is deceptive in this case.

To summarize: the ten-parameter models can be used with care, especially when they are derived from not-a-dense-enough network of gauges. A sample of the different models is presented in Table 6.1 for the average year of 1974-75. The rest of the Tables can be found in Appendix H.

Using the GIS module (AVRU), estimates for average and total volume of rainfall for Crete and its three regions for the different cases were obtained, as shown in Table 6.2. The four-parameter models were used for Crete, as well as the three divisions, while elevation-only models were used for Crete for comparison purposes. Moving from the one variable model to the three variable model resulted in a noticeable improvement in $R^2$ for Crete in all cases. Knowing that the highest raingauge (the Germiado gauge in the prefecture of Lassithi) is installed at an elevation of 905.4m, two values for average and total rainfall were estimated. The first value is the "conditional estimate", which is based on the assumption that elevations higher than the 905.4m value are considered 905.4m when using the MLR models. The "unconditional estimate" is obtained by using elevation values as they are. The relatively larger influence of elevation on rainfall estimates, in addition to the lack of information about precipitation behavior above the 905.4m level were the reasons behind the differentiation. In other words, although the models were derived based on information obtained from gauges installed on elevations of 0m to 905.4m, they still are considered applicable on elevations higher than the 905.4m limit. According to the generated DEM, about 15% of the elevations are above the 905.4m level. The mean elevation above 905.4m is 1310m. The GIS module provides the user with the choice of a conditional or unconditional estimate based on a DEM of a resolution of 1km*1km. The results show that the difference between conditional and unconditional estimates is obviously caused by the number of cells with elevations that are greater than 905.4m in the DEM. The unconditional volume estimates are, on average, higher by 4.6%, 5.9%, and 4.9% for Northern, Southern, and Eastern Crete, respectively. For the whole island, there is also an increase of 5.5% using elevation-only models, and 5.9% using three-variable models. Results also show that the north receives approximately 45% of the total rain, while the south receives 31%, and the east 24%.

Based on the parameter significance analysis alone, new models were derived to examine the effect of eliminated (insignificant) parameters on the results. The results show that, although some models provided comparable results to the original models for estimating areal rainfall, they failed to provide reliable models for Northern Crete for the different cases. These models are not recommended for point (i, j) estimates (which are regarded as the strength of the MLR models) due to the fact that negative results were obtained at some locations.

Upon examining the individual influence of the different variables on the models, it was found that due to the unique shape of the island and the new coordinate system (refer to Figure 1) high values for the latitude parameter ($\beta_3$) as well as high negative values for the parameter ($\beta_o$) are obtained. The models adjust to this condition in the western part by introducing positive values for ($\beta_3$), adding a large negative number for ($\beta_o$) to equalize that effect. This was clearly noticed in the case of the wet year (1986-87) models, where latitude is a key variable in explaining rainfall for that year. Two types of wet years can be distinguished for Crete. One type can be referred to as "conservative", as in the case of 1977-78, since it conserves the elevation-precipitation correlation. In other words, the increase in precipitation amounts collected is homogeneously distributed and correlated over the island with the variation in elevation of the recording gauge. An $R^2$ of 47% is obtained and precipitation-elevation gradient (slope) of 1.2 mm/m is estimated. The second type can be referred to as "aspect-driven", as in the case of 1986-87, due to the fact that the gauges in Northern Crete recorded almost double the precipitation of those in Southern Crete. An $R^2$ of 14% for the elevation-precipitation correlation was obtained and precipitation-elevation gradient of 0.6 mm/m was estimated.

Based on results reported in Chapter 3, for a typical dry year, the island of Crete would receive up to 800mm of rainfall. For an average year, between 800 to 1100mm and for a wet year the island would receive a rainfall that is greater than 1100mm. Based on these values, as shown in Figure 6.16, the range of elevation-precipitation gradient ( 1) for a dry year is 0.6 to 0.75 mm/m, rising to 1.0 mm/m for an average year and up to 1.4 mm/m for a typical wet year. The range of longitude-precipitation gradient ( 2) for a dry year is -1.9 to -2.6 mm/km, up to –3.6 mm/km for an average year and -5.1 mm/km for a typical wet year. The range of latitude-precipitation gradient ( 3) for a dry year is 10 to 13.3 mm/km, rising to 18.0 mm/km in an average year and up to 25.0 mm/km in a typical wet year. Details for wet and dry years are shown below:

| | | | | | | | | |
|---|---|---|---|---|---|---|---|---|
| wet years | 1967-68 | 1968-69 | 1975-76 | 1977-78 | 1980-81 | 1981-82 | 1984-85 | 1986-87 |
| areal rainfall | 1206mm | 1346 | 1211 | 1480 | 1163 | 1185 | 1174 | 1285 |
| dry years | 1969-70 | 1973-74 | 1976-77 | 1985-86 | 1989-90 | 1992-93 | | |
| areal rainfall | 791mm | 778 | 827 | 736 | 618 | 769 | | |

Figure 6.16 also shows the degree of interaction between the parameters (i.e. the influence of a particular parameter decreases when additional parameters are added to the model). For example, introducing latitude in addition to elevation reduces the parameter ($\beta_1$). For a certain value of areal rainfall, ($\beta_2$) is at its lowest value when the elevation and latitude variables are added to the model. It is at its highest value when only longitude models are used.

Table 6.3 shows the influence of each individual variable on the model output for an average year (1974-75) for Crete and its divisions when employing elevation only; elevation and longitude; elevation and latitude; longitude and latitude; and elevation, longitude and latitude. The results show that there is a noticeable increase in the coefficient of determination from the one-variable model to the three-variable model. Although the three-variable model provided more reasonable estimates, the models based on elevation and longitude provided a more physically meaningful interpretation of the effect of each variable. For example, looking at the model of Crete, a mean areal rain of 736 mm is expected over the island, with an increase of 69 mm/100m of elevation and a decrease of 1.65 mm/km of longitude (i.e. from west to east). Very poor $R^2$ values are obtained when using only longitude and latitude models.

To compare the different interpolation techniques, the "fictitious-point" method (refer to Section 5.2.2.4) has been used. In this case the MLR models, as a spatial interpolation technique, are considered superior to the conventional spatial interpolation techniques such as Spline, IDW and Kriging. Figure 6.17 illustrates the difference in average estimates according to the different methods as well as the spatial distribution of rainfall across the island. The estimates ranged from 799mm, using IDW, to 944mm using MLR. The spatial distribution of the MLR for three divisions is considered to be a reasonable one, yielding a mean annual precipitation of 913mm for the average year 1974-75.

### 6.7.2 Medium-Scale (watersheds)

As previously indicated, introducing latitude and longitude, in addition to elevation, as independent variables improved the estimates when studying the Gerapotamou basin. Three basins were used as test cases to compare the MLR model results with the spatial interpolation techniques and to examine the effect of spatial extent on the output. The selected basins were used to represent different divisions of Crete with relatively dense raingauge networks. As shown in Figure 6.18, the basins are Gerapotamou (with 9 gauges and area of 602 $km^2$) and Anapodiaris (with 9 gauges and area of 520 $km^2$), both of which represent the South. Giofyro (with 3 gauges and area of 189 $km^2$), which represents the North. No basins represented the far east or the far west due to the lack of gauges. A comparable analysis was held by using four different MLR models derived from data sets representing: the whole island (Crete), the division where the basin is located, the gauges located inside the basin, and the gauges located inside and outside the basin. The models were applied to the basins to estimate conditional and unconditional areal rain and rain volume. For Gerapotamou basin, the larger extent is represented by the rectangle in Figure 6.18, with an area of 1738 $km^2$ including 24 gauges; for Anapodiaris basin, the larger extent is of an area of 1706 $km^2$, containing 23 gauges (excluding the Kapsaloi gauge); and the larger extent for Giofyro basin occupies an area of 1023 $km^2$ surrounding 14 gauges

(excluding the Iraklio B gauge). The results, from which the following can be concluded, are summarized in Table 6.4. As in the case of larger scale analysis, the models based on elevation and longitude mostly provide more physically meaningful interpretations of the effect of each variable. The precipitation-elevation gradient is higher in the north than in both the south and east. Both conditional and unconditional estimates for Giofyro basin are the same because the highest elevation in the basin is 808.5 m, which is less than the 905.4 m limit. The difference between the lowest and highest estimates for average rainfall ranged from 13% to 26%, with the values estimated by the 3-variable models derived from the larger extent are in an intermediate position.

Figure 6.19 shows a comparison between MLR models and spatial interpolation techniques for the Gerapotamou basin. When the gauges located inside the basin were considered, the estimates ranged from 698 mm using IDW to 782 mm using MLR. Estimates for gauges located inside the larger extent ranged from 701 mm using IDW to 763 mm using MLR. Notice the slight difference in the spatial distribution between the two cases of MLR compared to the two cases for each of the other spatial interpolation techniques.

Figure 6.20 shows the thirteen gauges located in and around the Anapodiaris basin, from which annual data for thirty years (from 1967-68 to 1996-97) were obtained and used to derive MLR models. The models were then applied for each year to estimate the areal rain and volume for that particular basin based on the two scenarios of conditional and unconditional assumptions. The values obtained show a cyclic behavior on a downward trend for the areal estimates of a -3.67 mm/year, which corresponds to a -1.9 $Mm^3$/year change in the rain volume (refer to Figure 6.21). The shaded area of this figure represents the output of thirty MLR models (one for each year) developed for this basin. The unshaded areas represent the de-trended precipitation values. Based on the conditional and unconditional assumptions, the average rain over the thirty years is 805 to 855 mm/year (or 420 to 445 $Mm^3$/year).

### 6.7.3 Small-Scale (sub-basins)

Following the delineation of sub-basins using ArcView GIS, another form of analysis was carried out for the Giofyro basin. The MLR models, together with the GIS module, were used to estimate both areal rain and the mean elevation for the sub-basins. It is clear that, for an average year, mountainous sub-basins receive more rain than coastal basins. Figure 6.22 shows that sub-basins (B6, B7, and B8), which occupy the highest elevations, collect greater amounts of rain than the rest of the sub-basins. A strong positive correlation existed that relates the mean elevation and the average rain. The slope of the line (0.79 mm/m) is comparable to the results obtained for Giofyro basin shown in Table 6.4.

In addition to estimating areal rain for areal extents (Crete, Northern Crete, Southern Crete, Eastern Crete, Anapodiaris Basin, Gerapotamou Basin, Giofyro Basin and subbasins), the developed GIS module also provides the means for estimating areal rain for ranges of elevation, as shown in Table 6.5. In all three basins, elevations that are higher than 600m occupied around 28% of the area of the basin. However, Gerapotamou basin collects more rain for that range due to the fact that its highest elevation is 2300m. The highest elevation for Anapodiaris is 2067m, and for Giofyro basin is 809m. Based on an average year, the elevation range of 300 to 600m in the Grapotamou basin receives almost 45% of the amount of rain that falls on the elevation range of 600m and higher. Generally, most of the precipitation falls between the elevations 300 m to 600 m.

Regression models were also derived for every year for the thirty year period 1967-97. Out of the 77 gauges available, only 42 gauges recorded data for that period. The analysis was based on the data from these 42 gauges. Their locations are shown in Figure 6.23. Precipitation data were also collected from a set of 13 storage gauges (see Figure 6.23) that were mostly installed on relatively higher elevations. The gauges were read once a year due to accessibility problems. The models developed were used to estimate precipitation at those locations as shown in Table 6.6.

*Generally*, the results can be considered satisfactory due to the sparse raingauge network employed in the analysis, as well as the uncertainty associated with the data collected from the storage gauges as readings are done only once per year.

*Spatially*, the results obtained can be ranked as: good for the gauges Aloides, Gerakari, Idi-1, Kato Horio, Kato Metoxi, Omalos Chania, and Thripti; average for the gauges Idi-2 and Vistagi; and bad for the gauges Idi-3, Kathro, Omalos-1, and Omalos-2. There was a relatively high overestimation by the models for Kathro, Omalos-1, and Omalos-2, while there was a relatively high underestimation for Idi-3. Estimated values using MLR were compared with those obtained by using spatial interpolation techniques. In all cases, estimates using MLR were closest to the observed values. Figure 6.24 shows an example for the year 1995-96, when all observed records were available for all gauges which were compared to estimates obtained using the spatial interpolation trechniques. Case (a) is MLR estimates, (b) Spline_Regularized, (c) Spline_Tension, (d) IDW, (e) Kriging, and (f) 2$^{nd}$ Order Polynomial.

*Temporally*, there was a general overestimation by the models for all years especially the years 1985-86 and 1996-97. The observed records for the year 1977-78 were significantly underestimated especially for the gauges Idi-1, Idi-2, Idi-3, and Vistagi (they are located in

the middle of the island). The models, however, overestimated the records of 1977-78 for the gauges Kato Metoxi and Omalos-1 (they are both located at the eastern part of the island).

New models were developed for the regions of the island (North, South, and East - refer to Figure 6.2) as an attempt to enhance the estimates. Results show that the new models provided some improvement, however the observed records for the year 1977-78 were still not matched as shown in Table 6.7.

## 6.8 Conclusion

The multiple linear regression (MLR) method has been used to develop models to estimate the amount and the spatial distribution of orographic precipitation for complex terrain such as that of the island of Crete in Greece using elevation, latitude and longitude. This can be considered a new spatial interpolation technique that provided comparable results to those of the conventional spatial interpolation techniques such as Spline, IDW, and Kriging. The MLR models were derived and applied using a GIS. The use of MLR in conjunction with GIS provides the flexibility and accuracy in estimating both areal and point precipitation for different scales with minimum user intervention. The MLR technique was found to be superior for estimating precipitation at point (ungauged) locations. Negative values for point precipitation estimated using the other conventional spatial interpolation techniques are not uncommon, especially if the rain gauges network is not dense enough (sparse). This problem can be avoided by using the appropriate MLR models which yield not only positive but reasonable values as well. The MLR provides realistic estimates for mean areal precipitation for the island of Crete: 700 ± 100 mm, 950 ± 150 mm, and 1300 ± 200 mm for dry, average and wet years, respectively. Elevation-rainfall gradients are: 0.45 to 0.6 mm/m, 0.6 to 0.9 mm/m, and 0.9 to 1.3 mm/m for dry, average and wet years, respectively. Of this, 44% falling on the northern, 33% on the southern and 23% on the eastern parts of the island for a typical average year.

The 3-variable models are easier and more acceptable, especially when dealing with a relatively small number of rain gauges. The more parameters used, the more the degrees of freedom are compromised. In some cases, however, the 10-parameter models are regarded as more informative. As for the case study, the island of Crete, different models were derived that were used for different scales that ranged from large (the island), medium (watersheds), and small (sub-basins). Results show that Crete could receive around 950mm ($8*10^9$ $m^3$) of rain for an average year, with the north sharing 45%, the south 31%, and the east 24% of that amount. These analyses should be of value for the purpose of water resources planning and management in those regions where the dominating type of rain is orographic.

Integrating GIS with statistical models, represented in this case by the multiple linear regression method, can enhance the capabilities of the GIS. The development of the ArcView Regression Utility (AVRU) enables the user of modelling precipitation, or any other spatial hydrologic response variable, using three spatial variables (i.e. altitude, longitude, and latitude). ArcView Avenue scripts, Fortran, IMSL Stat Library, ArcView Dialog Designer, and Batch Programming were used effectively and interactively to create this new tool. The result is a linear (in the parameters) model that is used to estimate mean areal precipitation and total precipitation volume over any specified region using its digital elevation model (DEM). The results show that due to the uncertainty associated with the data from storage gauges (yearly values), the comparison between observed and estimated values can neither be used to verify the models nor to provide specific recommendation for installing recording gauges on those higher altitudes. However, the differences detected between estimated and observed values can provide general guidelines for both the models and the collected data. As a result the following should be considered: (a) Investigate the site where the gauge is installed to determine the degree of exposure. Evaporation and wind currents cause the largest error by diverting falling rain away from the instrument. (b) Conduct an experiment by installing low-cost standard gauges on higher altitudes for a short period of time to improve/verify the models. (c) Errors: read the documentation of the gauge to see if there is any changes in the surroundings, the observer, the location of the gauge (gauge has moved) or the gauge type. Mechanical errors are also a factor. A human error in documenting the right observation should also be investigated.

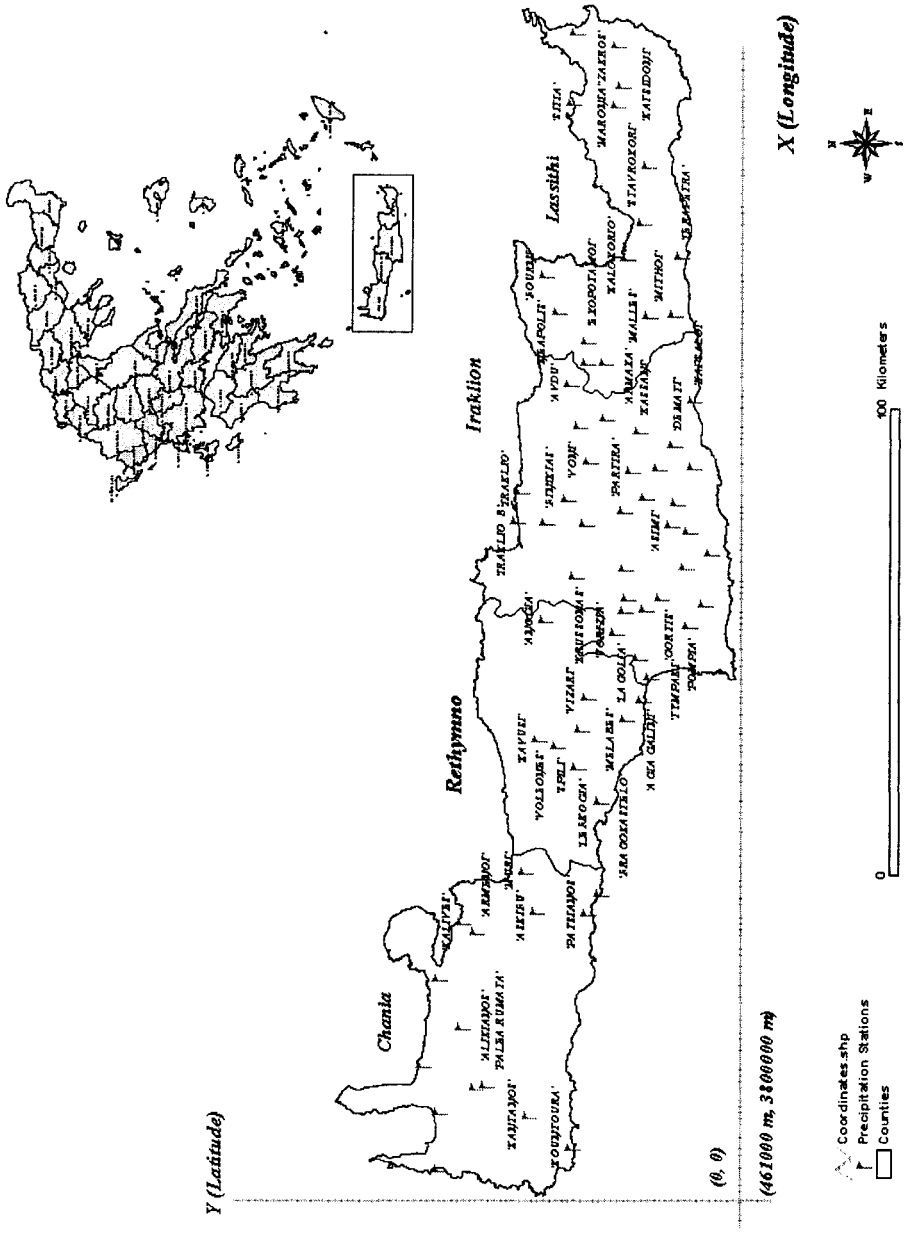


**Figure 6.1:** Precipitation stations in the four prefectures of Crete.

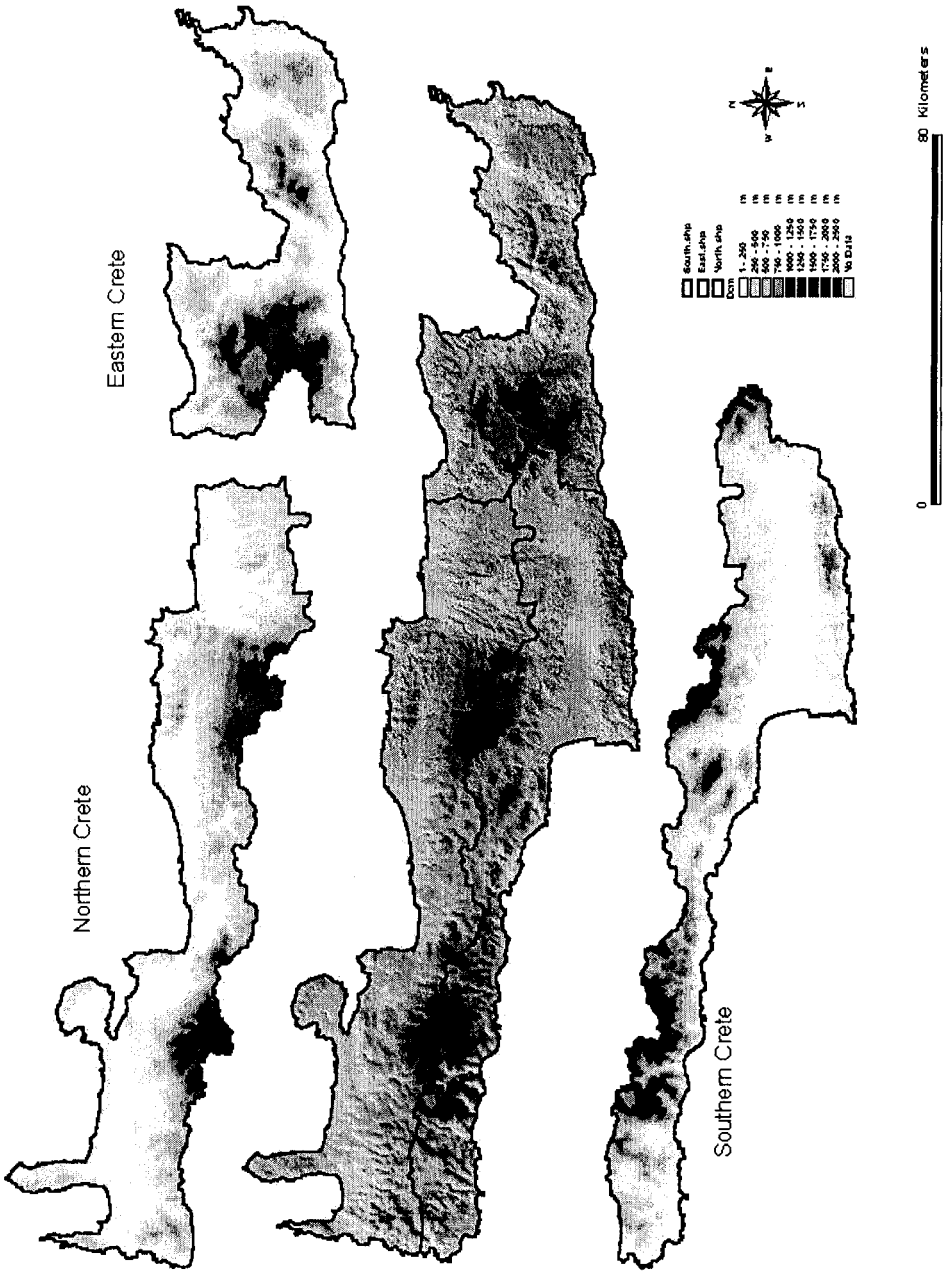


**Figure 6.2:** The Digital Elevation Model (DEM) of Crete and the three divisions.

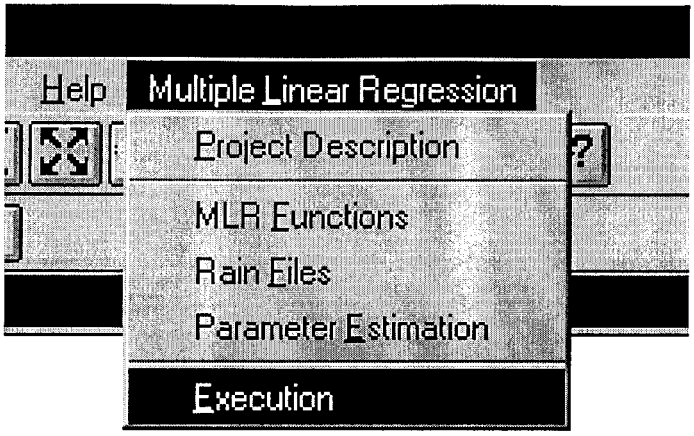


**Figure 6.3:** The main drop-down menu representing the ArcView Regression Utility.

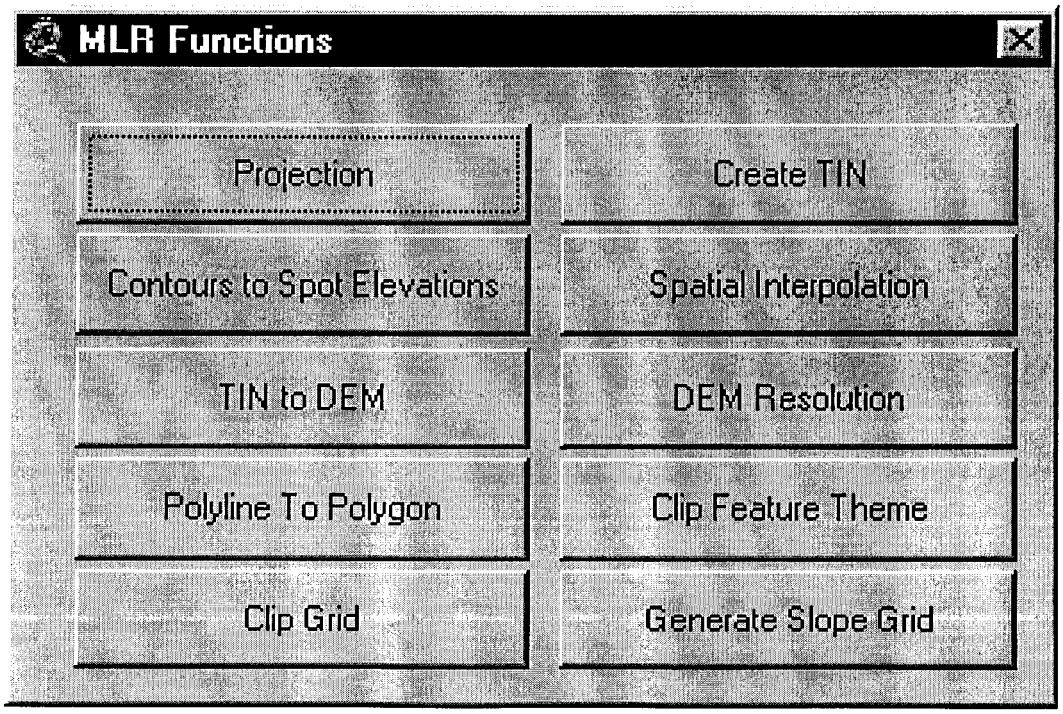


**Figure 6.4:** The "MLR functions" dialog representing module 1.

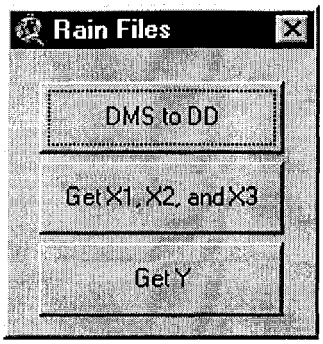


**Figure 6.5:** The "rain files" dialog representing module 2.

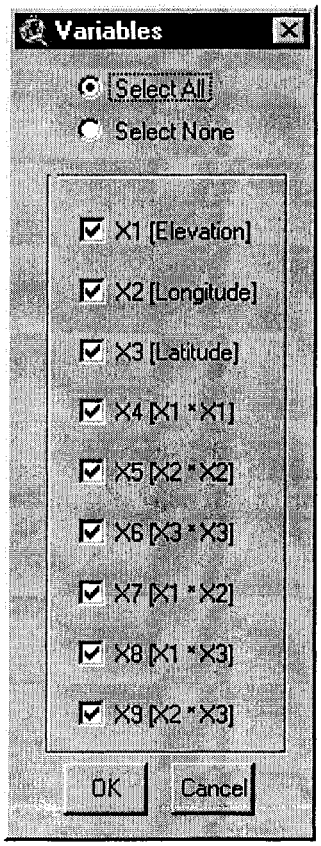


**Figure 6.6:** The "variables" dialog representing the parameter generator module (module 3).

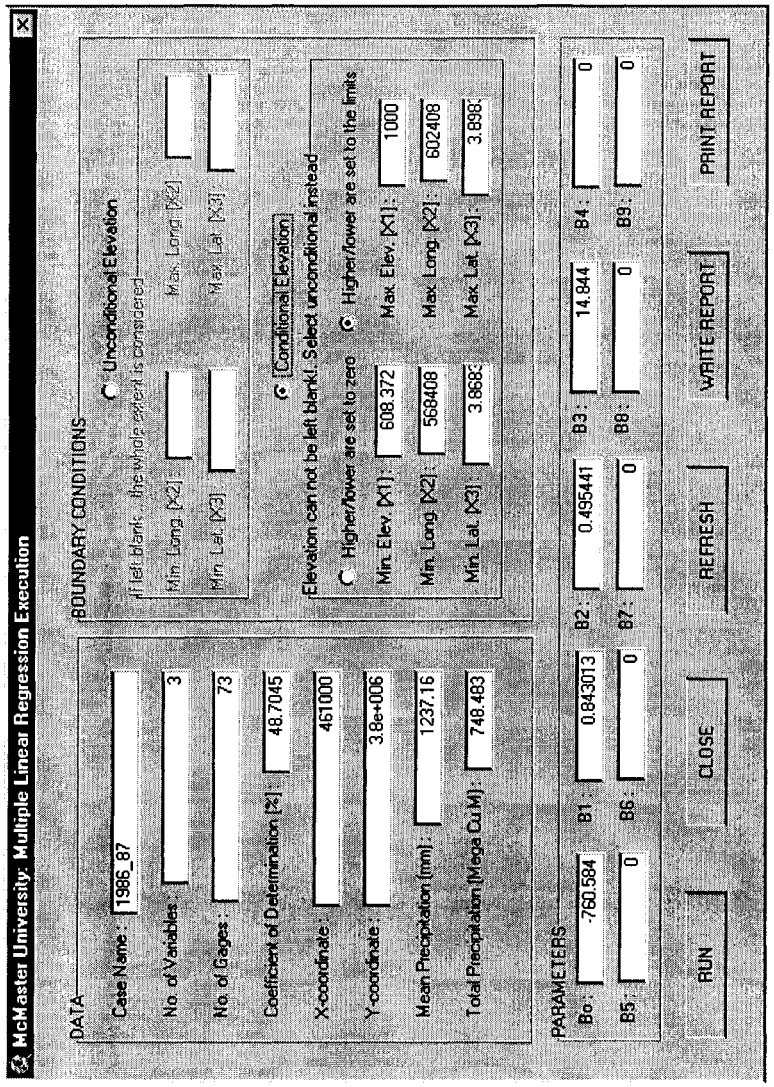


**Figure 6.7:** The "multiple linear regression execution" dialog representing modules 4 and 6.

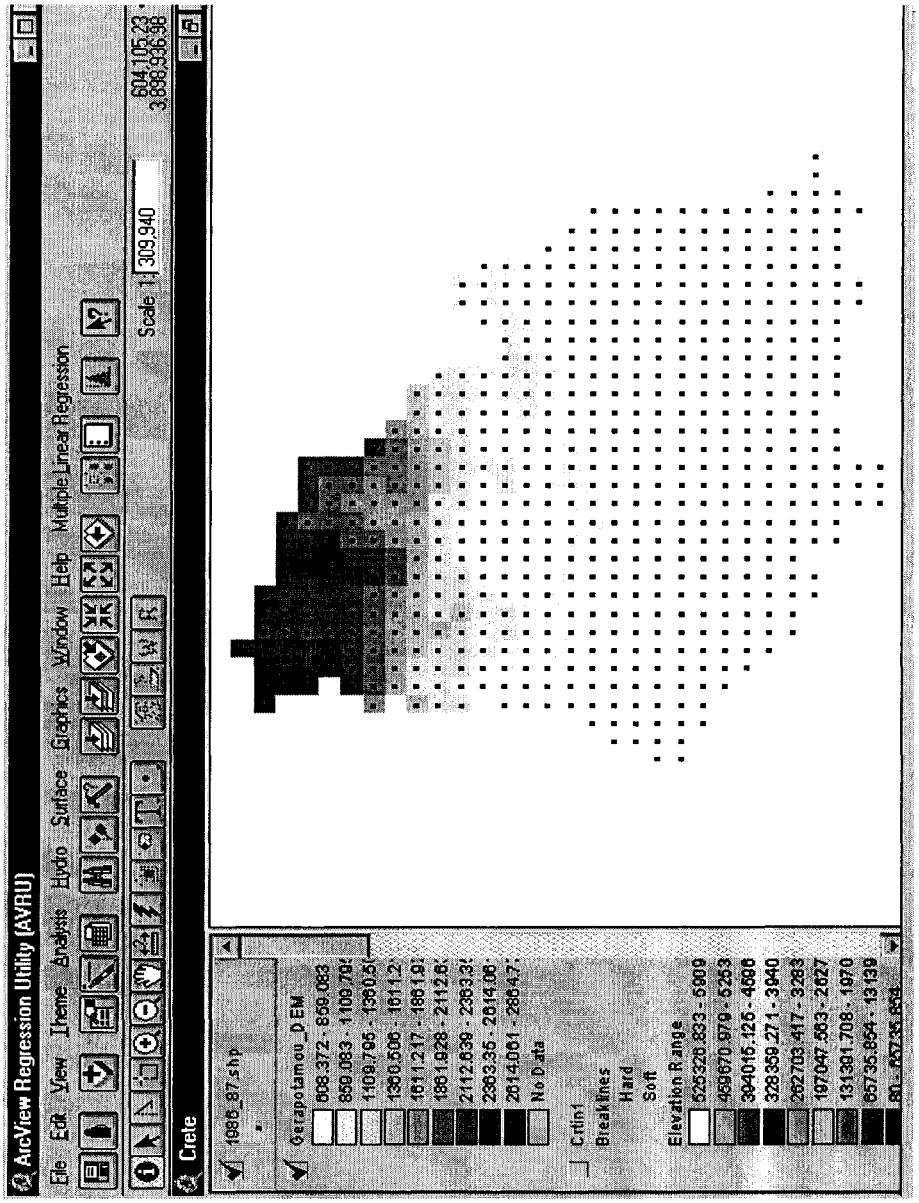


**Figure 6.8:** Visual output for a basin in Crete (Gerapotamou basin) representing module 5.

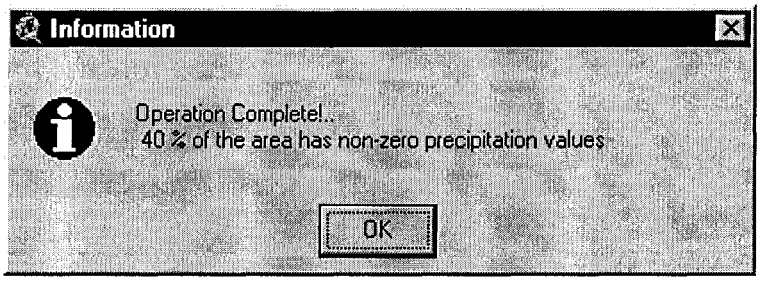


**Figure 6.9:** This message shows following execution to inform the user of the operation completion and the percentage of area that has precipitation values.

1 .. General Information
---
Case Name: 1986_87
Number of Variables: 3
Number of Gauges: 73
Coefficient of Determination: 48.7045 %
The X-coordinate: 461000 m
The Y-coordinate: 3.8e+006 m
Bo: -760.584
B1: 0.843013
B2: 0.495441
B3: 14.844
B4: 0
B5: 0
B6: 0
B7: 0
B8: 0
B9: 0

2 .. Boundary Conditions
---
Unconditional Elevation Case
Minimum Elevation: 608.372 m
Maximum Elevation: 2864.77 m
Minimum Longitude: 568408 m
Maximum Longitude: 602408 m
Minimum Latitude: 3.86832e+006 m
Maximum Latitude: 3.89832e+006 m

3 .. Grid Information
---
Elevation Grid Name: Gerapotamou_DEM
Mean Elevation: 1065.19 m
Average Slope as Percentage: 7.46999 %
Average Slope in Degrees: 4.24133 degrees

4 .. MLR Results
---
Mean Areal Precipitation :1412.36 mm
Total Precipitation: 854.478 Mega Cubic Meter

END OF REPORT

**Figure 6.10:** A sample report for one case that is generated using the MLR executor dialog.

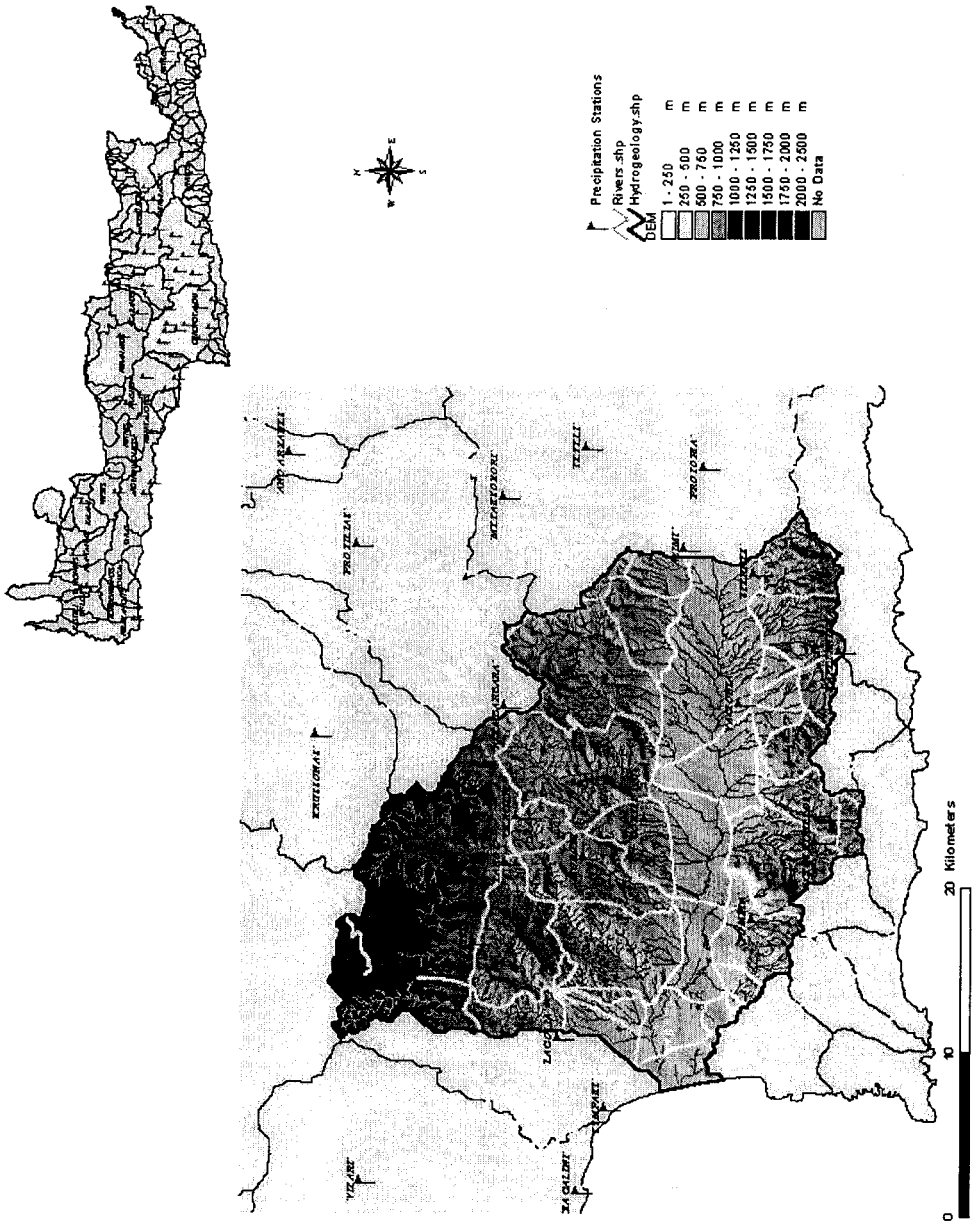


**Figure 6.11:** Roads, streams, and topography in Gerapotamou basin.

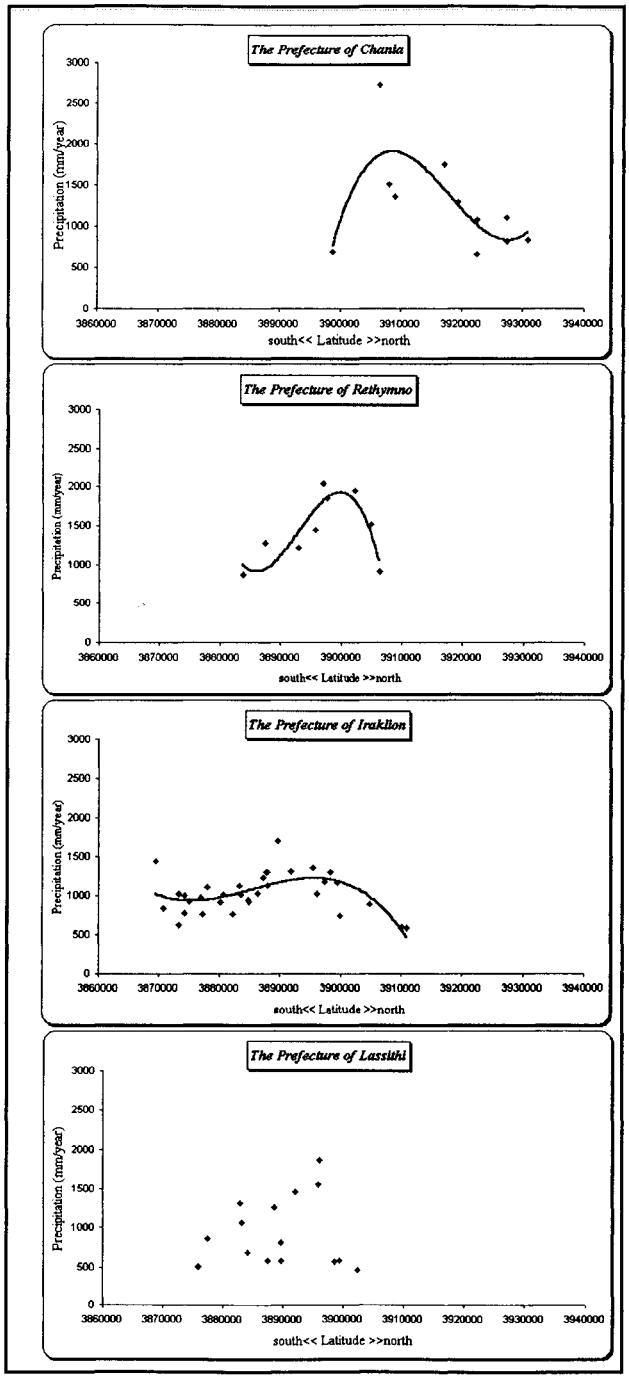


**Figure 6.12:** The variation of precipitation with latitude in the four prefectures.

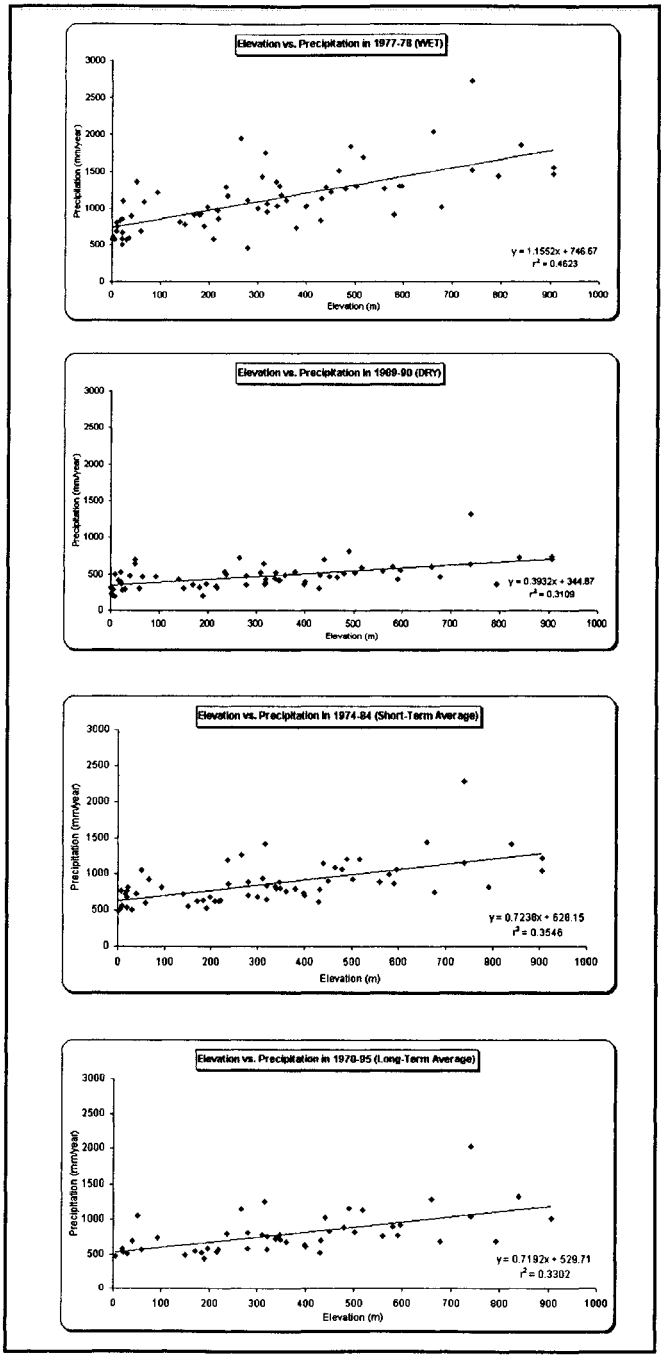


**Figure 6.13:** The degree of association between elevation and precipitation using different data sets for Crete.

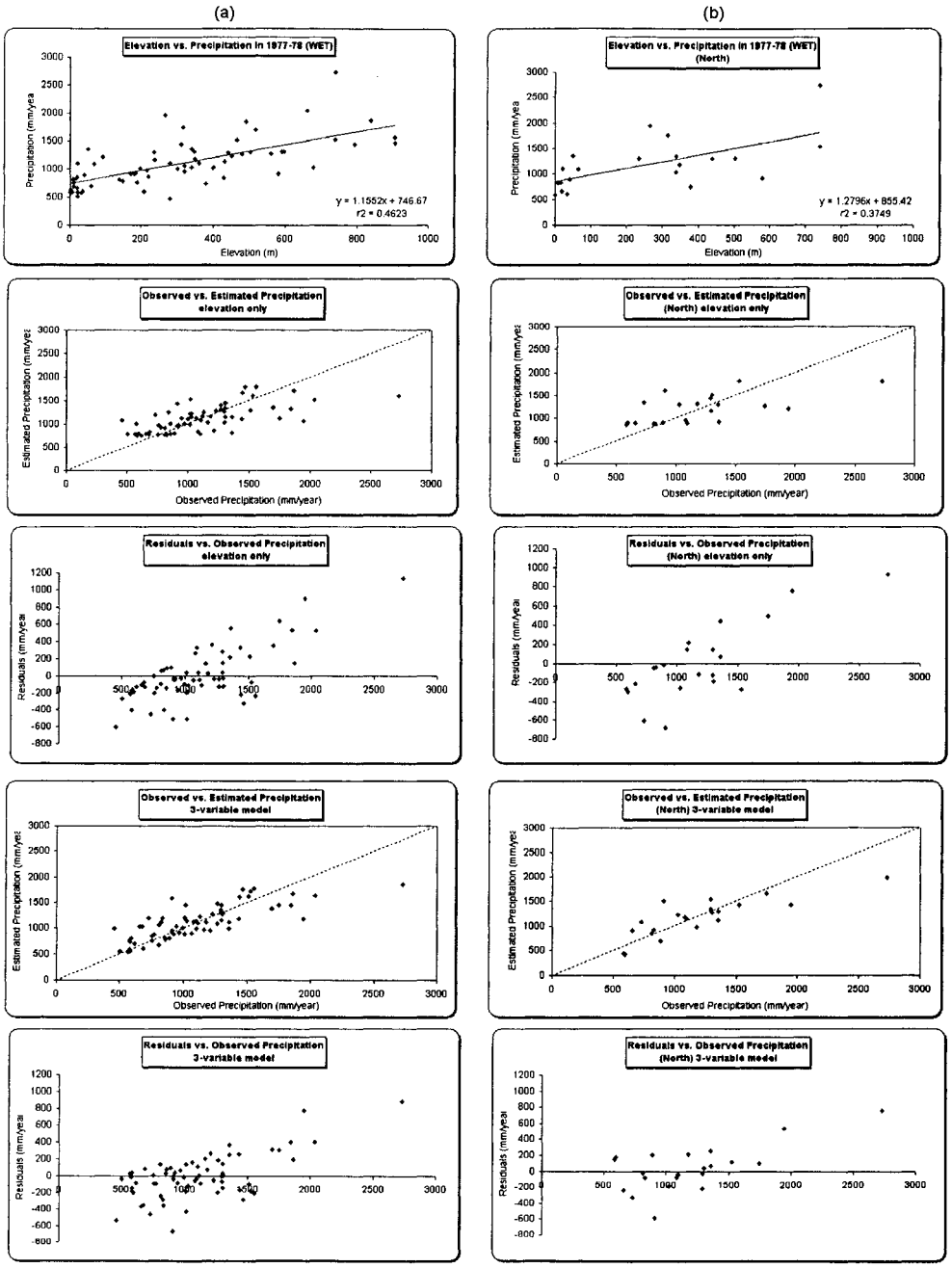


**Figure 6.14a:** Using the water year of 1977-78 as an example, observed vs estimated precipitation plots as well as residual plots were generated for the two cases of elevation only and three-variable models for Crete and Northern Crete.

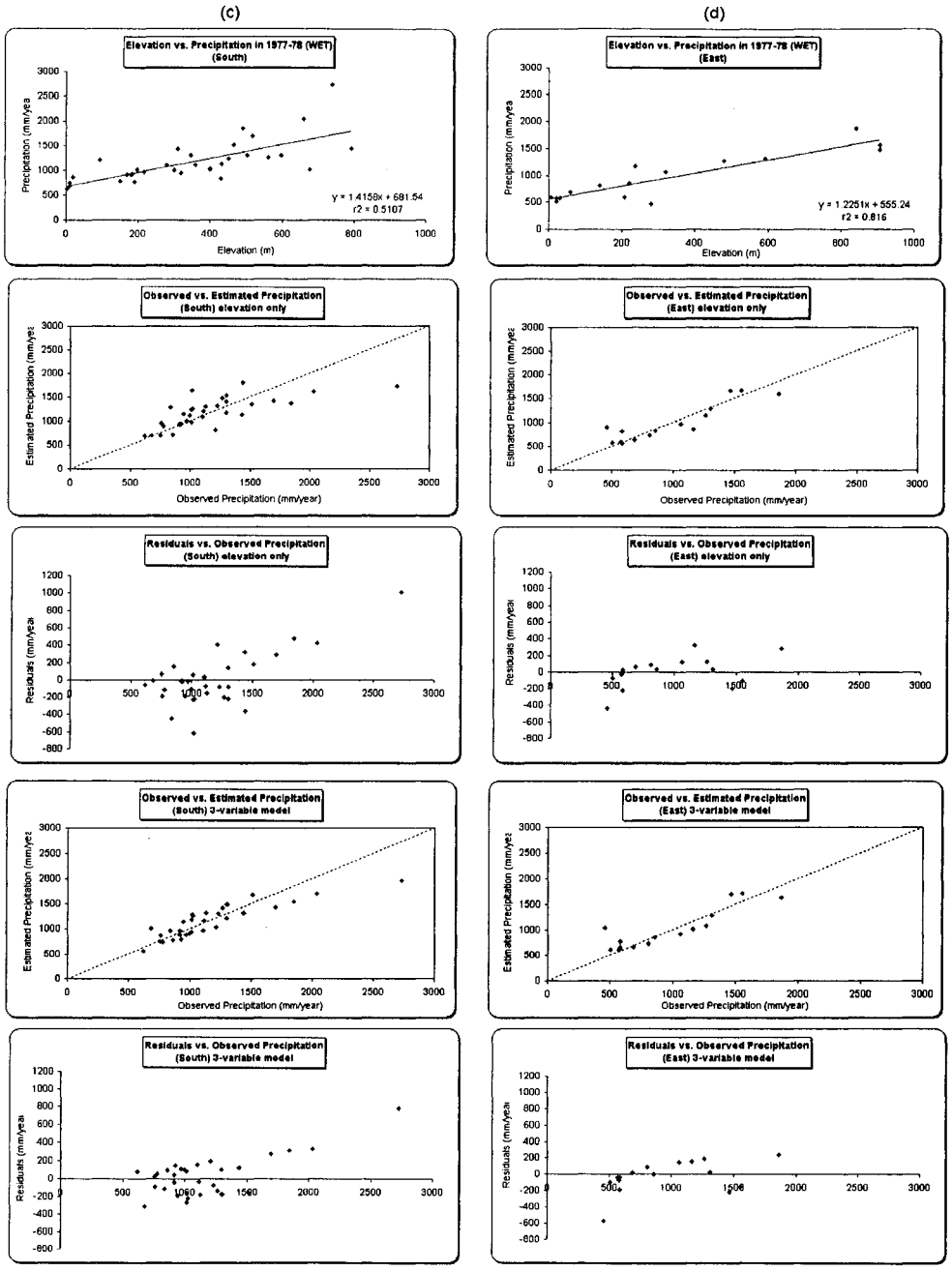


**Figure 6.14b:** Using the water year of 1977-78 as an example, observed vs estimated precipitation plots as well as residual plots were generated for the two cases of elevation only and three-variable models for Southern and Eastern Crete.

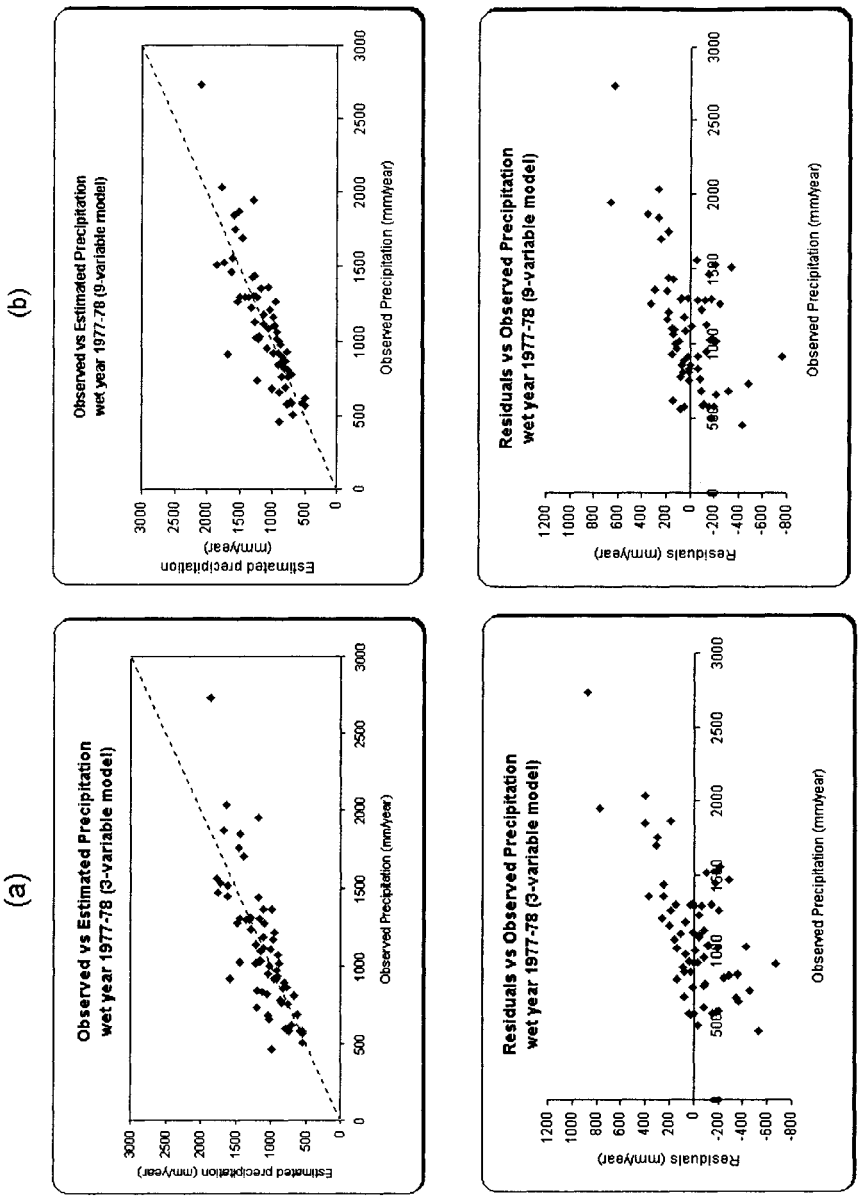


**Figure 6.15:** For Northern Crete, and based on the year 1977-78, a comparison between the output of (a) 4-parameter model and (b) 10-parameter model - is illustrated.

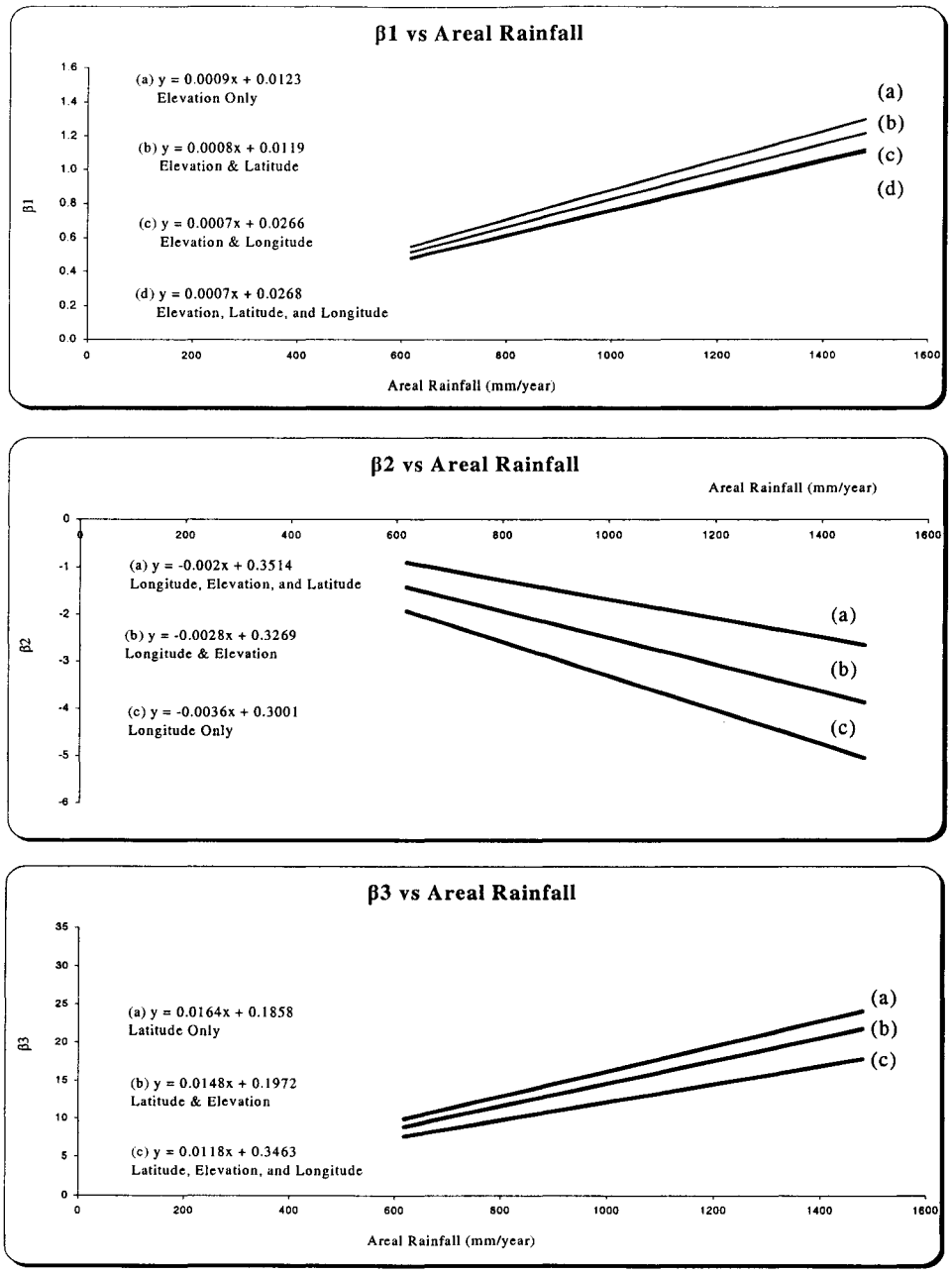


**Figure 6.16:** The relation between the different parameters and areal rain.

**Figure 6.17:** A comparison between MLR models and spatial interpolation techniques.

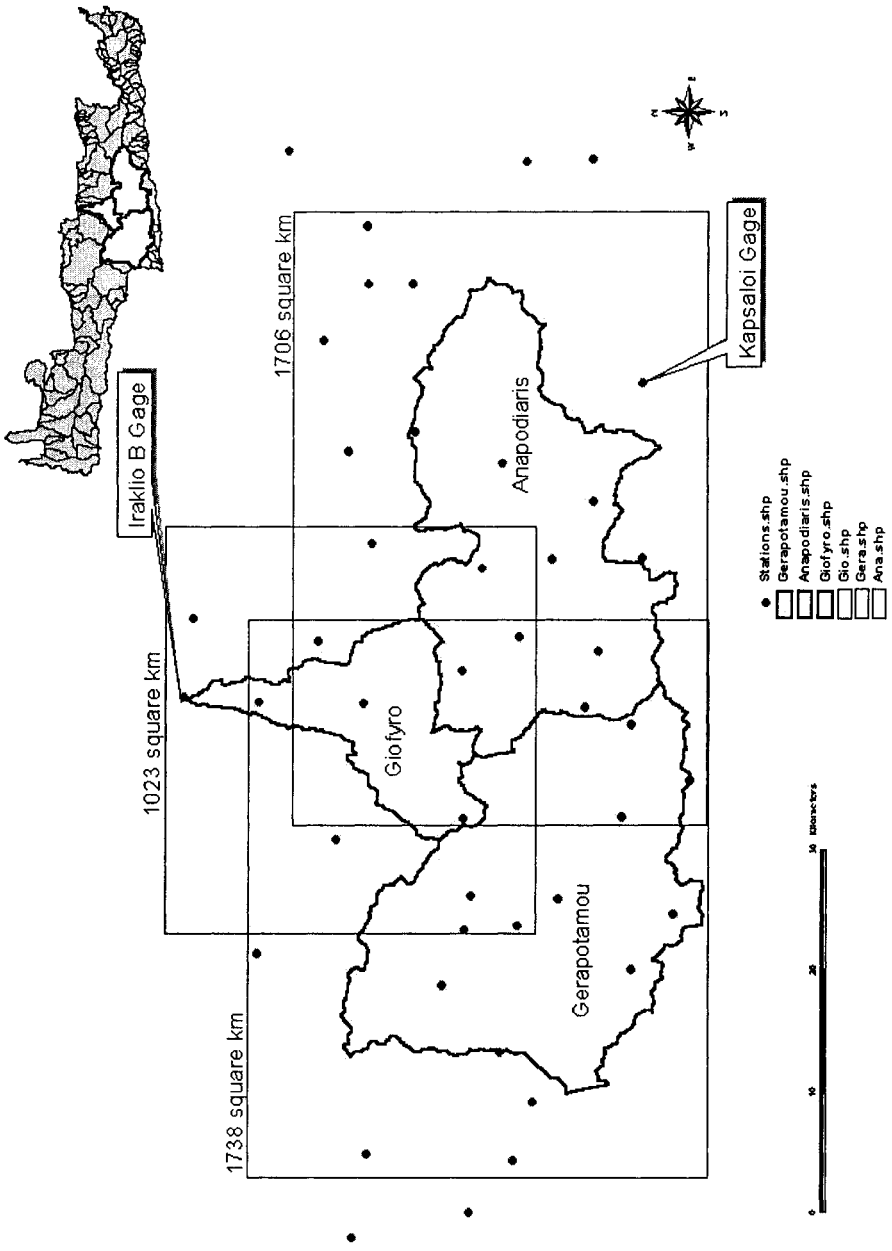


**Figure 6.18:** An illustration of the spatial extents of the basins under study and their respective rain gauges.

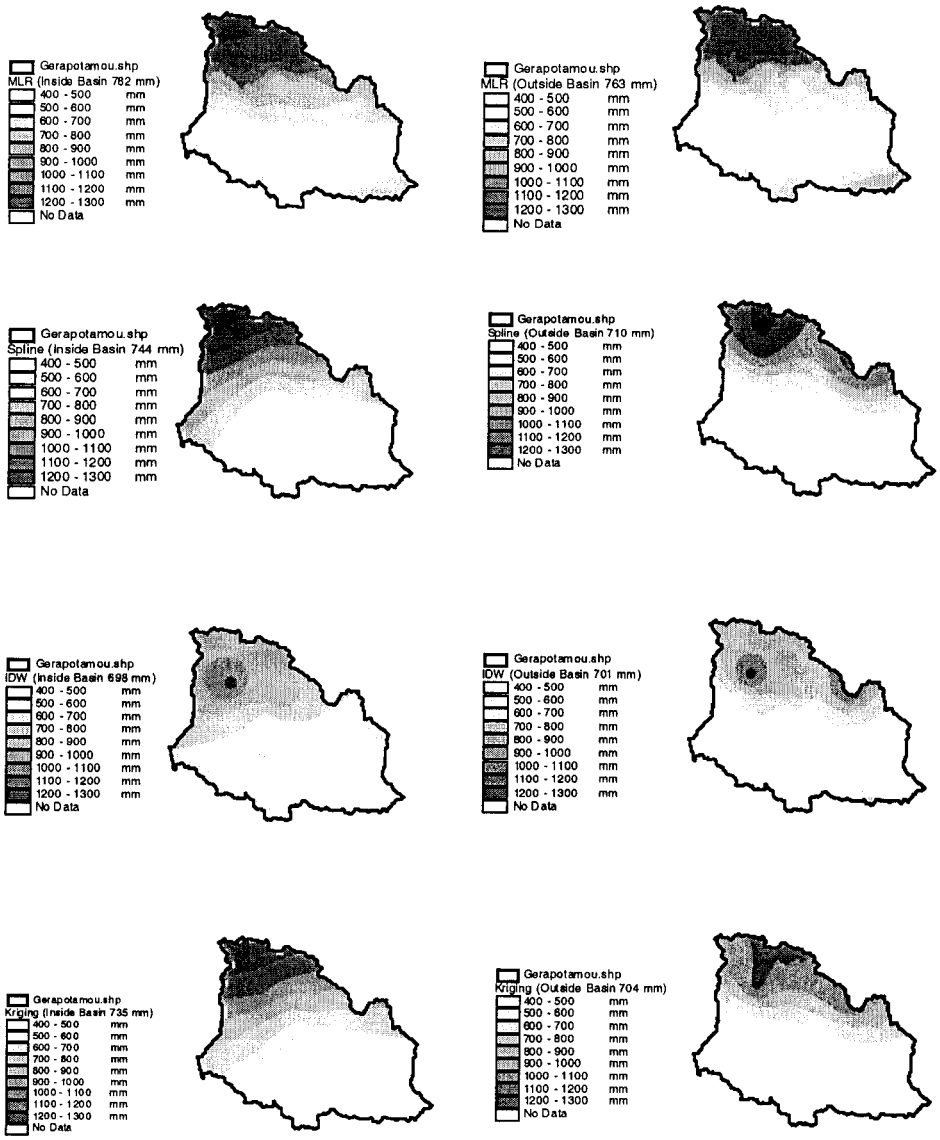


**Figure 6.19:** A comparison between MLR models and conventional spatial interpolation techniques for Gerapotamou basin.

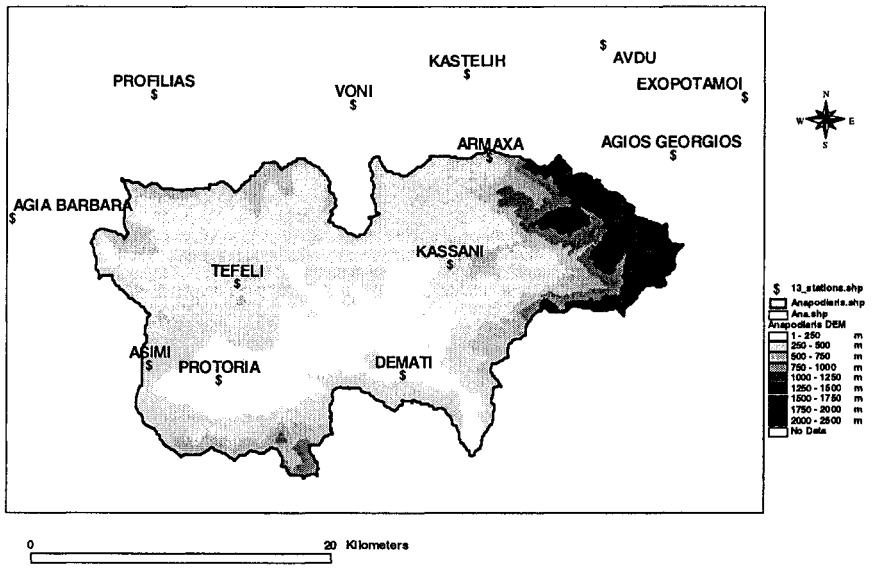


**Figure 6.20:** Anapodiaris basin and the 13 gauges with a common set of data for 30 years (1967-68 to 1996-97).

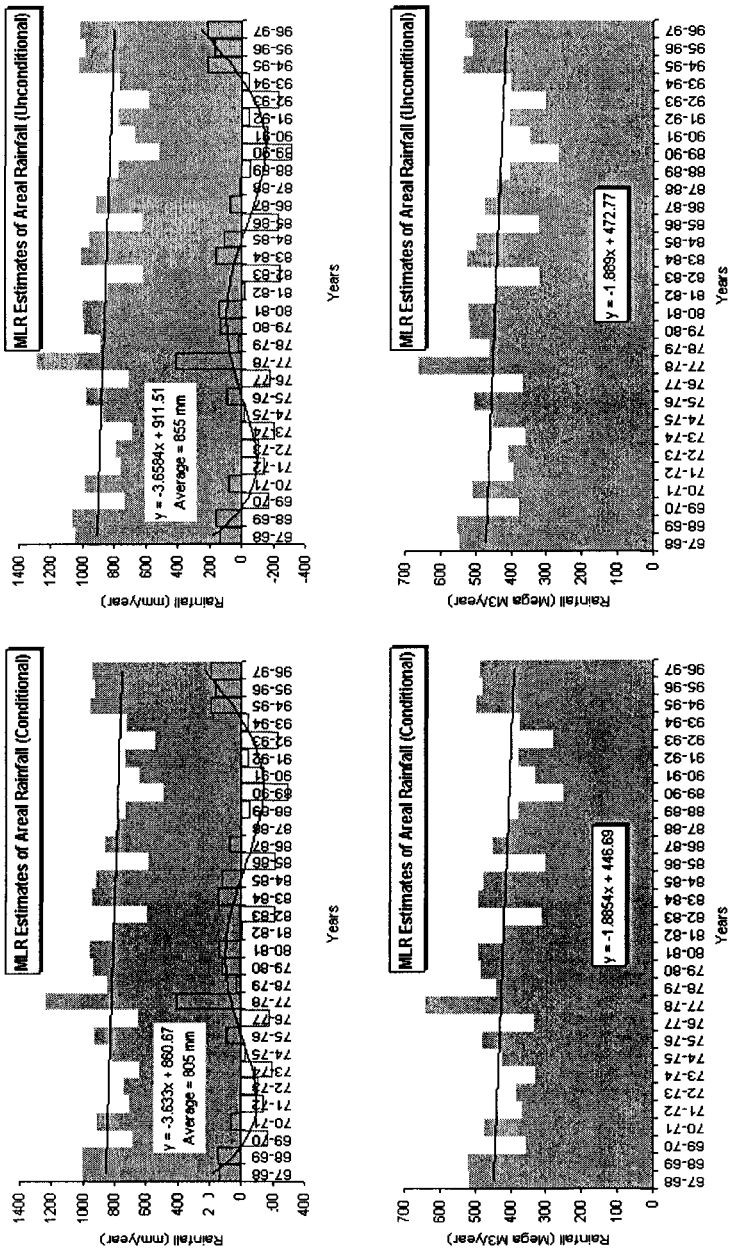


**Figure 6.21:** Estimated yearly areal rainfall for Anapodiaris basin based on the conditional and unconditional criteria for elevation.

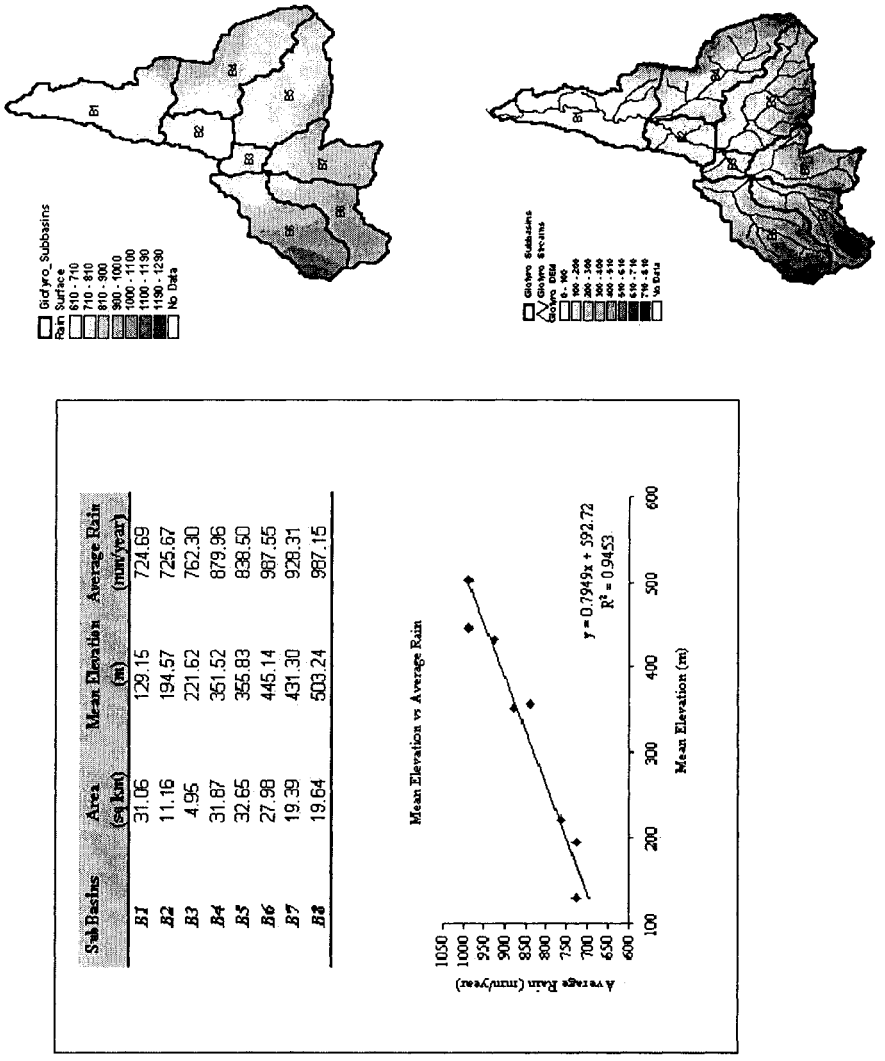


| Sub Basins | Areal (sq km) | Mean Elevation (m) | Average Rain (mm/year) |
|---|---|---|---|
| *B1* | 31.06 | 129.15 | 724.69 |
| *B2* | 11.16 | 194.57 | 725.67 |
| *B3* | 4.95 | 221.62 | 762.30 |
| *B4* | 31.87 | 351.52 | 879.96 |
| *B5* | 32.65 | 355.83 | 838.50 |
| *B6* | 27.98 | 445.14 | 987.55 |
| *B7* | 19.39 | 431.30 | 928.31 |
| *B8* | 19.64 | 503.24 | 987.15 |

**Figure 6.22:** Estimated areal rainfall for Giofyro sub-basins using MLR for an average year.

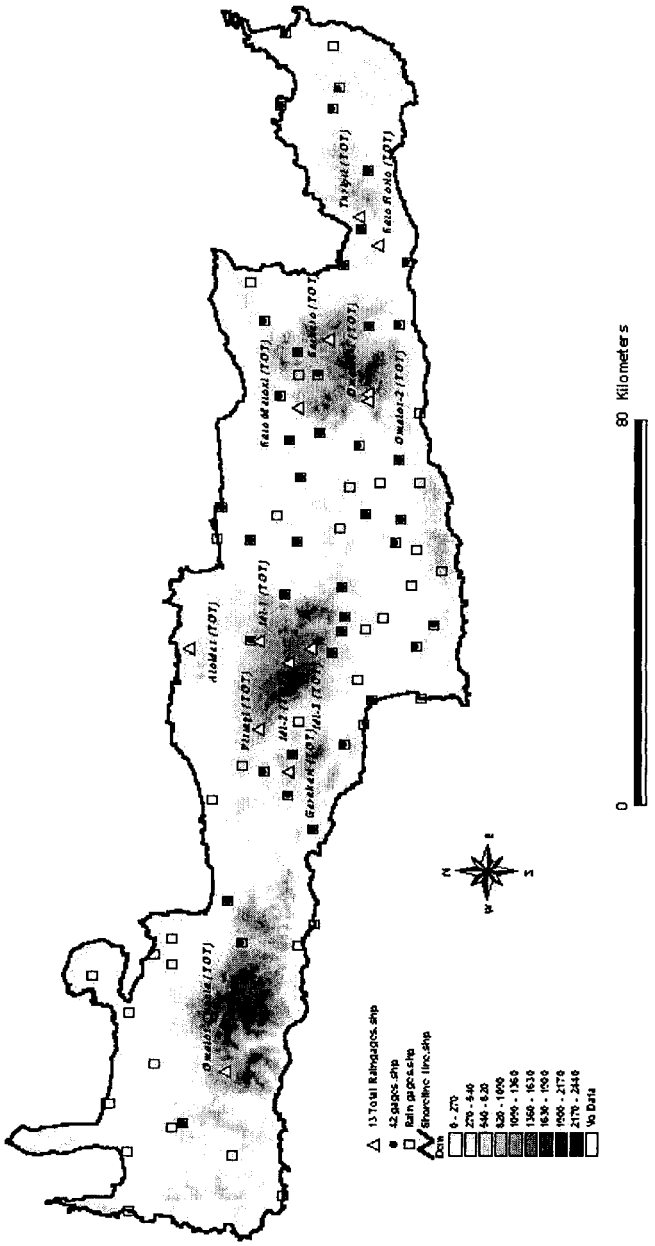


**Figure 6.23:** The gauges used in the analysis. 13 gauges that recorded annual precipitation, 42 gauges that recorded for the period of 1960 to 1995, and a total of 77 gauges that cover the island.

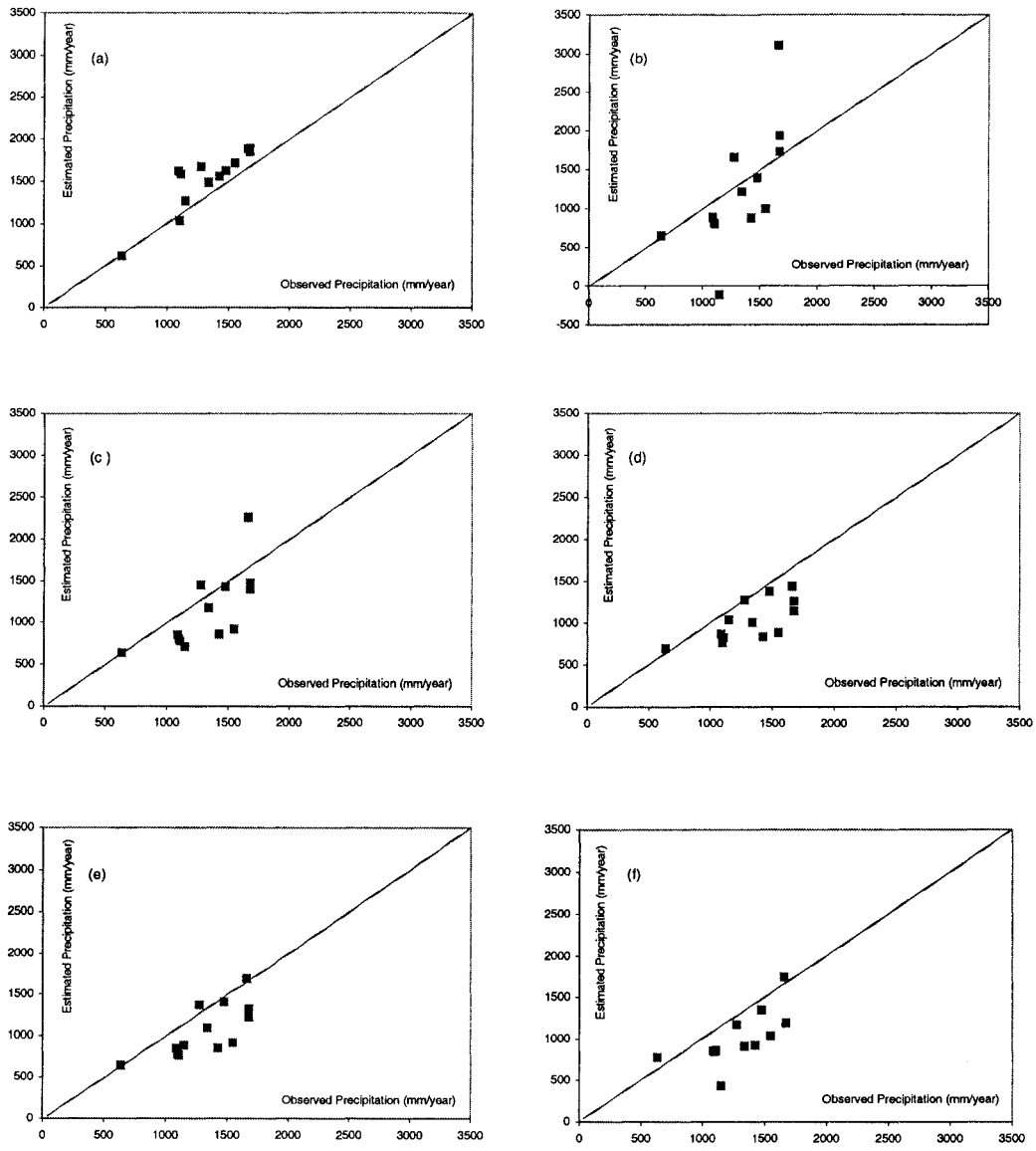


**Figure 6.24:** A comparison between observed precipitation for the water year 1995-96 and estimated values using the MLR models and spatial interpolation techniques.

**Table 6.1:** The different multiple linear regression models for Crete and its three divisions for the year1974-75.

| Data Set | Spatial Extent | No. of Stations | Boundary Conditions: Flow (X1) | Boundary Conditions: Longitude (X2) | Boundary Conditions: Longitude Long (m) | Boundary Conditions: Latitude (X3) | Boundary Conditions: Latitude Lat (m) | β0 | β1 | β2 | β3 | β4 | β5 | β6 | β7 | β8 | β9 | R2 (%) | Is The Model Significant as a ..... Model? Descriptive | Is The Model Significant as a ..... Model? Predictive |
|---|---|---|---|---|---|---|---|---|---|---|---|---|---|---|---|---|---|---|---|---|
| 1977-78 (Wet Year) | Crete | 67 | 0 ≤ (X1) ≤ 905 m | 45 ≤ X2 ≤ 244 km | 464,917.5 ≤ Lo ≤ 705,498 | 69 ≤ X3 ≤ 131 km | 3,869,421.5 ≤ La ≤ 3,938,976 | 655.8 | 1.24 | -2.15 | 3.76 | - | - | - | - | - | - | 61.8 | YES | YES |
| | | | | | | | | 479.4 | 1.76 | -2.03 | 4.85 | -0.0007 | - | - | - | - | - | 62.9 | YES | YES |
| | | | | | | | | 491.8 | 1.77 | -2.16 | 4.77 | -0.0007 | 0.0005 | - | - | - | - | 62.9 | YES | YES |
| | | | | | | | | -2523.0 | 1.46 | -3.83 | 74.67 | -0.0004 | 0.0037 | -0.3703 | - | - | - | 66.9 | YES | YES |
| | | | | | | | | -2168.0 | 1.85 | -2.66 | 64.13 | -0.0002 | 0.0029 | -0.3137 | -0.0039 | - | - | 68.2 | YES | YES |
| | | | | | | | | -1231.0 | 0.80 | -2.56 | 46.40 | -0.0002 | 0.0023 | -0.2328 | -0.0032 | 0.0104 | - | 68.6 | YES | YES |
| | | | | | | | | -7316.0 | 1.56 | 17.60 | 149.12 | 0.0001 | -0.0113 | -0.6596 | -0.0047 | 0.0006 | -0.1716 | 70.5 | YES | YES |
| | North | 20 | 0 ≤ (X1) ≤ 748 m | 13 ≤ X2 ≤ 153 km | 473,828.5 ≤ Lo ≤ 541,595 | 88 ≤ X3 ≤ 131 km | 3,887,874.5 ≤ La ≤ 3,938,976 | 5761.0 | 0.74 | -9.94 | -36.43 | - | - | - | - | - | - | 63.4 | YES | NO |
| | | | | | | | | 7694.0 | -1.14 | -11.83 | -49.77 | 0.0023 | - | - | - | - | - | 67.2 | YES | NO |
| | | | | | | | | 7956.0 | -1.28 | -14.31 | -51.32 | 0.0025 | 0.0133 | - | - | - | - | 67.3 | NO | NO |
| | | | | | | | | -3262.0 | -1.76 | -21.98 | 170.20 | 0.0031 | 0.0482 | -1.0426 | - | - | - | 74.6 | YES | NO |
| | | | | | | | | 3494.0 | 0.03 | -14.27 | 29.00 | 0.0023 | 0.0260 | -0.3672 | -0.0128 | - | - | 77.1 | NO | NO |
| | | | | | | | | 39321.0 | -23.42 | -8.21 | -580.90 | 0.0043 | -0.0109 | 2.2010 | -0.0079 | 0.2013 | - | 80.6 | NO | NO |
| | | | | | | | | 36759.0 | -22.78 | -1.40 | -541.00 | 0.0043 | -0.0158 | 2.0440 | -0.0087 | 0.1959 | -0.0530 | 80.6 | YES | NO |
| | South | 30 | 0 ≤ (X1) ≤ 792 m | 45 ≤ X2 ≤ 182 km | 464,917.5 ≤ Lo ≤ 562.2,758 | 69 ≤ X3 ≤ 108 km | 3,869,421.5 ≤ La ≤ 3,908,176 | -978.3 | 1.05 | 0.62 | 19.91 | - | - | - | - | - | - | 71.9 | YES | YES |
| | | | | | | | | -1093.1 | 0.73 | 1.01 | 21.24 | 0.0004 | - | - | - | - | - | 72.2 | YES | YES |
| | | | | | | | | -1641.0 | 0.71 | 11.33 | 23.57 | 0.0004 | -0.0564 | - | - | - | - | 83.8 | YES | YES |
| | | | | | | | | 4531.0 | 0.21 | 17.60 | -137.28 | 0.0007 | -0.0746 | 0.9797 | - | - | - | 87.2 | YES | YES |
| | | | | | | | | 3538.0 | 0.40 | 16.80 | -112.47 | 0.0009 | -0.0683 | 0.8286 | -0.0025 | - | - | 87.4 | YES | YES |
| | | | | | | | | 4168.0 | -0.74 | 16.13 | -121.14 | 0.0009 | -0.0686 | 0.9528 | -0.0004 | 0.0107 | - | 87.5 | YES | YES |
| | | | | | | | | -454.0 | -2.36 | 45.98 | -49.40 | 0.0009 | -0.1041 | 0.5987 | 0.0058 | 0.0218 | -0.2675 | 88.1 | YES | YES |
| | East | 18 | 0 ≤ (X1) ≤ 986 m | 168 ≤ X2 ≤ 244 km | 621,158.5 ≤ Lo ≤ 705,498 | 78 ≤ X3 ≤ 182 km | 3,876,861.5 ≤ La ≤ 3,902,388 | 669.5 | 1.09 | -2.28 | 4.71 | - | - | - | - | - | - | 89.6 | YES | YES |
| | | | | | | | | 468.4 | 1.79 | -1.92 | 5.23 | -0.0006 | - | - | - | - | - | 91.9 | YES | YES |
| | | | | | | | | -2505.0 | 1.94 | 24.97 | 8.07 | -0.0009 | -0.0668 | - | - | - | - | 92.5 | YES | YES |
| | | | | | | | | -5104.0 | 1.91 | 27.68 | 61.00 | -0.0009 | -0.0731 | -0.2940 | - | - | - | 92.7 | YES | YES |
| | | | | | | | | -3604.0 | 0.39 | 15.37 | 59.40 | -0.0006 | -0.0473 | -0.2832 | 0.0064 | - | - | 92.9 | YES | YES |
| | | | | | | | | -3867.0 | 0.14 | 17.98 | 61.80 | -0.0007 | -0.0525 | -0.3039 | 0.0052 | 0.0065 | - | 92.9 | YES | YES |
| | | | | | | | | -388.0 | -2.36 | -10.18 | 50.40 | -0.0010 | -0.0691 | -0.6561 | 0.0091 | 0.0288 | 0.3667 | 93.3 | YES | NO |

**Table 6.2:** 3-variable MLR models for Crete and its divisions for the different years.

| Data Set | Spatial Extent | Number of Stations | Bo | β1 | β2 | β3 | R2 (%) | Conditional Average Rain (mm) | Conditional Total Rain (Giga M3) | Unconditional Average Rain (mm) | Unconditional Total Rain (Giga M3) |
|---|---|---|---|---|---|---|---|---|---|---|---|
| 1977-78 (Wet Year) | Crete | 67 | 746.67 | 1.16 | - | - | **46.2** | **1360.9** | **11.27** | **1450.1** | **12.01** |
| | North | 20 | 655.80 | 1.24 | -2.15 | 3.76 | **61.8** | 1437.9 | 11.91 | 1533.6 | 12.70 |
| | South | 30 | 5761.00 | 0.74 | -9.94 | -35.43 | **63.4** | 1365.8 | 4.56 | 1421.0 | 4.74 |
| | East | 18 | -978.30 | 1.05 | 0.62 | 19.91 | **71.9** | 1464.8 | 3.94 | 1558.7 | 4.20 |
| 1986-87 (Wet Year) | Crete | 65 | 809.00 | 0.57 | - | - | **13.5** | **1109.4** | **9.19** | **1153.0** | **9.55** |
| | North | 21 | -1121.20 | 0.88 | 0.82 | 18.17 | **53.1** | 1238.9 | 10.26 | 1306.9 | 10.82 |
| | South | 28 | 3763.00 | 0.75 | -7.27 | -19.58 | **47.7** | 1361.9 | 4.54 | 1417.7 | 4.73 |
| | East | 17 | -1340.50 | 0.73 | 0.42 | 21.45 | **65.7** | 1038.5 | 2.80 | 1103.9 | 2.97 |
| | | | -920.40 | 0.67 | 1.67 | 15.36 | **61.2** | 1164.2 | 2.48 | 1206.2 | 2.57 |
| 1989-90 (Dry Year) | Crete | 64 | 344.87 | 0.39 | - | - | **31.1** | **553.9** | **4.59** | **584.3** | **4.84** |
| | North | 21 | -240.80 | 0.49 | -0.01 | 5.89 | **54.6** | 601.2 | 4.98 | 639.0 | 5.30 |
| | South | 27 | 1505.00 | 0.46 | -2.43 | -7.79 | **46.6** | 666.1 | 2.22 | 700.4 | 2.34 |
| | East | 17 | -681.60 | 0.32 | 1.10 | 10.07 | **61.2** | 509.0 | 1.37 | 537.7 | 1.45 |
| | | | -122.50 | 0.44 | 0.03 | 4.57 | **90.2** | 536.5 | 1.14 | 564.1 | 1.20 |
| 1974-75 (Average Year) | Crete | 66 | 536.00 | 0.65 | - | - | **43.6** | **982.1** | **7.31** | **932.4** | **7.72** |
| | | | 50.60 | 0.74 | -0.84 | 6.04 | **68.4** | 944.2 | 7.82 | 1001.3 | 8.29 |
| | North | 19 | 3468.10 | 0.62 | -6.39 | -20.18 | **82.9** | 995.1 | 3.32 | 1041.2 | 3.47 |
| | South | 30 | -543.60 | 0.62 | 0.38 | 11.60 | **72.5** | 886.3 | 2.39 | 941.8 | 2.54 |
| | East | 18 | 364.30 | 0.59 | -1.15 | 3.98 | **88.3** | 816.8 | 1.74 | 853.8 | 1.82 |
| Short-Term Average | Crete | 62 | 628.15 | 0.72 | - | - | **35.5** | **1013.0** | **8.39** | **1068.9** | **8.85** |
| | | | -88.00 | 0.90 | -0.92 | 8.35 | **64.3** | 1108.8 | 9.19 | 1179.3 | 9.77 |
| | North | 18 | 3949.00 | 0.89 | -8.31 | -22.68 | **70.4** | 1187.0 | 3.96 | 1253.3 | 4.18 |
| | South | 28 | -738.50 | 0.66 | 0.24 | 14.95 | **74.6** | 1000.9 | 2.70 | 1060.0 | 2.85 |
| | East | 17 | 85.00 | 0.75 | -0.02 | 5.17 | **83.4** | 958.0 | 2.04 | 1005.1 | 2.14 |
| Long-Term Average | Crete | 49 | 529.71 | 0.72 | - | - | **33.0** | **912.0** | **7.55** | **967.6** | **8.01** |
| | | | -516.50 | 0.66 | -1.50 | 14.16 | **74.0** | 1061.2 | 8.79 | 1112.2 | 9.21 |
| | North | 11 | 2504.00 | 0.62 | -7.32 | -9.32 | **67.9** | 1185.4 | 3.95 | 1231.6 | 4.11 |
| | South | 25 | -503.10 | 0.60 | -2.18 | 15.07 | **83.4** | 980.3 | 2.64 | 1034.0 | 2.78 |
| | East | 14 | -83.50 | 0.72 | 0.29 | 5.78 | **84.4** | 890.0 | 1.90 | 935.1 | 1.99 |

**Table 6.3:** Examining the individual influence of the different predictor variables on estimating average and total rain for the year 1974-75.

| Spatial Extent | Number of Stations | βo | β1 | β2 | β3 | R2 (%) | Conditional: Average Rain (mm) | Conditional: Total Rain (Giga M3) |
|---|---|---|---|---|---|---|---|---|
| Crete (x1) | 66 | 536.00 | 0.65 | - | - | **43.6** | 882.10 | 7.31 |
| Crete (x1, x2) | | 735.99 | 0.69 | -1.65 | - | **59.5** | 913.34 | 7.56 |
| Crete (x1, x3) | | -234.72 | 0.74 | - | 7.92 | **65.6** | 945.02 | 7.83 |
| Crete (x2, x3) | | 527.07 | - | -0.86 | 3.50 | **13.9** | 773.22 | 6.40 |
| Crete (x1, x2, x3) | | 50.60 | 0.74 | -0.84 | 6.04 | **68.4** | 944.20 | 7.82 |
| North (x1) | 19 | 651.83 | 0.79 | - | - | **47.4** | 1042.07 | 3.48 |
| North (x1, x2) | | 843.27 | 1.00 | -2.95 | - | **71.4** | 1103.79 | 3.68 |
| North (x1, x3) | | -243.41 | 1.03 | - | 7.55 | **53.5** | 1109.93 | 3.70 |
| North (x2, x3) | | 5438.31 | - | -8.36 | -35.12 | **69.7** | 837.06 | 2.79 |
| North (x1, x2, x3) | | 3458.10 | 0.62 | -6.39 | -20.18 | **82.9** | 995.10 | 3.32 |
| South (x1) | 30 | 472.85 | 0.65 | - | - | **46.2** | 844.14 | 2.27 |
| South (x1, x2) | | 647.08 | 0.70 | -1.64 | - | **56.0** | 891.75 | 2.40 |
| South (x1, x3) | | -416.86 | 0.63 | - | 10.57 | **72.3** | 890.41 | 2.40 |
| South (x2, x3) | | -806.53 | - | 1.63 | 15.41 | **34.0** | 730.57 | 1.97 |
| South (x1, x2, x3) | | -543.60 | 0.62 | 0.38 | 11.60 | **72.5** | 886.30 | 2.39 |
| East (x1) | 18 | 472.37 | 0.66 | - | - | **84.7** | 834.39 | 1.78 |
| East (x1, x2) | | 718.93 | 0.61 | -1.15 | - | **86.4** | 820.91 | 1.75 |
| East (x1, x3) | | 117.67 | 0.64 | - | 3.98 | **86.7** | 828.35 | 1.76 |
| East (x2, x3) | | 928.06 | - | -4.37 | 6.98 | **40.0** | 684.66 | 1.46 |
| East (x1, x2, x3) | | 364.30 | 0.59 | -1.15 | 3.98 | **88.3** | 816.80 | 1.74 |

**Table 6.4:** MLR models for Crete basins for the year 1974-75.

| Spatial Extent | Area (sq.km) | Mean Elevation (m) | Average Slope (m/km) | Models Used | Number of Stations | Bo | β1 | β2 | β3 | R2 (%) | Conditional Average Rain (mm) | Conditional Total Rain (Mega M3) | Unconditional Average Rain (mm) | Unconditional Total Rain (Mega M3) |
|---|---|---|---|---|---|---|---|---|---|---|---|---|---|---|
| Gerapotamos | 602 | 471 | 170 | Crete (x1) | 66 | 536.00 | 0.65 | - | - | 43.6 | 843 | 506 | 897 | 541 |
| | | | | Crete (x1, x2) | | 735.99 | 0.69 | -1.65 | - | 59.5 | 860 | 519 | 918 | 554 |
| | | | | Crete (x1, x3) | | -234.72 | 0.74 | - | 7.92 | 65.6 | 765 | 461 | 827 | 499 |
| | | | | Crete (x1, x2, x3) | | 50.60 | 0.74 | -0.84 | 6.04 | 68.4 | 790 | 477 | 852 | 514 |
| | | | | South (x1) | 30 | 472.86 | 0.65 | - | - | 46.2 | 778 | 469 | 832 | 502 |
| | | | | South (x1, x2) | | 647.08 | 0.70 | -1.64 | - | 56.0 | 778 | 469 | 836 | 504 |
| | | | | South (x1, x3) | | -416.86 | 0.63 | - | 10.57 | 72.3 | 745 | 449 | 798 | 481 |
| | | | | South (x1, x2, x3) | | -543.60 | 0.62 | 0.38 | 11.60 | 72.5 | 745 | 449 | 796 | 480 |
| | | | | inside (x1) | 9 | 371.52 | 0.97 | - | - | 53.8 | 827 | 449 | 908 | 548 |
| | | | | inside (x1, x2) | | 1495.17 | 0.84 | -8.76 | - | 63.8 | 813 | 490 | 884 | 533 |
| | | | | inside (x1, x3) | | -823.57 | 0.48 | - | 16.87 | 86.3 | 784 | 473 | 824 | 497 |
| | | | | inside (x1, x2, x3) | | -290.51 | 0.47 | -3.42 | 15.54 | 87.8 | 782 | 471 | 821 | 495 |
| | | | | inside & out (x1) | 24 | 492.08 | 0.63 | - | - | 50.7 | 786 | 475 | 841 | 507 |
| | | | | inside & out (x1, x2) | | 853.03 | 0.67 | -2.96 | - | 55.3 | 804 | 485 | 860 | 519 |
| | | | | inside & out (x1, x3) | | -246.74 | 0.58 | - | 8.80 | 75.8 | 748 | 451 | 797 | 480 |
| | | | | inside & out (x1, x2, x3) | | 106.25 | 0.62 | -2.86 | 8.75 | 80.2 | 763 | 460 | 815 | 491 |
| Anapodiaris | 520 | 455 | 167 | Crete (x1) | 66 | 536.00 | 0.65 | - | - | 43.6 | 880 | 457 | 921 | 478 |
| | | | | Crete (x1, x2) | | 735.99 | 0.69 | -1.65 | - | 59.5 | 861 | 442 | 894 | 464 |
| | | | | Crete (x1, x3) | | -234.72 | 0.74 | - | 7.92 | 65.6 | 817 | 424 | 863 | 448 |
| | | | | Crete (x1, x2, x3) | | 50.60 | 0.74 | -0.84 | 6.04 | 68.4 | 815 | 423 | 861 | 447 |
| | | | | South (x1) | 30 | 472.86 | 0.65 | - | - | 46.2 | 816 | 423 | 856 | 444 |
| | | | | South (x1, x2) | | 647.08 | 0.70 | -1.64 | - | 56.0 | 770 | 399 | 814 | 422 |
| | | | | South (x1, x3) | | -416.86 | 0.63 | - | 10.57 | 72.3 | 794 | 412 | 833 | 432 |
| | | | | South (x1, x2, x3) | | -543.60 | 0.62 | 0.38 | 11.60 | 72.5 | 805 | 418 | 844 | 438 |
| | | | | inside (x1) | 9 | 390.03 | 0.72 | - | - | 52.5 | 771 | 400 | 816 | 423 |
| | | | | inside (x1, x2) | | 353.51 | 0.72 | 0.25 | - | 52.6 | 771 | 400 | 816 | 423 |
| | | | | inside (x1, x3) | | -132.22 | 0.38 | - | 7.59 | 85.2 | 700 | 363 | 729 | 376 |
| | | | | inside (x1, x2, x3) | | -232.47 | 0.16 | -1.96 | 13.20 | 86.8 | 647 | 336 | 657 | 341 |
| | | | | inside & out (x1) | 22 | 433.09 | 0.67 | - | - | 69.9 | 789 | 409 | 830 | 431 |
| | | | | inside & out (x1, x2) | | 39.37 | 0.60 | 2.81 | - | 73.6 | 788 | 409 | 825 | 428 |
| | | | | inside & out (x1, x3) | | -189.46 | 0.62 | - | 7.48 | 83.7 | 759 | 394 | 797 | 414 |
| | | | | inside & out (x1, x2, x3) | | -175.73 | 0.62 | -0.18 | 7.61 | 83.7 | 758 | 393 | 797 | 414 |
| Glopyro | 189 | 341 | 163 | Crete (x1) | 66 | 536.00 | 0.65 | - | - | 43.6 | 846 | 151 | 846 | 151 |
| | | | | Crete (x1, x2) | | 735.99 | 0.69 | -1.65 | - | 59.5 | 839 | 150 | 839 | 150 |
| | | | | Crete (x1, x3) | | -234.72 | 0.74 | - | 7.92 | 65.5 | 873 | 156 | 873 | 156 |
| | | | | Crete (x1, x2, x3) | | 50.60 | 0.74 | -0.84 | 6.04 | 68.4 | 861 | 154 | 861 | 154 |
| | | | | North (x1) | 19 | 661.83 | 0.79 | - | - | 47.4 | 1028 | 184 | 1028 | 184 |
| | | | | North (x1, x2) | | 843.27 | 1.00 | -2.95 | - | 71.4 | 913 | 164 | 913 | 164 |
| | | | | North (x1, x3) | | -243.41 | 1.03 | - | 7.55 | 53.5 | 962 | 172 | 962 | 172 |
| | | | | North (x1, x2, x3) | | 3458.10 | 0.62 | -6.39 | -20.18 | 82.9 | 957 | 171 | 957 | 171 |
| | | | | inside (x1) | 3 | 591.73 | 0.67 | - | - | 36.3 | 911 | 163 | 911 | 163 |
| | | | | inside (x1, x2) | | - | - | - | - | - | - | - | - | - |
| | | | | inside (x1, x3) | | - | - | - | - | - | - | - | - | - |
| | | | | inside (x1, x2, x3) | | - | - | - | - | - | - | - | - | - |
| | | | | inside & out (x1) | 13 | 454.66 | 0.78 | - | - | 55.3 | 828 | 148 | 828 | 148 |
| | | | | inside & out (x1, x2) | | 1259.00 | 0.65 | -5.51 | - | 67.8 | 807 | 145 | 807 | 145 |
| | | | | inside & out (x1, x3) | | -368.36 | 1.09 | - | 7.59 | 62.5 | 881 | 158 | 881 | 158 |
| | | | | inside & out (x1, x2, x3) | | 371.40 | 1.00 | -6.33 | 9.40 | 78.6 | 870 | 156 | 870 | 156 |

**Table 6.5:** Estimated areal rainfall for the basins for different elevation ranges for an average year.

| Elevation Range | | Giofyro Basin | Anapodiaris Basin | Gerapotamou Basin |
|---|---|---|---|---|
| E <= 300 M | % of Basin Area | 15% | 12% | 32% |
| | Average Rain | 680 mm | 575 mm | 564 mm |
| 300 M < E < 600 M | % of Basin Area | 57% | 60% | 40% |
| | Average Rain | 830 mm | 700 mm | 720 mm |
| E >= 600 M | % of Basin Area | 28% | 28% | 28% |
| | Average Rain | 1045 mm | 1090 mm | 1230 mm |

**Table 6.6:** Observed and estimated yearly precipitation values for the 13 storage gauges.

| No | 1 | 2 | 3 | 4 | 5 | 6 | 7 | 8 | 9 | 10 | 11 | 12 | 13 |
|---|---|---|---|---|---|---|---|---|---|---|---|---|---|
| English-Name | Alaides (TOT) | Gerakari (TOT) | Idi-1 (TOT) | Idi-2 (TOT) | Idi-3 (TOT) | Kathara (TOT) | Kato Horio (TOT) | Kato Metoxi (TOT) | Omalos Chania (TOT) | Omalos-1 (TOT) | Omalos-2 (TOT) | Thripti (TOT) | Vistagi (TOT) |
| Code | RG31 | RG33 | RG3 | RG7 | RG30 | RG38 | RG37 | RG39 | RG40 | RG34 | RG35 | RG36 | RG32 |
| Prefecture | Rethymno | Rethymno | Rethymno | Rethymno | Rethymno | Lassithi | Lassithi | Lassithi | Chania | Irakilio | Irakilio | Lassithi | Rethymno |
| Longitude | 024:52:20E | 024:35:40E | 024:53:16E | 024:52:20E | 024:50:26E | 025:34:46E | 025:47:20E | 025:25:08E | 023:54:20E | 025:27:14E | 025:26:00E | 025:51:22E | 024:41:00E |
| latitude | 35:22:20N | 35:12:12N | 35:15:00N | 35:13:06N | 35:12:15N | 35:08:50N | 35:03:28N | 35:11:16N | 35:20:50N | 35:04:40N | 35:04:00N | 35:05:18N | 35:15:50N |
| Epsg87.X | 578283.9 | 452778.2 | 573606.0 | 576283.9 | 575225.0 | 642004.4 | 661531.3 | 627845.8 | 490863.8 | 630904.6 | 629393.6 | 667435.2 | 551757.6 |
| Epsg87.Y | 3916306.1 | 3897949.9 | 3903382.7 | 3897978.9 | 3897999.3 | 3890502.2 | 3881266.1 | 3895987.2 | 3909639.2 | 3883076.2 | 3883076.2 | 3894925.7 | 3903410.0 |
| Elevation (X1 in m) | 480.0 | 1000.0 | 1150.0 | 1450.0 | 1360.0 | 1150.0 | 180.0 | 1150.0 | 1050.0 | 1360.0 | 1300.0 | 700.0 | 1040.0 |
| Long (X2 in km) | 117.3 | 91.8 | 118.8 | 117.3 | 114.2 | 181.0 | 200.5 | 186.8 | 29.7 | 169.9 | 168.4 | 206.4 | 100.6 |
| Lat (X3 in km) | 116.3 | 97.9 | 103.4 | 93.7 | 98.0 | 90.5 | 81.3 | 96.0 | 109.6 | 83.1 | 83.1 | 84.9 | 103.4 |
| Agency | YEB | YEB | YEB | YEB | YEB | YEB | YEB | YEB | YEB | YEB | YEB | YEB | YEB |
| Start Date | 1/1/65 | 1/1/68 | 1/1/68 | 1/1/68 | 1/1/68 | 1/1/66 | 1/1/66 | 1/1/68 | 1/1/65 | 1/1/68 | 1/1/95 | 1/1/66 | 1/1/68 |
| End Date | 1/1/96 | 1/1/96 | 1/1/96 | 1/1/96 | 1/1/96 | 1/1/96 | 1/1/96 | 1/1/96 | 1/1/96 | 1/1/96 | 1/1/96 | 1/1/96 | 1/1/96 |
| 1968.69 | -999.99 | -999.99 | 1910.00 | 2020.00 | 1810.00 | 1550.00 | -999.99 | 1625.00 | -999.99 | -999.99 | -999.99 | -999.99 | -999.99 |
| Estimated | 1732.43 | 2037.99 | 2283.39 | 2440.45 | 2417.14 | 1883.61 | 474.95 | 2029.90 | 2472.30 | 1966.72 | 1929.29 | 1169.95 | 2196.49 |
| 1969.70 | -999.99 | 1005.00 | 920.00 | 1215.00 | 1340.00 | 940.00 | -999.99 | 1130.00 | -999.99 | 925.00 | -999.99 | -999.99 | 1180.00 |
| Estimated | 894.92 | 1155.53 | 1232.78 | 1359.72 | 1329.37 | 1053.18 | 360.95 | 1109.11 | 1358.17 | 1148.84 | 1121.19 | 708.31 | 1196.72 |
| 1970.71 | -999.99 | 1545.00 | 1510.00 | 1875.00 | 1915.00 | 1230.00 | -999.99 | 1435.00 | -999.99 | 1155.00 | -999.99 | -999.99 | 1790.00 |
| Estimated | 1316.42 | 1678.35 | 1820.91 | 1999.70 | 1959.80 | 1525.84 | 448.59 | 1672.64 | 2007.01 | 1656.63 | 1612.51 | 972.62 | 1758.80 |
| 1971.72 | -999.99 | 1200.00 | 1186.00 | 1430.00 | 1395.00 | 1105.00 | -999.99 | 1190.00 | -999.99 | 915.00 | -999.99 | -999.99 | 1440.00 |
| Estimated | 1015.02 | 1282.38 | 1395.19 | 1527.95 | 1498.75 | 1177.15 | 360.72 | 1249.81 | 1525.75 | 1273.36 | 1239.68 | 759.77 | 1345.58 |
| 1972.73 | -999.99 | 1136.00 | 1366.00 | 1436.00 | 1360.00 | 1190.00 | -999.99 | 1220.00 | -999.99 | 1110.00 | -999.99 | -999.99 | 1465.00 |
| Estimated | 1250.15 | 1425.45 | 1559.58 | 1638.91 | 1631.94 | 1286.90 | 461.17 | 1383.59 | 1716.46 | 1342.42 | 1310.27 | 860.27 | 1512.58 |
| 1973.74 | -999.99 | 915.00 | 1480.00 | 1155.00 | 1025.00 | 1060.00 | -999.99 | 1055.00 | -999.99 | 940.00 | -999.99 | -999.99 | 1030.00 |
| Estimated | 941.46 | 1176.01 | 1307.86 | 1434.53 | 1403.11 | 1159.53 | 400.63 | 1214.76 | 1348.55 | 1242.29 | 1209.78 | 786.01 | 1243.84 |
| 1974.75 | -999.99 | 1190.00 | 1180.00 | 1660.00 | 1450.00 | 840.00 | -999.99 | 1105.00 | -999.99 | 880.00 | -999.99 | -999.99 | 1285.00 |
| Estimated | 1068.57 | 1371.04 | 1460.80 | 1668.24 | 1572.95 | 1262.96 | 493.77 | 1324.62 | 1595.72 | 1374.01 | 1342.07 | 867.80 | 1417.75 |
| 1975.76 | -999.99 | 1415.00 | 1536.00 | 1690.00 | 1460.00 | 1280.00 | -999.99 | 1415.00 | -999.99 | 1140.00 | -999.99 | -999.99 | 1625.00 |
| Estimated | 1491.43 | 1718.49 | 1877.07 | 1987.97 | 1973.16 | 1565.52 | 567.76 | 1675.23 | 2054.19 | 1643.39 | 1603.87 | 1062.26 | 1818.14 |
| 1976.77 | -999.99 | 1065.00 | 1195.00 | 1315.00 | 1160.00 | 815.00 | -999.99 | 965.00 | -999.99 | 670.00 | -999.99 | -999.99 | 1225.00 |
| Estimated | 1064.16 | 1248.41 | 1407.54 | 1506.53 | 1489.79 | 1198.19 | 331.63 | 1271.36 | 1489.38 | 1248.83 | 1213.96 | 760.18 | 1341.36 |
| 1977.78 | -999.99 | 2090.00 | 3005.00 | 3240.00 | 3770.00 | 1310.00 | -999.99 | 1790.00 | -999.99 | 1305.00 | -999.99 | -999.99 | 3110.00 |
| Estimated | 1569.53 | 2093.84 | 2230.70 | 2480.73 | 2416.09 | 1947.21 | 748.70 | 2033.91 | 2421.68 | 2133.23 | 2082.52 | 1334.65 | 2160.12 |
| 1978.79 | -999.99 | 1270.00 | 1315.00 | 1515.00 | 1410.00 | 1070.00 | -999.99 | 1500.00 | -999.99 | 1025.00 | -999.99 | -999.99 | 1570.00 |
| Estimated | 1236.65 | 1511.90 | 1688.19 | 1842.20 | 1804.33 | 1515.41 | 563.09 | 1583.52 | 1715.88 | 1611.29 | 1568.72 | 1051.15 | 1603.01 |
| 1979.80 | -999.99 | 1450.00 | 1595.00 | 1715.00 | 1570.00 | 1155.00 | -999.99 | 1580.00 | -999.99 | 1050.00 | -999.99 | -999.99 | 1715.00 |
| Estimated | 1329.01 | 1599.36 | 1801.39 | 1956.13 | 1916.27 | 1524.95 | 607.94 | 1697.68 | 1806.86 | 1717.59 | 1671.72 | 1133.24 | 1703.86 |

**Table 6.6:** Continued

| No | 1 | 2 | 3 | 4 | 5 | 6 | 7 | 8 | 9 | 10 | 11 | 12 | 13 |
|---|---|---|---|---|---|---|---|---|---|---|---|---|---|
| English Name | Alolides (TOT) | Gerakari (TOT) | Idi-1 (TOT) | Idi-2 (TOT) | Idi-3 (TOT) | Kathara (TOT) | Kato Herle (TOT) | Kato Metexi (TOT) | Omalos Chania (TOT) | Omalos-1 (TOT) | Omalos-2 (TOT) | Thripti (TOT) | Vistagi (TOT) |
| Code | RG31 | RG33 | RG3 | RG7 | RG30 | RG38 | RG37 | RG39 | RG40 | RG34 | RG35 | RG36 | RG32 |
| 1980.81 | -999.99 | 1700.00 | 1400.00 | 2310.00 | 3360.00 | 1250.00 | -999.99 | 1350.00 | -999.99 | 1070.00 | -999.99 | -999.99 | 1150.00 |
| Estimated | 1249.56 | 1611.97 | 1703.69 | 1880.24 | 1835.96 | 1481.36 | 618.31 | 1546.44 | 1865.63 | 1615.37 | 1579.59 | 1035.88 | 1658.19 |
| 1981.82 | -999.99 | 1575.00 | 1600.00 | 1750.00 | 1700.00 | 925.00 | -999.99 | 1465.00 | -999.99 | 1375.00 | -999.99 | -999.99 | 1775.00 |
| Estimated | 1253.04 | 1503.27 | 1563.35 | 1670.89 | 1663.76 | 1275.36 | 546.52 | 1362.95 | 1811.10 | 1368.20 | 1341.65 | 879.50 | 1547.96 |
| 1982.83 | -999.99 | 1200.00 | 1525.00 | 2000.00 | 1445.00 | 900.00 | -999.99 | 1000.00 | -999.99 | 750.00 | -999.99 | -999.99 | 1500.00 |
| Estimated | 1067.69 | 1351.37 | 1498.67 | 1648.44 | 1612.45 | 1304.94 | 403.86 | 1374.48 | 1573.85 | 1405.64 | 1366.57 | 856.66 | 1428.59 |
| 1983.84 | -999.99 | 1665.00 | 1350.00 | 1650.00 | 1650.00 | 1400.00 | -999.99 | 1225.00 | -999.99 | 1225.00 | -999.99 | -999.99 | 1425.00 |
| Estimated | 1222.40 | 1479.36 | 1636.78 | 1771.79 | 1739.80 | 1461.87 | 591.71 | 1528.58 | 1890.94 | 1547.92 | 1509.66 | 1034.07 | 1562.30 |
| 1984.85 | -999.99 | 1550.00 | 1600.00 | 1700.00 | 1900.00 | 1100.00 | -999.99 | 1000.00 | -999.99 | 1000.00 | -999.99 | -999.99 | 1900.00 |
| Estimated | 1318.26 | 1602.98 | 1730.83 | 1875.93 | 1842.24 | 1520.89 | 654.21 | 1592.54 | 1840.91 | 1623.00 | 1586.38 | 1093.01 | 1671.86 |
| 1985.86 | 1105.00 | 900.00 | 900.00 | 1100.00 | 1150.00 | 1000.00 | -999.99 | 925.00 | -999.99 | 755.00 | -999.99 | -999.99 | -999.99 |
| Estimated | 1305.61 | 1378.96 | 1461.22 | 1496.05 | 1496.29 | 1297.24 | 823.53 | 1356.67 | 1552.06 | 1320.50 | 1300.32 | 1052.34 | 1433.98 |
| 1986.87 | 1255.00 | 1500.00 | 1700.00 | 1650.00 | 1540.00 | 910.00 | 860.00 | 1425.00 | -999.99 | 800.00 | -999.99 | 1360.00 | 1405.00 |
| Estimated | 1863.70 | 1697.67 | 1936.32 | 1966.22 | 1979.22 | 1645.07 | 853.56 | 1767.99 | 2003.09 | 1644.21 | 1603.86 | 1154.59 | 1849.74 |
| 1987.88 | 970.00 | 1400.00 | -999.99 | 1800.00 | 1900.00 | 1325.00 | 490.00 | 1140.00 | -999.99 | 1020.00 | -999.99 | 900.00 | 1220.00 |
| Estimated | 1044.90 | 1436.63 | 1556.72 | 1763.10 | 1703.29 | 1423.12 | 550.24 | 1465.47 | 1608.17 | 1668.03 | 1528.23 | 952.74 | 1496.71 |
| 1988.89 | 1065.00 | 1075.00 | 1225.00 | 1450.00 | 1360.00 | 875.00 | 563.00 | 1150.00 | -999.99 | 925.00 | -999.99 | 975.00 | 1265.00 |
| Estimated | 1069.30 | 1298.90 | 1403.00 | 1521.30 | 1496.50 | 1191.05 | 432.61 | 1261.66 | 1533.08 | 1277.43 | 1246.51 | 801.62 | 1368.80 |
| 1989.90 | 750.00 | 850.00 | 975.00 | -999.99 | 1050.00 | 575.00 | 256.00 | 750.00 | -999.99 | 660.00 | -999.99 | 464.00 | 825.00 |
| Estimated | 742.83 | 883.34 | 969.75 | 1041.26 | 1027.77 | 825.12 | 250.66 | 876.49 | 1042.61 | 874.11 | 862.06 | 554.15 | 933.77 |
| 1990.91 | 825.00 | 950.00 | 1350.00 | 1450.00 | 1100.00 | 860.00 | 462.00 | 1000.00 | -999.99 | 700.00 | -999.99 | 840.00 | 960.00 |
| Estimated | 988.37 | 1134.46 | 1240.04 | 1315.68 | 1302.47 | 1074.49 | 460.04 | 1134.86 | 1316.03 | 1124.52 | 1089.14 | 764.36 | 1196.64 |
| 1991.92 | 1100.00 | 1115.00 | 1610.00 | 2475.00 | 2175.00 | 1050.00 | 572.00 | 1300.00 | -999.99 | 625.00 | -999.99 | 899.00 | 1100.00 |
| Estimated | 1280.46 | 1396.28 | 1544.52 | 1602.24 | 1602.36 | 1279.97 | 476.30 | 1378.21 | 1676.25 | 1315.67 | 1284.27 | 868.49 | 1493.22 |
| 1992.93 | 850.00 | 950.00 | 1100.00 | -999.99 | 1000.00 | 765.00 | 350.00 | 1025.00 | -999.99 | 500.00 | -999.99 | 670.00 | 775.00 |
| Estimated | 932.57 | 1122.37 | 1208.24 | 1256.33 | 1262.26 | 974.76 | 295.50 | 1051.39 | 1373.54 | 1042.51 | 1016.54 | 617.52 | 1178.70 |
| 1993.94 | 925.00 | 1225.00 | 1360.00 | 1310.00 | 1465.00 | 995.00 | 474.00 | 1175.00 | -999.99 | 800.00 | -999.99 | 780.00 | 975.00 |
| Estimated | 1116.87 | 1435.26 | 1549.10 | 1706.96 | 1669.70 | 1313.07 | 421.45 | 1388.34 | 1700.45 | 1428.83 | 1392.02 | 855.69 | 1497.41 |
| 1994.95 | 950.00 | 1125.00 | 1660.00 | 1475.00 | 1475.00 | 1150.00 | 537.00 | 1460.00 | -999.99 | 815.00 | -999.99 | 972.00 | 1175.00 |
| Estimated | 1275.80 | 1566.49 | 1771.34 | 1936.62 | 1895.42 | 1611.80 | 583.86 | 1678.93 | 1758.91 | 1712.18 | 1666.09 | 1118.04 | 1662.20 |
| 1995.96 | 1150.00 | 1475.00 | 1550.00 | 1675.00 | 1675.00 | 1340.00 | 636.00 | 1425.00 | 1660.00 | 1630.00 | 1110.00 | 1100.00 | 1275.00 |
| Estimated | 1262.51 | 1630.29 | 1713.64 | 1867.45 | 1844.57 | 1484.69 | 614.98 | 1554.21 | 1880.26 | 1616.78 | 1580.90 | 1035.14 | 1668.38 |
| 1996.97 | 1400.00 | 1400.00 | 1500.00 | 1475.00 | 1475.00 | 1040.00 | 512.00 | 1455.00 | 2370.00 | 810.00 | 820.00 | 883.00 | 1690.00 |
| Estimated | 1950.12 | 1830.32 | 2001.95 | 2133.31 | 2117.10 | 1607.45 | 431.09 | 1742.36 | 2253.07 | 1704.83 | 1658.35 | 994.70 | 1941.92 |

Note: -999.99 = unavailable record

**Table 6.7:** A comparison between observed precipitation values, estimated precipitation values using Crete models, and estimated precipitation values using regional models.

| No | Region | English-Name | Code | Prefecture | X1 | X2 | X3 | 1974-75 | 1977-78 | 1986-87 | 1989-90 |
|---|---|---|---|---|---|---|---|---|---|---|---|
| | Observed | | | | | | | -999.99 | -999.99 | 1255.00 | 750.00 |
| 1 | Crete | Aloides (TOT) | RG31 | Rethymno | 460.0 | 117.28 | 116.34 | 1068.57 | 1589.53 | 1663.70 | 742.83 |
| | North | | | | | | | 646.19 | 813.81 | 977.49 | 524.41 |
| | Observed | | | | | | | 1190.00 | 2090.00 | 1500.00 | 850.00 |
| 2 | Crete | Gerakari (TOT) | RG33 | Rethymno | 1000.0 | 91.78 | 97.95 | 1371.04 | 2093.84 | 1697.67 | 883.34 |
| | South | | | | | | | 1247.49 | 2078.78 | 1529.07 | 721.58 |
| | Observed | | | | | | | 1180.00 | 3005.00 | 1700.00 | 975.00 |
| 3 | Crete | Idi-1 (TOT) | RG3 | Rethymno | 1150.0 | 118.81 | 103.38 | 1460.80 | 2230.70 | 1936.32 | 969.75 |
| | North | | | | | | | 1325.67 | 1768.22 | 1737.55 | 936.75 |
| | Observed | | | | | | | 1660.00 | 3290.00 | 1650.00 | -999.99 |
| 4 | Crete | Idi-2 (TOT) | RG7 | Rethymno | 1450.0 | 117.28 | 93.73 | 1609.24 | 2480.73 | 1966.22 | 1041.28 |
| | North | | | | | | | 1716.21 | 2347.38 | 2162.63 | 1152.65 |
| | Observed | | | | | | | 1450.00 | 3770.00 | 1540.00 | 1050.00 |
| 5 | Crete | Idi-3 (TOT) | RG30 | Rethymno | 1350.0 | 114.23 | 97.97 | 1572.95 | 2416.09 | 1979.22 | 1027.77 |
| | North | | | | | | | 1588.18 | 2153.55 | 2026.85 | 1081.37 |
| | Observed | | | | | | | 840.00 | 1310.00 | 910.00 | 575.00 |
| 6 | Crete | Katharo (TOT) | RG38 | Lassithi | 1150.0 | 181.00 | 90.50 | 1262.95 | 1947.21 | 1645.07 | 825.12 |
| | East | | | | | | | 1194.84 | 1936.58 | 1542.49 | 800.44 |
| | Observed | | | | | | | -999.99 | -999.99 | 880.00 | 256.00 |
| 7 | Crete | Kato Horio (TOT) | RG37 | Lassithi | 180.0 | 200.53 | 81.29 | 493.77 | 748.70 | 653.56 | 290.66 |
| | East | | | | | | | 563.41 | 791.35 | 783.64 | 334.58 |
| | Observed | | | | | | | 1105.00 | 1790.00 | 1425.00 | 750.00 |
| 8 | Crete | Kato Metoxi (TOT) | RG39 | Lassithi | 1150.0 | 166.85 | 96.00 | 1324.62 | 2033.91 | 1767.99 | 876.49 |
| | East | | | | | | | 1233.00 | 1994.74 | 1603.25 | 825.06 |
| | Observed | | | | | | | -999.99 | -999.99 | -999.99 | -999.99 |
| 9 | Crete | Omalos Chania (TOT) | RG40 | Chania | 1050.0 | 29.66 | 109.64 | 1595.72 | 2421.68 | 2003.09 | 1042.61 |
| | South | | | | | | | 1390.49 | 2325.51 | 1790.22 | 786.94 |
| | Observed | | | | | | | 880.00 | 1305.00 | 800.00 | 560.00 |
| 10 | Crete | Omalos-1 (TOT) | RG34 | Iraklio | 1350.0 | 169.90 | 83.08 | 1374.01 | 2133.23 | 1644.21 | 874.11 |
| | South | | | | | | | 1321.65 | 2198.59 | 1498.34 | 768.18 |
| | Observed | | | | | | | -999.99 | -999.99 | -999.99 | -999.99 |
| 11 | Crete | Omalos-2 (TOT) | RG35 | Iraklio | 1300.0 | 168.39 | 83.08 | 1342.07 | 2082.52 | 1603.86 | 852.08 |
| | South | | | | | | | 1290.07 | 2145.15 | 1461.21 | 750.71 |
| | Observed | | | | | | | -999.99 | -999.99 | 1360.00 | 464.00 |
| 12 | Crete | Thripti (TOT) | RG36 | Lassithi | 700.0 | 206.44 | 84.93 | 867.60 | 1334.65 | 1154.59 | 554.15 |
| | East | | | | | | | 877.90 | 1361.83 | 1197.81 | 578.94 |
| | Observed | | | | | | | 1285.00 | 3110.00 | 1405.00 | 825.00 |
| 13 | Crete | Vistagi (TOT) | RG32 | Rethymno | 1040.0 | 100.76 | 103.41 | 1417.75 | 2160.12 | 1849.74 | 933.77 |
| | North | | | | | | | 1372.25 | 1865.25 | 1785.72 | 930.07 |

Note: -999.99 = unavailable record

# CHAPTER 7

# IRRIGATION WATER DEMAND ASSESSMENT

In the first part of this chapter, the design, development, and application of a hydroinformatic system for estimating evapotranspiration is presented. Reference evapotranspiration is calculated via the Penman-Monteith approach as well as the Class A pan evaporation records. Station- and grid-based methods for estimating reference evapotranspiration are developed and coupled to a geographic information system. The station-based method provides the user with evapotranspiration estimates at point locations, corresponding to meteorological stations within the study area. The grid-based method is developed in order to provide an improved understanding of the spatial variation in evapotranspiration. A graphical interface provides model execution and functionality for use in the management phase of the analysis. The island of Crete is used as a case study to illustrate the applicability of the system.

In the second part of the chapter, a GIS was also used to utilize spatially distributed and temporally averaged meteorological data, crop distributions, and crop coefficients in order to estimate irrigation requirements. The irrigation requirements were estimated as the difference between crop evapotranspiration and effective rainfall. Crop evapotranspiration was evaluated as the product of reference evapotranspiration and the crop coefficient. Reference evapotranspiration is calculated via the Penman-Monteith approach. Monthly effective rainfall was estimated from total monthly rainfall according to the method developed by the USDA Soil Conservation Service. The country of Greece as well as the island of Crete were both used as case studies.

## 7.1 Introduction

Evapotranspiration is the sum of the volume of water used by vegetation (transpired) and evaporated from the soil and the intercepted precipitation on vegetation (Singh, 1988). It plays an important role in our environment at global, regional, and local scales. Water entering the evaporation phase of the hydrological cycle becomes unavailable and cannot be recovered for further use (Brutsaert, 1982). In many areas where water resources are scarce, the calculation of this loss becomes imperative in the planning and management of irrigation practices. The shortage of water in the dry seasons for the different uses makes the accurate estimation of this loss very important. This is especially true when estimating the crop water requirements of agricultural areas. Despite its importance, the loss of water by evapotranspiration in the water balance calculation is one of the least understood components of the hydrologic cycle, which in turn, influences significantly the irrigation requirements estimation (Brutsaert, 1982; Jackson, 1985).

Evaporation and transpiration occur simultaneously and there is no easy way of distinguishing between the two processes (Allen et al., 1998). Transpiration consists of the vaporization of liquid water contained in plant tissues and the vapor removal to the atmosphere. Evaporation occurs at the top soil if the water is available. When the crop is small, water is predominantly lost by soil evaporation, but once the crop is well developed and completely covers the soil, transpiration becomes the main process. Smith et al (1997) defined the reference evapotranspiration as "the rate of evapotranspiration from a hypothetical reference crop with an assumed crop height (12 cm), a fixed crop surface resistance (70 s/m) and albedo (0.23) , closely resembling the evapotranspiration from an extensive surface of green grass cover of uniform height, actively growing, completely shading the ground with adequate water".

Numerous methods have been proposed for modelling evapotranspiration as described by Brutsaert (1982) and ASCE (1989). In general, the combination of energy balance/aerodynamic equations "provide the most accurate results as a result of their foundation in physics and basis on rational relationships" (ASCE, 1989).

GIS contains the unique functionality to manage and relate both spatial and tabular data. In doing so, this technology provides a structured formal data model that symbolically represents patterns and processes in our environment. As a result, this technology provides new ways in which to address, store information about, and display information that is relevant to the problem statement. These combine to provide enhanced decision support in terms of efficiency, application development, and data visualization.

## 7.2 Methodology

### 7.2.1 Reference Evapotranspiration

Reference evapotranspiration (ETo) is either directly measured using a lysimeter or estimated using climatological or pan evaporation data. Both methods of estimating ETo are incorporated in the system.

#### 7.2.1.1 The FAO Penman-Monteith approach

The Penman-Monteith approach for calculating reference evapotranspiration ($ET_o$) is used. It is a combination of both aerodynamic and radiation terms, as reported by Allen et al. (1998):

$$ET_o = \frac{0.408\Delta (R_n - G) + \gamma \frac{900}{T+273} U_2 (e_a - e_d)}{\Delta + \gamma (1 + 0.34 U_2)} \qquad (7.1)$$

where $ET_o$ is the reference evapotranspiration (mm $d^{-1}$); $R_n$ is the net radiation at crop surface

(MJ $m^{-2}$ $d^{-1}$); $G$ is the soil heat flux (MJ $m^{-2}$ $d^{-1}$); $T$ is the average temperature (°C); $U_2$ is the wind speed measured at 2.0m height (m $s^{-1}$); $(e_a-e_d)$ is the vapor pressure deficit (kPa); $\Delta$ is the slope vapor pressure curve (kPa °$C^{-1}$); $\gamma$ is the psychrometric constant (kPa °$C^{-1}$); and 900 is the conversion factor.

The different meteorological variables on the right hand side of equation (7.1) are either measured or estimated from other more readily available meteorological variables (for instance, sunshine hours rather than net or solar radiation). Although this method provides good estimates of evapotranspiration, it requires a large amount of data which can sometimes be a limitation and alters its popularity worldwide especially in developing countries. Note that if only mean temperature records are available, "the calculations can still be executed but some underestimation of Eto will probably occur due to the non-linearity of the saturation vapor pressure-temperature relationship. Using mean air temperature instead of maximum and minimum air temperatures yields a lower saturation vapor pressure ($e_a$), and hence a lower vapor pressure difference ($e_a$-$e_d$), and a lower reference evapotranspiration estimate" (Allen at al., 1998).

7.2.1.2 Pan Evaporation Coefficient ($K_p$)

ETo can be estimated from pan evaporation records using the simple equation:

$$ET_o = K_P * E_{pan} \tag{7.2}$$

where $ET_o$ is the reference evapotranspiration (mm $d^{-1}$); $K_p$ is the pan coefficient ( ); and $E_{pan}$ is the evaporation rate from a class "A" evaporation pan (mm $d^{-1}$).

Raghuwanshi and Wallender (1998) developed a new formula to estimate pan coefficient that, as they reported, is more accurate than Cuenca's (1989) or Snyder's (1992) formulas. The indicator regression technique is used to derive the formula as a function of fetch distance, wind speed and relative humidity. The model uses both qualitative (categorical) (wind speed and relative humidity) and quantitative (fetch length) data as independent variables to estimate ($K_p$) which is the dependent variable. The new equation is:

$$K_P = 0.5944 + 0.0242X_1 - 0.0583X_2 - 0.1333X_3 - 0.2083X_4 + 0.0812X_5 + 0.1344X_6 \tag{7.3}$$

where $K_p$ is the pan coefficient ( ); $X_1$ is the ln (natural logarithm) of fetch distance in meters; $X_2$, $X_3$, *and* $X_4$ are the wind speed categories of 175-425, 425-700 and >700 in km $day^{-1}$, respectively. These variables are assigned values of one or zero depending upon their

presence. A zero value for these variables represented a wind run of <175 km $d^{-1}$; $X_5$ *and* $X_6$ are the relative humidity categories of 40-70 % and ≥70 %, respectively. These variables are assigned values of one or zero depending upon their presence. A zero value for these variables represented a relative humidity of ≤40 %.

Note that since most of wind speed data are compiled in (m $s^{-1}$), all wind speed records were multiplied by 86.4 to convert to km $d^{-1}$ to suit the methodology units. Figure 7.1a shows the influence of each factor on the estimated value of $K_p$.

7.2.2 Effective Precipitation

Effective precipitation is the portion of total precipitation which is useful for crop production. As previously mentioned, effective precipitation is estimated according to the method of the USDA Soil Conservation Service (Dastane, 1974). The method assumes that crops can use almost 60 to 80 percent of the precipitation up to 250 mm/month. Over 250 mm/month, the crops benefit from only 10 percent of that amount as shown in Figure 7.1b. In other words, as precipitation increases, its efficiency decreases:

$$\begin{aligned} P_{eff} &= P_{tot}\,(125-0.2P_{tot})/125 && \text{for } P_{tot} < 250\text{mm} \\ P_{eff} &= 125 + 0.1\,P_{tot} && \text{for } P_{tot} > 250\text{mm} \end{aligned} \qquad (7.4)$$

where $P_{eff}$ is the effective precipitation in millimeters per month and $P_{tot}$ is the total precipitation in millimeters per month.

Effective precipitation values are then linearly interpolated to daily values. It should be noted that in this study, due to lack of soil properties data, rainfall losses due to deep percolation and surface runoff are not being directly taken into account in the actual soil moisture content of the root zone. The USDA SCS method accounts for some of the losses. No daily rain data is available and the gauges used are of the cylindrical weighing type with a diameter of 10 cm. The addition of oil, which forms a film on the surface, prevents excessive evaporation losses.

7.2.3 Irrigation Requirements

Irrigation requirements are then calculated after the Cropwat program (Smith, 1992) by:

$$Irr = A\Sigma_{i=1}^{365}(ET_{0_i} * K_c - P_{eff_i}) \qquad (7.5)$$

where *Irr* is the irrigation requirements ($m^3$ $year^{-1}$); *A* is the crop area in stremmas (1 stremma = 1000 $m^2$); $ET_o$ is the reference evapotranspiration (mm $d^{-1}$); $k_c$ is the crop coefficient ( );

and $P_{eff}$ is the effective rainfall (mm $d^{-1}$).

The crop coefficients are used in determining each crop's actual evapotranspiration. These values may vary based on the crop characteristics, planting date, crop development and phenology, the length of growing season, and local climatic conditions (Doorenbos and Pruitt, 1977). Only positive values for *Irr* are considered since negative values indicate that only precipitation can cover the crop needs.

## 7.3 Study Areas

### 7.3.1 Greece

Greece covers an area of 130000 $km^2$ and is located in the Mediterranean region at the south of Europe and facing northern Africa as shown in Figure 7.2a. The result of the country's geographical location can be seen in its climate range with mild winters and sub-tropically warm summers cooled by a system of seasonal breezes popularly called "meltemia". An outstanding feature of the Greek climate is its ample sunshine hours, which is about 3,000 hours per year. In recent times, water demand has significantly increased in Greece, raising concerns on the availability of this resource for irrigation purposes. Government agencies agree that water consumption constitutes only a small percentage, estimated at approximately 5 percent of the total annual precipitation. The northwestern region of Greece, which is a mountainous region, receives most of the annual precipitation, imposing technical and economic constraints on the transport of this resource to other parts. In many areas, such as the coastal districts and throughout the southeastern regions, a severe water imbalance occurs. This is especially true during summer months when these districts experience seasonal fluctuations in precipitation at times when the water demand is at its maximum. These uneven spatial and temporal distributions, although common in many Mediterranean countries, have significant impact when compounded by the water demands associated with high population densities, intensive agricultural activities, tourism industry, and high surface run-off (Marecos do Monte et al., 1996).

Meteorological data were compiled by the Hellenic National Meteorological Service for 38 meteorological stations representing the country as shown in Figure 7.2b. This data set included information on wind speed, precipitation, air temperature, relative humidity and sunshine hours. Time series data were manually entered into database tables. The GIS coverages used in this study were based upon maps developed by the Greek Army Geographical Service.

Greece is divided politically into 51 counties as shown in Figure 7.3a. Data on arable and irrigated lands and category of cultivated crops were reported by county by the Ministry of Agriculture of Greece for the years 1963, 1971, 1981, 1991, and 1992. The Ministry also

provided the distribution percentage of the different crops for each of the four main categories (trees, grapes, vegetables, and crops). This information was integrated into the database by relating the statistics for each county to the corresponding feature contained within the counties' database layer.

According to water resources legislation, Greece is divided into 14 hydrologic compartments for water administration and management reasons as shown in Figure 7.3b. The compartments are placed into two groups according to their geographical location as follows: (1) West Rumeli, Epirus, Thessaly, West Macedonia, Central Macedonia, East Macedonia, and Thrace are located to the northern part of the country; and (2) West Pelponnesus, North Pelponnesus, East Pelponnesus, Attica, East Rumeli, Crete, and Aegean Isles constitute the southern part. The 38 representative meteorological stations of Greece are distributed so that at least one station will represent a hydrologic compartment.

Planting dates, growing season duration, and crop coefficients for each crop were obtained for both Northern and Southern Greece by the National Foundation for Agriculture Research Institute of Iraklion and from the literature (Doorenbos and Pruitt, 1977; Papazafiriou, 1984; ASCE, 1989) and after consultation with the Ministry of Agriculture of Greece.

### 7.3.2 Crete

The island of Crete, one of Greece's hydrologic compartments, is located at the most southern point of Greece. Approximately 7% of the total irrigated land in the country of Greece is located on the island of Crete. In spite of adequate precipitation, the increased demand for water for agricultural use in Crete, which consists of approximately 80% of the water use, cannot be always met (Angelakis and Diamadopoulos, 1995).

There has been little emphasis on quantifying the variation in climatic conditions and/or the relative distribution of irrigated areas and their respective impact on irrigation estimates on the island of Crete. The water use for irrigation requirements in Crete was estimated at 200 $Mm^3$ for the year 1980 (Ministry of Industry, 1989).

The island of Crete has a total area of 8265 $km^2$ (which is almost 6.3% of the area of Greece) with an agricultural area of 3205 $km^2$. The island is divided into four counties (Lassithi, Iraklio, Rethymno, and Chania). In the county of Iraklio (2626 $km^2$) the most of the agricultural activity takes place while the remaining counties in order of agricultural activity, are: Lassithi (1810 $km^2$), Chania (2342 $km^2$) and Rethymno (1487 $km^2$). The counties are divided into 20 regions and 567 municipalities, as shown in Figure 7.4. Information on four main categories of crop (i.e. trees, grapes, vegetables and crops) are as follows: (a) trees occupy approximately 64% of the irrigated land in Crete, representing

almost 20% of the total area under trees in Greece; (b) 30% of the grapes in Greece are grown in Crete, covering 12% of the island's irrigated land; (c) 7% of the vegetable (green) area in Greece is located in Crete, representing approximately 10% of the island's irrigated land; and (d) 1% of the crop area in Greece is located in Crete, constituting 14% of the irrigated land in Crete.

The data on irrigated land and category of crop were collected from the records of the municipalities, which were made available by the Ministry of Agriculture of Greece for the year 1991, as shown in Table 7.1. All areas are reported in units of stremmas (one stremma = 1000 $m^2$). The irrigated land for the year 1991 was estimated at 789 $km^2$, which corresponds to 26% of the overall agricultural land (Agricultural Statistics of Greece, 1991). The spatial distribution of the irrigated land and the four categories of crop are shown in Figures 7.5a to 7.5d. The biggest share of the irrigated areas of the four main categories of crops (trees, grapes, vegetables, and crops on arable land) are in the county of Iraklion, which contains 38% of the irrigated area under trees, 89% of the area under grapes, 43% of the vegetable area, and 43% of the area under crops. The county of Lassithi comes in second place, Chania comes third, and the county of Rethymno comes last.

Figure 7.5a shows that the largest area under trees is in the region of Kydonias (943) in the prefecture of Chania, which represents around 16% of the total irrigated land under trees in Crete. The municipality of Males, in the prefecture of Lassithi, was found to contain the largest irrigated area of trees, which is about 11.4% of the trees area in Lassithi and 3.2% of the total trees area in Crete. Figure 7.5b shows that the largest area under grapes can be found in the region of Monofatsiou (914), in the prefecture of Iraklion, which represents around 30% of the total irrigated land under grapes in Crete. The municipality of Iraklio, in the prefecture of Iraklion, was found to contain the largest irrigated area of grapes, which is about 8% of the grapes area in Iraklion and 7.1% of the total grapes area in Crete. Figure 7.5c shows that the largest vegetable area can be found in the region of Ierapetras (921), in the prefecture of Lassithi, which represents around 13% of the total irrigated land under vegetables in Crete. The municipality of Males, in the prefecture of Lassithi, was found to contain the largest irrigated area of vegetables, which is about 25.4% of the vegetable area in Lassithi and 6.2% of the total vegetable area in Crete. Figure 7.5d shows the largest area under crops can be found in the region of Monofatsiou (914), in the prefecture of Iraklion, which represents around 17% of the total irrigated land under crops in Crete. The municipality of Agios Georgios, in the prefecture of Lassithi, was found to contain the largest irrigated area of crops, which is about 12.5% of the crops area in Lassithi and 3% of the total crops area in Crete.

Monthly meteorological data was compiled by the Hellenic National Meteorological Service for 54 meteorological stations for periods up to 50 years representing the island (refer

to Figure 7.6a). The locations of the stations were provided in degrees, minutes, and seconds. Counties with higher agricultural activity (Eastern Crete) was covered by more stations. The available records ranged from 12 to 50 years. The gauges were located at different elevations ranged from mean sea level (MSL) in the county of Iraklion to 905 m above MSL for the county of Lassithi. Spatial data is handled through the use of the software ArcView GIS where a database was created for that purpose. The database included information on spot elevations for the island, shoreline, counties, location of stations (x, y, z), and monthly data for relative humidity, sunshine hours, maximum temperature, minimum temperature, mean temperature, wind speed, and pan evaporation. GIS layers were generated for the meteorological stations where their locations were identified (after conversion from DMS) by decimal degrees. The layers were then projected using the Transverse Mercator projection and the GRS 80 Spheroid with a Central Meridian of 24°, Scale Factor of 0.9996, and False Easting of 500000. This projection is also referred to as EGSA units. From the spot elevation values together with a 20m contour map, a Digital Elevation Model (DEM) was also generated as shown in Figure 7.6b.

Again, the meteorological data was compiled by the Hellenic National Meteorological Service for ten meteorological stations representing the island (refer to Figure 7.4). This data set included information on relative humidity, sunshine hours, maximum temperature, minimum temperature, mean temperature, and wind speed. Based on the methodology described above, preliminary graphs were developed which show the time series of reference evapotranspiration and effective precipitation for those representative stations (as shown in Figure 7.7). The graphs best describe the severe water shortages that occur in summer months.

## 7.4 The ArcView GIS Project

### 7.4.1 Approach

The system is developed within ArcView GIS. The components of this system include (1) the FAO Penman-Monteith Method for reference evapotranspiration, (2) the pan coefficient model, (3) database, (4) a Graphic User Interface, and (5) Display functionality. Two approaches are proposed in determining the reference evapotranspiration which are referred to as station-based method and grid-based method.

#### 7.4.1.1 Station-based Method

This method provides the user with evapotranspiration estimates at point locations, corresponding to meteorological stations within the study area, where the required climatic and precipitation data have been collected. The user may assign representative stations to management areas, such as a watershed or administrative district, and proceed to calculate

ETo. Using the The ArcView GIS programming language (AVENUE) calculation procedures are contained within the GIS. This minimizes the need for pre- and post-processors since the numerical model directly accesses input data from within the database structure connected to the GIS. Input requirements are 7 shapefiles representing the location of the meteorological stations that record relative humidity, wind speed, sunshine hours, mean temperature, maximum temperature, minimum temperature, and pan evaporation (in case of using the Pan Evaporation method). For the station-based method, the number and location of the stations should be the same for all shapefiles. The attribute table of one of the shapefiles should contain, in addition to "elevation" and "name", information about "fetch length" in meters and "latitude" in decimal degrees for all stations.

#### 7.4.1.2 Grid-based Method

This method enables estimates of the spatial variation in evapotranspiration to be acquired at a field level by providing data for a network of grid points at a user-specified resolution. This "distributed" concept is an extension of the station-based method in that instead of having one or two points within the model, the same calculations are performed for thousands of individual points. The analysis procedure and methodology are identical to the station-based application, however, model input has been descritized through interpolation functions over the study area. Although, different interpolation methods can result in slightly different results, Hashmi and Garcia (1998) emphasized the use of the "distributed" concept to minimize the errors associated with the spatial and temporal variability of evapotranspiration parameters. The grid-based method is more convenient if the spatial distribution of the stations that record the meteorological parameters is different. However, if the stations that recorded one of the meteorological parameters are sparse, interpolation problems may arise. Input requirements are 7 shapefiles representing the location of the meteorological stations that record relative humidity, wind speed, sunshine hours, mean temperature, maximum temperature, minimum temperature, pan evaporation (in case of using the Pan Evaporation method), and the DEM. For the grid-based method, the number and location of the stations do not have to be the same for all shapefiles. The attribute table of one of the shapefiles should again contain, in addition to "elevation" and "name", information about "fetch length" in meters and "latitude" in decimal degrees for all stations.

### 7.4.2 GIS Module Structure

Seventy nine Avenue scripts and two dynamic link libraries (dlls) were used to build the system. The main folder that holds the ArcView project and the two dlls also contains two sub-folders containing information about the spatial and temporal distribution of the monthly data. The spatial distribution folder contains two separate storage locations for

storing shapefiles related to the station-based method and grid-based method. The temporal distribution folder contains seven storage locations for storing time series data for relative humidity, wind speed, sunshine hours, mean temperature, maximum temperature, minimum temperature, and pan evaporation as shown in Figure 7.8. Although the data can be updated regularly, these locations should not be changed. The ArcView project recognizes these locations at all times leading to accurate extraction of time series data at the outset of the project execution. The names of the stations in the attribute table of the shapefile in ArcView should match the names of the stations in the temporal distribution folder. The written routines within ArcView match each name in the attribute table with the names in the folder prior to data extraction. After extracting the monthly data based on a user-specified selection of the year of concern, the data is linearly interpolated into daily values and stored in text format prior to the execution of the different methods. If the year is a leap year, it is interpolated over 366 days, otherwise 365 days. The system consists of three modules and can be executed from a drop-down menu as shown in Figure 7.9. The flow chart-like diagram in Figure 7.10 shows instances of the sequence of execution steps in each case of the station- or grid- based methods. The pop-up menus and messages are meant to function as a guide to the user.

#### 7.4.2.1 Project Description

This module informs the user of the different parts of the system (documentation of the project) using many graphic illustrations. The file is viewed as an HTML file (help.htm).

#### 7.4.2.2 Station-based Method

*Penman-Monteith Method.* The system is structured so that it allows the calculation of ETo using mean, maximum, and minimum temperature or only mean temperature. The calculations are carried out for each day of the specified year and the results are stored in text format.

*Pan Evaporation Method.* Similarly, the calculations are carried out for each day of the specified year and the results are stored in text format and the user is then presented with a message informing of execution completion.

*User Control.* The user is then prompted to specify the day of concern. The corresponding ETo values are then extracted for each station, copied to the attribute table of the active shapefile, and then added to the point theme in the active view so that each point (station) is labeled with the calculated value for ETo as shown in Figure 7.11, which represents ETo values for September 20$^{th}$ 1986 using the station-based Penman-Monteith method with only average temperature records.

*Clean Work Directory.* A typical run would result in a number of text files stored in the working directory. This option is available to enable the user of erasing the unnecessary files after ensuring that the calculations were correct. Using Penman-Monteith method, the number of text files (N) is determined as:

$$N = 3 + 20 * \text{the number of stations} \quad (7.6)$$

For example, if 7 stations are used in the calculations, a total of 143 text files are generated taking up almost 0.5 MB of memory. The user can then erase all files except ( N = 1 + the number of stations). Similarly, using Pan Coefficient method, the number of text files (N) is determined as:

$$N = 1 + 4 * \text{the number of stations} \quad (7.7)$$

For example, if 7 stations are used in the calculations, a total of 29 text files are generated taking up almost 0.1 MB of memory. The user can then erase all files except ( N = 1 + the number of stations).

#### 7.4.2.3 Grid-based Method

*Penman-Monteith Method.* The system is structured in a way that allows the calculation of ETo using mean, maximum, and minimum temperature as well as only mean temperature. Unlike the station-based method, the calculations are carried out for only one user-specified day of the specified year and the results are stored in text format. The number of stations recording the various meteorological parameters can differ noting that denser networks are preferable. Figure 7.12 shows the resulting ETo grid for the same day using grid-based Penman-Monteith method with only average temperature records.

*Pan Evaporation Method.* Similarly, the calculations are carried out for only one user-specified day of the specified year and the results are stored in text format and the user is presented with a message informing of execution completion. In both methods (grid-based PenMon and grid-based Pan), the user has the choice of selecting the cell size and interpolation technique of the resulting ETo grid.

## 7.5 Analysis, Results and Discussion

### 7.5.1 The GIS Project

For the station-based method, only 7 stations were used (Ierapetra, Iraklion, KasteliEMY, Rethymno, Sitia, Suda, and Tympaki). However, for the grid-based method, different number of stations were used (35 for evaporation, 25 for relative humidity, 21 for sunshine hours, 53 for mean temperature, 30 for minimum and maximum temperature, and

12 for wind speed). Although, the station-based method provides estimates for every day of the year, it requires information for all stations involved in the analysis. On the other hand, the grid-based method provides estimates for one day for each run, but any number of stations can be used.

The station-based method was run for the water year 1986-87 (meaning September 15, 1986 to September 14, 1987) using the Penman-Monteith method (both max, mean, and min temperature records and only mean temperature) in addition to the Pan Evaporation Coefficient method. The results were verified using manual as well as spreadsheet calculations. Generally, and as shown in Figure 7.13, estimates using the Penman-Monteith method are higher than estimates using the Pan Evaporation Coefficient method. Using only mean temperature records resulted in somewhat underestimation of ETo estimates compared to using mean, max, and min temperature, as previously mentioned.

The grid-based method was run for the day September 20$^{th}$ 1986 using the Penman-Monteith method (both max, mean, and min temperature records and only mean temperature) in addition to the Pan Evaporation Coefficient. As shown in Figure 7.14, estimates using the Penman-Monteith method are higher than estimates using the Pan Evaporation Coefficient method except for the station of Ierapetra. And again using only mean temperature records resulted in lower estimates of ETo compared to using mean, max, and min temperature. Estimates using the grid-based Penman-Monteith method showed, in some cases, large differences from estimates using the station-based Penman-Monteith method due to the lack of meteorological stations that recorded wind speed, sunshine hours, and relative humidity, which led to spatial interpolation-related problems. Note that there is not a great difference between estimates obtained from station-based and grid-based methods for both Pan Coefficient method and Penman-Monteith method using only average temperature records. That can be attributed to the fact that less number of generated grids which were used as input to both methods. This means that for sparse stations, reducing the number of grids involved in the calculations reduces the error in the results.

### 7.5.2 Greece

#### 7.5.2.1 Meteorological Data

*Consistency.* In some cases, the meteorological data were obtained from different government agencies. Only data sets for those stations that showed reasonable or no deviation from one source to the other were considered. As for precipitation, available records for neighboring stations were used to check consistency using the double-mass curve analysis (Kohler, 1949; Gray, 1973).

*Format and Units.* Data was converted to format that is suitable for the GIS, such as text files and database files. Units were checked for consistency with the methodology requirement.

7.5.2.2 Crop Distribution

As mentioned earlier, numerical values for the irrigated land were obtained for the 51 counties of Greece for the years 1963, 1971, 1981, 1991 and 1992. The crop distribution was provided as a percentage of the irrigated land for each county for the year 1991. The irrigated land and crop distribution were then converted from county-based to hydrologic compartment-based. The conversion was done using the spatial analysis capabilities of GIS in two steps: (1) by evaluating the percentage of each county in each hydrologic compartment, as shown in Table 7.2; and (2) by using the percentage of crop distribution for each county and the percentage of each county in the respective hydrologic compartment to estimate the crop distribution in the hydrologic compartment. Table 7.3 shows an example for the calculation of the crop distribution in Compartment (1) for the year 1991. The hydrologic compartment-based crop distribution was then obtained for the years 1963, 1971, 1981 and 1992. Two implicit assumptions were made in order to obtain those crop distributions: (1) the county-based crop distribution as percentage of the irrigated land is valid for the period from 1963 to 1992; and (2) each one of the crop types is distributed in the county in such a way that if 10 percent of the area under tree cultivation in the county of Evritania is apple trees and 90 percent of that specific county is located in the compartment of West Central Greece, it is then estimated that 90% of the apple trees are located in that compartment.

7.5.2.3 Crop Coefficients

Crop coefficients ($K_c$) are used to relate each crop evapotranspiration ($ET_c$) to a standardized crop evapotranspiration ($ET_o$). Two sets of planting data, growing season, and crop coefficients for each crop, which distinguish between North and South Greece, were integrated into the database. Due to a lack of information, average values of crop coefficients may be used instead of the actual crop coefficient, which normally varies with the stage of crop development. Since there was a noticeable difference in the results obtained by using average or actual crop coefficients, as shown in Figure 7.15, an effort was made to accumulate information from which actual crop coefficients were extracted and used.

7.5.2.4 Calculations and Results

Using the Penman-Monteith method, daily irrigation requirements were calculated and summed up to estimate yearly requirements. Results revealed a noticeable variation in irrigation requirement estimates based on the different stations within the same hydrologic compartment. Higher estimates were mostly obtained at the coastal locations, whereas lower estimates were obtained at mountainous areas. Maximum, minimum, and mean estimates were obtained for the hydrologic compartments that were represented by more than one

meteorological station. An average estimate of 3539 $Mm^3$ of irrigation water was obtained for the year 1991, as shown in Table 7.4 (the range is 3,009 to 4,068 $Mm^3$). Water consumption data in Greece, according to final use for agricultural purposes, was 5,355 $Mm^3$ for the same year (Angelakis and Diamadopoulos, 1995). This large difference is due to irrigation efficiency, which in this case is estimated at 66 percent. The large range of the irrigation requirements estimates can be referred to: (1) the representativeness of the stations for each hydrologic compartment; (2) the method of estimating effective rainfall; and 3) the values used for each crop coefficient.

Table 7.4 shows the estimated irrigation water requirements per category of crop for different years during the period 1963 to 2020. Based on a linear increase in irrigated land in Greece, as shown in Figure 7.16, a yearly increase in irrigation water consumption (at 100 percent efficiency) ranging from 57 to 75 $Mm^3$ is estimated. Again the range in values is influenced by the meteorological stations used to represent the hydrologic compartments. It is estimated that by the year 2020, the total irrigated land will be 18,835 $km^2$ and an average irrigation water volume of 5,510 $Mm^3$ will be required at 100 percent irrigation efficiency. Table 7.5 shows the irrigation requirements for the 14 hydrologic compartments by year 2020 and Figure 7.17 graphically illustrates these results. The compartment of Thessaly (8) had the highest total irrigation water requirements followed by East Macedonia (11), Thrace (12), Crete (13) and East Roumelli (7). The irrigation requirements for crops were highest in Thessaly (8) followed by East Macedonia (11) and Thrace (12) while for trees the highest were in Crete (13) and West Macedonia (9).

### 7.5.3 Crete

As concluded in the previous section, the island of Crete was represented by the stations of Iraklion and Rethymno, which posed questions about the credibility of this representation. The irrigation requirements for the year 1991 based on stations of Iraklion and Rethymno were estimated at 390 $Mm^3$ and 227 $Mm^3$, respectively, with an average of 308 $Mm^3$. Among the fourteen hydrologic compartments of Greece, the island of Crete was ranked as the third highest compartment with respect to the average irrigation water consumption per unit area (as shown in Table 7.6). This water demand can be accounted for by the large areas of trees and grapes, which require relatively higher amounts of irrigation water. According to the formula (Irrigation = A * Eto * Kc - A * $P_{eff}$ ), effectiveness of precipitation implies the degree of contribution of precipitation to satisfy the crop needs. Crete was also ranked eighth in the effectiveness of precipitation, as shown in Table 7.7. Preliminary results based on the ten representative meteorological stations showed the difference between calculated mean annual reference evapotranspiration and mean annual precipitation, as shown in Table 7.8. The analysis included several combinations of stations representing different parts of the island to improve the irrigation water requirement estimate.

One approach was to assign each of the ten stations to represent the whole island. The second approach was to use seven sets of two stations each to represent the two prefectures in Western and Eastern Crete. For example, in one case the station of Sitia represented the prefectures of Lassithi and Iraklion, while the station of Alikianos represented the prefectures of Chania and Rethymno. In another case the station of Paxia Ammos represented the prefectures of Lassithi and Iraklion, while the station of Lefkogia represented the prefectures of Chania and Rethymno, and so on. In the third approach, six sets of four meteorological stations each were to represent the whole island in such a way that each station represented a prefecture. For example, the prefecture of Lassithi was represented by the station of Sitia in one case and the station of Paxia Ammos in another case. The other three prefectures have been similarly represented. In the fourth approach, two sets of six meteorological stations each represented the island. The fifth approach assigned four sets of eight meteorological stations each to represent the whole area. And finally, each of the group of ten stations was assigned to represent one region or more, according to its geographical location.

7.5.3.1 Based on Individual Meteorological Stations

Each of the ten meteorological stations was assigned to represent the whole island. Different estimates were obtained, which ranged from a maximum of 497 $Mm^3$/year, for the station of Ierapetra, to a minimum of 227 $Mm^3$/year, for the station of Rethymno (as shown in Figure 7.18). The irrigation water requirements are higher in east southeast Crete due to meteorological conditions, i.e., precipitation decreases from west to east. Detailed irrigation demand estimates for the year 1991 based on the stations of Iraklio (390 $Mm^3$) and Rethymno (227 $Mm^3$) are given in Table 7.9.

7.5.3.2 Based on Two Meteorological Stations

The prefectures of Lassithi and Iraklion and the prefectures of Rethymno and Chania were represented by seven different pairs of stations. The first set consisted of the stations of Sitia and Alikianos respectively; resulting in an estimate of 322 $Mm^3$. The second set consisted of the stations of Paxia Ammos and Lefkogia, resulting in an irrigation water requirements estimate of 397 $Mm^3$. In the third set, by assigning the stations of Ierapetra and Rethymno the estimate was 414 $Mm^3$ while in the fourth set by assigning the stations of Zaros and Chania the estimate was 335 $Mm^3$ Finally, by using the stations of Iraklion and Kandanos, the estimate was 369 $Mm^3$. Two more sets were used, which resulted in the extreme requirements. The stations of Ierapetra and Chania resulted in a maximum of 445 $Mm^3$, while the stations of Sitia and Rethymno resulted in a minimum of 299 $Mm^3$.

7.5.3.3 Based on Four Meteorological Stations

Six sets of four meteorological stations, each representing the four prefectures of

Crete, were chosen to estimate the irrigation water requirements for the whole island. Calculations for reference evapotranspiration and effective precipitation were carried out. Daily and monthly irrigation water requirements for the different crops based on the four stations were obtained. The crop distribution (Table 7.1) and the irrigation water requirements for the four prefectures were also evaluated and the total irrigation requirements were estimated at :

(a) 375 $Mm^3$ based on the south stations of Zaros, Ierapetra, Lefkogia, and Kandanos;
(b) 355 $Mm^3$ based on the stations of Zaros, Paxia Ammos, Lefkogia, and Kandanos;
(c) 350 $Mm^3$ based on the north stations of Iraklion, Sitia, Rethymno, and Chania;
(d) 343 $Mm^3$ based on the stations of Iraklion, Sitia, Rethymno, and Alikianos;
(e) 320 $Mm^3$ based on the stations of Sitia, Zaros, Rethymno, and Alikianos; and
(f) 390 $Mm^3$ based on the stations of Ierapetra, Iraklion, Lefkogia, and Chania.

The station combinations (e) and (f) resulted in minimum and maximum requirements, respectively.

7.5.3.4 Based on Six Meteorological Stations

Two sets of six meteorological stations each to represent the whole island resulting in the highest and lowest estimates for irrigation requirements. The set of stations Sitia, Iraklion, Zaros, Rethymno, Lefkogia, and Alikianos resulted in a low estimate of 331 $Mm^3$, and the stations of Ierapetra, Iraklion, Zaros, Lefkogia, Chania, and Kandanos resulted in a high estimate of 390 $Mm^3$.

7.5.3.5 Based on Eight Meteorological Stations

Two sets of eight meteorological stations each were chosen to represent the 20 regions of Crete as follows:

*Alikianos or Chania* to represent the regions Apokoronou, Kissamou, and Kydonias.
*Ierapetra or Paxia Ammos* to represent the regions Ierapetras, Mirabelou, Lassithiou, and Fiannou.
*Iraklion* to represent the regions Maleviziou, Pediados, and Temenous.
*Kandanos* to represent the regions Sfakion and Selinou.
*Lefkogia* to represent the regions Agiou Vasiliou, and Amariou.
*Rethymno* to represent the regions Mylopotamou and Rethymno.
*Sitia* to represent the region Sitias.
*Zaros* to represent the regions Kenourgiou, Monofatsiou, and Pyrgiotissis.

Crop distribution, reference evapotranspiration, daily and monthly irrigation requirements for the different crops, and the yearly irrigation water demand per unit area were calculated. The areas represented by the different stations varied from as small as 646

$km^2$ (represented by the station of Lefkogia) to as large as 1450 $km^2$ (represented by the station of Chania or Alikianos).

7.5.3.6 Based on Ten Meteorological Stations

The island of Crete was divided into 10 regions according to the distribution of the ten meteorological stations across the island (as shown in Figure 7.19). The crop distribution and the irrigation water requirements were also obtained. The irrigation water requirements were estimated at 359 $Mm^3$ for the year 1991. The areas represented by the different stations varied from 532 $km^2$ (represented by the station of Chania) to 1523 $km^2$ (represented by the station of Zaros). The irrigation water requirements for each municipality were also evaluated (as shown in Figure 7.20). Results show the variation of irrigation requirements within the 10 regions and reflect mainly the type of crop and size of irrigated land in each municipality. The correlation between the irrigated land for the four types of crop (shown in Figs 7.5a to 7.5d) and the findings shown in Figure 7.20 is evident.

The different approaches are best illustrated in Figure 7.21, where there is a convergence of the irrigation water requirements estimate to a narrower range with the use of more stations to represent smaller areas.

Figure 7.22 shows the irrigation requirements based on individual meteorological stations versus the longitude of the stations. Apart from the results based on the stations Rethymno and Sitia (which are located close to the sea and record higher humidity, which reduces the evapotranspiration estimate and consequently the irrigation requirements estimate), there appears to be an increase in the irrigation requirements per stremma from the western to the eastern part of the island.

A linear projected increase in irrigated land in the island of Crete resulted in a yearly increase in irrigation water requirements of 8 $Mm^3$, or 10 $Mm^3$ if results from the year 1963 are excluded (as shown in Figure 7.23). The rate of development in Crete prior to 1970, including the tourism industry, was not so fast and intense as it has been during the last 30 years. Increased development led to a faster growth in irrigated land after the 1970s. Based on these considerations, a yearly increase in irrigation water requirements closer to 10 $Mm^3$ may be more appropriate.

## 7.6 Conclusion

### 7.6.1 The GIS Project

Station- and grid-based methods for calculating reference evapotranspiration were developed and incorporated into a GIS. The FAO Penman-Monteith method as well as the

Pan Evaporation Coefficient method were employed for estimating ETo. The grid-based component of the system allowed evapotranspiration to be simulated on field-to-field basis by providing data for a network of grid points at a user-specified resolution. The application of this analysis method offers valuable information that is capable of providing decision support for the design of irrigation systems and planning future crop locations.

The system was applied to a case study in the island of Crete in Greece. Results showed that applying Penman-Monteith approach using only mean temperature records yielded lower estimates for ETo compared to those obtained by using the Penman-Monteith approach using mean, max, and min temperature. The Pan Evaporation Coefficient provided even lower estimates. It is generally recommended to use the Penman-Monteith method if enough meteorological data is available.

### 7.6.2 Greece

Present and future irrigation water amounts were estimated for the country of Greece using: (1) monthly data from 38 meteorological stations; (2) data on irrigated land for the years 1963, 1971, 1981, 1991, and 1992; and (3) crop distribution for the categories of trees, grapes, vegetables, and crops for the year 1991. The Penman-Monteith method was used for irrigation requirement estimation. Irrigation efficiency was evaluated at 66 percent based on the average irrigation requirements estimated by this approach. Average estimation of irrigation requirements for year 2020 at 66 percent irrigation efficiency was 8350 $Mm^3$ for a total irrigated land of 18835 $km^2$. Additional improvements of irrigation efficiency by 20 percent could result in 2000 $Mm^3$ in water savings by year 2020.

### 7.6.3 Crete

It was clear that assigning representative stations for smaller regions/catchments is more appropriate. The representative station is generally a station that is located at a moderate altitude and operating under average meteorological conditions. Information from those representative stations can also be spatially interpolated in order to provide meteorological and hydrological information in unrepresented locations.

Based on estimates obtained from individual stations, the following conclusions can be made: (a) based on meteorological data obtained at the station of Ierapetra, the highest estimate of irrigation water requirements was obtained (497 $Mm^3$/year), whereas an estimate based on the station of Rethymno's data is (227 $Mm^3$/year); (b) the representative station for the whole island which reflects an average estimate for irrigation water requirements is to be located in the prefecture of Iraklion due its location in the middle of the island, where most of the agricultural activities take place; (c) assigning a coastal station as a

representative station for the island is not recommended; and (d) excluding the stations of Sitia and Rethymno and assigning the station of (1) Ierapetra to represent the prefecture of Lassithi, (2) Lefkogia to represent the prefecture of Rethymno, (3) Iraklion to represent the north part and Zaros to represent the south part of the prefecture of Iraklion, and (4) Chania to represent the northern part, and Kandanos to represent the southern part of the prefecture of Chania resulted in an irrigation water requirements estimate of 390 $Mm^3$/year. This estimate can be considered the maximum total irrigation water requirements for the year 1991.

The irrigation water requirements for the island of Crete, based on ten representative meteorological stations for the year 1991, were estimated at 359 $Mm^3$. The station of Lefkogia provided estimates close to the ten-station estimate; therefore this station can be considered as the representative station for the island from the irrigation water requirements perspective. A yearly increase in irrigation water requirements of 8-10 $Mm^3$ may lead to an average estimate of irrigation water requirements of 591-647 $Mm^3$ for the year 2020.

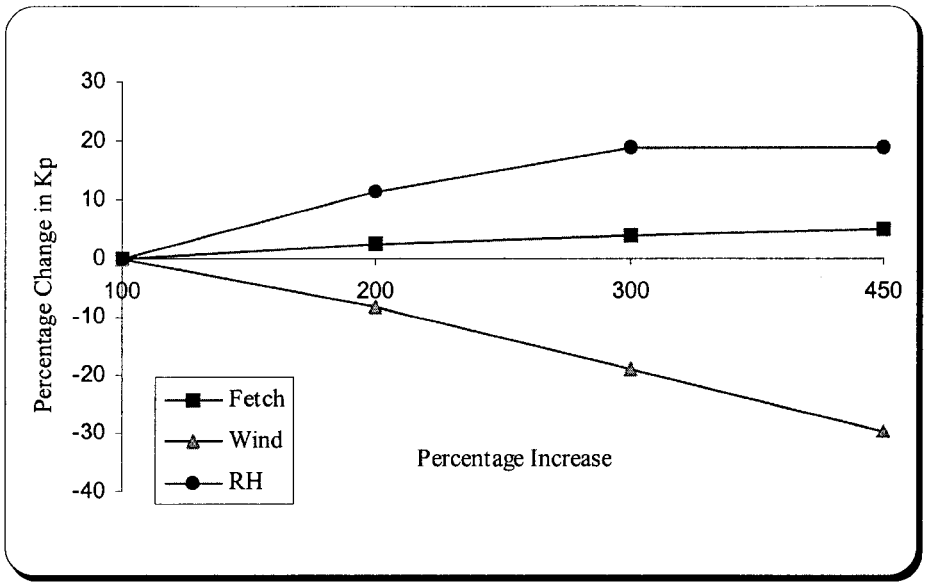


**Figure 7.1a:** Sensitivity analysis results for the Pan Evaporation Coefficient method.

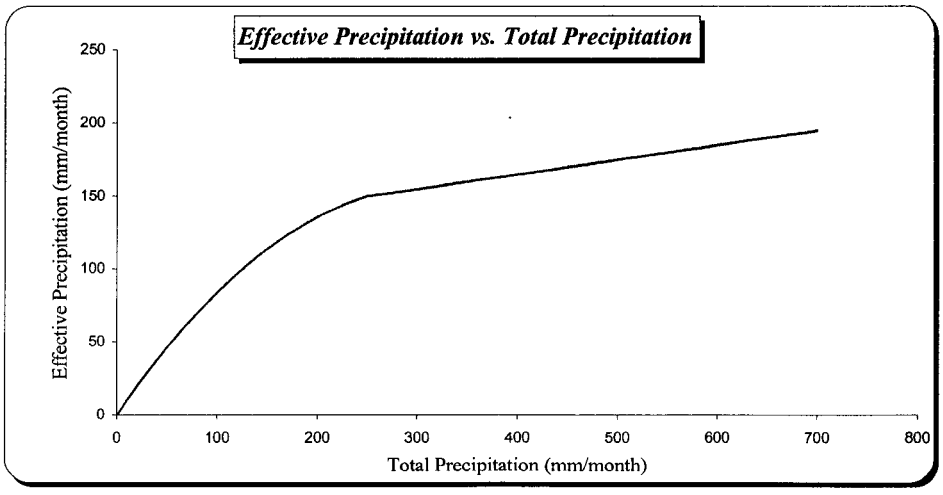


**Figure 7.1b:** Effective precipitation vs. total precipitation according to the USDA SCS method.

*(a)*


*(b)*

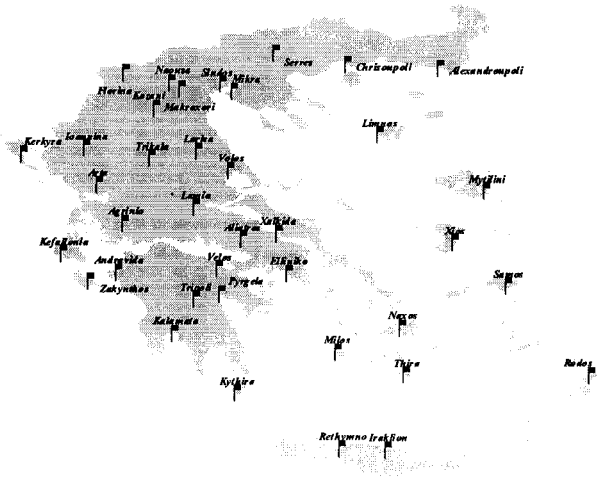

**Figure 7.2:** (a) The country of Greece and its neighbors in the Mediterranean region at the south of Europe and facing northern Africa. (b) The thirty eight meteorological stations representing Greece.

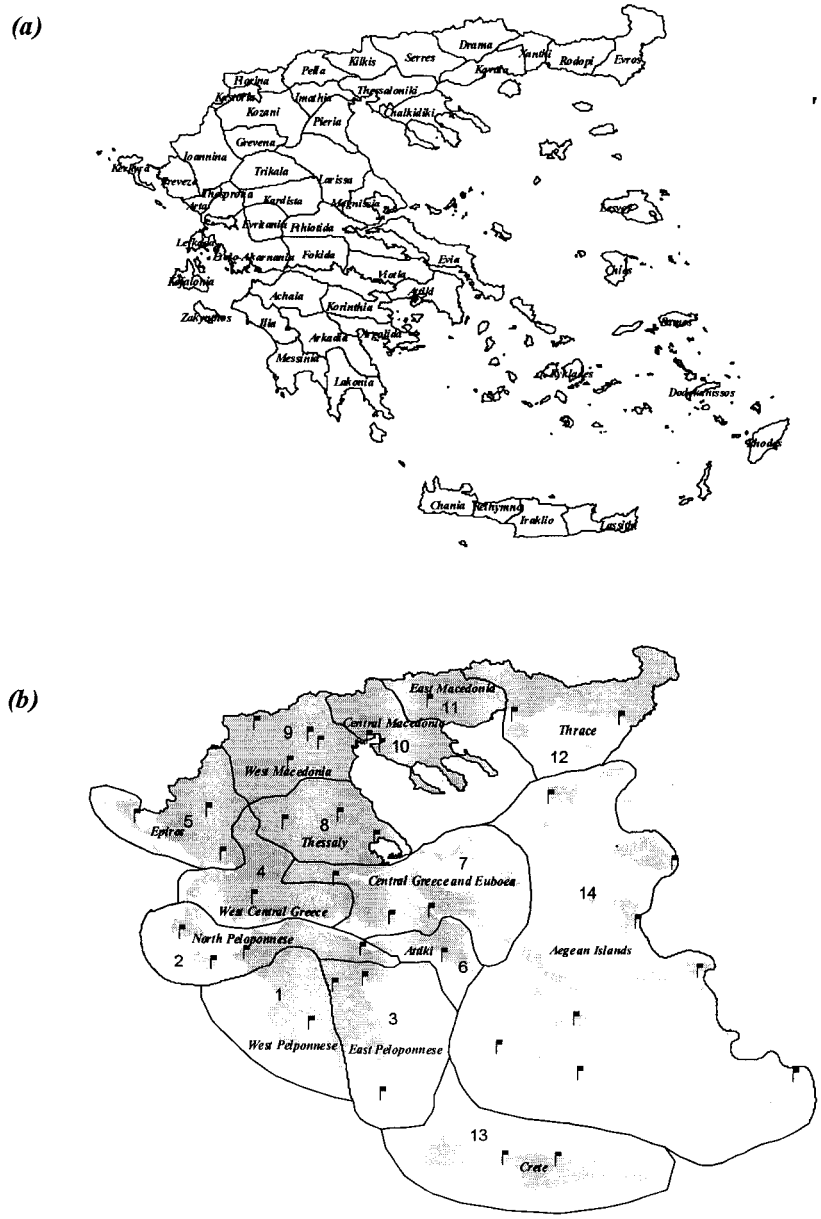


**Figure 7.3:** (a) The fifty one counties of Greece. (b) The fourteen hydrologic compartments of Greece.

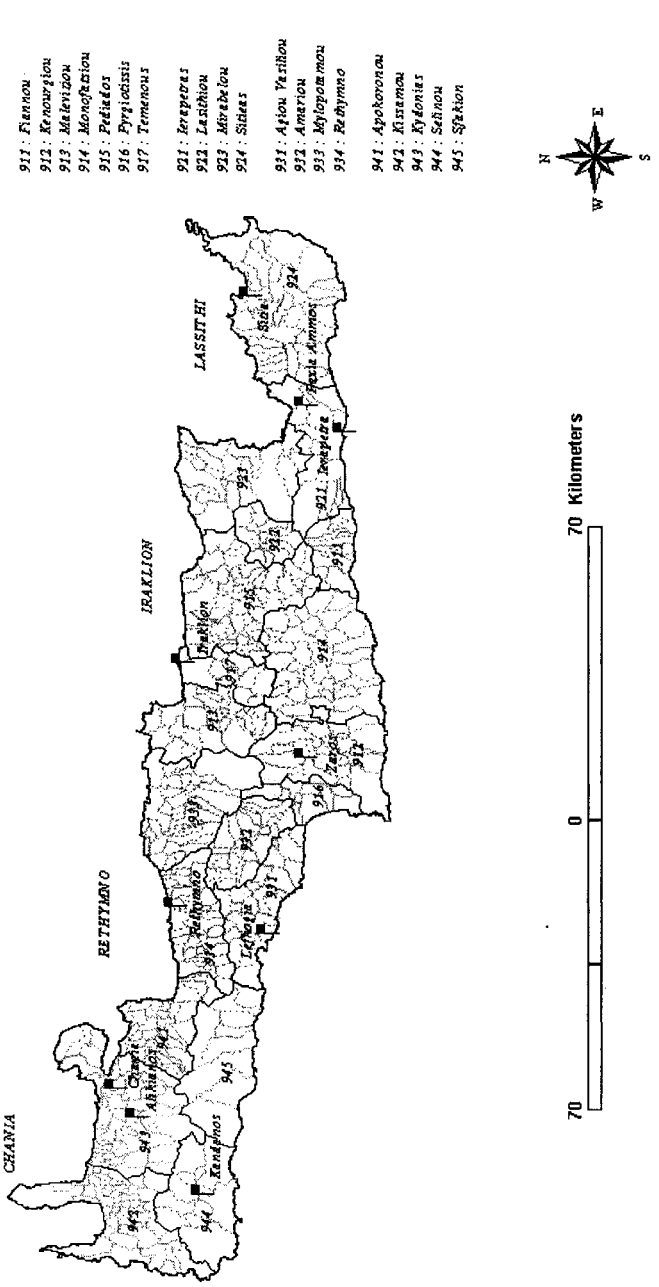


**Figure 7.4:** Crete is divided into 4 political counties (prefectures), 20 regions, and 567 municipalities.

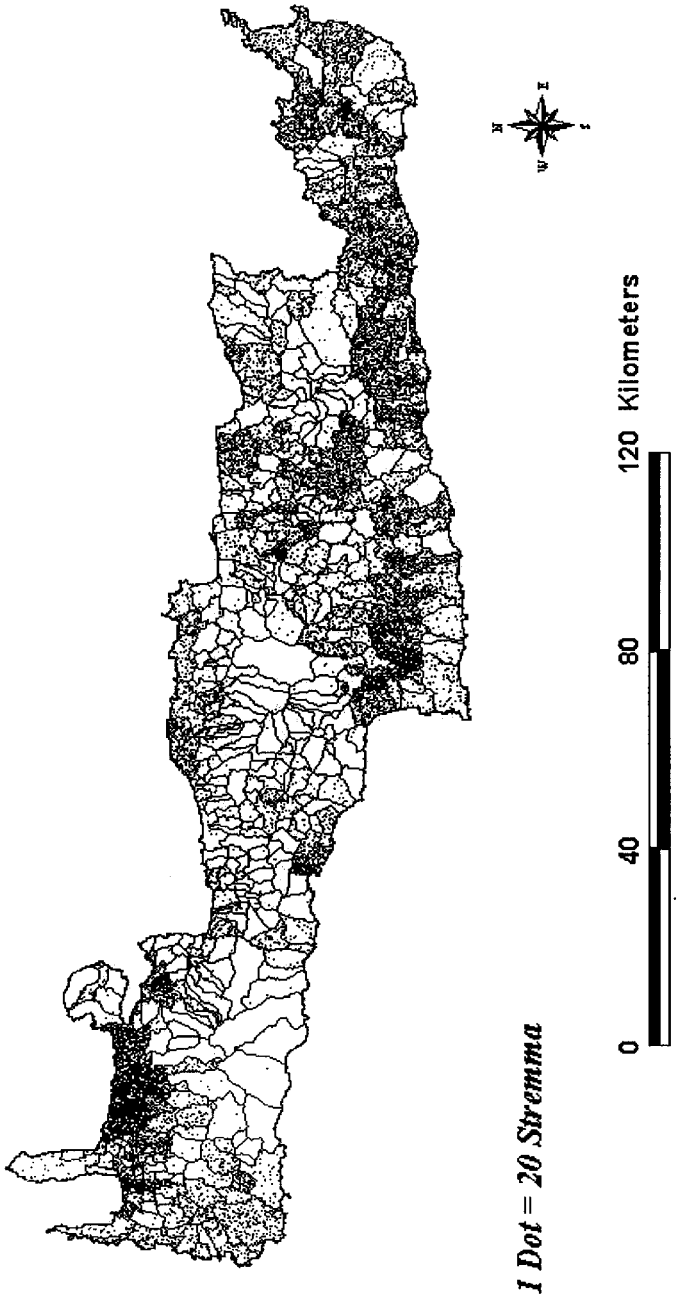


**Figure 7.5a:** Areas under trees in Crete.

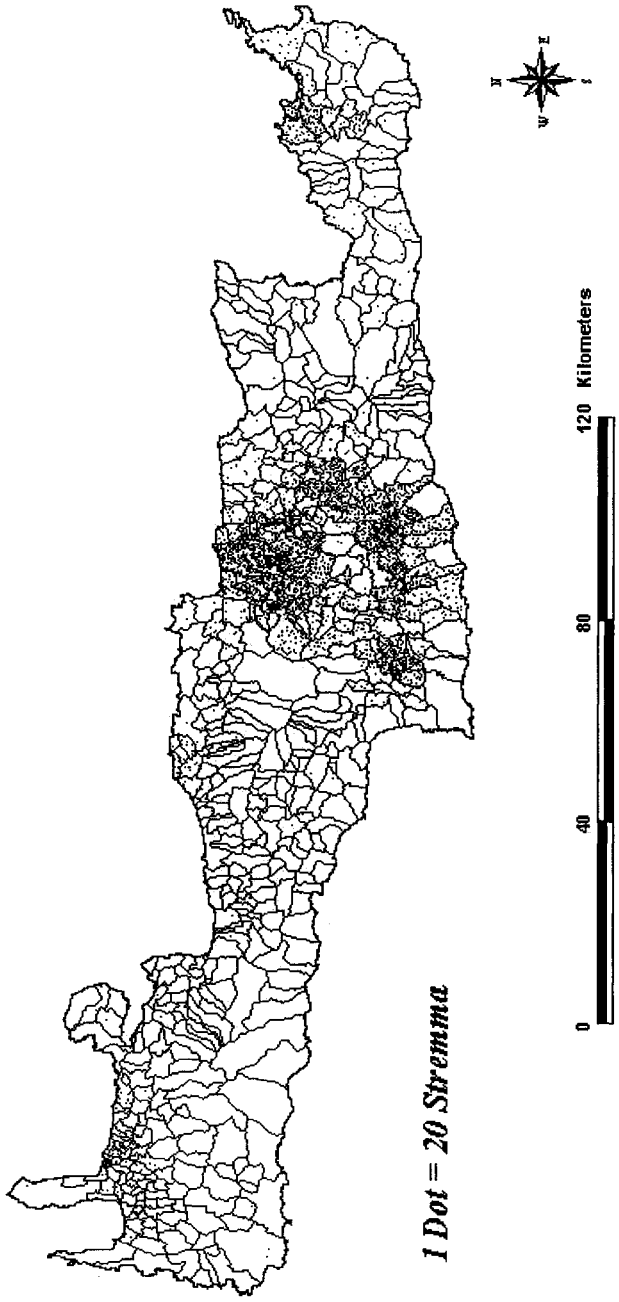


**Figure 7.5b:** Distribution of grapes in Crete.

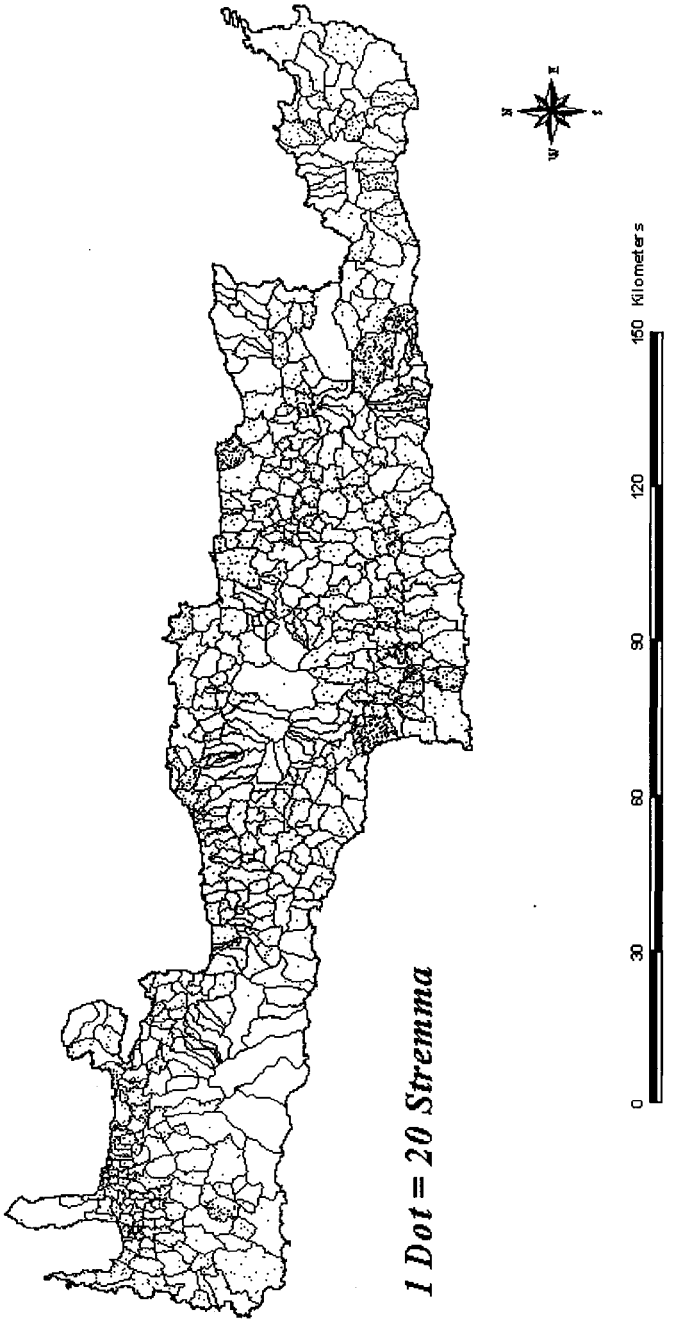


**Figure 7.5c:** Areas under vegetables.

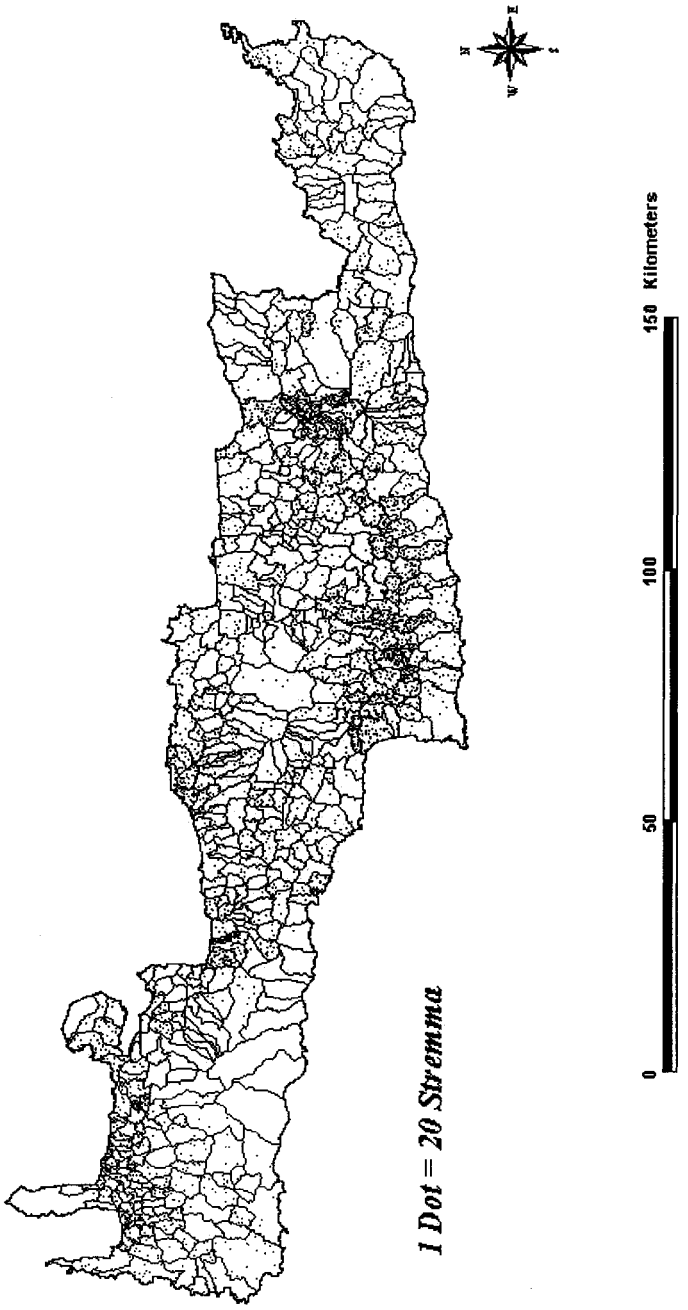


**Figure 7.5d:** Crops on arable land.

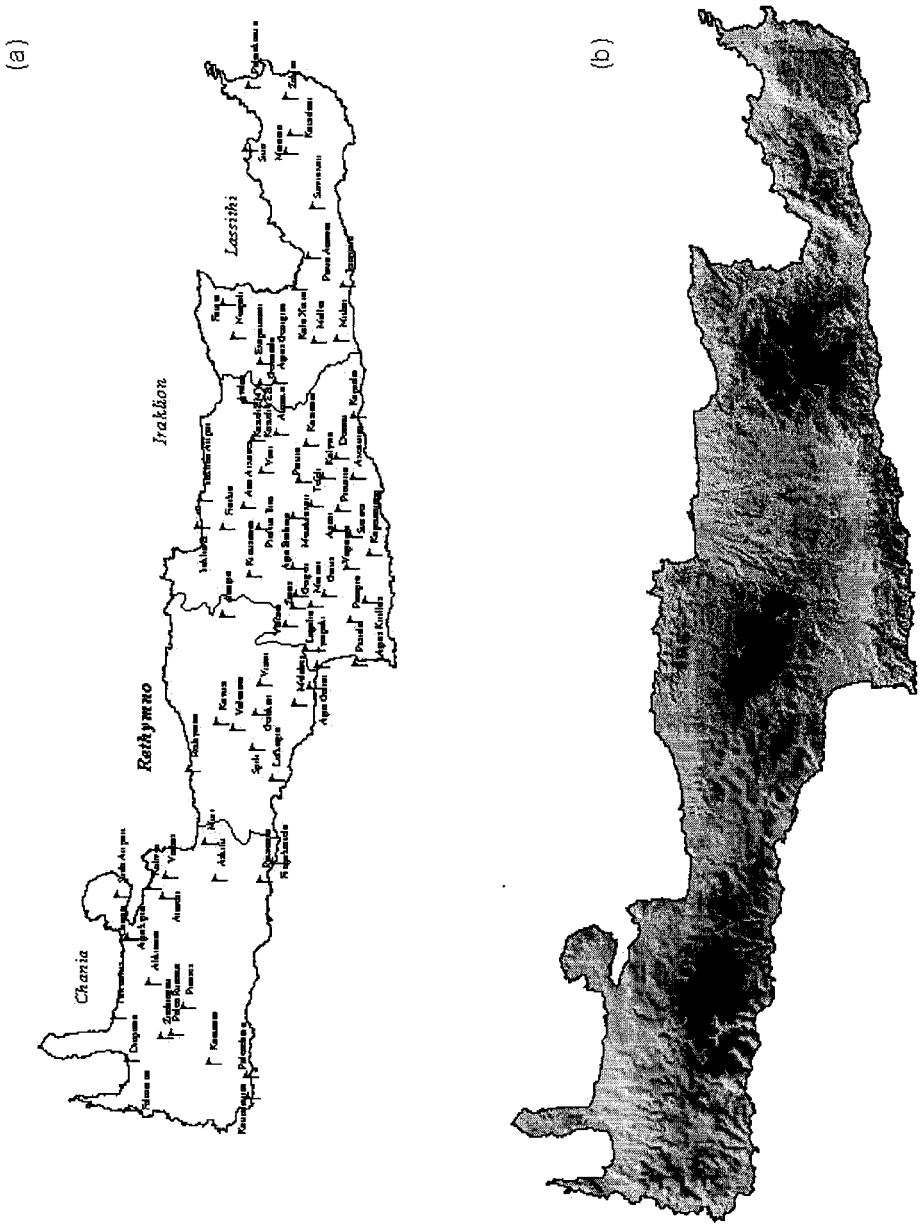


**Figure 7.6:** (a) Meteorological stations and rain gauges in Crete, (b) The digital elevation model for Crete.

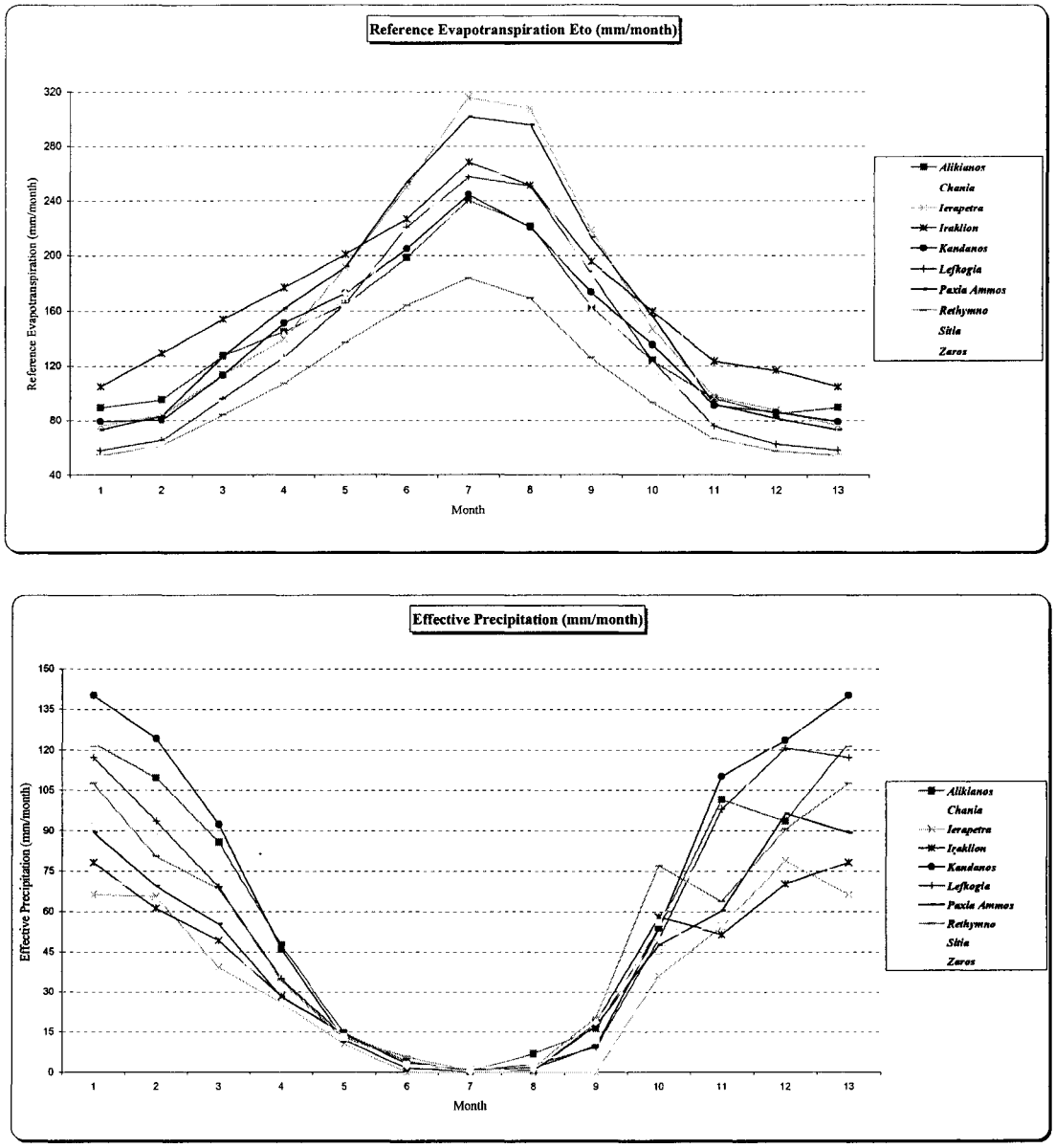


**Figure 7.7:** Monthly values for reference evapotranspiration and effective precipitation for the ten representative meteorological stations of Crete.

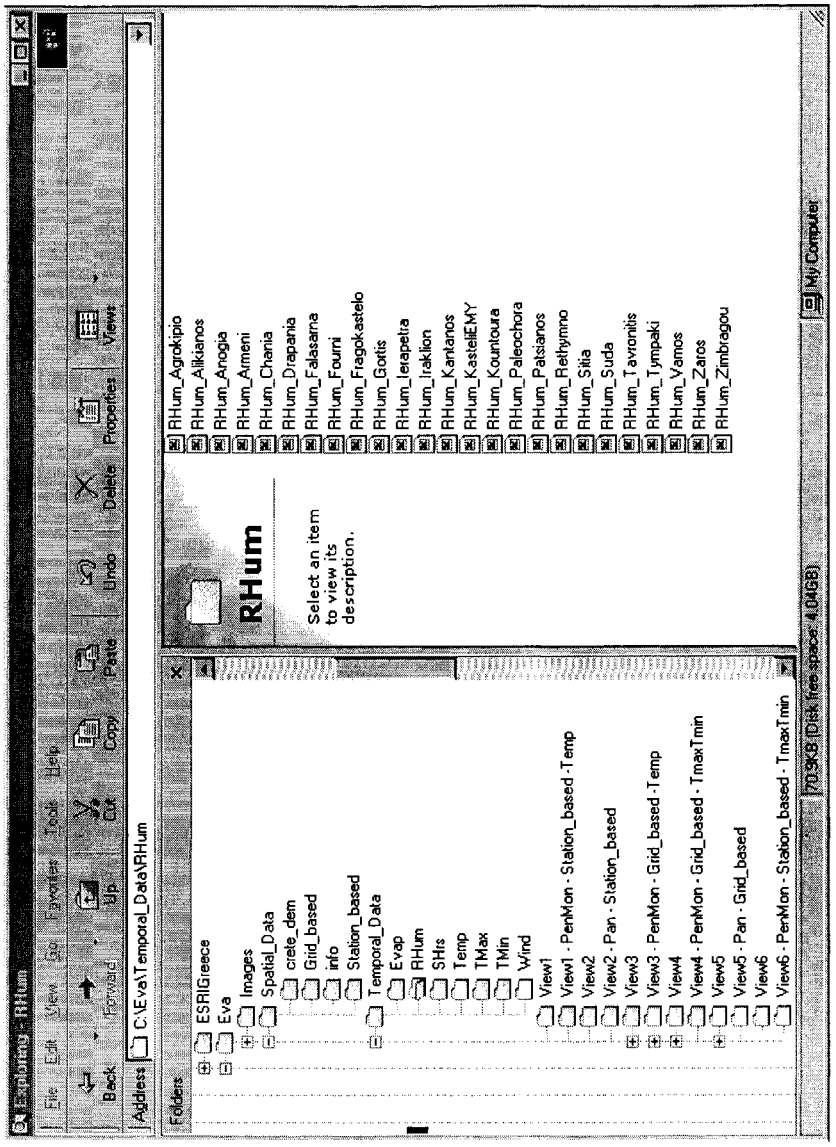


**Figure 7.8:** The database structure for the application of the GIS project.

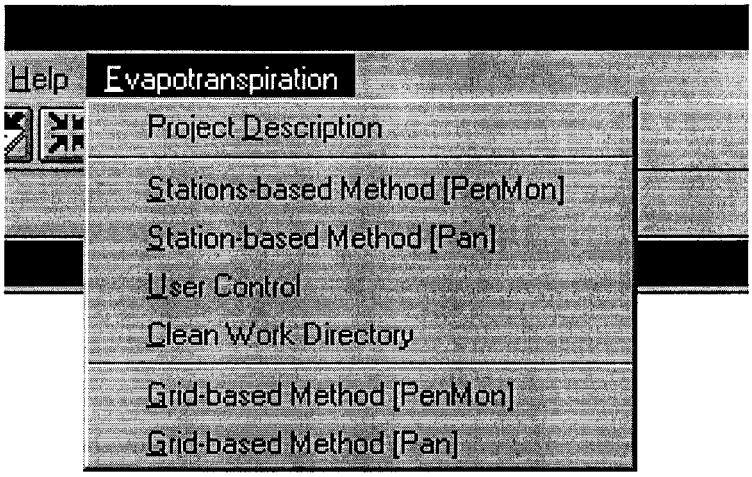


**Figure 7.9:** A drop-down menu representing the main module of the system.

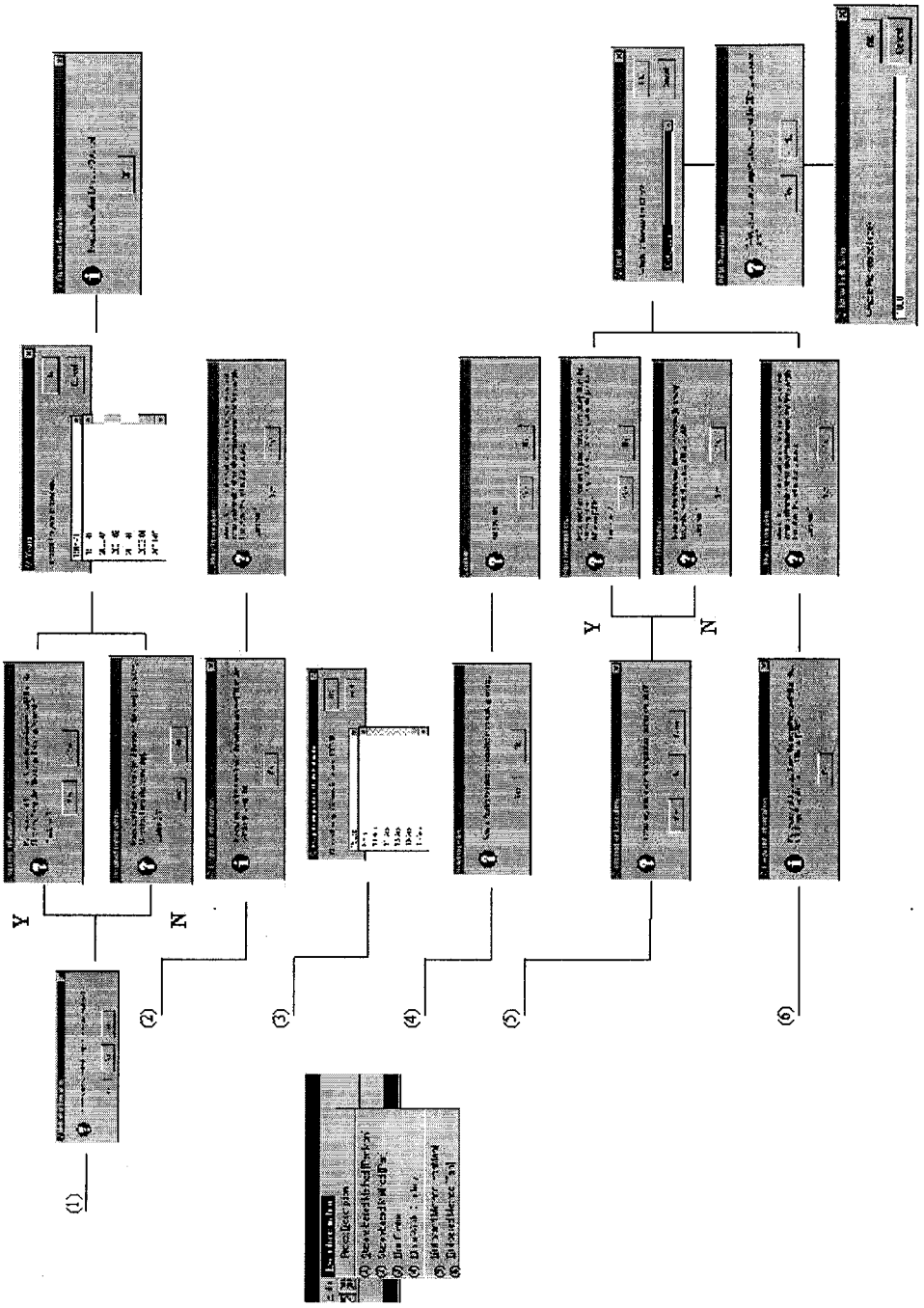


**Figure 7.10:** A flow chart-like diagram that shows the sequence of execution of the different modules.

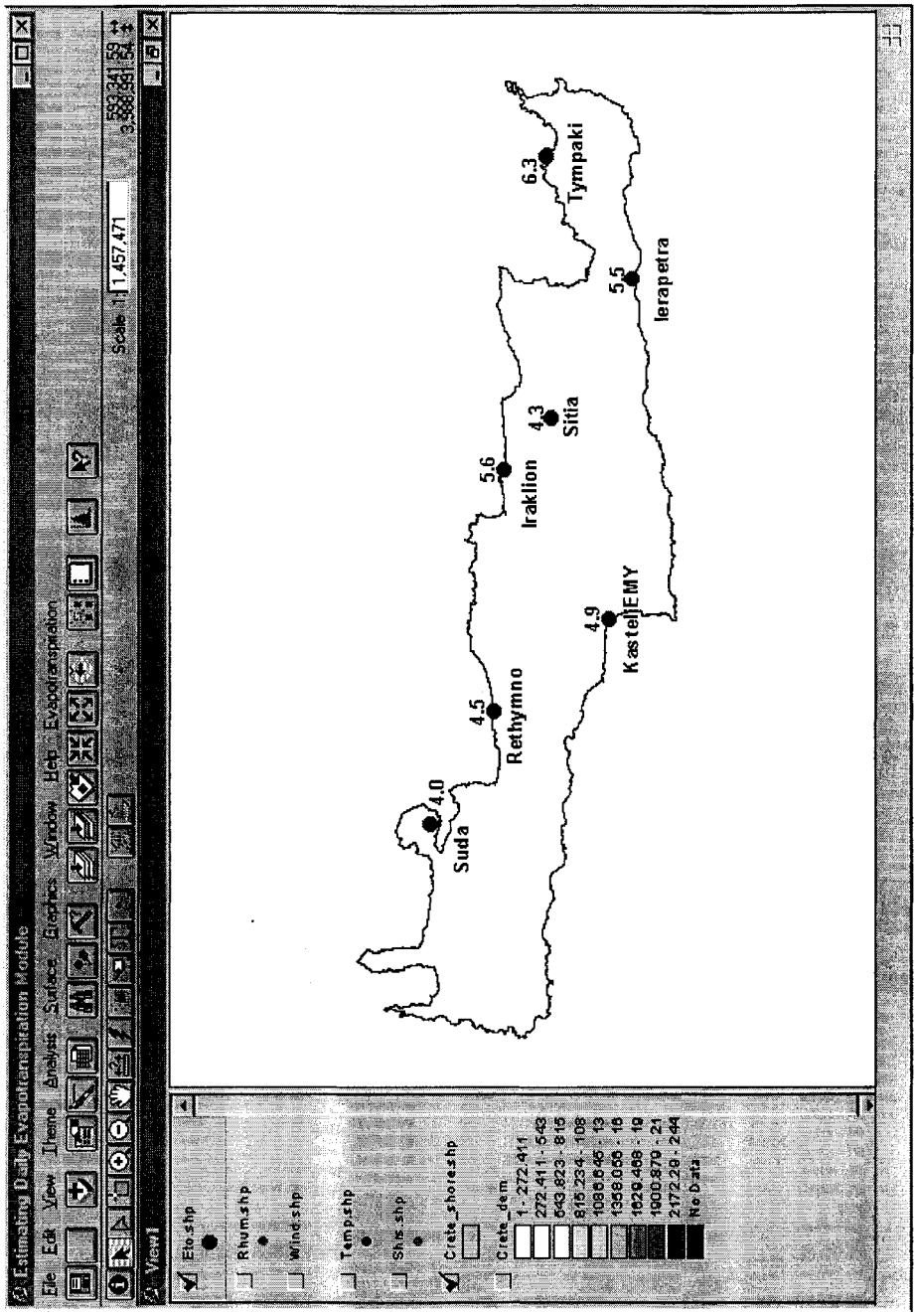


**Figure 7.11:** Point estimates of reference evapotranspiration at sample locations.

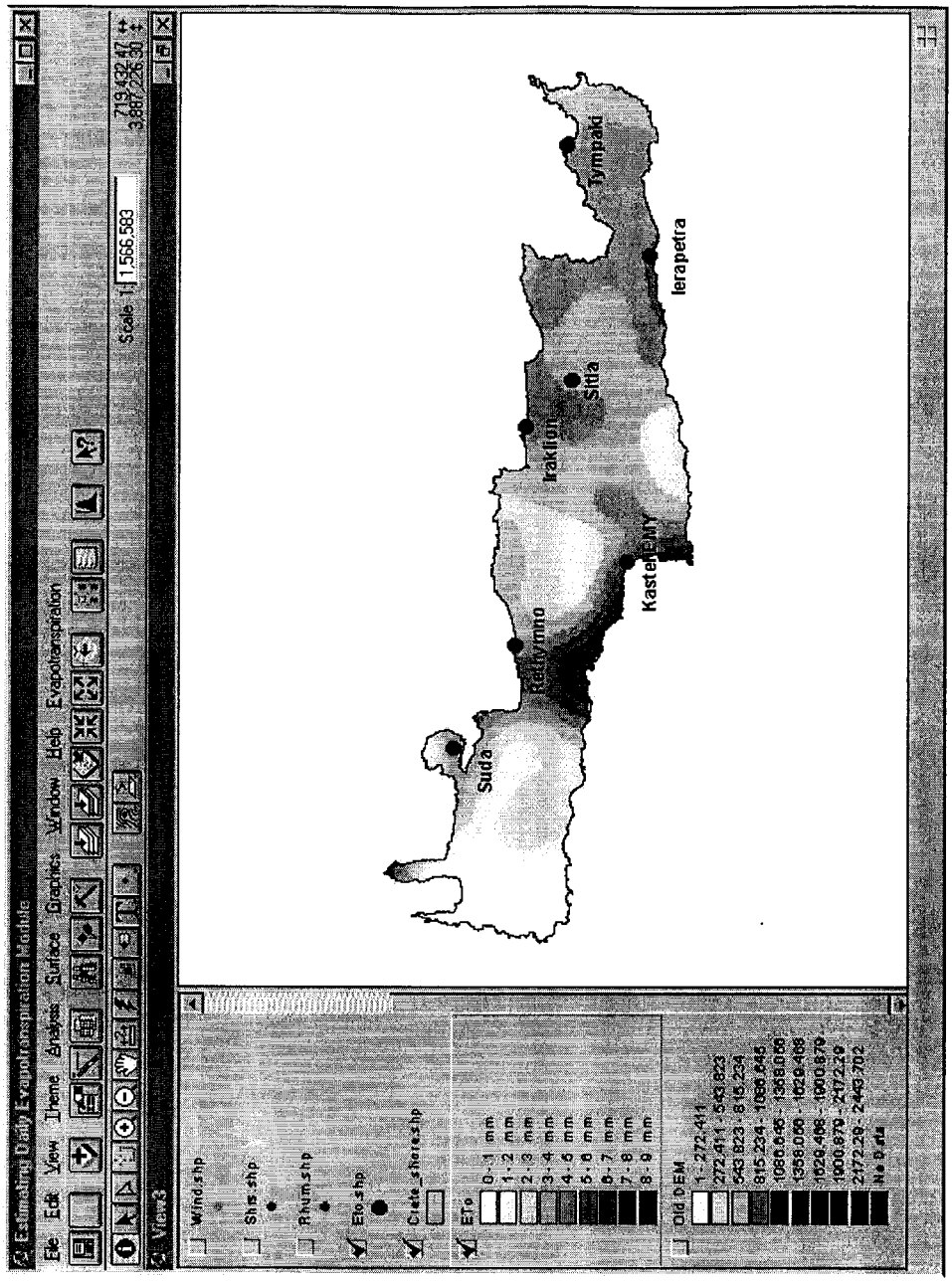


**Figure 7.12:** An ETo grid representing estimated values for the 20th of September 1986 using the grid-based method.

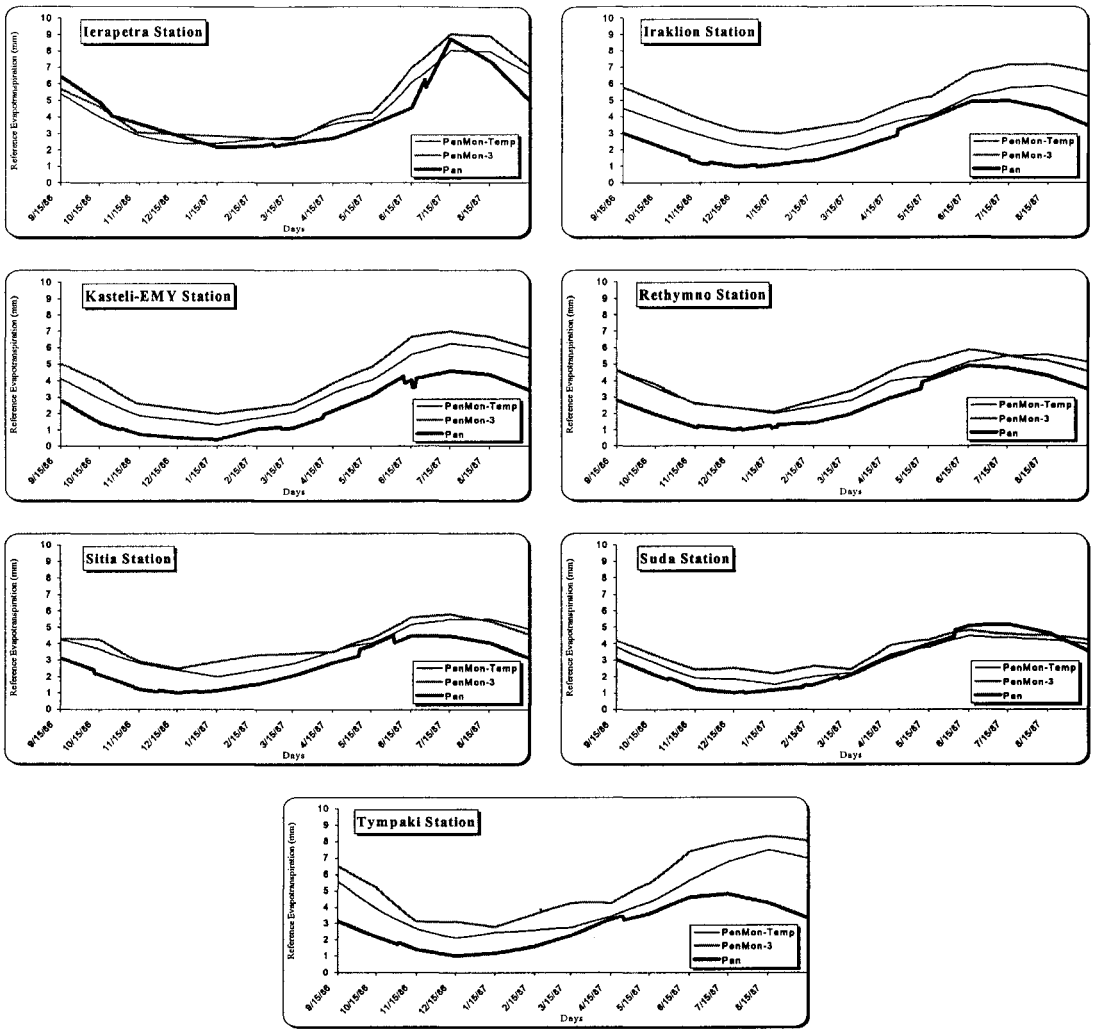


**Figure 7.13:** Reference evapotranspiration (ETo) estimates for the year 1986-87 using the station-based method at sample locations. [PenMon-Temp = Penman-Monteith method using mean temperature; PenMon-3 = Penman-Monteith method using the 3 temperatures (mean, maximum, and minimum); and Pan = the Pan Evaporation Coefficient method].

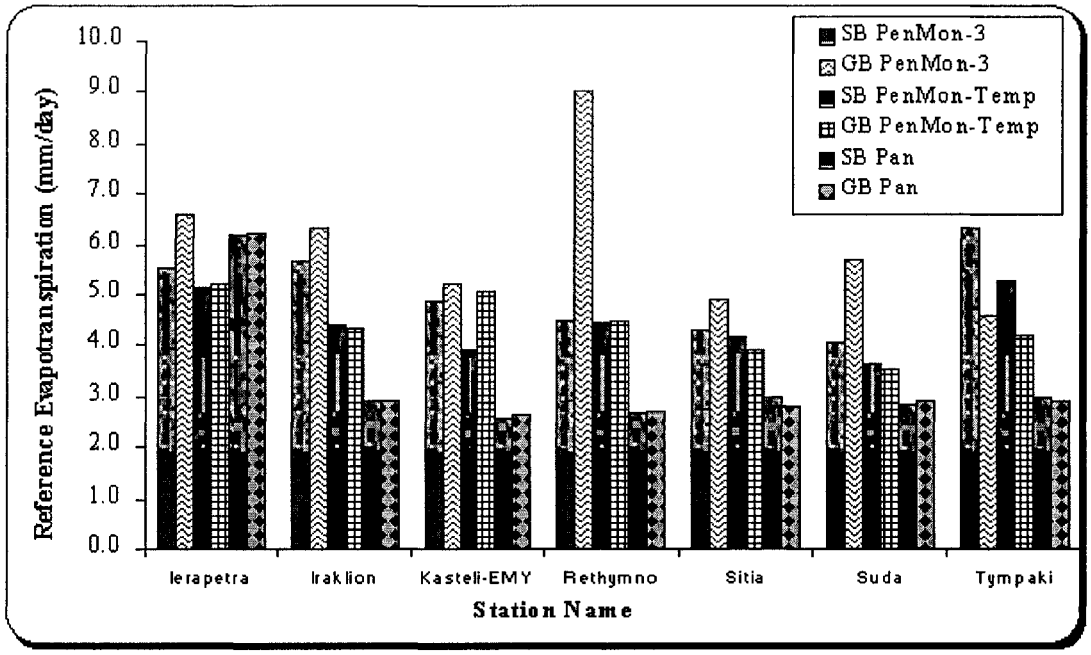


**Figure 7.14:** Reference evapotranspiration (ETo) estimates for September 20, 1986 using all methods at sample locations. [SB PenMon-3 = Station-based approach and using the Penman-Monteith method with the 3 temperatures (mean, maximum, and minimum); GB PenMon-3 = Grid-based approach and using the Penman-Monteith method with the 3 temperatures (mean, maximum, and minimum); SB PenMon-Temp = Station-based approach and using the Penman-Monteith method with mean temperature; GB PenMon-Temp = Grid-based approach and using the Penman-Monteith method with mean temperature; SB Pan = Station-based approach and using the Pan Evaporation Coefficient method; and GB Pan = Grid-based approach and using the Pan Evaporation Coefficient method].

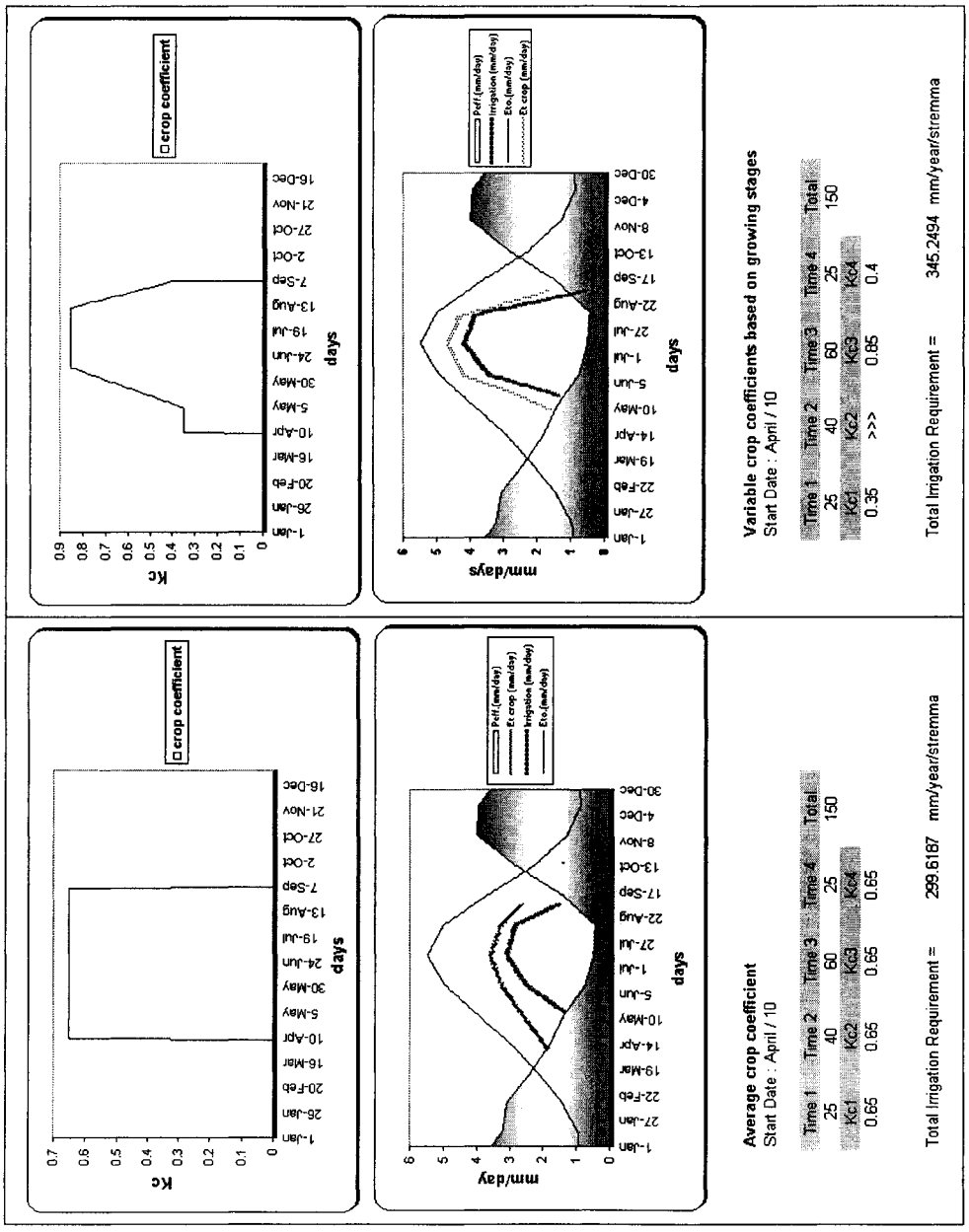


**Figure 7.15:** Average and actual crop coefficients for corn (station of Agrinio).

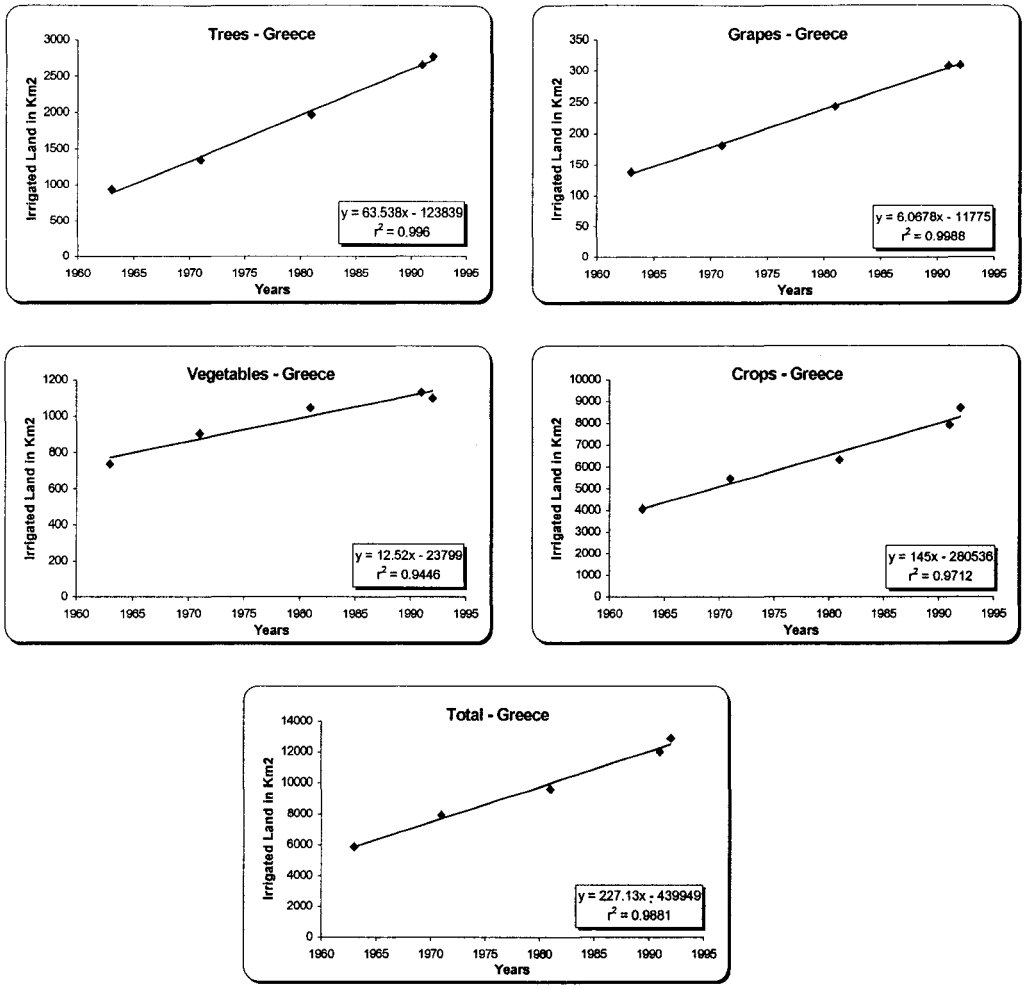


**Figure 7.16:** Linear projection of the irrigated lands in Greece.

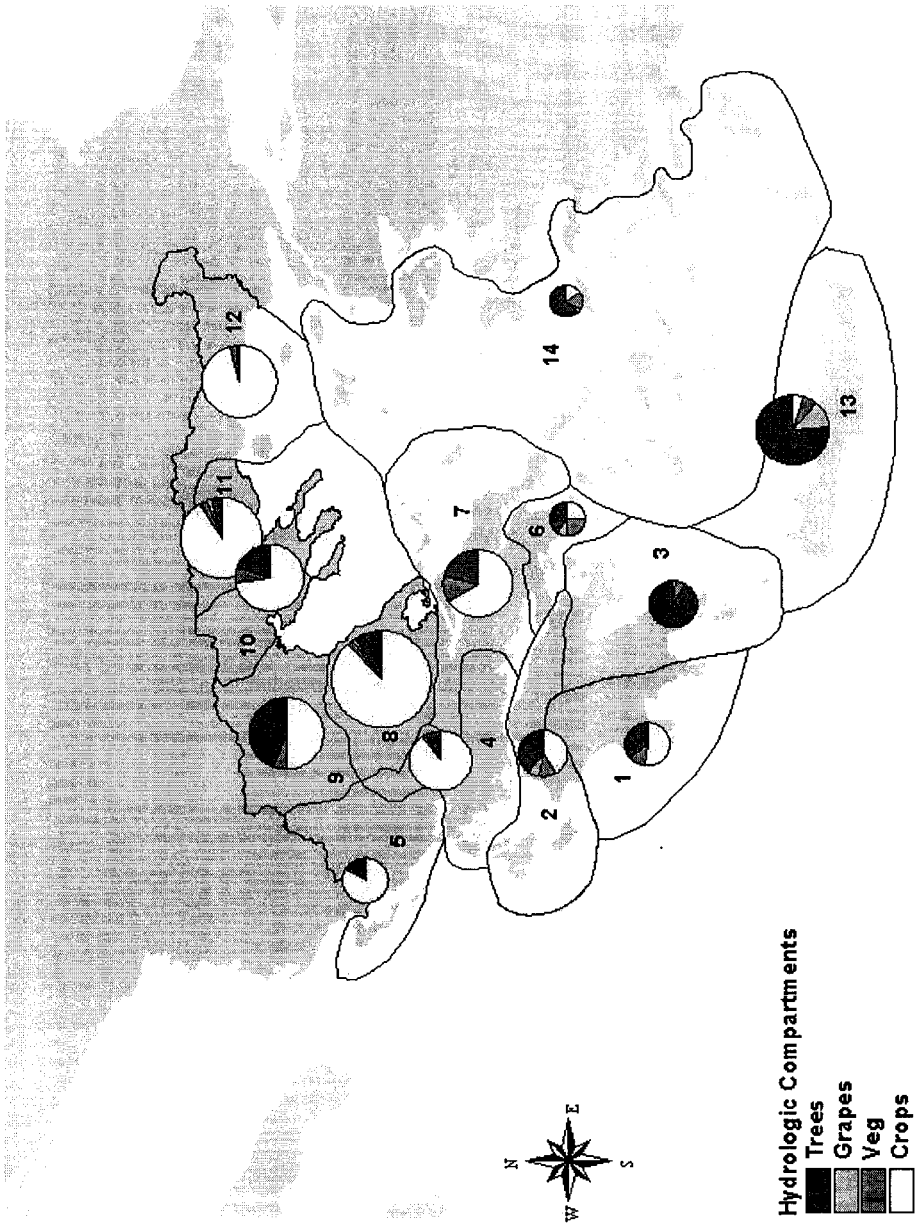


**Figure 7.17:** A multi-size pie chart illustration shows the variation in irrigation water demand for the different compartments.

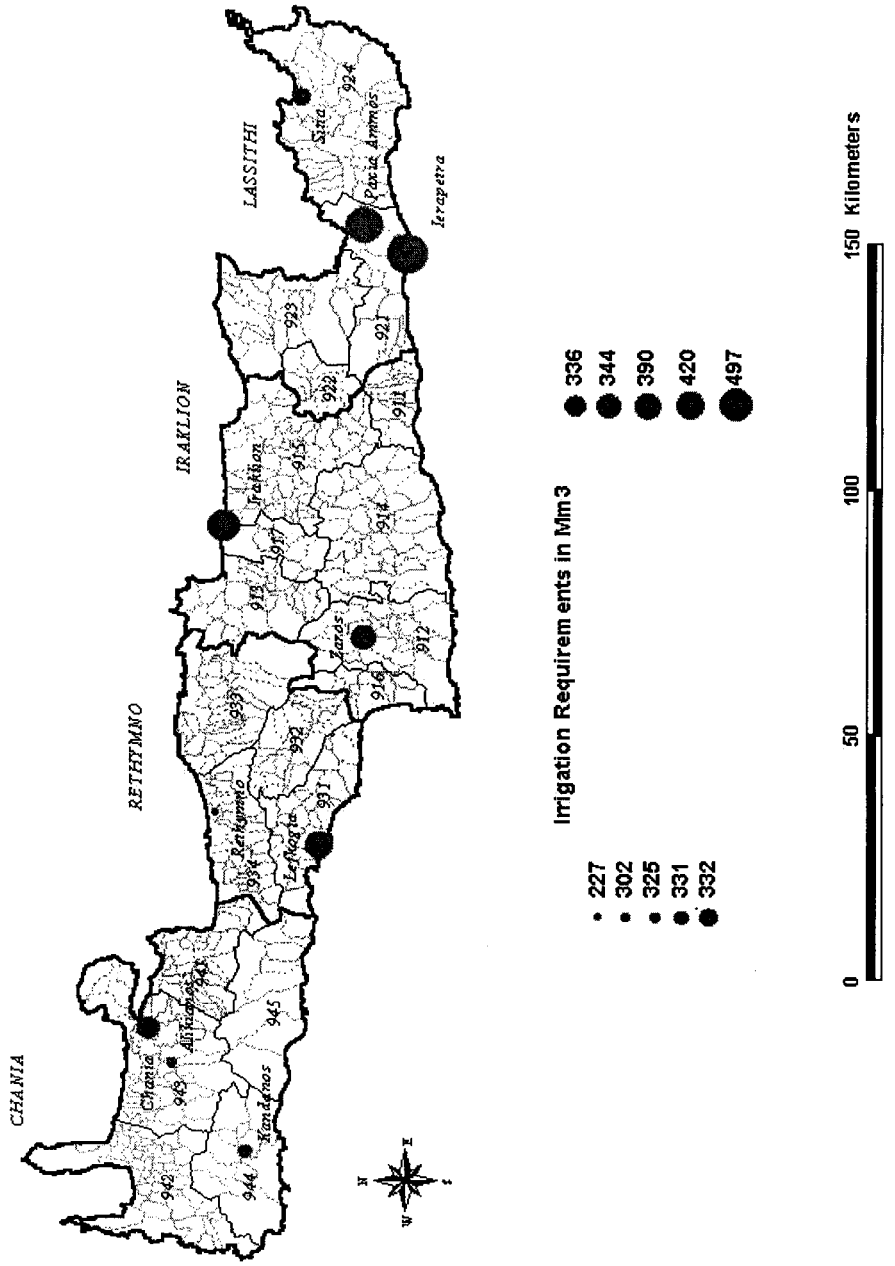


**Figure 7.18:** Irrigation water requirement estimates for the island of Crete based on individual stations.

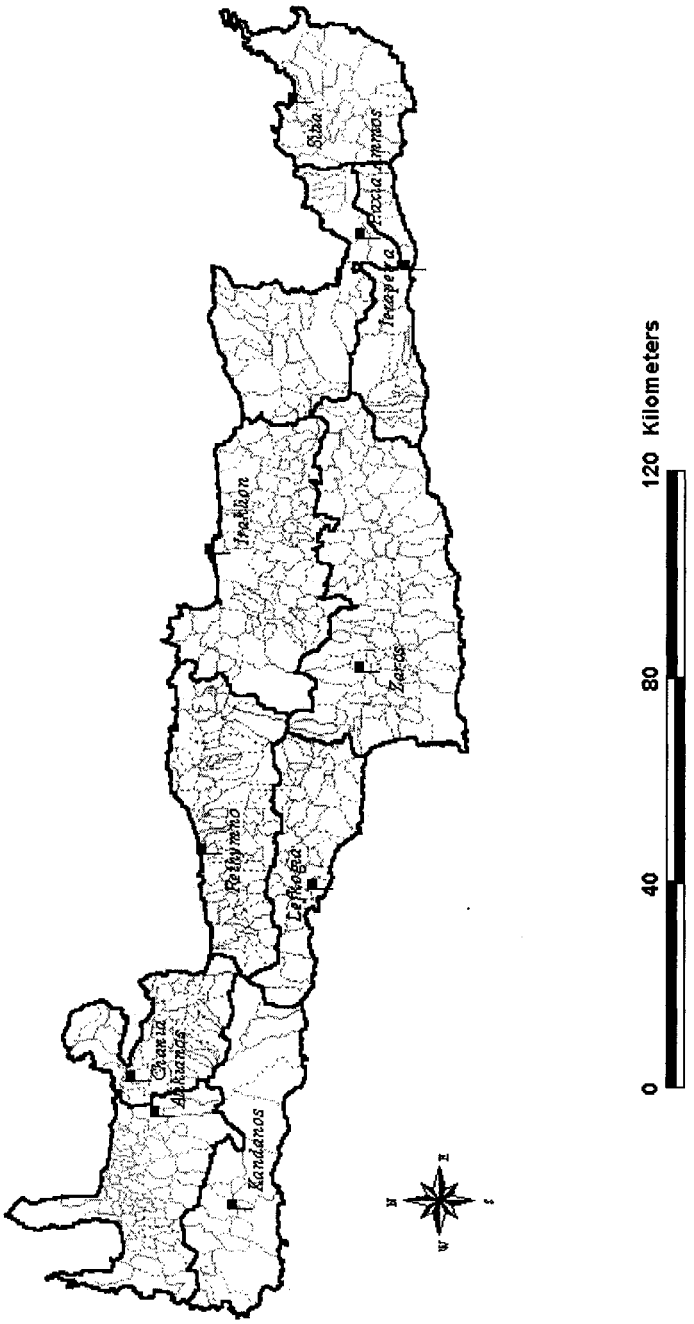


**Figure 7.19:** The ten regions of Crete and their representative stations.


**Figure 7.20:** Estimated irrigation water requirements by municipality based on ten stations for the year 1991.

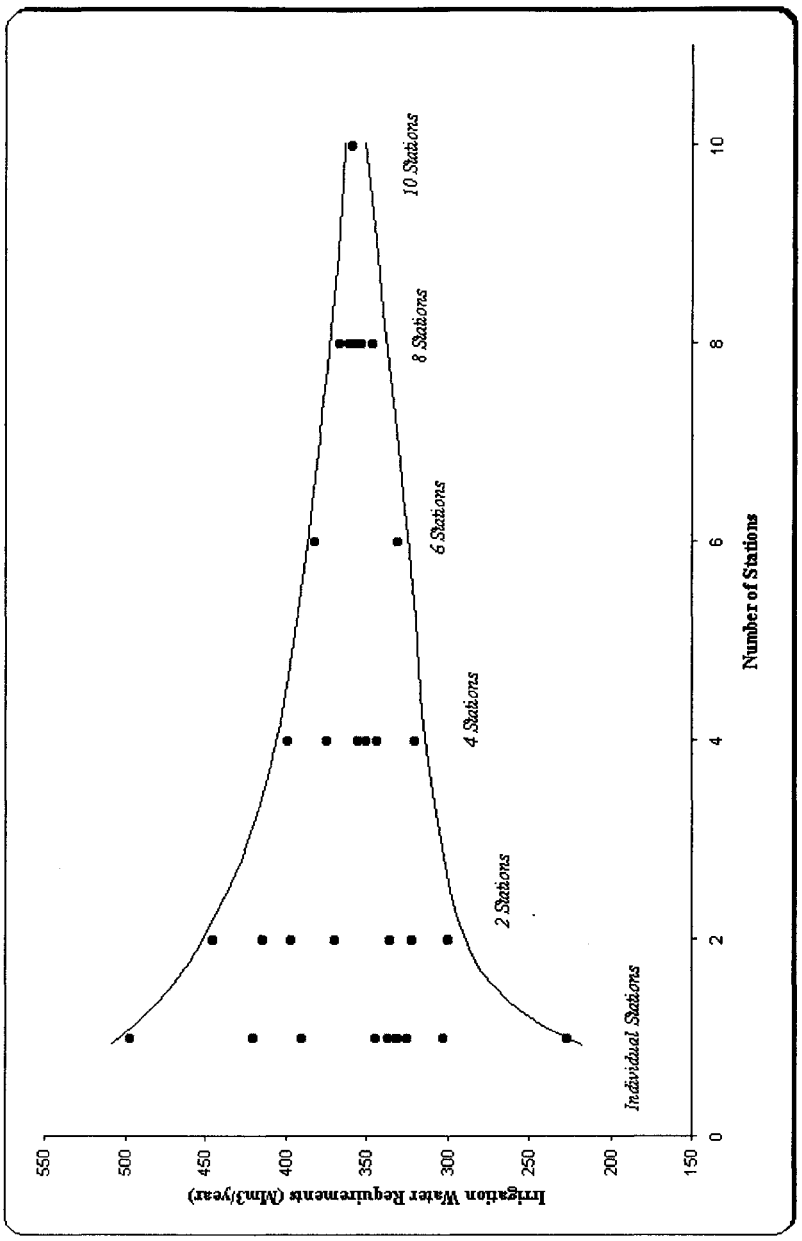


**Figure 7.21:** Estimated irrigation water requirements for the island of Crete utilizing the different approaches described in this chapter for the year 1991.

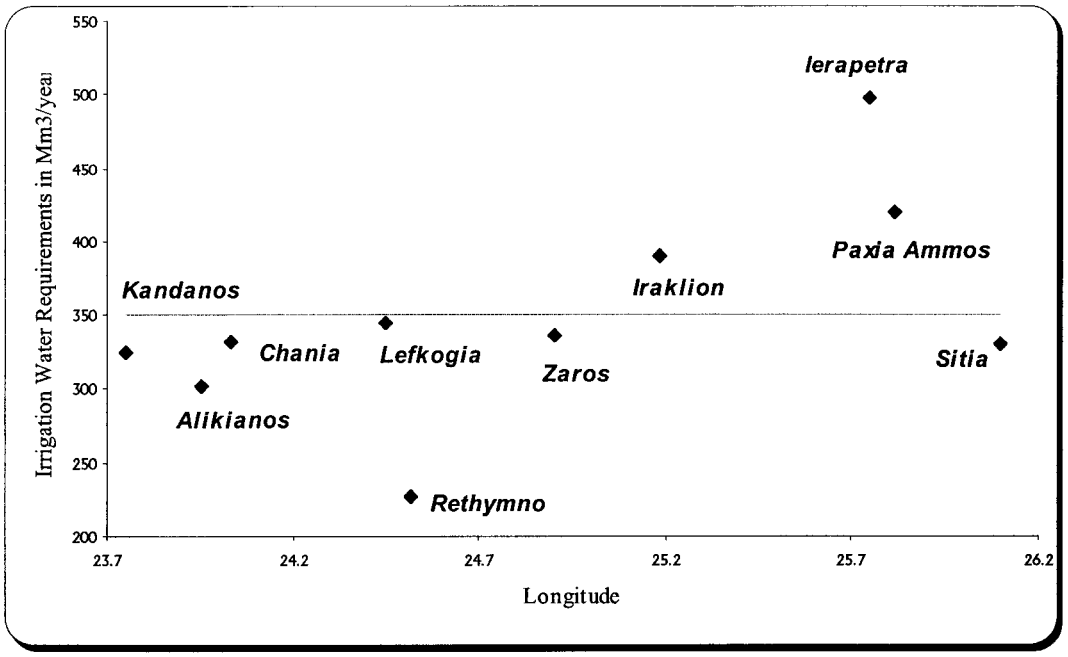


**Figure 7.22:** Estimated irrigation water requirements for the island of Crete based on individual stations against the longitude of those stations.

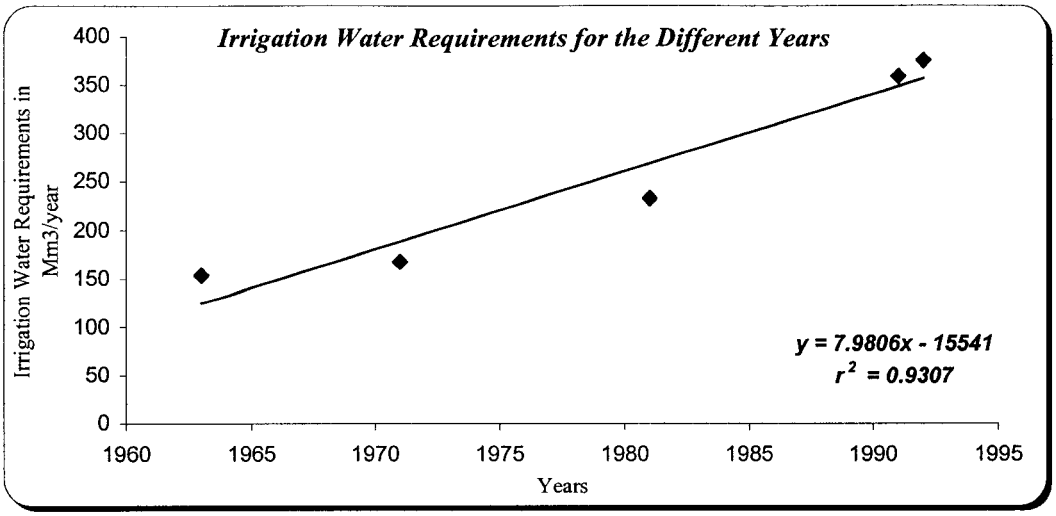


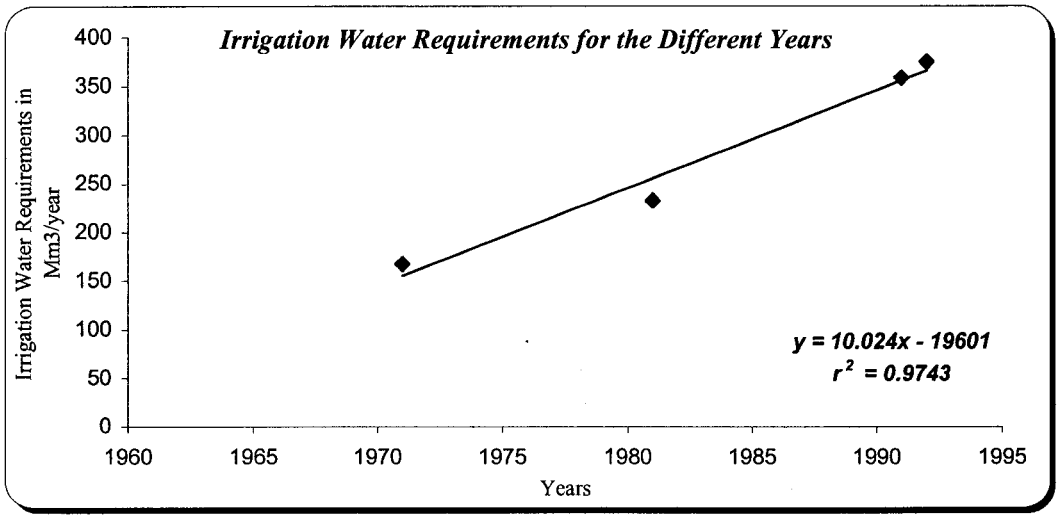


**Figure 7.23:** Projected irrigation requirements for the island. An annual increase of 10 Mm3 of water for irrigation purposes is estimated.

**Table 7.1:** Crop distribution in the four prefectures (counties) of Crete for the year 1991.

| | *IRAKLION* | *LASSITHI* | *RETHYMNO* | *XANIA* | *TOTAL* |
|---|---|---|---|---|---|
| **Trees** | **190224** | **137367** | **30101** | **133500** | **491192** |
| *Almonds* | 0.00 | 4807.85 | 0.00 | 0.00 | 4807.85 |
| *Apples* | 0.00 | 0.00 | 0.00 | 0.00 | 0.00 |
| *Apricots* | 475.56 | 2060.51 | 1204.04 | 0.00 | 3740.11 |
| *Avocado* | 475.56 | 0.00 | 0.00 | 1335.00 | 1810.56 |
| *Cherries* | 0.00 | 0.00 | 0.00 | 0.00 | 0.00 |
| *Chineese Goosberries* | 0.00 | 0.00 | 0.00 | 0.00 | 0.00 |
| *Citrus* | 1902.24 | 6868.35 | 602.02 | 13350.00 | 22722.61 |
| *Figtrees* | 0.00 | 0.00 | 0.00 | 0.00 | 0.00 |
| *Gum* | 0.00 | 0.00 | 0.00 | 0.00 | 0.00 |
| *Hazelnut* | 0.00 | 0.00 | 0.00 | 0.00 | 0.00 |
| *Olives* | 186419.52 | 119509.29 | 25886.86 | 116145.00 | 447960.67 |
| *Peach* | 475.56 | 1373.67 | 1204.04 | 2670.00 | 5723.27 |
| *Pears* | 475.56 | 2747.34 | 1204.04 | 0.00 | 4426.94 |
| *Plums* | 0.00 | 0.00 | 0.00 | 0.00 | 0.00 |
| *Pomegranate* | 0.00 | 0.00 | 0.00 | 0.00 | 0.00 |
| *Walnuts* | 0.00 | 0.00 | 0.00 | 0.00 | 0.00 |
| **Grapes** | **100209** | **7539** | **1185** | **3497** | **112430** |
| *Wine* | 15031.35 | 2261.70 | 185.55 | 1923.35 | 19401.95 |
| *Table-Use* | 20041.80 | 376.95 | 739.05 | 874.25 | 22032.05 |
| *Raisins* | 65135.85 | 4900.35 | 260.40 | 699.40 | 70996.00 |
| **Vegetables** | **33538** | **18867** | **9242** | **15551** | **77198** |
| *Artichokes* | 3018.42 | 1886.70 | 1663.56 | 1555.10 | 8123.78 |
| *Asparagus* | 0.00 | 0.00 | 0.00 | 0.00 | 0.00 |
| *Beans-Green* | 1341.52 | 1320.69 | 924.20 | 1166.33 | 4752.74 |
| *Cabbage* | 3018.42 | 1886.70 | 462.10 | 777.55 | 6144.77 |
| *Carrots* | 0.00 | 0.00 | 0.00 | 0.00 | 0.00 |
| *Cauliflower* | 1341.52 | 1509.36 | 924.20 | 1088.57 | 4863.65 |
| *Cuc. Autumn* | 0.00 | 0.00 | 0.00 | 0.00 | 0.00 |
| *Cuc. Greenhouse* | 0.00 | 0.00 | 0.00 | 1010.82 | 1010.82 |
| *Cuc. Open* | 5366.08 | 4716.75 | 323.47 | 466.53 | 10872.83 |
| *Chicory* | 0.00 | 0.00 | 0.00 | 0.00 | 0.00 |
| *Eggplants* | 0.00 | 1320.69 | 877.99 | 0.00 | 2198.68 |
| *Garlic* | 0.00 | 0.00 | 0.00 | 0.00 | 0.00 |
| *Leek* | 0.00 | 0.00 | 0.00 | 0.00 | 0.00 |
| *Lettuce* | 2347.66 | 754.68 | 924.20 | 466.53 | 4493.07 |
| *Okra* | 2012.28 | 754.68 | 277.26 | 311.02 | 3355.24 |
| *Onions-Dry* | 2347.66 | 1320.69 | 831.78 | 1166.33 | 5666.46 |
| *Peas* | 0.00 | 0.00 | 0.00 | 1088.57 | 1088.57 |
| *Spinach* | 0.00 | 0.00 | 0.00 | 1088.57 | 1088.57 |
| *Squash* | 2347.66 | 0.00 | 462.10 | 1166.33 | 3976.09 |
| *Strawberries* | 0.00 | 0.00 | 0.00 | 0.00 | 0.00 |
| *Tom. Autumn* | 0.00 | 0.00 | 0.00 | 0.00 | 0.00 |
| *Tom. Greenhouse* | 3353.80 | 2264.04 | 0.00 | 1555.10 | 7172.94 |
| *Tom. Industry* | 0.00 | 0.00 | 0.00 | 0.00 | 0.00 |
| *Tom. Open* | 7042.98 | 1132.02 | 1571.14 | 2643.67 | 12389.81 |
| **Crops on Arable Land** | **47469** | **25668** | **14399** | **20649** | **108185** |
| *Alfalfa* | 949.38 | 256.68 | 863.94 | 2064.90 | 4134.90 |
| *Barely* | 237.35 | 128.34 | 72.00 | 103.25 | 540.93 |
| *Broad Bean* | 4746.90 | 2053.44 | 1727.88 | 1238.94 | 9767.16 |
| *Clover* | 474.69 | 385.02 | 431.97 | 619.47 | 1911.15 |
| *Corn* | 0.00 | 0.00 | 0.00 | 309.74 | 309.74 |
| *Cotton* | 0.00 | 0.00 | 0.00 | 0.00 | 0.00 |
| *Crops for Grazing* | 0.00 | 0.00 | 0.00 | 309.74 | 309.74 |
| *Crops for Hay* | 949.38 | 770.04 | 0.00 | 1651.92 | 3371.34 |
| *Dry Beans* | 949.38 | 1283.40 | 719.95 | 516.23 | 3468.96 |
| *Groundnuts* | 0.00 | 0.00 | 0.00 | 0.00 | 0.00 |
| *Lentil* | 0.00 | 0.00 | 0.00 | 0.00 | 0.00 |
| *Melons* | 4034.87 | 1411.74 | 575.96 | 1342.19 | 7364.75 |
| *Oats* | 0.00 | 0.00 | 0.00 | 0.00 | 0.00 |
| *Pot. Autumn* | 6170.97 | 3850.20 | 719.95 | 1238.94 | 11980.06 |
| *Pot. Spring* | 13053.98 | 6417.00 | 4031.72 | 4542.78 | 28045.48 |
| *Pot. Summer* | 8781.77 | 8470.44 | 3455.76 | 2477.88 | 23185.85 |
| *Rice* | 0.00 | 0.00 | 0.00 | 0.00 | 0.00 |
| *Soya* | 0.00 | 0.00 | 0.00 | 0.00 | 0.00 |
| *Sugarbeets* | 0.00 | 0.00 | 0.00 | 0.00 | 0.00 |
| *Sunflower* | 0.00 | 0.00 | 0.00 | 0.00 | 0.00 |
| *Tobacco* | 0.00 | 0.00 | 0.00 | 0.00 | 0.00 |
| *Vetch* | 0.00 | 0.00 | 0.00 | 0.00 | 0.00 |
| *Watermelons* | 6883.01 | 513.36 | 1727.88 | 4129.80 | 13254.05 |
| *Wheat* | 237.35 | 128.34 | 72.00 | 103.25 | 540.93 |
| **TOTAL** | **371440** | **189441** | **54927** | **173197** | **789005** |

**Table 7.2:** Percentages of county land in each hydrologic compartment.

| County | Area 1 | Area 2 | Area 3 | Area 4 | Area 5 | Area 6 | Area 7 | Area 8 | Area 9 | Area 10 | Area 11 | Area 12 | Area 13 | Area 14 |
|---|---|---|---|---|---|---|---|---|---|---|---|---|---|---|
| Attiki | | | | | | 90 | 10 | | | | | | | |
| Ftiotis-Akarnania | | | | 90 | 10 | | | | | | | | | |
| Viotia | | | | | | 10 | 90 | | | | | | | |
| Evia | | | | | | | 100 | | | | | | | |
| Evritania | | | | 90 | | | 5 | 5 | | | | | | |
| Fthiotida | | | | 5 | | | 90 | 5 | | | | | | |
| Fokida | | | | 90 | | | 10 | | | | | | | |
| Argolida | | | 100 | | | | | | | | | | | |
| Arkadia | 47 | | 53 | | | | | | | | | | | |
| Achaia | 21 | 79 | | | | | | | | | | | | |
| Ilia | 56 | 44 | | | | | | | | | | | | |
| Korinthia | | 95 | | | | 5 | | | | | | | | |
| Lakonia | 21 | | 79 | | | | | | | | | | | |
| Messinia | 100 | | | | | | | | | | | | | |
| Zakinthos | | 100 | | | | | | | | | | | | |
| Kerkyra | | | | | 100 | | | | | | | | | |
| Kefalonia | | 100 | | | | | | | | | | | | |
| Lefkada | | | | 100 | | | | | | | | | | |
| Arta | | | | | 100 | | | | | | | | | |
| Thesprotia | | | | | 100 | | | | | | | | | |
| Ioannina | | | | | 100 | | | | | | | | | |
| Preveza | | | | | 100 | | | | | | | | | |
| Karditsa | | | | 25 | | | | 75 | | | | | | |
| Larissa | | | | | | | | 100 | | | | | | |
| Magnesia | | | | | | | 10 | 90 | | | | | | |
| Trikala | | | | 28 | 5 | | | 67 | | | | | | |
| Grevena | | | | | | | | 10 | 90 | | | | | |
| Drama | | | | | | | | | | | 54 | 46 | | |
| Imathia | | | | | | | | | 83 | 17 | | | | |
| Thessaloniki | | | | | | | | | | 90 | 10 | | | |
| Kavala | | | | | | | | | | | 90 | 10 | | |
| Kastoria | | | | | 10 | | | | 90 | | | | | |
| Kilkis | | | | | | | | | | 95 | 5 | | | |
| Kozani | | | | | | | | | 100 | | | | | |
| Pella | | | | | | | | | 90 | 10 | | | | |
| Pieria | | | | | | | | 5 | 95 | | | | | |
| Serres | | | | | | | | | | | 100 | | | |
| Florina | | | | | | | | | 100 | | | | | |
| Chalkidiki | | | | | | | | | | 100 | | | | |
| Evros | | | | | | | | | | | | 100 | | |
| Xanthi | | | | | | | | | | | 60 | 40 | | |
| Rodopi | | | | | | | | | | | | 100 | | |
| Dodekanissos | | | | | | | | | | | | | | 100 |
| Kyklades | | | | | | 5 | | | | | | | | 95 |
| Lesvos | | | | | | | | | | | | | | 100 |
| Samos | | | | | | | | | | | | | | 100 |
| Chios | | | | | | | | | | | | | | 100 |
| Idealio | | | | | | | | | | | | | 100 | |
| Lassithi | | | | | | | | | | | | | 100 | |
| Rethymno | | | | | | | | | | | | | 100 | |
| Xania | | | | | | | | | | | | | 100 | |

**Table 7.3:** Crop distribution under the four main categories of crops in Compartment (1).

| Region / Trees | Area 1 | almonds | apples | apricots | avocado | cherries | chinese-gooseberries | citrus | figtrees |
|---|---|---|---|---|---|---|---|---|---|
| Arkadia | 47 | 2 | 5 | 5 | | 2.5 | | | |
| Achaia | 21 | 2.5 | | | | 5 | | 20 | |
| Elia | 56 | | | 1 | | | | 12 | |
| Lakonia | 21 | | | 1.5 | | | | 9.5 | 4 |
| Mesinia | 100 | | | 0.5 | | 0.5 | | 2 | 6 |

| Region / Trees | Area 1 | gum | hazelnut | olives | peaches | pears | plums | pomegranate | walnut |
|---|---|---|---|---|---|---|---|---|---|
| Arkadia | 47 | | | 75 | 3 | 2 | | | 5.5 |
| Achaia | 21 | | | 64 | | 4.5 | | | 4 |
| Elia | 56 | | | 86 | | 1 | | | |
| Lakonia | 21 | | | 83.5 | 1.5 | | | | |
| Mesinia | 100 | | | 91 | | | | | |

| Region / Grapes | Area 1 | wines | table use | raisins |
|---|---|---|---|---|
| Arkadia | 47 | 50 | 50 | |
| Achaia | 21 | 28 | 17 | 55 |
| Elia | 56 | 5 | 80 | 15 |
| Lakonia | 21 | 83 | 16 | 1 |
| Mesinia | 100 | 2 | 80 | 18 |

| Region / Vegetables | Area 1 | artichokes | asparagus | beans-green | cabbage | carrots | cauliflower | cu.-aut. | cu.-spr. | cucum-open | dandelion | eggplants | garlic |
|---|---|---|---|---|---|---|---|---|---|---|---|---|---|
| Arkadia | 47 | | | 8.5 | 8 | | 6 | | | 6 | | 7 | 5 |
| Achaia | 21 | | | 10 | 6.5 | 8.5 | | | | 10 | | 3 | 3 |
| Elia | 56 | | | 9 | 3 | 4 | 3 | | | 5 | | | 5 |
| Lakonia | 21 | 3.5 | | | 5.5 | 8.5 | 9 | | | 10 | | 7 | |
| Mesinia | 100 | 4 | | 19 | 7 | 6 | 6 | | | 4 | | 5 | |

| Region / Vegetables | Area 1 | green-pea | leek | lettu.-spr. | okra | onions-dry | spinach | squash | strawberries | tom.-greenhouse | tom.-indus. | tom.-open |
|---|---|---|---|---|---|---|---|---|---|---|---|---|
| Arkadia | 47 | | | 18 | 5 | 6 | | 5.5 | | | 4 | 21 |
| Achaia | 21 | | | 3 | 10 | 7 | | 5 | | | 14 | 20 |
| Elia | 56 | | | 5 | | 4 | | 6 | | 4 | 45 | 7 |
| Lakonia | 21 | 5 | | 4 | | 23 | | 3.5 | | | | 21 |
| Mesinia | 100 | 5 | 6 | 3 | | 5 | | 7 | | 6 | | 17 |

| Region / Crops | Area 1 | alfalfa | barley | clover | corn | cotton | crops-grazing | dry-beans | grass-cut-hay | kukia | lentil | melons | nuts |
|---|---|---|---|---|---|---|---|---|---|---|---|---|---|
| Arkadia | 47 | 10 | 1 | | 30 | | | 10 | 3 | 10 | | | |
| Achaia | 21 | 15 | 1 | 2 | 16 | | 4 | 4.5 | 20 | | | | |
| Elia | 56 | 7 | 0.5 | 1.5 | 43 | 1.5 | 3 | 2.5 | 10 | | | 2 | |
| Lakonia | 21 | 25 | 0.5 | 4 | 20 | | 10 | 3 | 8 | 1.5 | | 4 | |
| Mesinia | 100 | 10 | 0.5 | 3 | 15 | | 4 | 2.5 | 4 | | | 4 | 8 |

| Region / Crops | Area 1 | oats | pota.-aut. | pota.-spr. | pota.-sum. | rice | soya | sugarbeets | sunflower | tobacco | vetch | watermelons | wheat |
|---|---|---|---|---|---|---|---|---|---|---|---|---|---|
| Arkadia | 47 | | | | 35 | | | | | | | | 1 |
| Achaia | 21 | | | 13 | 17 | | | | | | 0.5 | 6 | 1 |
| Elia | 56 | | | 15 | | | | | | | | 13 | 1 |
| Lakonia | 21 | | 3 | 8 | 6 | | | | | 1.5 | | 5 | 0.5 |
| Mesinia | 100 | | 10 | 15 | 15 | 1.5 | | | | | | 7 | 0.5 |

**Table 7.4:** Estimated irrigation water requirements per category of crop in $Mm^3$

| | | 1963 | 1971 | 1981 | 1991 | 1992 | 2020 |
|---|---|---|---|---|---|---|---|
| Trees | Max | 373 | 511 | 731 | 1012 | 1055 | 1695 |
| | Mean | 312 | 430 | 616 | 845 | 881 | 1414 |
| | Min | 251 | 349 | 500 | 678 | 707 | 1136 |
| Grapes | Max | 40 | 57 | 79 | 95 | 93 | 148 |
| | Mean | 35 | 49 | 67 | 81 | 80 | 126 |
| | Min | 30 | 40 | 54 | 67 | 66 | 104 |
| Vegetables | Max | 229 | 257 | 274 | 302 | 298 | 368 |
| | Mean | 194 | 219 | 235 | 259 | 255 | 317 |
| | Min | 158 | 182 | 196 | 215 | 211 | 266 |
| Crops | Max | 1440 | 1898 | 2127 | 2659 | 2942 | 4093 |
| | Mean | 1243 | 1651 | 1878 | 2354 | 2599 | 3653 |
| | Min | 1045 | 1404 | 1628 | 2048 | 2256 | 3215 |
| Total | Max | 2083 | 2723 | 3211 | 4068 | 4389 | 6304 |
| | Mean | 1783 | 2349 | 2795 | 3539 | 3815 | 5510 |
| | Min | 1484 | 1976 | 2378 | 3009 | 3241 | 4719 |

**Table 7.5:** Estimated irrigation water requirements per hydrologic compartment for the year 2020 in $Mm^3$.

| No. | Compartments | Trees | Grapes | Vegetables | Crops | Total |
|---|---|---|---|---|---|---|
| 1 | West Pelponnesus | 62 | 1 | 20 | 92 | 176 |
| 2 | North Pelponnesus | 84 | 14 | 25 | 87 | 211 |
| 3 | East Pelponnesus | 187 | 1 | 12 | 6 | 206 |
| 4 | West Rumeli | 31 | 0 | 8 | 328 | 368 |
| 5 | Epirus | 26 | 0 | 6 | 151 | 184 |
| 6 | Attica | 37 | 9 | 23 | 23 | 92 |
| 7 | East Rumeli | 98 | 3 | 59 | 313 | 472 |
| 8 | Thessaly | 92 | 10 | 22 | 856 | 981 |
| 9 | West Macedonia | 240 | 0 | 32 | 276 | 547 |
| 10 | Central Macedonia | 87 | 5 | 30 | 336 | 457 |
| 11 | East Macedonia | 28 | 11 | 21 | 611 | 672 |
| 12 | Thrace | 8 | 1 | 15 | 533 | 556 |
| 13 | Crete | 386 | 67 | 29 | 30 | 511 |
| 14 | Aegean Isles | 49 | 3 | 15 | 11 | 77 |
| | **Total** | **1415** | **126** | **317** | **3653** | **5511** |

**Table 7.6:** Ranking the fourteen hydrologic compartments of Greece according to average irrigation requirements
[Rank 1 = the highest consumption, and Rank 14 = the lowest consumption].

| Compartments Year 1991 | Irrigation Water Requirements (Mm3/Year) | Irrigated Area (Stremma) | Average Irrigation Water Requirements (m3 / stremma/year) | Rank |
|---|---|---|---|---|
| Area 1 | 113 | 528504 | 214 | 12 |
| Area 2 | 145 | 609226 | 237 | 10 |
| Area 3 | 157 | 424713 | 369 | 4 |
| Area 4 | 202 | 995452 | 203 | 14 |
| Area 5 | 131 | 623526 | 210 | 13 |
| Area 6 | 61 | 153181 | 399 | 2 |
| Area 7 | 363 | 995570 | 364 | 5 |
| Area 8 | 574 | 1865997 | 308 | 7 |
| Area 9 | 390 | 1617061 | 241 | 9 |
| Area 10 | 309 | 911054 | 340 | 6 |
| Area 11 | 391 | 1286996 | 304 | 8 |
| Area 12 | 246 | 1043567 | 236 | 11 |
| **Area 13** | **308** | **789005** | **390** | **3** |
| Area 14 | 135 | 182354 | 741 | 1 |

**Table 7.7:** Ranking the fourteen hydrologic compartments of Greece according to the effectiveness of precipitation
[Rank 1 = the highest efficiency, and Rank 14 = the lowest efficiency].

| Compartments Year 1991 | Average Irrigation Water Requirements (mm/year) | Average Yearly Precipitation (mm/year) | Total Water Losses Due to Evapotranspiration (mm/year) | Effectiveness of Precipitation (%) | Rank |
|---|---|---|---|---|---|
| Area 1 | 214 | 781 | 996 | **78** | **3** |
| Area 2 | 237 | 802 | 1039 | **77** | **4** |
| Area 3 | 369 | 539 | 908 | **59** | **9** |
| Area 4 | 203 | 937 | 1140 | **82** | **1** |
| Area 5 | 210 | 965 | 1174 | **82** | **2** |
| Area 6 | 399 | 364 | 763 | **48** | **13** |
| Area 7 | 364 | 375 | 739 | **51** | **12** |
| Area 8 | 308 | 506 | 813 | **62** | **7** |
| Area 9 | 241 | 601 | 842 | **71** | **5** |
| Area 10 | 340 | 455 | 795 | **57** | **11** |
| Area 11 | 304 | 422 | 726 | **58** | **10** |
| Area 12 | 236 | 553 | 789 | **70** | **6** |
| **Area 13** | **390** | **574** | **964** | **60** | **8** |
| Area 14 | 741 | 371 | 1112 | **33** | **14** |

**Table 7.8:** A comparison between the calculated mean annual reference evapotranspiration and mean annual precipitation for each of the ten representative meteorological stations representing Crete.

| Station Name | Elevation (m) | Mean Annual Precipitation in mm | Calculated Mean Annual Reference Evapotranspiration in mm |
|---|---|---|---|
| ***Alikianos*** | 18 | 809 | 1749 |
| ***Chania*** | 62 | 548 | 1680 |
| ***Ierapetra*** | 16 | 422 | 2029 |
| ***Iraklion*** | 38 | 486 | 2108 |
| ***Kandanos*** | 466 | 944 | 1752 |
| ***Lefkogia*** | 80 | 755 | 1689 |
| ***Paxia Ammos*** | 50 | 554 | 2031 |
| ***Rethymno*** | 5 | 662 | 1304 |
| ***Sitia*** | 6 | 485 | 1673 |
| ***Zaros*** | 343 | 813 | 1654 |

**Table 7.9:** Estimated irrigation water requirements for each crop type for the year 1991 based on the stations of Iraklion and Rethymno.

| AREA 13 (Crete) | Iraklion | Rethymno |
|---|---|---|
| CROP TYPE | Mm3/year | Mm3/year |
| TREES | 270.63 | 157.32 |
| ALMONDS | 2.01 | 0.99 |
| APPLES | 0.00 | 0.00 |
| APRICOTS | 3.08 | 1.82 |
| AVOCADO | 1.49 | 0.88 |
| CHERRIES | 0.00 | 0.00 |
| CHINEESE GOOSBERRIES | 0.00 | 0.00 |
| CITRUS | 17.04 | 10.03 |
| FIGTREES | 0.00 | 0.00 |
| GUM | 0.00 | 0.00 |
| HAZELNUT | 0.00 | 0.00 |
| OLIVES | 238.34 | 138.44 |
| PEACH | 5.12 | 3.05 |
| PEARS | 3.55 | 2.11 |
| PLUMS | 0.00 | 0.00 |
| POMEGRANATE | 0.00 | 0.00 |
| WALNUTS | 0.00 | 0.00 |
| GRAPES | 48.93 | 30.23 |
| WINES | 7.77 | 5.11 |
| TABLE USE | 8.96 | 5.45 |
| RAISINS | 32.21 | 19.66 |
| VEGETABLES | 33.70 | 19.32 |
| ARTICHOKES | 7.25 | 3.95 |
| ASPARAGUS | 0.00 | 0.00 |
| BEANS-GREEN | 1.00 | 0.31 |
| CABBAGE | 2.57 | 1.76 |
| CARROTS | 0.00 | 0.00 |
| CAULIFLOWER | 2.03 | 1.39 |
| CUC. AUTUMN | 0.00 | 0.00 |
| CUC. GREENHOUSE | 0.18 | 0.03 |
| CUC. OPEN | 5.30 | 3.44 |
| CHICORY | 0.00 | 0.00 |
| EGGPLANTS | 1.17 | 0.74 |
| GARLIC | 0.00 | 0.00 |
| LEEK | 0.00 | 0.00 |
| LETTUCE | 0.76 | 0.27 |
| OKRA | 1.52 | 0.82 |
| ONIONS DRY | 1.86 | 0.77 |
| PEAS | 0.32 | 0.15 |
| SPINACH | 0.20 | 0.07 |
| SQUASH | 1.48 | 0.90 |
| STRAWBERRIES | 0.00 | 0.00 |
| TOM. AUTUMN | 0.00 | 0.00 |
| TOM. GREENHOUSE | 0.35 | 0.00 |
| TOM. INDUSTRY | 0.00 | 0.00 |
| TOM. OPEN | 7.70 | 4.72 |
| CROPS ON ARABLE LAND | 36.57 | 20.36 |
| ALFALFA | 3.98 | 2.60 |
| BARLEY | 0.15 | 0.05 |
| BROAD BEAN | 2.52 | 0.95 |
| CLOVER | 1.91 | 1.19 |
| CORN | 0.20 | 0.13 |
| COTTON | 0.00 | 0.00 |
| CROPS FOR GRAZING | 0.02 | 0.00 |
| CROPS FOR HAY | 0.99 | 0.35 |
| DRY BEANS | 1.43 | 0.93 |
| GROUND NUTS | 0.00 | 0.00 |
| LENTIL | 0.00 | 0.00 |
| MELONS | 3.00 | 1.75 |
| OATS | 0.00 | 0.00 |
| POT. AUTUMN | 2.53 | 1.00 |
| POT. SPRING | 2.06 | 0.02 |
| POT. SUMMER | 12.21 | 8.20 |
| RICE | 0.00 | 0.00 |
| SOYA | 0.00 | 0.00 |
| SUGARBEETS | 0.00 | 0.00 |
| SUNFLOWER | 0.00 | 0.00 |
| TOBACCO | 0.00 | 0.00 |
| VETCH | 0.00 | 0.00 |
| WATERMELONS | 5.41 | 3.14 |
| WHEAT | 0.15 | 0.05 |
| TOTAL | 389.84 | 227.23 |

# CHAPTER 8

# A GIS PRE-PROCESSOR FOR POLLUTANT TRANSPORT MODELLING

A GIS pre-processor was developed to produce bathymetric and shoreline data of different resolution for open and closed boundary as input to a three-dimensional hydrodynamic/pollutant transport model to simulate the currents and pollutant transport in lakes and coastal areas. The pre-processor operates within ArcView GIS. The use of this GIS module facilitates the implementation of different pollutant transport scenarios, which in turn can significantly contribute to the decision-making process concerning one of the most contemporary environmental problems. The development and applicability of the pre-processor is illustrated through a test case for Suda Bay in Crete, Greece. More test cases for selected bays located around Greece are also presented.

## 8.1 Introduction

Water quality problems have been identified in many coastal areas around the world. The environmental degradation of the coastal areas has been attributed to municipal and industrial discharges. In addition to sanitary sewers and sewage treatment plant submerged discharges, a number of storm and combined sewer overflow (CSO) and major tributaries (creeks, rivers), have significant impacts on the water quality of coastal areas. During a heavy rainfall event, the runoff from roads and buildings is collected in the combined storm and sanitary sewers where it is transported to the sewage treatment facility. If the demand on the plant is too high, the excess runoff and raw sewage in the sewers is redirected to outfalls located along the shoreline. In fact, it is not uncommon to hear of beach closures in a number of coastal areas around the world after a heavy rain event due to high levels of pollution.

Most of today's models require as input a gridded dataset giving a complete model of the spatial distribution of each input parameter. Numerical grid generation is becoming a fairly common tool for use in the numerical solution of partial differential equations on arbitrarily shaped regions. It is the function of the grid to make the best use of the number of points (sampling stations) that are available. The numerical solution of partial differential equations requires some discretization of the field into a collection of points or elemental volumes (cells). The discretization must conform to the boundaries of the region in such a way that boundary conditions can be accurately represented (Thompson et al. 1985).

In this chapter, an ArcView GIS project is developed and used to prepare ASCII input files representing the bathymetric grid and shorelines necessary for running a 3D hydrodynamic/pollutant transport model and for post-processing purposes (represented in this case by the graphics package Tecplot® v8.0 for visualizing). The depths of the different

locations in the domain are spatially interpolated from contours and/or spot depths. The 3D hydrodynamic/pollutant transport model (IDOR3D) is a DOS-based educational and research program developed at McMaster University.

## 8.2 3D Hydrodynamic/Pollutant Transport Model

Description of the governing equations, boundary conditions, and numerical analysis techniques can be found in Shen et al. (1995).

## 8.3 The ArcView GIS Project

The ArcView project, in its basic format, is a collection of views, tables, scripts, layouts, and charts as shown in Figure 8.1a. The saved project, with all its contents, is transferable under the condition that the source location of the themes displayed in the views is transferred along with it. Upon opening the project, all information is retrieved and redisplayed in the same fashion.

The GIS module developed can read digital hydrographic files, which represent the definition of the bathymetry of the computational domain. Since the hydrographic files are in decimal degrees (geographic projection), projecting them in the appropriate projection is the first step in order to properly link all details and any additional information. Upon completing projection, the files are then: 1) converted to ArcView shapefiles; 2) filtered to remove any information that, for this application, is deemed irrelevant (for example, rivers); 3) edited to fix any errors and erase any unnecessary features (i.e. moving any spot depths points to inside the shoreline, trim shoreline, ...etc); and 4) manipulated to match the desired features by the module to generate grids (i.e. convert contours to points, convert shoreline from polygon to polyline, merge islands and shoreline, ...etc).

The written scripts are then run consecutively to perform the grid generation, which also has been designed to prompt the user with dialogs and messages for guidance and interaction. The depth grids may be defined for either the full extent (Figure 8.1b) or a sub area (Figure 8.1c) of the available input data. The module also allows the user to specify both the grid cell size (Figure 8.1d) and the type of interpolation technique. The depth grids can also be generated for open or closed boundary conditions (Figure 8.2).

After collecting all necessary information from the user through prompts and messages, the program starts executing the task of generating the depth grid. The execution time depends exclusively on the type of interpolation technique used, the extent of the area under study, and the cell size of the grid. Larger areas and smaller cell size definitely increase execution time. Kriging interpolation, for example, normally requires more time than Spline and IDW. The user is informed of the completion of the operation when a message is

displayed on the screen. The ASCII file is then generated, together with a visual presentation of the grid. Another process initiates by running a series of ArcView scripts that converts the shoreline (including islands) to points separated at user-specified spacing. The text file is then generated. The hydrodynamic model IDOR3D requires additional processing of files once the shore and bathymetric files have been generated. The following steps are necessary for running the IDOR3D model

(a) The bottom topography of the computational domain must be defined. The depths of the domain are interpolated from the topography file, created by ArcView GIS and an additional program is run to generate a depth grid.

(b) Generation of two files that contain information about each grid (column) within the larger grid system. The depths in each column are expressed as cells. The number of cells in a column is directly related to the depth of water at that point, and the number of layers is defined in a file, which specifies the thickness of each layer.

(c) To define the simulation, IDOR3D reads two parameter files. The first file provides IDOR3D with information such as simulation length, date and time of simulation, time series locations, time levels when variables about the whole water body are to be saved, as well as wind and source characteristics. The second file defines the physical characteristics of the body of water provided by experts such as diffusivity, viscosity, water density, drag coefficient, etc.

### 8.3.1 Test Case

The island of Crete in the country of Greece was used as a test case during the process of developing the project. The island of Crete is located between latitudes 34° and 36° North and longitudes 23° and 27° East as shown in Figure 8.3a. The length of Crete coastline is estimated at 1,000 km. The highest point on the island is approximately 2,500 meters above mean sea level, while the deepest point around the island is approximately -2,500 meters as shown in Figure 8.3b. The island has an area of 8265 $Km^2$ and is located in the southern part of Greece as shown in Figure 8.4. Suda Bay (area of interest, Figure 8.4) is located at the northwestern part of the island and is exposed to effluent from ten outlets, including an outlet of water course, an outlet during heavy rainfall, five outlets of public parking grounds, and three outlets of untreated industrial sewage. Figure 8.5 shows a satellite image of the bay as well as a photograph taken from the northwestern side of the bay, where, as will be seen in a following section, the pollutant source is located. The GIS coverages used in this study, including shoreline and spot depths of the bay, were based on maps developed by the Greek Army Geographical Service (1:12,500) in the form of ARC/INFO export files.

### 8.3.2 Generating Bathymetric Grid (dpthgis.dat)

The ARC/INFO export files (*.e00) are imported as ARC/INFO coverages using the "IMPORT 71" utility provided by ArcView. The coverages are then added to the project and

converted to ArcView shapefiles. The user is then prompted to define the analysis extent, which can be for the full or part of the extent. Open or closed boundary conditions may be imposed during the grid generation stage, which is a closed all around except for the east side (sub area of extent). The user is then presented with a dialog, where they can determine the desired cell size of the grid and confirm the analysis extent. The program is then executed to generate the depth grid. For organizational purposes, the project has been equipped with an automatic tool to generate working directories for each view. For example, all work performed in the view "suda_all" is stored in a directory with the same name. A visual presentation of the grid, as shown in Figure 8.6, is generated and added to the view.

As shown in Figure 8.7, bathymetry grids have been generated using different cell sizes of 50, 100, 200, 300, 400, and 500m (a cell size of 50m is a square grid of 50m*50m). It is clear that as the cell size increases, the shape of the grid does not seem to conform to the shoreline and small islands in the area, which can produce erratic modeling results. A 50m or 100m grid is more acceptable than 200m and 300m grids; while 400m and 500m grids are not desirable due to the coarse representation of bathymetry and the compromising of the shoreline and islands. This is especially true in the case of islands, which are no longer represented in the case of the 500m grid. The header of the generated "dpthgis.dat" file includes the following information:

| | | |
|---|---|---|
| NCOLS | number of columns | IMAX |
| NROWS | number of rows | JMAX |
| Xllcorner | x-coordinate of the origin | |
| Yllcorner | y-coordinate of the origin | |
| Cellsize | the dimension of the square cell | |
| NODATA_value | are ground points (not covered with water) | -9999 |

### 8.3.3 Generating Shoreline Points (shore.dat)

As indicated earlier, the second group of scripts is executed to convert the shoreline (including islands, if they exist) to points separated at user-specified spacing which is 50 meters in this case. The "shore.dat" text file is then generated (refer to Figure 8.8). This file takes the following form:

| | | |
|---|---|---|
| MZONE | Number of zones [>1 if there are islands] | loops from 1 to MZONE |
| MIMAX(M) | Number of points in the zone | |
| X(MI), Y(MI) | locations of points in the zone | loops from 1 to MIMAX |

### 8.3.4 Input File Requirements – Pre-Processing Procedure

The hydrodynamic model IDOR3D requires additional pre-processing of files once the shore and bathymetric files have been generated. The following steps are necessary for running the model:

- Generate the *Depth.dat* file
- Generate the *Column.dat and Cell.dat* file
- Definition of Simulation Parameters

The first two steps are done from within ArcView GIS by using direct commands to execute the related programs. The third step includes manual input/generation of parameters/files.

Using the file (dpthgis.dat) as input, the Fortran program "Deprd.exe" generates a new file (Depth.dat). The depth.dat file is a new format of the dpthgis.dat file. The program: 1) converts all no-data values (-9999) to (0); 2) converts all negative values to positive (i.e. multiplies all values in the dpthgis.dat file by –1); and 3) arranges all depth values in blocks. The number of blocks equals the number of rows and in each block the number of values equals the number of columns. The first block in the depth.dat file is the last row of the grid (i.e. the last row of the dpthgis.dat file).

Two other programs (Column.exe and Cell.exe) are then run to create two grid/depth files called "Column.dat" and "Cell.dat", which are used in the main program (idor3d.exe). The column file contains information about each grid (column) within the larger grid system. The depths in each column are expressed as cells. The number of cells in a column is directly related to both the depth of water at that point and the number of layers defined in the *zinter.dat* file, which specifies the thickness of each layer.

The simulation is defined in the third step when IDOR3D reads two parameter files, the *Paruser* and *Parexp* data files. An *input* file (*.inp) provides the program with a list of data files available to be read. Not all of the files listed in the input file are necessary; thus necessity is determined by how the simulation is defined.

The *Paruser.Dat* file provides IDOR3D with information such as simulation length, date and time of simulation, time series locations, time levels at which variables about the whole water body are to be saved, as well as wind and source characteristics. The *Parexp.Dat* file defines the physical characteristics of the body of water provided by experts, such as density, diffusivity, viscosity, water density, drag coefficient, etc.

The number of files that can potentially be used by the model can be quite large, depending on the complexity of the simulation and the availability of data regarding the particular study area. However, for very simple cases, the model is capable of running with the following files: Dpthgis.dat, Depth.dat, Zinter.dat, Column.dat, Cell.dat, Paruser.dat, Parexpt.dat, Souloc.dat, Idor.txt, 001Files.INP.

The *Souloc.dat* file contains source information, such as the number of sources, their location within the grid, the direction of discharge, flowrate, temperature, concentration and the dilution factor. If there is a continuous discharge, all information is read here. For variable discharge a source file with variable flow and concentration data is needed. The *Idor.txt* file contains information regarding the warm-up time. The shore.dat file, generated by the GIS, is not required in order to run the model, however, it is necessary during the post-processing of the results.

8.3.5 Output File Requirements – Post-Processing Procedure

During the course of a simulation, the following three files are created by the IDOR3D program and will store specific information

- 001.suv - Stores grid, depth, vector, and concentration data for the entire study area for the times specified in the Paruser.dat file.
- 001.kin - Stores the kinetic energy of the study area over the simulation period.
- 001.tim - Stores the concentration levels at pre-determined locations (i.e. specified in Paruser.dat) for the duration of the run.

To generate time series plots that can be viewed in Tecplot, the program "Vartiargno12.exe" reads the 001.tim file and creates a data file for each location specified in the *Paruser.dat* file. These files will take on the form <Location>.con. For example the file 13_29.con is a time series file generated by the "Vartiargno12.exe" program for the (I, J) grid point 13,29 on the grid. This file can now be loaded into Tecplot.

Run the "Transarg .exe" program to view both contour and vector data in Tecplot. This program will read the *Shore.dat* file, which contains X and Y values that are based on the UTM coordinate system. It will convert those values to (I, J) grid coordinates before writing the shoreline information to each vector file generated.

"Transarg .exe" program will also read the 001.suv file and format the data into vector files for each time period specified. For example, if one time interval at hour 24 is defined in the *Paruser.Dat* file, then the "Transarg .exe" program will create one vector file with the name 001a24.vec. The '001' is the run code, while the 'a' character stands for average depth. The user has the option of choosing a layer or viewing the depth average. If, for example, layer 3 is chosen, then the vector file created is given the name 001324.vec. These files can then be loaded into Tecplot for viewing.

8.3.6 Simulation

The model simulated the hydrodynamic conditions in Suda Bay over a three-day (72 hr) period under a constant northwest wind of 5 m/s and an open boundary to the east. A

single submerged source, located along the northwest shoreline of the bay, will provide the contaminant loading for the simulation. The bay has been vertically discretized into 12 layers (1, 3, 5, 8, 13, 18, 28, 40, 60, 80, 100, 120m). Since the effluent will be discharged into the bay under hydraulically stable conditions, a 36 hour warm-up period will preceed the start of the simulation. Two different scenarios will be considered for this case study. The first will be a continuous discharge of pollutant from the source. The release of the contaminant will coincide with the start of the simulation (i.e. after the 36 hour warm-up period). The other scenario involves a variable discharge from the source. Twenty-four hours after the simulation begins, the source will discharge effluent into the bay for a two-hour period. The source will discharge a pollutant with a concentration of 10000 ppm and a flow rate of $2m^3/s$ in both scenarios. The transport of the pollutant through the bay under both constant and variable discharge conditions will be analyzed using contour/vector plots and concentration time series plots.

The purpose of a warm-up period under constant wind conditions is to allow the bay time to set-up into hydraulically stable conditions. Without it the simulation would begin with the bay completely at rest (i.e. all current velocities are zero), which is physically unrealistic. The application of a constant wind to the simulation provides the opportunity to examine the stability of the model and the results. After 36 hours, the flow is fully established (i.e. the kinetic energy is constant). Figure 8.9 shows the circulation features of Suda Bay under a 5 m/s northwestern wind for the two grids used 100m and 200m. Although both plots show similar circulation patterns, the 100m grid requires more computation time. In spite of this, the 100m grid better conforms to the shoreline.

Vector/contour plots are generated for specific times of the simulation. During the post-processing procedure, the "Transarg .exe" program will generate these vector files for any depth (i.e. layer), including the depth averaged. The depth averaged current distribution (as shown in Figure 8.9) is represented with uniform velocity vectors to show the current patterns more clearly. The use of reference vectors is not desirable due to the very low velocities that occur in the deep regions of the bay. Figure 8.10 examines the current distribution at various depths of Suda Bay. For the 100m grid, the surface layer in Figure 8.10a shows a consistent vector pattern moving from northwest to southeast based on a constant northwest wind. The currents in Figures 8.10b and 8.10c illustrate the return flow that is expected along the bay bottom. Figure 8.10c in particular shows a strong return flow near the mouth of the bay and dissipating velocities as the current moves west into the bay and into deeper water.

As stated earlier, two simulations were run; one with a constant discharge from the source and the other with a variable source condition. That is, the effluent was discharged

from the source located at the bottom layer of the bay for a period of two hours only. The discharge from both simulations was $2m^3/s$, and the concentration of the pollutant was 10000 ppm. Figure 8.11a shows the concentration time series for the source with a constant discharge. The source is submerged therefore the concentration at the bottom layer is greater than at the surface. The effluent is continuously discharged throughout the entire length of simulation therefore the concentration at the source should eventually level off and remain constant. The variable discharge simulation was run for the same time period, however, the pollutant was released for two hours only. Figure 8.11b shows the concentration time series. The pollutant was not released until 24 hours after the simulation began. The plot shows a sharp peak in concentration for that two-hour period. The levels then dissipate as the plume moves along from the source and through the bay. The initial dilution for both the continuous and variable discharge is approximately 25:1.

The model was setup to examine the plume behavior of both the constant and variable discharge simulations by 1) defining specific times when vector and contour information regarding the bay is to be saved, and 2) using reference points to analyze pollution levels over the simulation length for different locations within the bay. Figure 8.12 shows "snapshots" of plume concentration contours at the surface, based on a continuous discharge from the source, for 1, 6, and 12 hours after the initial release of the effluent. As the time advances, the plume and the distance it covers are transported in the wind direction to cover larger area. Within 12 hours the plume has spread 2 kilometers into the bay. Two reference points were chosen in order to examine the concentration levels at these locations over the length of the simulation. Figure 8.13a is a concentration time series plot at reference point one (RP1), which is located approximately 700m away from the source. The second reference point (RP2) is 1500m away from the source and is shown if Figure 8.13b. In both cases, the plume has reached the surface, therefore higher concentrations are seen along the upper layers. The concentration levels at RP2 are roughly one half that of RP1. This makes sense, since the wind is constant and the distance between RP1 and RP2 is roughly equal to the distance between RP1 and the source.

The results from the variable discharge simulation are represented in Figures 8.14 and 8.15. They follow the same format as the continuous discharge scenario. The plume concentration contours at the surface for 1, 6, and 12 hours after the initial release from the source are also shown in Figure 8.14. Since the effluent is released for two hours only, the plume moves sluggishly away from the source and dilutes over time as the pollutant mixes with the ambient fluid (i.e. water). Concentration levels are higher along the surface due to the jet discharging into a stratified body of water. The plume rises until the material comes into equilibrium with the density of the ambient at that location. Figure 8.15 shows the concentration time series for RP1 and RP2 as the plume moves through the bay. The

concentration at RP1 peaks at 24ppm, approximately 4 hours after the initial release of the pollutant and 28 hours after the start of the simulation. RP2 peaks approximately 8 hours after the initial release of the contaminant, while RP1 concentration level has been reduced, by a factor of 3, to 8ppm. The concentration levels for RP1 and RP2 are considerably less than those found under the continuous discharge scenario simply because less pollutant (only 2 hours worth) is being discharged into the bay. For this reason, the pollutant will dilute at a faster rate.

## 8.4 More Test Cases

Greece is located between latitudes 34° and 42° North and longitudes 20° and 27° East. It has an area of 131,944 $km^2$ and contains a population of about 10 million. The length of the Greek coastline is estimated at 15,000 $km^2$. The highest peak in Greece is at an altitude 2,917 meters, which is the summit of Mount Olympus (the Pantheon). The deepest point in Greece (and the Mediterranean) is off the south tip of the Peloponnese and is called the Oinousai (Inousses) Pit. This point is 4,850 meters deep. Selected coastal areas in Greece, as shown in Figure 8.16, were chosen as test cases to illustrate the functionality of coupling the 3D model with the GIS module. In addition to the availability of the data, the coastal areas were selected to reflect: a) different boundary conditions, b) various sizes (areas), and c) different locations around the country. The data was obtained from hydrographic files which, mostly, included information on spot depths, bathymetric contours, shorelines, islands, and rivers. Figure 8.17 shows an example of a hydrographic file for the Thessaloniki bay (map section B), which was processed through the GIS module to a proper format for generating the bathymetric file. Five areas around the island of Crete were also selected. Area E, the coast of the whole island and four coastal areas on the north shore of Crete. These cases were run for the island employing different modeling scenarios that include one, two, three, and four open boundaries. Information from the DEM of the island can provide information, as shown in Figure 8.18, of point sources discharging in the near shore of the island. For complicated shorelines, small cell sizes are generally preferred in order for the grid to conform to the shore. Figure 8.19a shows a 1000m-grid for the Amvrakikos bay (map section A), while Figure 8.19b shows a 50m-grid for the same area. Notice the difference in the northwestern part of the bay, which is enlarged on both figures in the insets.

## 8.5 Results and Discussion

A number of simulations were performed on the various bays in Greece. Figure 8.20 shows the current distribution at the surface and at a depth of 20m based on a 5m/s NW wind in Thessaloniki bay (map section B) located in north Greece. The wind-induced currents produce a consistent flow pattern at the surface and generate a return flow at a depth of 20m. Figure 8.21 examines the surface layer current patterns for Kalloni bay (map section C) under

a constant 5m/s wind applied from the SW and the NW. Eddy currents form at the surface under both wind conditions as a result of the geometry of the bay, which is long and narrow. Figure 8.22 illustrates the bathymetry and surface layer flow distribution under a constant 5m/s NW wind for the Saronikos bay near Athens (map section D). The uniform depth averaged current patterns are represented in Figure 8.23 along with referenced depth averaged flow for the NE corner of the bay. A number of eddy currents are prevalent within the extent of the domain due to the presence of islands, small inlets and the bathymetry of the bay.

As previously mentioned and due to the availability of additional bathymetric data for the island of Crete, five runs, employing different boundary and pollutant source conditions, were performed for the island in the areas shown in Figure 8.24. The distribution of the surface layer currents around the Island of Crete (map section E) under a NW wind is illustrated in Figure 8.25. A section along the north shore of the island (north of the Iraklion prefecture) was also considered in order to simulate the surface flow based on a NW and NE wind. Figure 8.26 describes the bathymetry and current patterns at the surface and at a depth of 200m for Agios Nikolaos bay based on a NW wind. As expected the currents at the surface are driven by the wind and a return flow is prevalent at a depth of 200m following the bottom topography of the bay.

The two bays located along the north shore of Chania region were used to examine the hydrodynamics and pollutant transport of a hypothetical contaminant discharged under various conditions. Kasteli bay (map section E4) was used to simulate the fate of a pollutant discharged over a four-hour period. Chania bay (map section E3) was used to examine the transport of a pollutant discharged continuously from a source for the entire simulation from two different locations. The first scenario to consider involves Kasteli bay. As shown in Figure 8.27, a watershed is discharging through two streams into the bay, which could be regarded as a source of pollution that can cause environmental problems in the near shore areas. Three reference points (i.e. RP1, RP2 and RP3) are positioned downstream (i.e. east) of the source (river outlet) in order to determine the concentration levels at these points over the entire length of the simulation. RP1 and RP2 are located (side-by-side) at a distance of 200m from the source, which is defined as a surface discharge. RP3 is situated 1.5 km downstream of the source and 200m offshore. RP1 is positioned on the shore and RP2 is 200m offshore north of RP1. The purpose of this arrangement is to compare the concentration levels along the shore with levels just off shore. A NW wind is applied to the bay under isothermal conditions for a period of 72 hours. A contaminant with a concentration of 10000ppm is released 24 hours after the simulation begins at a rate equal to $1 m^3/s$ over a four-hour period.

Figure 8.28 shows the movement of the plume 6, 10 and 20 hours after the initial

release of the pollutant. The plume is restricted in moving along the shoreline due to the currents generated by the NW wind. The contaminant is transported downstream as a plug flow and it takes approximately twenty hours (from the initial release of the pollutant) for the slug to pass over RP3, which is 1.5 km away from the source. A comparison of the depth-averaged time series concentration levels at the three reference points and the source is shown in Figure 8.29a. Based on the results, the pollutant exhibits a higher concentration at RP1 (i.e. along the shore) than at RP2, which is expected due to the location of the source and the alongshore currents. Figure 8.29b shows the concentration time series at the source for various layers. The water depth at this point is approximately 5m. Under isothermal conditions the depth-averaged concentration is approximately 400 ppm; this suggests an initial dilution of 25:1.

The second scenario involves another bay in the region of Chania referred to as Chania bay (map section E3). Two cases will be used to examine the behavior of a contaminant discharged continuously into the bay from a submerged source at two different locations.

Case 1: corresponds to a source positioned 2Km offshore and approximately 900m NW of a small island. The depth of the source is 27m (see Figure 8.30).

Case 2: simulates the pollutant transport discharged from a source 10m deep, situated 250m offshore and 800m SW of the island (see Figure 8.32). The purpose behind the two different orientations of the source is to analyze the movement of the contaminant with respect to the island. A NW wind of 5m/s was applied to both cases in order to produce similar hydrodynamic conditions in the bay. The source released a pollutant with a concentration of 1000ppm at a rate of $1m^3/s$. For both cases three reference locations are used (i.e. RP1, RP2 and RP3). RP1 is located between the mainland and the east side of the island. RP2 and RP3 are defined further east, approximately 4 km and 7 km respectively from the source and 700m offshore.

Figure 8.30 describes the source and reference point locations as well as the movement of the pollutant 12 and 48 hours after the start of the simulation for Case 1. Due to the current patterns generated by the NW wind and the position of the source, the pollutant moves eastward around the north side of the island and then travels back towards the shore. Figure 8.31 shows the concentration time series at the source for Case 1 at different layers under isothermal conditions. The concentration is considerably higher at the bottom layer compared to the surface layer because temperature is not considered under isothermal conditions therefore more mixing occurs. A comparison of the depth-averaged concentration time series for the three reference points is shown in Figure 8.31b. As expected the

concentration at RP1 is lower than RP2 and RP3 due to its location. Based on the position of RP1 only the outer edge of the plume flows over this point, therefore levels will be much lower. Under isothermal conditions the concentration at RP2 and RP3 reach the same constant level (equal to 1.5ppm) since RP3 although is further away from the source as compared with RP2 but is in lower depth of 12 m versus 18 m. The plume movement for Case 2 is described in Figure 8.32 and suggests that a large amount of the contaminant will travel between the island and the mainland. In both cases the pollutant accumulates in the SE corner of the bay based on this particular NW wind pattern.

Figure 8.33 shows the concentration time series for the new source location (which is located at a depth of 10m) under both isothermal and stratified conditions for Case 2. The initial dilution is approximately 22:1 and 13:1, respectively. The dilution is less under stratified conditions due to the buoyant forces of the pollutant generated by temperature and density differences, which reduces the amount of mixing due to the contaminant moving quickly to the surface.

The behavior of the contaminant downstream of the source is analyzed by investigating the time series concentrations for the three reference points. Figure 8.34 shows the concentration levels for RP1, RP2 and RP3 over the entire length of the simulation under isothermal and stratified conditions for Case 2. Unlike Case 1 where the concentration at RP1 was quite low (see Figure 8.31b), due to the new source location RP1 records much higher concentration levels than RP2 and RP3. This makes sense since most of the pollutant now moves between the small island and the Island of Crete and directly over RP1.

## 8.6 Conclusion

A case of an interaction between science, engineering and information technology is presented in this chapter. The increasing urbanization of coastal watersheds accompanied by the increasing levels of pollutants introduced to the waterways require a higher level of awareness among decision makers to ensure clean and safe water for drinking and recreation purposes (engineering component). This GIS pre-processor (information technology) should promote the successful and accurate application of sophisticated hydrodynamic/pollutant transport simulation (science component) through a simple and straightforward graphic user interface. The use of this decision support system was illustrated through multi-case scenarios involving a number of coastal areas in Greece. The different scenarios involved different: (a) grid sizes and bay sizes, (b) wind cases (magnitude and direction), (c) pollutant releases, and (d) open boundary conditions.

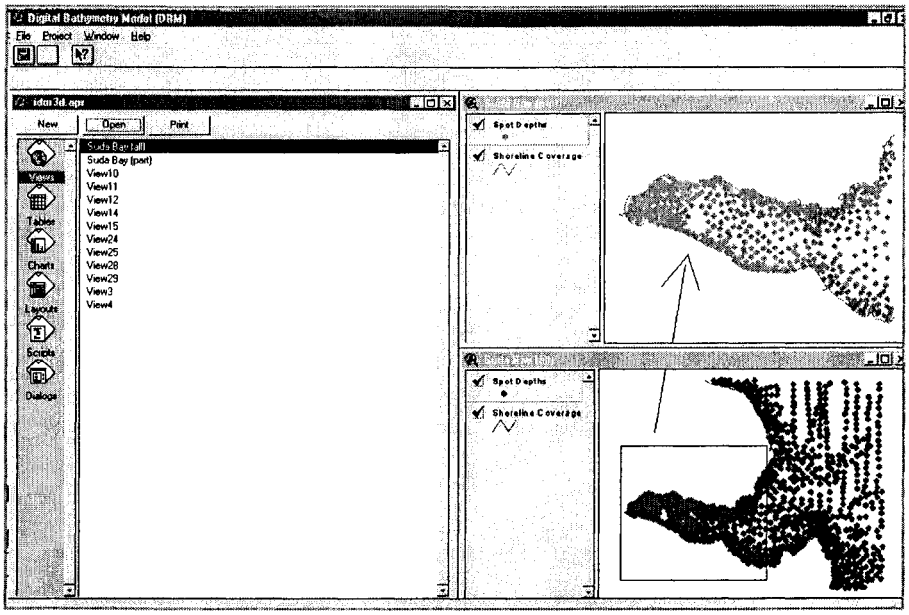


**Figure 8.1a:** Components of an ArcView GIS project.

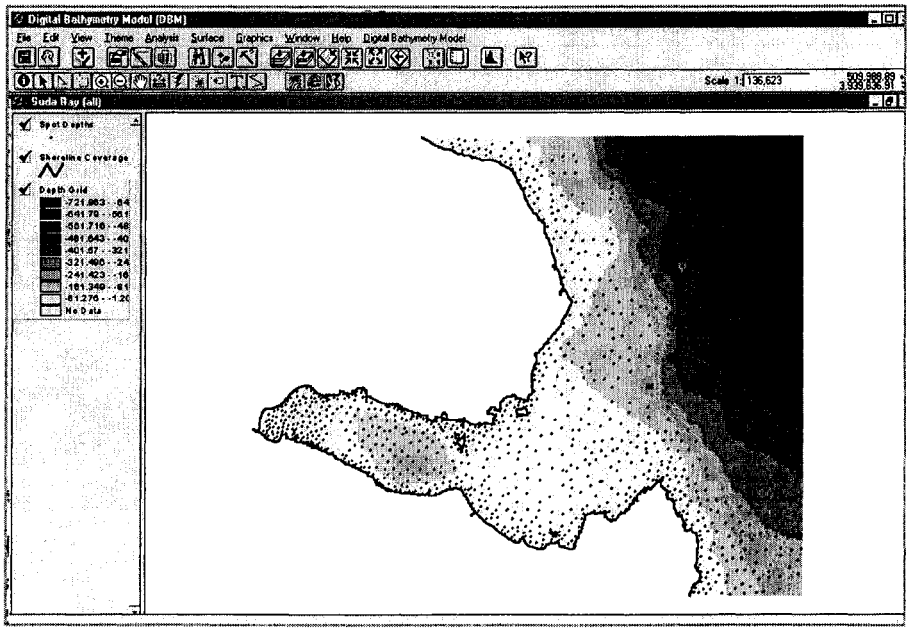


**Figure 8.1b:** The full extent of Suda bay.

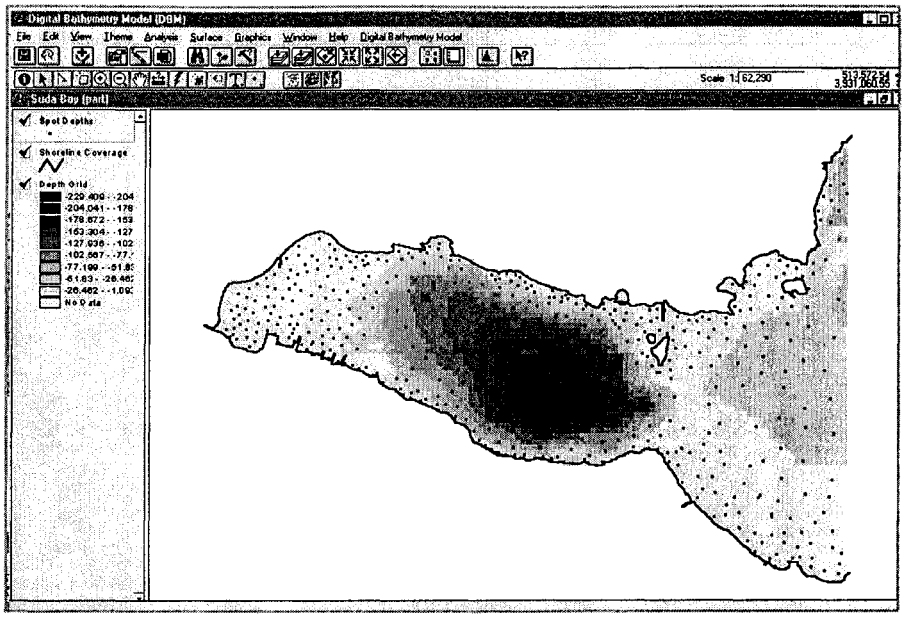


**Figure 8.1c:** Part of Suda bay.

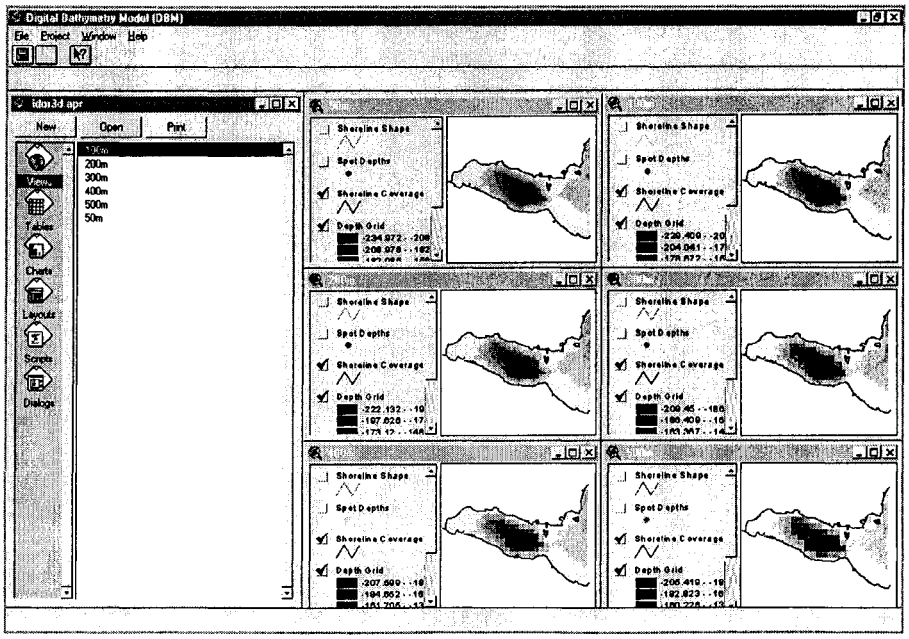


**Figure 8.1d:** Bathymetric grids with different cell sizes for the partial extent of Suda bay.

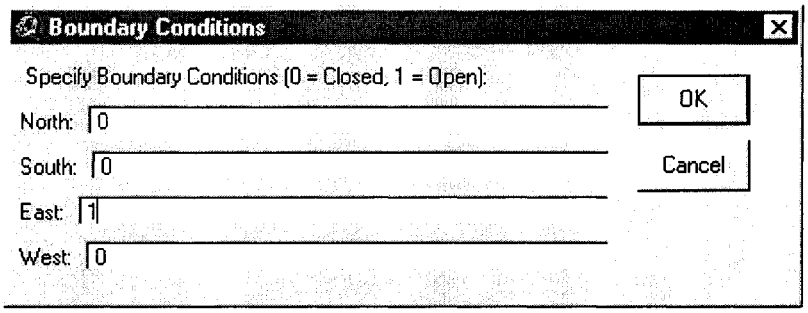


**Figure 8.2:** Boundary conditions pop-up menu for Suda bay.

(a

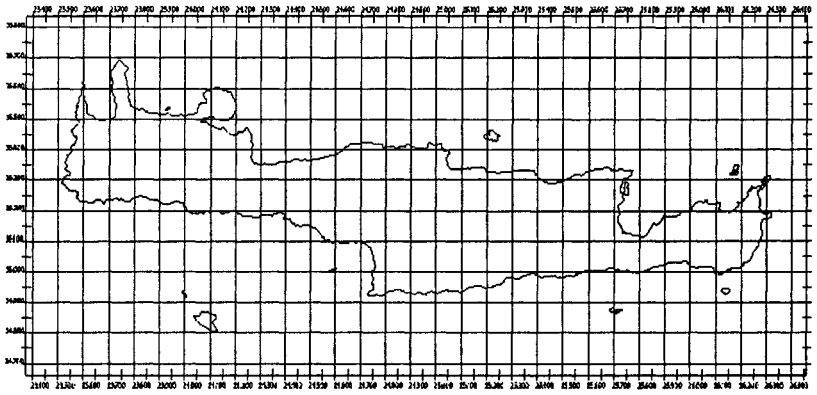

(b

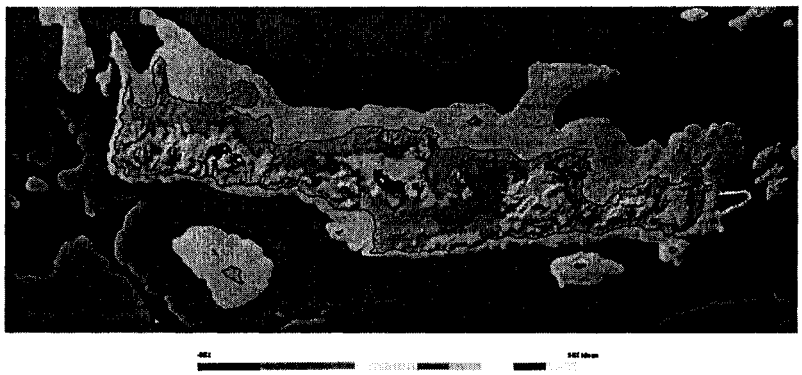

**Figure 8.3:** (a) The geographic location of the island of Crete between latitudes 34° and 36° North and longitudes 23° and 27° East. (b) Digital Elevation Model (DEM) and the Digital Bathymetry Model (DBM) of Crete.

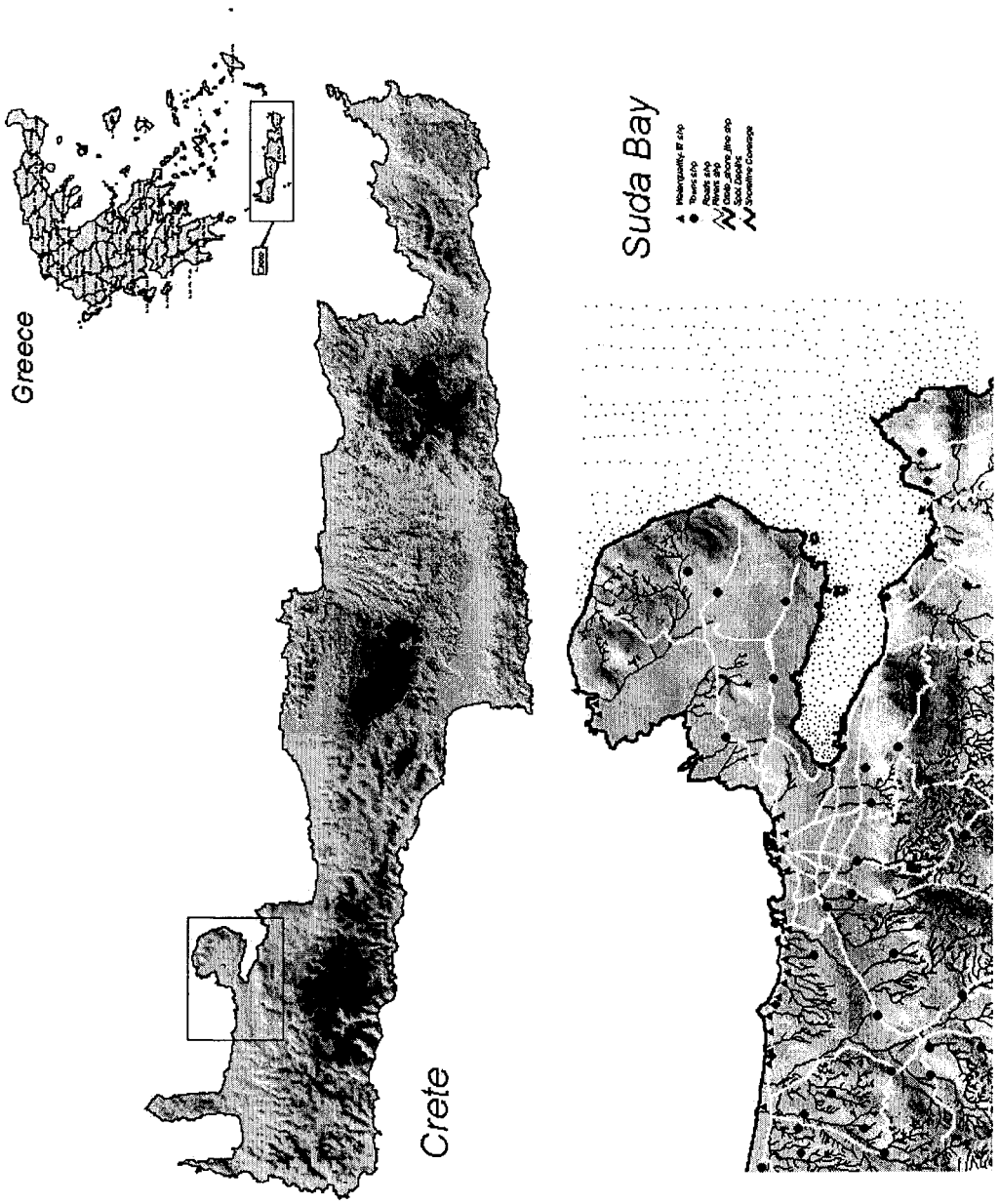


**Figure 8.4:** Location of the island of Crete with respect to the country of Greece and the location of Suda bay with respect to the island.

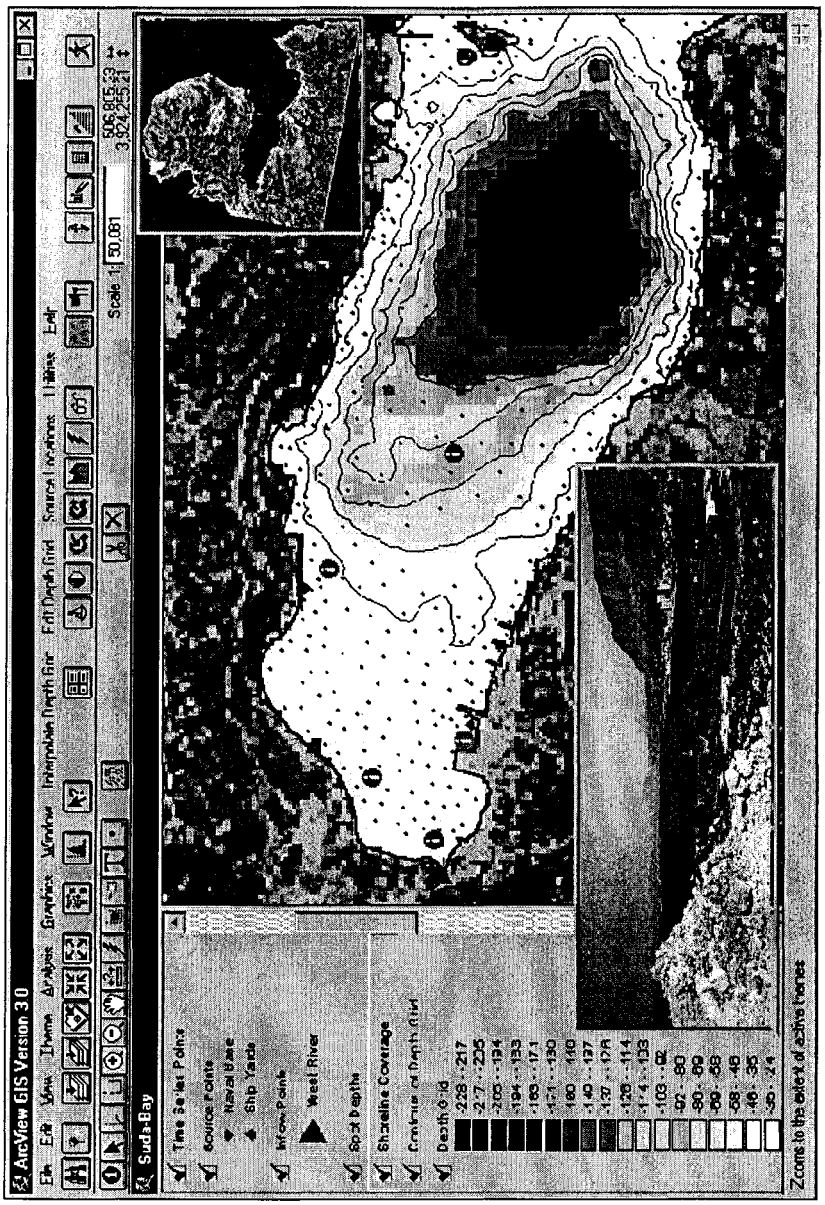


**Figure 8.5:** A superimposed bathymetric grid over a satellite image for the partial extent of Suda bay.

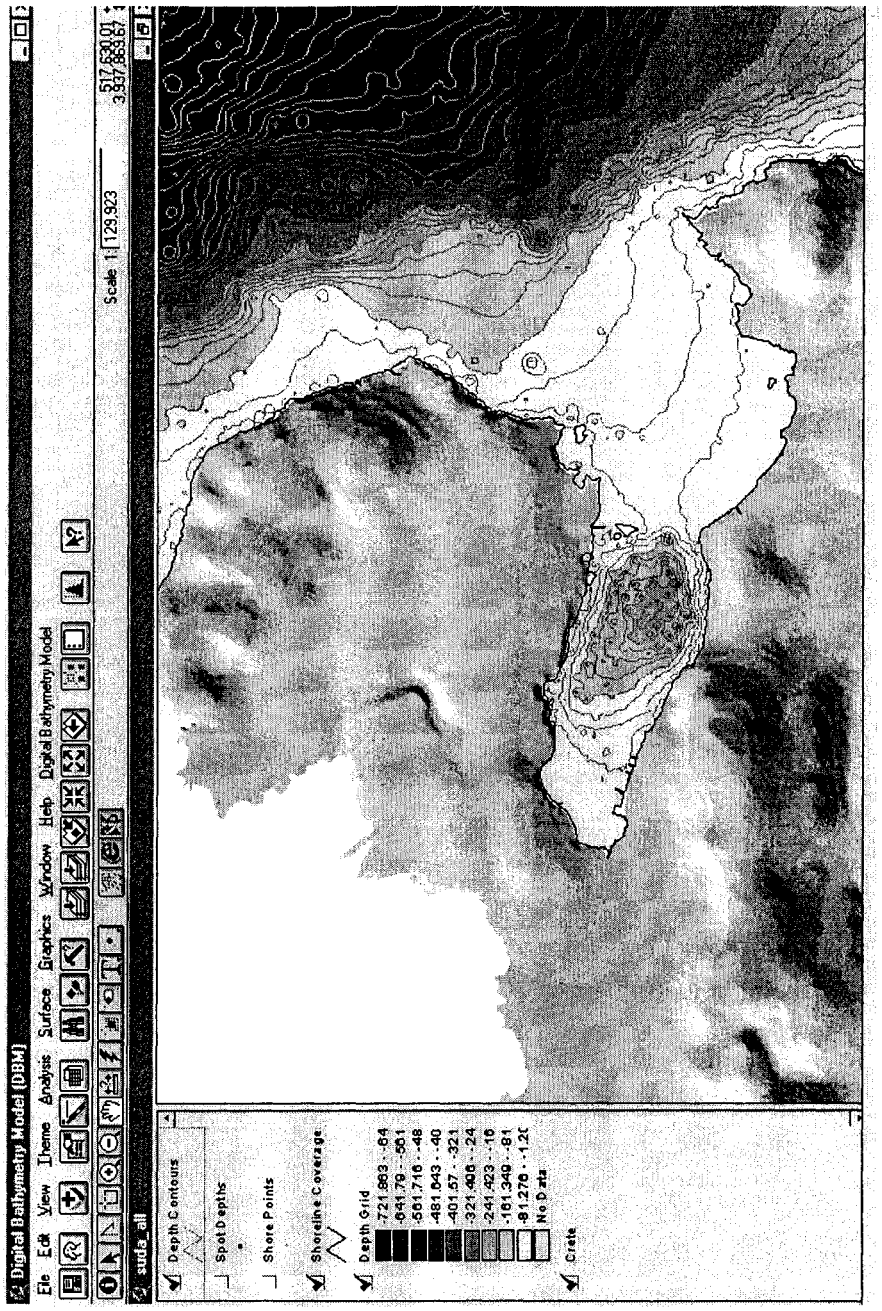


**Figure 8.6:** A visual presentation of bathymetry (grid and contours) together with the digital elevation model of the island.

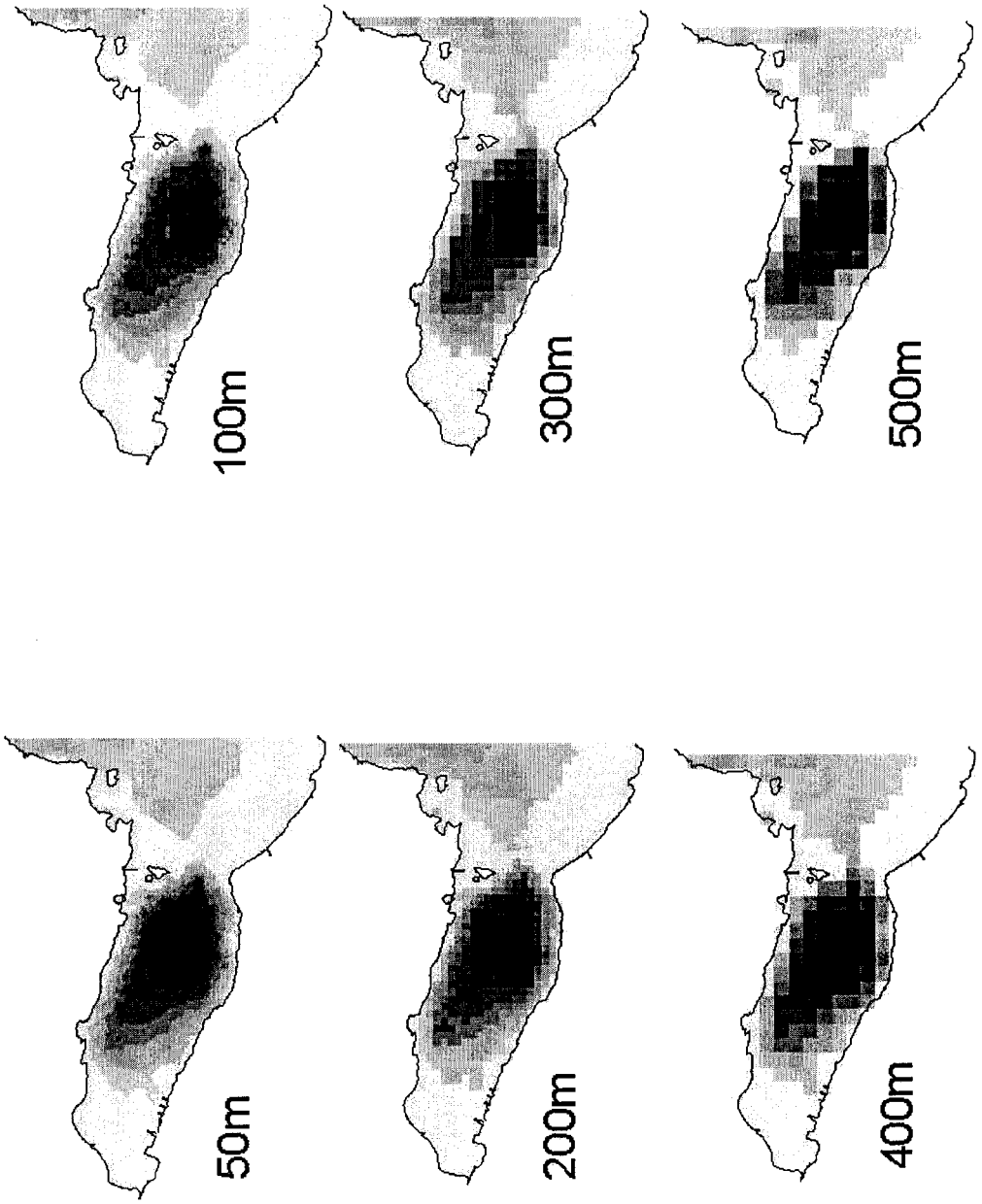


**Figure 8.7:** Bathymetric grids generated for the partial extent of Suda bay using different cell sizes.

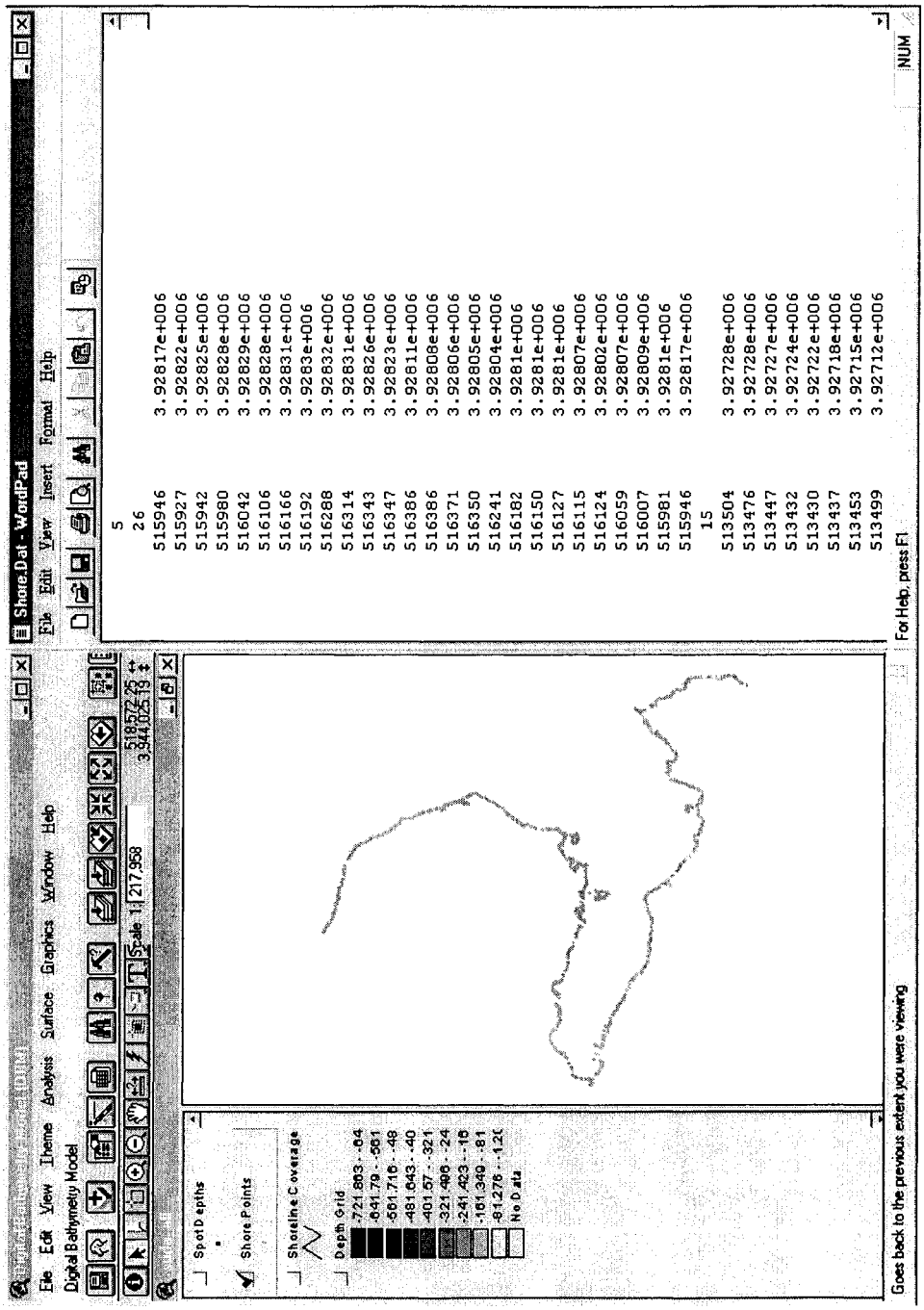


**Figure 8.8:** The shoreline of the bay shown as an ArcView GIS shapefile as well as an ASCII file.

a)

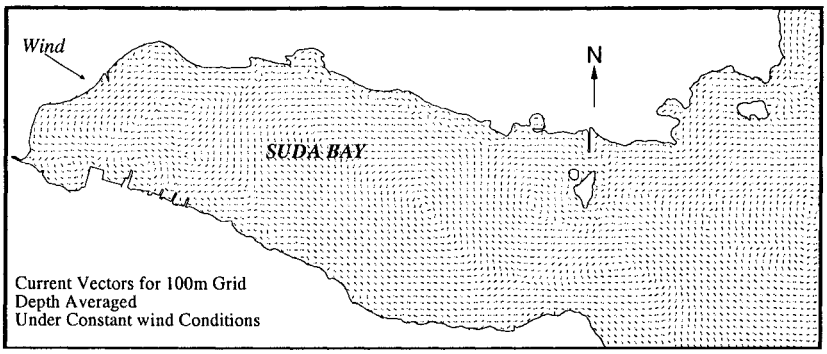


b)

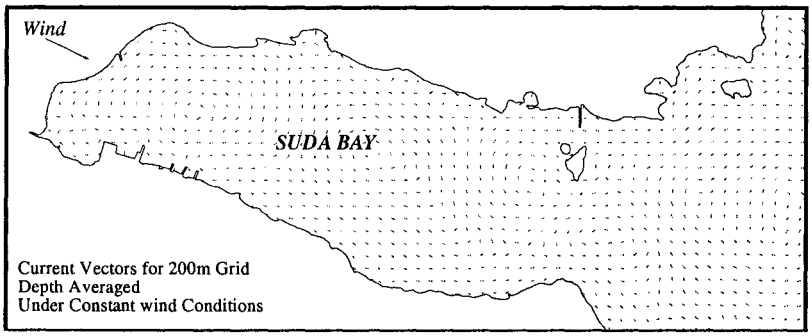


**Figure 8.9:** Shows a) depth averaged vector distribution under constant wind conditions for the 100m grid and b) the 200m grid. All vectors are represented by a uniform length.

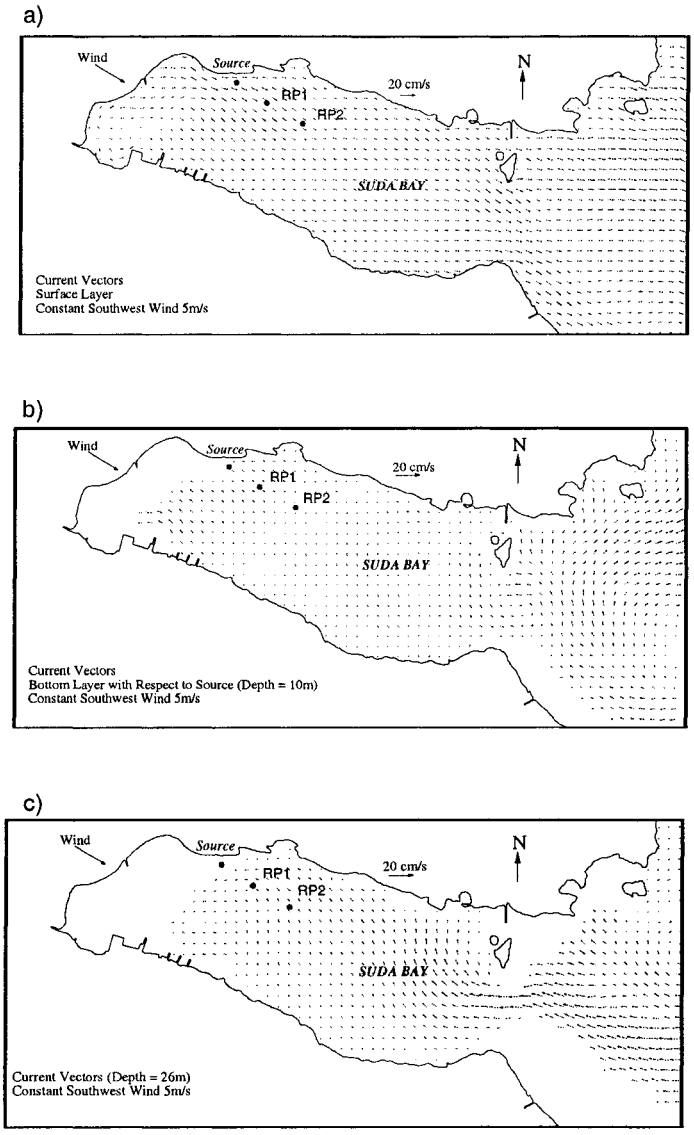


**Figure 8.10:** Shows the current disribution in the bay for the 100m grid at various depths based on constant wind conditions. a) Surface layer vectors, b) at a depth = 10m, and c) at a depth = 26m.

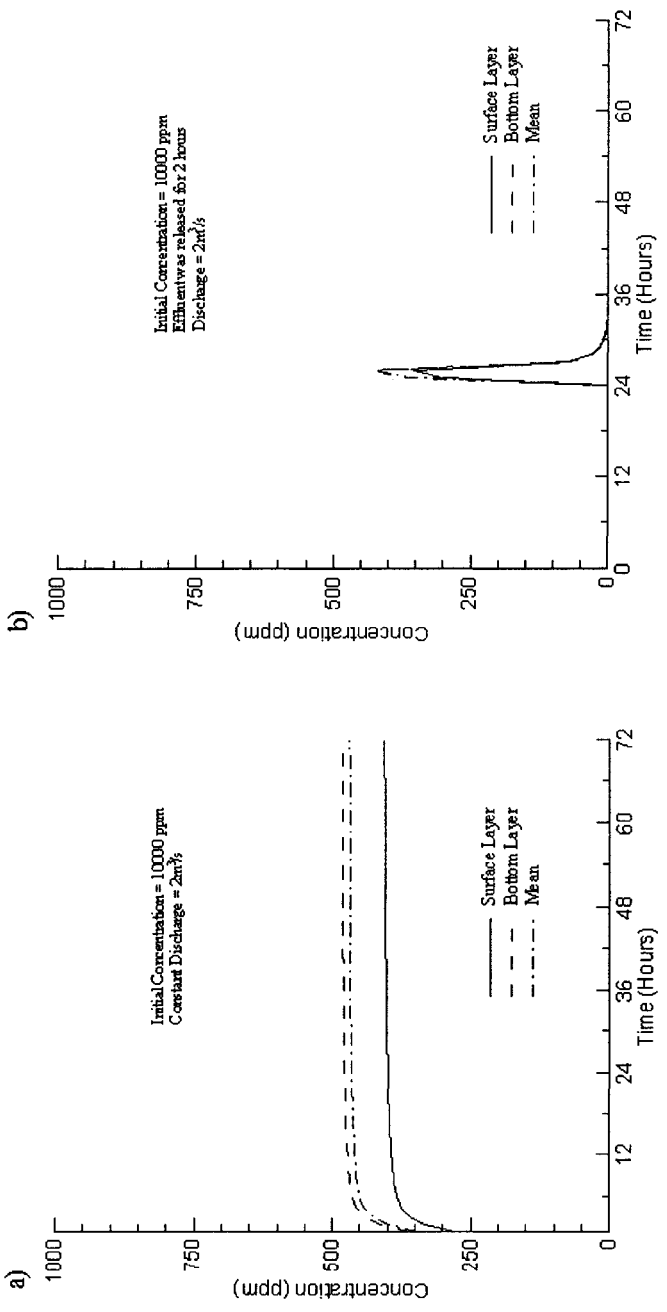


**Figure 8.11:** Concentration time series at the source. a) constant discharge of effluent from source, b) variable pulse discharge of effluent from the source.

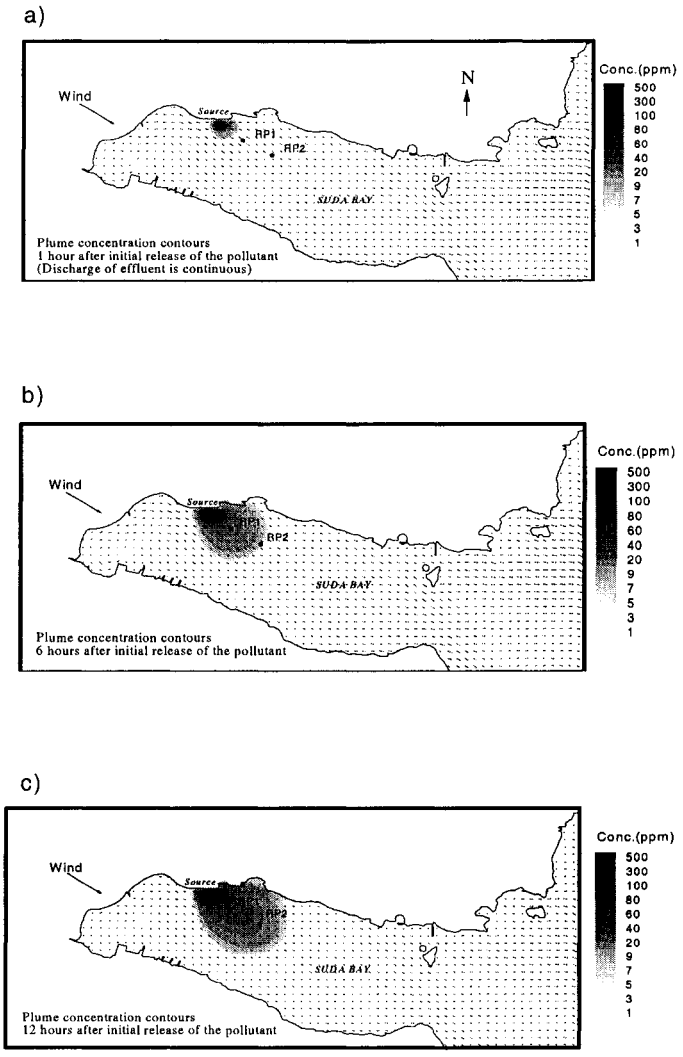


**Figure 8.12:** Plume concentration contours at various times based on a continuous discharge of effluent from the source. a) 1 hour after the initial release of the pollutant, b) 6 hours after the initial release of the pollutant, c) 12 hours after the initial release of the pollutant.

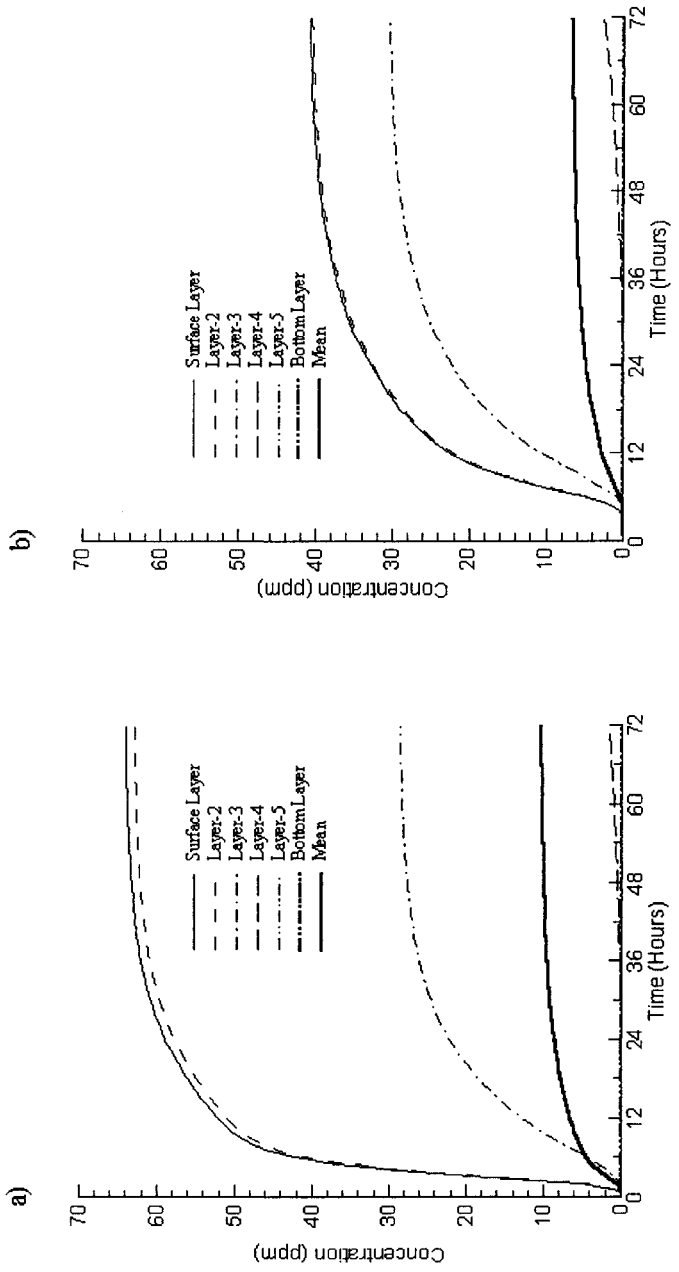


**Figure 8.13:** Concentration time series for, a) reference point 1, and b) reference point 2 as effluent from source is discharged continuously.

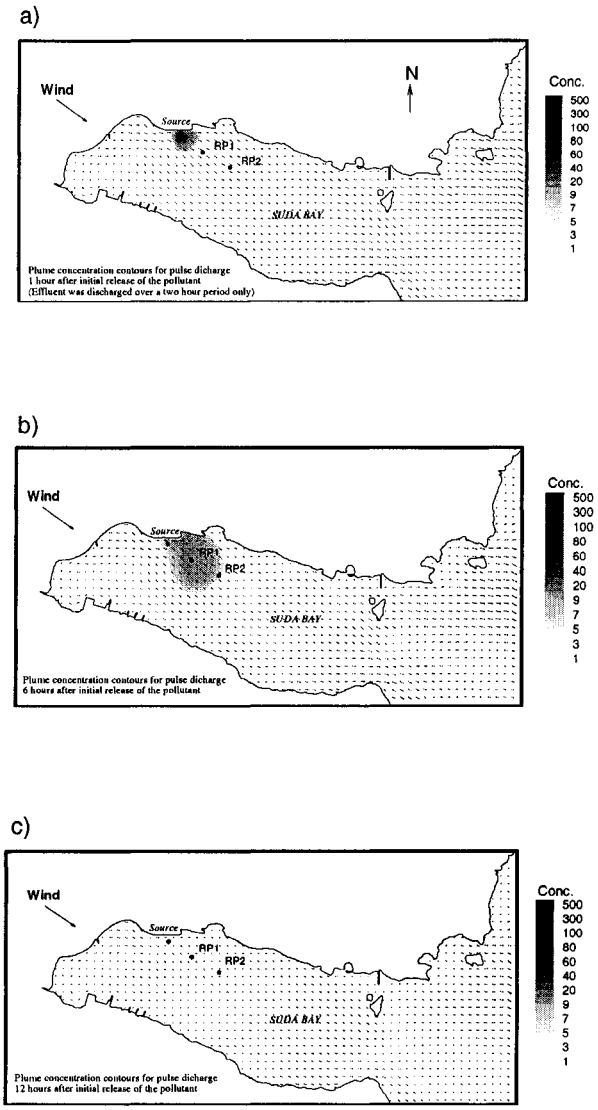


**Figure 8.14:** Plume concentration contours at various times based on a 2 hour pulse discharge from the source. a) 1 hour after initial release of the pollutant, b) 6 hours after initial release of the pollutant, and c) 12 hours after initial release of the pollutant.

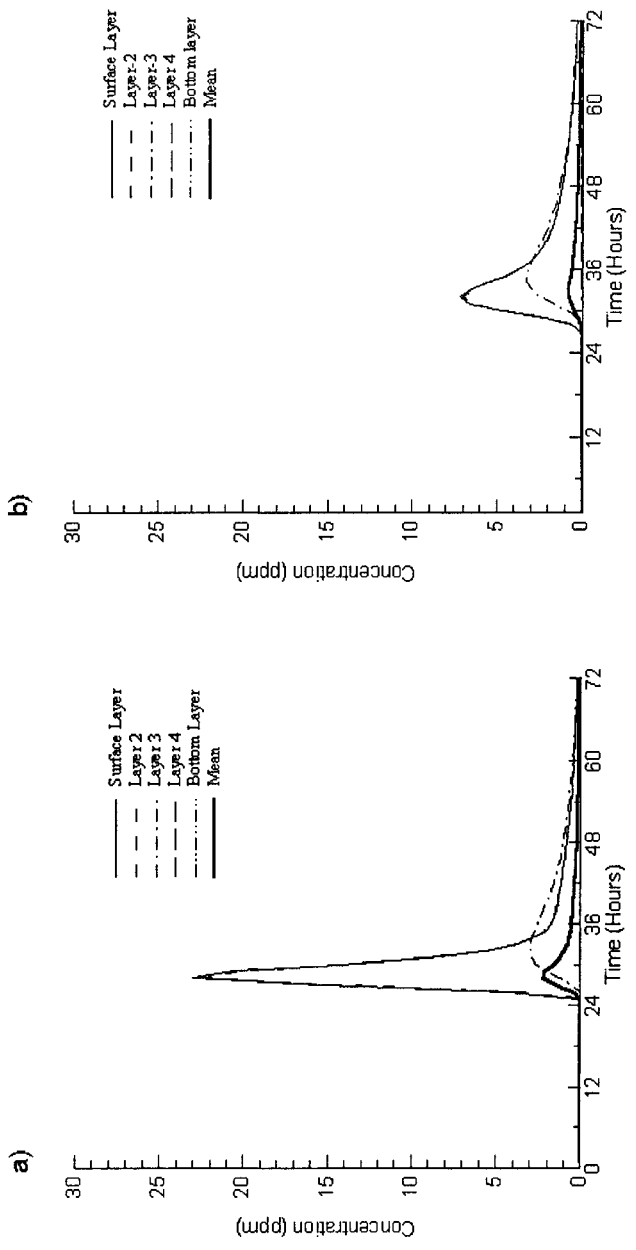


**Figure 8.15:** Concentration time series for, a) reference point 1, and b) reference point 2 as effluent from the source is discharged over a 2 hour period only (pulse).

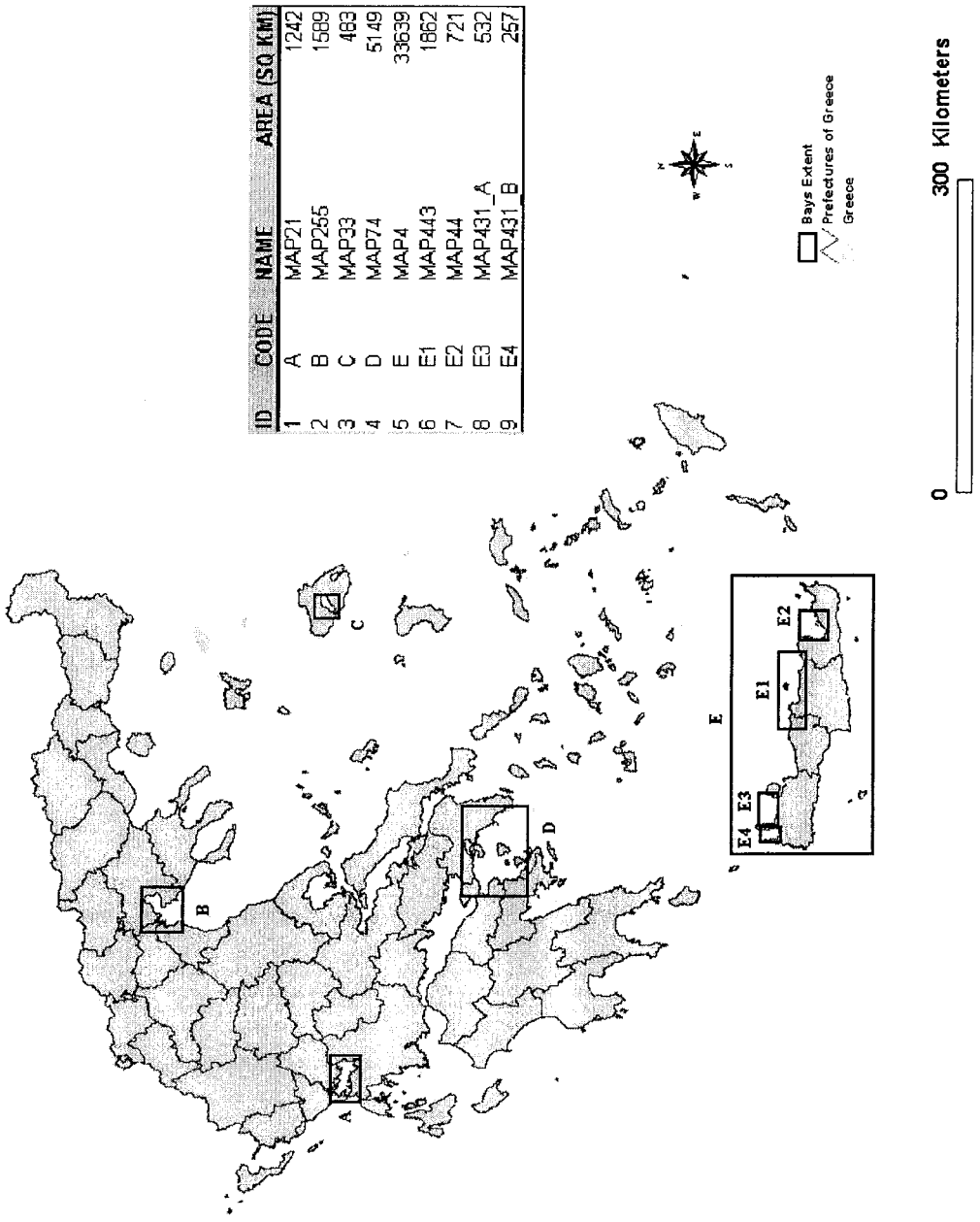


**Figure 8.16:** Selected bays in Greece.

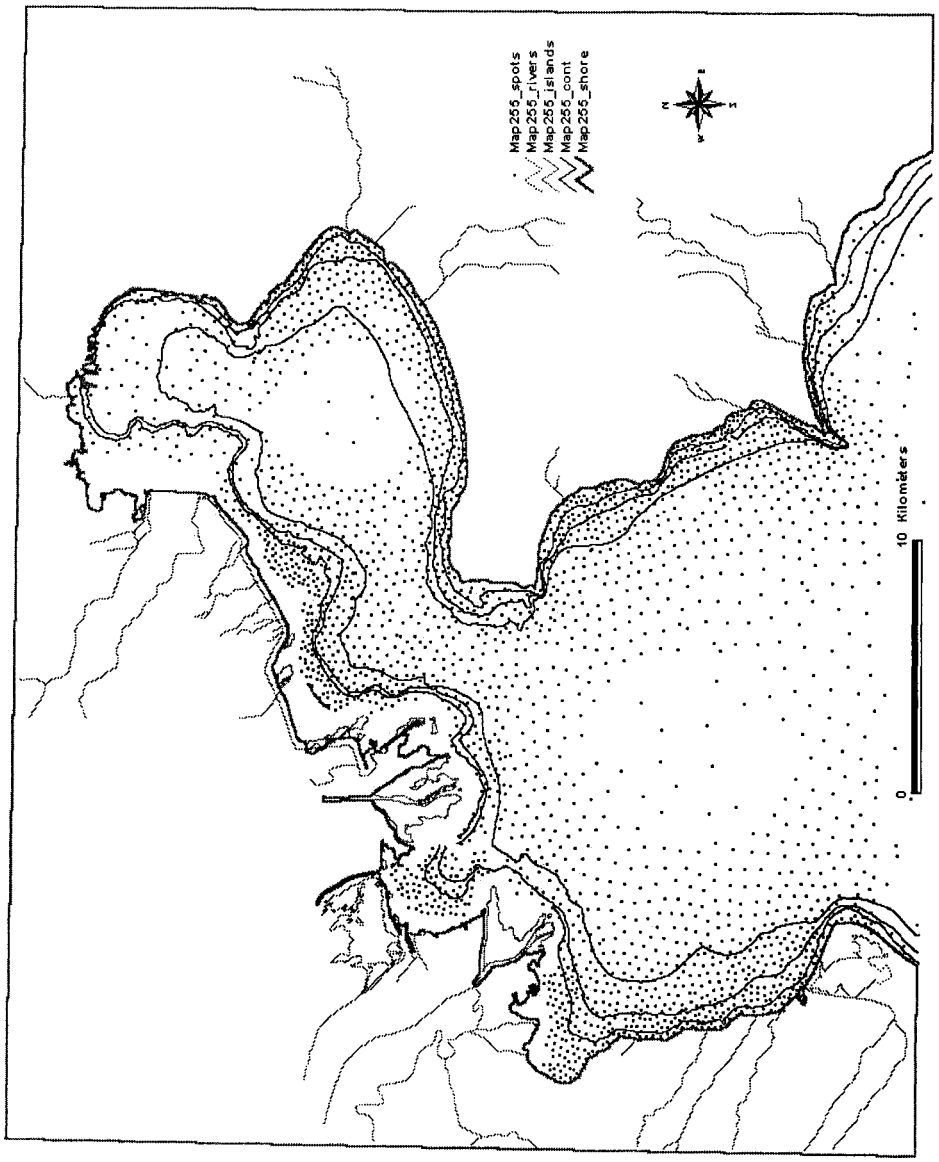


**Figure 8.17:** A hydrographic file for the Thessaloniki bay.

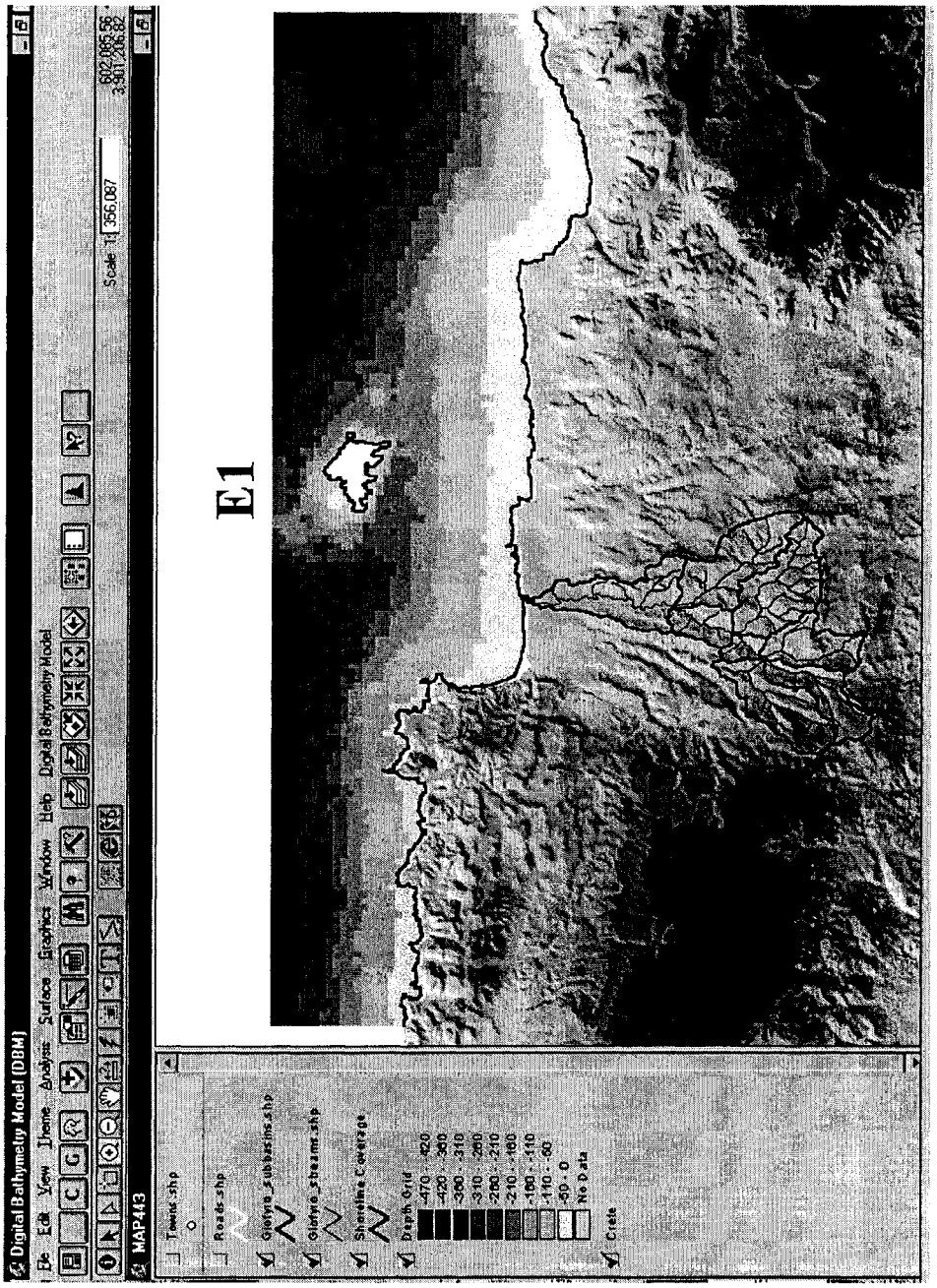


**Figure 8.18:** A digital bathymetry model (DBM) together with a digital elevation model (DEM) for the north shore of the Iraklion prefecture.

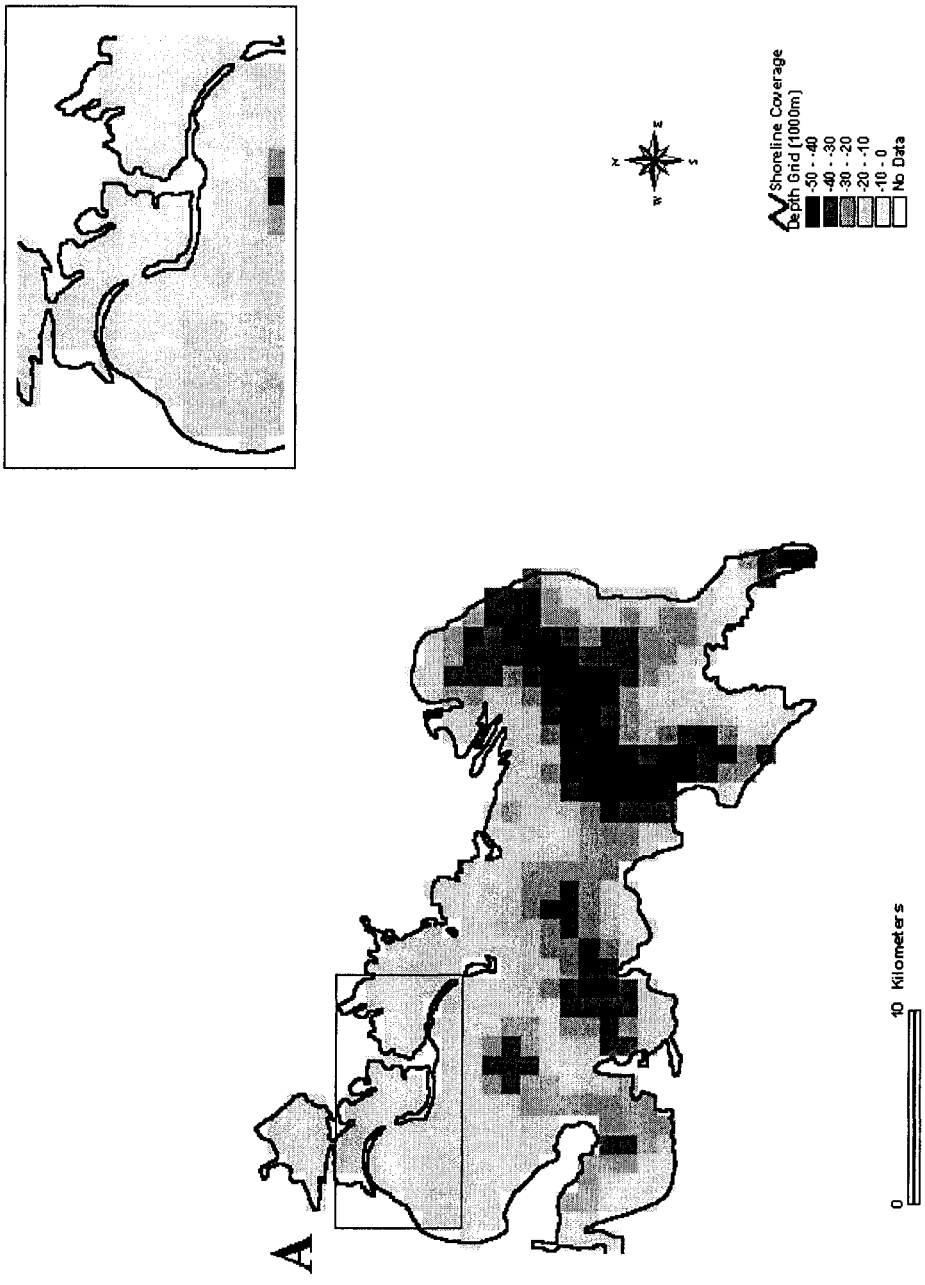


**Figure 8.19a:** A 1000m-grid for the Amvrakikos bay.

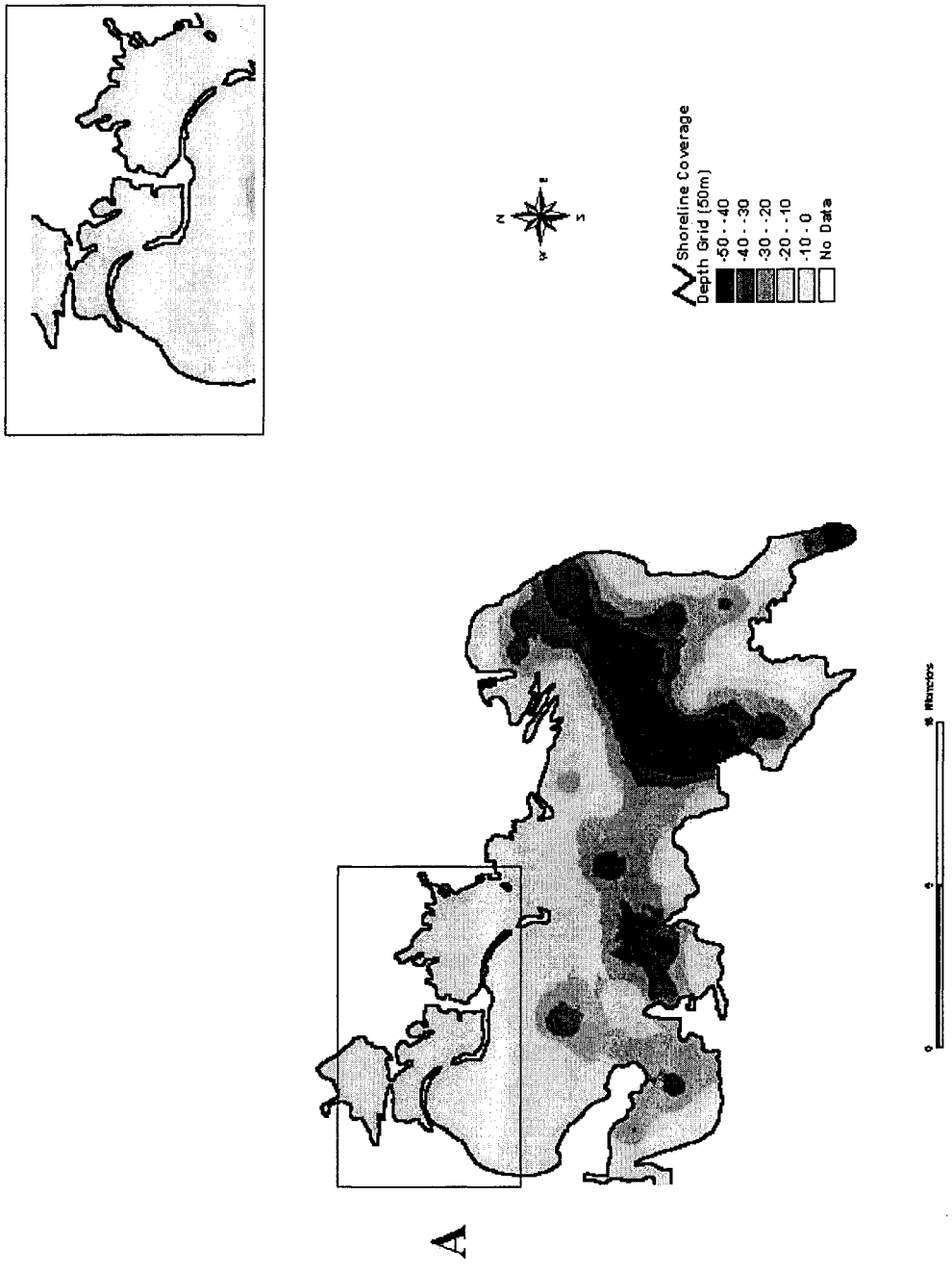


**Figure 8.19b:** A 50m-grid for the Amvrakikos bay.

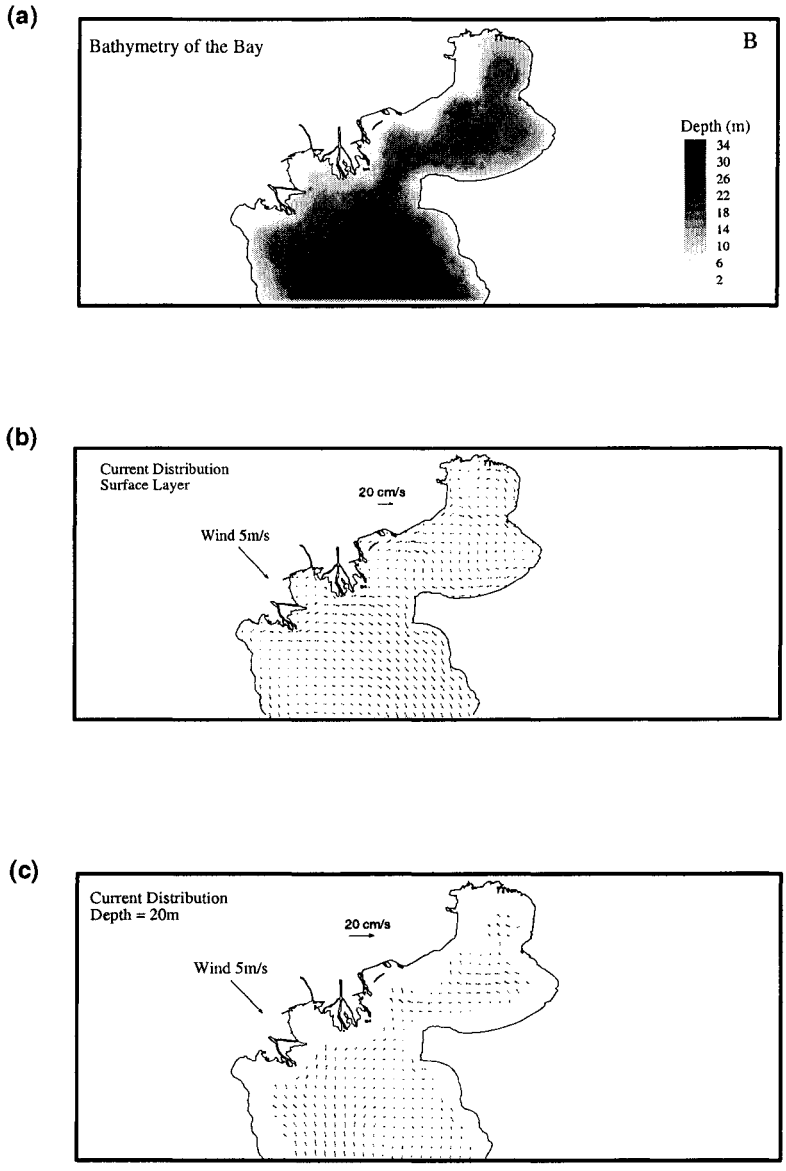


**Figure 8.20:** Shows the bathymetry of Thessaloniki bay (Section B) and the current distribution at the surface and at a depth = 20m based on a NW wind = 5m/s.

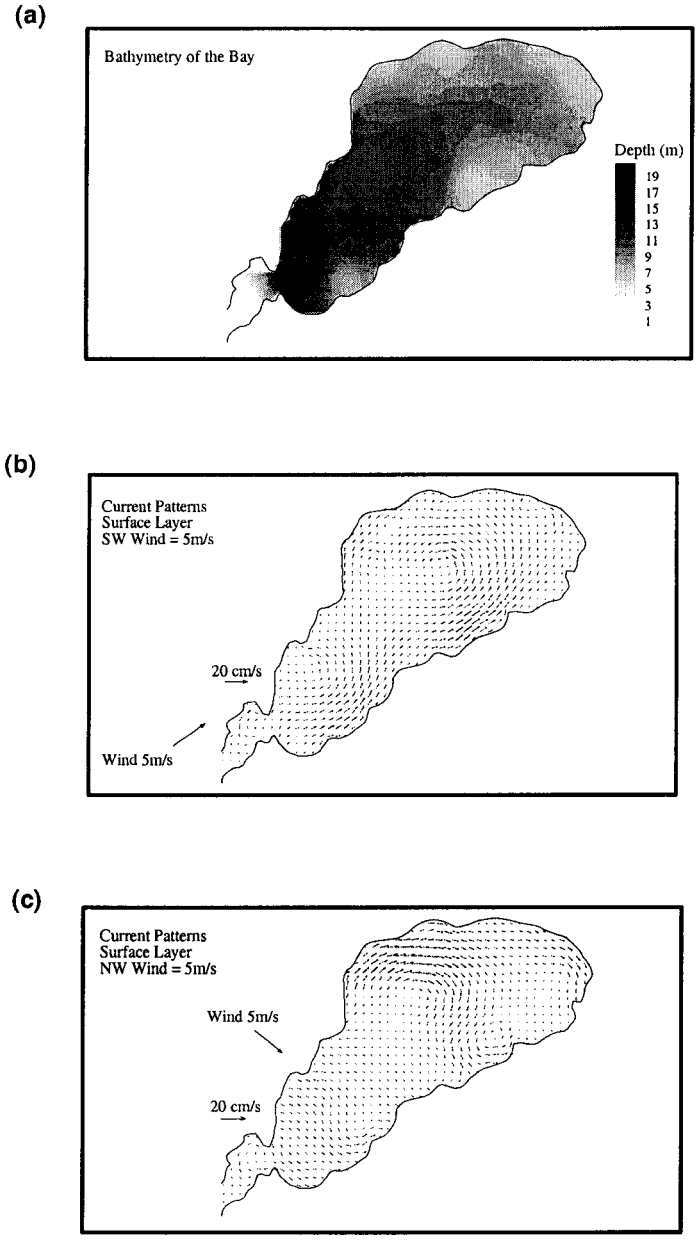


**Figure 8.21:** Shows the bathymetry of Kalloni bay (Section C) and the current distribution based on a 5m/s SW and NW wind direction.

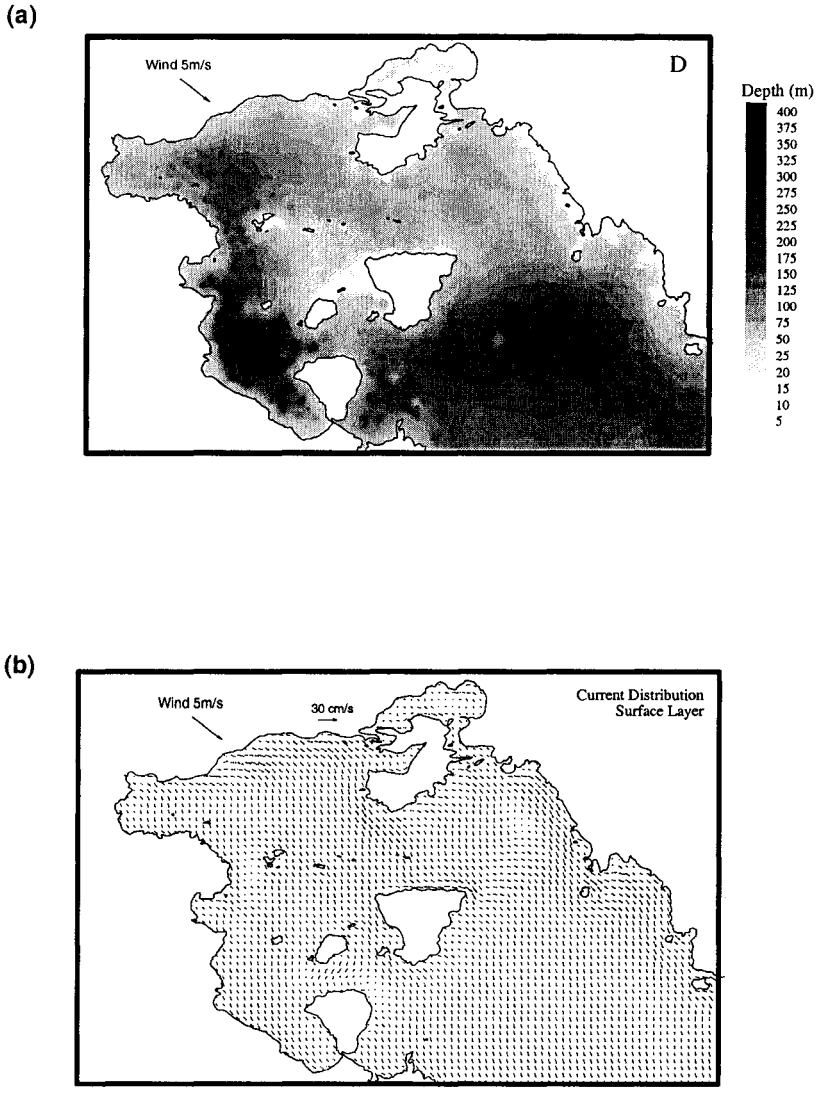


**Figure 8.22:** Shows: a) the bathymetry of Saronikos bay (Section D) and b) the surface layer current patterns for a 5m/s NW wind.

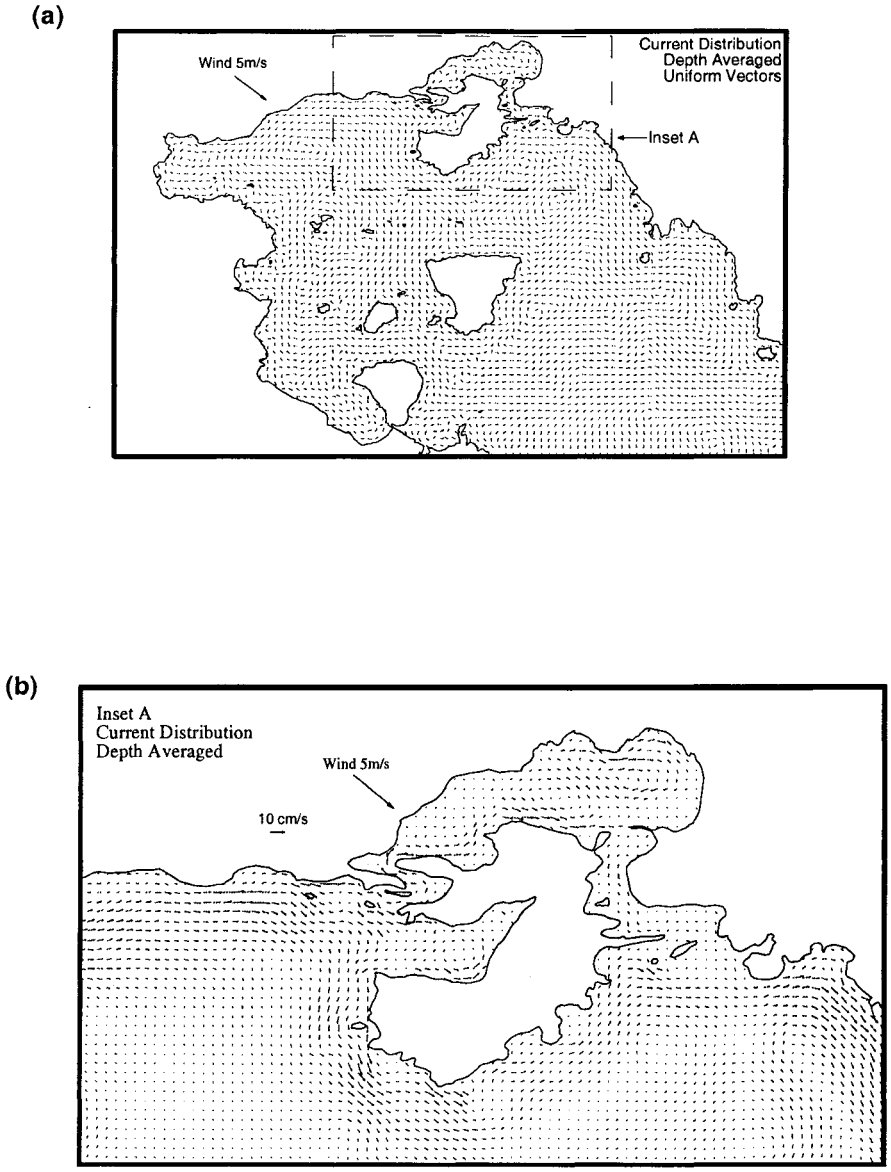


**Figure 8.23:** Describes: (a) the depth averaged current patterns for Saronikos bay (Section D) using uniform vectors for the entire bay; and (b) actual magnitude vectors for the NE corner of the bay.

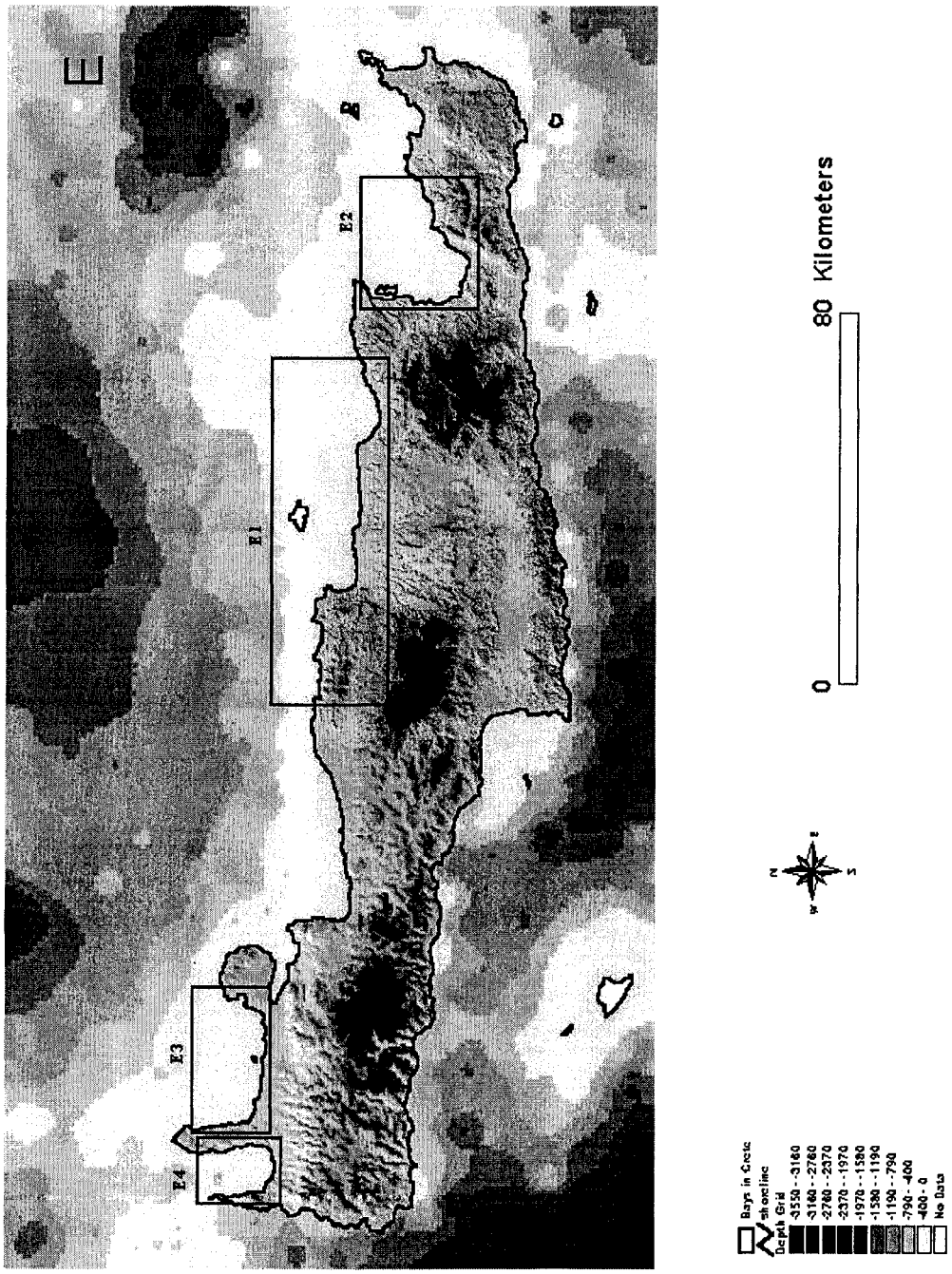


**Figure 8.24:** The DBM and DEM of the island of Crete and its selected bays.

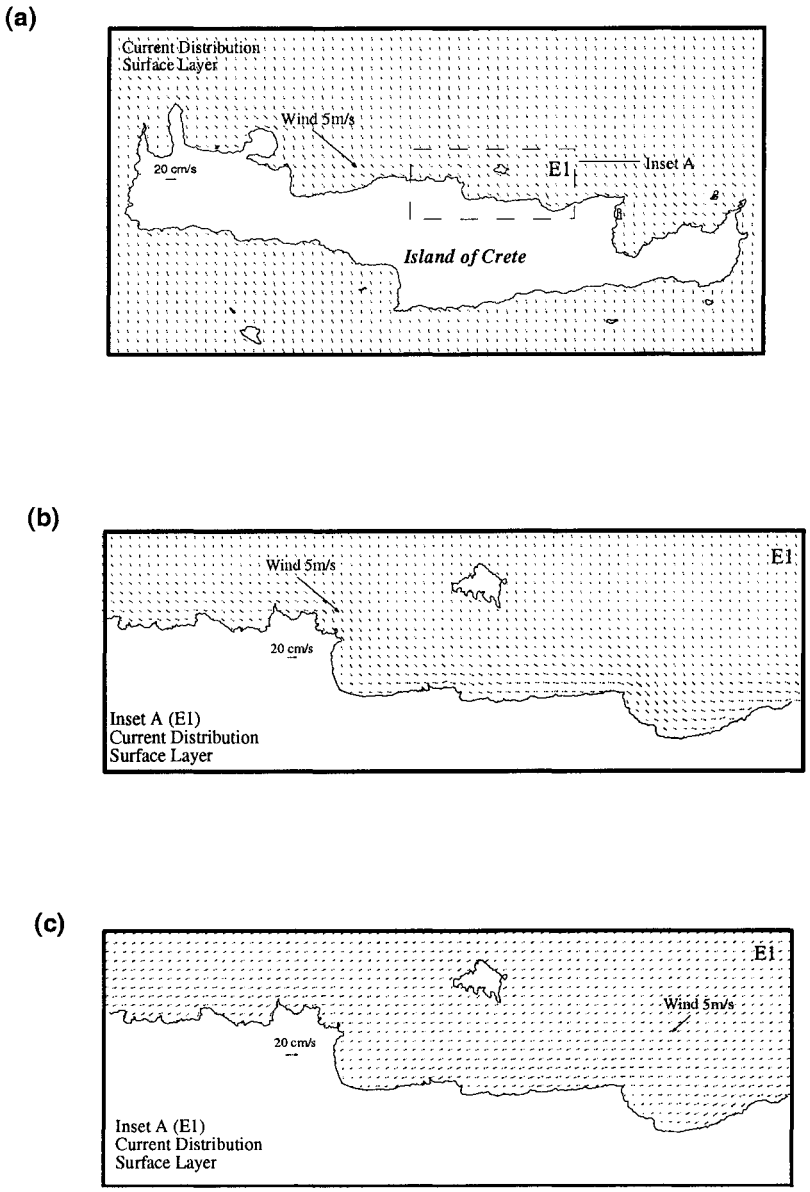


**Figure 8.25:** The surface layer current patterns around the Island of Crete (Section E) and a section (E1) of the northshore of Crete for a 5m/s NW wind.

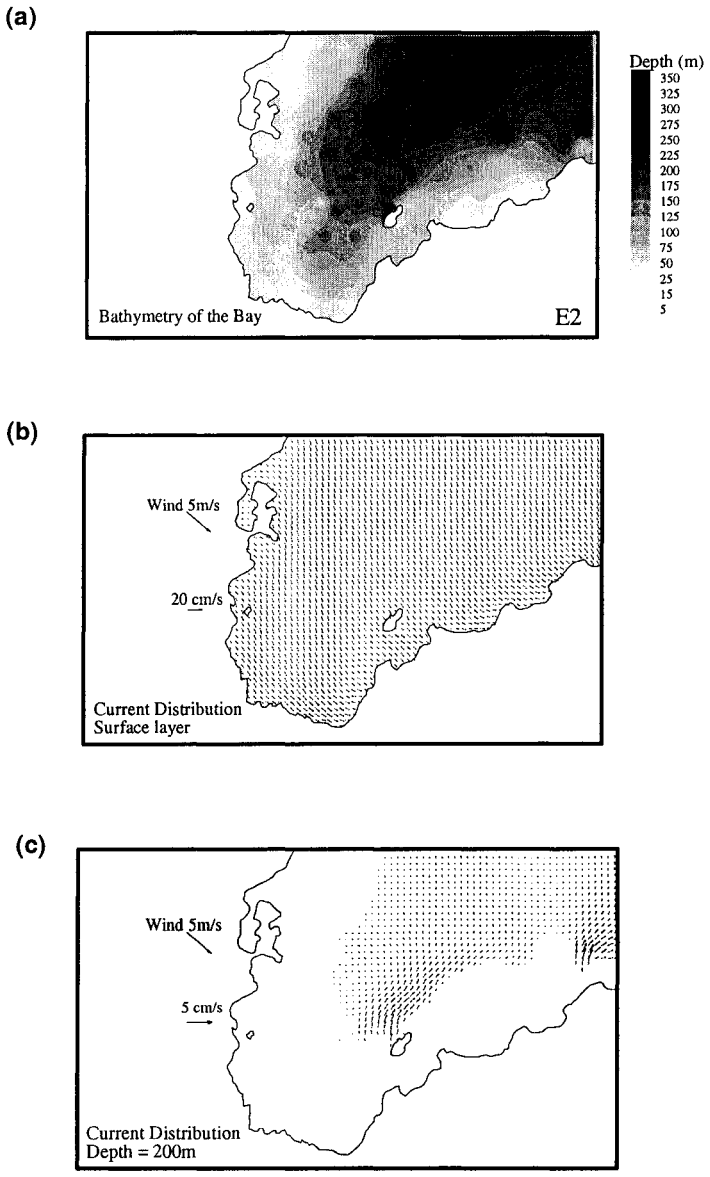


**Figure 8.26:** The bathymetry of Agios Nikolaos bay (Section E2) and the current patterns at the surface layer and at a depth = 200m for a 5m/s NW wind.

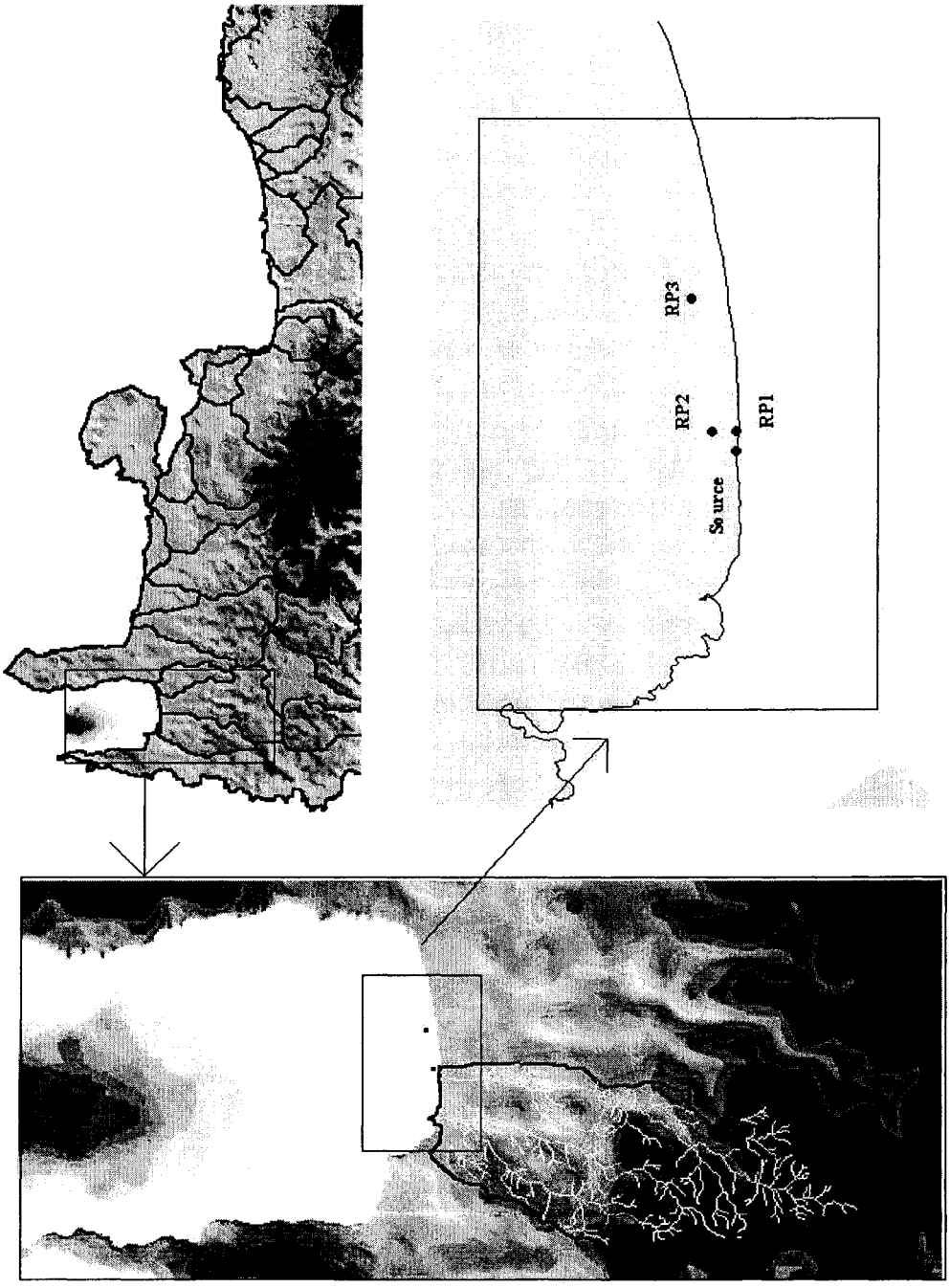


**Figure 8.27:** A watershed discharging to Kasteli bay through two streams.

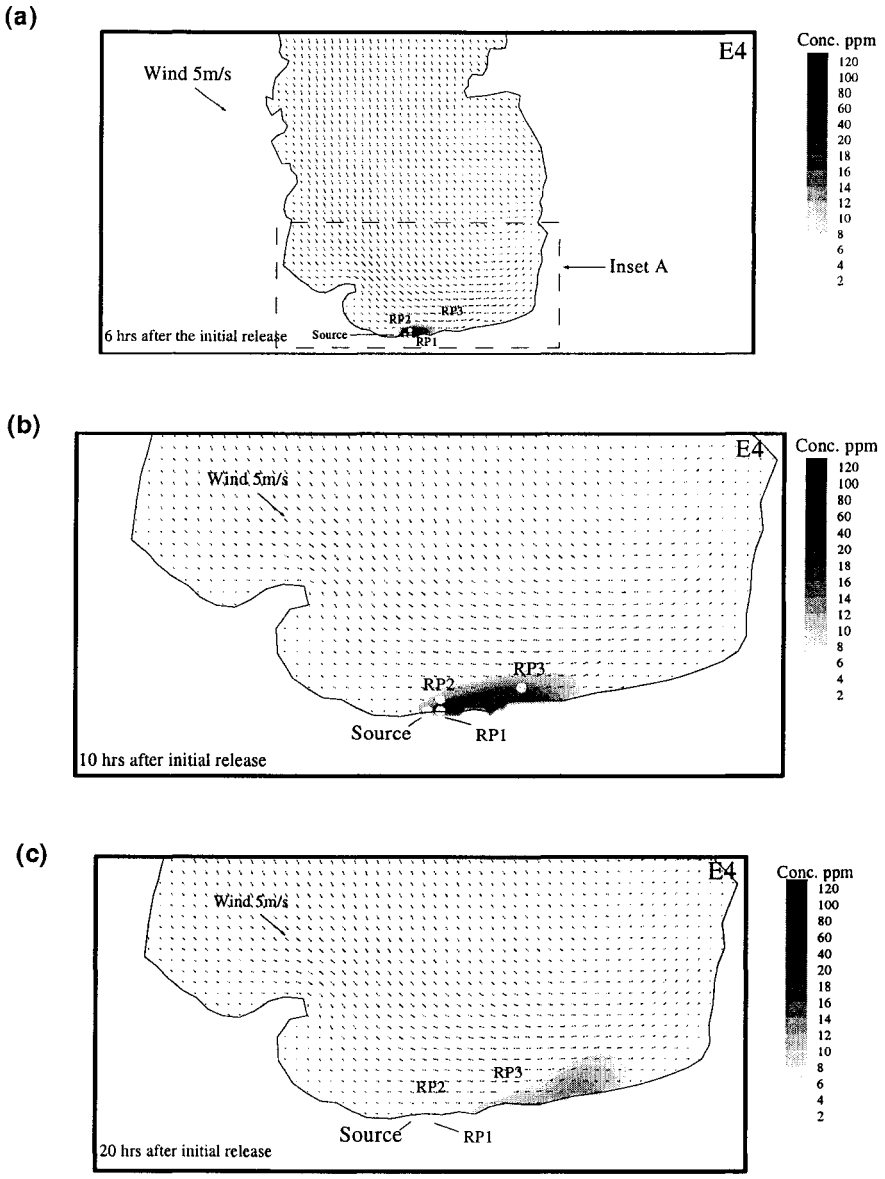


**Figure 8.28:** Current distribution and pollutant concentration contours at the surface layer of Kasteli bay under sea isothermal conditions and a 5m/s NW wind.

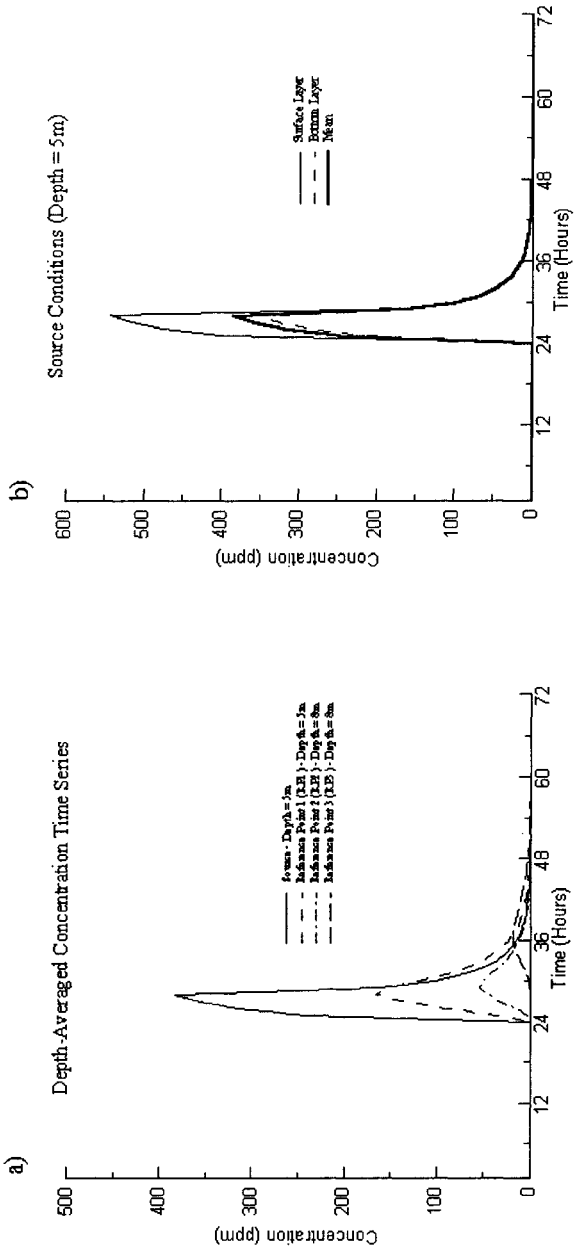


**Figure 8.29:** Concentration time series for a conservative pollutant released for a period of 4 hrs into Kasteli bay under sea isothermal conditions and a 5m/s NW wind.

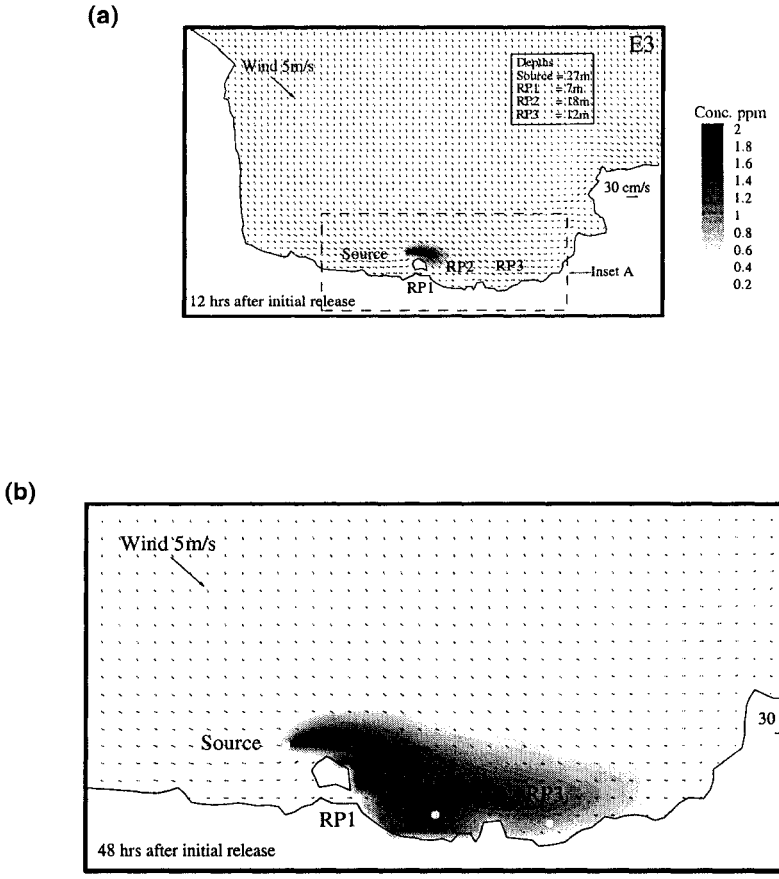


**Figure 8.30:** Case 1 – Current distribution and pollutant concentration contours at the surface layer for a continuous conservative pollutant released with a concentration of 1000ppm from a submerged source at a depth of 27m, in Chania bay under sea isothermal conditions and a 5m/s NW wind.

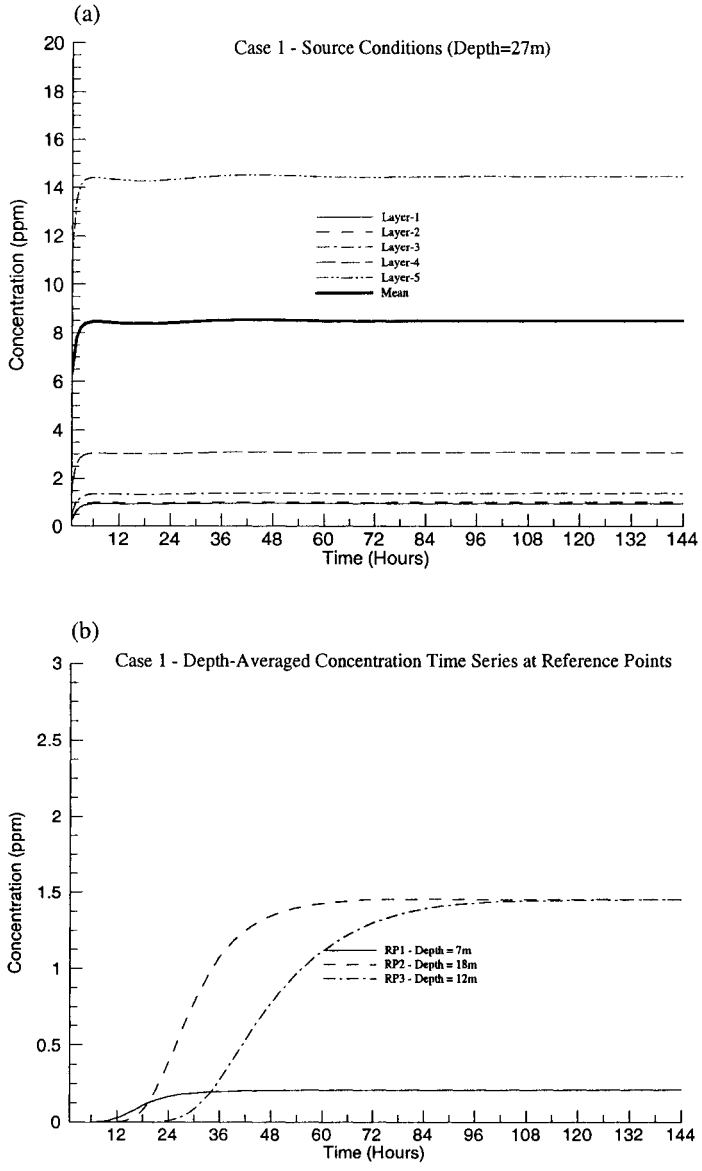


**Figure 8.31:** Case 1 – Concentration time series for a continuous conservative pollutant released with a concentration of 1000ppm into Chania bay under sea isothermal conditions and a 5m/s NW wind.

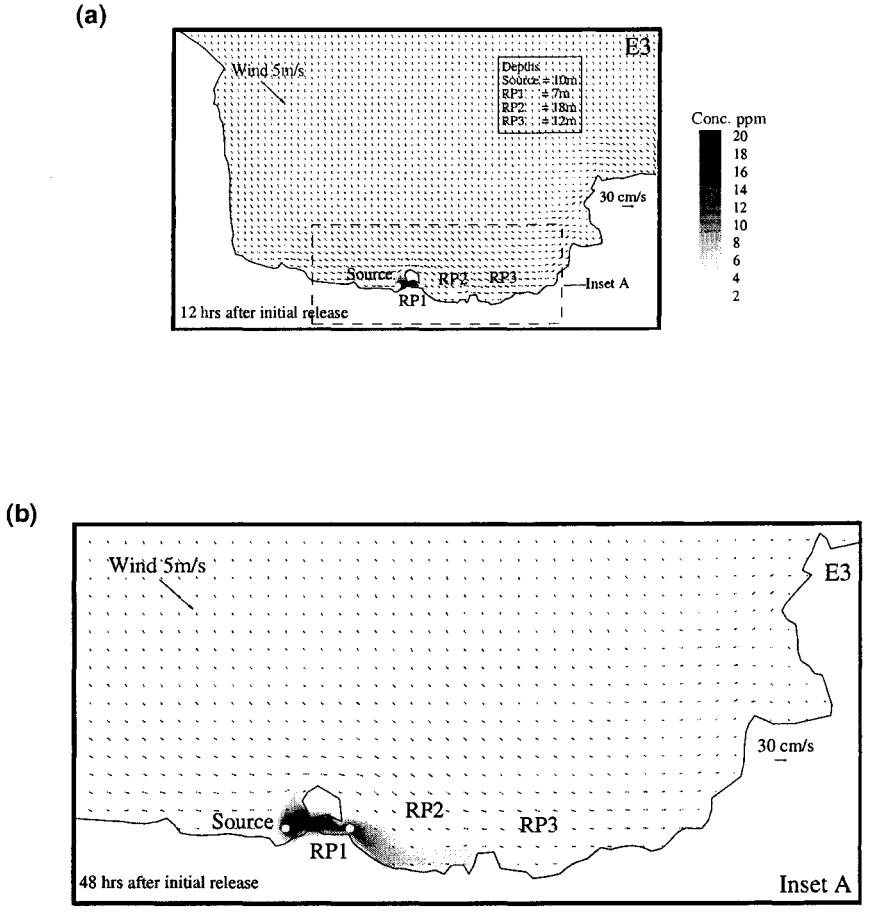


**Figure 8.32:** Case 2 - Current distribution and pollutant concentration contours at the surface layer for a continuous conservative pollutant released with a concentration of 1000ppm from a submerged source at a depth of 10m, in Chania bay under sea isothermal conditions and a 5m/s NW wind.

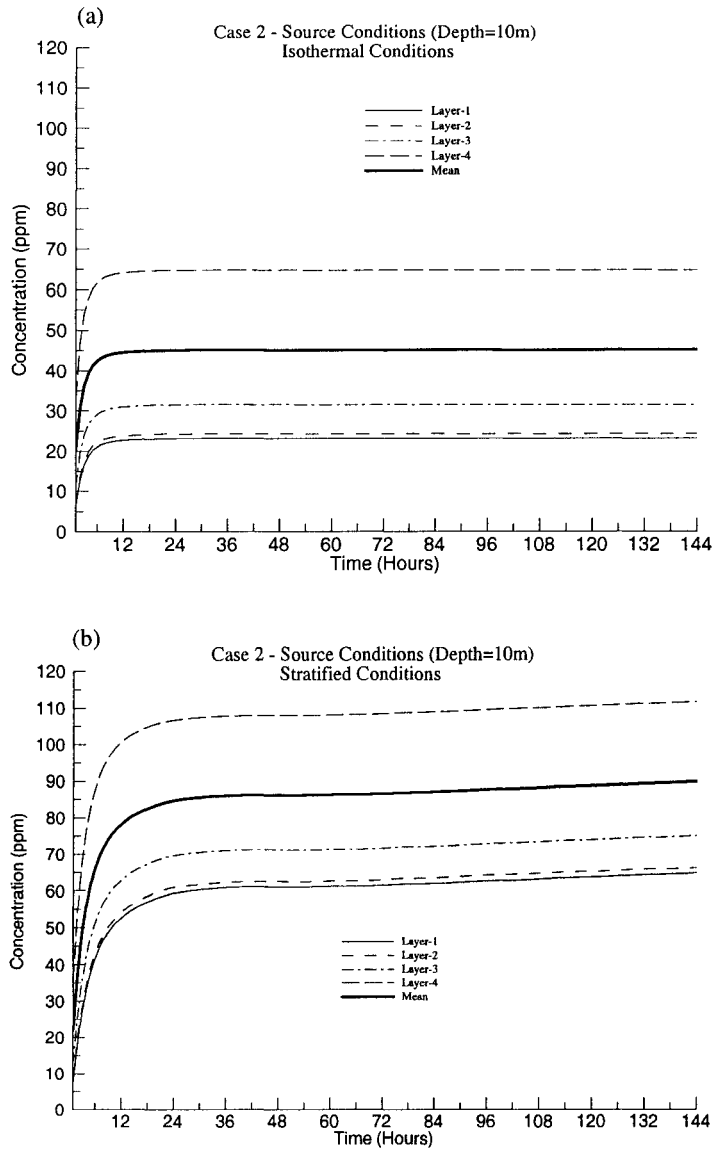


**Figure 8.33:** Case 2 - Concentration time series for a continuous conservative pollutant released with a concentration of 1000ppm into Chania bay under a) isothermal and b) stratified conditions.

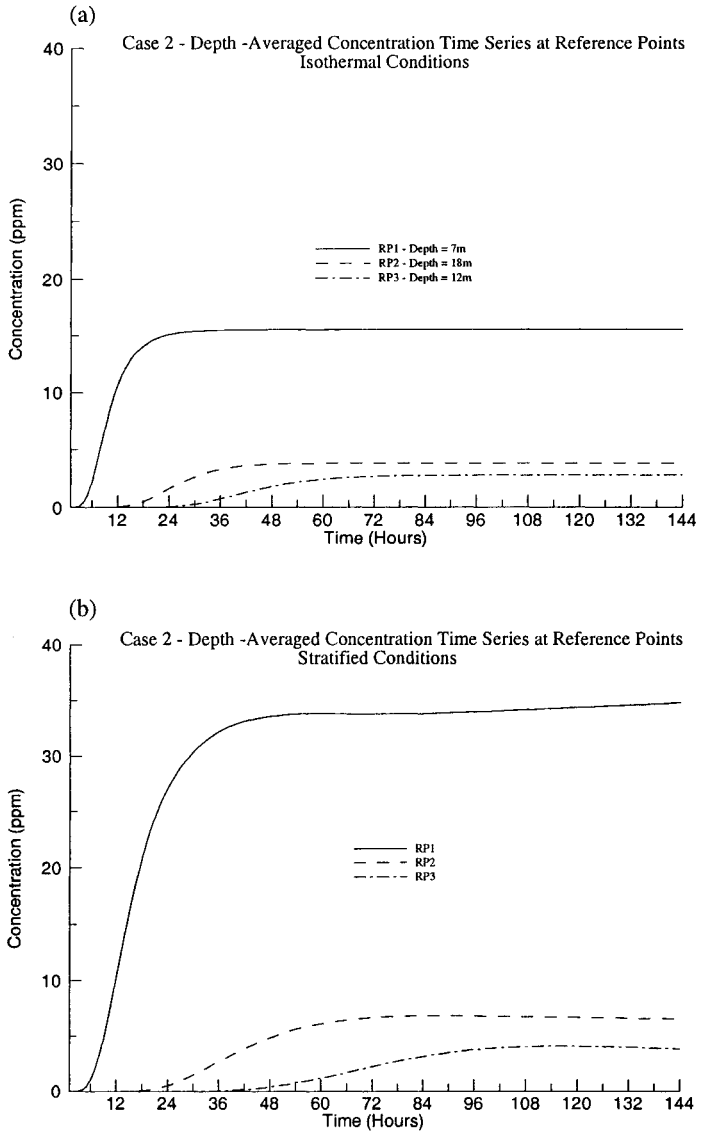


**Figure 8.34:** Case 2 – Depth-averaged concentration time series for a continuous conservative pollutant released with a concentration of 1000ppm into Chania bay under a) isothermal and b) stratified conditions.

# CHAPTER 9

# ACHIEVEMENTS AND RECOMMENDATIONS

## 9.1 Achievements of the Present Study

In this study, the interaction between a variety of disciplines such as information technology, surface hydrology, water resources management, and coastal modelling had been successfully achieved and documented. Serious investigation of the potential of geographic information systems led to the development of a number of algorithms, which were used to shed the light on some of the current challenges in the areas mentioned above. The outcome of this study can be classified into three groups (components): innovative (original), engineering, and software (hydroinformatics) components.

The original component is best illustrated in: (1) investigating the spatial and temporal variation of annual rainfall on the island of Crete (chapter 3), (2) modelling annual orographic rainfall using the multiple linear regression method (chapter 6), and (3) comparing station- and grid-based methods when estimating reference evapotranspiration (chapter 7).

1) Investigating the spatial and temporal variation of annual rainfall on the island of Crete revealed that while most rainfall records showed a downward trend in rainfall over 30 years with higher negative rainfall gradients at the higher elevations, those slopes were not significant. Trend analysis results for Palea Rumata station (county of Chania) indicate a downward trend that is significant at $p<0.05$, while for Anogia station (county of Rethymno) is not significant at $p<0.05$ but significant at $p<0.1$.

- [*Naoum, S., and Tsanis, I.K., 2003. Temporal And Spatial Variation of Annual Rainfall on the Island of Crete, Greece. Hydrological Processes vol. 17, (accepted, to appear)*]

2) Modelling annual orographic rainfall using multiple linear regression provided better estimates/predictions of rainfall at un-gauged locations than the conventional spatial interpolation techniques, which, in turn, resulted in more realistic spatial distribution of rainfall. The MLR estimates for mean areal precipitation and elevation-rainfall gradient for the island of Crete are: 600 mm (0.4mm/m), 950 mm (0.7 mm/m) to 1400 mm (up to1.2 mm/m) for a typical dry, average and wet year, respectively. Of this, 45% falls on the northern, 31% on the southern and 24% on the eastern parts of the island.

- [*Naoum, S., and Tsanis, I.K., 2003. Orographic Precipitation Modelling With Multiple Linear Regression. Journal of Hydrologic Engineering (ASCE)*, (accepted, to appear)]

3) Comparing reference evapotranspiration estimates obtained by using the Penman-Montieth and Class A Pan Evaporation methods and both the station- and grid-based

approaches provided the decision support necessary as to which method and approach to use. The configuration of the meteorological stations network may determine the procedure that should be followed to obtain reasonable estimates for reference evapotranspiration. Generally, the grid-based approach is recommended if a relatively dense networks of meteorological stations exist.

- [*Naoum, S., and Tsanis, I.K., 2003. Hydroinformatics In Evapotranspiration Estimation. Environmental Modelling and Software, vol. 18, number 3, pages 261-271*]

The engineering component included various elements such as statistical, surface hydrology, program design, and data analysis elements. This component is best documented in: (1) studying the spatial and temporal variation of rainfall (chapter 3), (2) assessing raingauge worth in an existing network (chapter 4), (3) ranking spatial interpolation techniques (chapter 5), (4) estimating irrigation requirements for different scales (chapter 7), and (5) the GIS pre-processor for coastal modelling (chapter 8).

1) Studying the spatial and temporal variation of annual rainfall on the island of Crete helped in identifying the wet, average, and dry years for this area. The study also provided estimates for 2, 5, and 10 year rainfall return period.

- [*Naoum, S., and Tsanis, I.K., 2003. Temporal And Spatial Variation of Annual Rainfall on the Island of Crete, Greece. Hydrological Processes, vol. 17,* (accepted, to appear)]

2) Assessing raingauge worth within an established network provided the decision support needed if a decision to be made to reduce the number of gauges within a network. This means eliminating redundant gauges while maintaining an efficient network.

- [*Naoum, S., and Tsanis, I.K., 2003. Integrating Multi-criteria Analysis and GIS for Assessing Raingauge Worth Within an Established Network. Journal of American Water Resources Association*]

3) Ranking spatial interpolation techniques in large and small networks also provided the decision support required to evaluate the available spatial interpolation techniques for large and small networks. This, in turn, improves the spatial distribution of any hydrological variable (e.g. precipitation) which means more accurate input to distributed hydrological models.

- [*Naoum, S., and Tsanis, I.K., 2003. Ranking Spatial Interpolation Techniques Using A GIS-based DSS. Global NEST (Network for Environmental Science and Technology): The International Journal, vol. 5, number 1,* (accepted, to appear)]
- [*Naoum, S., and Tsanis, I.K., 2003. A Hydroinformatic Approach to Assess Interpolation Techniques In High Spatial and Temporal Resolution. Journal of Canadian Water Resources Association*]

4) Estimating irrigation requirements for different scales provided an inspiration and support

for the use of the grid approach to better estimate irrigation requirements. Zooming in from large scale with limited number of meteorological stations to smaller scales with more "representative" meteorological stations was a successful approach to confirm this claim.

- [*Tsanis, I.K., Naoum, S., and Boyle, S.J., 2002. A GIS Interface Method Based on Reference Evapotranspiration and Crop Coefficients for the Determination of Irrigation Requirements. Journal of International Water Resources Association, vol. 27, number 2, pages 233-242*]
- [*Tsanis, I.K., and Naoum, S., 2003. The Effect of Spatially Distributed Meteorological Parameters on Irrigation Water Demand Assessment. Advances in Water Resources, vol. 26, number 3, pages 311-324*]

5) Developing the GIS pre-processor for coastal modelling provided more accurate input to pollutant transport models.

- [*Naoum, S., Tsanis, I.K., and Fullarton, M., 2003. A GIS Pre-Processor For Pollutant Transport Modelling. Journal of Environmental Modelling and Software,* (accepted, to appear)]
- [*Tsanis, I.K., Naoum, S., and Fullarton, M., 2002. Coastal Modelling With A GIS Bathymetric Module. Global NEST (Network for Environmental Science and Technology): The International Journal, vol. 4, number 1, pages 51-74*]

The software component is achieved through the development of a number of hydroinformatics where the tight coupling approach was used with ArcView GIS such as: (1) the integration of multi-criteria analysis and GIS to assess raingauge worth within an established network (chapter 4), (2) assessing spatial interpolation techniques using a GIS (chapter 5), (3) the multiple linear regression GIS module using spatial variables to model orographic rainfall (chapter 6), (4) estimating reference evapotranspiration (chapter 7), and (5) the GIS pre-processor for coastal modelling (chapter 8).

Within these hydroinformatics, statistical methods were used for:
1) the integration of multi-criteria analysis and GIS to assess raingauge worth within an established network [*Naoum, S., and Tsanis, I.K., 2003. Integrating Multi-criteria Analysis and GIS for Assessing Raingauge Worth Within an Established Network. Journal of American Water Resources Association*].
2) assessing spatial interpolation techniques using a GIS [*Naoum, S., and Tsanis, I.K., 2003. Ranking Spatial Interpolation Techniques Using A GIS-based DSS. Global NEST (Network for Environmental Science and Technology): The International Journal, vol. 5, number 1,* (accepted, to appear)] and [*Naoum, S., and Tsanis, I.K., 2003. A Hydroinformatic Approach to Assess Interpolation Techniques In High Spatial and Temporal Resolution. Journal of Canadian Water Resources Association*]

3) the multiple linear regression GIS module using spatial variables to model orographic rainfall [*Naoum, S., and Tsanis, I.K., 2002. A Multiple Linear Regression GIS Module Using Spatial Variables to Model Orographic Rainfall. Journal of Hydroinformatics,* (accepted, to appear)].
And mathematical and statistical models as in estimating reference evapotranspiration [*Naoum, S., and Tsanis, I.K., 2003. Hydroinformatics In Evapotranspiration Estimation. Environmental Modelling and Software, vol. 18, number 3, pages 261-271*].

## 9.2 Recommendations for Future Work

Naturally, and as an extension to this work, a recommendation to continue developing hydroinformatics using GIS is reasonable. However, the successful continuation of this research, if desired, requires some dedicated effort and fund to the professional programming and documentation of the systems developed in this study. As these systems become larger, as a result of introducing new components, the proper programming and documentation will help in keeping track of the different modules and ensure the smooth integration and update of any new additions.

Generally, the suggested components that can provide interesting topics for future consideration share the idea of integrating GIS with methods/models/concepts such as Water Evaluation and Planning System (WEAP) or Artificial Neural Networks (ANNs) for forecasting the fluctuation of groundwater table with precipitation.
Other ideas could be:

1. Fully integrating IDOR3D with GIS.
2. Integrating OBMs, a GIS hydrological distributed model (using raingauge records or radar data and including a water quality component), and IDOR3D GIS.
3. Integrating GIS with the following:
    1. estimating missing records using the normal-ratio method.
    2. record extension by MOVE1.
    3. data consistency by double-mass curve analysis.
    4. testing goodness of fit.
    5. checking for outliers.
    6. frequency analysis and estimating return periods.
    7. an algorithm to recognize the dry, average, and wet years.
4. Closely investigating the correlation between meteorological parameters and reference evapotranspiration estimates.
5. Studying the effect of using different interpolation techniques or cell sizes for the purpose of assessing networks.
6. Developing an interactive system that can take into account the change in the global raingauge network when assessing an existing network.

7. Using dummy variables to estimate the monthly precipitation.
8. Using time as an explanatory (independent) variable as a part of the MLR models.
9. Using MLR to estimate the monthly precipitation.
10. Verifying the spatial interpolation techniques using radar data.
11. Verifying the spatial interpolation techniques using hydrologic modelling and comparing the results with measured flows.

## REFERENCES

Abbott, M.B., 1994. Hydroinformatics: A Copernican revolution in hydraulics. *Journal of Hydraulic Research*, 32:3-13.

*Agricultural Statistics of Greece*, 1991. Hellenic Statistical Services.

Allen, R.G., Pereira, L.S., Raes, D., and Smith, M., 1998. Crop evapotranspiration - guidelines for computing crop water requirements. *FAO Irrigation and Drainage Paper No. 56,* Food and Agriculture Organization of the United Nations, Rome, Italy.

Alter, J.C.,1919. Normal precipitation in Utah. *Monthly Weather Review*, 47:633-636.

Alvarez, F., and Henry, W.K., 1970. Rain-gauge spacing and reported rainfall. *Bulletin of the International Association of Scientific Hydrology*, XV(1):97-107.

Angelakis, A.N., and Diamadopoulos, E., 1995. Water resources management in Greece: current status and prospective outlook. *Water Science and Technology,* 32(9-10):267-272.

ASCE, 1989. Evapotranspiration and irrigation water requirements. *ASCE-Manuals and Reports on Engineering Practice* - No. 70 Eds. Jensen, M.E., Burman, R.D., and Allen, R.G., American Society of Civil Engineers, New York, New York.

Banta, RM., 1990. The role of mountain flows in making clouds. Atmospheric processes over complex terrain. *Meteorological Monographs, NO. 45, American Meteorological Society* 173-228.

Barrows, H.K.,1933. Precipitation and runoff and altitude relations for Connecticut river. *Transactions of American Geophysical Union*, 14:396-406.

Barry, R.G., and Chorley, R.J.,1976. *Atmosphere, Weather, and Climate.* 3rd Edition. Methuen, 432 pages.

Bay Area Restoration Council (BARC), 2002. (*http://www.hamiltonharbour.ca/pdf/ reports/TSH_ report _20 02. pdf*). Accessed June 22nd 2002.

Boyle, S.J., and Tsanis, I.K., 1998. IDOR$^{2D}$GIS - A closely coupled hydrodynamic/pollutant transport GIS model. *The 18$^{th}$ Annual ESRI International User Conference*, San Diego, California, USA.

Boyle, S.J., Tsanis, I.K., and Kanaroglou, P.S., 1998. Developing geographic information systems for land use impact assessment in flooding conditions. *Journal of Water Resources Planning and Management (ASCE)*, (2):89-98.

Bradsley, W.E, and Manly, B.F., 1985. Note on selecting an optimum raingauge subset. *Journal of Hydrology*, (76):197-201.

Bras, R.L., and Rodrigues-Iturbe, I., 1976. Rainfall network design for runoff prediction. *Water Resources Research*, (12):1197-1208.

Brimicombe, A. J., and Bartlett, J. M., 1996. Linking geographic information systems with hydraulic simulation modelling for flood risk assessment: the Hong Kong approach. *GIS and Environmental Modelling*, Goodchild M. F., ed., Oxford University Press, New York, N.Y., 165-168.

Brutsaert, W.H., 1982. *Evaporation into the Atmosphere*. D. Reidel Publishing Company. Dordrecht, Holland.

Burns, J.I.,1953. Small-scale topographic effects on precipitation distribution in San Dimas experimental forest. *Transactions of American Geophysical Union*, 34:761-768.

Burrough, P. A., 1986. *Principles of Geographic Information Systems for Land Assessment*. Oxford University Press, New York.

Burrough, P. A., Van Rijn, R., and Rikken, M., 1996. Spatial data quality and error analysis issues: GIS functions and environmental modelling. In: *GIS and Environmental Modelling*: Progress and Research Issues, M. R. Goodchild et al. (Editors). GIS World, Inc., Fort Collins, Colorado.

Charbonneau, R., 1979. Use of principal component analysis to identify homogeneous precipitation stations for optimal interpolation. *Water Resources Research*, 15(6):1841-1850.

Chow, V.T., Maidment, D.R., and Mays, L.W., 1988. *Applied Hydrology*. McGraw-Hill Inc., New York.

Chua, S.H., and Bras R.L., 1982. Optimal estimators of mean areal precipitation in regions of orographic influence. *Journal of Hydrology*, 57:23-48.

Creutin, J.D., and Obled, C., 1982. Objective analyses and mapping techniques for rainfall fields: an objective comparison. *Water Resources Research*, (18):413-431.

Cuenca, R.H., 1989. *Irrigation System Design: An Engineering Approach.* Prentice-Hall, Englewood Cliffs, N.J.

Daly, C., Neilson, R.P., and Phillips, D.L., 1994. A statistical-topographic model for mapping climatological precipitation over mountainous terrain. *Journal of Applied Meteorology*, 33(2):140-158.

Daniels, H.E., 1950. Rank correlation and population models. *Journal of the Royal Statistical Society* B, (12):171-81

Dastane, N.G., 1974. Effective Rainfall. *FAO Irrigation and Drainage Paper 25*, Food and Agriculture Organization of the United Nations, Rome, Italy.

Delhomme, J.P., 1978. Kriging in the hydrosciences. *Advances in Water Resources,* 1(5):251-266.

Desi, F., Czelani, R., and Rackoczi, F., 1965. On determining the rational density of precipitation measuring networks. *Proceedings of the WMO/IASH Symposium on the Design of Hydrological Networks*, Quebec, IASH, 67:127-129.

Dingman, S.L., Reynolds, S., and Reynolds, R.C., 1988. Application of kriging to estimating mean annual precipitation in a region of orographic influence. *Water Resources Bulletin*, (24):329-339.

Doorenbos, J., and Pruitt, P.W., 1977. Crop water requirements. *FAO Irrigation and Drainage Paper 24 (revised)*, Food and Agriculture Organization of the United Nations, Rome, Italy.

Draper, N.R., and Smith, H., 1998. *Applied Regression Analysis.* John Wiley & Sons, Inc.

Dubois, G., 1998. Spatial interpolation comparison 97: forward and introduction. *Journal of Geographic Information and Decision Analysis*, 2(2):1-10.

Eagleson, P.S., 1967. Optimum density of rainfall networks. *Water Resources Research*, 3(4):1021-1033.

Englund, E.J., 1990. A variance of geostatisticians. *Journal of Mathematical Geology*, (22): 417-455.

Fan, Y., and Duffy, C.J., 1991. Estimating space-time precipitation and temperature fields in mountainous terrain: Wasatch Range, *Utah. American Geophysical Union Fall Meeting Program and Abstracts*. San Francisco, CA., American Geophysical Union.

Fortin, J.P., Bobee, B., and Villeneuve, J.P., 1978. An integrated approach to network design. *Paper presented at the Chapman Conference on the Design of Hydrologic Data Networks*, AGU, Tucson, Ariz., Dec. 11-14.

Franke, R., 1982. Smooth interpolation of scattered data by local thin plate splines. *Journal of Computation and Mathematics with Applications*, 8(4):273-281.

Gallopoulos, E., Houstis, E.N. and Rice, J.R., 1992. *Future Research Directions in Problem Solving Environments for Computational Science*. Report of a Workshop on Research Directions in Integrating Numerical Analysis, Symbolic Computing, Computational Geometry, and Artificial Intelligence for Computational Science. CSRD Report 1259, Center for Supercomputing Research and Development: Urbana, Illinois, Oct. 1992.

Genton, M.G, Furrer, R., 1998. Analysis of rainfall data by simple good sense: is spatial statistics worth the trouble?. *Journal of Geographic Information and Decision Analysis,* 2(2):11-17.

Goodchild, M.F., 1996. The spatial data infrastructure of environmental modelling. In: *GIS and Environmental Modelling: Progress and Research Issues*, M. R. Goodchild et al. (Editors). GIS World, Inc., Fort Collins, Colorado.

Gray, D.M., 1973. *Handbook on the Principles of Hydrology*. Secretariat, Canadian National Committee for the International Hydrological Decade. National Research Council of Canada.

Greene, R.G., and Cruise, J.F., 1995. Urban watershed modelling using geographic information systems. *Journal of Water Resources Planning and Management (ASCE)*, 121(4):318-325.

Hashmi, M.A., and Garcia, L.A., 1998. Spatial and temporal errors in estimating regional evapotranspiration. *Journal of Irrigation and Drainage Engineering (ASCE)*, 124(2):108-114.

Hay, L.E., Branson, M.D., and Leavesly, G.H., 1991. The effects of scale on precipitation estimates from an orographic precipitation model. *American Geophysical Union Fall Meeting Program and Abstracts*. San Francisco, CA., American Geophysical Union.

He, C., Shi, C., Yang, C., and Agosti, B.P., 2001. A windows-based GIS-AGNPS interface. *Journal of the American Water Resources Association*, 37: (2):395-406.

Heine, G.W., 1986. A controlled study of some two-dimensional interpolation method. *The Computer Oriented Geological Society (COGS) Computer Contributions*, 2: (2): 60-72.

Hendrick, R.L., and Comer, G.H., 1970. Space variations of precipitation and implications for raingauge network design. *Journal of Hydrology*, (10):151-163.

Hershfeld, D.M., 1965. On the spacing of raingauges. *Symposium Design of Hydrological Networks*, IASH, (65):72-79.

Hibbert, A.R.,1977. Distribution of precipitation on rugged terrain in central Arizona. *Hydrology and Water Resources Arizona Southwest*, 7:163-173.

Hirsch, R.M., 1982. A comparison of four stream-flow record extension techniques. *Water Resources Research*, 18:1081-1088.

Hirsch, R.M, Alexander, R.B., Smith, R.A., 1991. Selection of methods for the detection and estimation of trends in water quality. *Water Resources Research*, 27(5):803-813.

Hoffmann, W., 1974. Objectives and Approaches in Hydrological Network Planning and Design. *WMO Publications*, (433):9-14.

Houghton, J.G., 1979. A model for orographic precipitation in the north-central Great basin. *Monthly Weather Review*, 107:1462-1475.

Hutchinson, P., 1969. Estimation of rainfall in sparsely gauged areas. *International Association of Hydrologic Sciences Bulletin*, (14):101-120.

Jackson, R.D., 1985. Evaluating evapotranspiration at local and regional scales. *Proceedings of the IEEE*, 73(6).

Jelinski, D.E., Goodchild, M.F., and Steyaert, L.T., 1994. Multiple roles for GIS in global change research: towards a research agenda. In: *Environmental Information Management and Analysis: Ecosystem to Global Scales*, W. K. Michener et al. (Editors). Taylor and Francis, Bristol, Pennsylvania, pp. 40-56.

Jenson, S.K., Domingue, J.O., 1988. Extracting topographic structure from digital elevation data for geographic information system analysis. *Photogrammetric Engineering and Remote Sensing*, 54(11):1593-1600.

Kendall, M.G., 1907. *Rank Correlation Methods*. First Edition. Charles Griffin, London.

Kendall, R.G., Petrie, A.G., 1962. The frequency of thunder storm days in Canada. *Meteorological Branch, Department of Transportation, CIR-3688, TEC-418*, June 1962.

Kohler, M.A., 1949. On the use of double-mass analysis for testing the consistency of meteorological records and for making required adjustments. *Bulletin of American Meteorological Society*, 30(5):188-189.

Lichy, C., 1998. A multidirectional and multifunctional gateway between GIS and hydrodynamic models. *Hydroinformatics 98*, Copenhagen, Denmark.

Maidment, D.R., 1993. *Handbook of Hydrology*, McGraw-Hill, 1400 pp.

Maidment, D.R., 1996. Environmental modelling within GIS. In: *GIS and Environmental Modelling: Progress and Research Issues*, M. R. Goodchild et al. (Editors). GIS World, Inc., Fort Collins, Colorado.

Mann, H.B., 1945. Non-parametric tests against trend. *Econometrica*, 13:245-259.

Marecos do Monte, M.H.F., Angelakis, A.N., and Asano, T., 1996. Necessity and basis for the establishment of european guidelines on wastewater reclamation and reuse in the Mediterranean region. *Water Science and Technology*, 30(10-11):319-332.

Marwitz, J.D., 1987. Deep orographic storms over the Sierra Nevada. Part I: thermodynamic and kinematic structure. *Journal of Atmospheric Sciences*, 44:159-173.

Matheron, G., 1971. *The Theory of Regionalized Variables and Its Applications*. Cahiers du Centre de Morphologie Mathematique, Ecole des Mines, 211 pages.

McBratney, A.B, Webster, R., 1986. Choosing functions for semi-variograms of soil properties and fitting them to sampling estimates. *Journal of Soil Science*, (37):617-639.

Ministry of Industry, 1989. *Water Resources of Greece.* Athens (in Greek).

Mitas, L, Mitasova, H., 1988. General variational approach to the interpolation problem. *Journal of Computation and Mathematics with Applications*, 16:(12):983-992.

Montgomery, D.C., Runger, G.C., 1994. *Applied Statistics and Probability for Engineers*. John Wiley & Sons, Inc.

Naranjo, E., and Larsen, H., 1998. An integrated model to assess pollution loads with the use of GIS and numerical models. *Hydroinformatics 98*, Copenhagen, Denmark.

Nicks, A.D., 1963. Field evaluation of rain gauges network design principles. *The IASH Symposium Design of Hydrological Network*, (67):82-93.

Oke, T.R., 1987. *Boundary Layer Climates*. Second Edition. University Press, Cambridge; 435.

Oliver, M.A., 1990. Kriging: A method of interpolation for geographical information systems. *International Journal of Geographic Information Systems*, 4(4):313-332.

Orville, H.D., 1965. A numerical study of the initiation of cumulus clouds over mountainous terrain. *Journal of Atmospheric Sciences* 22: 684-699.

Orville, H.D., 1968. Ambient wind effects on the initiation and development of cumulus clouds over mountains. *Journal of Atmospheric Sciences,* 25: 385-403.

Paniconi, C., Kleinfeldt, S., Deckmyn, J., and Giacomelli, A., 1999. Integrating GIS and data visualization tool for distributed hydrologic modelling. *Transactions in GIS*, 3(2):97-118

Papazafiriou, Z., 1984. *Principles and Practice of Irrigation*. Thessaloniki (in Greek).

Patankar, S.V., 1980. *Numerical heat transfer and fluid flow*. Hemisphere, Washington D.C.

Paulhus, J.L.H., Kohler, M.A., 1952. Interpolation of missing precipitation records. *Monthly Weather Review,* 80(8):129-134.

Peck, E.L., and Schaake, J.C., 1990. Network design for water supply forecasting in the west. *Water Resources Bulletin*, 26:87-99.

Peck, E.L., and Brown, M.J., 1962. An approach to the development of isohyetal maps for mountainous areas. *Journal of Geophysical Research*, 67:681-694.

Phillips, D.L., Dolph, J., and Marks, D., 1992. A comparison of geostatistical procedures for spatial analysis of precipitation in mountainous terrain. *Agricultural and Forest Meteorology*, 58:119-141.

Pilon, P.J., Condie, R., Harvey, K.D., 1985. Consolidated frequency analysis package (CFA). *Water Resources Branch, Inland Waters Directorate*, Environment Canada, Ottawa, Ontario, Canada.

Raghuwanshi, N.S., and Wallender, W.W., 1998. Converting from pan evaporation to evapotranspiration. *Journal of Irrigation and Drainage Engineering (ASCE)*, 124(5):275-277.

Reed, W.G., and Kincer, J.B., 1917. The preparation of precipitation charts. *Monthly Weather Review*, 45:233-235.

Rodda, J.C., Dowing, R.A., and Law, F.M., 1976. *Systematic Hydrology*. Butterworths, London.

Ross, M.A., and Tara, P.D., 1993. Integrated hydrologic modelling with geographic information systems. *Journal of Water Resources Planning and Management (ASCE)*, 2(19):129-140.

Royle, A.G., Clausen F.L., and Frederiksen, P., 1981. Practical universal kriging and automatic contouring. *Geoprocessing*, 1(11):377-394.

Schermerhorn, V.P.,1967. Relations between topography and annual precipitation in western Oregon and Washington. *Water Resources Research*, 3:707-711.

Sevruk, B., 1982. Methods of correction for systematic error in point precipitation measurement for operational use. *WMO Tech. Note. WMO-589*, Operational Hydrology Report (21); 91 pages.

Sharp, A.L., Owens, W.J., and Gibbs, A.E., 1961. A comparison of method for estimating precipitation of watershed, *forty-Second Annual Meeting of the American Geophysical Union.*

Shen H., Tsanis I.K. and D'Andrea M., 1995. A three-dimensional hydrodynamic/pollutant transport simulation model for the nearshore areas of Lake Ontario, *Journal of Great Lakes Research,* 21(2):161-177.

Shifter, Z., 1981. *A Kinematic Storm Model for Urban Drainage Study.* Master's Thesis. Department of Civil Engineering, McMaster University, Hamilton, Ontario, Canada.

Singh, V.P., 1988. *Hydrologic System - Rainfall-Runoff Modelling Vol. 1.* Prentice Hall, Englewood Cliffs, New Jersey.

Singh, V.P., 1992. *Elementary Hydrology.* Prentice-Hall Inc., Englewood Cliffs, N.J.

Smith, M., 1992. Cropwat: a computer program for irrigation planning and management. *FAO Irrigation and Drainage Paper 46*, Food and Agriculture Organization of the United Nations, Rome, Italy.

Smith, M., Allen, R., and Pereira, L., 1997. Revised FAO methodology for crop water requirements. *Land and Water Development Division.* FAO, Rome, Italy.

Smith, R.B., 1979. The influence of mountains on the atmosphere. *Advances in Geophysics, Academic Press*, 21:87-230.

Snyder, R.L., 1992. Equation for pan evaporation to evapotranspiration conversion. *Journal of Irrigation and Drainage Engineering (ASCE)*, 118(6):977-980.

Spearman, C., 1904. The proof and measurement of association between two things. *American Journal of Psychology*, 15: 72-101.

Spreen, W.C., 1947. A determination of the effect of topography upon precipitation. *Transactions of American Geophysical Union*, 28:285-290.

Stafford, S.G., Brunt, J.W., Michener, W.K., 1994. Integration of scientific information management and environmental research. In: *Environmental Information Management and Analysis: Ecosystem to Global Scales*, W. K. Michener et al. (Editors). Taylor and Francis, Bristol, Pennsylvania, pp. 1-19.

Steyaert, L. T., and Goodchild, M. F., 1994. Integrating geographic information systems and environmental simulation models: A Status Review. In: *Environmental Information Management and Analysis: Ecosystem to Global Scales*, W. K. Michener et al. (Editors). Taylor and Francis, Bristol, Pennsylvania, pp. 333-355.

Stole, T., 1972. The relative efficiency of the density of raingauge networks. *Journal of Hydrology*, (15):193-208.

Strebel, D.E., Meeson, B.W., and Nelson, A.K., 1994. Scientific information systems: a conceptual framework. In: *Environmental Information Management and Analysis: Ecosystem to Global Scales*, W. K. Michener et al. (Editors). Taylor and Francis, Bristol, Pennsylvania, pp. 59-85.

Sui, D.Z., and Maggio, R.C., 1999. Integrating GIS with hydrological modelling: practices, problems, and prospects. *Computers, Environment and Urban Systems* 23:33-51.

Tabios III, G.Q., Salas, J.D., 1985. A comparative analysis of techniques for spatial interpolation of precipitation. *Water Resources Bulletin, American Water Resources Association* 21(3):365-380.

Taylor, K., Walker, G., and Abel, D., 1999. A framework for model integration in spatial decision support systems. *International Journal of Geographic Information Sciences*, 13(6):533-555.

Thiessen, A. H., 1911. Precipitation for large areas. *Monthly Weather Review*, (39):1082-1084.

Thompson, J.F., Warsi, Z.U.A., and Mastin, C.W., 1985. *Numerical Grid Generation: Foundation and Applications*. Elsevier Science Publishing Co., Inc.

Tsanis, I.K., 1999. Real-time rainfall prediction and storm tracking for Hamilton-Wentworth region. *A "Final Report" submitted to the Regional Municipality of Hamilton-Wentworth*, August 1999.

Tsanis, I.K., and Gad, M.A., 2001. A GIS precipitation method for analysis of storm kinematics. *Environmental Modelling and Software,* 16(3): 273-281.

Tsanis, I.K., Valeo, C., Wu, J., and Boyle, S., 1996. Managing contaminated sediments using a hydrodynamic model and a GIS. *Environmental Technology*, 17:877-883.

Tung, Y.K., 1983. Point rainfall estimation for a mountainous region. *Journal of Hydraulic Engineering (ASCE)*, 109(10):1386-1393.

U.S. Water Resources Council (now called Interagency Advisory Committee on Water Data) 1981. Guidelines for determining flood flow frequency. *Bulletin 17B, U.S. Geological Survey*, Reston, VA.

Watkins, Jr., D.W. and McKinney, D.C., 1995. Recent development associated with decision support systems in water resources. *Environmental and Water Resources Engineering Program, Department of Civil Engineering, University of Texas at Austin.*

Watson, D.F, and Philip, G.M., 1985. A refinement of inverse distance weighted interpolation. *Geo-Processing*, (2):315-327.

Watt, I.E.M., 1956. Distribution of rainfall over a small area in the tropics. *Symposium International Congress Zone, Thunderstorms, Tropical Clouds*, Vol 13.

Zawadzki, I.I., 1973. Errors and fluctuations of raingauge estimates of areal rainfall. *Journal of Hydrology*, (18):243-255.

# APPENDIX A: PUBLICATIONS

## (Refereed Journal Papers)

**Published**

1. Tsanis, I.K., Naoum, S., and Boyle, S.J., 2002. A GIS Interface Method Based on Reference Evapotranspiration and Crop Coefficients for the Determination of Irrigation Requirements. *Journal of International Water Resources Association*, vol. 27, number 2, pages 233-242.

2. Tsanis, I.K., and Naoum, S., 2003. The Effect of Spatially Distributed Meteorological Parameters on Irrigation Water Demand Assessment. *Advances in Water Resources*, vol. 26, number 3, pages 311-324.

3. Tsanis, I.K., Naoum, S., and Fullarton, M., 2002. Coastal Modelling With A GIS Bathymetric Module. *Global NEST (Network for Environmental Science and Technology): The International Journal*, vol. 4, number 1, pages 51-74.

4. Naoum, S., and Tsanis, I.K., 2003. Hydroinformatics In Evapotranspiration Estimation. *Environmental Modelling and Software,* vol. 18, number 3, pages 261-271.

**In press**

5. Naoum, S., and Tsanis, I.K., 2003. Temporal And Spatial Variation of Annual Rainfall on the Island of Crete, Greece. *Hydrological Processes*, vol. 17, pages..-..

6. Naoum, S., and Tsanis, I.K., 2002. A Multiple Linear Regression GIS Module Using Spatial Variables to Model Orographic Rainfall. *Journal of Hydroinformatics.*

7. Naoum, S., and Tsanis, I.K., 2003. Ranking Spatial Interpolation Techniques Using A GIS-based DSS. *Global NEST (Network for Environmental Science and Technology): The International Journal*, vol. 5, number 1, pages ..-..

8. Naoum, S., and Tsanis, I.K., 2003. Orographic Precipitation Modelling With Multiple Linear Regression. *Journal of Hydrologic*

*Engineering (ASCE).*

9. Naoum, S., Tsanis, I.K., and Fullarton, M., 2003. A GIS Pre-Processor For Pollutant Transport Modelling. *Journal of Environmental Modelling and Software.*

**Submitted**

10. Naoum, S., and Tsanis, I.K., 2003. Integrating Multi-criteria Analysis and GIS for Assessing Raingauge Worth Within an Established Network. *Journal of American Water Resources Association.*

11. Naoum, S., and Tsanis, I.K., 2003. A Hydroinformatic Approach to Assess Interpolation Techniques In High Spatial and Temporal Resolution. *Journal of Canadian Water Resources Association.*

**To be submitted**

12. Naoum, S., and Tsanis, I.K., 2003. A Hydroinformatics Approach to Assess Raingage Worth Within an Established Network. Journal of Environmental Modelling and Software.

12. Naoum, S., Tsanis, I.K., and Fullarton, M., 2003. A GIS Pre-Processor For Pollutant Transport Modelling. Journal of Environmental Modelling and Software.

13. Naoum, S., 2003. Interpolation Techniques Assessment In High Spatial and Temporal Resolution. Journal of Hydroinformatics.

**(Conference Papers)**

14. Tsanis, I.K., and Naoum, S., 2002. Spatial Precipitation with GIS. *GIS Users Conference, Athens, Greece*, 7-8 November 2002.

15. Naoum, S., and Tsanis, I.K., 2003. Estimating Rainfall at Ungauged Locations using Topographical and Geographical Features by Means of Multiple Linear Regression. *The 8th Conference on Environmental Science and Technology*, Lemnos Island, Greece, 8-10 September, 2003.

## APPENDIX B: PROJECTION

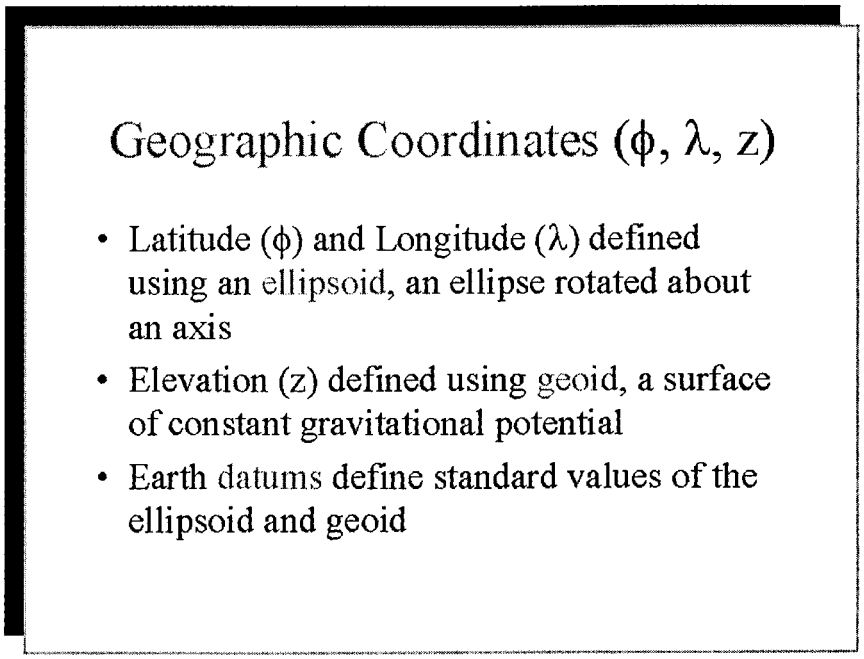


**Figure 1**

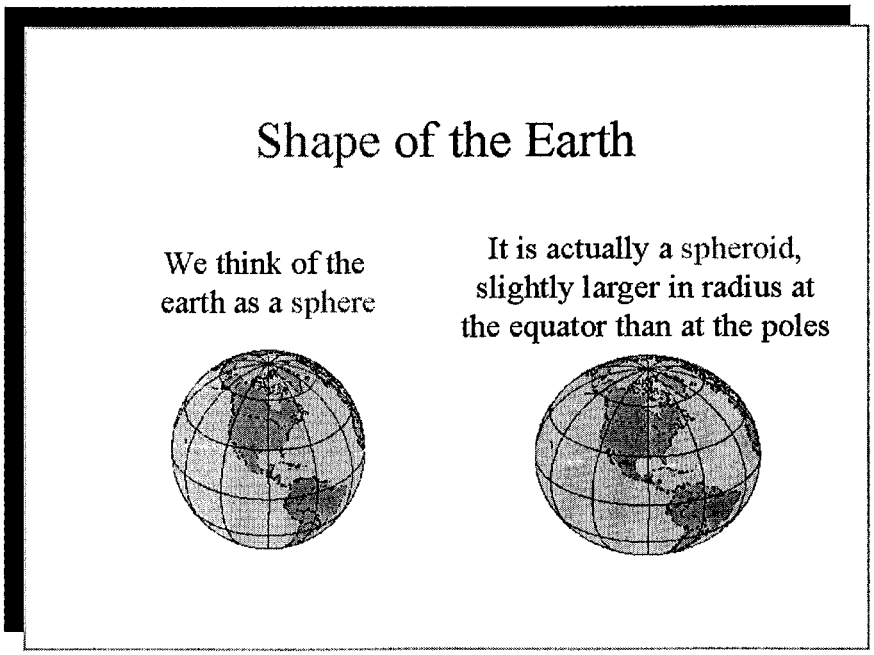


**Figure 2**

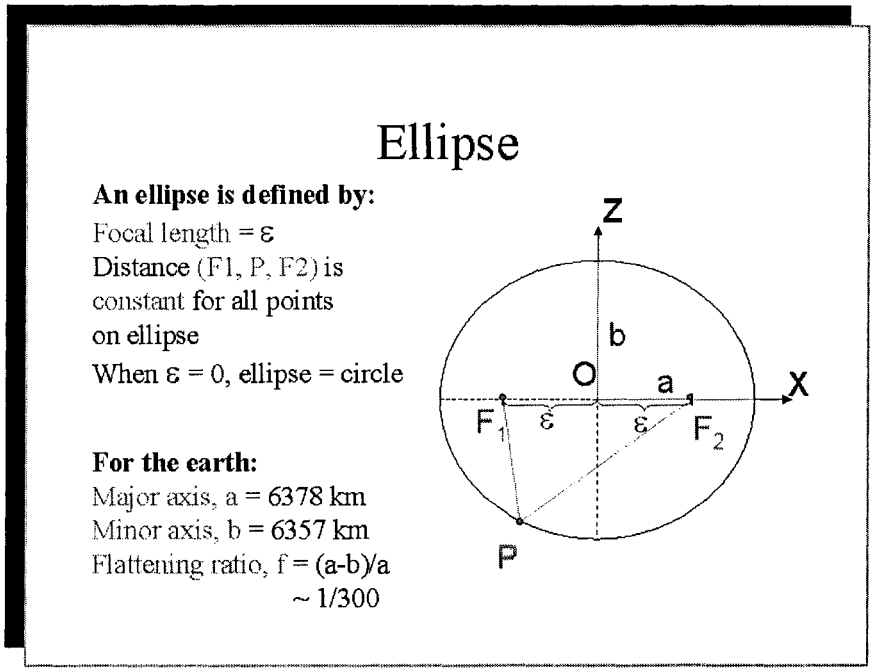


**Figure 3**

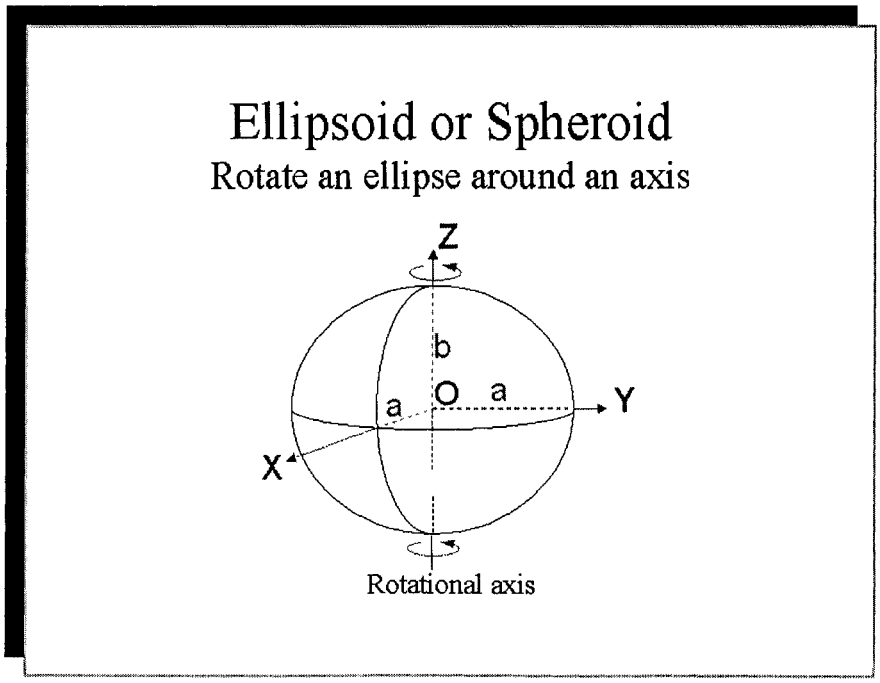


**Figure 4**

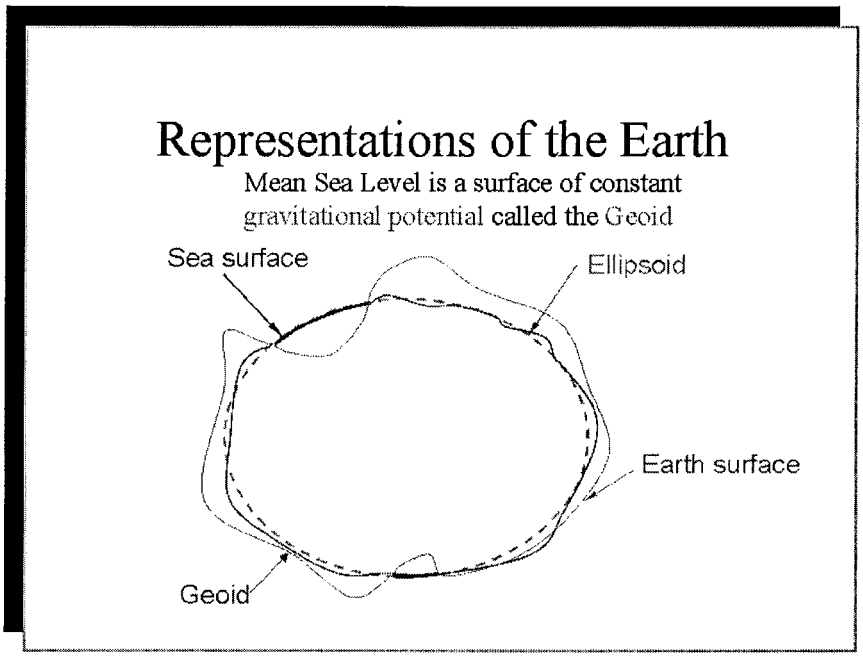


**Figure 5**

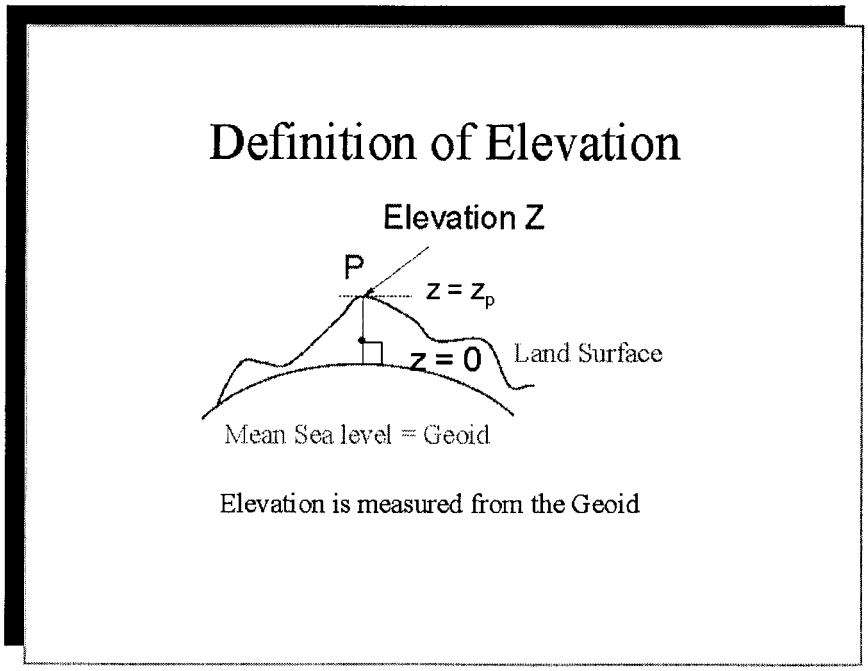


**Figure 6**

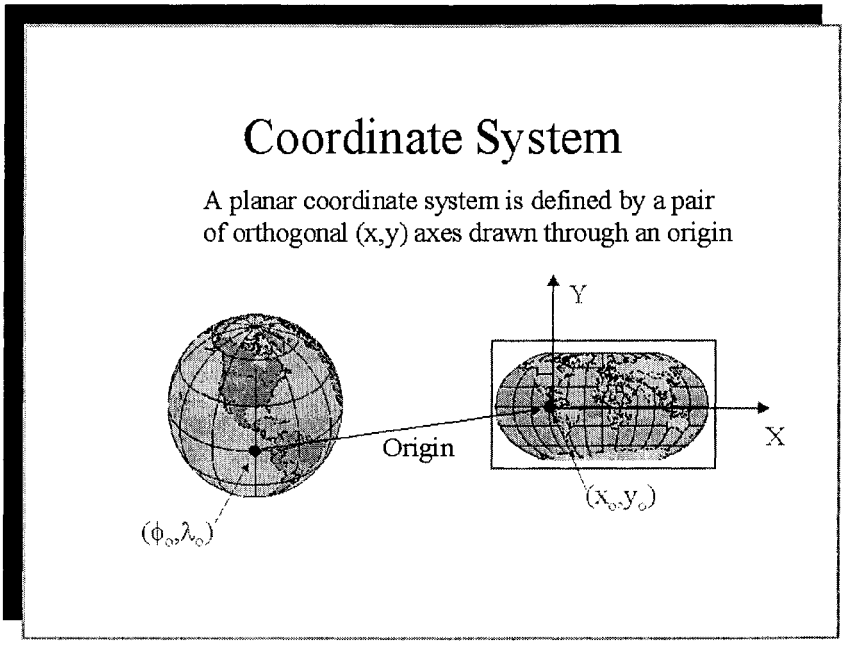


**Figure 7**

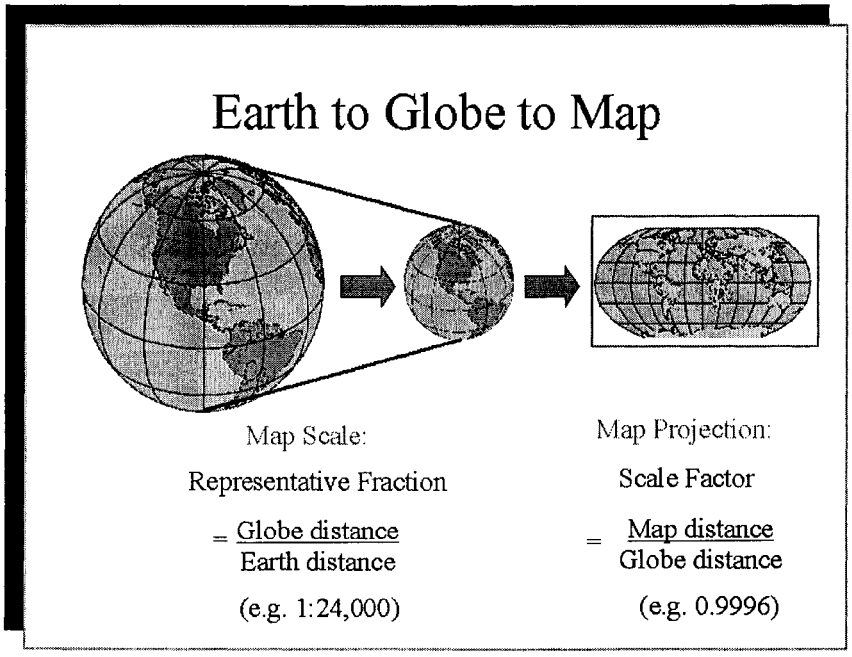


**Figure 8**

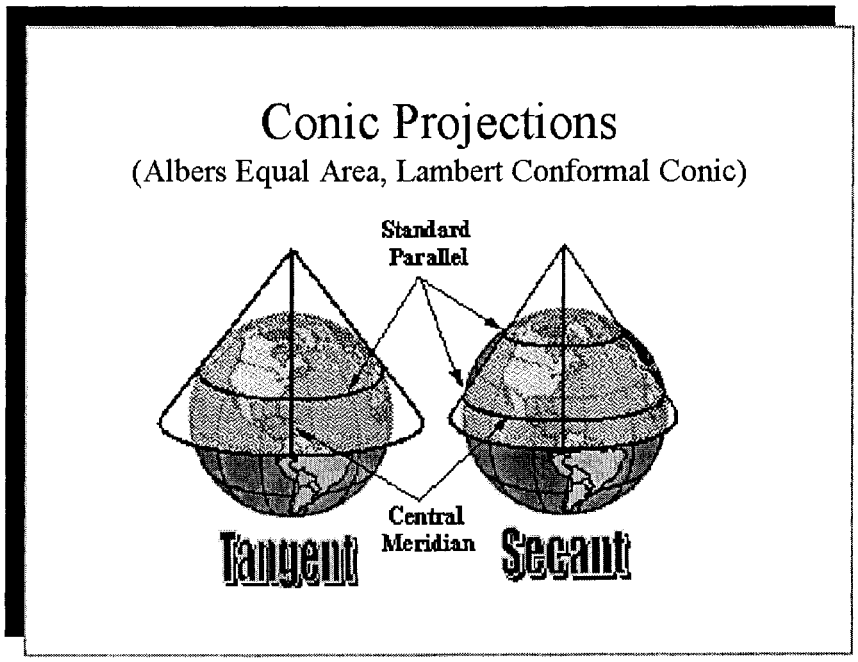


**Figure 9**

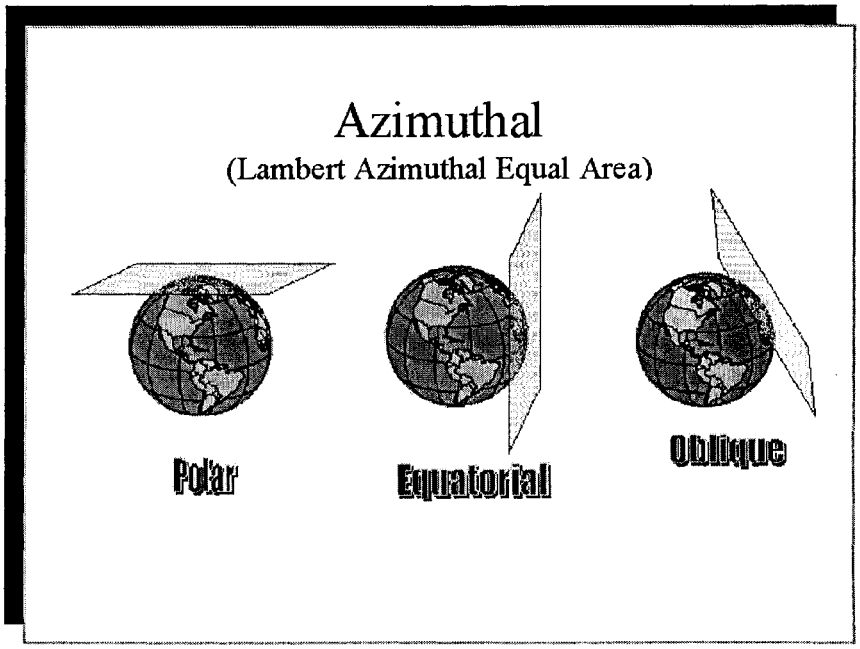


**Figure 10**

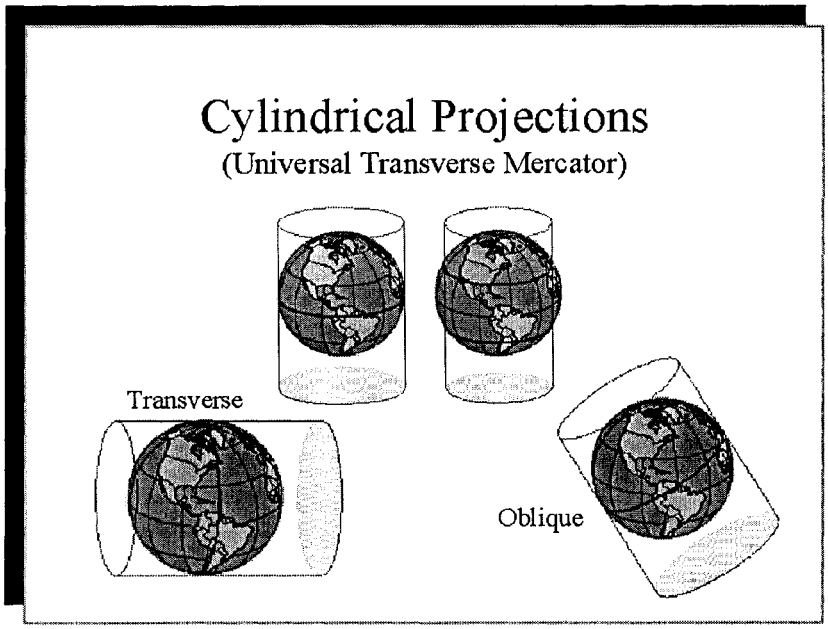


**Figure 11**

**UTM:**

The Universal Transverse Mercator (UTM) projection is used to define horizontal, positions world-wide by dividing the surface of the Earth into 6 degree zones, each mapped by the Transverse Mercator projection with a central meridian in the center of the zone. UTM zone numbers designate 6 degree longitudinal strips extending from 80 degrees South latitude to 84 degrees North latitude. UTM zone characters designate 8 degree zones extending north and south from the equator. Eastings are measured from the central meridian (with a 500km false easting to insure positive coordinates). Northings are measured from the equator (with a 10,000km false northing for positions south of the equator).

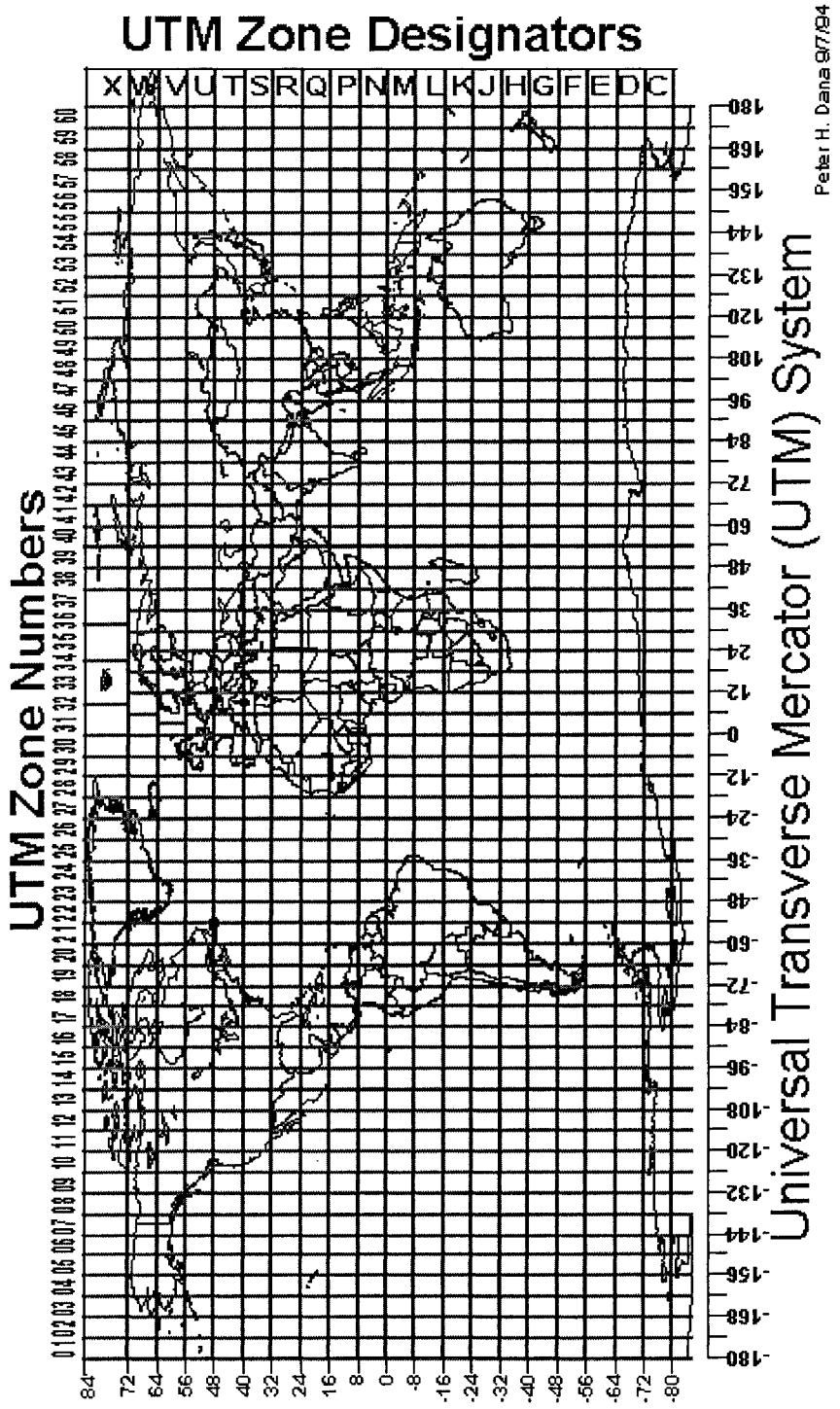
UTM Zone Designators
X W V U T S R Q P N M L K J H G F E D C
UTM Zone Numbers
01 02 03 04 05 06 07 08 09 10 11 12 13 14 15 16 17 18 19 20 21 22 23 24 25 26 27 28 29 30 31 32 33 34 35 36 37 38 39 40 41 42 43 44 45 46 47 48 49 50 51 52 53 54 55 56 57 58 59 60
84 72 64 56 48 40 32 24 16 8 0 -8 -16 -24 -32 -40 -48 -56 -64 -72 -80
180 168 156 144 132 120 108 96 84 72 60 48 36 24 12 0 -12 -24 -36 -48 -60 -72 -84 -96 -108 -120 -132 -144 -156 -168 -180
Universal Transverse Mercator (UTM) System
Peter H. Dana 9/7/94

## APPENDIX C: DEM, FLOW DIRECTION GRID, FLOW ACCUMULATION GRID, WATERSHEDS AND STREAM NETWORK

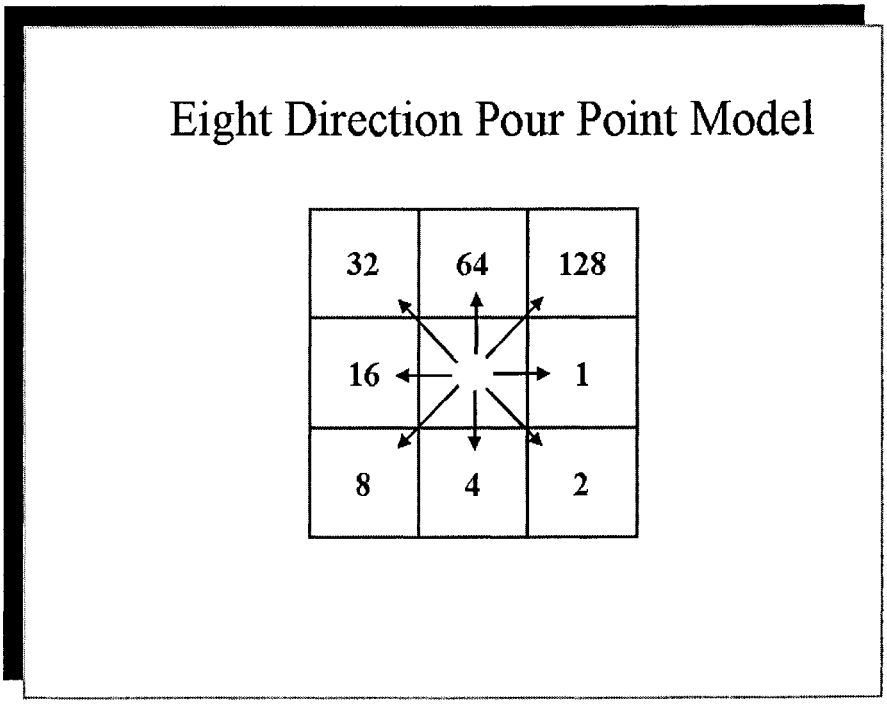


**Figure 1**

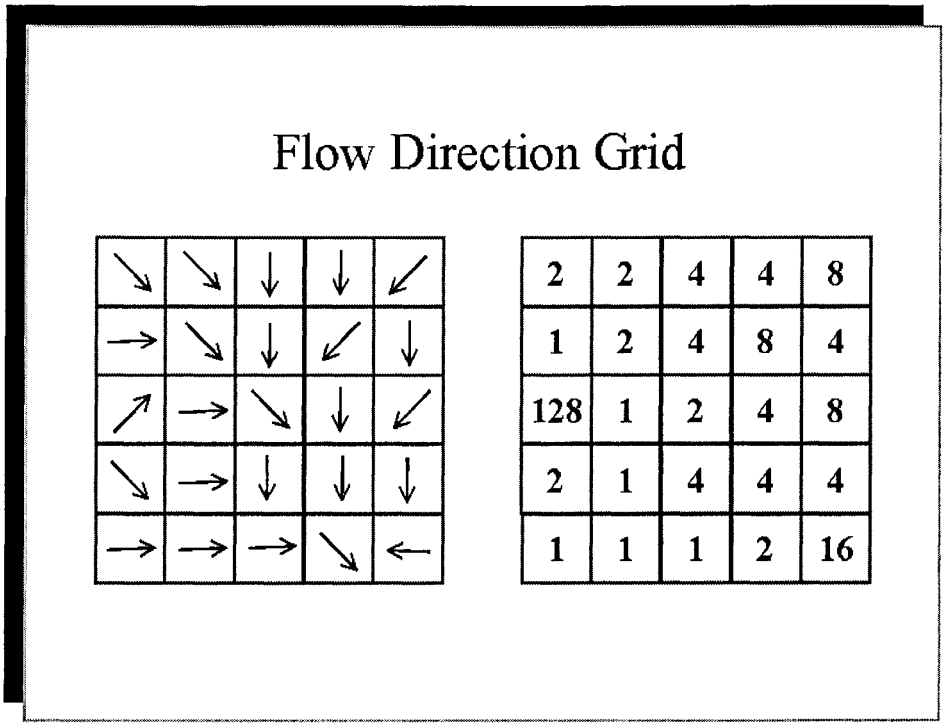


**Figure 2**

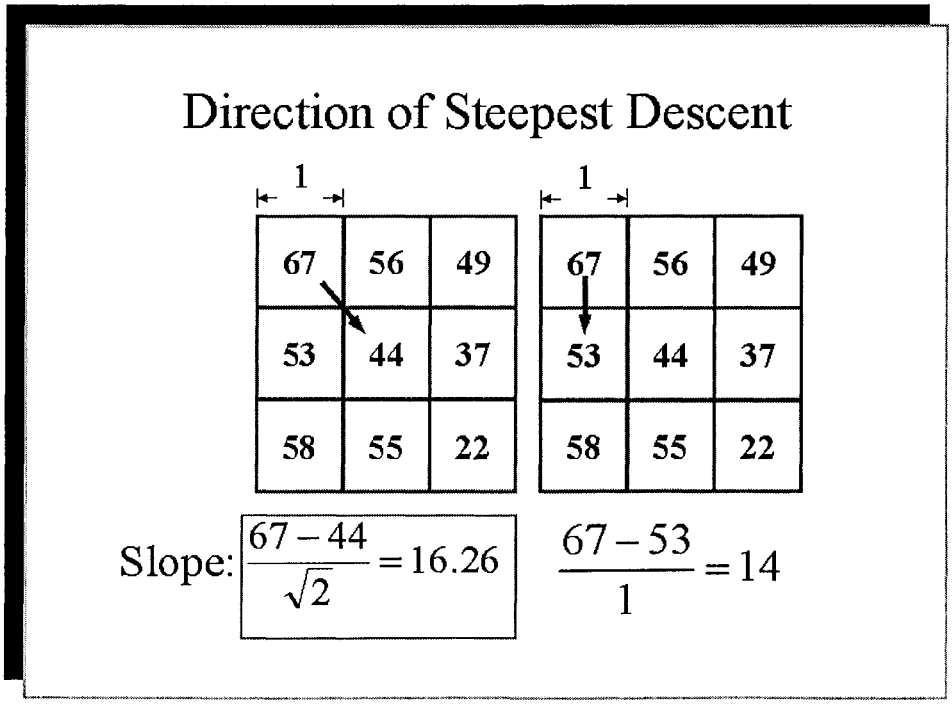


**Figure 3**

## Flow Accumulation Grid

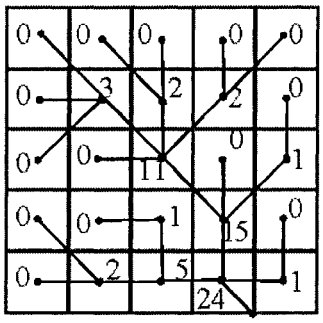


| | | | | |
|---|---|---|---|---|
| 0 | 0 | 0 | 0 | 0 |
| 0 | 3 | 2 | 2 | 0 |
| 0 | 0 | 11 | 0 | 1 |
| 0 | 0 | 1 | 15 | 0 |
| 0 | 2 | 5 | 24 | 1 |

to Grid calculator

**Figure 4**

## Flow Accumulation > 5 Cell Threshold

| | | | | |
|---|---|---|---|---|
| 0 | 0 | 0 | 0 | 0 |
| 0 | 3 | 2 | 2 | 0 |
| 0 | 0 | 11 | 0 | 1 |
| 0 | 0 | 1 | 15 | 0 |
| 0 | 2 | 5 | 24 | 1 |

**Figure 5**

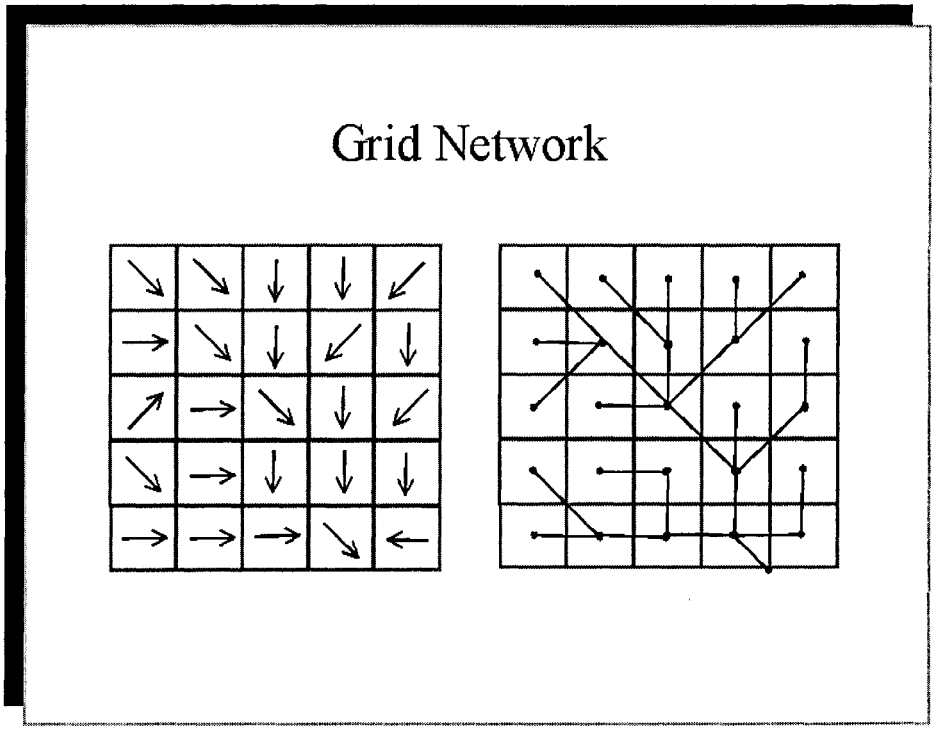


**Figure 6**

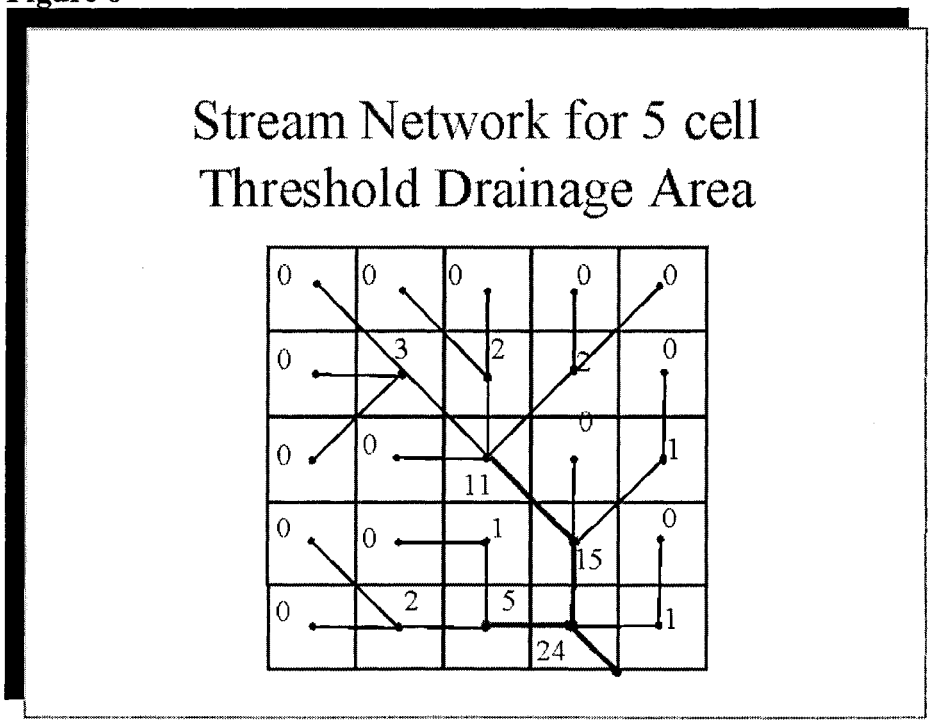


**Figure 7**

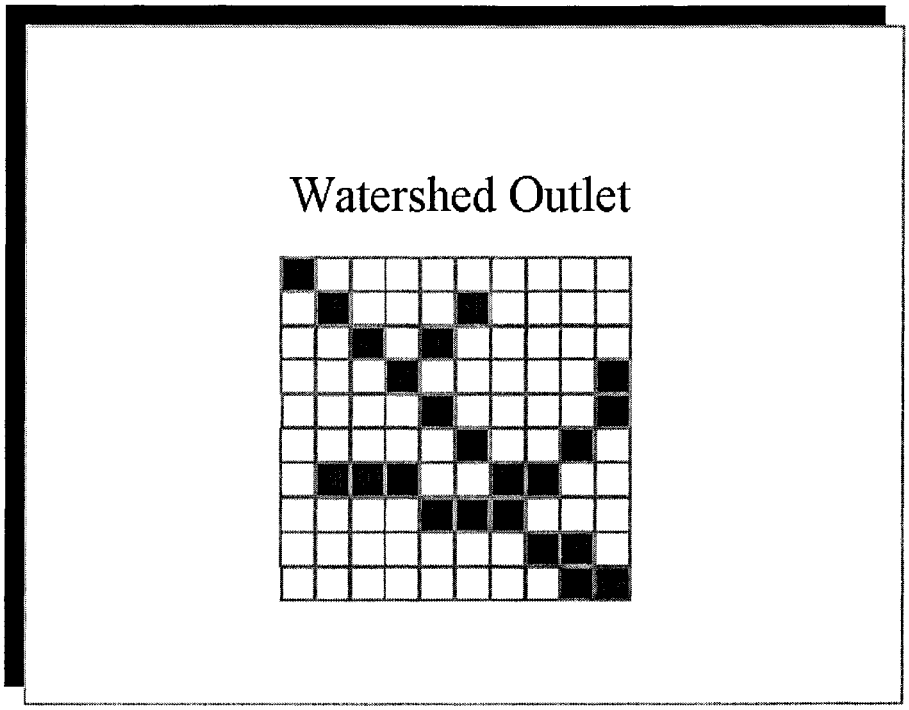


**Figure 8**

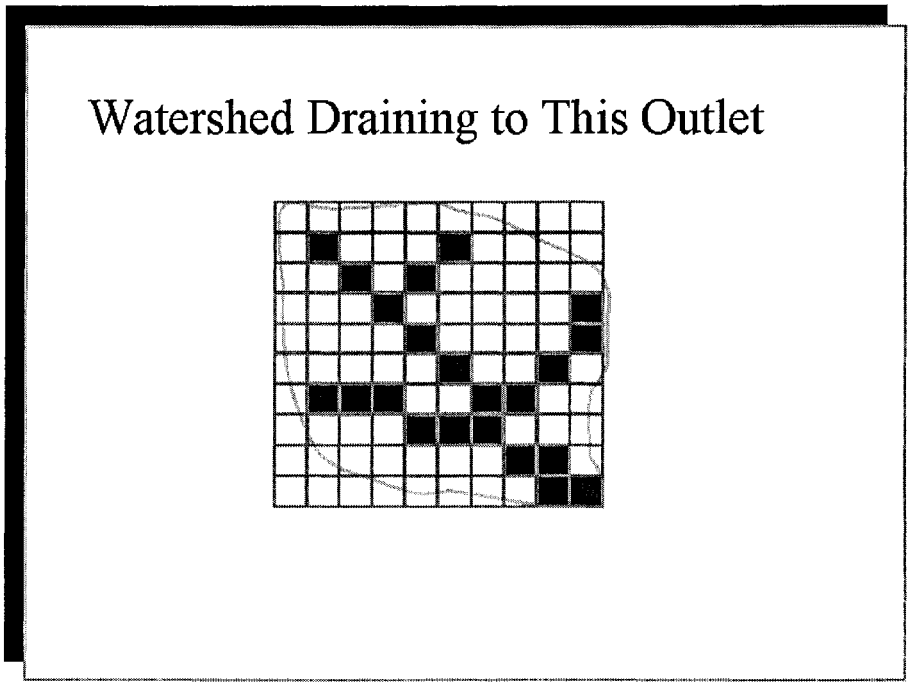


**Figure 9**

# APPENDIX D: SPATIAL INTERPOLATION TECHNIQUES IN ARCVIEW GIS

## 1. Spline (Regularized and Tension)

Spline interpolation is referred to as the basic minimum curvature technique or thin plate interpolation as it possesses two main features: (a) the surface must pass exactly through the data points, and (b) the surface must have minimum curvature. The latter is accomplished by minimizing the cumulative sum of the squares of the second derivative terms of the surface, taken over each point on the surface. Rapid changes in gradient or slope (the first derivative) may occur in the vicinity of the data points; hence this model becomes unsuitable for estimating second derivative (curvature).

The Regularized option, identified in the aType argument, modifies the minimization criterion so that the third derivative terms are incorporated into the minimization criteria. The aWeight argument specifies the weight attached to the third derivative terms during minimization. Higher values of this term lead to smoother surfaces. Values between 0 and 1 are suitable. Using the Regularized option ensures a smooth surface, together with smooth first-derivative surfaces. This technique is useful if the second derivative of the interpolated surface needs to be computed. For the purpose of this analysis, the weight was taken as "1" and the number of neighboring points used is "8".

The Tension option, identified in the aType argument, modifies the minimization criterion so that first-derivative terms are incorporated into the minimization criteria. The aWeight argument specifies the weight attached to the first-derivative terms during minimization. A weight of 0 results in the basic thin plate Spline interpolation. Using a larger value of weight reduces the stiffness of the plate, and, as it approaches infinity, the surface approximates the shape of a membrane, or rubber sheets passing through the points. For the purpose of this analysis, the weight was taken as "1" and the number of neighboring points used is "8". The Regularized option usually produces more smooth surfaces than those created with the Tension option. Higher values used for the weight parameter produce smoother surfaces in the Regularized option.

**2. Inverse distance weighted (IDW)**

Inverse distance weighted (IDW) interpolation determines cell values using a linearly weighted combination of a set of sample points. The weight is a function of inverse distance. IDW allows the user to control the significance of known points upon the interpolated values, based upon their distance from the output point. The interpolation can be shifted from local to global by changing the power. A larger power will result in less influence from surrounding points, i.e., nearby data will have the most influence, and the surface will have more detail (be less smooth). The power is a positive, real number. A common value is 2.

The characteristics of the interpolated surface can also be controlled by limiting the input points for calculating each interpolated point. The input can be limited by the number of sample points to be used (specified as a variable Radius object), or by a radius (specified as a fixed Radius object), within which all points are to be used in the calculation of the interpolated locations. The radius object to be used is identified through the Radius argument. The output value from a cell using IDW is limited to the range of values used to interpolate. Because the IDW is a weighted distance average, the average cannot be greater than the highest, or less than the lowest, input. Therefore, it cannot create ridges or valleys if these extremes have not already been sampled. The influence of an input point on an interpolated value is isotropic. Since the influence of an input point on an interpolated value is distance related, IDW is not "ridge preserving". The best results from IDW are obtained when sampling is sufficiently dense with regard to the local variation the user is attempting to simulate. If the sampling of input points is sparse or very uneven, the results may not sufficiently represent the desired surface. For the purpose of this analysis, the Radius is specified as variable and the number of points used is "8".

**3. Kriging** (Ordinary: Spherical, Circular, Exponential, Gaussian, and Linear) (Universal: Universal1 and Universal2)

Unlike the other interpolation models, Kriging involves an interactive investigation of the spatial behavior of the phenomenon before generating the output surface. It is based on the regionalized variable theory, which assumes that the spatial variation in the

phenomenon is statistically homogeneous throughout the surface; that is, the same pattern of variation can be observed at all locations on the surface. This hypothesis of spatial homogeneity is fundamental to the regionalized variable theory. Data sets known to have spikes or abrupt changes are not appropriate for the Kriging technique. In some cases, the data can be pre-stratified into regions of uniform surface behavior for separate analysis.

The spatial variation is quantified by the semi-variogram. The semi-variogram is estimated by the sample semi-variogram, which is computed from the input point data set. The value of the sample semi-variogram for a separation distance, referred to as the lag, is the average squared difference in value between pairs of input sample points separated by that distance. The sample semi-variogram is calculated from the sample data with the equation:

$$\gamma(h) = \frac{1}{2n} \sum_{i=1}^{n} \{Z(X_i) - Z(X_i - h)\}^2 \qquad (D.1)$$

where h: is the separation distance (the lag); n: is the number of pairs of sample points separated by distance h; z: is the spatial variation of the phenomenon (rainfall, elevation, etc.) The semi-variogram is modeled by fitting a theoretical function to the sample semi-variogram. There are several important features worth noting in the sample semi-variogram. At relatively short lag distances of (h), the semi-variance is small. It increases, however, with the distance between the pairs of sample points. At a distance referred to as the range, the semi-variance levels off to a relatively constant value, referred to as the sill. This implies that beyond this range distance, the variation in (z) values is no longer spatially correlated. Within the range, the z-value variation is smaller when the pairs of sample points are closer together.

The extent of the horizontal axis of the semi-variogram is determined by the distance between the most widely separated pair of points in the input sample data. The maximum distance separating the pairs of points used to fit the mathematical function is determined by the Radius object specified in the aRadius argument. The aGrid.MakeKriging request offers

two types of surface estimators: Ordinary Kriging and Universal Kriging. Ordinary Kriging is represented by the SPHERICAL, CIRCULAR, EXPONENTIAL, GAUSSIAN, and LINEAR methods. With these options, available through the aType argument, Kriging uses the mathematical function specified with the method argument to fit a line or curve to the semi-variance data in the semi-variogram. Ordinary Kriging assumes that the variation in (z) values is free of any structural component (drift). These five models are provided to ensure that the necessary conditions of the variogram model are satisfied, which is not always possible with interactive "manual" variogram fitting. In this analysis, the range used is "8000 m" and the number of points is "8".

Universal Kriging, represented by the UNIVERSAL1 and UNIVERSAL2 methods, assumes that the spatial variation across the surface has a structural component (drift). Drift is a systematic change in the cell values at a particular scale. This scale is related to the radius of the search area. The goal is to change the search radius to find the scale at which the drift can be detected and the variance is lowest. Therefore, it is not recommended that a variable Radius object be created for Universal Kriging. UNIVERSAL1 uses a first order polynomial to approximate the drift, while UNIVERSAL2 uses a second order.

### 4. Trend Surface

The linear trend surface interpolator creates a floating-point grid. It uses a polynomial regression to fit a least-squares surface to the input points. This allows the user to control the order of the polynomial used to fit the surface. Trend interpolation is easy to understand by considering a first-order polynomial. A first-order linear trend surface interpolation simply performs a least-squares fit of a plane to the set of input points. Trend surface interpolation creates smooth surfaces. The surface generated will seldom pass through the original data points since it performs a best fit for the entire surface. When an order higher than 1 is used, the interpolator may generate a grid whose minimum and maximum might exceed the minimum and maximum of the input points.

As the order of the polynomial is increased the surface being fitted becomes

progressively more complex. A higher order polynomial will not always generate the most accurate surface, since it is dependent upon the data. The lower the RMS error, the more closely the interpolated surface represents the input points. The most common order of polynomials is 1 through 3 (2 in this paper).

## 5. Theissen Polygons

Theissen polygons are probably the most common approach for modeling the spatial distribution of rainfall. The approach is based on defining the area closer to a gage then any alternate gage and the assumption that the best estimate of rainfall on that area is represented by the point measurement at the gage. Because the basis of the model is geometry and gage location, implementation of Theissen polygons in a GIS environment is not difficult. However, an impact of the use of Theissen polygons is the development of discontinuous surfaces defining the rainfall depth over the area under study. This effect arises at the boundaries of the polygons where a discrete change in rainfall depth occurs.

# APPENDIX E: QUESTIONS AND ANSWERS

## 1. Can you explain the MOVE1 method (a numerical example)?

In this exercise, a time series (y), which represents monthly precipitation data, should be filled using another complete time series (x).

| no. | month | y | x | $(y_i - \bar{y})^2$ | $(x_i - \bar{x})^2$ | $\tilde{y}_i = a + bx_i$ |
|---|---|---|---|---|---|---|
| 1 | 9 | 200 | 400 | 75625 | 360000 | |
| 2 | 10 | 300 | 600 | 30625 | 160000 | |
| 3 | 11 | 400 | 800 | 5625 | 40000 | |
| 4 | 12 | 500 | 1000 | 625 | 0 | |
| 5 | 1 | 600 | 1200 | 15625 | 40000 | |
| 6 | 2 | 700 | 1400 | 50625 | 160000 | |
| 7 | 3 | 600 | 1400 | 15625 | 160000 | |
| 8 | 4 | 500 | 1200 | 625 | 40000 | |
| 9 | 5 | ***na*** | 1000 | | | ***475*** |
| 10 | 6 | ***na*** | 800 | | | ***384.8612*** |
| 11 | 7 | ***na*** | 600 | | | ***294.7224*** |
| 12 | 8 | ***na*** | 400 | | | ***204.5836*** |

| $\bar{y} = 475$ | $\bar{x} = 1000$ | $s_{yy} = \sum (y_i - \bar{y})^2 = 195000$ | $s_{xx} = \sum (x_i - \bar{x})^2 = 960000$ |
|---|---|---|---|

| | |
|---|---|
| $s_{yy} / s_{xx}$ | = 0.203125 |
| $b = \sqrt{s_{yy}} / s_{xx}$ | = 0.450694 |
| $a = \bar{y} - b\bar{x}$ | 475-0.450694*1000 = 24.306 |

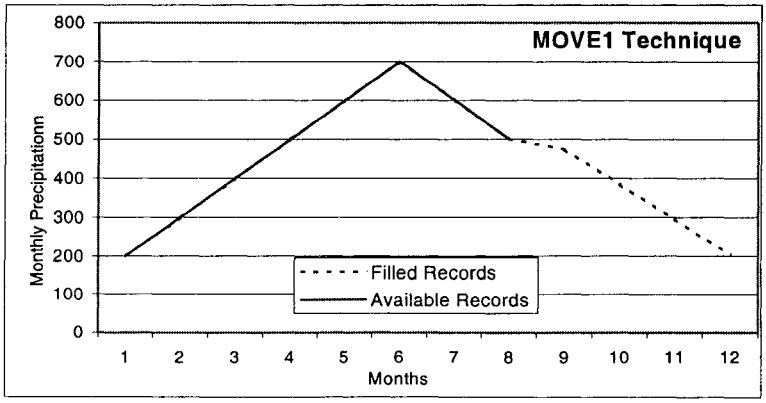

**2. What is the Least Squares method? And how the parameters are estimated? What is weighted LS? Residual plots?**

Minimizing the sum of squares of errors. A parameter is the amount of increase in a dependent variable if the independent variable is increased by a unit while all other parameters are held at a zero value. Parameters are estimated by regressing each independent variable against the other and determining the residuals and then regressing the dependent variable against the sets of residuals. Weighted LS is used when the variance of the residuals is not the same. Residual plots can be generated as residuals versus observed or estimated values.

**3. What is the difference between trend surface technique and the MLR?**

The trend surface is a polynomial regression while MLR is linear regression.

**4. What is the fetch distance?**

It is the distance over which the wind is blowing. It can be calculated by knowing the wind speed and the time it had been blowing for.

**5. What is the relation between current speed and wind speed in Figure 8.20?**

Current speed is approximately 3 to 6 % of wind speed.

**6. What are the different types of rain?**

Cyclonic precipitation: results from the lifting of air converging into a low pressure area, or cyclone.

Convective precipitation: is caused by the rising of warmer, lighter air in colder denser surroundings.

Orographic precipitation: results from mechanical lifting over mountain barriers.

**7. What is continentality?**

When clouds move inland from the coast, they become isotopically depleted progressively, as a result of their loss of moisture. The isotopic signatures also reflect the topography of the continent. Mountain chains deplete the clouds too, because of orographically forced rainout. The degree of continentality, as defined by the isotopes, is a function of the effect of the steep temperature gradient between the ocean and the interior especially in winter. This leads to progressive isotopic depletion, as precipitable water is lost with the passage of air inland. This process prevails for as long as the ocean is the dominant moisture source and re-evaporated moisture does not play a major role.

**8. What are network densities for urban, rural, mountain, etc areas?**

The following minimum densities of precipitation networks have been recommended by

WMO (1974) for general hydrometeorological purposes:

1. For flat regions of temperate, Mediterranean, and tropical zones, 600 to 900 $km^2$ per station.
2. For mountainous regions of temperate, Mediterranean, and tropical zones, 100 to 250 $km^2$ per station.
3. For small mountainous islands with irregular precipitation 25 $km^2$ per station.
4. For arid and polar zones, 1500 to 10000 $km^2$ per station.

**9. What is adjusted $R^2$?**

Adjusted $R^2$ is a lower estimate for $R^2$ and equals = $1- (1-R^2)[(n-1)/(n-p)]$. The less parameters you use the less difference it is between the real $R^2$ and the adjusted one.

**10. What is a statistical model and an empirical model? What are other kinds of models?**

***A statistical model*** is a relationship between variables by means of parameters (the parameters are the quantitative impact of variables on a certain process). But we fit a model to data from a sample almost always to make a statement about the model in the population. ***An empirical model*** is a simple relationship that locally approximate the true functions over a limited region. Frequently the mechanism underlying a process is not understood sufficiently well, or is too complicated, to allow an exact model to be derived from theory. Other models are:

***A deterministic model*** is a model that doesn't consider randomness. A given input always produces the same output and is used to make forecasts.

***A stochastic model*** has outputs that are at least partially random and is used to make predictions.

**11. Talk about the effect of aspect and altitude.**

The following chart shows a hypothetical mountain and the effect of meteorological precipitation on it. As can be seen from this example, when there is a flux in meteorological precipitation, a vertical shift in moisture regime occurs. Whereas in flat non-mountainous regions, a horizontal shift of moisture regime occurs. This example shows how it is possible for plants to survive periods of environmental flux on mountains by transposing their distribution vertically, whereas on flat areas they would possibly die out. Laps Rate is of importance when considering evolutionary processes on mountains.

Meteorological precipitation is not the only environmental factor which shows this tendency. As is known, temperatures drop as altitude increases, and the eastern slopes are usually cooler than the western slopes. The Laps Rate of air is highly variable, being affected by radiation, convection and condensation processes. In times of temperature fluctuations, plants might either become transposed vertically, or gradually change their preference of

aspect. In this respect, vagile plants with a short life expectancy are able move from one habitat to another as observed in periods of drought caused by El Niño.

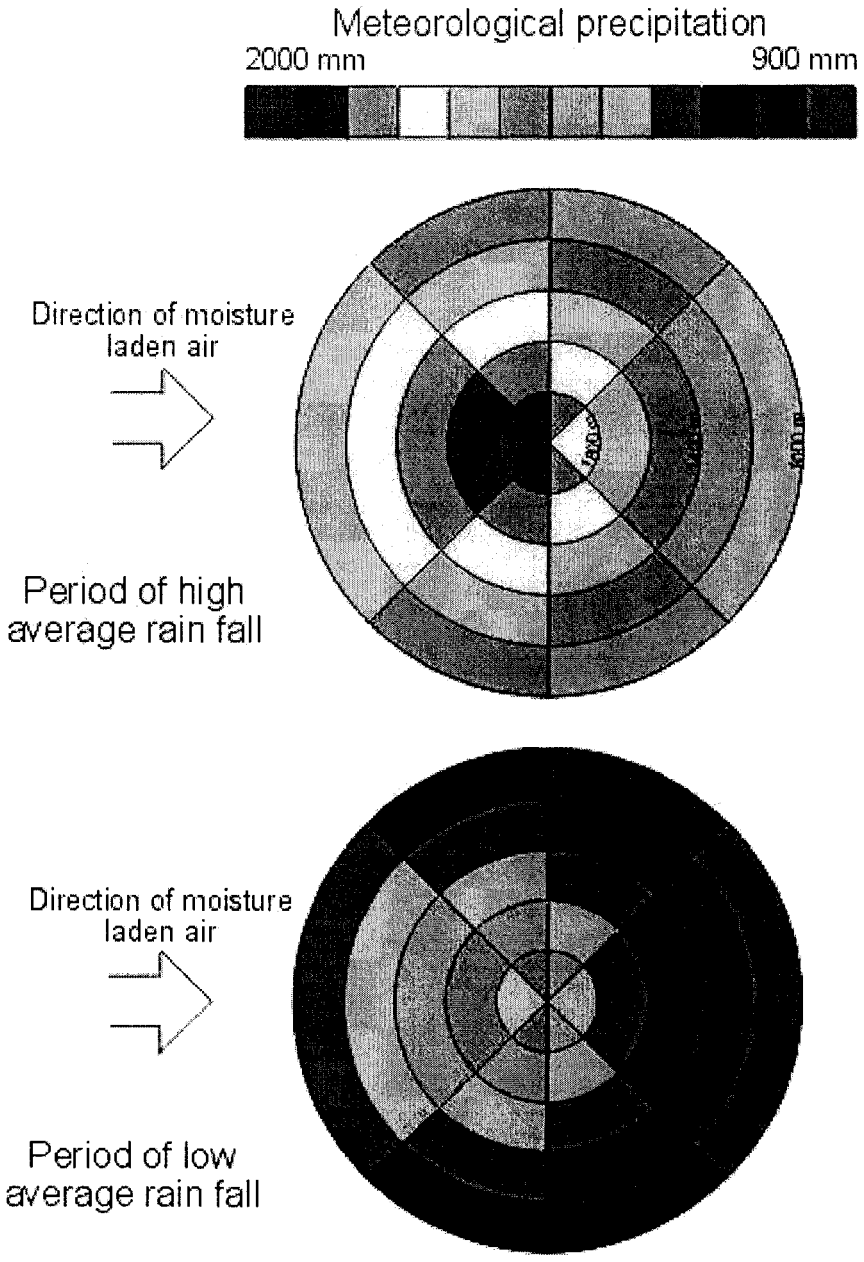

## 12. Give an example formula for precipitation and reference evapotranspiration in Crete?

**Peff**

| x | y |
|---|---|
| 1 | 140 |
| 2 | 125 |
| 3 | 92 |
| 4 | 45 |
| 5 | 15 |
| 6 | 5 |
| 7 | 0 |
| 8 | 5 |
| 9 | 10 |
| 10 | 55 |
| 11 | 110 |
| 12 | 123 |
| 13 | 140 |

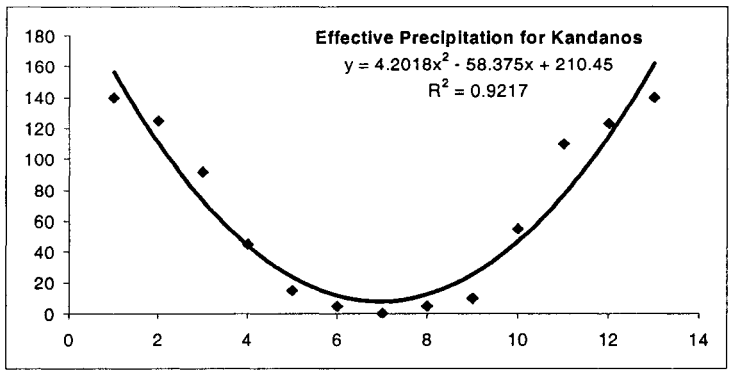


**Eto**

| x | y |
|---|---|
| 1 | 80 |
| 2 | 85 |
| 3 | 120 |
| 4 | 140 |
| 5 | 190 |
| 6 | 250 |
| 7 | 320 |
| 8 | 310 |
| 9 | 220 |
| 10 | 150 |
| 11 | 100 |
| 12 | 90 |
| 13 | 70 |

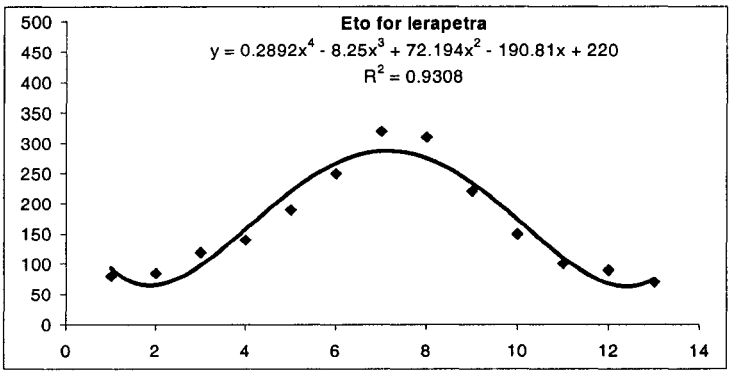


## 13. Why does Spline give negative values sometimes?

The problem with Spline is that it tries to fit a smooth curvature to the data points. If there is abrupt changes in data values within a short distance, the interpolation results may not be very accurate and reliable. There could be 3 potential reasons for obtaining negative values:

1) a big difference in data values
2) not enough sampling in space
3) there is a big unmonitored area between the last sampling locations and the border of the region.

To resolve the problem, I can suggest either of 2 solutions. The two solutions are actually aiming at the same goal and that is to avoid the risk of extrapolation by:

1) trying to get more samples close to the border all around the region (from the inside) over which you are interpolating, or
2) drawing a new (imaginary) border line that will be right outside the external sampling points. See figure below.

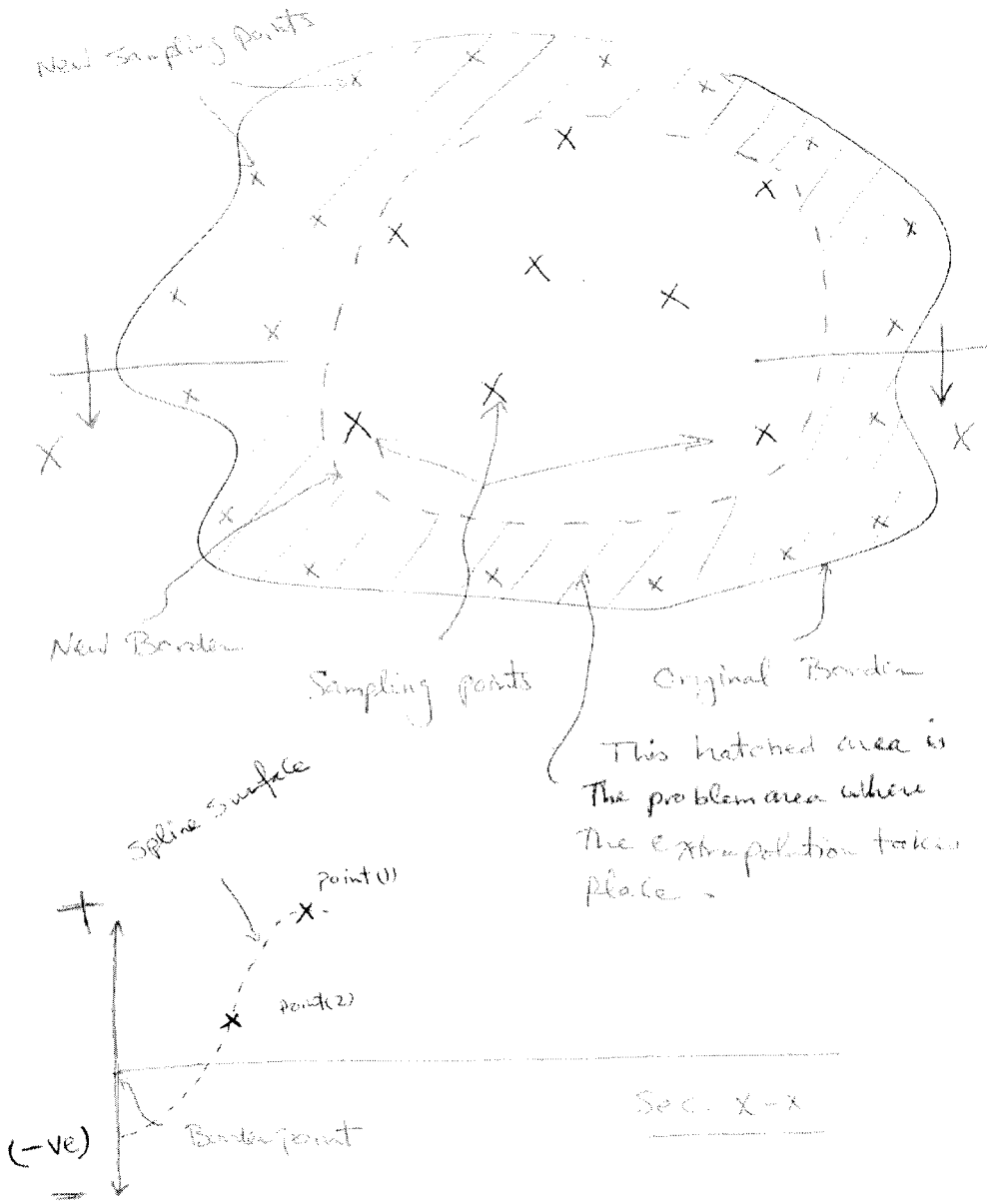

**14. What are the statistics used for error analysis and frequency analysis?**

$$\text{StDev} = \sqrt{\frac{(x_i - \bar{x})^2}{n-1}} \qquad \text{StError} = \frac{\text{StDev}}{\sqrt{n}}$$

$$\text{CoefOfVar} = \frac{\text{StDev}}{\text{Mean}} \qquad \text{MeanAbsError} = \frac{|x_{obs} - x_{est}|}{n}$$

$$\text{StDevAbsError} = \sqrt{\frac{(|e_i| - \bar{e})^2}{n-1}} \qquad \text{VarAbsError} = \frac{(|e_i| - \bar{e})^2}{n-1}$$

$$\text{RMSE} = \sqrt{\frac{(x_{est} - x_{obs})^2}{n}}$$

Statistical Significance for t-test

| | | | |
|---|---|---|---|
| (1) one-sided test | rejection region | $p \geq \alpha$ | (e.g. $\mu > \mu_o$) |
| (2) two-sided test | rejection region | $p \geq \alpha/2$ | (e.g. $\mu \neq \mu_o$) |

$$\text{CoeffOfSkewness} = \frac{n\sum_{i=1}^{n}(x_i - \bar{x})^3}{(n-1)(n-2)s^3}$$

$$\text{CoeffOfKurtosis} = \frac{n^2(n+1)\sum_{i=1}^{n}(x_i - \bar{x})^4}{(n-1)(n-2)(n-3)s^4}$$

**Kurtosis**

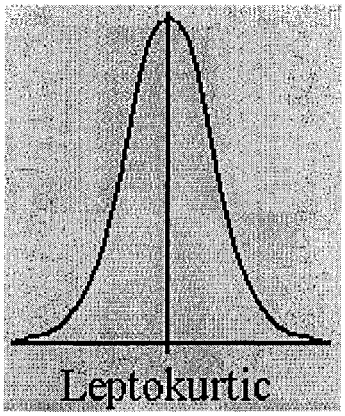


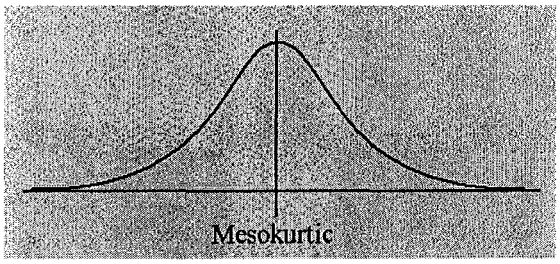


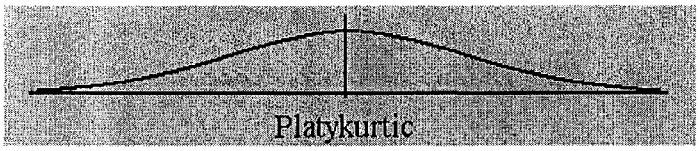


**Skewness**

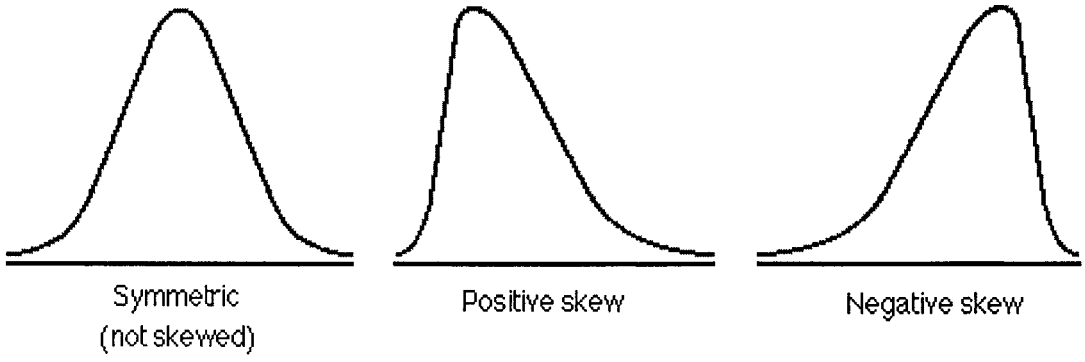

## APPENDIX F: MORE FIGURES FOR CHAPTER 4

*Continue: Figures 4.14 and 4.15*

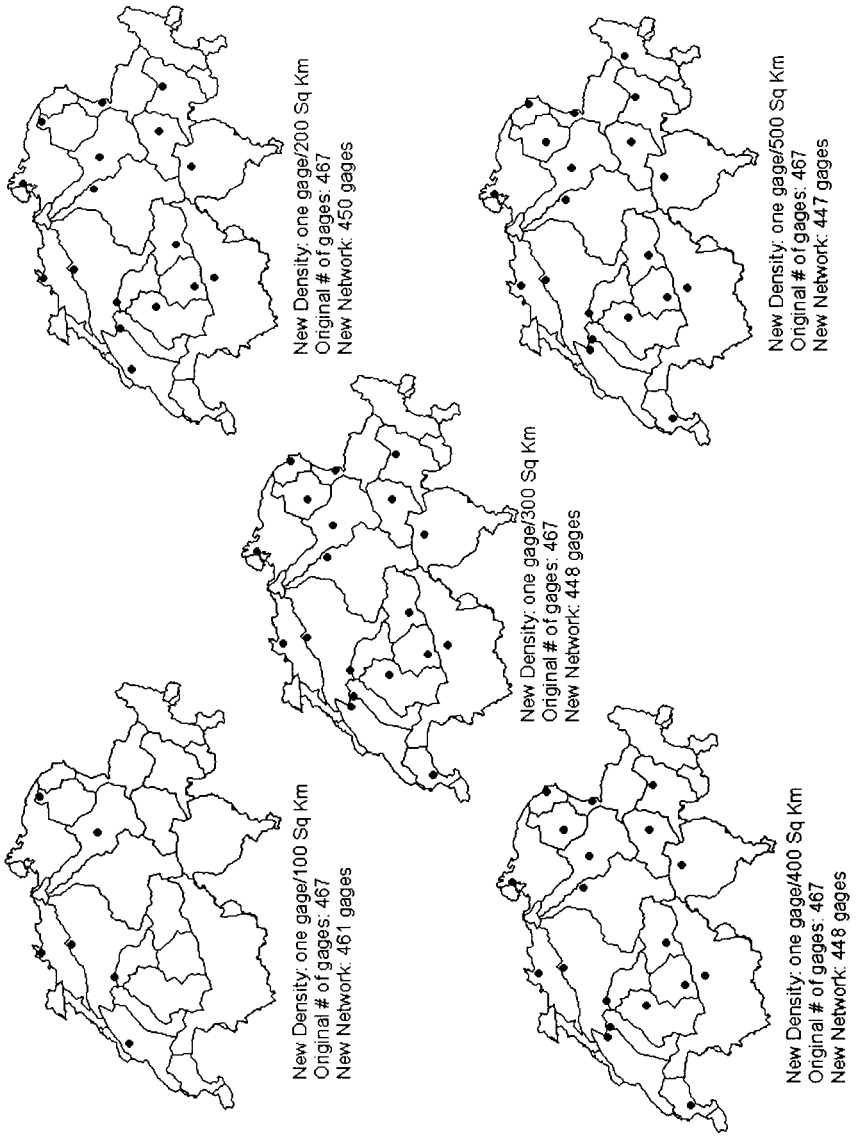


**Figure 4.14a:** Based on the VAR approach, the candidate gauges for removal based on the criterion: eliminate one gauge per watershed/subnetwork

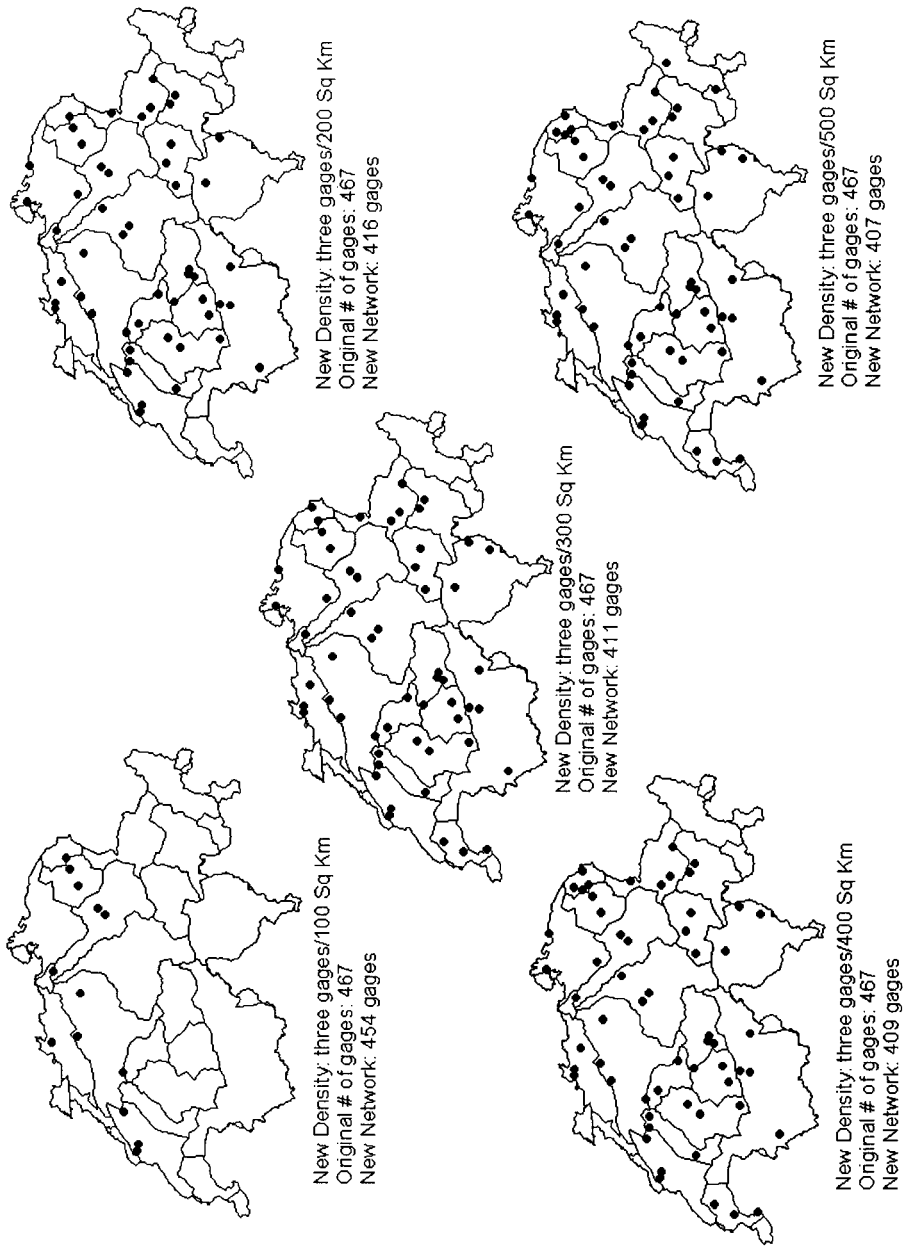


**Figure 4.14c:** Based on the VAR approach, the candidate gauges for removal based on the criterion: eliminate three gauges per watershed/subnetwork.

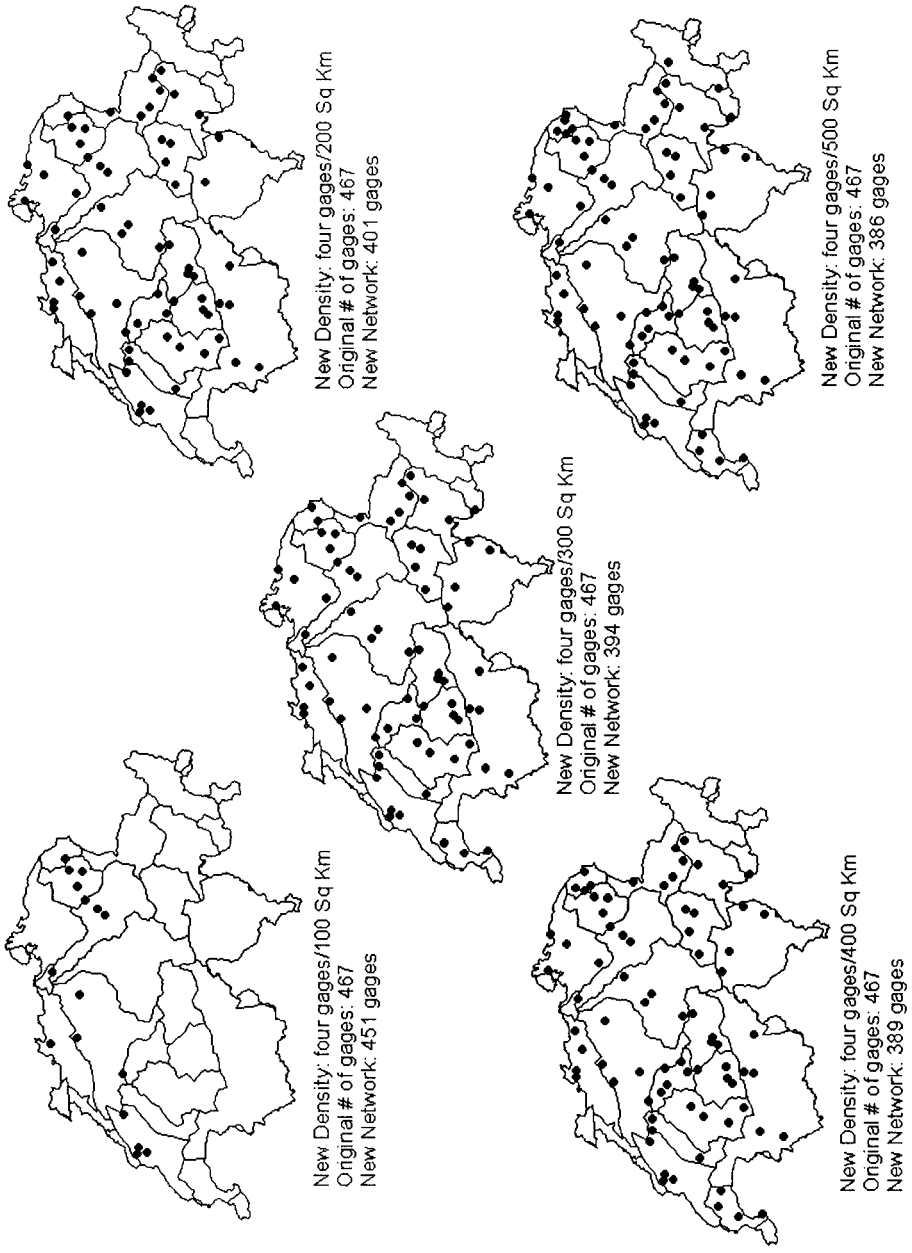


**Figure 4.14d:** Based on the VAR approach, the candidate gauges for removal based on the criterion: eliminate four gauges per watershed/subnetwork.

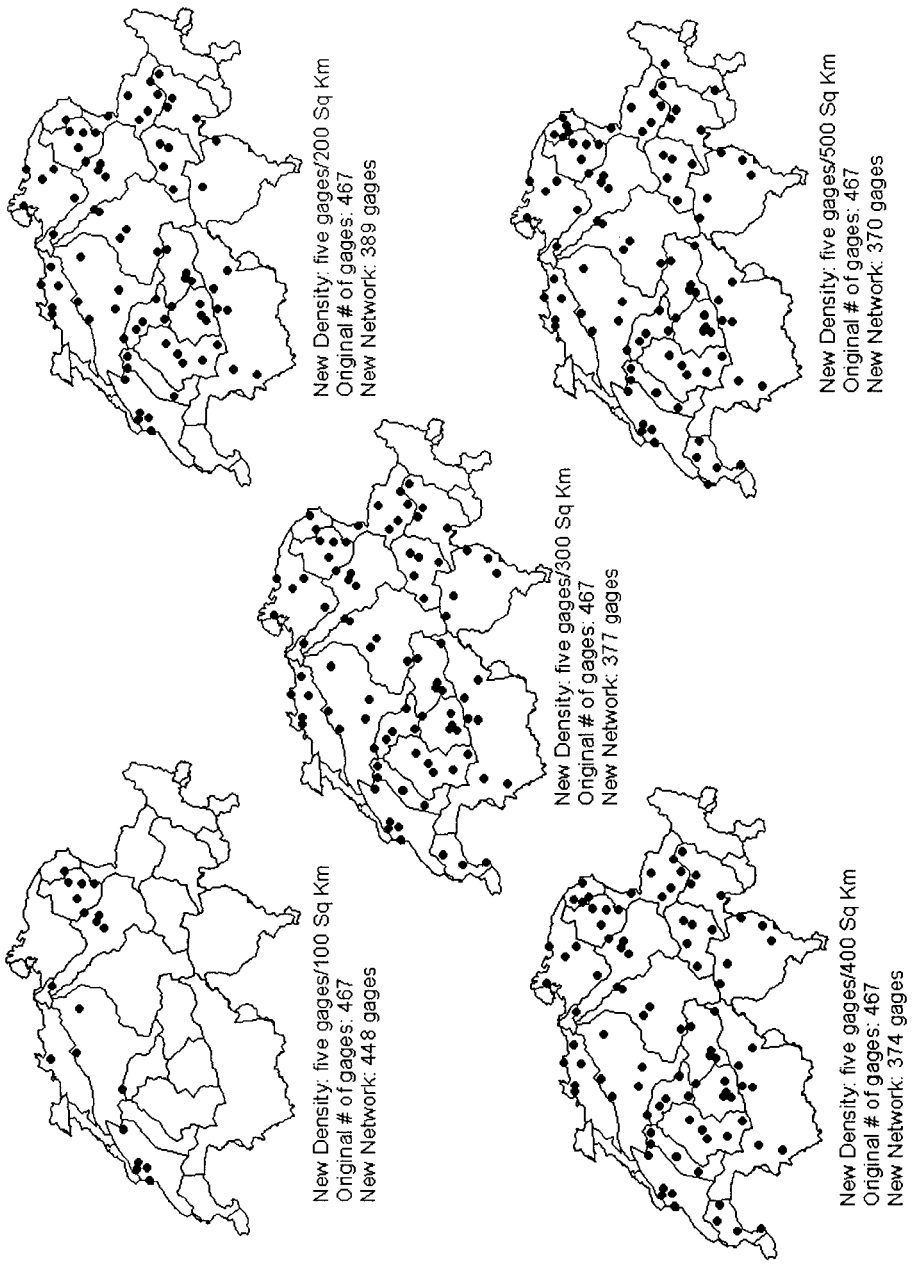


**Figure 4.14e:** Based on the VAR approach, the candidate gauges for removal based on the criterion: eliminate five gauges per watershed/subnetwork.

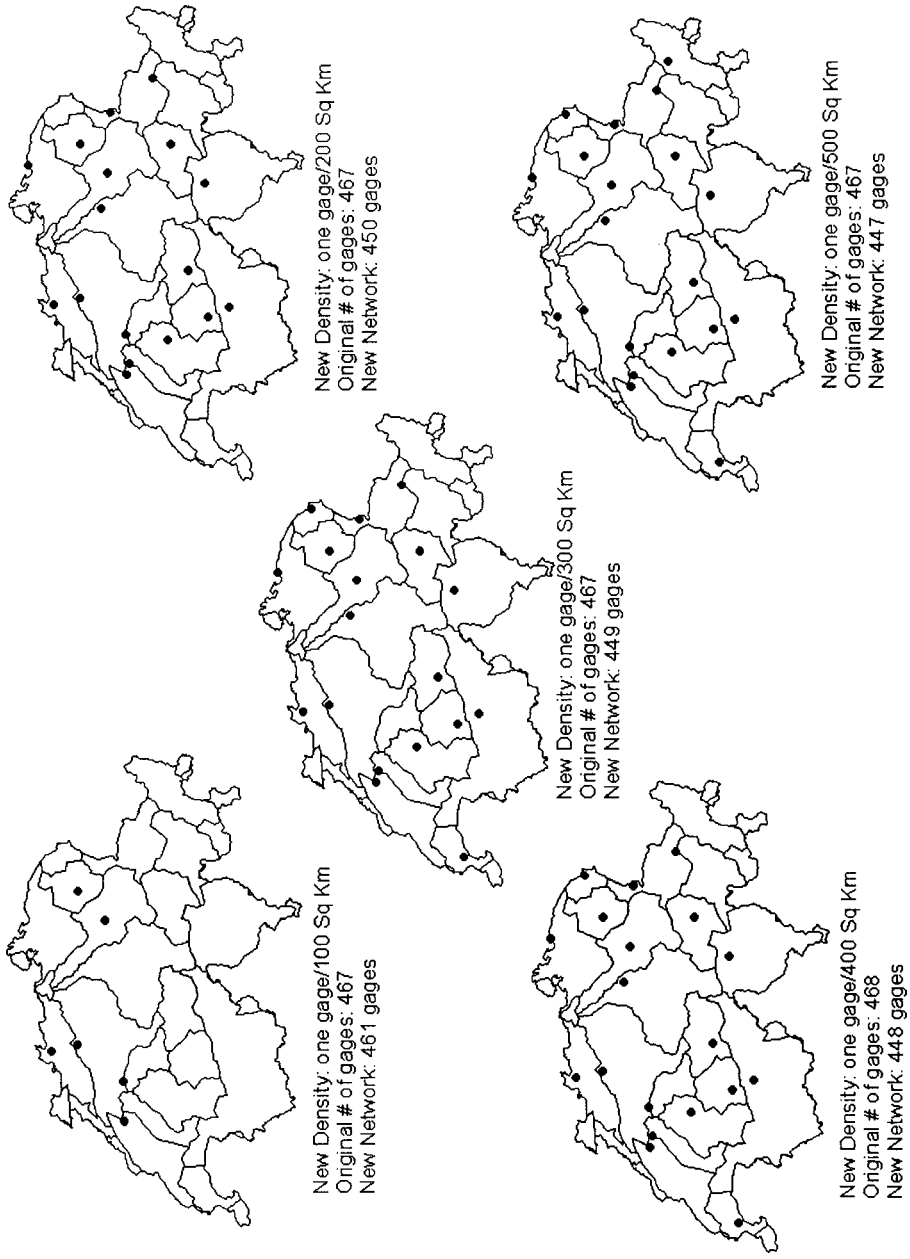


**Figure 4.15a:** Based on the STDEV approach, the candidate gauges for removal based on the criterion: eliminate one gauge per watershed/subnetwork.

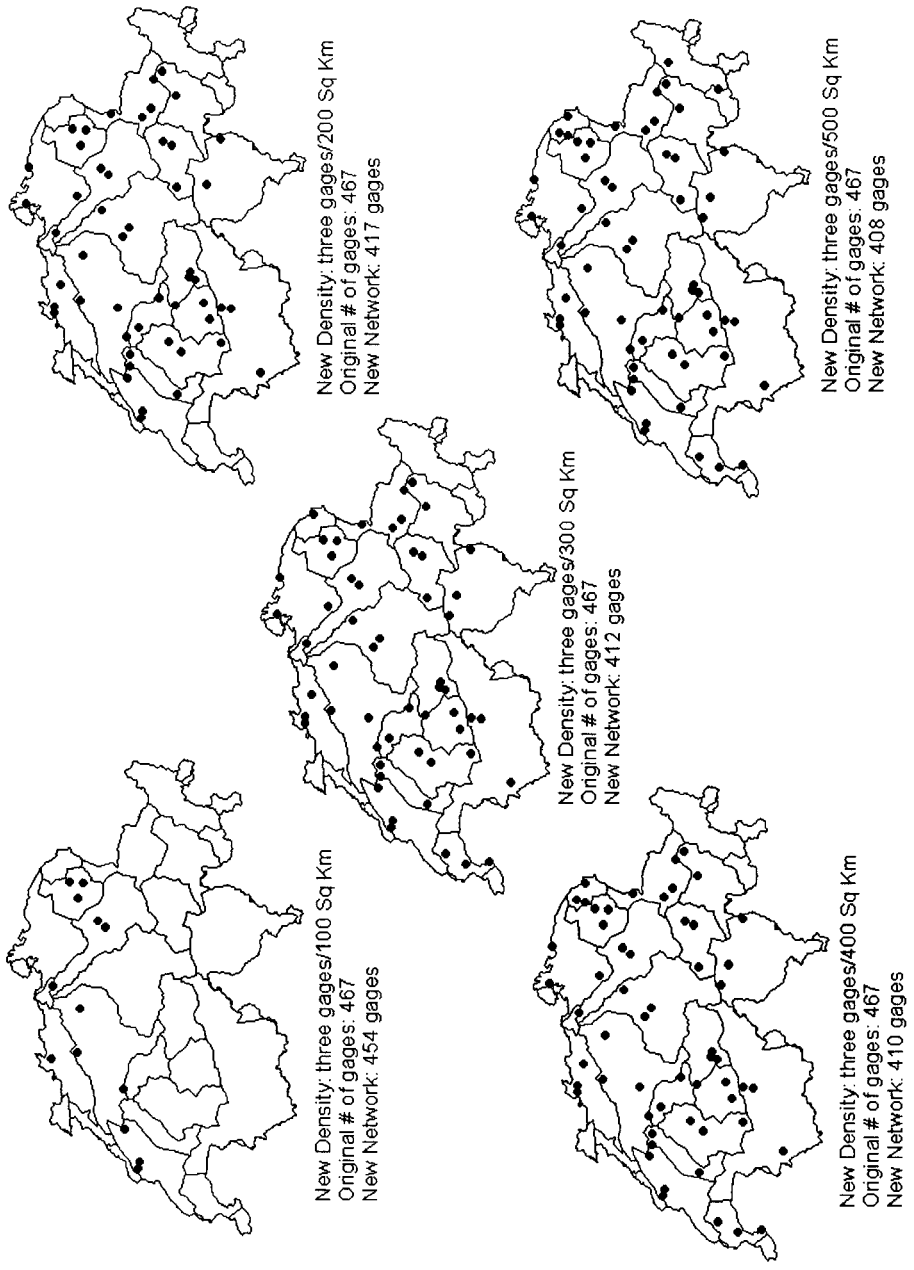


**Figure 4.15c:** Based on the STDEV approach, the candidate gauges for removal based on the criterion: eliminate three gauges per watershed/subnetwork.

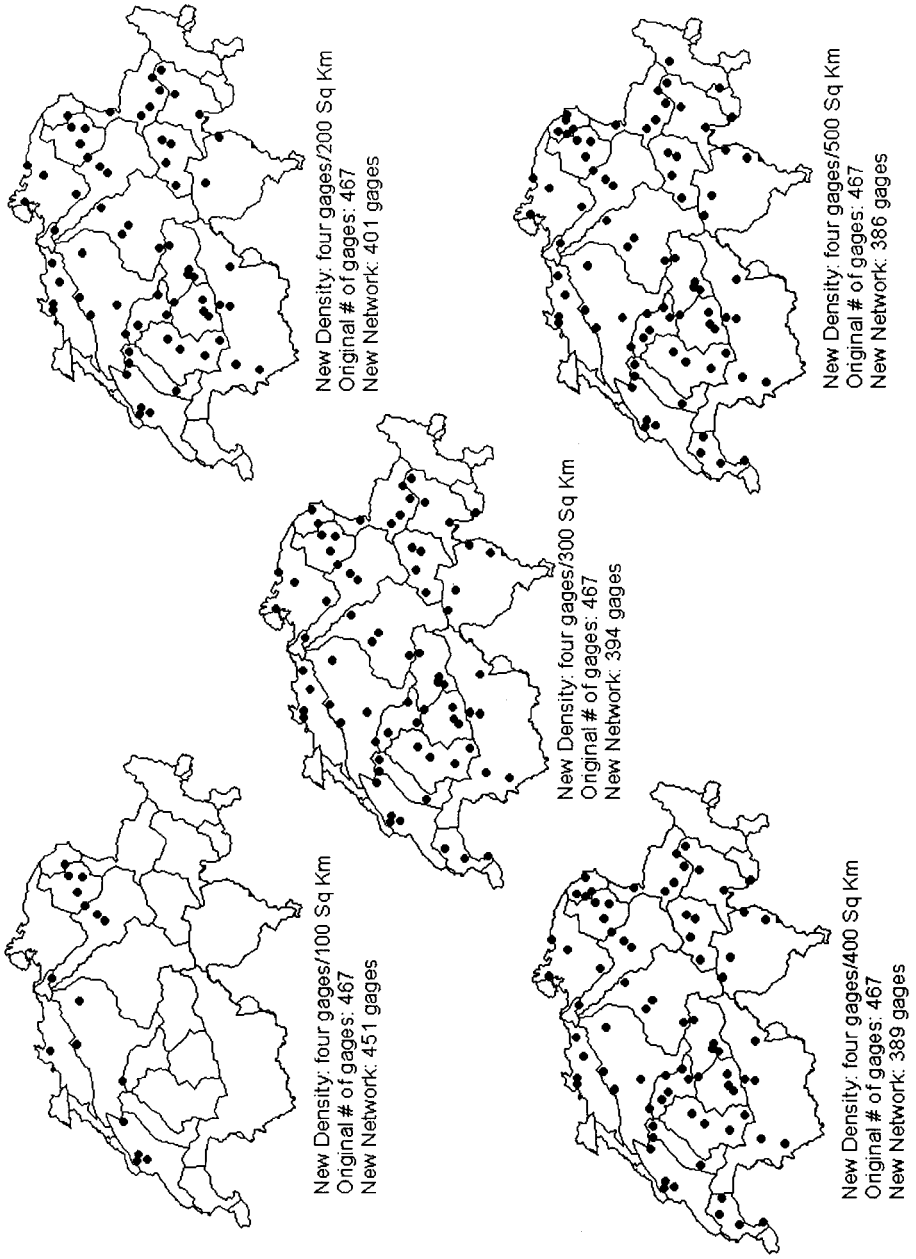


**Figure 4.15d:** Based on the STDEV approach, the candidate gauges for removal based on the criterion: eliminate four gauges per watershed/subnetwork.

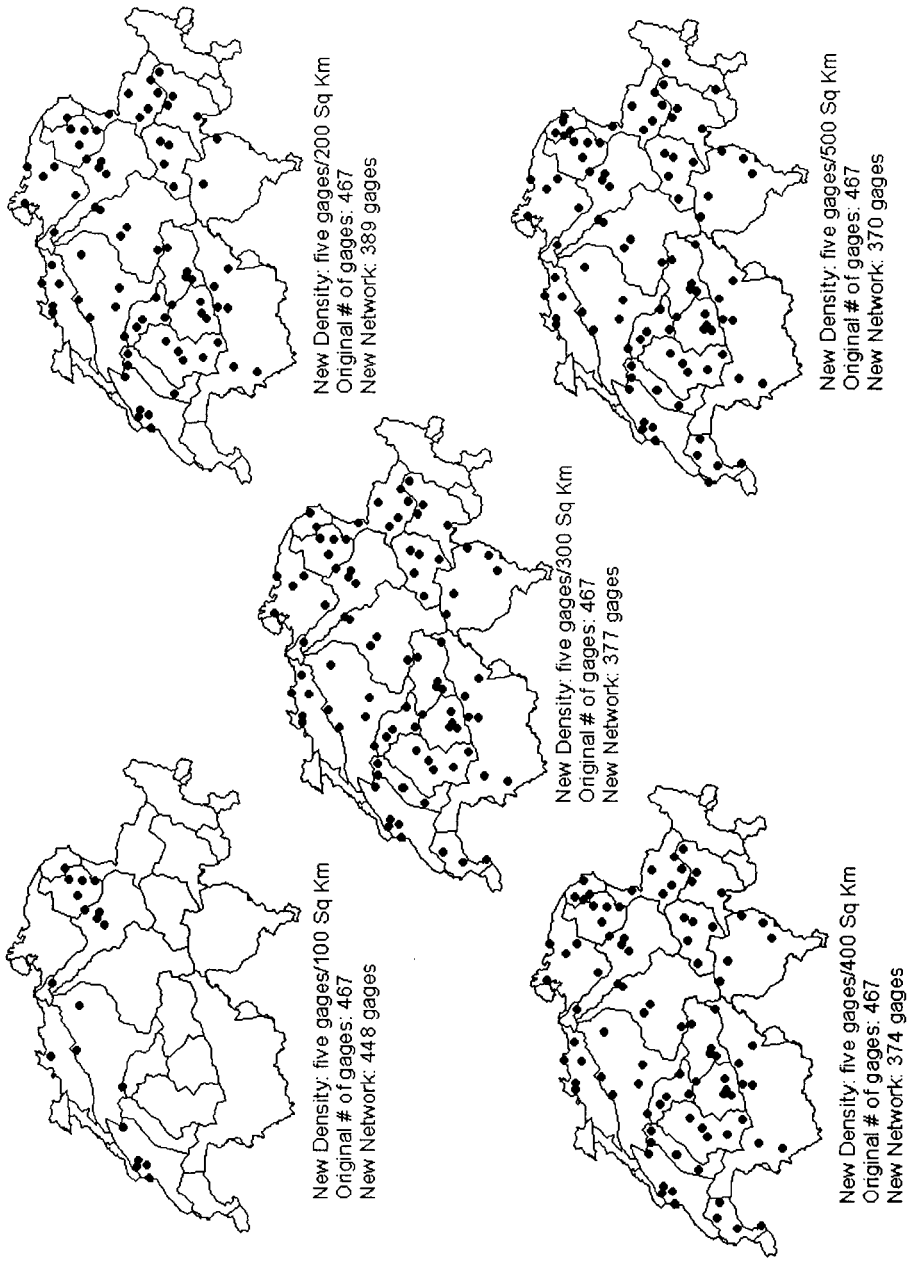


**Figure 4.15e:** Based on the STDEV approach, the candidate gauges for removal based on the criterion: eliminate five gauges per watershed/subnetwork.

# APPENDIX G: MORE FIGURES FOR CHAPTER 5

## G.1 Urbanization

Many parts of the world now are being urbanized. The majority of the population live in or near cities. Big cities mean big development over large areas, which can certainly have an impact on the local water supply. It's not that hard to imagine that as cities grow, things happen that can harm the quality of the local water resources. That is why most governments must take measures to protect rivers, streams, lakes and aquifers when small towns grow into big cities.

Refer to this web-site http://royal.okanagan.bc.ca/mpidwirn/urbanization/urbanization.html for more information about urbanization, where these excerpts were taken from:

### G.1.1 Environmental Impacts of Urbanization

Environmental problems associated with urbanization tend to be similar in both developed and developing countries. For most cities in developed countries, population growth is beginning to level off. In the developing world, rates of population growth in urban areas is increasing as more and more people move from rural areas in search of jobs and better living conditions. For example, Mexico City, Cairo, Jakarta, Delhi, Bombay, Karachi, Sao Paulo, Beijing and Shanghai are predicted to more than double their population size from 1985 to the year 2025.

Atmosphere and Climate

Urbanization can not only alter local climate but it can also pollute the atmosphere.

1. Climate. Temperature, winds, and precipitation patterns can all be altered due to urbanization.

a) Temperature. The temperature of a city is often warmer than that of surrounding rural areas. Temperature contrast is usually slight but differences can be as high as 10 degrees Celsius in some areas. Because of this, cities are often referred to as urban heat islands. As an urban area grows, a regional heat island can develop impacting regional climate. Temperature increases can result from numerous factors.

i) Roads, roofs, and buildings conduct more heat than vegetated areas. Energy builds up during the day and this stored heat is then released back to the atmosphere at night, increasing temperatures at the surface.

ii) The construction of roads, parking lots and buildings acts to waterproof the surface of a city. Channeled precipitation quickly drains into nearby storm sewers away from the surface. Less moisture available for evaporation (which is a cooling effect) means more radiation can go into heating.

iii) There are a number of heat sources within a city that can contribute to increased temperatures. Combustion of fossil fuels for industry, transportation and heating as well as human metabolism are all very concentrated in a city and supply extra heat to the atmosphere.

b) Cloudiness and Precipitation. Urban climates are generally cloudier and experience more precipitation than their rural counterparts. The air pollution, associated with large cities provides many particles that act as nuclei for cloud droplets, influencing cloud and precipitation development. In addition, convection currents associated with urban heat islands cause cooling and condensation of water vapor.

c) Wind. The buildings in an urban area provide a landscape that is more rough than vegetative cover. Surface roughness has a major impact on the speed and structure of wind near the surface of the earth. Closely spaced buildings reduce surface winds to almost nothing. With more irregular spaced buildings, eddies can develop at the corner of the building that blow down to ground level.

2. Air Pollution. Air pollution is a major problem associated with most urban areas. It is believed that more than 1.1 billion people reside in cities with extremely poor air quality. Sources of air pollution include industrial and vehicle emissions and energy production. Often, energy use per capita is less in an urbanized area than in a rural area due to energy efficient apartments, attached housing and mass transit. The sheer number of people involved, however, still makes urban areas major contributors to air pollution. Some problems include photochemical smog, acid rain, and the enhanced greenhouse effect. One study revealed that 40 % of the total North American carbon dioxide emissions came from 50 urban areas. The circulation patterns associated with an urban heat island creates a dome over the city, trapping pollutants. Concentrations of pollutants such as suspended particulate matter can be thousands of times greater than rural areas.

Water Resources

Urbanization can alter several aspects of the hydrosphere. Urban development causes changes in hydrology, depletion of supplies and aquatic pollution.

1. Hydrology. Urbanization completely alters the landscape of an area, impacting local hydrology. Roads, parking lots and buildings do not absorb precipitation as vegetation does which increases runoff. In addition the water quickly drains from streets into storm sewers. Often wetlands, which efficiently act to absorb excess water, are filled in. The development of floodplains for homes and industry, remove land where excess runoff could go. With all the excess runoff and lack of adequate disposal places, there is an increase in both the number and magnitude of floods. The removal of vegetation from stream banks for

development, leaves the water exposed to the elements so that it is warmer in the summer and colder in the winter.

2. Consumption. Urban areas obtain their water from either surface sources or from ground water supplies. Not only does an increasing population put more demand on water resources but urbanized areas generally have a greater water demand per capita than rural areas. In most urban areas the price of water is relatively low (due to government subsidies) so there is no incentive for conservation. In addition, a lot of water is lost due to old, leaky distribution systems. Those cities without easy access to surface water supplies often use ground water. This can lead to land subsidence and salinization if withdrawal rates exceed the rate of recharge.

3. Water Pollution. There are many ways that urbanization contributes to the pollution of both surface and ground water. The dumping of wastes into waterways is common as they dilute and disperse pollutants. The current volume of wastes added is far beyond the capacity of these waters for effective dilution and dispersal. Over 220 million urban residents do not have access to clean drinking water. Some sources of aquatic pollution include industry, sewage, runoff and sediment.

Industry. Often industry is concentrated in urban areas, particularly in the developing world. Tanneries, metal plating operations, pulp mills and refineries contribute things such as PCB's, dioxins, pesticides, grease, oil, acids and heavy metals. In many areas of the world, industrial water pollution is declining due to government regulations on discharges.

Sewage. In an urban area, sewage can be a major source of water pollution. Sewage is a source of nutrients that can lead to eutrophication of lakes. Sewage also contains many pathogens such as cholera bacterium, hepatitis virus, and salmonellae all of which are hazardous to human health. In the developing world, 90% of the sewage are discharged, untreated into surface waters. Treatment usually removes only the pathogens so the nutrients remain to pollute the water.

Sediment. The construction of things such as buildings and streets result in substantial erosion. In fact, erosion rates can be 20,000 to 40,000 times higher than vegetated areas. Sediments end up in waterways reducing biological activity. Physically, sediments can build up in waterways causing floods. Finally, sediment pollution is not aesthetically pleasing.

Runoff. Urban runoff pollutes waterways as it contains pollutants from hundreds of sources. As water travels over the surface it picks up pollutants from cars, fertilizers, pesticides, etc. Most of the time, runoff often enters waterways without treatment.

Soils and Landscapes

Approximately 1% of the Earth's total land surface is urbanized. This small amount of land, however, has changed drastically from its original state. Further urban expansion will destroy many more valuable habitats. Urban expansion today is often as urban sprawl, low density developments that consume vast quantities of land. The conversion of a natural landscape to an urban area is essentially an irreversible process. Some habitats that are at risk due to urbanization include:

Agricultural lands. Often agriculture and cities develop in similar areas -- flat, well-drained soils close to water. Unfortunately expanding urban areas are consuming agricultural land. Agriculture then develops in new areas that may not be as productive. In Ontario, for instance, the destruction of 1 hectare of prime farmland means the agricultural development of 3 hectares of prairie land to obtain the same amount of productivity.

Coastal ecosystems such as wetlands, swamps, marshes and tidal flats. These areas are all very vulnerable to human development. Coastal areas are very popular for urban development. Currently over 1 billion people inhabit these areas. Often these ecosystems are drained and filled in prior to development. Wetlands act as a natural flood control, support many different species and are effective in filtering out pollutants. Development of these areas not only eliminates their productivity but can lead to enhanced coastal erosion.

Hillsides. As a city develops, it may run out of room and begin to develop on steep hillsides. This is common in developing countries, as squatters have nowhere else to live. Hills are unstable and subject to considerable erosion and landslides without native vegetation.

In addition to destroying habitats, urbanization impacts the soil. Development of an agricultural area for agricultural purposes causes the loss of fertile topsoil. The disposal of wastes is often in land disposal sites. Some of this garbage can contaminate soils rendering it useless in the future. Vehicular traffic contaminates soils with cadmium, lead, nickel, oil and grease. Road salt applied in the winter can also contaminate nearby soils. Paving over the surface prevents air and moisture from getting into the soil that is vital for micro-organisms and plant roots.

Plants and Animals

The main impact urbanization has on plants and animals is loss of habitat. Loss of suitable habitat can result from pollution, physical destruction, altering of local climate, or modification with grasses and shrubs. Habitat loss can cause some native species to become endangered or in severe cases extinct. In some cases, however, urbanization alters the habitat such that native and non-native species can flourish. For example, urbanization caused

populations of some species of birds and squirrels to be above their natural levels. Some plant species can also thrive in an urban environment, demonstrating their ability to survive even under harsh conditions. In fact, it is not uncommon to see mosses on walls of buildings or dandelions pushing through cracks in the concrete.

G.1.2 Benefits of Urbanization

There are several environmental advantages to urban areas. These advantages include:

Land and Habitat Reservation. Urban areas that grow upwards rather than outwards use up less land, preserving the rural areas surrounding the city. Unfortunately, this is not the trend in North America, where low density urban sprawl is devouring the land neighboring the cities. Compact development also means less land devoted to roads and parking lots as they become unnecessary, leaving more room for green space.

Increased Energy Efficiency. Urban developments provide the opportunity for increased energy efficiency for a number of reasons. First, apartments and attached housing require less energy for both heating and cooling when compared to single housing units. In compact developments, industry, shopping and leisure activities are all relatively close, serviced easily by walking or mass transit. Mass transit consumes only a fraction of the energy per person when compared to a personal automobile.

Efficient Waste Management Systems. In areas with high population densities, the development of waste management programs is often more economical and practical than in spread out areas. In a city, recycling programs become worthwhile as there is a large quantity of materials available. Both small and large industries in urban areas can benefit economically from recycling.

Increased Access to Education, Jobs, Health Care and Social Services. Increased education is a benefit of urbanization. Education informs more people about environmental issues and possible remedies. Most urban areas have significantly lower birth rates than rural areas, by as much as 3 to 4 times. Lower birth rates remove the environmental pressures caused by a growing population.

G.1.3 Sustainable Urban Development

Sustainable development as defined by the Brundtland Commission (a commission chartered by the United Nations) is "development which meets present needs without compromising the ability of future generations to achieve their needs and aspirations." As the previous section illustrates, urbanization offers numerous environmental benefits when designed properly. To achieve sustainability, urban areas must implement conservation incentives and develop areas with minimal impact to the environment. A city should attempt to implement the following in order to become sustainable:

1. Compact Development. To meet the housing requirements of a growing population urban areas should grow upwards rather than outwards. In order to achieve this, development must shift from single detached homes to multifamily housing. Increased population density provides the opportunities for increased energy efficiency and more green space.

2. Conserve Natural Habitats. Wetlands, meadows, marshes and groves, are not only a source of beauty but they are also very functional. They provide habitat for wildlife, keep air fresh, filter out pollutants and provide flood control. In order for wildlife to survive in an urban environment there must be a suitable habitat.

3. Cautious Development Plans. Natural features should be protected when an area is developed. Avoid urban development is valleys as they are vulnerable to erosion and the fertile topsoil is very suitable for agriculture. Develop with the contours of the land, thereby reducing erosion and landslides.

4. Provide Ample Green Space. Growing trees in the city can improve air quality, moderate climate, stabilize soils and provide habitat for bird species. Grow plants abandoned lots, rooftops and window sills. Plants serve to supplement food sources, provide habitat for wildlife species, and are aesthetically pleasing.

5. Encourage Water Conservation. Currently water use is very high in urban areas. Artificially low water prices, due to government subsidies, provide no incentive for conservation. Raising prices to reflect true costs of treatment and distribution and by installing meters encourages people to conserve.

6. Discourage the Use of Motor Vehicles. Motor vehicles require a lot of energy, contribute to air pollution and require large amounts of land for roads and parking lots. By designing a city that is compact with most things within walking distance reduces dependency on motor vehicles. This conserves energy, reduces air and to some extent water pollution and saves land.

7. Initiate Recycling Programs. Recycling is possible for many different types of wastes. Sewage effluents, solid waste and hazardous waste can all be recycled for other uses.

G.2 Floods and Flash Floods (Rain and Ice Melt)

When it rains heavily, there may be floods or flash floods. Flash floods occur in mountain streams - often in canyons; or flooding of dry washes. But they do happen in cities as well. Flash floods can occur even though it's not raining where you are. It may be raining hard farther upstream. It is raining so hard, water can not sink into the ground. It rushes down the mountainside to the stream. The stream can't carry all the water, so it floods. A flash flood may come at you as a high wave of water.

Floods also occur at the beginning of the Spring season when ice starts to melt. The rate of melting of ice depends on the rate of temperature increase.

While it is not the focus of our topic, there is also another type of floods that is worth mentioning. Coastal flooding is the inundation of land areas along the oceanic coast that is caused by sea waters over and above normal tidal action. Such flooding can originate from the ocean front, back bays, etc.

G.3 Warning Systems and Combined Sewer Overflows (CSOs)

By its very nature, wet weather issues are complex. Unlike municipal wastewater, overflow events are random occurrences controlled by storm events. The consequences of these overflows are highly variable pollutant loads and difficult to assess impacts on the environment.

During a storm, excessive combined sewer overflows (CSOs), if uncontrolled, may overload a sewer system and result in flooding or untreated discharge to streams and lakes. Wastewater treatment plants with combined sewers can also be burdened to the point where a severe loss of treatment efficiency occurs or the effluent flows become great enough that it becomes life threatening and the sewerage flow is allowed to by-pass the treatment plant and be discharged directly to the receiving body of water. Sewage discharged without treatment is a source of biological, chemical and aesthetic pollution. These overflow events pose a threat to water quality, aquatic life, human health, and properties.

Many municipalities are working to develop new, or improve existing, early warning systems to ensure proper and safe disposal of sewer water in case of extreme rain events.

G.4 The Region

The Greater Toronto Area (GTA) (Figure 1) is spatially partitioned into six Regional Municipalities namely, Metropolitan Toronto (now City of Toronto), Durham, York, Peel, Halton and Hamilton-Wentworth (Figure 1). Each of these regions can in turn be spatially partitioned in a number of local municipalities. The Regional Municipality of Hamilton-Wentworth (The Region) is comprised of the cities of Hamilton and Stoney Creek, the towns of Ancaster, Dundas, and Flamborough, and the township of Glanbrook (Figures 2 to 7). For more information about the municipalities, refer to the link http://www.jpint.utoronto.ca/gta96/reg6.html. Figures 1 to 7 are copied from this website. Stirrup et al. (1997) stated in their study that The Region operates and maintains a large combined sewer system in the Great Lakes basin. During dry weather and small storm events, two large interceptor sewers convey all sanitary and storm flows to the Woodward Avenue wastewater treatment plant. Larger rainfall events, specifically high intensity summer thunderstorms, generate flows which exceed the design capacity of the sanitary interceptors and result in combined sewer overflows to Hamilton Harbour and Cootes Paradise, which ultimately discharge to Lake Ontario. The Region is implementing a comprehensive program for reducing the pollution caused by these overflows. This program includes the construction

of several off-line detention storage facilities and the implementation of a real-time control system for combined sewer overflow reduction. Real-time control will enable maximum utilization of the storage available within the combined sewer network and help reduce the frequency and volume of combined sewer overflows. New hydrologic and hydraulic simulation models have been specially developed for this project to help identify, test and implement optimal real-time control strategies. The study discusses some of the more important aspects related to the design and implementation of the Region's real-time control system, and focuses mainly on the development of these hydrologic and hydraulic simulation models. The region is developing a Real Time Control (RTC) system to help reduce combined sewer overflows (CSOs) to local receiving waters. Knowledge of rainfall and resulting flows at key points in the region's combined sewer system is essential to minimize CSOs. The region has set up a monitoring network of nine gauges to provide data for rainfall and flow forecasting. Accurate gridded rainfall information is needed to compute expected rainfall intensities at ungauged locations as input to hydrologic/hydraulic distributed models of the region and its combined sewer system. In hydrologic modeling, the random spatial variability of rainfall is often accounted for by spatial interpolation techniques with varying degrees of complexity. This results in better prediction of rainfall storms in real time for flood warning systems and the minimization of the discharge of untreated sewage into the receiving water bodies. The Region is located on the west end of Lake Ontario as shown in Figure 8.

G.5 Station-based and Grid-based Approaches

The station-based approach is mainly using the records at point locations, corresponding to rain-gauges within the study area. Rain-gauges may be assigned to represent management areas, such as watersheds or administrative districts. This approach is a standard procedure when running "lumped models". The grid-based method enables estimates of the spatial variation in precipitation to be acquired at a field level by providing data for a network of grid points at a user-specified resolution. This "distributed" concept is an extension of the station-based method in that instead of having one or two points within the model, the same calculations are performed for thousands of individual points (represented by the small red flags "imaginary gauges" in Figure 9). This is a standard procedure when running "distributed models".

G.6 References

Stirrup, M., Z. Vitasovic and E. Strand (1997). Real-Time Control of Combined Sewer Overflows in Hamilton-Wentworth Region. *Water Quality Research Journal of Canada*, 32(1): 155-168.

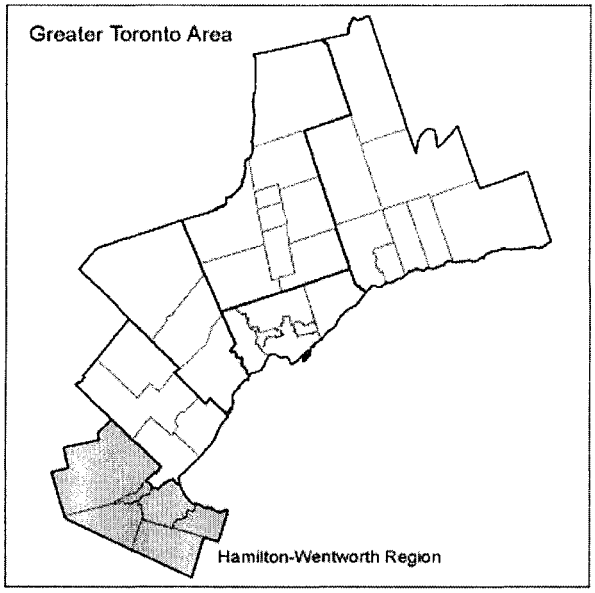


Figure 1

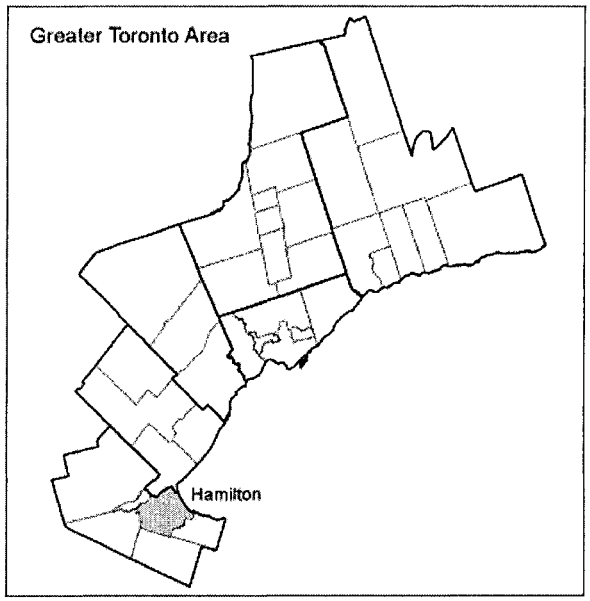


Figure 2

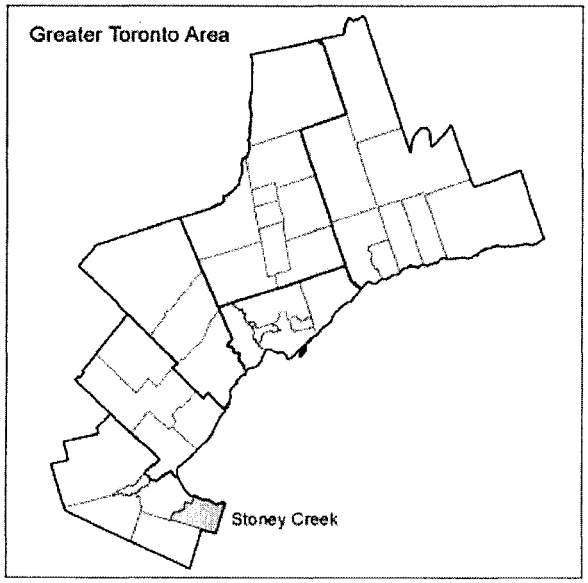


Figure 3

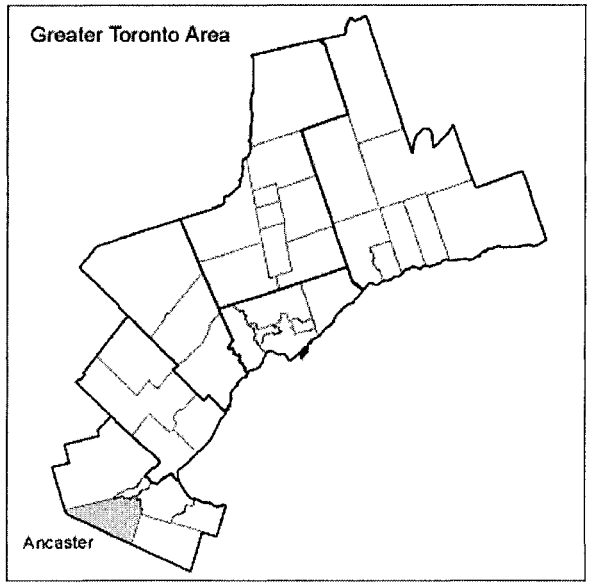


Figure 4

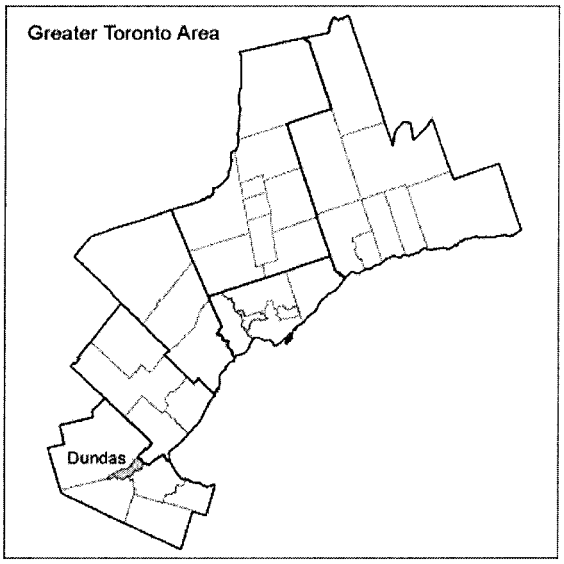


Figure 5

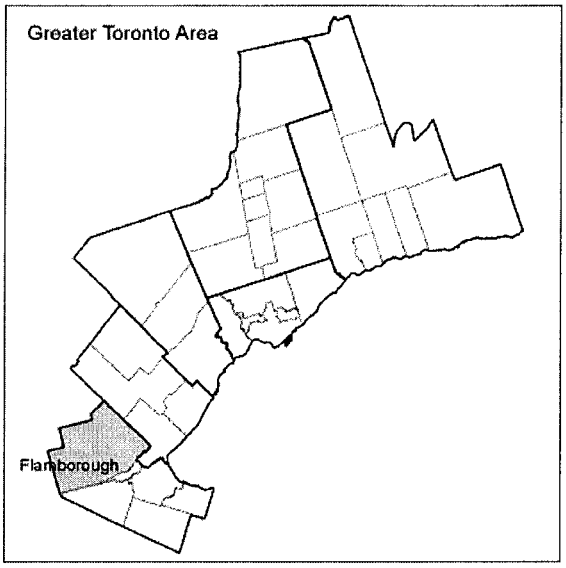


Figure 6

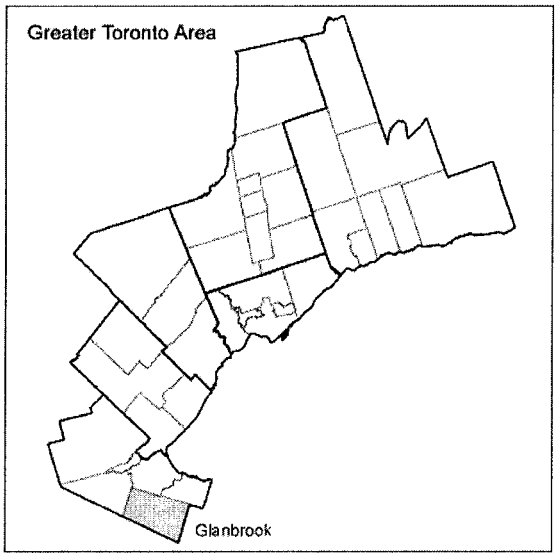


Figure 7

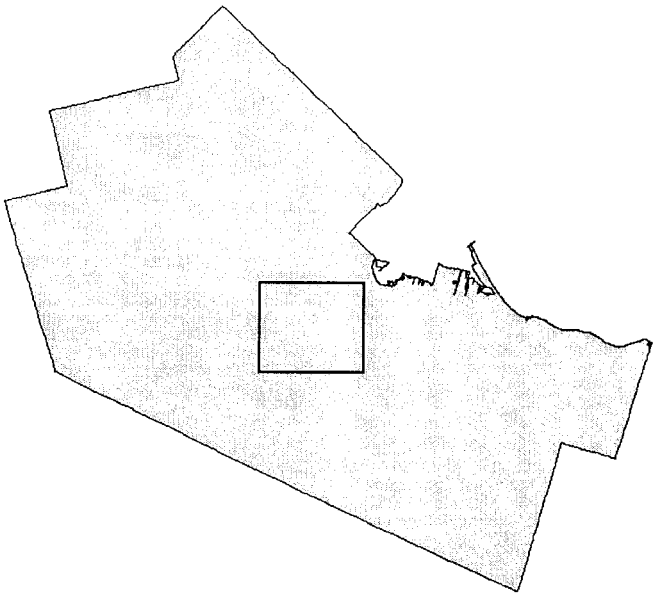

Figure 8

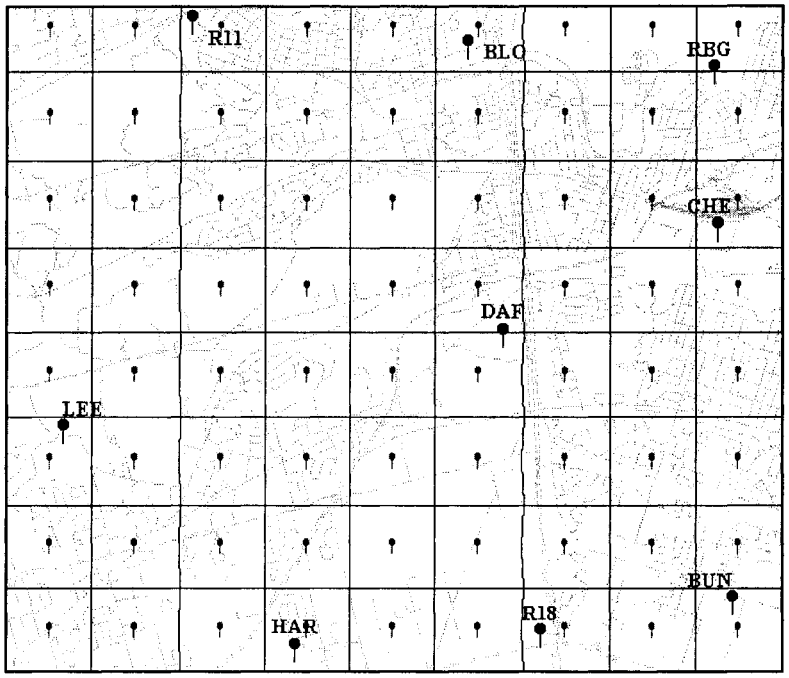


Figure 9

# APPENDIX H: MORE TABLES FOR CHAPTER 6

## *Continue: Tables 6.1*

| Data Set | Spatial Extent | No. of Stations | Boundary Conditions: Elev (X1) | Longitude (X2) | Latitude (X3) | Lat (m) | β0 | β1 | β2 | β3 | β4 | β5 | β6 | β7 | β8 | β9 | R2 (%) | Is The Model Significant as a ..... Model? Descriptive | Predictive |
|---|---|---|---|---|---|---|---|---|---|---|---|---|---|---|---|---|---|---|---|
| 1977-78 (Wet Year) | Crete | 67 | 0 ≤ E (X1) ≤ 905 m | 45 ≤ X2 ≤ 244 km | 69 ≤ X3 ≤ 134 km | 3,869,4215 ≤ L ≤ 3,930,876 | 655.8 | 1.24 | -2.15 | 3.76 | - | - | - | - | - | - | 61.8 | YES | YES |
| | | | | | | | 478.4 | 1.76 | -2.03 | 4.85 | -0.0007 | - | - | - | - | - | 62.9 | YES | YES |
| | | | | | | | 491.8 | 1.77 | -2.16 | 4.77 | -0.0007 | 0.0005 | - | - | - | - | 62.9 | YES | YES |
| | | | | | | | -2523.0 | 1.46 | -3.83 | 74.67 | -0.0004 | 0.0037 | -0.3703 | - | - | - | 66.9 | YES | YES |
| | | | | | | | -2168.0 | 1.85 | -2.66 | 64.13 | -0.0002 | 0.0029 | -0.3137 | -0.0039 | - | - | 68.2 | YES | YES |
| | | | | | | | -1231.0 | 0.80 | -2.56 | 46.40 | -0.0002 | 0.0023 | -0.2328 | -0.0032 | 0.0104 | - | 68.6 | YES | YES |
| | | | | | | | -7316.0 | 1.56 | 17.80 | 149.12 | 0.0001 | -0.0113 | -0.6686 | -0.0047 | 0.0008 | -0.1716 | 70.5 | YES | YES |
| | North | 20 | 0 ≤ E (X1) ≤ 748 m | 13 ≤ X2 ≤ 163 km | 86 ≤ X3 ≤ 134 km | 3,887,8745 ≤ L ≤ 3,938,876 | 5761.0 | 0.74 | -9.94 | -35.43 | - | - | - | - | - | - | 63.4 | YES | NO |
| | | | | | | | 7694.0 | -1.14 | -11.83 | -49.77 | 0.0023 | - | - | - | - | - | 67.2 | YES | NO |
| | | | | | | | 7956.0 | -1.28 | -14.31 | -51.32 | 0.0025 | 0.0133 | - | - | - | - | 67.3 | NO | NO |
| | | | | | | | -3282.0 | -1.76 | -21.96 | 170.20 | 0.0031 | 0.0462 | -1.0426 | - | - | - | 74.6 | YES | NO |
| | | | | | | | 3494.0 | 0.03 | -14.27 | 29.00 | 0.0023 | 0.0260 | -0.3672 | -0.0128 | - | - | 77.1 | NO | NO |
| | | | | | | | 39321.0 | -23.42 | -9.21 | -580.90 | 0.0043 | -0.0109 | 2.2010 | -0.0079 | 0.2013 | - | 80.6 | NO | NO |
| | | | | | | | 36759.0 | -22.78 | -1.40 | -541.00 | 0.0043 | -0.0158 | 2.0440 | -0.0087 | 0.1959 | -0.0530 | 80.6 | YES | NO |
| | South | 30 | 0 ≤ E (X1) ≤ 792 m | 4 ≤ X2 ≤ 182 km | 69 ≤ X3 ≤ 188 km | 3,869,4215 ≤ L ≤ 3,906,170 | -978.3 | 1.05 | 0.62 | 19.91 | - | - | - | - | - | - | 71.9 | YES | YES |
| | | | | | | | -1093.1 | 0.73 | 1.01 | 21.24 | 0.0004 | - | - | - | - | - | 72.2 | YES | YES |
| | | | | | | | -1641.0 | 0.71 | 11.33 | 23.57 | 0.0004 | -0.0064 | - | - | - | - | 83.8 | YES | YES |
| | | | | | | | 4531.0 | 0.21 | 17.60 | -137.26 | 0.0007 | -0.0746 | 0.9797 | - | - | - | 87.2 | YES | YES |
| | | | | | | | 3538.0 | 0.40 | 16.80 | -112.47 | 0.0009 | -0.0683 | 0.8286 | -0.0025 | - | - | 87.4 | YES | YES |
| | | | | | | | 4168.0 | -0.74 | 16.13 | -121.14 | 0.0009 | -0.0686 | 0.8528 | -0.0004 | 0.0107 | - | 87.5 | YES | YES |
| | | | | | | | -454.0 | -2.36 | 45.98 | -49.40 | 0.0009 | -0.1041 | 0.5987 | 0.0068 | 0.0218 | -0.2675 | 88.1 | YES | YES |
| | East | 18 | 6 ≤ E (X1) ≤ 905 m | 160 ≤ X2 ≤ 244 km | 76 ≤ X3 ≤ 182 km | 3,875,8515 ≤ L ≤ 3,902,368 | 669.5 | 1.09 | -2.28 | 4.71 | - | - | - | - | - | - | 89.6 | YES | YES |
| | | | | | | | 488.4 | 1.79 | -1.92 | 5.23 | -0.0008 | - | - | - | - | - | 91.9 | YES | YES |
| | | | | | | | -2505.0 | 1.94 | 24.97 | 8.07 | -0.0009 | -0.0658 | - | - | - | - | 92.5 | YES | YES |
| | | | | | | | -5104.0 | 1.91 | 27.68 | 61.00 | -0.0009 | -0.0731 | -0.2940 | - | - | - | 92.7 | YES | YES |
| | | | | | | | -3604.0 | 0.39 | 15.37 | 59.40 | -0.0006 | -0.0473 | -0.2832 | 0.0064 | - | - | 92.9 | YES | YES |
| | | | | | | | -3967.0 | 0.14 | 17.96 | 61.80 | -0.0007 | -0.0525 | -0.3039 | 0.0052 | 0.0065 | - | 92.9 | YES | YES |
| | | | | | | | -388.0 | -2.36 | -10.18 | 50.40 | -0.0010 | -0.0691 | -0.6561 | 0.0091 | 0.0288 | 0.3667 | 93.3 | YES | NO |

| Data Set | Spatial Extent | No. of Stations | Boundary Conditions | | | | | | | | | | | | | | | | | Is The Model Significant as a ..... Model? | |
|---|---|---|---|---|---|---|---|---|---|---|---|---|---|---|---|---|---|---|---|---|---|
| | | | Elev (X1) | Longitude (X2) | Latitude (X3) | | βo | β1 | β2 | β3 | β4 | β5 | β6 | β7 | β8 | β9 | R2 (%) | Descriptive | Predictive |
| 1986-87 (Wet Year) | Crete | 65 | 0 ≤ E (X1) ≤ 905 m | 1 ≤ X2 ≤ 244 km | Long (m) | Lat (m) | -1121.2 | 0.88 | 0.82 | 18.17 | - | - | - | - | - | - | 53.1 | YES | YES |
| | | | | | 464,716≤ Lo ≤705,496 | 3,869,421≤ La ≤3,930,876 | -1158.9 | 0.98 | 0.84 | 18.41 | -0.0001 | - | - | - | - | - | 53.2 | YES | YES |
| | | | | | | | -1121.2 | 0.99 | 0.47 | 18.18 | -0.0001 | 0.0014 | - | - | - | - | 53.2 | YES | YES |
| | | | | | | | -4279.0 | 0.62 | -1.48 | 92.04 | 0.0002 | 0.0051 | -0.3915 | - | - | - | 58.7 | YES | YES |
| | | | | | | | -3734.0 | 1.06 | -0.08 | 77.03 | 0.0005 | 0.0043 | -0.3113 | -0.0048 | - | - | 61.0 | YES | YES |
| | | | | | | | -2002.0 | -0.83 | 0.02 | 44.88 | 0.0005 | 0.0036 | -0.1665 | -0.0035 | 0.0182 | - | 62.1 | YES | YES |
| | | | | | | | -6583.0 | -0.42 | 16.12 | 121.70 | 0.0008 | -0.0070 | -0.4836 | -0.0049 | 0.0126 | -0.1368 | 63.5 | YES | YES |
| | North | 21 | 0 ≤ E (X1) ≤ 748 m | 1 ≤ X2 ≤ 153 km | 464,716≤ Lo ≤813,595 | 3,895,526≤ La ≤3,939,876 | 3763.0 | 0.75 | -7.27 | -19.58 | - | - | - | - | - | - | 47.7 | NO | NO |
| | | | | | | | 6050.0 | -1.55 | -9.36 | -36.65 | 0.0029 | - | - | - | - | - | 56.5 | NO | NO |
| | | | | | | | 4813.0 | -0.80 | 5.68 | -29.73 | 0.0017 | -0.0868 | - | - | - | - | 68.2 | YES | NO |
| | | | | | | | -3522.0 | -1.14 | 0.61 | 131.99 | 0.0021 | -0.0615 | -0.7536 | - | - | - | 73.6 | YES | NO |
| | | | | | | | 3170.0 | 0.41 | 5.51 | -3.40 | 0.0017 | -0.0681 | -0.1125 | -0.0133 | - | - | 78.2 | YES | NO |
| | | | | | | | 26102.0 | -15.18 | 8.05 | -368.40 | 0.0031 | -0.0903 | 1.4920 | -0.0082 | 0.1313 | - | 80.4 | YES | NO |
| | | | | | | | -13231.0 | -7.28 | 130.20 | 218.90 | 0.0032 | -0.1870 | -0.8490 | -0.0204 | 0.0668 | -0.9344 | 81.9 | YES | NO |
| | South | 28 | 0 ≤ E (X1) ≤ 792 m | 4 ≤ X2 ≤ 182 km | 464,716≤ Lo ≤622,750 | 3,868,421≤ La ≤3,908,170 | -1340.5 | 0.73 | 0.42 | 21.45 | - | - | - | - | - | - | 65.7 | YES | YES |
| | | | | | | | -1527.2 | 0.15 | 1.09 | 23.72 | 0.0007 | - | - | - | - | - | 66.7 | YES | YES |
| | | | | | | | -2018.0 | -0.06 | 10.43 | 26.11 | 0.0009 | -0.0503 | - | - | - | - | 77.9 | YES | YES |
| | | | | | | | -686.0 | -0.18 | 11.82 | -8.63 | 0.0010 | -0.0543 | 0.2119 | - | - | - | 78.1 | YES | YES |
| | | | | | | | -1333.0 | -0.07 | 11.35 | 7.50 | 0.0011 | -0.0504 | 0.1137 | -0.0016 | - | - | 78.1 | YES | YES |
| | | | | | | | 2228.0 | -6.69 | 7.73 | -41.00 | 0.0015 | -0.0523 | 0.2457 | 0.0069 | 0.0614 | - | 83.3 | YES | YES |
| | | | | | | | -3201.0 | -8.56 | 42.77 | 43.20 | 0.0014 | -0.0939 | -0.0521 | 0.0171 | 0.0743 | -0.3142 | 84.4 | YES | YES |
| | East | 17 | 9 ≤ E (X1) ≤ 905 m | 160 ≤ X2 ≤ 244 km | 621,158≤ Lo ≤705,496 | 3,877,380≤ La ≤3,902,380 | -920.4 | 0.67 | 1.67 | 15.36 | - | - | - | - | - | - | 61.2 | YES | NO |
| | | | | | | | -1073.4 | 0.95 | 1.88 | 16.16 | -0.0003 | - | - | - | - | - | 61.9 | NO | NO |
| | | | | | | | -10594.0 | 1.48 | 87.03 | 26.01 | -0.0008 | -0.2080 | - | - | - | - | 75.3 | YES | NO |
| | | | | | | | -28335.0 | 1.60 | 110.41 | 368.30 | -0.0011 | -0.2683 | -1.8740 | - | - | - | 83.1 | YES | NO |
| | | | | | | | -18572.0 | -4.53 | 55.06 | 294.60 | 0.0004 | -0.1497 | -1.4716 | 0.0254 | - | - | 89.9 | YES | NO |
| | | | | | | | -17497.0 | -6.54 | 61.58 | 259.80 | -0.0001 | -0.1601 | -1.3330 | 0.0202 | 0.0374 | - | 92.2 | YES | NO |
| | | | | | | | -19048.0 | -4.77 | 82.67 | 244.40 | 0.0002 | -0.1373 | -0.8936 | 0.0173 | 0.0208 | -0.3201 | 92.7 | YES | NO |

| Data Set | Spatial Extent | No. of Stations | Boundary Conditions Elev (X1) | Longitude (X2) | Long (m) (X3) | Latitude Lat (m) | β0 | β1 | β2 | β3 | β4 | β5 | β6 | β7 | β8 | β9 | R2 (%) | Is The Model Significant as a ..... Model? Descriptive | Predictive |
|---|---|---|---|---|---|---|---|---|---|---|---|---|---|---|---|---|---|---|---|
| 1989-90 (Dry Year) | Crete | 64 | 0 ≤ E (X1) ≤ 905 m | 1 ≤ X2 ≤ 244 km | 461,7185 ≤ E ≤ 570,5,496 | 3,869,4215 ≤ N ≤ 53,930,876 | -240.8 | 0.49 | -0.01 | 5.89 | - | - | - | - | - | - | 54.6 | YES | YES |
| | | | | | | | -271.6 | 0.57 | 0.01 | 6.09 | -0.0001 | - | - | - | - | - | 54.8 | YES | YES |
| | | | | | | | -498.2 | 0.48 | 2.32 | 7.44 | 0.0000 | -0.0069 | - | - | - | - | 58.1 | YES | YES |
| | | | | | | | -1927.9 | 0.29 | 1.45 | 40.88 | 0.0001 | -0.0073 | -0.1772 | - | - | - | 63.3 | YES | YES |
| | | | | | | | -1685.5 | 0.53 | 2.13 | 33.86 | 0.0002 | -0.0076 | -0.1391 | -0.0024 | - | - | 66.1 | YES | YES |
| | | | | | | | -995.3 | -0.26 | 2.12 | 20.83 | 0.0002 | -0.0078 | -0.0802 | -0.0017 | 0.0078 | - | 67.2 | YES | YES |
| | | | | | | | -3433.0 | 0.02 | 10.33 | 62.08 | 0.0004 | -0.0132 | -0.2514 | -0.0024 | 0.0043 | -0.0699 | 68.9 | YES | YES |
| | North | 21 | 0 ≤ E (X1) ≤ 740 m | 1 ≤ X2 ≤ 153 km | 461,7185 ≤ E ≤ 581,3,595 | 3,867,8745 ≤ N ≤ 53,930,876 | 1505.0 | 0.46 | -2.43 | -7.79 | - | - | - | - | - | - | 46.6 | NO | NO |
| | | | | | | | 2483.0 | -0.53 | -3.32 | -15.08 | 0.0012 | - | - | - | - | - | 52.9 | NO | NO |
| | | | | | | | 1768.0 | -0.09 | 5.37 | -11.09 | 0.0006 | -0.0501 | - | - | - | - | 58.2 | YES | NO |
| | | | | | | | -2539.0 | -0.27 | 2.75 | 72.47 | 0.0008 | -0.0371 | -0.3695 | - | - | - | 73.8 | YES | NO |
| | | | | | | | 1823.0 | 0.74 | 5.95 | -15.77 | 0.0005 | -0.0414 | 0.0284 | -0.0087 | - | - | 81.5 | YES | NO |
| | | | | | | | 6030.0 | -2.12 | 6.41 | -86.40 | 0.0008 | -0.0454 | 0.3228 | -0.0077 | 0.0241 | - | 81.8 | YES | NO |
| | | | | | | | -26493.0 | 4.41 | 107.38 | 415.70 | 0.0009 | -0.1255 | -1.6130 | -0.0178 | -0.0292 | -0.7726 | 86.0 | YES | NO |
| | South | 27 | 0 ≤ E (X1) ≤ 792 m | 4 ≤ X2 ≤ 162 km | 464,9165 ≤ E ≤ 582,2,750 | 3,869,4215 ≤ N ≤ 53,908,170 | -881.6 | 0.32 | 1.10 | 10.07 | - | - | - | - | - | - | 61.2 | YES | NO |
| | | | | | | | -658.1 | 0.36 | 1.02 | 9.79 | -0.0001 | - | - | - | - | - | 61.3 | YES | NO |
| | | | | | | | -940.3 | 0.26 | 6.16 | 11.24 | 0.0000 | -0.0275 | - | - | - | - | 79.9 | YES | YES |
| | | | | | | | -553.0 | 0.22 | 6.55 | 1.18 | 0.0001 | -0.0287 | 0.0613 | - | - | - | 80.0 | YES | YES |
| | | | | | | | 215.0 | 0.10 | 7.10 | -17.91 | -0.0001 | -0.0333 | 0.1770 | 0.0019 | - | - | 80.6 | YES | YES |
| | | | | | | | 746.0 | -0.83 | 6.59 | -25.37 | -0.0001 | -0.0336 | 0.1989 | 0.0035 | 0.0087 | - | 81.2 | YES | NO |
| | | | | | | | -1706.0 | -1.73 | 22.91 | 12.33 | -0.0001 | -0.0631 | 0.0678 | 0.0070 | 0.0150 | -0.1464 | 82.4 | YES | NO |
| | East | 17 | 3 ≤ E (X1) ≤ 986 m | 160 ≤ X2 ≤ 244 km | 621,1685 ≤ E ≤ 705,498 | 3,873,2805 ≤ N ≤ 53,902,360 | -122.5 | 0.44 | 0.03 | 4.57 | - | - | - | - | - | - | 90.2 | YES | YES |
| | | | | | | | -108.2 | 0.36 | 0.01 | 4.57 | 0.0001 | - | - | - | - | - | 90.4 | YES | YES |
| | | | | | | | -1572.0 | 0.36 | 14.18 | 5.42 | 0.0001 | -0.0365 | - | - | - | - | 91.9 | YES | YES |
| | | | | | | | -3632.0 | 0.29 | 12.07 | 58.02 | 0.0001 | -0.0312 | -0.2955 | - | - | - | 93.0 | YES | YES |
| | | | | | | | -4280.0 | -1.11 | 6.80 | 86.87 | 0.0004 | -0.0223 | -0.4465 | 0.0063 | - | - | 95.2 | YES | YES |
| | | | | | | | -4334.0 | -2.00 | 11.06 | 79.71 | 0.0000 | -0.0291 | -0.4348 | 0.0029 | 0.0199 | - | 97.0 | YES | YES |
| | | | | | | | -4327.0 | -1.94 | 11.76 | 77.93 | 0.0000 | -0.0270 | -0.4072 | 0.0028 | 0.0192 | -0.0165 | 97.0 | YES | YES |

| Data Set | Spatial Extent | No. of Stations | Boundary Conditions: Elev (X1) | Longitude (X2) | Long (m) | Latitude (X3) | Lat (m) | β0 | β1 | β2 | β3 | β4 | β5 | β6 | β7 | β8 | β9 | R2 (%) | Is The Model Significant as a .....Model? Descriptive | Predictive |
|---|---|---|---|---|---|---|---|---|---|---|---|---|---|---|---|---|---|---|---|---|
| Short-Term Average | Crete | 62 | 6 ≤ E (X1) ≤ 905 m | 4 ≤ X2 ≤ 244 km | 464,9175 ≤ Lo ≤ 705,498 | 69 ≤ X3 ≤ 131 km | 3,869,4215 ≤ La ≤ 53,939,876 | -88.0 | 0.90 | -0.92 | 8.35 | - | - | - | - | - | - | 64.3 | YES | YES |
| | | | | | | | | -192.3 | 1.15 | -0.86 | 9.02 | -0.0003 | - | - | - | - | - | 64.7 | YES | YES |
| | | | | | | | | -111.7 | 1.18 | -1.61 | 8.53 | -0.0003 | 0.0028 | - | - | - | - | 64.8 | YES | YES |
| | | | | | | | | -2249.0 | 0.99 | -2.48 | 57.00 | -0.0002 | 0.0041 | -0.2538 | - | - | - | 68.3 | YES | YES |
| | | | | | | | | -1636.5 | 1.39 | -0.90 | 40.61 | 0.0001 | 0.0027 | -0.1675 | -0.0047 | - | - | 71.9 | YES | YES |
| | | | | | | | | -62.0 | -0.77 | -1.04 | 12.33 | 0.0000 | 0.0023 | -0.0440 | -0.0029 | 0.0211 | - | 73.7 | YES | YES |
| | | | | | | | | -3579.0 | -0.56 | 11.44 | 71.43 | 0.0002 | -0.0054 | -0.2878 | -0.0037 | 0.0178 | -0.1080 | 75.1 | YES | YES |
| | North | 18 | 8 ≤ E (X1) ≤ 740 m | 13 ≤ X2 ≤ 153 km | 473,8295 ≤ Lo ≤ 613,595 | 88 ≤ X3 ≤ 131 km | 3,887,8745 ≤ La ≤ 53,939,875 | 3949.0 | 0.89 | -8.31 | -22.68 | - | - | - | - | - | - | 70.4 | NO | NO |
| | | | | | | | | 4958.0 | -0.24 | -9.11 | -30.12 | 0.0014 | - | - | - | - | - | 73.2 | YES | NO |
| | | | | | | | | 4688.0 | -0.05 | -6.14 | -28.47 | 0.0011 | -0.0165 | - | - | - | - | 73.6 | YES | NO |
| | | | | | | | | -4154.0 | -0.67 | -11.98 | 142.73 | 0.0018 | 0.0159 | -0.7956 | - | - | - | 81.4 | YES | NO |
| | | | | | | | | 2943.0 | 1.36 | -2.72 | -10.88 | 0.0013 | -0.0016 | -0.0451 | -0.0173 | - | - | 89.7 | YES | NO |
| | | | | | | | | -1483.0 | 4.24 | -3.31 | 63.70 | 0.0011 | 0.0041 | -0.3560 | -0.0185 | -0.0246 | - | 89.7 | YES | NO |
| | | | | | | | | -14087.0 | 5.19 | 45.70 | 255.80 | 0.0013 | -0.0400 | -1.0870 | -0.0214 | -0.0321 | -0.3760 | 89.9 | YES | NO |
| | South | 28 | 9 ≤ E (X1) ≤ 792 m | 4 ≤ X2 ≤ 162 km | 464,9175 ≤ Lo ≤ 622,750 | 69 ≤ X3 ≤ 108 km | 3,869,4215 ≤ La ≤ 53,988,170 | -738.5 | 0.66 | 0.24 | 14.95 | - | - | - | - | - | - | 74.6 | YES | YES |
| | | | | | | | | -789.9 | 0.50 | 0.43 | 15.57 | 0.0002 | - | - | - | - | - | 74.7 | YES | YES |
| | | | | | | | | -1153.0 | 0.35 | 7.34 | 17.34 | 0.0003 | -0.0372 | - | - | - | - | 86.2 | YES | YES |
| | | | | | | | | 1541.0 | 0.11 | 10.15 | -52.95 | 0.0005 | -0.0454 | 0.4286 | - | - | - | 87.7 | YES | YES |
| | | | | | | | | 330.0 | 0.31 | 9.26 | -22.75 | 0.0006 | -0.0380 | 0.2450 | -0.0030 | - | - | 88.2 | YES | YES |
| | | | | | | | | 2306.0 | -3.37 | 7.25 | -49.66 | 0.0009 | -0.0391 | 0.3182 | 0.0033 | 0.0341 | - | 91.2 | YES | YES |
| | | | | | | | | -1396.0 | -4.64 | 31.14 | 7.76 | 0.0009 | -0.0675 | 0.1152 | 0.0083 | 0.0428 | -0.2142 | 92.1 | YES | YES |
| | East | 17 | 6 ≤ E (X1) ≤ 905 m | 168 ≤ X2 ≤ 244 km | 621,1585 ≤ Lo ≤ 705,498 | 77 ≤ X3 ≤ 102 km | 3,877,3905 ≤ La ≤ 53,902,380 | 85.0 | 0.75 | -0.02 | 5.17 | - | - | - | - | - | - | 83.4 | YES | YES |
| | | | | | | | | -182.0 | 1.25 | 0.36 | 6.57 | -0.0005 | - | - | - | - | - | 85.9 | YES | YES |
| | | | | | | | | -5142.0 | 1.53 | 44.72 | 11.70 | -0.0008 | -0.1084 | - | - | - | - | 90.1 | YES | YES |
| | | | | | | | | -9869.0 | 1.56 | 50.95 | 102.90 | -0.0009 | -0.1244 | -0.4993 | - | - | - | 90.7 | YES | YES |
| | | | | | | | | -5995.0 | -0.88 | 28.98 | 73.60 | -0.0003 | -0.0774 | -0.3396 | 0.0101 | - | - | 91.9 | YES | YES |
| | | | | | | | | -4859.0 | -2.99 | 35.86 | 37.00 | -0.0006 | -0.0884 | -0.1933 | 0.0046 | 0.0394 | - | 94.8 | YES | YES |
| | | | | | | | | -2972.0 | -5.13 | 10.18 | 55.79 | -0.0012 | -0.1162 | -0.7281 | 0.0081 | 0.0596 | 0.3896 | 95.8 | YES | YES |

| Data Set | Spatial Extent | No. of Stations | Boundary Conditions: Elev (X1) | Longitude (X2) | Longitude Long (m) | Latitude (X3) | Latitude Lat (m) | β0 | β1 | β2 | β3 | β4 | β5 | β6 | β7 | β8 | β9 | R2 (%) | Is The Model Significant as a ..... Model? Descriptive | Predictive |
|---|---|---|---|---|---|---|---|---|---|---|---|---|---|---|---|---|---|---|---|---|
| Long-term Average | Crete | 49 | 6 ≤ E (X1) ≤ 905 m | 18 ≤ X2 ≤ 244 km | 479,746≤ Lo ≤705,496 | 69 ≤ X3 ≤ 117 km | 3,869,421≤ La ≤3,917,260 | -516.5 | 0.66 | -1.50 | 14.16 | - | - | - | - | - | - | 74.0 | YES | YES |
| | | | | | | | | -437.7 | 0.40 | -1.60 | 13.96 | 0.0003 | - | - | - | - | - | 74.4 | YES | YES |
| | | | | | | | | 126.0 | 0.55 | -6.97 | 11.13 | 0.0002 | 0.0186 | - | - | - | - | 77.2 | YES | YES |
| | | | | | | | | -2266.0 | 0.49 | -9.72 | 71.27 | 0.0003 | 0.0264 | -0.3404 | - | - | - | 78.9 | YES | YES |
| | | | | | | | | -2340.0 | 0.69 | -8.94 | 71.15 | 0.0003 | 0.0251 | -0.3405 | -0.0015 | - | - | 79.2 | YES | YES |
| | | | | | | | | -1195.0 | -0.64 | -8.90 | 50.36 | 0.0003 | 0.0249 | -0.2513 | -0.0008 | 0.0133 | - | 80.4 | YES | YES |
| | | | | | | | | -3664.0 | -0.33 | 2.25 | 86.95 | 0.0004 | 0.0166 | -0.3804 | -0.0017 | 0.0098 | -0.0899 | 81.4 | YES | YES |
| | North | 11 | 40 ≤ E (X1) ≤ 740 m | 18 ≤ X2 ≤ 153 km | 479,746≤ Lo ≤613,595 | 88 ≤ X3 ≤ 117 km | 3,887,874≤ La ≤3,917,260 | 2504.0 | 0.62 | -7.32 | -9.32 | - | - | - | - | - | - | 67.9 | YES | NO |
| | | | | | | | | 3680.0 | -0.95 | -8.23 | -17.70 | 0.0019 | - | - | - | - | - | 74.8 | NO | NO |
| | | | | | | | | 3772.0 | -1.01 | -9.34 | -18.15 | 0.0020 | 0.0059 | - | - | - | - | 74.8 | NO | NO |
| | | | | | | | | -30856.0 | -1.30 | -39.96 | 733.90 | 0.0023 | 0.1322 | -3.8622 | - | - | - | 94.9 | NO | NO |
| | | | | | | | | -24646.0 | -0.42 | -31.25 | 596.80 | 0.0020 | 0.1026 | -3.1620 | -0.0066 | - | - | 96.1 | NO | NO |
| | | | | | | | | -59977.0 | 18.54 | -40.12 | 1213.30 | 0.0008 | 0.1585 | -5.8260 | -0.0108 | -0.1658 | - | 97.3 | NO | NO |
| | | | | | | | | 14926.0 | 15.25 | -422.40 | 170.50 | -0.0014 | 0.5308 | -2.3260 | 0.0081 | -0.1348 | 2.8700 | 99.6 | NO | NO |
| | South | 25 | 20 ≤ E (X1) ≤ 792 m | 80 ≤ X2 ≤ 162 km | 648,774≤ Lo ≤822,750 | 69 ≤ X3 ≤ 98 km | 3,869,421≤ La ≤3,897,768 | -503.1 | 0.60 | -2.18 | 15.07 | - | - | - | - | - | - | 83.4 | YES | YES |
| | | | | | | | | -565.7 | 0.39 | -1.93 | 15.84 | 0.0003 | - | - | - | - | - | 83.6 | YES | YES |
| | | | | | | | | -1260.0 | 0.23 | 7.09 | 17.73 | 0.0005 | -0.0360 | - | - | - | - | 84.0 | YES | YES |
| | | | | | | | | 1621.0 | 0.12 | 13.71 | -63.92 | 0.0005 | -0.0582 | 0.5003 | - | - | - | 85.3 | YES | YES |
| | | | | | | | | 1067.0 | 0.66 | 13.71 | -52.85 | 0.0008 | -0.0491 | 0.4329 | -0.0063 | - | - | 86.7 | YES | YES |
| | | | | | | | | 2297.0 | -2.51 | 8.50 | -58.19 | 0.0008 | -0.0394 | 0.3864 | 0.0008 | 0.0282 | - | 88.8 | YES | YES |
| | | | | | | | | -2286.0 | -4.04 | 40.37 | 9.26 | 0.0007 | -0.0772 | 0.1689 | 0.0066 | 0.0391 | -0.2625 | 90.7 | YES | YES |
| | East | 14 | 6 ≤ E (X1) ≤ 905 m | 160 ≤ X2 ≤ 244 km | 821,158≤ Lo ≤705,496 | 77 ≤ X3 ≤ 102 km | 3,877,390≤ La ≤3,902,380 | -83.5 | 0.72 | 0.29 | 5.78 | - | - | - | - | - | - | 84.4 | YES | YES |
| | | | | | | | | -155.2 | 0.85 | 0.44 | 6.08 | -0.0001 | - | - | - | - | - | 84.6 | YES | NO |
| | | | | | | | | -4061.0 | 1.03 | 36.66 | 10.13 | -0.0003 | -0.0668 | - | - | - | - | 88.3 | YES | NO |
| | | | | | | | | -7573.0 | 1.07 | 39.93 | 78.60 | -0.0004 | -0.0976 | -0.3754 | - | - | - | 88.8 | YES | NO |
| | | | | | | | | -3214.0 | -1.20 | 18.54 | 36.80 | 0.0002 | -0.0516 | -0.1467 | 0.0093 | - | - | 90.2 | NO | NO |
| | | | | | | | | -3174.0 | -3.64 | 27.48 | 19.51 | -0.0006 | -0.0633 | -0.1279 | 0.0003 | 0.0529 | - | 96.0 | YES | NO |
| | | | | | | | | -2880.0 | -3.91 | 23.94 | 21.40 | -0.0006 | -0.0675 | -0.1967 | 0.0010 | 0.0549 | 0.0542 | 96.0 | YES | NO |